



This is to certify that the
dissertation entitled

THE REGIO-AND STEREOSELECTIVE SYNTHESIS OF 2,3,5-
TRISUBSTITUTED TETRAHYDROFURANS VIA CYCLIZATION OF
EPOXY DIOLS AND TOTAL SYNTHESIS OF THE PROPOSED
STRUCTURE OF MUCOXIN

presented by

Radha Sridhar Narayan

has been accepted towards fulfillment
of the requirements for the

Ph. D. degree in Chemistry


Major Professor's Signature

1/26/2004

Date

LIBRARY
Michigan State
University

PLACE IN RETURN BOX to remove this checkout from your record.
TO AVOID FINES return on or before date due.
MAY BE RECALLED with earlier due date if requested.

DATE DUE	DATE DUE	DATE DUE

THE REGIO-AND STEREOSELECTIVE SYNTHESIS OF 2,3,5-TRISUBSTITUTED
TETRAHYDROFURANS VIA CYCLIZATION OF EPOXY DIOLS AND TOTAL
SYNTHESIS OF THE PROPOSED STRUCTURE OF MUCOXIN

By

Radha Sridhar Narayan

A DISSERTATION

Submitted to
Michigan State University
in partial fulfillment of the requirements
for the degree of

DOCTOR OF PHILOSOPHY

Department of Chemistry

2004

1. The first part of the document is a list of names and titles, including "The Hon. Mr. Justice" and "The Hon. Mr. Justice".

2. The second part of the document is a list of names and titles, including "The Hon. Mr. Justice" and "The Hon. Mr. Justice".

3. The third part of the document is a list of names and titles, including "The Hon. Mr. Justice" and "The Hon. Mr. Justice".

4. The fourth part of the document is a list of names and titles, including "The Hon. Mr. Justice" and "The Hon. Mr. Justice".

5. The fifth part of the document is a list of names and titles, including "The Hon. Mr. Justice" and "The Hon. Mr. Justice".

6. The sixth part of the document is a list of names and titles, including "The Hon. Mr. Justice" and "The Hon. Mr. Justice".

7. The seventh part of the document is a list of names and titles, including "The Hon. Mr. Justice" and "The Hon. Mr. Justice".

8. The eighth part of the document is a list of names and titles, including "The Hon. Mr. Justice" and "The Hon. Mr. Justice".

9. The ninth part of the document is a list of names and titles, including "The Hon. Mr. Justice" and "The Hon. Mr. Justice".

10. The tenth part of the document is a list of names and titles, including "The Hon. Mr. Justice" and "The Hon. Mr. Justice".

ABSTRACT

THE REGIO-AND STEREOSELECTIVE SYNTHESIS OF 2,3,5-TRISUBSTITUTED TETRAHYDROFURANS VIA CYCLIZATION OF EPOXY DIOLS AND TOTAL SYNTHESIS OF THE PROPOSED STRUCTURE OF MUCOXIN

By

Radha Sridhar Narayan

This dissertation describes the development of a method for the stereoselective synthesis of 2,3,5-trisubstituted tetrahydrofurans (THFs), and the application of this method towards the total synthesis of mucoxin – a nonclassical annonaceous acetogenin. The synthesis also features a novel cyclization of a 1,2,5 triol system resulting in the formation of a 2,5-disubstituted THF.

Our interest in the synthesis of variously substituted THFs stems from the recent discovery of arachidonic acid tetrahydrofuran diols (AA-THF diols) – a novel class of secondary metabolites of AA. A total of 24 regio- and stereoisomeric THF diols can be formed from arachidonic acid. The chemical synthesis of these metabolites was undertaken in order to access them as single compounds for further biological studies. Our method involves the acid promoted cyclization of epoxy diols containing directing groups with different electronic properties. Depending upon the choice of the directing groups and the acid promoter, several regio- and stereoisomeric THF diols could be accessed from a common precursor. These studies are described in Chapter I.

Chapter II includes a survey of the structure, classification and biological activity of annonaceous acetogenins. Representative total syntheses of several members of this family of natural products are also discussed.

The later chapters discuss the application of our epoxy diol cyclization methodology towards the total synthesis of mucoxin. Mucoxin, the first example of an annonaceous acetogenin containing a hydroxylated THF ring, has shown highly potent cytotoxic activity of against human tumor cell lines. The synthesis of the left hand portion of mucoxin is described in Chapter III. The core THF diol unit was constructed using a thiophenyl directing group in the epoxy diol cyclization. Further, preliminary studies on the coupling of the left and right hand fragments are also discussed.

The completion of the total synthesis is described in Chapter IV. The disubstituted THF ring in mucoxin was constructed using a novel orthoester mediated cyclization of 1,2,n triols. The butenolide ring was introduced using the previously known thiophenyl lactone, to complete the synthesis. However, the spectral data for the synthetic material did not match that reported for the natural product. After analyzing data for both natural as well as synthetic compounds, and conformational analysis using molecular mechanics, we have proposed an alternative structure for the natural product.

To Sridhar

ACKNOWLEDGEMENTS

This dissertation would be incomplete without the mention of all those who contributed to my successful graduate career. Babak has been an enthusiastic and fun advisor to work with. Since I am his first graduate student, we both have gone through five years of learning and teaching together. I thank him for being extremely kind and supportive throughout. He always let me be independent and explore my own ideas. His encouragement and confidence in me has helped me achieve goals that at times seemed out of reach.

I would like to thank Profs. Maleczka, Wulff, and Weliky for serving on my committee and their advise on several occasions. I also thank Prof. Tepe for his help with my postdoctoral proposal and Prof. Hollingsworth for – among other things – a generous gift of 2-deoxy-D-ribose.

All the past and present group members have been my good friends. I especially thank Chryssoula and Courtney for their help and friendship. Jennifer has been a great colleague and neighbor to work with. I enjoyed her company working late hours in the lab and numerous interesting discussions we had. I also thank Qifei, Rachael, Montserrat, Ben, Marina, Tao and Jun for the fun time we shared.

Dr. Daniel Holmes has been extremely helpful with the NMR spectroscopy. The crucial NMR analysis toward the end would not have been possible without his assistance and active interest.

I extend my very special thanks to Prof. William Roush at the University of Michigan for his help on numerous occasions throughout my graduate career.

I am grateful for the support of my parents and the rest of the family, which has been crucial to my success. Their love and faith has helped me overcome all hurdles and pursue my goals tirelessly.

Finally, I thank my husband Sridhar for his constant encouragement every step of the way. His suggestions and advice have helped a great deal. I truly appreciate his unconditional love and support.

10

F:DT

10

1

...

1

•

100

100

 \vdots

;

1

10

1

;

11

142P

1

211

1

2.

1

•

•

;

;

;

1

1

1

 $\frac{1}{2}$

11

:

;

•

•

•

1

1

TABLE OF CONTENTS

List of Tables	ix
List of Figures	x
List of Schemes	xiv
Key to Symbols and Abbreviations	xvi
CHAPTER I	
Method development for the stereoselective synthesis of 2,3,5-trisubstituted tetrahydrofurans	1
A. Introduction	1
1. Novel metabolites of arachidonic acid	1
2. Stereoselective synthesis of 2,3,5 trisubstituted THFs – a brief review	6
B. Regio- and stereoselective synthesis of 2,3,5 THFs <i>via</i> cyclization of methylene interrupted epoxy diols	10
1. Method design	10
2. Background on regiocontrol in cyclization of epoxy alcohols	13
3. Method development	17
C. A novel method for the oxidative cleavage of olefins	35
D. Experimental	40
1. Experimental section for synthesis of 2,3,5 trisubstituted THFs	41
2. Experimental section for the oxidative cleavage of olefins	58
E. References	62
CHAPTER II	
The annonaceous acetogenins: structure, biological activity and total syntheses	67
A. Historical background	67
B. Structure and proposed biogenesis	68
C. Biological activity	71
1. <i>In vitro</i> studies	72
2. <i>In vivo</i> studies	73
3. Activity against multidrug resistant (MDR) cells	73
4. Pesticidal activity	74
D. Mechanism of action	75
E. Structure-activity relationships	77
F. Classical vs. nonclassical acetogenins	80
G. Total synthesis of the annonaceous acetogenins	81
1. Multiple intramolecular Williamson etherification strategy	84
2. Epoxide cascade strategy	88
3. Biomimetic ‘naked carbon skeleton’ strategy	89
4. Step-growth oligomerization strategy	90

10
11
12

13

14

15

16

17

18

19

20

21

22

23

24

25

26

27

5. Sequential, modular strategy	91
6. Miscellaneous	94
H. References	100

CHAPTER III

Synthesis of the left hand fragment (C12-C34) of mucoxin and preliminary studies on its coupling with the right hand fragment	105
A. Introduction	105
B. Retrosynthesis	108
C. Evaluation of the proposed intermolecular regio- and stereoselective epoxide opening strategy	119
1. Design and synthesis of chiral allylic alcohol III-3	119
a) Synthesis of a model allylic alcohol	145
b) Determination of the enantiomeric excess and the absolute configuration of diol III-59	148
2. Synthesis of vinylic epoxide III-4	152
3. Attempted intermolecular epoxide opening	157
D. Experimental section	172
E. References	211

CHAPTER IV

Total synthesis of the proposed structure of mucoxin	219
A. Revised strategies for the coupling of left- (C13-C37) and right-hand (C1-C12) fragments of mucoxin	219
1. Evaluation of coupling strategies involving organozinc additions	222
2. Conventional organometallic addition using chelation control to couple the two halves of mucoxin	229
B. Completion of the total synthesis of the proposed structure of mucoxin	244
C. Comparison of spectroscopic data and conclusions	258
D. Experimental section	280
E. References	319

APPENDIX	324
----------	-----

LIST OF TABLES

Table I-1: OsO ₄ – Oxone [®] mediated cleavage of complex olefins	38
Table II-1: Relative tumor growth inhibition (ED ₅₀ mg / mL) for representative acetogenins compared to adriamycin	72
Table II-2: LT ₅₀ values for German cockroach fifth instars	74
Table III-1: Optimization of the Sharpless asymmetric epoxidation of III-64	133
Table III-2: Cyclization of III-5 under various conditions	139
Table III-3: Synthesis of model allylic alcohol III-140	148
Table III-4: Preliminary attempts at optimization of the coupling of III-4 and III-140	158
Table IV-1: Optimization of the chelation controlled addition	232
Table IV-2: Mosher's ester analysis of IV-99 and IV-100	251
Table IV-3: Mosher's ester analysis of IV-101 and IV-102	253
Table IV-4: Mosher's ester analysis of IV-105 and IV-106	255
Table IV-5: Comparison of ¹ H NMR chemical shifts of bis-THF portions (C8-C17) of natural mucoxin vs. IV-117	261
Table IV-6: Comparison of ¹ H chemical shifts of bis-THF portions (C8-C17) of natural mucoxin vs. IV-122	264

LIST OF FIGURES

Figure I-1: Pathways of arachidonic acid metabolism	1
Figure I-2: Proposed biosynthesis of AA-THF-diols	3
Figure I-3: Regio- and stereoisomers of AA-THF-diols	5
Figure I-4: Intramolecular oxymercuration strategy for the construction of 2,3,5 trisubstituted THFs	7
Figure I-5: Roush's three component coupling approach to trisubstituted THFs	8
Figure I-6: Iodoetherification of alkene diols to stereoselectively access hydroxylated THFs	8
Figure I-7: Intramolecular iodoetherification of C6 allyl pyranosides used by Mootoo	9
Figure I-8: Sugimura's β -silyl cation cyclization tactic	9
Figure I-9: Cyclization pathways of methylene interrupted epoxydiol I-29	11
Figure I-10: Synthetic scheme to access enantiopure epoxy diols	11
Figure I-11: Conventional Baldwin vs. Warren's hybrid nomenclature for epoxide ring opening	12
Figure I-12: The first report of epoxy alcohol cyclization to construct THF ring by Kishi	13
Figure I-13: Nicolaou's strategy for <i>endo</i> over <i>exo</i> selectivity in epoxide ring opening	14
Figure I-14: Cyclizations of <i>trans</i> vinylic epoxides	14
Figure I-15: Cyclizations of <i>cis</i> vinylic epoxides	15
Figure I-16: Hirama's π -allyl palladium cyclization strategy	16
Figure I-17: Use of catalytic antibodies to achieve <i>endo</i> selective epoxide opening	16
Figure I-18: Mukai's alkynyl epoxide cyclization <i>via</i> cobalt complexation	17
Figure I-19: Proposed in situ deprotection – cyclization of epoxy diol	18
Figure I-20: Cyclic ethers derived from epoxy sulfide I-100 <i>via</i> episulfonium intermediate	28
Figure I-21: Warren's phenylthio polyol cyclization strategy for synthesis of THFs and THPs	29
Figure I-22: Possible equilibration between activated epoxy sulfide I-100 and the corresponding episulfonium ion	33
Figure I-23: Isomeric THF diols available from a common precursor I-93	34
Figure I-24: Oxidative cyclization of linoleic acid to produce THF diols	36
Figure II-1: Uvaricin – the first acetogenin isolated from <i>Uvaria accuminata</i> (Annonaceae)	68
Figure II-2: Generic structure of a binuclear acetogenin	68
Figure II-3: Classification and representative structures of acetogenins	69
Figure II-4: Proposed biosynthetic pathways for two main classes of acetogenins	71
Figure II-5: Some acetogenins that showed high <i>in vivo</i> cytotoxicity profiles	73
Figure II-6: Annonin I	75
Figure II-7: Model of bis-THF acetogenins interacting with complex I in mitochondrial membrane (Ref. 35)	76
Figure II-8: NADH-oxidase inhibitory potencies of bullatacin analogs	79

Figure II-9: The first total synthesis of an acetogenin, (+)-(3 <i>6-epi</i>)- <i>ent</i> -uvaricin	82
Figure II-10: Trost's synthesis of (+)-squamocin K (key retrosynthetic disconnections)	84
Figure II-11: Trost's synthesis of (+) - squamocin K	85
Figure II-12: Marshall's stereoselective S _E 2' addition approach to oxygenated THF precursors	86
Figure II-13: Marshall's synthesis of bullanin	87
Figure II-14: Hoyer's synthesis of (+)-parviflorin	88
Figure II-15: Syn and anti oxidative cyclizations of hydroxy olefin	89
Figure II-16: McDonald's biomimetic oxidative cyclization strategy	90
Figure II-17: Casiraghi's iterative vinologous aldol reaction strategy	91
Figure II-18: Proposed mechanisms for metal mediated oxidative cyclization of hydroxy olefins	92
Figure II-19: Sinha and Keinan's library synthesis of bis - THF core units	93
Figure II-20: Koert's modular strategy to construct bis - and tris - THF system	94
Figure II-21: Jacobsen's synthesis of muconin	95
Figure II-22: Tanaka's stereodivergent strategy for construction of adjacent bis-THF systems	97
Figure II-23: Evans' synthesis of mucocin	98
 Figure III-1: Mucoxin	 105
Figure III-2: Mucoxin: retrosynthetic analysis	108
Figure III-3: Grubbs' tandem olefin metathesis - hydrogenation protocol	109
Figure III-4: Common tactics used for regiocontrol in intermolecular epoxide opening reactions	111
Figure III-5: Sharpless' protocol for C3 selective epoxide ring opening of 2,3 epoxy alcohols	112
Figure III-6: Hirama's conditions for regio-and stereoselective addition of aromatic alcohols to highly functionalized vinyl epoxides	113
Figure III-7: Trost's strategy for 1,2 addition of alcohols to vinylic epoxides	114
Figure III-8: Trialkyl stannanes proved inefficient as electrophiles in Trost's studies	114
Figure III-9: Trost's two-component catalyst system for asymmetric allylic alkylation of alcohols	115
Figure III-10: A representative example of regio-and stereoselective ring opening of sugar derived oxiranes	115
Figure III-11: Mioskowski's conditions for stereoselective S _N 2 addition of alcohols to vinyl epoxides	116
Figure III-12: Lautens' protocol for S _N 2 substitution of vinylic epoxides by alcohols under mild conditions	116
Figure III-13: Jacobsen's strategy to construct the THF ring of muconin	118
Figure III-14: Isomeric THF diols available from a common epoxy diol precursor	119
Figure III-15: Stereochemical similarities and differences between the target THF unit III-3 and an available precursor III-56	120
Figure III-16: A route to transform III-57 to the target allylic alcohol III-3	120
Figure III-17: Proposed synthesis of the left hand (C13-C34) fragment of mucoxin	121
Figure III-18: Schlosser's β-oxido ylide route to <i>trans</i> alkenols	124
Figure III-19: Curran's self-oxidizing protecting group	129

Figure III-20: An <i>endo</i> selective epoxide opening of III-108 to generate 3-hydroxylated trisubstituted THF III-109	134
Figure III-21: Cyclization of an epoxy sulfide derived from 2-deoxy-D-ribose (Chapter I) via episulfonium ion formation	135
Figure III-22: Stereoisomeric THF diols originating from <i>trans</i> alcohol III-64	136
Figure III-23: <i>Cis</i> -vinyl epoxide may exhibit reduced <i>endo</i> -selectivity during intramolecular cyclization reaction	137
Figure III-24: Payne like equilibration of epoxy sulfide III-121 under acidic conditions	139
Figure III-25: Rayner's conditions for intermolecular trapping of episulfonium ions	140
Figure III-26: Possible route for cyclization of epoxy sulfides under acidic conditions; <i>endo</i> / <i>exo</i> notation is relative to epoxide.	141
Figure III-27: Comparison of structures of epoxy sulfides III-5 and III-29	142
Figure III-28: 1,2 vs. 1,3 Chelation control in addition of vinyl magnesium bromide to aldehyde III-139	147
Figure III-29: Mnemonic device for Sharpless asymmetric dihydroxylation reaction as applied to <i>trans</i> olefin III-102	149
Figure III-30: A positively helical system comprises of two interacting chromophores twisted in a clockwise direction going from the front to the back chromophore	150
Figure III-31: ECCD spectrum of III-146 in MeCN	152
Figure III-32: Design of an epoxy sulfide substrate for regioselective ring opening by alcohols	163
Figure III-33: Regio- and stereoselective alkyl group transfer to epoxy sulfides	165
Figure III-34: Cyclic sulfates and sulfites as epoxide surrogates	168
Figure III-35: S _N 2 displacement of allylic electrophiles with alkoxides	169
Figure IV-1: Original regio- and stereoselective intermolecular epoxide opening strategy	219
Figure IV-2: General representation of the revised strategy	220
Figure IV-3: Design of the new synthetic strategy	222
Figure IV-4: Chelation controlled vs. Felkin-Anh transition state for reduction of ketone IV-18	227
Figure IV-5: Revised stepwise strategy to assemble fragments IV-8 , IV-32 and IV-35	230
Figure IV-6: Sharpless' mechanism for vanadium catalyzed epoxidation of allylic alcohols	235
Figure IV-7: Kishi's transition state analysis to explain the diastereoselectivity observed in directed epoxidation of bis-homoallylic alcohols	236
Figure IV-8: Application of Kishi's T.S. models to bis-homoallylic alcohol IV-50	237
Figure IV-9: Representative examples of Shi asymmetric epoxidation of <i>cis</i> olefins	238
Figure IV-10: Proposed radical intermediate during oxygen transfer step in Jacobsen epoxidation	239
Figure IV-11: Sharpless' protocol for stereospecific conversion of vicinal diols into epoxides	240
Figure IV-12: Proposed one pot cyclization of triols (IV-76) to the corresponding cyclic hydroxy ethers (IV-78)	241

Figure IV-13: Assembly of the real aldehyde (IV-86) and partially functionalized right hand piece IV-87	244
Figure IV-14: Empirical mnemonic device for the asymmetric dihydroxylation reaction	246
Figure IV-15: Application of the asymmetric dihydroxylation mnemonic to olefin IV-85	247
Figure IV-16: nOe correlations in IV-101 and IV-105 containing <i>trans</i> and <i>cis</i> di-substituted THF rings respectively	254
Figure IV-17: Mucoxin: synthetic and originally proposed structures	258
Figure IV-18: Comparison of partial ¹ H NMR spectra of the natural mucoxin and IV-117	260
Figure IV-19: Comparison of partial ¹ H NMR spectra of natural mucoxin and IV-122	263
Figure IV-20: HRMS fragmentation pattern of the tris-TMS derivative of mucoxin. (* = observed peak)	265
Figure IV-21: nOe correlations in the two synthetic diastereomers	265
Figure IV-22: Intramolecular hydrogen bonding in mucoxin as proposed by McLaughlin	266
Figure IV-23: Truncated stereoisomeric bis-THF analogs of proposed structure of mucoxin	267
Figure IV-24: Low energy conformations of <i>cis-threo</i> isomer IV-123	268
Figure IV-25: Karplus equation plot for vicinal oxygenated systems	269
Figure IV-26: Low energy conformations of <i>cis-erythro</i> isomer IV-124	271
Figure IV-27: Low energy conformations of <i>trans-threo</i> isomer IV-125	273
Figure IV-28: Low energy conformations of <i>trans-erythro</i> isomer IV-126	274
Figure IV-29: Jimenezin: proposed structure (IV-125) vs. real structure (IV-126)	275
Figure IV-30: Possible alternative structure of mucoxin	276
Figure IV-31: Synthesis of hydroxy THF (C12-C34) portion and its union with iodide IV-87 via chelation controlled addition	277
Figure IV-32: Completion of the total synthesis	278
Figure IV-33: Summary of structure proof of synthetic material (IV-117)	279

LIST OF SCHEMES

Scheme I-1: Spontaneous 5- <i>exo</i> cyclization of free epoxy diol	19
Scheme I-2: Synthesis of acetonide protected epoxy diols	19
Scheme I-3: Various acids screened for deprotection – cyclization of I-89 and I-91	20
Scheme I-4: Synthesis of silyl protected epoxy diols	21
Scheme I-5: Preparation of epoxy diols with different pendant groups	23
Scheme I-6: Acid catalyzed cyclization of epoxy alcohols I-94 and I-95	24
Scheme I-7: Cyclization of epoxy diols containing electron withdrawing and neutral pendant groups	25
Scheme I-8: Cyclization of vinylic epoxy diol	26
Scheme I-9: Absence of equilibration between vinyl THF I-109 and THP I-110 under the cyclization conditions	27
Scheme I-10: Epoxy sulfide cyclization	30
Scheme I-11: Cyclization of I-100 in polar and nonpolar media using different acids	31
Scheme I-12: Absence of equilibration between phenylthio THFs I-123 and I-124 (products prior to acetylation) under the cyclization conditions	32
Scheme I-13: Cyclization of diastereomeric epoxy sulfide I-125	33
Scheme I-14: The OsO ₄ – Oxone [®] method for the oxidative cleavage of olefins	37
Scheme I-15: Plausible mechanism of OsO ₄ – Oxone [®] mediated cleavage of olefins	39
Scheme III-1: Proposed intermolecular epoxide opening strategy	118
Scheme III-2: Alkyne zipper reaction strategy	123
Scheme III-3: Propargylic ester strategy	123
Scheme III-4: Application of Schlosser's method to synthesize <i>trans</i> alcohol III-62	125
Scheme III-5: Iodide alkynylation route	127
Scheme III-6: Synthesis of <i>trans</i> homoallylic alcohol III-62	128
Scheme III-7: Attempted use of Curran's self-oxidizing protecting groups in our system	129
Scheme III-8: Synthesis of the differentially protected triol III-104	131
Scheme III-9: Selective deprotection of the PMB group in III-104	131
Scheme III-10: Synthesis of allylic alcohol III-64	132
Scheme III-11: Use of the Hata reagent to install the thiophenyl pendant group	134
Scheme III-12: BF ₃ •OEt ₂ mediated cyclization of the epoxy sulfide III-5 using previously optimized conditions	138
Scheme III-13: Cyclization of three different epoxy sulfides under the same conditions	142
Scheme III-14: Another attempt to improve the <i>endo</i> selectivity in the cyclization of III-5	143
Scheme III-15: Preparation of the aldehyde III-135	144
Scheme III-16: Synthesis of a model aldehyde III-139	146
Scheme III-17: Synthesis of dibenzoate derivatives of the diol III-103 for ECCD analysis	151
Scheme III-18: preparation of the three component coupling partners, III-6 and III-8	153

Scheme III-19: Synthesis of bromomethylacrylic acid III-149	154
Scheme III-20: Synthesis of vinylic epoxide III-4	156
Scheme III-21: A trial intermolecular ring opening of the vinylic epoxide III-4 using Mioskowski's conditions	157
Scheme III-22: Synthesis of simplified model vinylic epoxides and an allylic alcohol	159
Scheme III-23: Further optimization studies on the ring opening using model systems	160
Scheme III-24: Application of Lautens' conditions to model systems	160
Scheme III-25: Screening of various acid catalysts for S_N2 opening of the model epoxide	161
Scheme III-26: Attempted epoxide opening reactions using a tributyl tin ether	163
Scheme III-27: Synthesis and acid catalyzed intermolecular coupling reaction of an epoxy sulfide with an alcohol nucleophile	164
Scheme III-28: Attempted preparation and reaction of a trialkoxy aluminum with the epoxy sulfide III-189	166
Scheme III-29: Attempted alkoxy group transfer to the epoxy sulfide III-189	167
Scheme III-30: Attempted preparation and ring opening of cyclic sulfates and sulfites	168
Scheme III-31: Attempted preparation and displacement reactions of allylic triflate and tosylate	170
 Scheme IV-1: Synthesis of the model iodide	 223
Scheme IV-2: Attempted organozinc additions to aldehyde IV-8	224
Scheme IV-3: Synthesis of ketone IV-18 via organozinc addition to acid chloride IV-17	225
Scheme IV-4: Attempted addition of epoxy iodide IV-20 to acid chloride IV-17 via the the organozinc reagent	226
Scheme IV-5: Attempted hydride reduction reactions of ketone IV-18	228
Scheme IV-6: Model studies on HWE olefination approach	228
Scheme IV-7: Synthesis of the requisite homoallylic halides	230
Scheme IV-8: Synthesis of bis-homoallylic alcohol IV-50	233
Scheme IV-9: Feasibility studies of the new strategy described in Figure IV-5	234
Scheme IV-10: One pot cyclization of a model triol IV-82	243
Scheme IV-11: Synthesis of the real bis-homoallylic alcohol (IV-85)	245
Scheme IV-12: Application of triol cyclization method to the real system	247
Scheme IV-13: Chiral alcohols (IV-85 and IV-98) used in Mosher's ester analysis	249
Scheme IV-14: Synthesis of Mosher's esters of IV-85	250
Scheme IV-15: Synthesis of α -SPh lactones IV-111 and IV-112	256
Scheme IV-16: Completion of the total synthesis of proposed structure of mucoxin (IV-117)	257
Scheme IV-17: Synthesis of C36 epimer of IV-117	258
Scheme IV-18: Synthesis of (8,9- <i>epi</i>) IV-117	262

KEY TO SYMBOLS AND ABBREVIATIONS

AA	arachidonic acid
Ac	acetyl
AcOH	acetic acid
acac	acetoacetate
Bn	benzyl
BOC-ON	2-(<i>tert</i> -butoxycarbonyloxyimino)-2-phenylacetonitrile
Bu ₂ BOTf	dibutylboron trifluoromethanesulfonate
CI	chemical ionization
CSA	camphorsulfonic acid
δ	chemical shift (parts per million)
D	dextro (denotes configurational relationship with (<i>R</i>)-(+)-glyceraldehyde)
DDQ	2,3-dichloro-5,6-dicyano-1,4-benzoquinone
DEAD	diethyl azodicarboxylate
DET	diethyl tartrate
DIAD	diisopropyl azodicarboxylate
DIBAL-H	diisobutylaluminum hydride
DIPT	diisopropyl tartrate
DMAP	4-(dimethylamino)pyridine
DMF	dimethylformamide
DMP	Dess–Martin periodinane (oxidation reagent)
de	diastereomeric excess
dr	diastereomeric ratio
ECCD	exciton coupled circular dichroism
ee	enantiomeric excess
EE	1-ethoxyethyl
equiv.	equivalent(s)
Et ₂ O	diethyl ether
EtOAc	ethyl acetate
EtOH	ethanol
g	gram(s)
h	hour
HMPA	hexamethylphosphoramide
HRMS	high resolution mass spectrometry
Hz	Hertz
Im	imidazole
ⁱ Pr	isopropyl
IR	infrared spectrum
<i>J</i>	coupling constant
KHMDS	potassium hexamethyldisilylazide
L	levo (denotes configurational relationship with (<i>S</i>)-(–)-glyceraldehyde)

[illegible]

LAH	lithium aluminum hydride
LDA	lithium diisopropylamide
M	molar (concentration)
mCPBA	4-chloroperbenzoic acid
MeCN	acetonitrile
MeOH	methanol
Ms	methane sulfonate
MS	mass spectrometry
<i>m/z</i>	mass to charge ratio
NBS	<i>N</i> -bromosuccinamide
NCS	<i>N</i> -chlorosuccinamide
NMR	nuclear magnetic resonance
OAc	acetate
OTf	trifluoromethanesulfonate
PCC	pyridinium chlorochromate
PMB	<i>para</i> -methoxybenzyl
PPTS	pyridinium <i>p</i> -toluenesulfonic acid
pTSA	<i>para</i> -toluenesulfonic acid
<i>R</i>	rectus (Cahn-Ingold-Prelog system)
<i>S</i>	sinister (Cahn-Ingold-Prelog system)
SAD	Sharpless asymmetric dihydroxylation
SAE	Sharpless asymmetric epoxidation
TBAF	tetrabutylammonium fluoride
TBAI	tetrabutylammonium iodide
TBDPS	<i>t</i> -butyldiphenylsilyl
TBS	<i>t</i> -butyldimethylsilyl
TBHP	<i>t</i> -butyl hydroperoxide
TES	triethylsilyl
TFA	trifluoroacetic acid
TBSOTf	<i>t</i> -butyldimethylsilyl trifluoromethanesulfonate
THF	tetrahydrofuran
THP	tetrahydropyran
TMS	trimethylsilyl
TMSOTf	trimethylsilyl trifluoromethanesulfonate
TPAP	tetrapropylammonium perruthenate
TsOH	<i>para</i> -toluenesulfonic acid

127

128

129

130

131

132

CHAPTER I

METHOD DEVELOPMENT FOR THE STEREOSELECTIVE SYNTHESIS OF 2,3,5-TRISUBSTITUTED TETRAHYDROFURANS

A. Introduction

1. Novel metabolites of arachidonic acid

Arachidonic acid (AA) is a C20 polyunsaturated fatty acid found in phosphatidylinositol and other phospholipids as a C2 ester of glycerol. AA is stored in a

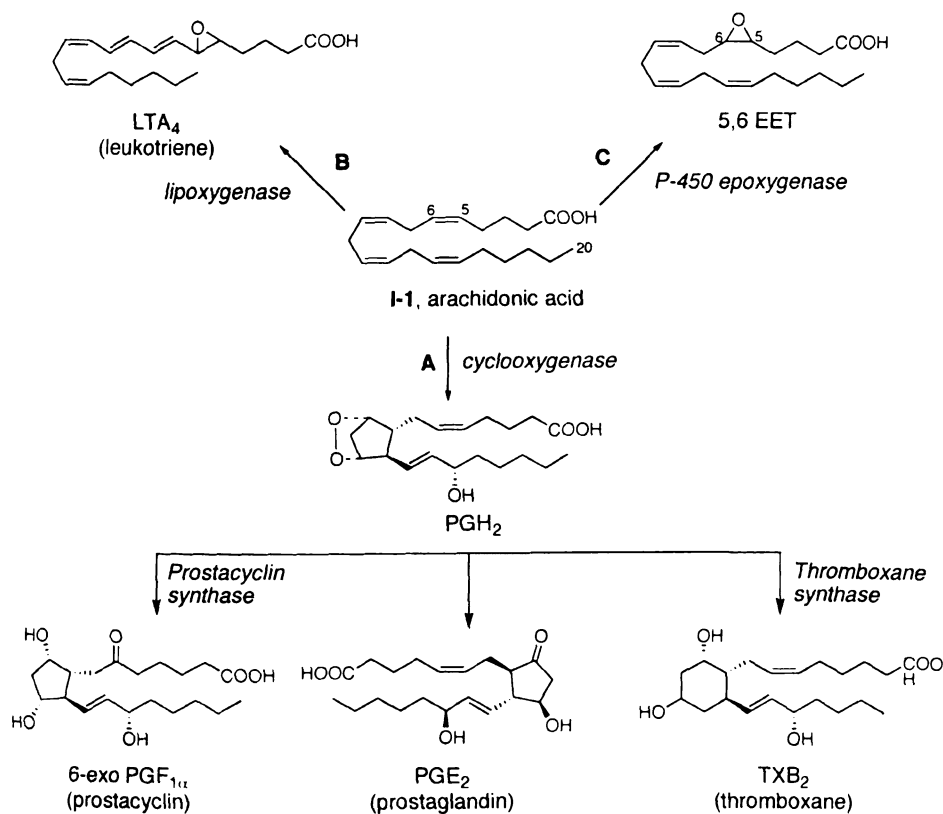


Figure I-1: Pathways of arachidonic acid metabolism

variety of cell membranes and as a response to physiological or pathological stimuli, is released into the cells by hydrolytic cleavage of phospholipids.¹ Once liberated, depending on the parent cell type, AA is metabolized *via* one of the three pathways (A, B or C, Figure I-1). Each pathway involves a class of enzymes that oxidatively metabolize AA.² Cyclooxygenases (path A) and lipoxygenases (path B) are responsible for formation of prostanoids (which include prostacyclins, prostaglandins, and thromboxanes) and leukotrienes, respectively. Each class of metabolites is comprised of a large number of compounds (collectively called as eicosanoids) with great diversity of structures and functions.³ Figure I-1 shows only a representative structure of each class. In fact, in humans, AA is the most important precursor of prostaglandins and related secondary metabolites. Eicosanoids have profound physiological effects including the onset of pain and fever, regulation of blood pressure and blood clotting, control of sleep/wake cycle and inflammatory response.⁴⁻⁶ Due to this, a large body of pharmacological research has targeted the enzymes and receptors involved in AA metabolism.⁷⁻¹⁰

Of all the AA metabolic pathways, P-450 epoxxygenase route (path C, Figure I-1) is least scrutinized. Known metabolites along this path include regioisomeric AA monoepoxides (such as 5, 6 EET, Figure I-1) and the corresponding diols formed by the action of epoxide hydrolases.¹¹⁻¹³ Though less explored, these metabolites have also been shown to possess important biological activities. 5,6 EET, for example, is a potent stimulator of prolactin release and an effective vasodilator.^{14,15} 11,12 DHET – 11,12 diol of AA (not shown) is Na⁺/K⁺ ATPase inhibitor.¹³

Recently, a novel class of AA metabolites — termed as arachidonic acid tetrahydrofuran diols (AA-THF-diols) has been discovered.¹⁶ It has been proposed that AA-THF-diols, (box in Figure I-2) are formed along the P-450 epoxigenase path as depicted in Figure I-2.¹⁷ Since monoepoxides and the corresponding diols of AA are well preceded, it is conceivable that diepoxides (and even higher order epoxides) and their hydrolyzed products may be formed *via* the same metabolic path. Accordingly, Moghaddam et al. found that when monoepoxides of AA (**I-2** and **I-3**, Figure I-2) were exposed to clofibrate* treated mouse liver microsomes, mixtures of regioisomeric diepoxides (**I-4**) were generated.¹⁷ Also, treatment of synthetically prepared regioisomeric diepoxides of AA with the microsomes resulted in formation of the corresponding AA-THF diols *via* cyclization of adjacent diepoxides (**I-7** and **I-8**). These

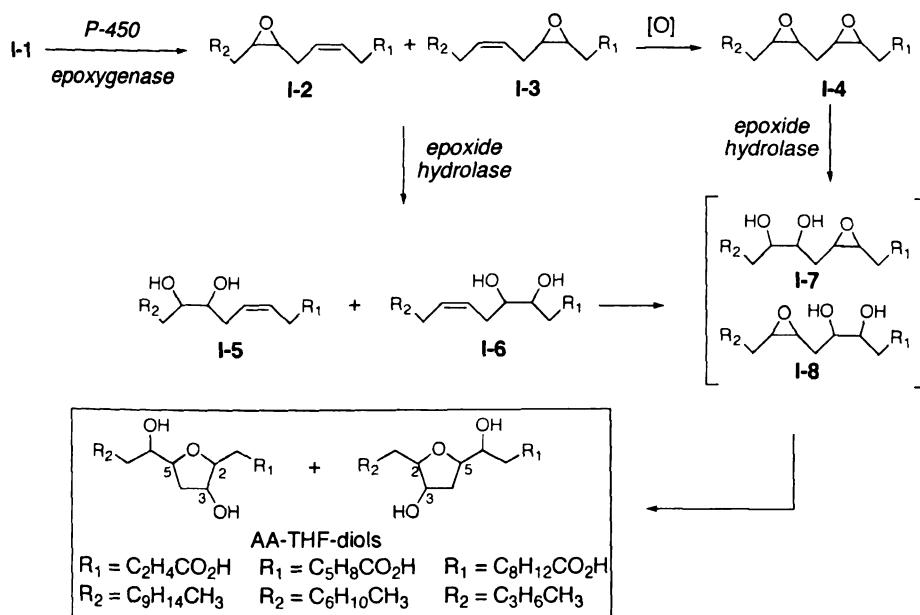


Figure I-2: Proposed biosynthesis of AA-THF-diols

* Clofibrate is an inducer of P-450 epoxigenase and epoxide hydrolase.

novel structures generated *in vitro*, were identified by comparison of their GC/MS fragmentation with that of synthetic samples AA-THF diols prepared *via* mCPBA epoxidation and subsequent acidic hydrolysis of AA. Based on these *in vitro* studies, a plausible biochemical route to AA-THF-diols was proposed (Figure I-2).

Later, it was also shown that the proposed AA-THF-diols are biosynthesized *in vivo*.¹⁶ Lipids isolated from liver extracts of clofibrate treated mice were derivatized to their α -pentafluorobenzyl esters, which were then transformed to the corresponding TMS ethers to facilitate GC/MS analysis. Comparison of the mass fragmentation of these derivatives with similar derivatives of synthetically prepared AA-THF-diols confirmed their presence in the liver extracts.

Our primary interest in AA-THF-diols stems from their interesting biological activity.¹⁶ When rat pulmonary alveolar epithelial cells were incubated with AA-THF-diols, a rapid increase in intracellular Ca^{+2} ion concentration was observed (as detected by fluorescence measurements). This finding is significant in view of the crucial role of intracellular Ca^{+2} ion levels in controlling physiological processes such as signal transduction, protein phosphorylation and cell homeostasis. Interestingly, in the same assays, AA did not show any detectable Ca^{+2} influx, while AA-diepoxides showed a limited degree of potency, possibly due to their slow hydrolysis to AA-THF-diols. These preliminary studies prompted us to initiate a program to further investigate biological activity of AA-THF-diols, conduct SAR studies and delineate their precise mode of action at the molecular level.

The primary bioassays (*vide supra*) were carried out using reigo- and stereoisomeric mixtures of AA-THF-diols. As shown in Figure I-2, from three pairs of

200

201

202

203

204

205

206

207

208

209

210

211

212

213

214

215

216

217

218

219

220

221

222

223

224

225

adjacent diepoxides of AA, six regioisomeric AA-THF-diols would be produced. Since the starting epoxides are *cis*, only two configurations about the THF ring, namely, all-*cis* and 2,3-*cis*-5-*trans* are possible. Taken together, twenty four different regio- and stereoisomers of AA-THF-diols can exist (Figure IV-3, enantiomers not shown). Our proposed biological studies in this area, required access to these THF diols as regio- and stereodefined single compounds. During earlier studies,¹⁷ it was found that isomeric mixture AA-THF-diols (obtained *via* epoxidation and subsequent acid catalyzed cyclization of AA) could be separated only into two fractions, viz., all-*cis* and 2,3-*cis*-5-*trans* stereoisomers (Figure IV-3). The separation was carried out using HPLC and the fractions were not amenable to any further purification. We therefore decided to access

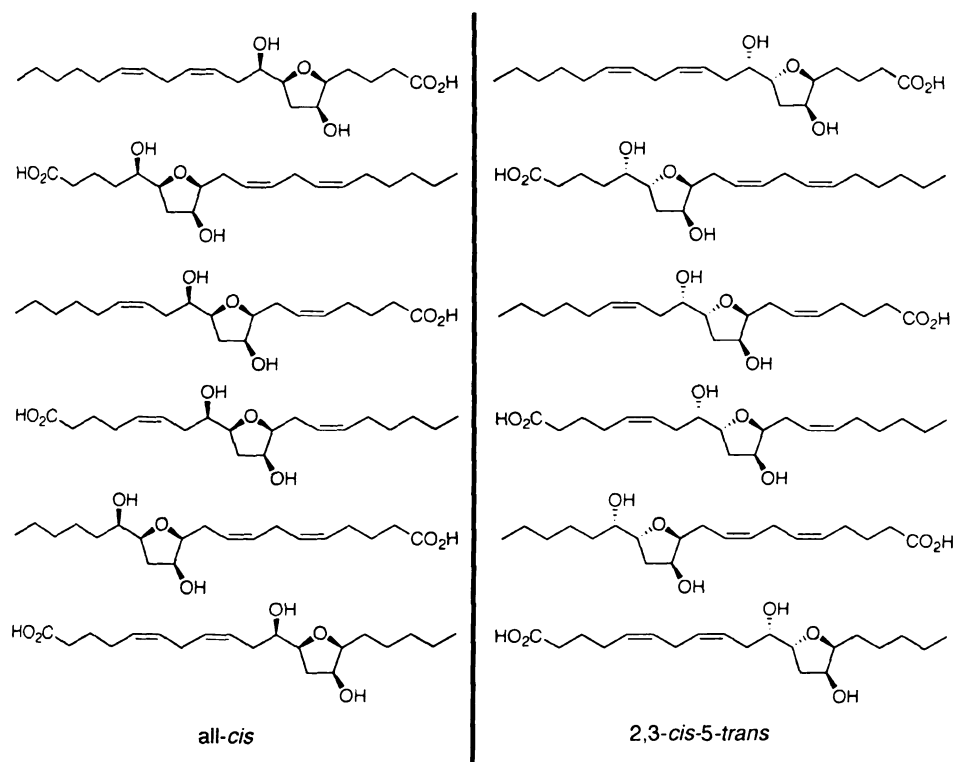


Figure I-3: Regio- and stereoisomers of AA-THF-diols

9-1

200

100

50

25

12.5

6.25

3.125

1.5625

0.78125

0.390625

0.1953125

0.09765625

0.048828125

0.0244140625

0.01220703125

0.006103515625

0.0030517578125

0.00152587890625

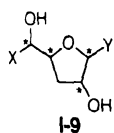
0.000762939453125

0.0003814697265625

0.00019073486328125

regio- and stereoisomerically pure compounds by way of chemical synthesis.

2. Stereoselective synthesis of 2,3,5 trisubstituted THFs – a brief review



Total synthesis of AA-THF-diols would also allow access to structurally diverse analogs such as unnatural stereoisomers or variants containing modified aliphatic appendages to facilitate SAR studies. We felt that a straightforward way to exercise regiocontrol in the total synthesis of AA-THF-diols would be to first construct the THF diol core represented by general description **I-9**. The functional group handles (X and Y) would then be elaborated to install the desired side chains. In this way, unnatural analogs containing modified side chains would be easily accessed. The THF-diol fragments of type **I-9** when constructed in enantiopure forms should lead to the corresponding AA-THF-diols and / or analogs in regio- and stereodefined manner.

Thus, attention was focused on stereoselective synthesis of the trisubstituted THF-diol intermediates. In order to introduce stereodiversity in the synthesis, we were looking for a versatile route that will allow access to all possible stereoisomers of **I-9** in a quick and efficient manner. Stereoselective synthesis of 2,5 disubstituted THFs is an extensively studied area due to their presence in polyether antibiotics, annonaceous acetogenins and other medicinally and biologically relevant natural products containing such THF moieties.¹⁸⁻²¹ Trisubstituted THFs, on the other hand are relatively less explored motifs. Methods for stereoselective construction of 3-hydroxy-2,3,5 substituted THFs have appeared in the last few years. Representative syntheses of such trisubstituted THF are described below.

Landaïs and co-workers used β -hydroxyhomoallylsilanes (**I-10**, Figure I-4) for mercury mediated electrophilic cyclization to construct 2,3,5 trisubstituted THFs in good diastereoselectivities.²² The stereocontrol in the ring closure step arose from the preferential equatorial disposition of the silicon substituent in the chair like transition

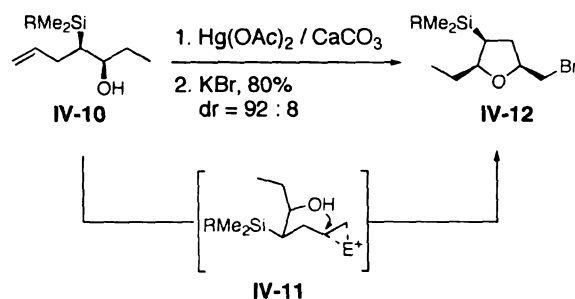


Figure I-4: Intramolecular oxymercuration strategy for the construction of 2,3,5 trisubstituted THFs

state (**I-11**). Stereospecific conversion of the C-Si bond to the C-O bond allowed access to the corresponding all-*cis* hydroxytetrahydrofuran.

Roush has developed a highly convergent three component coupling strategy for stereoselective construction of 2,3,5 trisubstituted THFs *via* the net [3+2] cycloaddition of allyl silanes with aldehydes (Figure I-5).²³ Chiral allylsilanes (**I-13**) obtained *via* allylboration of the corresponding aldehyde (not shown) are treated with the second aldehyde in presence of a Lewis acid to furnish trisubstituted THF units in high diastereoselectivities. The THF product arises through trapping of the developing positive charge on the silicon-bearing carbon by the aldehyde oxygen, concomitant with a 1,2 silyl migration. In case of $\text{BF}_3 \cdot \text{OEt}_2$ coordinated aldehyde, the reaction proceeds *via* synclinal transition state **I-14**, in which steric interactions between R and BF_3 are minimized leading to the 2,5-*cis* THF **I-15**. On the other hand, in presence of chelating

20

21

22

23

24

25

26

27

28

29

30

31

Lewis acids such as SnCl_4 , **I-16** is proposed to be the lowest energy pathway producing 2,5-*trans* THF **I-17** as the major diastereomer. Fleming-Tamao oxidation to access hydroxy THFs was demonstrated on silyl substituted THFs (substrates similar to **I-15** and **I-17**) in the same report.

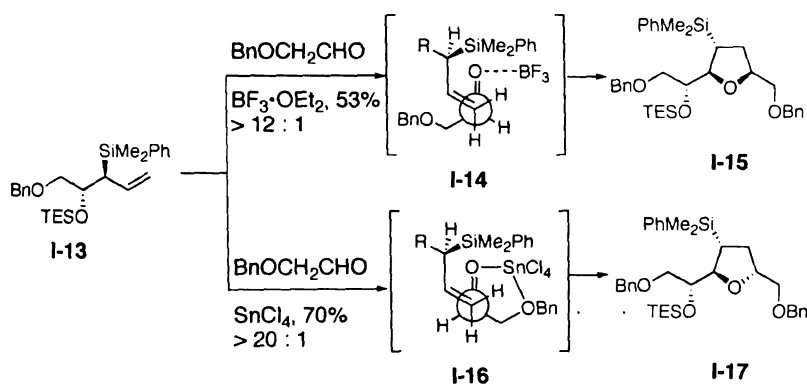


Figure I-5: Roush's three component coupling approach to trisubstituted THFs

The cyclization of alkene diols such as **I-18** (Figure I-6) by way of iodoetherification has been reported by Guindon and coworkers as a general method to prepare the corresponding 2,3,5 trisubstituted THFs (**I-21**) with complete diastereoselectivity.²⁴ In the cyclization of **I-18**, two transition states **I-19** and **I-20** were invoked to explain the observed 2,3-*trans* selectivity (**I-21**). Alternative transition states involving the opposite face of olefin (and thus leading to 2,5-*cis* isomer) are disfavored

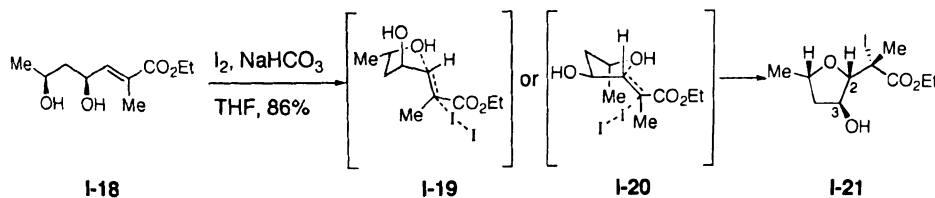


Figure I-6: Iodoetherification of alkene diols to stereoselectively access hydroxylated THFs

due to A 1,3-strain between the allylic hydroxyl and olefin methyl substituent. The overall 2,3,5 stereochemical relationship depends upon the configuration of the participating carbinol center.

Intramolecular iodoetherification approach was also used by Mootoo and co-workers for cyclization of C6 allylated pyranoside substrates (**I-22** and **I-24**, Figure I-7).²⁵ Ether ring closure is accompanied by pyranoside opening under the reaction conditions. Diastereoselectivity of the cyclization was found to be dependent upon configuration of the allylic carbinol center.

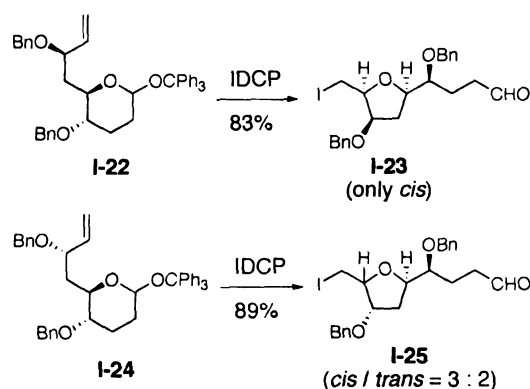


Figure I-7: Intramolecular iodoetherification of C6 allyl pyranosides used by Mootoo

In the total synthesis of (–)-*trans*-kumausyne, the trisubstituted hydroxy THF core (**I-28**, Figure I-8) was constructed *via* $\text{BF}_3 \cdot \text{OEt}_2$ promoted allylsilane addition to substituted glyceraldehyde (**I-26**).²⁶ Intermediate β -silyl cation (**I-27**) is trapped by

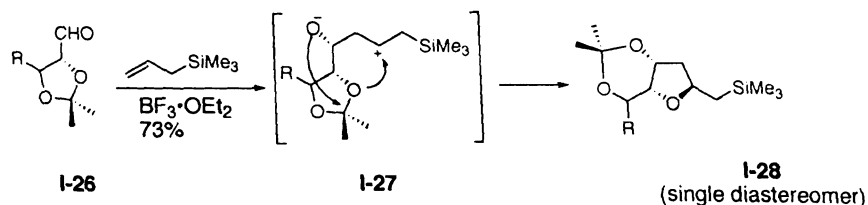


Figure I-8: Sugimura's β -silyl cation cyclization tactic

The diagram illustrates a two-dimensional square lattice. The horizontal and vertical distances between adjacent lattice points are labeled 'a'. The diagonal distance between lattice points, representing next-nearest neighbors, is labeled 'b'. Arrows indicate the direction of interactions between these points.

15

444

3 R.

267

10

1

1

14

internal oxygen nucleophile resulting in thermodynamically more stable 2,5-*trans* THF

(**I-28**)

Although the above mentioned and other related methods²⁷⁻³² afford 3-hydroxy-2,3,5-trisubstituted THFs in good diastereoselectivities and yields, they suffer from lack of versatility. In most strategies, the stereoselectivity is substrate derived rather than reagent derived. Depending upon the chirality of existing stereocenter(s) in the substrate, a specific diastereomer is obtained. Thus, an inherent limitation on these methods is the inability to provide various stereoisomeric THFs starting from a common precursor. Clearly, these methods were unsuitable to quickly access our requisite trisubstituted THF-diols scaffolds in a stereodivergent manner.

B. Regio- and stereoselective synthesis of 2,3,5 THFs *via* cyclization of methylene interrupted epoxy diols

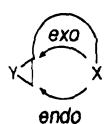
1. Method design

Upon re-examination of the proposed biosynthesis of AA-THF-diols (Figure I-2), we thought that cyclization of methylene interrupted epoxydiol systems such as **I-29** (Figure I-9) would serve our purpose. Pathways **a** and **b** lead to the trisubstituted THFs with desired relative disposition of hydroxyl groups while **c** would result in a THP ring formation. Design of the epoxydiol (**I-29** with elements to achieve regiocontrol in the cyclization, should lead to regio- and stereoisomerically complementary THFs **I-30** and **I-31*** from a common precursor. Oxygenated stereocenters in the epoxydiol substrate

* Generation of THF **I-30** involves inversion at C2 whereas that of THF-**I-31** involves inversion at C1. The hybrid *exo* / *endo* nomenclature is explained later in the same section.

1.0
2.0
3.0
4.0
5.0
6.0
7.0
8.0
9.0
10.0

Baldwin's empirical rules for ring closure have served to explain and reliably predict regioselectivities in cyclization reactions.^{35,36} In case of opening of three-membered rings to form cyclic structures, (**I-38**), the rules lie between those for tetrahedral and trigonal systems and the *exo* mode is generally favored.



I-38

Applying Baldwin's rules to epoxydiol **I-29** (Figure I-11 (left)), path **a** being a 5-*exo* (**I-33**) closure is expected to be favored over path **b** involving a 5-*endo* cyclization. On the other hand, according to Warren's modified hybrid

nomenclature, path **b** would be labeled as 5-*exo* / 6-*endo* closure (Figure I-11 (right)).³⁷ This terminology originates from viewing the ring closure from two different perspectives. Ignoring the C4-O bond (**I-41**) the ring closure can be classified as 5-*exo* since the rupturing bond (C5-O) is *exo* to the incipient five-membered ring. However, if C4-C6 bond is disregarded the cyclization (**I-42**) resembles a 6-*endo* closure. Whether this hybrid ring closure terminology is just a matter of semantics or it has actual effects on the outcome of cyclization remains unclear from Warren's studies. In the

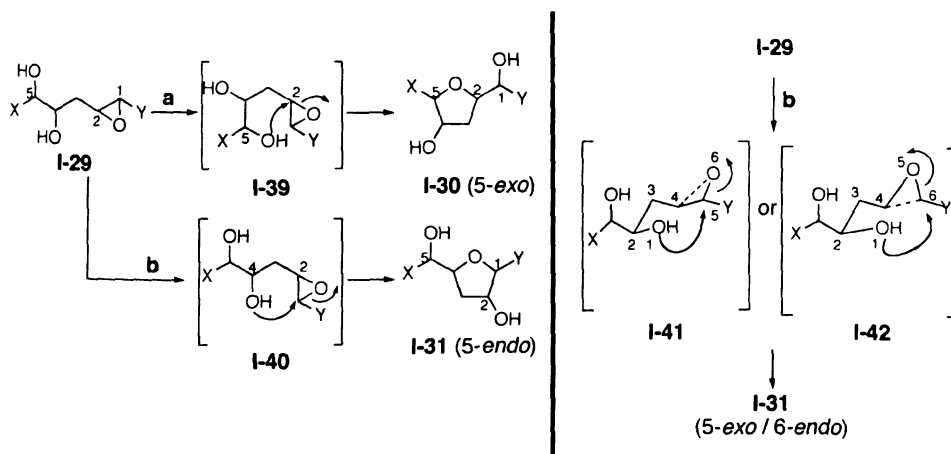


Figure I-11: Conventional Baldwin vs. Warren's hybrid nomenclature for epoxide ring opening

present discussion, the conventional Baldwin's nomenclature is used for clarity.

2. Background on regiocontrol in cyclization of epoxy alcohols

Regioselective cyclization of epoxy alcohols has been extensively exploited for construction of cyclic ethers widely found in biologically relevant natural products.¹⁸⁻²¹ Application of this approach to obtain small (5-7 membered) cyclic ethers was first used by Kishi in the total synthesis of lasalocid A (Figure I-12).^{38,39} Basic hydrolysis of epoxy acetate **I-43** and treatment of the resultant epoxy alcohol with acetic acid afforded the cyclized product **I-44** via 5-*exo* mode. Interestingly, the desired product was actually hydroxy THP ring (**I-47**), which is the disfavored 6-*endo* ring closure product of **I-43**. Thus, the hydroxy THF (**I-44**) was isomerized to the hydroxy THP (**I-47**) via hydrolysis of oxonium intermediate **I-46**.

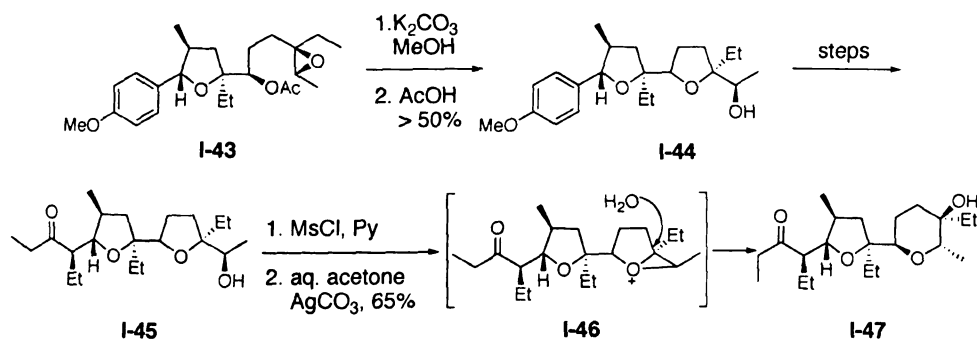


Figure I-12: The first report of epoxy alcohol cyclization to construct THF ring by Kishi

About a decade later, Nicolaou reported a strategy for activation of *endo* epoxide ring opening pathway over the *exo* counterpart (Figure I-13).^{40,41} By placement of a π system next to the epoxide, incipient carbocation at the proximal epoxide carbon (**I-49**, path a) is stabilized due to conjugation of the electron deficient orbital with the π orbitals. The partial positive charge at the distal carbon (**I-51**, path b) on the other hand, enjoys no

such extra stabilization. Thus, the *endo* opening path (**a**) leading to THP **I-50** is preferred over the *exo* mode (**b**) leading to THF **I-52**.

Accordingly, *trans* epoxide **I-53** (Figure I-14) containing a vinyl appendage afforded the corresponding 6-*endo* product **I-54** with complete regioselectivity and

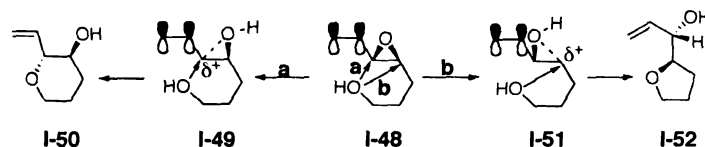


Figure I-13: Nicolaou's strategy for *endo* over *exo* selectivity in epoxide ring opening excellent yields, whereas the *trans* alkyl epoxide exclusively produced the 5-*exo* product (**I-55**). Both cyclizations proceeded with complete stereochemical inversion at the reacting carbon. In case of oxepane generation from *trans* vinyl epoxy alcohol **I-56**, the *endo* selectivity was slightly reduced. However, the selectivity could be improved by using a chlorinated vinyl group, possibly due to better stabilization of the positive charge.

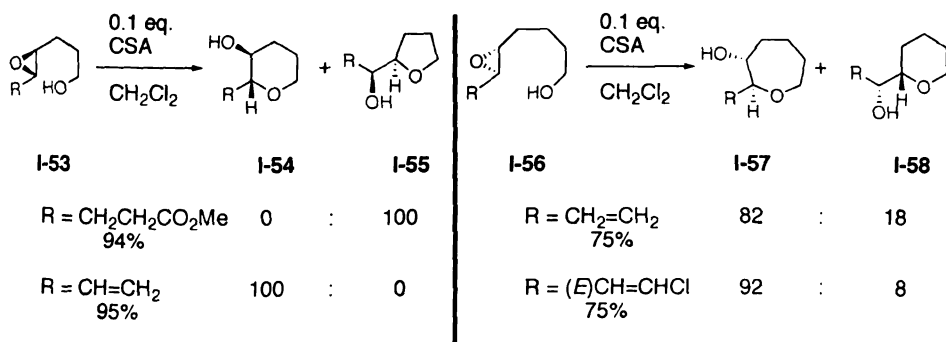


Figure I-14: Cyclizations of *trans* vinylic epoxides

This strategy however, was not successful in case of *cis* epoxides. *Cis*-vinyl epoxide **I-59** (Figure I-15) furnished the corresponding *endo* (**I-60**) and *exo* (**I-61**) products with almost no selectivity (THP : THF = 44 : 56).⁴¹ A slight improvement in the

7.1

7.2

7.3

7.4

7.5

7.6

7.7

7.8

7.9

7.10

7.11

7.12

7.13

7.14

7.15

7.16

7.17

7.18

7.19

7.20

7.21

7.22

7.23

7.24

7.25

ratio was achieved again by using chlorinated vinylic substituent. For larger oxepane rings, the selectivities further depleted. In case of unsubstituted vinyl appendage, oxepane **I-63** was obtained as a 1:1 mixture of *cis* and *trans* isomers (not shown). Thus, this technique failed to regioselectively produce *cis* THPs and oxepanes.

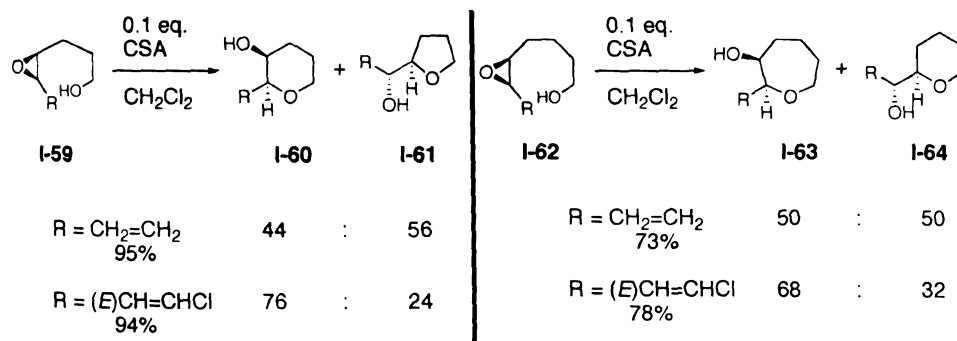


Figure I-15: Cyclizations of *cis* vinylic epoxides

After Nicolaou's reports, several other strategies to achieve *endo* selectivity in epoxide opening were published. Hirama, in 1990, developed palladium catalyzed stereospecific cyclization of hydroxy epoxides (Figure I-16).⁴² *Trans* (**I-65**) and *cis* (**I-69**) epoxy silyl ethers afforded the corresponding *cis* and *trans* THPs (**I-67** and **I-72**, respectively) in excellent yields and stereoselectivity. It was proposed that TBAF treatment of the starting epoxy silyl ether generates ammonium alkoxide species, which is a good nucleophile in subsequent palladium catalyzed allylic etherification. Both, generation of the π -allyl palladium species as well as the ring closure involve complete stereochemical inversion

27

28

29

30

31

32

33

34

35

36

37

38

39

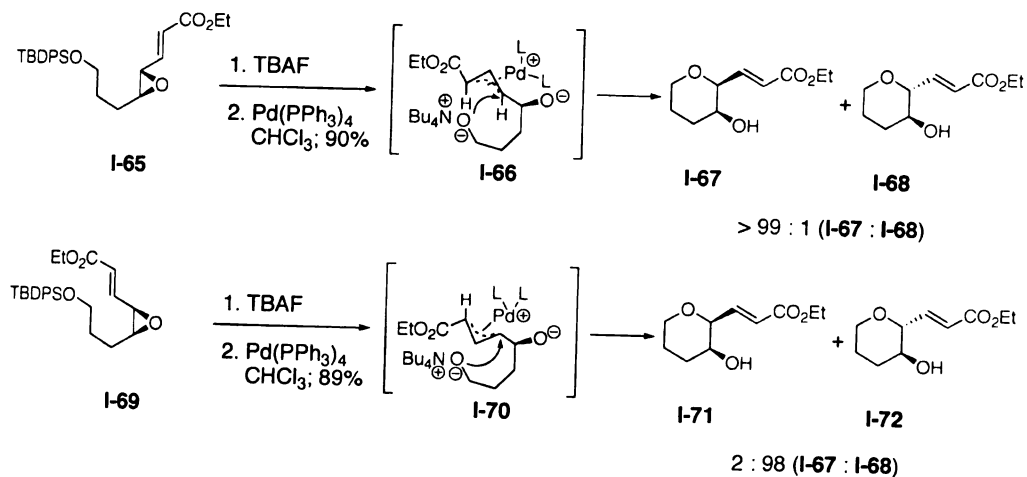


Figure I-16: Hirama's π -allyl palladium cyclization strategy

thus leading to observed diastereoselectivities.

Lerner and Janda demonstrated the utility of catalytic antibodies to facilitate chemically disfavored transformations by achieving forbidden 6-*endo* route in intramolecular epoxide opening reactions (Figure I-17).⁴³ *Trans* epoxide (**I-73**) was regioselectively cyclized to the THP (**I-75**) using monoclonal catalytic antibodies raised against *N*-oxide **I-76**. The antigen (**I-76**) closely mimics the TS (**I-74**) along the 6-*endo* epoxide opening path and thus produced antibodies that facilitated organization of the reaction geometry to prefer THP formation. Also, in the process racemic epoxide **I-73** was resolved producing one enantiopure hydroxy THP (**I-75**). This elegant technique, however is substrate specific and thus cannot be used as a general method in organic

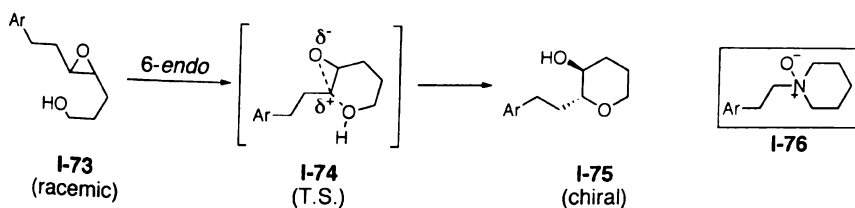


Figure I-17: Use of catalytic antibodies to achieve *endo* selective epoxide opening

synthesis.

Mukai and co-workers developed $\text{Co}_2(\text{CO})_8$ mediated cyclization of alkynyl epoxy alcohols to favor the 6-*endo* opening (Figure I-18).⁴⁴ The strategy involved initial formation of a cobalt complex of the epoxy alkyne (**I-78**). The complexed epoxide in presence of a Lewis acid underwent ring opening to produce the olefin intermediate (**I-79**) *via* anchimeric assistance of the antiperiplanar C-Co bond. Attack of the hydroxyl group onto the available face of the olefin led to the corresponding THP (**I-80**) with net retention of configuration at the propargylic carbon.

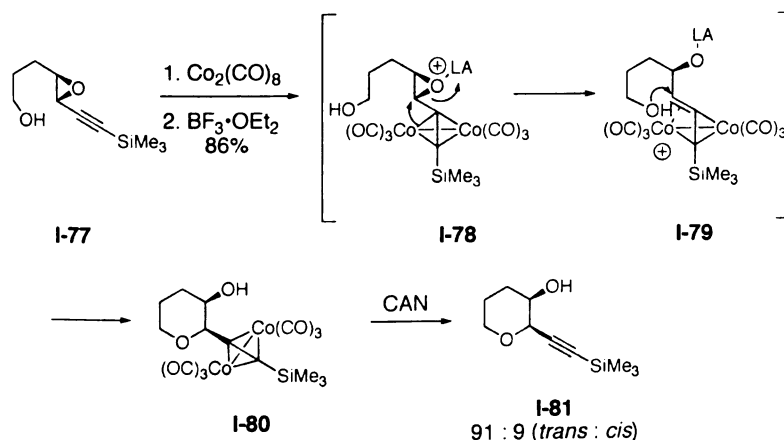


Figure I-18: Mukai's alkynyl epoxide cyclization *via* cobalt complexation

From the above discussion it may be stated that epoxide ring opening by an internal hydroxy nucleophile usually prefers the *exo* route, the selectivity however can be channeled along the *endo* pathway by use of vinylic or alkynyl directing groups.

3. Method development

To our knowledge, all studies in the context of regiocontrol in intramolecular epoxide opening have involved systems containing a single hydroxyl group available for

nucleophilic attack and hence only two competing (*vide supra*) paths in the cyclization event. Our epoxy diol system **I-29** (Figure I-9) presents an added level of complexity in that there are two *endo* (**b** and **c**) and an *exo* path (**a**) available.* The 5-*exo* path being the most preferred, should be easily accessible. On the other hand, even if the system is designed to promote *endo* cyclization, the relative preference between 5-*endo* and 6-*endo* processes would be hard to predict if both the hydroxyls are equally available for cyclization. Thus, selectively accessing either of the two *endo* routes appeared challenging due to their competition with each other in addition to the more preferred 5-*exo* pathway.

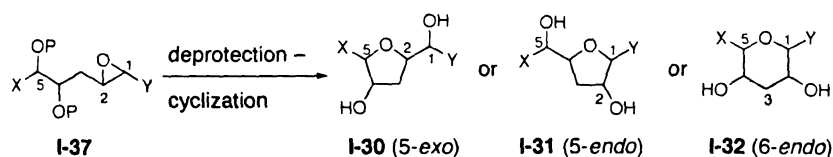


Figure I-19: Proposed in situ deprotection – cyclization of epoxy diol

From the outset, to avoid spontaneous cyclization of the free epoxy diol (*vide infra*), we decided to synthesize protected epoxy diol systems (**I-37**, Figure I-19) containing suitable control elements (such as protecting group **P** and directing functionality **Y**). The goal was to optimize conditions that would accomplish one pot diol deprotection and regio- and stereoselective cyclization reactions.

* Although, in principle, a 4-*exo* pathway is also possible, it is almost never encountered.

100

101

102

103

104

105

106

107

108

109

110

111

112

113

114

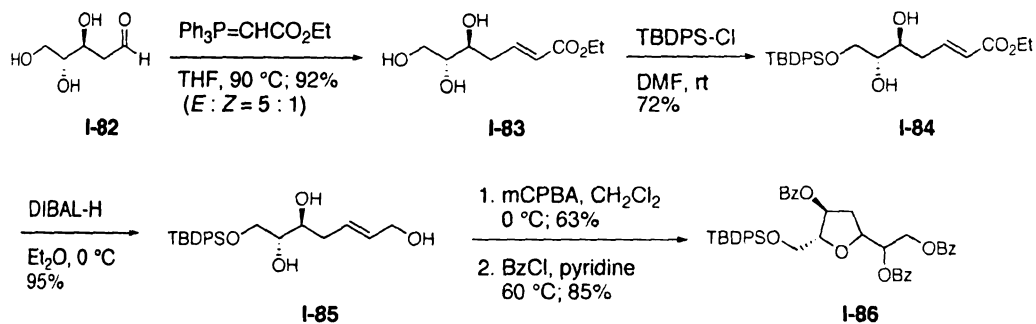
115

116

117

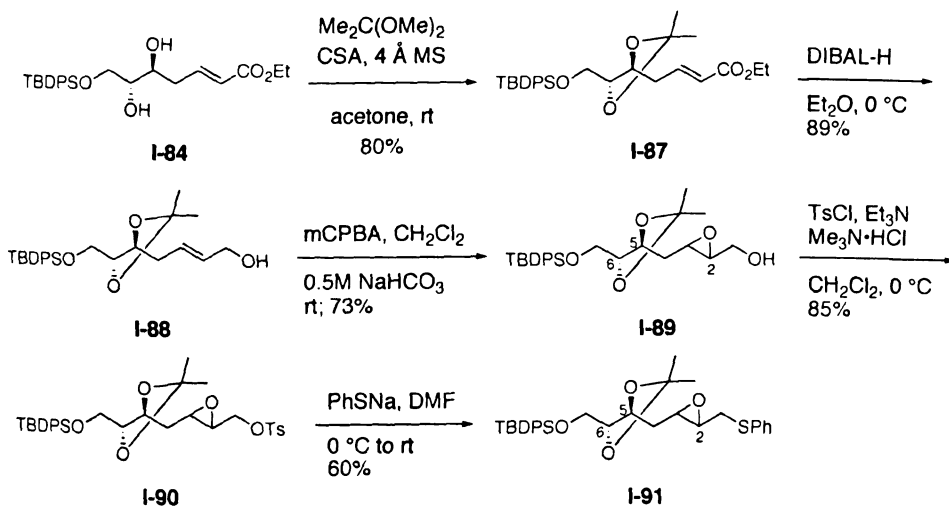
118

119



Scheme I-1: Spontaneous 5-*exo* cyclization of free epoxy diol

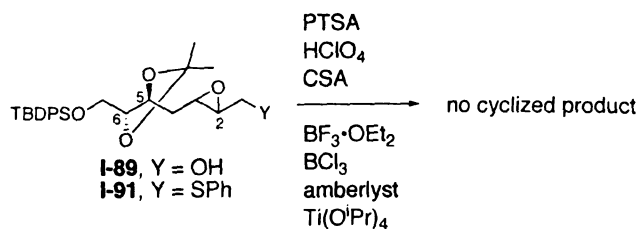
Since the critical issue to be addressed was regiocontrol in the proposed cyclization reactions, we decided to quickly access the requisite epoxy diol substrate from commercially available 2-deoxy-D-ribose (**I-82**, Scheme I-1). Wittig olefination of **I-82** using (carbethoxymethylene)triphenylphosphorane afforded α,β unsaturated ester **I-83** in good (5 : 1) diastereoselectivity.⁴⁵ After silyl protection of the primary hydroxyl group (72%) and subsequent DIBAL-H reduction (95%) the corresponding triol (**I-85**) was isolated as a single diastereomer. mCPBA epoxidation of **I-85** directly produced the corresponding cyclized product *via* 5-*exo* route as expected, which was characterized as



Scheme I-2: Synthesis of acetonide protected epoxy diols

THF **I-86** (1 : 1 mixture of isomers) after perbenzoylation.

Next, protected epoxy diols **I-89** and **I-91** were examined in order to evaluate the possibility of controlling the regioselectivity of cyclization. Based on simple molecular models, it appeared that the C5 oxygen of acetonide (**I-89** and **I-91**) might be sterically less hindered and hence more available for the nucleophilic attack. In that case, the corresponding 5-*endo* product would be obtained preferentially. Also due to neighboring group participation of the phenylthio group* in **I-91**, C2 might be selectively activated over C3 toward nucleophilic attack leading to *endo* cyclized product(s). The acetonides were accessed by protection of the diol functionality prior to epoxidation. However, all attempted *in situ* acetonide cleavage – epoxide opening reactions of **I-89** and **I-91** (Scheme I-3) using various protic and Lewis acids promoters resulted in either decomposition or recovery of the starting materials.

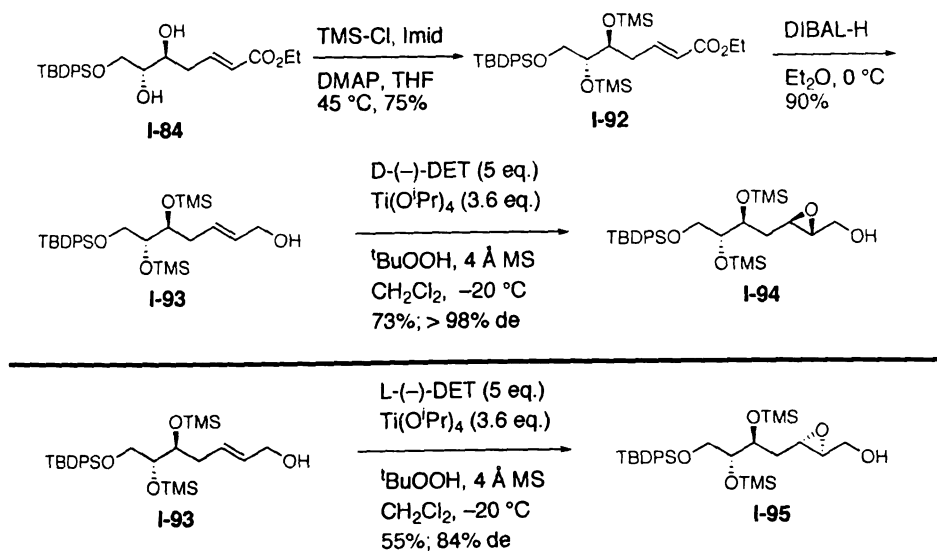


Scheme I-3: Various acids screened for deprotection – cyclization of **I-89** and **I-91**

We next turned to the more easily cleaved trimethylsilyl groups to protect the diol functionality (Scheme I-4). Accordingly, the available diol **I-84** was protected as bis-TMS ether **I-92**. During the silylation reaction, it was critical to maintain a 1:1 stoichiometry of TMSCl and Et₃N to avoid intramolecular Michael addition of the hydroxyl group on to the α,β unsaturated ester to produce the corresponding THF ring.

* This phenomenon is discussed in more detail later in this section.

DIBAL-H reduction of **I-92** afforded allylic alcohol **I-93** (90%). In order to simplify analysis of cyclization products we decided to prepare diastereomerically pure epoxides **I-94** and **I-95** using the Sharpless asymmetric epoxidation.



Scheme I-4: Synthesis of silyl protected epoxy diols

The SAE reaction proved tricky due to the acid sensitivity of the TMS protecting groups in the substrate. When standard catalytic conditions⁴⁶ (10 mol% Ti(OⁱPr)₄, 12 mol% DET) were utilized, the epoxidation was not complete even after prolonged reaction times (24 – 48 h). In addition, products arising from silyl deprotection were observed, probably as a result of prolonged exposure to the Lewis acidic conditions. On the other hand, when **I-93** was treated with 1 equiv. of Ti(OⁱPr)₄ and 1.2 equiv. of DET, the starting olefin was completely consumed within a few hours. Unfortunately, the yield of the desired epoxide was only about 30%, and considerably larger amounts of silyl deprotected products were recovered. After considerable optimization, we found that the epoxidation could be efficiently promoted using super-stoichiometric quantities of

reagents (3.6 equiv. $\text{Ti}(\text{O}^i\text{Pr})_4$, 5 equiv. DET).⁴⁷ Under these conditions epoxide **I-94** was obtained as a single diastereomer in 73% yield (in case of D-(-)-DET). We believe that the short reaction time (2 h) was crucial in suppressing the silyl deprotection pathway that plagued our earlier attempts. Under similar conditions, L-(+)-DET gave lower (55%) yield of epoxide **I-94**, with a diastereomer ratio of 92 : 8.

Using silyl protected epoxy diol systems, we hoped to be able to control the regioselectivity of cyclization by varying electronic properties epoxide pendant groups. Accordingly, derivatives **I-96** through **I-100** were prepared *via* standard transformations (Scheme I-5). Oxidation of epoxy alcohol **I-94** using usual protocols such as Swern, $\text{SO}_3 \cdot \text{Py}$ and Dess–Martin periodinane reactions afforded the desired aldehyde **I-96** in low (up to 40%) along with TMS cleaved by products. After some experimentation we found that by buffering the DMP reaction with pyridine,⁴⁸ the yield could be increased to 90%. Aldehyde **I-96** was treated with the ylide generated from methyltriphenylphosphonium bromide to generate vinylic epoxide **I-97** in moderate yield. Subsequent catalytic hydrogenation of **I-97** provided straightforward access to alkyl substituted epoxide **I-98**.

1
2
3
4
5
6
7
8
9
10
11
12
13
14
15
16
17
18
19
20
21
22
23
24
25
26
27
28
29
30
31
32
33
34
35
36
37
38
39
40
41
42
43
44
45
46
47
48
49
50
51
52
53
54
55
56
57
58
59
60
61
62
63
64
65
66
67
68
69
70
71
72
73
74
75
76
77
78
79
80
81
82
83
84
85
86
87
88
89
90
91
92
93
94
95
96
97
98
99
100
101
102
103
104
105
106
107
108
109
110
111
112
113
114
115
116
117
118
119
120
121
122
123
124
125
126
127
128
129
130
131
132
133
134
135
136
137
138
139
140
141
142
143
144
145
146
147
148
149
150
151
152
153
154
155
156
157
158
159
160
161
162
163
164
165
166
167
168
169
170
171
172
173
174
175
176
177
178
179
180
181
182
183
184
185
186
187
188
189
190
191
192
193
194
195
196
197
198
199
200
201
202
203
204
205
206
207
208
209
210
211
212
213
214
215
216
217
218
219
220
221
222
223
224
225
226
227
228
229
230
231
232
233
234
235
236
237
238
239
240
241
242
243
244
245
246
247
248
249
250
251
252
253
254
255
256
257
258
259
260
261
262
263
264
265
266
267
268
269
270
271
272
273
274
275
276
277
278
279
280
281
282
283
284
285
286
287
288
289
290
291
292
293
294
295
296
297
298
299
300
301
302
303
304
305
306
307
308
309
310
311
312
313
314
315
316
317
318
319
320
321
322
323
324
325
326
327
328
329
330
331
332
333
334
335
336
337
338
339
340
341
342
343
344
345
346
347
348
349
350
351
352
353
354
355
356
357
358
359
360
361
362
363
364
365
366
367
368
369
370
371
372
373
374
375
376
377
378
379
380
381
382
383
384
385
386
387
388
389
390
391
392
393
394
395
396
397
398
399
400
401
402
403
404
405
406
407
408
409
410
411
412
413
414
415
416
417
418
419
420
421
422
423
424
425
426
427
428
429
430
431
432
433
434
435
436
437
438
439
440
441
442
443
444
445
446
447
448
449
450
451
452
453
454
455
456
457
458
459
460
461
462
463
464
465
466
467
468
469
470
471
472
473
474
475
476
477
478
479
480
481
482
483
484
485
486
487
488
489
490
491
492
493
494
495
496
497
498
499
500
501
502
503
504
505
506
507
508
509
510
511
512
513
514
515
516
517
518
519
520
521
522
523
524
525
526
527
528
529
530
531
532
533
534
535
536
537
538
539
540
541
542
543
544
545
546
547
548
549
550
551
552
553
554
555
556
557
558
559
560
561
562
563
564
565
566
567
568
569
570
571
572
573
574
575
576
577
578
579
580
581
582
583
584
585
586
587
588
589
590
591
592
593
594
595
596
597
598
599
600
601
602
603
604
605
606
607
608
609
610
611
612
613
614
615
616
617
618
619
620
621
622
623
624
625
626
627
628
629
630
631
632
633
634
635
636
637
638
639
640
641
642
643
644
645
646
647
648
649
650
651
652
653
654
655
656
657
658
659
660
661
662
663
664
665
666
667
668
669
670
671
672
673
674
675
676
677
678
679
680
681
682
683
684
685
686
687
688
689
690
691
692
693
694
695
696
697
698
699
700
701
702
703
704
705
706
707
708
709
710
711
712
713
714
715
716
717
718
719
720
721
722
723
724
725
726
727
728
729
730
731
732
733
734
735
736
737
738
739
740
741
742
743
744
745
746
747
748
749
750
751
752
753
754
755
756
757
758
759
760
761
762
763
764
765
766
767
768
769
770
771
772
773
774
775
776
777
778
779
780
781
782
783
784
785
786
787
788
789
790
791
792
793
794
795
796
797
798
799
800
801
802
803
804
805
806
807
808
809
810
811
812
813
814
815
816
817
818
819
820
821
822
823
824
825
826
827
828
829
830
831
832
833
834
835
836
837
838
839
840
841
842
843
844
845
846
847
848
849
850
851
852
853
854
855
856
857
858
859
860
861
862
863
864
865
866
867
868
869
870
871
872
873
874
875
876
877
878
879
880
881
882
883
884
885
886
887
888
889
890
891
892
893
894
895
896
897
898
899
900
901
902
903
904
905
906
907
908
909
910
911
912
913
914
915
916
917
918
919
920
921
922
923
924
925
926
927
928
929
930
931
932
933
934
935
936
937
938
939
940
941
942
943
944
945
946
947
948
949
950
951
952
953
954
955
956
957
958
959
960
961
962
963
964
965
966
967
968
969
970
971
972
973
974
975
976
977
978
979
980
981
982
983
984
985
986
987
988
989
990
991
992
993
994
995
996
997
998
999
1000

Q. 1

Q. 2

Q. 3

Q. 4

Q. 5

Q. 6

Q. 7

Q. 8

Q. 9

Q. 10

Q. 11

Q. 12

Q. 13

Q. 14

Q. 15

Q. 16

Q. 17

Q. 18

Q. 19

Q. 20

Q. 21

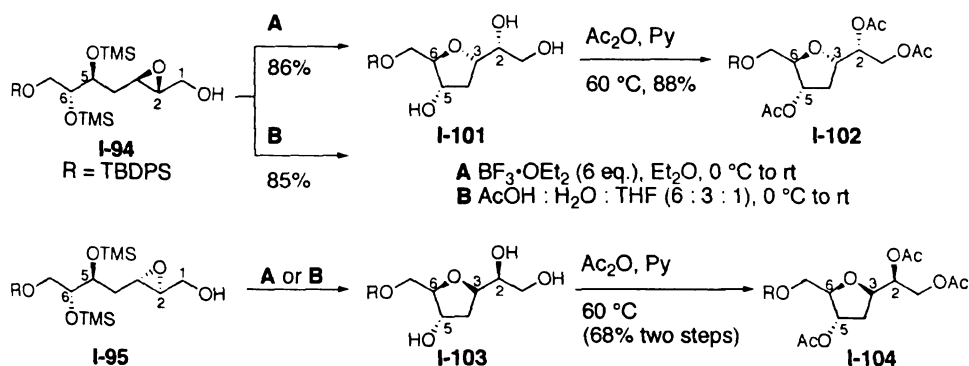
Q. 22

Q. 23

Q. 24

Q. 25

was characterized by COSY experiments as the expected 5-*exo* product after peracetylation to **I-102**. Also, lack of nOe correlations in **I-102** across the THF ring suggested *trans* relation between H₃ and H₆, in agreement with complete stereochemical inversion at C3. The same results were obtained when deprotection-cyclization of **I-94** was triggered by aqueous acetic acid.⁵² The diastereomeric epoxide (**I-95**) after similar acid treatments (**A** and **B**, Scheme I-6) also efficiently afforded the corresponding 5-*exo* product with inversion of configuration at C3. Thus, the stereochemical relationship between the diol and the epoxide was inconsequential to regio- and stereochemical outcome of the cyclization reaction and two stereochemically complementary THF diols (**I-101** and **I-103**)* were accessed.

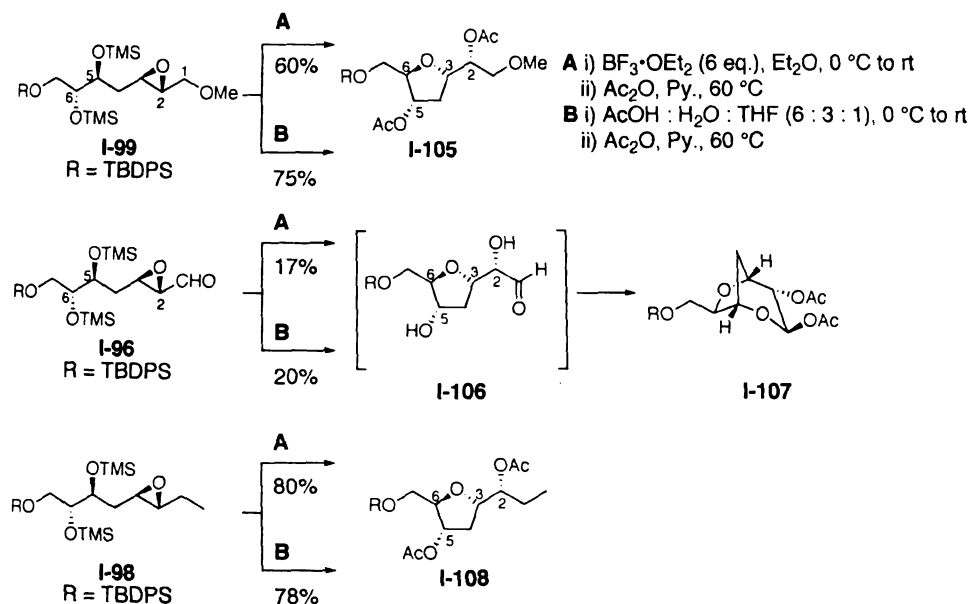


Scheme I-6: Acid catalyzed cyclization of epoxy alcohols **I-94** and **I-95**

Along similar lines, methoxy substituted epoxy diol **I-99** produced the corresponding 5-*exo* product (**I-105**). In this case, however cyclization under protic conditions was more efficient than using Lewis acid promoter (Scheme I-7). Substrate

* Although **I-101** and **I-103** are tetraols, the primary hydroxyl groups are considered as functional group handles. The cyclization products of all the epoxy diols under consideration would be referred to as THF or THP diols.

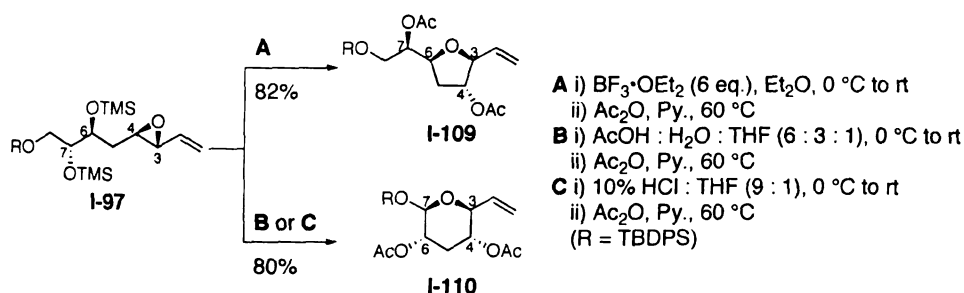
I-96 was designed to obtain 5-*exo* THF diol with a more versatile functional group handle (an aldehyde appendage). Unfortunately, under both Lewis and Bronsted acidic conditions, most of the starting material decomposed and only small amounts of the desired 5-*exo* product (**I-106**) were obtained. Interestingly, the *exo* product, after acetylation was isolated as bicyclic acetoxy acetal **I-107** generated by intramolecular addition of C5-OH to the aldehyde functionality.



Scheme I-7: Cyclization of epoxy diols containing electron withdrawing and neutral pendant groups

Alkyl substituted epoxide **I-98**, would serve to evaluate Warren's suggestion that conventional intramolecular *endo* opening of three-membered rings might have an *exo* component that is likely to influence regioselectivity in their cyclization reactions (*vide supra*).³⁷ Since both epoxide carbons (**I-98**) are electronically similar, the major product should be the result of most favored alignment of the forming and breaking bonds. As shown in Scheme I-7, irrespective of the nature of acid promoter, 5-*exo* product **I-108**

was obtained as a single regio- and stereoisomer. Our results with **I-98** clearly indicate that the hybrid terminology has no particular advantage in terms of predictability of the regiochemical outcome of the cyclization, at least in case of epoxides. Also, **I-98** electronically resembles the epoxy diol intermediates in the proposed biosynthesis of AA-THF-diols (**I-7** and **I-8**, Figure I-2). Complete 5-*exo* selectivity in cyclization of **I-98** suggests that non-enzymatic *in vivo* cyclization of **I-7** and **I-8** likely proceeds exclusively via 5-*exo* path to generate regioisomeric the AA-THF-diols.

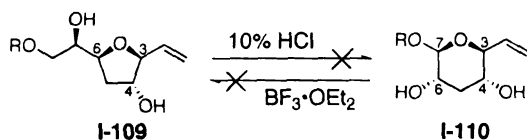


Scheme I-8: Cyclization of vinylic epoxy diol

Using vinyl epoxide **I-97** (Scheme I-8), we hoped to direct the cyclization along the *endo* pathway via stabilization of developing positive charge at C3.^{40,41} In $\text{BF}_3 \cdot \text{OEt}_2$ promoted deprotection–cyclization, the 5-*endo* product (**I-109**) was obtained as a single diastereomer with complete regioselectivity. While this was initially attributed to faster formation of a five-membered ring relative to a six-membered ring, curiously in polar protic media the 6-*endo* product (**I-110**) was selectively obtained. Moreover, the strength of protic acids did not affect the selectivity (**B** and **C**, Scheme I-8).

Semiempirical calculations (PM3 force field, Spartan V.5.1.3) indicated **I-110** (6-*endo* THP product prior to acetylation, Scheme I-9) to be slightly more stable (*ca.* 2 Kcal / mol) than **I-109** (5-*endo* THF product). This raised the possibility that **I-109** is initially

produced in aqueous acidic conditions and is then isomerized to the THP (**I-110**). To test this proposition, **I-109** was exposed to 10% HCl in THF. However, no isomerization of the THF to **I-110** was observed and the former was quantitatively recovered. Similarly, the THP (**I-110**) did not isomerize to the THF when treated with $\text{BF}_3 \cdot \text{OEt}_2$. Thus, clearly, formation of both the rings under the reaction conditions was irreversible. These experiments suggest that the cyclization reactions may be operative under kinetic rather than thermodynamic control.



Scheme I-9: Absence of equilibration between vinyl THF **I-109** and THP **I-110** under the cyclization conditions

Thus, it is likely that the TMS groups are cleaved at comparable rates (and hence equally available for nucleophilic attack) and in a nonpolar medium, 5-*endo* T.S. is the lower energy path while in a polar protic medium, the 6-*endo* T.S. is energetically favored. Another possible scenario is that the two silyl groups are cleaved at different rates in different media, i.e., under nonpolar conditions (**A**, Scheme I-8) C6-OTMS (**I-97**) is cleaved faster and therefore is readily available for the ring closure as compared to C7-OTMS and vice versa. Though factors controlling the regioselectivity are not clear at present, we were nevertheless able to access THF diol **I-109**, which is regio- and stereochemically distinct from those prepared earlier (**I-101** and **I-103** Scheme I-6). In addition THP diol **I-110** was also obtained in complete regio- and diastereoselectivity.

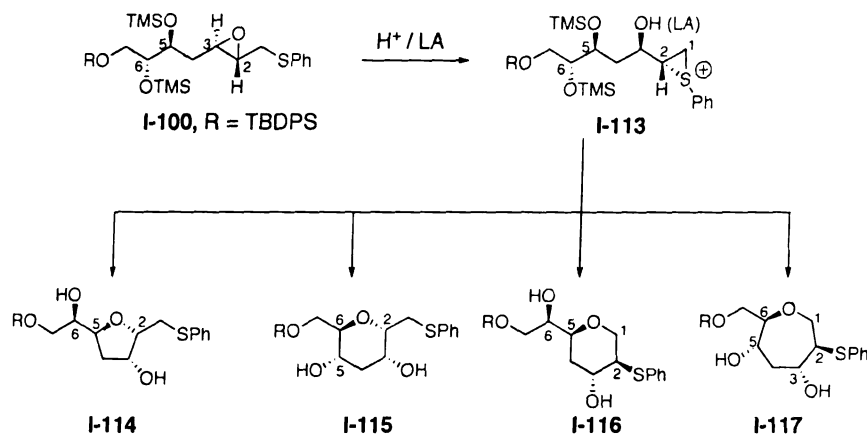


Figure I-20: Cyclic ethers derived from epoxy sulfide **I-100** via episulfonium intermediate

We next turned to explore cyclization reactions of epoxy diol **I-100** containing phenylthio directing group (from now on referred to as epoxy sulfide). It was anticipated that under acidic conditions, the epoxy sulfide would generate an episulfonium ion (**I-113**, Figure I-20) via neighboring group participation of the phenyl thio group.⁵³⁻⁵⁵ The two potential sites for nucleophilic attack in **I-113** are C1 and C2. Depending upon which nucleophile (C5-OH or C6-OH) participates in the cyclization, four regioisomeric products (**I-114** through **I-117**) can be generated. **I-114** and **I-115** are the 5-*endo* and 6-*endo* cyclization products with respect to the original epoxy sulfide **I-100**, and 5-*exo* and 6-*exo* with respect to the episulfonium ion **I-113**. For consistency in the discussion **I-114** and **I-115** will be referred to as 5-*endo* and 6-*endo* products. THP **I-116** and oxepane **I-117** arise from cyclization reactions at C1, which are *endo* paths with respect to the episulfonium intermediate (**I-113**).

If conditions could be found that would favor the formation of **I-114** and / or **I-115** over **I-116** and / or **I-117**, this strategy would constitute a novel tactic to achieve

endo over *exo* selectivity in epoxide opening reactions. An added advantage of this technique is the stereochemical outcome of the cyclization. During the formation of **I-114** and **I-115** from the epoxysulfide (**I-100**) via **I-113**, the configuration at C2 is retained as a result of double inversion. Thus, stereochemical relation between C2 and C3 in the two cyclic ethers is complementary to that if a single inversion were involved (for example by using vinyl epoxide substrates). Moreover, thiophenylmethyl group in **I-114** and **I-115** can be easily transformed into an aldehyde functionality,^{56,57} which is a versatile functional group handle.

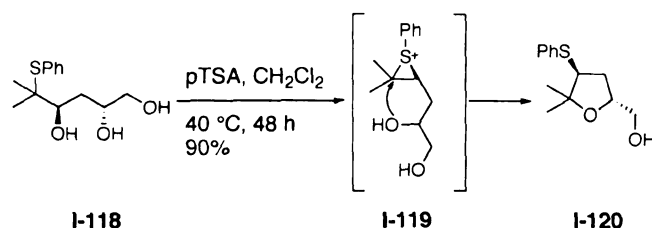
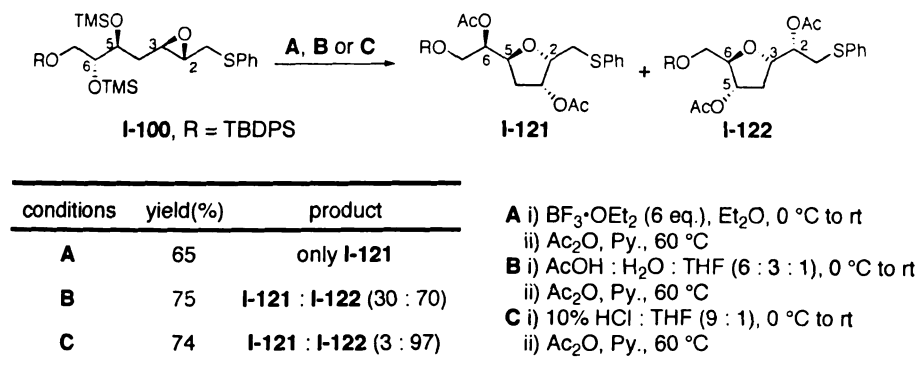


Figure I-21: Warren's phenylthio polyol cyclization strategy for synthesis of THFs and THPs

Warren has used phenylthio polyol systems to construct THF and THP rings through episulfonium intermediates.⁵⁸ A representative example is shown in Figure I-21.⁵⁹⁻⁶¹ Prolonged exposure of triol **I-118** to acid at 40 °C afforded THF **I-120** as a single regioisomer. **I-120** was shown to be the thermodynamic product and the THP formed by attack of the primary hydroxyl group was converted to **I-120** under the reaction conditions. Intermediacy of an episulfonium ion was clearly established due to migration of the phenylthio group. Under the reaction conditions, attack at the more substituted carbon of the episulfonium ion was usually observed. A similar method for stereospecific synthesis of THFs using phenylthio diols has been developed by

Williams.⁶² However, the use of a phenylthio directing group in the intramolecular opening of epoxides containing internal nucleophiles in the context of heterocycle synthesis is not known.



Scheme I-10: Epoxy sulfide cyclization

Scheme I-10 depicts the results of the epoxy sulfide (**I-100**) cyclization under the standard conditions (**A**, **B** and **C**) used earlier. Gratifyingly, the 5-*endo* product **I-121** was obtained with using BF_3 in CH_2Cl_2 *via* nucleophilic attack at C2 was obtained by the liberated C5 hydroxyl. The structure was determined by COSY analysis of the peracetylated derivative (**I-121**, Scheme I-10). Also, 1D NOESY experiments indicated a *cis* relationship between H_2 and H_3 , which confirmed a net retention of configuration at C2. Therefore, it was concluded that **I-121** is formed *via* the corresponding episulfonium intermediate (**I-113**, Figure I-20).

However, a mixture of regioisomeric THFs was obtained upon treatment of **I-100** with aqueous acetic acid and the products were characterized as **I-121** and **I-122** (30:70) using the same NMR techniques. **I-122** is the 5-*exo* product originating from the parent

400
1000
1000
1000
1000
1000
1000

1000

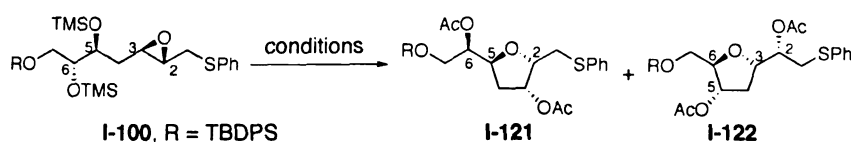
1000

1000

1000

1000

epoxy sulfide (by ring opening at C3) without the involvement of the episulfonium ion. Surprisingly, stronger protic acid (10% HCl, **C**, Scheme I-10) almost completely reversed the regioselectivity to afford the 5-*exo* THF diol **I-122** as the only isolated product.* Also treatment of **I-100** with PPTS in EtOH led to the formation of **I-122** as the major product (**I-121** : **I-122** = 5:95 as determined by GC). Aqueous PPTS mediated cyclization also afforded **I-122** as the major product, although the reaction was much slower (50% complete in 24 h).



conditions	yield(%)	I-121 : I-122
H ₂ SO ₄ , EtOH	81	8 : 92
pTSA, EtOH	83	6 : 94
AcOH, EtOH	82	8 : 92
HF·Py, EtOH	95	9 : 91
PPTS, EtOH	73	3 : 97
pTSA, CH ₂ Cl ₂	95	95 : 5
TFA, CH ₂ Cl ₂	89	90 : 10
HF·Py, CH ₂ Cl ₂	80	78 : 22

Scheme I-11: Cyclization of **I-100** in polar and nonpolar media using different acids

Scheme I-11 shows data collected by Dr. Meenakshi Sivakumar.⁶³ Simultaneous deprotection – cyclization reaction of **I-100** was carried out using various acids in polar (EtOH) and nonpolar (CH₂Cl₂) solvents. The results indicate that irrespective of the acid strength, the direct cyclization of the epoxy sulfide by 5-*exo* path was favored in polar

* The 97 : 3 ratio of **I-122** : **I-121** in **C** (Scheme I-10) was determined by GC.

2010

2011

2012

2013

2014

2015

2016

2017

2018

2019

2020

2021

2022

2023

2024

2025

2026

2027

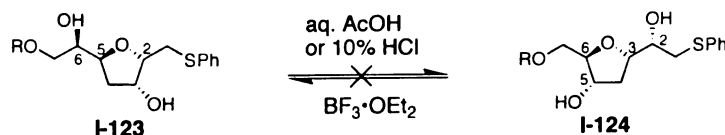
2028

2029

2030

medium whereas in a protic environment, cyclization of the episulfonium at C2 was the preferred route.

Semiempirical calculations (Spartan 5.3.1, AM1 force field) showed **I-124** (Scheme I-12) to be lower in energy (*ca.* 2 Kcal / mol) than **I-123**. However, **I-123** when treated aqueous acids does not isomerize to **I-124** thereby ruling out the possibility that under polar protic conditions, the 5-*endo* product was initially formed and then slowly equilibrated to **I-123**. Similarly **I-123** in presence of $\text{BF}_3 \cdot \text{OEt}_2$ did not convert to **I-124**. These experiments indicated that the cyclization reactions are operative under kinetic control as in the case of the vinyl epoxide .



Scheme I-12: Absence of equilibration between phenylthio THFs **I-123** and **I-124**

(products prior to acetylation) under the cyclization conditions

One possible explanation to the preferential formation of the 5-*exo* product in polar protic media is that the episulfonium formation is prevented due to solvation of the phenylthio group. It is conceivable that the lone pair on sulfur atom is engaged in hydrogen bonding with the protic solvent and hence is not available for anchimeric assistance to generate the episulfonium ion. The extent of such hydrogen bonding and hence extent of episulfonium formation is likely to depend on overall polarity of the medium.

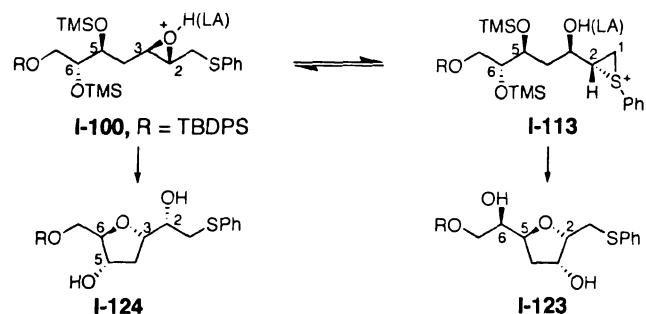
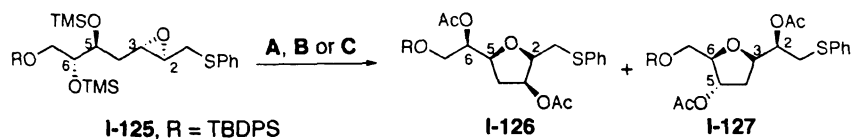


Figure I-22: Possible equilibration between activated epoxy sulfide **I-100** and the corresponding episulfonium ion

Another likelihood is that activated epoxy sulfide **I-100** and the episulfonium (**I-113**) exist in a dynamic equilibrium. Both species are trapped by different hydroxyl groups and the relative rates of intramolecular trapping might be different. This rate difference could be either due to difference in inherent reactivities of **I-100** and **I-113** or in the availability of the nucleophiles. The availability of nucleophiles may in turn depend upon the relative rates of silyl deprotection and the steric environment. Overall, the nature of the reaction medium may influence the availability of the nucleophiles and therefore relative rates of cyclization of **I-100** vs. **I-113**.



conditions	yield(%)	I-126 : I-127
A	65	(97 : 3)
B	75	(20 : 80)
C	74	(5 : 95)

- A** i) $\text{BF}_3 \cdot \text{OEt}_2$ (6 eq.), Et_2O , 0 °C to rt
 ii) Ac_2O , Py., 60 °C
B i) $\text{AcOH} : \text{H}_2\text{O} : \text{THF}$ (6 : 3 : 1), 0 °C to rt
 ii) Ac_2O , Py., 60 °C
C i) 10% $\text{HCl} : \text{THF}$ (9 : 1), 0 °C to rt
 ii) Ac_2O , Py., 60 °C

Scheme I-13: Cyclization of diastereomeric epoxy sulfide **I-125**

W

22

Al

one

the

the

the

the

the

the

the

the

the

the

the

the

the

the

the

the

the

the

the

the

the

the

We also investigated the cyclization reactions of diastereomeric epoxy sulfide **I-125**, and obtained results similar to that in case of **I-100**. Under Lewis acidic conditions (A, Scheme I-13) the 5-*endo* product (**I-126**) was obtained with excellent regioselectivity whereas using 10% HCl, the selectivity was reversed to access the 5-*exo* product (**I-127**). Since the outcome of the cyclization is independent of the epoxide stereochemistry, THF diols **I-121** and **I-126**, which are regio- and stereochemically distinct from the earlier THF diols (**I-101**, **I-103** and **I-111**), could be obtained. Thus, using diastereomeric epoxy sulfide systems **I-100** and **I-125**, a total of five different THF diols could be accessed.

To summarize, as part of our research program directed toward the total synthesis and biological studies of recently discovered metabolites of arachidonic acid (AA-THF-diols), we needed to access THF diol cores represented by **I-9** in stereodefined forms. In the present study, a versatile strategy for regio- and stereoselective synthesis of such THF diols has been developed.⁶⁴

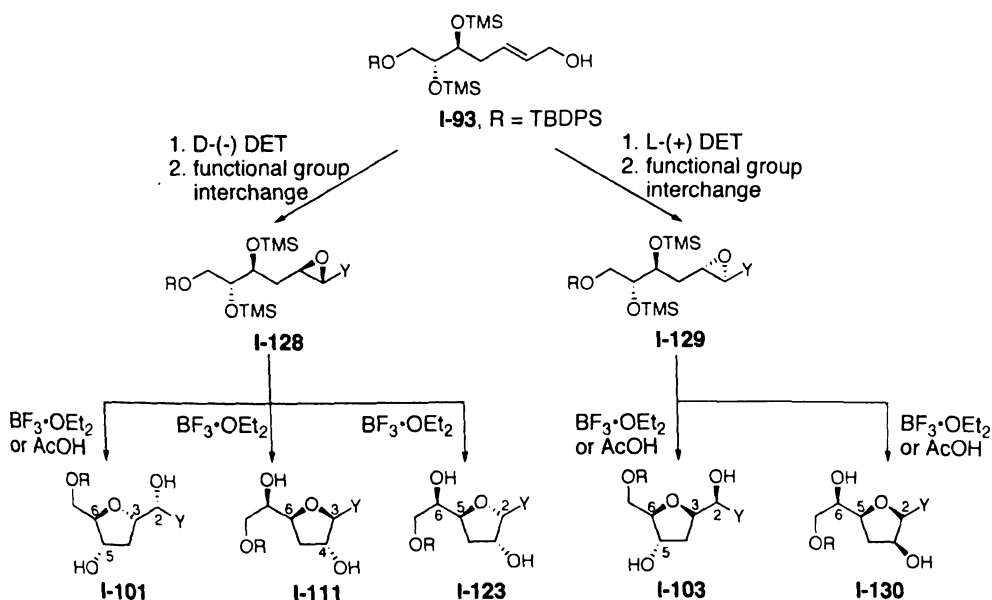
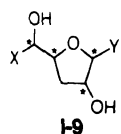


Figure I-23: Isomeric THF diols available from a common precursor **I-93**

0
1
2
3
4
5
6
7
8
9
A
B
C
D
E
F
G
H
I
J
K
L
M
N
O
P
Q
R
S
T
U
V
W
X
Y
Z
[
\
]
^
_
`
a
b
c
d
e
f
g
h
i
j
k
l
m
n
o
p
q
r
s
t
u
v
w
x
y
z
{
|
}
~
_

Our approach is based on the regiocontrolled cyclization of methylene interrupted epoxy diols such as **I-128** and **I-129** (Figure I-23) that contain a directing group (Y) adjacent to the epoxide. Substrates **I-128** and **I-129** were accessed in enantiopure forms by Sharpless asymmetric epoxidation of the allylic alcohol (**I-93**) derived from 2-deoxy-D-ribose. Depending upon the electronic properties of the pendant group (Y) and nature of the acid promoter, five regio- and stereoisomerically complementary THF diols (Figure I-23) were selectively accessed from a single precursor (**I-93**). Since the cyclization in all cases was completely stereospecific, the remaining isomers can be obtained simply by changing the relative configuration between the diol and the epoxide. With the enantiomerically pure THF diol cores in hand, we intend to pursue the total synthesis of THF-diols derived from arachidonic acid (*vide supra*).

This method has been also applied to the total synthesis of mucoxin – a non classical acetogenin. These studies are the subject of Chapters III and IV.

C. A novel method for the oxidative cleavage of olefins

In the course of related work on the synthesis of 2,3,5-tisubstituted tetrahydrofuran diols, a coworker Benjamin Travis attempted to prepare these compounds *via* the direct oxidative cyclization of 1,4-dienes such as methyl linoleate (Figure I-24).⁶⁵ He found that treatment of 1,4-dienes with catalytic OsO₄ in the presence of stoichiometric amounts of various co-oxidants such as KMnO₄ and Oxone® (potassium peroxymonosulfate) produced the requisite THF diols. However, the yields did not attain useful levels. The poor yield of the desired products in these reactions was attributed to competing over-oxidation of the olefin functionalities, resulting in C–C bond cleavage. Thus, carboxylic acids were obtained as the major side products.

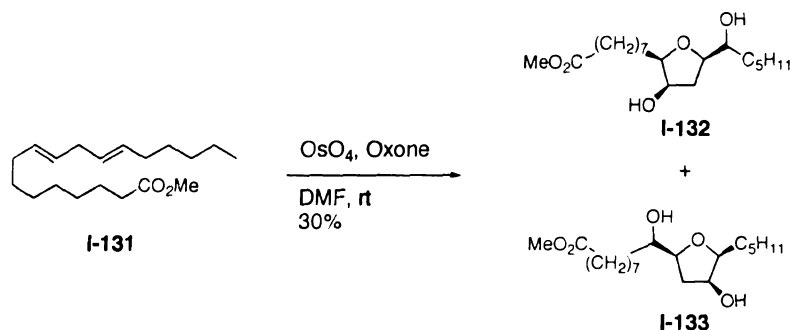
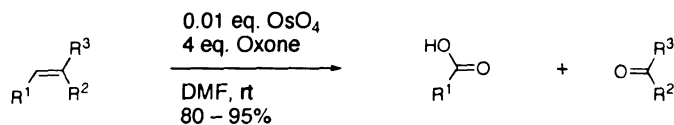


Figure I-24: Oxidative cyclization of methyl linoleate to produce THF diols

Upon further investigation, it became apparent that this Oxone[®] mediated oxidative cleavage of olefins was a fairly general process and was, in effect, an alternative method for the ozonolysis of olefins. Such a method would be useful, since safety concerns preclude the use of ozonolysis for large-scale processes. In fact, serious accidents due to explosions have been reported in some instances.⁶⁶⁻⁶⁸ Ozonolysis is also operationally difficult, requiring specialized equipment for the generation of ozone. Therefore, a safer and simpler chemical alternative is desirable.

The traditional alternative to ozonolysis involves the dihydroxylation of olefins, followed by the cleavage of the resulting vicinal diols. The dihydroxylation is effected using high-valent oxides of transition metals such as manganese, osmium, ruthenium or tungsten. The 1,2-diols are then cleaved using the Lemieux–Johnson protocol or its variants.⁶⁹⁻⁷³ However, the direct oxidative cleavage of olefins without the intermediacy of 1,2-diols is not as common.⁷⁴⁻⁷⁶ It should be noted that the oxidative cleavage of osmate esters – which are precursors to 1,2-diols during dihydroxylation – has been previously observed, although the process has not been optimized for the direct cleavage



Scheme I-14: The OsO₄ – Oxone[®] method for the oxidative cleavage of olefins

of olefins.⁷⁷

Preliminary optimization of the OsO₄ – Oxone[®] cleavage reaction was done by B. Travis, who demonstrated that simple alkyl and aryl olefins (such as stilbene, styrene, cyclohexene, and 1-decene) smoothly underwent cleavage to the corresponding carboxylic acids. My contribution to this study was the evaluation of the scope of this method, especially on more functionalized olefins, and on olefins with different substitution patterns. We were also interested in exploring the effect of electron density on reactivity of olefins toward oxidative cleavage.

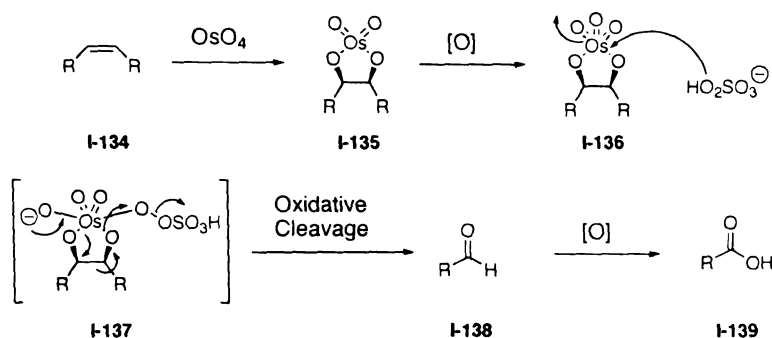
Table I-1 shows the scope of this oxidative cleavage method on a wide variety of olefin substrates.⁷⁸ All mono- and disubstituted olefins underwent cleavage smoothly to afford the corresponding carboxylic acid or ketone products (entries 1–5). In case of tri- and tetrasubstituted olefins (entries 7–9), low yields of the desired products were obtained under standard conditions. The major products in these cases were the 1,2-diols, presumably as a result of slow cleavage of the osmate ester intermediates. This problem was overcome by the addition of 4 equivalents of solid NaHCO₃ to the reaction mixture. The addition of bicarbonate likely helps reduce the acidity of the medium, thus slowing down the osmate ester hydrolysis pathway.

Cyclohexenone (entry 6) afforded pentanedioic acid, most probably *via* an intermediate α-keto carboxylic acid, which undergoes decarboxylation under the

Entry	Substrate	Product	Yield
1			R=H, 85% R=Ac, 93%
2			R=H, 44% R=CHO, 34%
3			80%
4			91%
5			95%
6			92%
7			82%
8			80%
9			85%
10			67%
11			60%
12		recovered SM (96%)	—

Table I-1: OsO₄ – Oxone[®] mediated cleavage of complex olefins

oxidative reaction conditions. Baeyer–Villiger type oxidative cleavage of α -dicarbonyl compounds by peroxo reagents has been previously reported^{79,80} and is likely to be operating in the oxidation of enones. In case of nootkatone (entry 11), more electron rich and sterically available exo olefin reacted preferentially. Lastly, alkyne (entry 12) proved to be immune to oxidative cleavage and was recovered unscathed.



Scheme I-15: Plausible mechanism of OsO_4 – Oxone[®] mediated cleavage of olefins

We believe that 1,2 diols may not be intermediates in this reaction path for two reasons. First, the oxidative cleavage proceeds efficiently under anhydrous conditions, which would not promote hydrolysis of the osmate ester. Second, styrene glycol when subjected to the reaction conditions was recovered quantitatively.

A plausible mechanism of this oxidative cleavage process is depicted in Scheme I-15. Oxone is thought to be involved at three different stages – (i) oxidation of the initial osmate ester (**I-135**) to Os(VIII) species **I-136**, (ii) oxidative cleavage of **I-136** to the aldehyde **I-138**, and (iii) independent oxidation of the aldehyde to carboxylic acid **I-139**.

Thus, a general, simple and mild method for the generation of carboxylic acids and ketones directly from olefins was established.⁷⁸ The optimized conditions involved the treatment of the starting olefins with 0.01 equivalents of OsO_4 and 4 equivalents of Oxone[®] in DMF (Scheme I-14). These reactions were typically complete within three to four hours at room temperature, and yields were typically high (80 – 95%). Further mechanistic studies on this reaction and its extension to prepare aldehydes and esters by similar C–C cleavage of olefins is being explored by B. Travis and other co-workers.

D. Exp

6.2.2

7.1.1

7.1.2

7.1.3

7.1.4

7.1.5

7.1.6

7.1.7

7.1.8

7.1.9

7.1.10

7.1.11

7.1.12

7.1.13

7.1.14

7.1.15

7.1.16

7.1.17

7.1.18

D. Experimental

General Procedures

All reactions were carried out in flame-dried glassware under an atmosphere of dry nitrogen or argon. 4 Å molecular sieves were dried at 160 °C under vacuum prior to use. Unless otherwise mentioned, solvents were purified as follows. THF and Et₂O were either distilled from sodium benzophenone ketyl or used as is from a solvent purification system. CH₂Cl₂, toluene, CH₃CN and Et₃N were distilled from CaH₂. DMF, diglyme, and DMSO were stored over 4 Å mol. sieves and distilled from CaH₂. All other commercially available reagents and solvents were used as received.

¹H NMR spectra were measured at 300, 500 or 600 MHz on a Varian Gemini-300, a Varian VXR-500 or a Varian Inova-600 instrument respectively. Chemical shifts are reported relative to residual solvent (δ 7.27, 2.50 and 4.80 ppm for CDCl₃, (CD₃)₂SO and CD₃OD respectively). ¹³C NMR spectra were measured at 125 MHz on a Varian VXR-500 instrument. Chemical shifts are reported relative to the central line of CDCl₃ (δ 77.0 ppm). Infrared spectra were recorded using a Nicolet IR/42 spectrometer FT-IR (thin film, NaCl cells). High-resolution mass spectra were measured at the University of South Carolina, Mass Spectrometry Laboratory using a Micromass VG-70s mass spectrometer. Optical rotations were measured on a Perkin–Elmer polarimeter (model 341) using a 1 mL capacity quartz cell with a 10 cm path length.

Analytical thin layer chromatography (TLC) was performed using Whatman glass plates coated with a 0.25 mm thickness of silica gel containing PF254 indicator, and compounds were visualized with UV light, potassium permanganate stain, *p*-

1. The first part of the document is a list of names and titles, including "The Hon. Mr. Justice" and "The Hon. Mr. Justice".

2. The second part of the document is a list of names and titles, including "The Hon. Mr. Justice" and "The Hon. Mr. Justice".

3. The third part of the document is a list of names and titles, including "The Hon. Mr. Justice" and "The Hon. Mr. Justice".

4. The fourth part of the document is a list of names and titles, including "The Hon. Mr. Justice" and "The Hon. Mr. Justice".

5. The fifth part of the document is a list of names and titles, including "The Hon. Mr. Justice" and "The Hon. Mr. Justice".

6. The sixth part of the document is a list of names and titles, including "The Hon. Mr. Justice" and "The Hon. Mr. Justice".

7. The seventh part of the document is a list of names and titles, including "The Hon. Mr. Justice" and "The Hon. Mr. Justice".

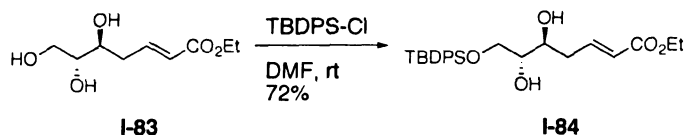
8. The eighth part of the document is a list of names and titles, including "The Hon. Mr. Justice" and "The Hon. Mr. Justice".

9. The ninth part of the document is a list of names and titles, including "The Hon. Mr. Justice" and "The Hon. Mr. Justice".

10. The tenth part of the document is a list of names and titles, including "The Hon. Mr. Justice" and "The Hon. Mr. Justice".

anisaldehyde stain, or phosphomolybdic acid in EtOH. Chromatographic purifications were performed using Silicycle 60 Å, 35-75 µm silica gel. All compounds purified by chromatography were sufficiently pure for use in further experiments, unless indicated otherwise. GC analysis was performed using HP (6890 series) GC system containing Altech SE-54, 30 m x 320 mm x 0.25 mm column. Analytical and semi-preparative HPLC normal phase separations were performed using HP 1100 series HPLC system.

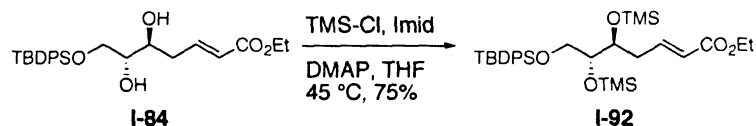
1. Experimental section for synthesis of 2,3,5 trisubstituted THFs



To a solution of **I-83**⁴⁵ (8.2 g, 0.04 mol) in DMF (30 mL), imidazole (3.0 g, 0.044 mol) and t-butylchlorodiphenylsilane (12 g, 0.044 mol) were added at room temperature. The mixture was stirred at room temperature for 3 h, after which time the reaction was quenched by adding H₂O and diluted with ethyl acetate. The layers were separated and the aqueous layer was extracted with ethyl acetate (3x100 mL). The organic layers were combined, dried over Na₂SO₄, filtered and concentrated. The *E* and *Z* isomers (approx. 5 : 1 ratio) were separated by flash column chromatography (ethyl acetate / hexanes = 20 / 80). The purified *E* isomer **I-84** was obtained as a yellow oil (72% yield).

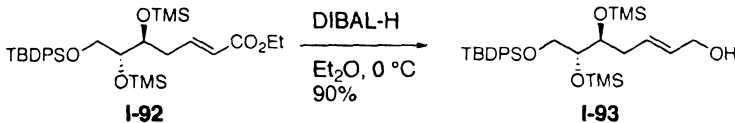
Data for **I-84**: ¹H NMR (500MHz, CDCl₃) δ 7.65-7.63 (m, 4 H), 7.45-7.37 (m, 6 H), 6.99-6.92 (m, 1 H), 5.87 (dt, *J* = 15.7, 1.4 Hz, 1 H), 4.17 (q, *J* = 7.07 Hz, 2 H), 3.80-3.79 (m, 3 H), 3.60-3.58 (m, 1 H), 2.60 (br-s, 1 H), 2.47-2.43 (m, 1 H), 2.37-2.32 (m, 1 H), 2.15 (br-s, 1 H), 1.27 (t, *J* = 7.07, 3 H), 1.06 (s, 9 H); ¹³C NMR (125 MHz, CDCl₃) δ 166.5, 145.1, 135.7, 132.9, 130.3, 128.1, 124.2, 73.5, 71.6, 64.8, 60.5, 36.1, 27.1, 19.4,

14.5; IR (neat, thin film), 3461, 3973, 2932, 2859, 1968, 1899, 1830, 1719, 1655, 1472, 1428, 1393, 1370, 1267, 1167, 1113, 1044, 824, 741, 702 cm^{-1} ; HRMS (CI) calcd for $\text{C}_{25}\text{H}_{34}\text{O}_5\text{Si}$, 460.2519 m/z ($\text{M} + \text{NH}_4$)⁺; observed, 460.2550 m/z .



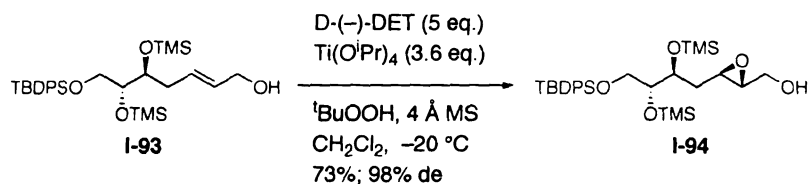
To a solution of **I-84** (0.5 g, 1.13 mmol) in THF (5 mL), imidazole (308 mg, 4.52 mmol), chlorotrimethylsilane (0.57 mL, 4.52 mmol) and cat. dimethylaminopyridine were added and the mixture was refluxed for 4 h. The reaction was cooled to room temperature, diluted with ethyl acetate and filtered. The precipitate was washed with ethyl acetate (200 mL). The filtrate was washed with H_2O and brine, dried over Na_2SO_4 , filtered and concentrated. The crude product was purified by flash column chromatography (ethyl acetate / hexane = 5/95) to isolate **I-92** as a colorless oil (75% yield).

Data for **I-92**: ^1H NMR (500MHz, CDCl_3) δ 7.67-7.65 (m, 4 H), 7.43-7.35 (m, 6 H), 6.99-6.93 (m, 1 H), 5.81 (d, $J = 14.2$ Hz, 1 H), 4.18 (q, $J = 7.1$, 2 H), 3.90-3.87 (m, 1 H), 3.75-3.72 (m, 1 H), 3.62-3.52 (m, 2 H), 2.41-2.26 (m, 2 H), 1.28 (t, $J = 7.1$, 3 H), 1.05 (s, 9 H), 0.07 (s, 9 H), 0.04 (s, 9 H); ^{13}C NMR (125 MHz, CDCl_3) δ 166.6, 147.3, 135.9, 133.6, 130.0, 128.0, 123.3, 72.7, 65.7, 60.2, 35.1, 27.1, 19.4, 14.5, 0.6, 0.5; IR (neat, thin film) 3086, 2957, 2896, 2859, 1982, 1893, 1824, 1722, 1657, 1474, 1429, 1368, 1318, 1252, 1113, 982, 841, 745, 702 cm^{-1} ; HRMS (CI) calcd for $\text{C}_{31}\text{H}_{50}\text{O}_5\text{Si}_3$, 587.3044 m/z ($\text{M} + \text{H}$)⁺; observed, 587.3030 m/z .



A solution of **1-92** (2 g, 3.4 mmol) in Et₂O (15 mL) was cooled to 0°C. To this, a solution of DIBAL-H (1.0 M in hexane, 13.6 mL) was added. The reaction was continued at 0°C and it was complete after 30 min. The reaction was quenched by adding saturated aqueous solution of Na-K tartrate (25 mL) and diluted with ether (50 mL). To this biphasic mixture, glycerol (0.7 mL) was added and the mixture was stirred vigorously for 8 h. The layers were separated and the aqueous layer was extracted with ether (2x50 mL). The organic layers were combined, dried over Na₂SO₄, filtered and concentrated. Purification after flash column chromatography led to **1-93** (1.66 g, 90% yield) as a colorless oil.

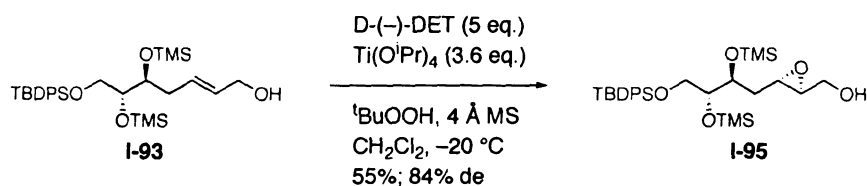
Data for **1-93**: ^1H NMR (500MHz, CDCl_3) δ 7.67-7.64 (m, 4 H), 7.41-7.34 (m, 6 H), 5.66-5.64 (m, 2 H), 4.07 (d, J = 4.6 Hz, 2 H), 3.76-3.71 (m, 2 H), 3.64 (dd, J = 10.6, 5.7 Hz, 1 H), 3.52 (dd, J = 10.4, 6.1 Hz, 1 H), 2.22-2.19 (m, 2 H), 1.04 (s, 9 H), 0.08 (s, 9 H), 0.01 (s, 9 H); ^{13}C NMR (125 MHz, CDCl_3) δ 135.9, 133.7, 131.3, 130.6, 129.8, 127.9, 73.8, 65.9, 64.1, 35.3, 27.1, 19.4, 0.7, 0.6; IR (neat, thin film) 3349, 3073, 2957, 2859, 1962, 1900, 1824, 1474, 1429, 1250, 1113, 972, 841, 702 cm^{-1} ; HRMS (CI) calcd for $\text{C}_{29}\text{H}_{48}\text{O}_4\text{Si}_3$, 545.2939 m/z ($\text{M} + \text{H}$) $^+$; observed, 545.2927 m/z .



To a round bottom flask charged with powdered, preactivated mol. sieves (50 mg), CH_2Cl_2 (2 mL) was added and cooled to -30°C . To this, $\text{Ti}(\text{O}^i\text{Pr})_4$ (0.4 mL, 0.132 mmol) was added followed by addition of D-(-)-DET (0.32 mL, 0.184 mmol in 1 mL CH_2Cl_2). This mixture was stirred at -30°C , under N_2 for 30 min after which time a solution of the allylic alcohol **I-93** (0.2 g, 0.368 mmol in 2 mL CH_2Cl_2) was added dropwise (over 30 min) to the reaction. This mixture was held for 45 min. at -20°C and *t*-BuOOH (0.50 mL, 0.184 mmol) was added to the reaction. Stirring was continued at -20°C for 2 h and quenched by adding saturated solutions of Na_2SO_4 (0.32 mL) and Na_2SO_3 (0.6 mL) and diluted with 10 mL ether. The mixture was stirred vigorously at room temperature for 3 h (yellow paste was formed in the reaction) and refrigerated overnight. The paste was diluted with anhydrous Et_2O (200 mL) and celite was added to it. This mixture was filtered on a celite pad using a sintered funnel. The yellow residue was further washed with anhydrous ether (200 mL) when it turned granular. The filtrate was concentrated and the crude product was purified by column chromatography (ethyl acetate / hexanes = 10 / 90). The epoxide **I-94** was obtained as a colorless oil (152 mg, 73% yield).

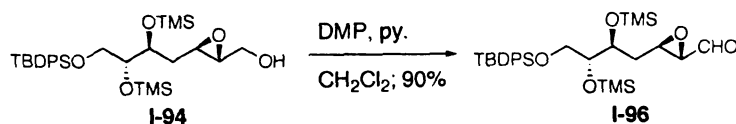
Data for **I-94**: $[\alpha]_{\text{D}}^{20.2} + 35.6$ (c 1.0, CHCl_3); ^1H NMR (500MHz, CDCl_3) δ 7.65-7.63 (m, 4 H), 7.42-7.35 (m, 6 H), 3.96-3.93 (m, 1 H), 3.88-3.86 (m, 1 H), 3.78-3.74 (m, 1 H), 3.60-3.55 (m, 2 H), 3.52-3.49 (m, 1 H), 3.05 (dt, $J = 5.9, 2.2$ Hz, 1 H), 2.84-2.82 (m, 1

H), 1.96-1.90 (m, 1 H), 1.57-1.48 (m, 2 H), 1.04 (s, 9 H), 0.06 (s, 9 H), 0.05 (s, 9 H); ^{13}C NMR (125 MHz, CDCl_3) δ 135.8, 133.6, 129.9, 127.9, 71.7, 65.7, 61.9, 58.4, 54.2, 34.6, 27.1, 19.4, 1.2, 0.4; IR (neat, thin film) 3418, 3071, 2957, 2864, 1962, 1893, 1824, 1590, 1472, 1428, 1252, 1111, 841, 747, 702 cm^{-1} ; HRMS (CI) calcd for $\text{C}_{29}\text{H}_{48}\text{O}_5\text{Si}_3$, 561.2888 m/z ($\text{M} + \text{H}$) $^+$; observed, 561.2881 m/z.



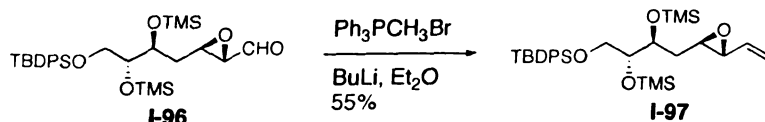
I-95 (114 mg, 0.02 mmol) was prepared from allylic alcohol **I-93** (200 mg, 0.37 mmol) following the same procedure as for **I-94** using L-(+)-DET.

Data for **I-95**: $[\alpha]_{\text{D}}^{20.2}$ -21.8 (c 0.73 CHCl_3); ^1H NMR (500MHz, CDCl_3) δ 7.66-7.65 (m, 4 H), 7.42-7.35 (m, 6 H), 4.06-4.04 (m, 1 H), 3.90-3.88 (m, 1 H), 3.78 (dt, $J = 6.4, 2.2$ Hz, 1 H), 3.61-3.57 (m, 1 H), 3.51 (d, $J = 2.7$, 1 H), 3.49 (d, $J = 2.3$ Hz, 1 H), 3.06-3.03 (m, 1 H), 2.89 (m, 1 H), 1.85-1.80 (m, 1 H), 1.67 (s (br), 1 H), 1.43 (ddd, $J = 14.4, 7.2, 2.6$ Hz, 1 H), 1.04 (s, 9 H), 0.1 (s, 9 H), 0.06 (s, 9 H); ^{13}C NMR (125 MHz, CDCl_3) δ 135.8, 133.5, 129.9, 127.9, 71.1, 65.3, 62.0, 59.4, 54.0, 34.1, 27.1, 19.3, 0.5, 0.4; IR (neat, thin film) 3430, 3073, 2957, 2859, 1967, 1900, 1821, 1590, 1474, 1429, 1252, 1113, 841, 743, cm^{-1} ; HRMS (CI) calcd for $\text{C}_{29}\text{H}_{48}\text{O}_5\text{Si}_3$, 561.2888 m/z ($\text{M} + \text{H}$) $^+$; observed, 561.2872 m/z.



Pyridine (50 μ L) was added to a mixture of Dess-Martin Periodinane (45 mg, 0.09 mmol) in CH_2Cl_2 (1.5 mL). To this, a solution of **I-94** (45 mg, 0.08 mmol) in 1.5 mL CH_2Cl_2 was added and the reaction was stirred at room temperature for 1 h after which time it was diluted with ether (15 mL). The reaction was quenched by adding satd. NaHCO_3 (5 mL) containing $\text{Na}_2\text{S}_2\text{O}_3$ (2.5 g) and the mixture was stirred for 5 min after which ether (15 mL) was added and the layers were separated. The ether layer was washed with H_2O (15 mL), dried over Na_2SO_4 , filtered and concentrated. The product was purified by column chromatography (ethyl acetate / hexanes = 5 / 95) to furnish the aldehyde **I-96** as a colorless oil (90% yield).

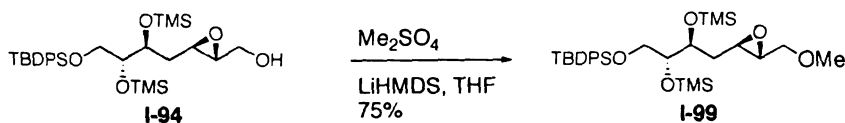
Data for **I-96**: ^1H NMR (500MHz, CDCl_3) δ 8.96 (d, J = 6.4 Hz, 1 H), 7.65-7.35 (m, 10 H), 3.99-3.96 (m, 1 H), 3.75 (dt, J = 6.3, 3.3 Hz, 1 H), 3.56 (dd, J = 10.6, 6.6 Hz, 1 H), 3.51 (dd, J = 10.6, 6.0 Hz, 1 H), 3.32 (dt, J = 5.8, 1.8 Hz, 1 H), 3.04 (dd, J = 6.3, 1.8 Hz, 1 H), 2.02-1.96 (m, 1 H), 1.57-1.53 (m, 1 H), 1.04 (s, 9 H), 0.05 (s, 9 H), 0.04 (s, 9 H); ^{13}C NMR (125 MHz, CDCl_3) δ 198.6, 135.8, 133.5, 130.0, 127.9, 76.7, 71.2, 65.6, 59.2, 55.1, 34.0, 27.1, 19.4, 0.5, 0.4; IR (neat, thin film) 3073, 2959, 2932, 2859, 1968, 1893, 1824, 1732, 1474, 1429, 1390, 1252, 1113, 843, 743, 702 cm^{-1} ; HRMS (CI) calcd for $\text{C}_{29}\text{H}_{46}\text{O}_5\text{Si}_3$, 559.2731 m/z ($M+H$) $^+$; observed, 559.2721 m/z .



A mixture of methyltriphenylphosphonium bromide (206 mg, 0.58 mmol) in THF (2 mL) was cooled to 0°C. To this, butyllithium (0.48 mmol, 0.13 mL of 0.25M solution

1.5 h. The reaction was filtered through a celite pad and the residue was washed with ethyl acetate. The filtrate was concentrated and the crude product was purified by flash column chromatography (ethyl acetate / hexanes = 1/99) to furnish alkyl epoxide **I-98** (60% yield) as a colorless film.

Data for **I-98**: ^1H NMR (500MHz, CDCl_3) δ 7.68-7.66 (m, 4 H), 7.44-7.36 (m, 6 H), 3.96-3.93 (m, 1 H), 3.78 (dt, $J = 5.8, 3.5$ Hz, 1 H), 3.63 (dd, $J = 6.2, 10.4$ Hz, 1 H), 3.53 (dd, $J = 6.2, 10.6$ Hz, 1 H), 2.83-2.80 (m, 1 H), 2.60 (dt, $J = 5.5, 2.2$ Hz, 1 H), 1.92 (ddd, $J = 14.2, 7.5, 5.3$ Hz, 1 H), 1.62-1.45 (m, 3 H), 1.06 (s, 9 H), 0.99 (t, $J = 7.5$ Hz, 2 H), 0.09 (s, 9 H), 0.07 (s, 9 H); ^{13}C NMR (125 MHz, CDCl_3) δ 135.6, 133.4, 129.7, 127.7, 71.8, 65.5, 59.9, 56.4, 35.1, 26.9, 25.1, 19.2, 9.9, 0.4, 0.3; IR (neat, thin film) 3076, 3961, 1736, 1429, 1250, 1113, 841, 742, 702 cm^{-1} .



A solution of **I-94** (51 mg, 0.09 mmol) in THF (0.7 mL) was cooled to 0 °C. To this solution $(\text{CH}_3)_2\text{SO}_4$ (50 μL , 0.52 mmol) and LiHMDS (140 μL of 1.0 M solution in THF) were added. After 2 h, the reaction was diluted with ethyl acetate (20 mL) and washed with H_2O (2x15 mL). The aqueous layer was extracted with ethyl acetate (2x20 mL). The organic layers were combined, dried over Na_2SO_4 , filtered and concentrated. The product **5e** was purified by flash column chromatography (ethyl acetate / hexanes = 5 / 95) as a colorless oil (75% yield).

241

242

243

244

245

246

247

248

249

250

251

252

253

254

255

256

257

258

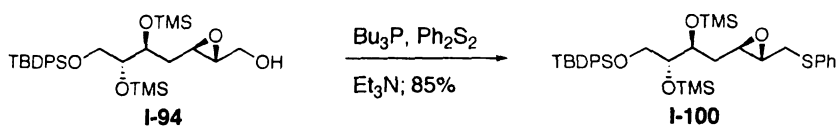
259

260

261

262

Data for **I-99**: ^1H NMR (500MHz, CDCl_3) δ 7.66-7.63 (m, 4 H), 7.42-7.34 (m, 6 H), 3.94-3.91 (m, 1 H), 3.77-3.73 (m, 2 H), 3.61-3.48 (m, 3 H), 2.93 (dt, $J = 5.9, 1.9$ Hz, 1 H), 2.79-2.77 (m, 1 H), 1.93-1.87 (m, 1 H), 1.53-1.49 (m, 1 H), 1.51 (s, 3 H), 1.04 (s, 9 H), 0.11 (s, 9 H), 0.06 (s, 9 H); ^{13}C NMR (125 MHz, CDCl_3) δ 135.8, 133.6, 129.8, 127.8, 71.9, 65.8, 63.3, 58.6, 54.5, 34.9, 27.1, 19.4, 0.6, 0.5; IR (neat, thin film) 3073, 2957, 2859, 192, 1893, 1824, 1589, 1474, 1429, 1252, 1113, 843, 747, 702 cm^{-1} .



To a solution of diphenyl disulphide (60 mg, 0.275 mmol) in triethyl amine (0.2 ml), tributyl phosphine (63 μL , 0.275 mmol) was added, stirred for 5 min. and cooled to 0°C . To this, a solution of the epoxyalcohol **I-94** (50 mg, 0.09 mmol) in triethyl amine (0.2 ml) cooled to 0°C was added dropwise. The reaction was allowed to warm to room temperature and stirred for 4 h. The reaction was diluted with ether (20 mL) and washed with H_2O (2x15 mL). The aqueous layer was extracted with ether (2x20 mL). **I-100** was purified by flash column chromatography (ethyl acetate / hexanes = 5 / 95) as a yellow oil in 85% yield.

Data for **I-100**: ^1H NMR (500MHz, CDCl_3) δ 7.66-7.63 (m, 4 H), 7.42-7.33 (m, 8 H), 7.27-7.23 (m, 2 H), 7.18-7.15 (m, 1 H), 3.89-3.86 (dt, $J = 7.6, 4.2$ Hz, 1 H), 3.75-3.72 (dt, $J = 6.0, 3.6$ Hz, 1 H), 3.57 (dd, $J = 10.6, 6.0$ Hz, 1 H), 3.48 (dd, $J = 10.6, 6.2$ Hz, 1 H), 3.07 (dd, 13.8, 5.2 Hz, 1 H), 2.95 (dd, 13.9, 5.3 Hz, 1 H), 2.87-2.83 (m, 2 H), 1.82-1.77 (m, 1 H), 1.52-1.47 (m, 1 H), 1.03 (s, 9 H), 0.06 (s, 9 H), 0.05 (s, 9 H); ^{13}C NMR (125

0.2

0.3

0.4

0.5

0.6

0.7

0.8

0.9

1.0

1.1

1.2

1.3

1.4

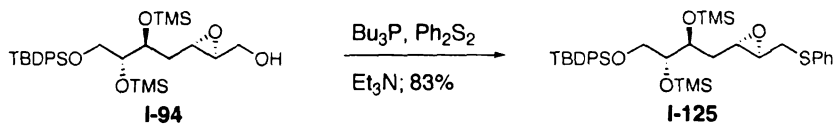
1.5

1.6

1.7

1.8

MHz, CDCl₃) δ 135.9, 133.6, 130.3, 129.9, 129.2, 127.9, 126.8, 71.7, 65.8, 57.5, 57.1, 36.7, 34.9, 27.1, 19.4, 0.6, 0. IR (neat, thin film) 3073, 2957, 2859, 1856, 1831, 1712, 1574, 1473, 1427, 1391, 1113, 941, 841, 741, cm⁻¹; HRMS (CI) calcd for C₃₅H₅₂O₄SSi₃, 653.2972 m/z (M+ H)⁺; observed, 653.2969 m/z.



I-125 was prepared following the same procedure as that for **I-100**.

Data for **I-125**: ^1H NMR (500MHz, CDCl_3) δ 7.65-7.62 (m, 4 H), 7.42-7.32 (m, 8 H), 7.28-7.25 (m, 2 H), 7.20-7.17 (m, 1 H), 3.98 (dt, $J = 5.0, 2.5$ Hz, 1 H), 3.73 (dt, $J = 6.3, 2.4$ Hz, 1 H), 3.47-3.45 (m, 1 H), 3.07 (dd, 13.9, 5.3 Hz, 1 H), 2.97 (dd, 13.9, 5.8 Hz, 1 H), 2.88 (dt, 2.0, 5.5 Hz, 1 H), 1.82-1.77 (m, 1 H), 1.21 (ddd, 18.3, 7.9, 2.9 Hz, 1 H), 1.02 (s, 9 H), 0.08 (s, 9 H), 0.07 (s, 9 H); ^{13}C NMR (125 MHz, CDCl_3) δ 135.9, 133.6, 129.8, 129.2, 127.9, 126.9, 71.7, 65.3, 57.9, 57.2, 36.9, 34.3, 27.1, 19.3, 0.6, 0.5. IR (neat, thin film) 3176, 2957, 2859, 1956, 1831, 1587, 1474, 1429, 1250, 1113, 943, 841, 741, cm^{-1} ; HRMS (CI) calcd for $\text{C}_{35}\text{H}_{52}\text{O}_4\text{SSi}_3$, 653.2972 m/z ($\text{M} + \text{H}$) $^+$; observed, 653.2965 m/z .

General Procedure for $\text{BF}_3 \cdot \text{Et}_2\text{O}$ Mediated Epoxide Opening Reactions:

A solution of the epoxide (0.088 mmol) in anhydrous Et₂O (1 mL) was cooled to 0 °C. BF₃•Et₂O (0.616 mmol) was added to this solution at 0 °C. The reaction was allowed to warm to the room temperature for 1 h. The reaction was quenched by adding H₂O. The mixture was diluted with ethyl acetate (10 mL) and washed with NaHCO₃.

(satd., 5 mL). The aqueous layer was extracted with ethyl acetate (2x10 mL). The organic layers were combined, dried over Na_2SO_4 , filtered and concentrated. The crude product was subjected to acetylation without purification.

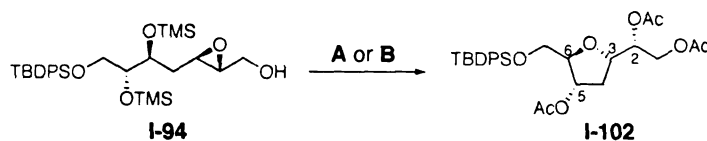
General Procedure for Protic Acid Mediated Epoxide Opening Reactions:

A solution of the epoxide (0.1 mmol) in THF (0.5 mL) was cooled to 0 °C. Aqueous protic acid ($\text{AcOH}:\text{H}_2\text{O}:\text{THF}$ (6:3:1) or 10% $\text{HCl}:\text{THF}$ (9 : 1) 3 mL) was added to the THF solution at 0 °C and the reaction was allowed to warm to room temperature for 3 h, after which time the reaction was diluted with ethyl acetate and neutralized by adding satd. NaHCO_3 solution. The aqueous layer was extracted with ethyl acetate (2x15 mL). The organic layers were combined, dried over Na_2SO_4 , filtered and concentrated. The crude product was subjected to acetylation without purification.

General Procedure for the Acetylation Reaction:

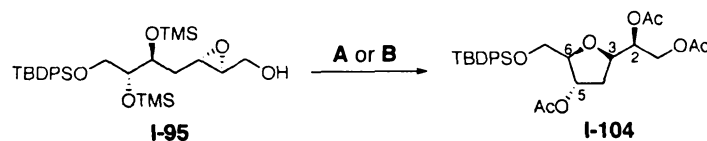
The crude cyclization product (0.11 mmol) was dissolved in pyridine (0.5 mL). Acetic anhydride (0.66 mmol) was added to the solution and the mixture was stirred at 60 °C for 4 h. The reaction was cooled to room temperature, diluted with ethyl acetate (15 mL) and washed with 10% HCl (2x10 mL). The aqueous layers were combined and extracted with ethyl acetate (2x15 mL). The organic layers were combined, dried over Na_2SO_4 , filtered and concentrated. The crude product was purified by flash column chromatography (hexanes/ethyl acetate).

Spectral data for cyclization products:



- A** i) $\text{BF}_3 \cdot \text{OEt}_2$ (6 eq.), Et_2O , 0 °C to rt
 ii) Ac_2O , Py., 60 °C, 75% (two steps)
B i) $\text{AcOH} : \text{H}_2\text{O} : \text{THF}$ (6 : 3 : 1), 0 °C to rt
 ii) Ac_2O , Py., 60 °C, 72% (two steps)

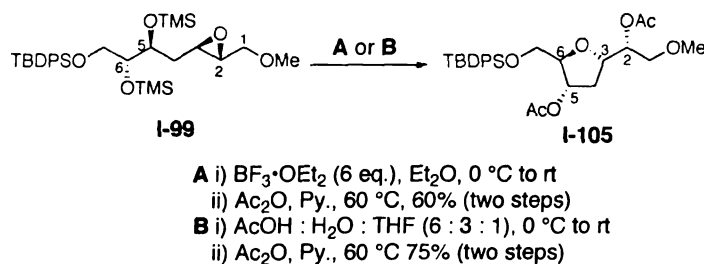
Data for **I-102**: $[\alpha]_{\text{D}}^{20.2} +46.9$ (c 1.7, CHCl_3); ^1H NMR (500MHz, CDCl_3) δ 7.66-7.63 (m, 4 H), 7.43-7.35 (m, 6 H), 5.34 (dt, $J = 4.5, 2.1$ Hz, 1 H), 5.15-5.11 (m, 1 H), 4.6 (dd, $J = 12.1, 2.7$ Hz, 1H), 4.31 (dt, $J = 7.8, 4.5$ Hz, 1 H), 4.15-4.10 (m, 2 H), 3.72 (dd, $J = 11.0, 3.3$ Hz, 1 H), 3.68 (dd, $J = 11.1, 4.2$ Hz, 1 H), 2.50-2.44 (m, 1 H), 2.05 (s, 6 H), 2.02 (s, 3 H), 1.91 (ddd, $J = 13.7, 4.4, 2.9$ Hz, 1 H), 1.03 (s, 9 H); ^{13}C NMR (125 MHz, CDCl_3) δ 170.9, 170.3, 135.8, 133.3, 130.1, 128.0, 85.1, 76.3, 72.7, 64.9, 63.2, 34.9, 27.0, 21.3, 21.2, 21.0, 19.4; IR (neat, thin film) 3070, 2932, 2859, 1984, 1903, 1744, 1429, 1370, 1237, 1113, 824, 743, 704 cm^{-1} ; HRMS (FAB) calcd for $\text{C}_{29}\text{H}_{39}\text{O}_8\text{Si}$, 543.2415 m/z ($\text{M}+\text{H}$) $^+$; observed, 543.2390 m/z.



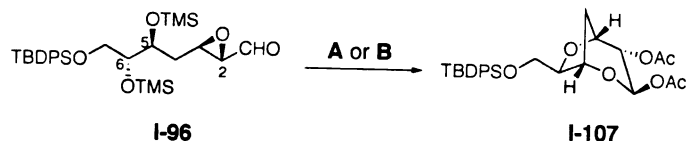
- A** i) $\text{BF}_3 \cdot \text{OEt}_2$ (6 eq.), Et_2O , 0 °C to rt
 ii) Ac_2O , Py., 60 °C, 80% (two steps)
B i) $\text{AcOH} : \text{H}_2\text{O} : \text{THF}$ (6 : 3 : 1), 0 °C to rt
 ii) Ac_2O , Py., 60 °C 76% (two steps)

Data for **I-104**: $[\alpha]_{\text{D}}^{20.2} +15.8$ (c 0.77, CHCl_3); ^1H NMR (500MHz, CDCl_3) δ 7.66-7.63 (m, 4 H), 7.42-7.34 (m, 6 H), 5.34-5.33 (m, 1 H), 5.09 (dt, $J = 5.9, 2.8$ Hz, 1 H), 4.3 (dd, $J = 12.2, 3.0$ Hz, 1 H), 4.19 (dt, $J = 10.2, 6.1$ Hz, 1 H), 4.12-4.08 (m, 1 H),

4.00-3.98 (m, 1 H) 3.74 (dd, $J = 11.0, 3.9$ Hz, 1 H), 3.62 (dd, $J = 11.0, 4.6$ Hz, 1 H), 2.09-2.02 (m, 2 H), 2.05 (s, 3 H), 2.03 (s, 3 H), 2.00 (s, 3 H), 1.03 (s, 9 H); ^{13}C NMR (125 MHz, CDCl_3) δ 170.8, 170.6, 170.2, 135.8, 133.3, 130.0, 128.0, 85.5, 76.3, 72.8, 64.2, 63.1, 35.5, 27.0, 21.3, 21.0, 19.4; IR (neat, thin film) 3073, 2932, 2859, 1975, 1906, 1746, 1429, 1370, 1237, 1113, 862, 802, 743, 704 cm^{-1} ; HRMS (FAB) calcd for $\text{C}_{29}\text{H}_{39}\text{O}_8\text{Si}$, 560.2680 m/z ($\text{M}+\text{NH}_4$) $^+$; observed, 560.2694 m/z .

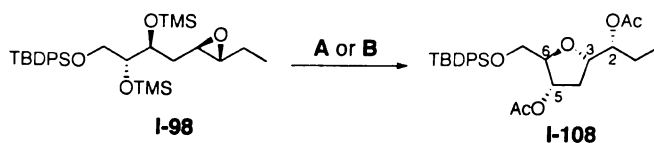


Data for **I-105**: $[\alpha]_{\text{D}}^{20.2} +31.8$ (c 1.0, CHCl_3); ^1H NMR (500 MHz, CDCl_3) δ 7.66-7.63 (m, 4 H), 7.42-7.35 (m, 6 H), 5.31 (dt, $J = 6.4, 2.7$ Hz, 1 H), 5.09 (m, 1 H), 4.32 (dt, $J = 7.9, 4.7$ Hz, 1 H), 4.09 (m, 1 H), 3.72 (dd, $J = 11.0, 3.6$ Hz, 1 H), 3.66 (dd, $J = 11.0, 4.4$ Hz, 1 H), 3.61 (dd, $J = 10.9, 3.2$ Hz, 1 H), 3.56 (dd, $J = 10.9, 5.6$ Hz, 1 H), 3.35 (s, 3 H), 2.45-2.40 (m, 1 H), 2.07 (s, 3 H), 2.05 (s, 3 H), 1.90 (ddd, $J = 13.9, 4.7, 3.0$ Hz, 1 H), 1.03 (s, 9 H); ^{13}C NMR (125 MHz, CDCl_3) δ 170.9, 170.5, 135.8, 133.4, 130.0, 128.0, 84.8, 76.3, 73.6, 71.8, 64.9, 59.5, 34.6, 27.0, 21.3, 19.4; IR (thin film) 3073, 3017, 2932, 2859, 1968, 1900, 1736, 1590, 1471, 1429, 1372, 1235, 1113, 1055, 762, 704 cm^{-1} ; HRMS (CI) calcd for $\text{C}_{28}\text{H}_{38}\text{O}_7\text{Si}$, 513.2309 m/z ($\text{M}-\text{H}$) $^-$; observed, 513.2306 m/z .



- A** i) $\text{BF}_3 \cdot \text{OEt}_2$ (6 eq.), Et_2O , 0 °C to rt
 ii) Ac_2O , Py., 60 °C, 17% (two steps)
B i) $\text{AcOH} : \text{H}_2\text{O} : \text{THF}$ (6 : 3 : 1), 0 °C to rt
 ii) Ac_2O , Py., 60 °C 20% (two steps)

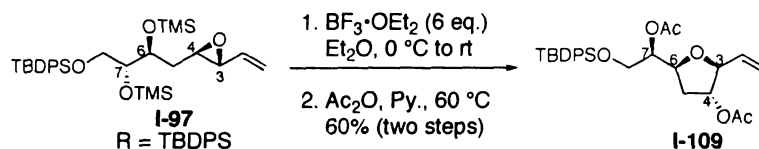
Data for **I-107**: $[\alpha]_{\text{D}}^{20.2} +45.6$ (c 0.9, CHCl_3); ^1H NMR (500MHz, CDCl_3) δ 7.62–7.59 (m, 4 H), 7.43–7.34 (m, 6 H), 6.00 (d, $J = 6.8$ Hz, 1 H), 4.66 (dd, $J = 6.8, 1.6$ Hz, 1 H), 4.57 (m, 1 H), 4.52–4.50 (m, 1 H), 4.34 (m, 1 H), 3.68 (dd, $J = 11.2, 3.8$ Hz, 1 H), 3.43 (dd, $J = 11.2, 6.6$ Hz, 1 H), 2.08 (s, 6 H), 2.06–2.11 (m, 2 H), 1.02 (s, 9 H); ^{13}C NMR (125 MHz, CDCl_3) δ 170.3, 169.6, 135.7, 133.1, 130.1, 128.0, 92.2, 82.3, 76.2, 74.2, 64.3, 33.9, 27.0, 21.7, 19.4; IR (neat, thin film) 3070, 2932, 2859, 1968, 1896, 1744, 1429, 1370, 1235, 1113, 897, 824, 758, 704 cm^{-1} ; HRMS (FAB) calcd for $\text{C}_{27}\text{H}_{34}\text{O}_7\text{Si}$, 537.1711 m/z ($\text{M}+\text{K}$) $^+$; observed, 537.1732 m/z .



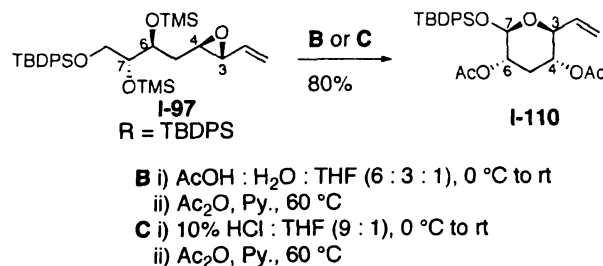
- A** i) $\text{BF}_3 \cdot \text{OEt}_2$ (6 eq.), Et_2O , 0 °C to rt
 ii) Ac_2O , Py., 60 °C, 80% (two steps)
B i) $\text{AcOH} : \text{H}_2\text{O} : \text{THF}$ (6 : 3 : 1), 0 °C to rt
 ii) Ac_2O , Py., 60 °C 78% (two steps)

Data for **I-108**: $[\alpha]_{\text{D}}^{20.2} +21.9$ (c 0.3, CHCl_3); ^1H NMR (500MHz, CDCl_3) δ 7.67
 7.62 (m, 4 H), 7.42–7.34 (m, 6 H), 5.32–5.30 (m, 1 H), 4.95 (ddd, $J = 8.3, 6.6, 4.0$ Hz, 1
 H), 4.18–4.14 (m, 1 H), 3.72 (dd, $J = 11.1, 3.5$ Hz, 1 H), 3.68 (dd, $J = 11.0, 4.3$ Hz, 1 H),
 2.45–2.39 (m, 1 H), 2.05 (s, 6 H), 1.86 (ddd, $J = 13.7, 5.7, 3.5$ Hz, 1 H), 1.73 (ddd, $J =$
 14.3, 7.5, 3.9 Hz, 1 H), 1.58–1.54 (m, 1 H), 1.03 (s, 9 H), 0.89 (t, $J = 7.5$ Hz, 3 H) ^{13}C

NMR (125 MHz, CDCl_3) δ 171.0, 170.7, 135.8, 133.4, 130.0, 128.0, 84.4, 80.0, 76.3, 76.0, 65.0, 34.6, 30.0, 27.0, 24.3, 21.3, 19.4, 9.6; IR (neat, thin film) 3071, 2928, 2857, 1975, 1887, 1740, 1590, 1462, 1429, 1370, 1242, 1113, 1020, 801, 741, 702 cm^{-1} .

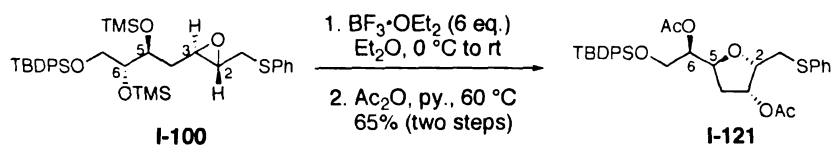


Data for **I-109**: $[\alpha]_{\text{D}}^{20.2} -12.0$ (c 0.3, CHCl_3); ^1H NMR (500MHz, CDCl_3) δ 7.65–7.63 (m, 4 H), 7.42–7.34 (m, 6 H), 5.82–5.75 (m, 1 H), 5.27–5.23 (m, 1 H), 5.20–5.16 (m, 1 H), 5.13–5.10 (m, 1 H), 4.96 (m, 1 H), 4.34–4.30 (m, 1 H), 3.81 (d, $J = 5.3$ Hz, 1 H), 2.07–2.03 (m, 1 H), 2.05, (s, 3 H), 2.02 (s, 3 H), 1.95–1.91, (m, 1 H), 1.03 (s, 9 H); ^{13}C NMR (125 MHz, CDCl_3) δ 170.7, 170.3, 136.0, 135.8, 133.5, 130.0, 127.9, 116.5, 84.8, 78.8, 74.8, 63.3, 33.4, 27.0, 21.3, 21.2, 19.4; IR (neat, thin film) 3072, 2932, 2858, 1746, 1590, 1474, 1429, 1374, 1235, 1113, 860, 823, 734, 704 cm^{-1} ; HRMS (FAB) calcd for $\text{C}_{28}\text{H}_{36}\text{O}_6\text{Si}$, 535.1918 m/z ($\text{M}+\text{K}$) $^+$; observed, 535.1912 m/z.

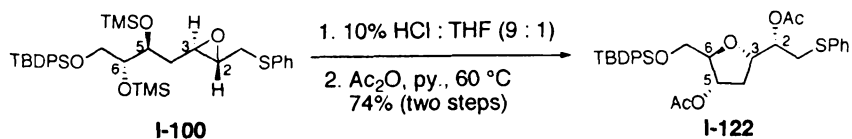


Data for **I-110**: $[\alpha]_{\text{D}}^{20.2} -12.0$ (c 0.3, CHCl_3); ^1H NMR (500MHz, CDCl_3) δ 7.69–7.63 (m, 4 H), 7.41–7.32 (m, 6 H), 5.81–5.75 (m, 1 H), 5.35–5.32 (m, 1 H), 5.23–5.20 (m, 1 H), 4.70 (ddd, $J = 11.2, 9.5, 4.8$ Hz, 1 H), 3.79–3.71 (m, 3 H), 3.43 (ddd, $J = 9.7, 4.5,$

2.2 Hz, 1 H), 2.58 (dt = 9.7, 4.5, 2.2 Hz, 1 H), 1.99 (s, 3 H), 1.93 (s, 3 H), 1.56-1.50 (m, 1 H), 1.02 (s, 9 H) ^{13}C NMR (125 MHz, CDCl_3) δ 169.8, 169.6, 135.9, 134.9, 133.8, 129.8, 127.8, 118.2, 80.5, 79.9, 69.9, 66.6, 63.4, 35.1, 26.9, 21.2, 21.1, 19.5; IR (neat, thin film) 3037, 2959, 2932, 2859, 1744, 1474, 1428, 1374, 1235, 1115, 995, 825, 798, 740, 706 cm^{-1} ; HRMS (CI) calcd for $\text{C}_{28}\text{H}_{36}\text{O}_6\text{Si}$, 497.2359 m/z ($\text{M}+\text{H}$) $^+$; observed, 497.2377 m/z .



Data for **I-121**: $[\alpha]_{\text{D}}^{20.2}$ - 37.5 (c 0.8, CHCl_3); ^1H NMR (500MHz, CDCl_3) δ 7.63-7.61 (m, 4 H), 7.43-7.33 (m, 8 H), 7.26-7.23 (m, 2 H), 7.19-7.15 (m, 1 H), 5.33-5.31 (m, 1 H), 5.10-5.07 (m, 1 H), 4.37 (dt, J = 9.0, 5.8 Hz, 1 H), 4.05-4.02 (m, 1 H), 3.77-3.72 (m, 2 H), 3.13 (dd, J = 13.5, 5.7 Hz, 1 H), 2.17-2.12 (m, 1 H), 2.05-2.00 (m, 3 H), 1.99 (s, 3 H), 1.95 (s, 3 H), 1.02 (s, 9 H) ^{13}C NMR (125 MHz, CDCl_3) δ 170.1, 170.0, 135.5, 133.1, 130.1, 129.8, 129.0, 127.7, 126.6, 80.3, 76.4, 74.9, 74.4, 62.7, 34.9, 32.8, 26.7, 21.0; IR (neat, thin film) 3073, 2932, 2859, 1956, 1900, 1744, 1588, 1474, 1429, 1373, 1230, 1113, 951, 823, 741, 704 cm^{-1} ; HRMS (CI) calcd for $\text{C}_{33}\text{H}_{40}\text{O}_6\text{SSi}$, 593.2393 m/z ($\text{M}+\text{H}$) $^+$; observed, 593.2383 m/z .



7

12

13

14

15

16

17

18

19

20

21

22

23

24

25

26

27

28

29

30

31

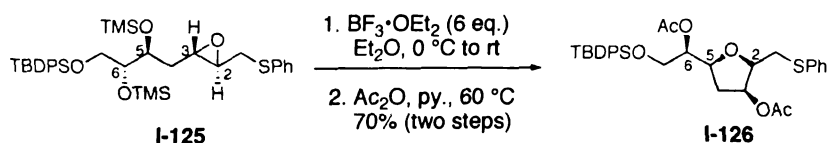
32

33

34

35

Data for **I-122**: $[\alpha]_D^{20.2}$ - 37.5 (c 0.8, CHCl_3); ^1H NMR (500MHz, CDCl_3) δ 7.66-7.60 (m, 4 H), 7.42-7.33 (m, 8 H), 7.27-7.23 (m, 2 H), 7.18-7.14 (m, 1 H), 5.29 (dt, J = 6.8, 2.5 Hz, 1 H), 5.12 (dt, J = 7.6, 3.4 Hz, 1 H), 4.32 (dt J = 7.8, 4.5 Hz, 1 H), 4.06 (m, 1 H), 3.70 (dd, J = 11.0, 3.6 Hz, 1 H), 3.65 (dd, J = 11.1, 4.2 Hz, 1 H), 3.38 (dd, J = 14.3, 3.4 Hz, 1 H), 3.07 (dd, J = 14.3, 7.5 Hz 1 H), 2.45-2.39 (m, 1 H), 2.00 (s, 3 H), 1.88 (s, 3 H), 1.85-1.84 (m, 1 H), 1.03 (s, 9 H); ^{13}C NMR (125 MHz, CDCl_3) δ 170.9, 170.3, 136.3, 135.8, 133.3, 130.2, 130.0, 129.1, 128.0, 126.5, 84.9, 79.2, 73.8, 64.9, 35.6, 34.7, 27.0, 21.3; IR (neat, thin film) 3073, 2932, 2859, 1962, 1891, 1742, 1588, 1472, 1428, 1370, 1239, 1113, 1026, 823, 740, 702 cm^{-1} ; HRMS (CI) calcd for $\text{C}_{33}\text{H}_{40}\text{O}_6\text{SSi}$, 621.2706 m/z ($\text{M} + \text{C}_2\text{H}_5$) $^+$; observed, 621.2702 m/z.



Data for **I-126**: $[\alpha]_D^{20.2}$ + 35.6 (c 1.0, CHCl_3); ^1H NMR (500 MHz, CDCl_3) δ 7.66-7.65 (m, 4 H), 7.44-7.35 (m, 8 H), 7.27-7.16 (m, 3 H), 5.25-5.22 (m, 1 H), 5.07 (dt, J = 7.0, 4.5 Hz, 1 H), 4.13 (dt, J = 7.7, 4.9 Hz, 1 H), 3.95 (ddd, J = 8.0, 5.8, 3.9 Hz, 1 H), 3.81 (d, J = 4.4 Hz, 1 H), 3.12 (dd, J = 13.7, 5.8 Hz, 1 H), 3.02 (dd, J = 13.7, 8.0 Hz, 1 H), 2.33-2.27 (m, 1 H), 2.01, (s, 3 H), 1.96 (s, 3 H), 1.89-1.85 (m, 1 H), 1.02 (s, 9 H); ^{13}C NMR (125 MHz, CDCl_3) δ 170.5, 170.4, 136.0, 135.8, 133.6, 130.1, 129.9, 129.2, 127.9, 126.7; IR (neat, thin film) 3074, 2932, 2859, 1962, 1900, 1742, 1588, 1473, 1428, 1373, 1242, 1113, 953, 823, 741, 702 cm^{-1} ; HRMS (CI) calcd for $\text{C}_{33}\text{H}_{40}\text{O}_6\text{SSi}$, 593.2393 m/z ($\text{M} + \text{H}$) $^+$; observed, 593.2377 m/z.

2. Experimental section for the oxidative cleavage of olefins

General Procedure for the Oxidative Cleavage of Mono and Disubstituted Olefins

(condition B):

The olefin (1 eq) was dissolved in DMF (0.2 M), and OsO_4 (0.01 eq, 2.5% in *t*BuOH) was added and stirred for 5 min. Oxone[®] (4 eq) was added in one portion and the reaction was stirred at RT for 3 h or until the solution becomes colorless. This usually marks the completion of the reaction, which was verified by TLC or GC. Na_2SO_3 (6 eq w/w) was added, to reduce the remaining Os(VIII), and stirred for an additional hour or until solution became dark brown / black. EtOAc was added to extract the products and 1N HCl was used to dissolve the salts. The organic extract was washed with 1N HCl (3x) and brine, dried over Na_2SO_4 , and the solvent was removed under reduced pressure to obtain the crude product. Products were purified by silica gel column chromatography.

General Procedure for the Oxidative Cleavage of Tri and Tetrasubstituted Olefins

(condition B):

The olefin (1 eq) was dissolved in DMF (0.2 M), and OsO_4 (0.01 eq, 2.5% in *t*BuOH) was added and stirred for 5 min. A solid mixture of Oxone[®] (4 eq) and NaHCO_3 (4 eq) was then added in one portion and the reaction was stirred at RT for 3 h or until solution becomes colorless. This usually marks the completion of the reaction, which

42.4

43.1

43.4

43.7

43.8

43.9

Spec

43.1

43.2

43.3

43.4

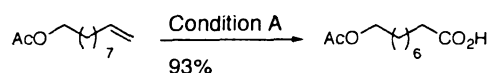
43.5

43.6

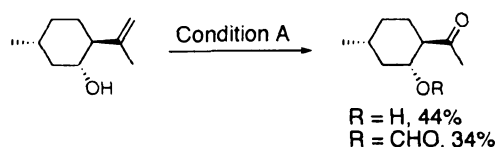
was verified by TLC or GC. Na_2SO_3 (6 eq w/w) was added, to reduce the remaining Os(VIII), and stirred for an additional hour or until solution became dark brown / black. EtOAc was added to extract the products and 1N HCl was used to dissolve the salts. The organic extract was washed with 1N HCl (3x) and brine, dried over Na_2SO_4 , and the solvent was removed under reduced pressure to obtain the crude product. Products were purified by silica gel column chromatography.

Spectral data:

Spectral properties of nonanoic acid (Table I-1, entry 1), *p*-methylbenzoic acid, *p*-nitrobenzoic acid, adipic acid, benzoic acid (entries 4–7), acetophenone and 3*R*-methyladipic acid (entries 9 and 10) match those reported by Aldrich and comparison to authentic samples.



^1H NMR (CDCl_3 , 300 MHz): δ 4.02 (t, 2H, $J=6.9$ Hz), 2.32 (t, 2H, $J=7.4$ Hz), 2.02 (s, 3H), 1.56-1.61 (m, 4H), 1.29 (bs, 8H); ^{13}C NMR (CDCl_3 , 75 MHz): δ 179.6, 171.4, 64.5, 33.9, 29.0, 28.9, 28.8, 28.4, 25.7, 24.5, 20.9; IR (neat, thin film) 3455, 2931, 2856 1739, 1737, 1242 cm^{-1} ; LRMS (70 eV, EI) m/z 199 $[\text{M}-\text{H}_2\text{O}]^+$, 157 $[\text{M}-\text{OAc}]^+$.

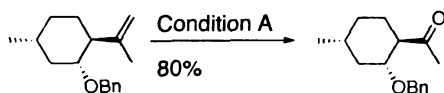


(1*R*, 2*R*, 5*R*)-2-Acetyl-5-methyl cyclohexanol (R = H):

^1H NMR (CDCl_3 , 300 MHz): δ 3.80 (ddd, 1H, $J=4.4, 9.6, 11.1$ Hz), 2.27 (ddd, 1H, $J=3.6, 9.6, 12.9$ Hz), 2.17 (s, 3H), 1.91-2.00 (m, 2H), 1.68-1.74 (m, 1H), 1.38-1.52 (m, 1H), 1.22-1.27 (m, 1H), 0.91-1.03 (m, 1H), 0.92 (d, 3H, $J=6.3$ Hz); ^{13}C NMR (CDCl_3 , 75 MHz): δ 212.9, 70.4, 58.5, 42.2, 34.0, 31.1, 29.2, 27.5, 22.0; IR (neat, thin film) 3417, 2952, 2927, 2869, 1705 cm^{-1} ; LRMS (70eV, EI) m/z 156 M^+ , 138 $[\text{M}-\text{H}_2\text{O}]^+$, 95 $[\text{M}-\text{H}_2\text{O}-\text{C}(\text{O})\text{Me}]^+$.

(1R, 2R, 5R)-2-Acetyl-5-methyl cyclohexanyl formate (R = CHO):

^1H NMR (CDCl_3 , 300 MHz): δ 7.95 (s, 1H), 5.06 (ddd, 1H, $J=4.4, 9.6, 11.2$ Hz), 2.59 (ddd, 1H, $J=6.9, 8.9, 14.5$ Hz), 2.15 (s, 3H), 2.11-2.13 (m, 1H), 1.93 (qd, 1H, $J=3.9, 6.9$ Hz), 1.68-1.77 (m, 1H), 1.50-1.62 (m, 1H), 1.27-1.41 (m, 1H), 0.87-1.06 (m, 4H); ^{13}C NMR (CDCl_3 , 75 MHz): δ 209.4, 160.3, 73.1, 55.2, 39.3, 33.3, 30.0, 29.3, 27.8, 21.7; IR (neat, thin film, cm^{-1}) 2952, 2929, 2869, 1728, 1178; LRMS (70 eV, EI) m/z 185 $[\text{M}+\text{H}]^+$, 149 $[\text{M}-\text{HCO}_2\text{H}]^+$; HRMS $[\text{M}+\text{H}]^+$ Calcd for $\text{C}_{10}\text{H}_{16}\text{O}_3$: 184.1099 m/z . Observed 184.1095 m/z .



^1H NMR (CDCl_3 , 300 MHz): δ 7.21-7.32 (m, 5H), 4.56 (d, 1H, $J=11.3$ Hz), 4.37 (d, 1H, $J=11.3$ Hz), 3.6 (dt, 1H, $J=6, 10.4$ Hz), 2.53 (ddd, 1H, $J=3.8, 10.1, 12.6$ Hz), 2.16 (s, 3H), 2.12-2.19 (m, 1H), 1.75 (qd, 1H, $J=3.6, 10.2$ Hz), 1.64-1.70 (m, 1H), 1.25-1.52 (m, 2H), 0.93 (d, 2H, $J=3.3$ Hz); ^{13}C NMR (CDCl_3 , 75 MHz): δ 212.3, 138.5, 128.2,

17

18

19

20

21

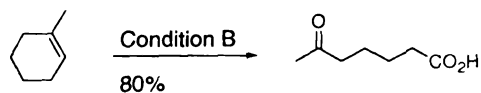
22

23

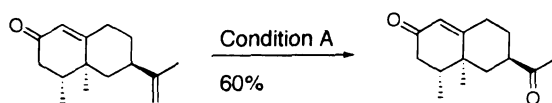
24

25

127.6, 127.4, 79.1, 70.9, 56.6, 39.4, 33.5, 30.9, 27.7, 22.1; IR (neat, thin film) 2950, 2927, 2867, 1739, 1712 cm^{-1} ; LRMS (70 eV, EI) m/z 228 $[\text{M}-\text{H}_2\text{O}]^+$, 140 $[\text{M}-\text{OBn}]^+$; HRMS $[\text{M}+\text{H}]^+$ Calcd. for $\text{C}_{16}\text{H}_{22}\text{O}_2$: 246.1620 m/z . Observed 246.1631 m/z .



^1H NMR (CDCl_3 , 300 MHz): δ 2.41-2.45 (m, 2H), 2.31-2.36 (m, 2H), 2.11 (s, 3H), 1.56-1.62 (m, 4H); ^{13}C NMR (CDCl_3 , 75 MHz): δ 208.8, 179.1, 43.2, 33.7, 29.9, 24.0, 22.9; IR (neat, thin film) 3455, 2939, 1714 cm^{-1} ; LRMS (70 eV, EI) m/z 144 M^+ , 126 $[\text{M}-\text{H}_2\text{O}]^+$.



^1H NMR (CDCl_3 , 300 MHz): δ 2.41-2.45 (m, 2H), 2.31-2.36 (m, 2H), 2.11 (s, 3H), 1.56-1.62 (m, 4H); ^{13}C NMR (CDCl_3 , 75 MHz): δ 208.8, 179.1, 43.2, 33.7, 29.9, 24.0, 22.9; IR (neat, thin film) 3455, 2939, 1714 cm^{-1} ; LRMS (70 eV, EI) m/z 144 M^+ , 126 $[\text{M}-\text{H}_2\text{O}]^+$.

E. References

1. Voet, D.; Voet, J. G.; 2nd ed.; J. Wiley & Sons: New York, 1995, pp 704-713.
2. Johnson, M.; Carey, F.; McMillan, R. M. *Essays Biochem.* **1983**, *19*, 40.
3. Needleman, P.; Turk, J.; Jakschik, B. A.; Morrison, A. R.; Lefkowitz, J. B. *Annu. Rev. Biochem.* **1986**, *55*, 69.
4. Hayaishi, O. *J. Biol. Chem.* **1988**, *263*, 14593.
5. Samuelsson, B. *Science* **1983**, *220*, 568.
6. Samuelsson, B.; Dahlen, S. E.; Lindgren, J. A.; Rouzer, C. A.; Serhan, C. N. *Science* **1987**, *237*, 1171.
7. Samuelsson, B. *Drugs* **1987**, *33*, 2.
8. Weissman, G. *Sci. Am.* **1991**, *264*, 84.
9. Ford-Hutchinson, A. W. *Trends Pharmacol. Sci.* **1991**, *12*, 68.
10. Taylor, G. W.; Clarke, S. R. *Trends Pharmacol. Sci.* **1986**, *7*, 100.
11. Capdevila, J. H.; Karara, A.; Waxman, D. J.; Martin, M. V.; Falck, J. R.; Guengerich, F. P. *J. Biol. Chem.* **1990**, *265*, 10865.
12. Oliw, E. H.; Guengerich, F. P.; Oates, J. A. *J. Biol. Chem.* **1982**, *257*, 3771.
13. Schwartzman, M. L.; Balazy, M.; Masferrer, J.; Abraham, N. G.; McGiff, J. C.; Murphy, R. C. *Proc. Natl. Acad. Sci. U. S. A.* **1987**, *84*, 8125.
14. Proctor, K. G.; Falck, J. R.; Capdevila, J. *Circ. Res.* **1987**, *60*, 50.
15. Cashman, J. R.; Hanks, D.; Weiner, R. I. *Neuroendocrinology* **1987**, *46*, 246.
16. Hammock, B. D., Personal communication.
17. Moghaddam, M. F.; Motoba, K.; Borhan, B.; Pinot, F.; Hammock, B. D. *Biochim. Biophys. Acta* **1996**, *1290*, 327.
18. Koert, U. *Synthesis* **1995**, 115.
19. Cardillo, G.; Orena, M. *Tetrahedron* **1990**, *46*, 3321.

20. Boivin, T. L. B. *Tetrahedron* **1987**, *43*, 3309.
21. Rao, A. S.; Paknikar, S. K.; Kirtane, J. G. *Tetrahedron* **1983**, *39*, 2323.
22. Andrey, O.; Landais, Y. *Tetrahedron Lett.* **1993**, *34*, 8435.
23. Micalizio, G. C.; Roush, W. R. *Org. Lett.* **2000**, *2*, 461.
24. Guindon, Y.; Soucy, F.; Yoakim, C.; Ogilvie, W. W.; Plamondon, L. *J. Org. Chem.* **2001**, *66*, 8992.
25. Seepersaud, M.; Blumenstein, M.; Mootoo, D. R. *Tetrahedron* **1997**, *53*, 5711.
26. Osumi, K.; Sugimura, H. *Tetrahedron Lett.* **1995**, *36*, 5789.
27. Larsen, C. H.; Ridgway, B. H.; Shaw, J. T.; Woerpel, K. A. *J. Am. Chem. Soc.* **1999**, *121*, 12208.
28. Shan, W. F.; Wilson, P.; Liang, W.; Mootoo, D. R. *J. Org. Chem.* **1994**, *59*, 7986.
29. Semmelhack, M. F.; Epa, W. R.; Cheung, A. W. H.; Gu, Y.; Kim, C.; Zhang, N.; Lew, W. *J. Am. Chem. Soc.* **1994**, *116*, 7455.
30. Tamaru, Y.; Hojo, M.; Kawamura, S.; Sawada, S.; Yoshida, Z. *J. Org. Chem.* **1987**, *52*, 4062.
31. Abeywickrema, A. N.; Beckwith, A. L. J.; Gerba, S. *J. Org. Chem.* **1987**, *52*, 4072.
32. Mukaiyama, T.; Hayashi, M.; Ichikawa, J. *Chem. Lett.* **1986**, 1157.
33. Johnson, R. A.; Sharpless, K. B. in *Catalytic Asymmetric Synthesis*; 2nd ed.; Ojima, I., Ed.; Wiley-VCH: New York, 2000, pp 357-398.
34. Johnson, R. A.; Sharpless, K. B. in *Catalytic Asymmetric Synthesis*; 2nd ed.; Ojima, I., Ed.; Wiley-VCH: New York, 2000, pp 231-280.
35. Baldwin, J. E. *J. Chem. Soc., Chem. Commun.* **1976**, 734.
36. Baldwin, J. E.; Cutting, J.; Dupont, W.; Kruse, L.; Silberman, L.; Thomas, R. C. *J. Chem. Soc., Chem. Commun.* **1976**, 736.
37. McIntyre, S.; Warren, S. *Tetrahedron Lett.* **1990**, *31*, 3457.
38. Nakata, T.; Schmid, G.; Vranesic, B.; Okigawa, M.; Smithpalmer, T.; Kishi, Y. *J. Am. Chem. Soc.* **1978**, *100*, 2933.

39. Nakata, T.; Kishi, Y. *Tetrahedron Lett.* **1978**, 2745.
40. Nicolaou, K. C.; Prasad, C. V. C.; Somers, P. K.; Hwang, C. K. *J. Am. Chem. Soc.* **1989**, *111*, 5330.
41. Nicolaou, K. C.; Prasad, C. V. C.; Somers, P. K.; Hwang, C. K. *J. Am. Chem. Soc.* **1989**, *111*, 5335.
42. Suzuki, T.; Sato, O.; Hirama, M. *Tetrahedron Lett.* **1990**, *31*, 4747.
43. Janda, K. D.; Shevlin, C. G.; Lerner, R. A. *Science* **1993**, *259*, 490.
44. Mukai, C.; Sugimoto, Y.; Ikeda, Y.; Hanaoka, M. *Tetrahedron* **1998**, *54*, 823.
45. Baskaran, S.; Vasu, J.; Prasad, R.; Kodukulla, K.; Trivedi, G. K.; Chandrasekhar, J. *Tetrahedron* **1996**, *52*, 4515.
46. Gao, Y.; Hanson, R. M.; Klunder, J. M.; Ko, S. Y.; Masamune, H.; Sharpless, K. B. *J. Am. Chem. Soc.* **1987**, *109*, 5765.
47. Reed, L. A.; Ito, Y.; Masamune, S.; Sharpless, K. B. *J. Am. Chem. Soc.* **1982**, *104*, 6468.
48. Dess, D. B.; Martin, J. C. *J. Am. Chem. Soc.* **1991**, *113*, 7277.
49. Nakagawa, I.; Hata, T. *Tetrahedron Lett.* **1975**, 1409.
50. Nakagawa, I.; Aki, K.; Hata, T. *J. Chem. Soc., Perkin Trans. I* **1983**, 1315.
51. Pettersson, L.; Frejd, T. *J. Chem. Soc., Chem. Commun.* **1993**, 1823.
52. Roush, W. R.; Russorodriguez, S. *J. Org. Chem.* **1987**, *52*, 598.
53. Gill, D. M.; Pegg, N. A.; Rayner, C. M. *J. Chem. Soc., Perkin Trans. I* **1993**, 1371.
54. Gill, D. M.; Pegg, N. A.; Rayner, C. M. *Tetrahedron* **1996**, *52*, 3609.
55. Miyauchi, H.; Nakamura, T.; Ohashi, N. *Bull. Chem. Soc. Jpn.* **1995**, *68*, 1731.
56. De Lucchi, O.; Miotti, U.; Modena, G. *Org. React. (N.Y.)* **1991**, *40*, 157.
57. Padwa, A.; Gunn, D. E., Jr.; Osterhout, M. H. *Synthesis* **1997**, 1353.
58. Fox, D. J.; House, D.; Warren, S. *Angew. Chem., Int. Ed.* **2002**, *41*, 2462.

59. House, D.; Kerr, F.; Warren, S. *Chem. Commun.* **2000**, 1779.
60. Fox, D. J.; House, D.; Kerr, F.; Warren, S. *Chem. Commun.* **2000**, 1781.
61. House, D.; Kerr, F.; Warren, S. *Chem. Commun.* **2000**, 1783.
62. Williams, D. R.; Phillips, J. G.; Barner, B. A. *J. Am. Chem. Soc.* **1981**, *103*, 7398.
63. Sivakumar, M.; Borhan, B. *Tetrahedron Lett.* **2003**, *44*, 5547.
64. Narayan, R. S.; Sivakumar, M.; Bouhlef, E.; Borhan, B. *Org. Lett.* **2001**, *3*, 2489.
65. Travis, B.; Borhan, B. *Tetrahedron Lett.* **2001**, *42*, 7741.
66. Dorofeev, S. B.; Eletskii, A. V.; Smirnov, B. M. *Dokl. Akad. Nauk. Sssr.* **1981**, *257*, 592.
67. Ogle, R. A.; Schumacher, J. L. *Process Saf Prog.* **1998**, *17*, 127.
68. Koike, K.; Inoue, G.; Fukuda, T. *J. Chem. Eng. Jpn.* **1999**, *32*, 295.
69. Lee, D. G.; Chang, V. S. *J. Org. Chem.* **1978**, *43*, 1532.
70. Ishii, Y.; Yamawaki, K.; Ura, T.; Yamada, H.; Yoshida, T.; Ogawa, M. *J. Org. Chem.* **1988**, *53*, 3587.
71. Henry, J. R.; Weinreb, S. M. *J. Org. Chem.* **1993**, *58*, 4745.
72. Antonelli, E.; D'Aloisio, R.; Gambaro, M.; Fiorani, T.; Venturello, C. *J. Org. Chem.* **1998**, *63*, 7190.
73. Sato, K.; Aoki, M.; Noyori, R. *Science* **1998**, *281*, 1646.
74. Kaneda, K.; Haruna, S.; Imanaka, T.; Kawamoto, K. *J. Chem. Soc., Chem. Commun.* **1990**, 1467.
75. Albarella, L.; Giordano, F.; Lasalvia, M.; Piccialli, V.; Sica, D. *Tetrahedron Lett.* **1995**, *36*, 5267.
76. Yang, D.; Zhang, C. *J. Org. Chem.* **2001**, *66*, 4814.
77. Sharpless, K. B.; Akashi, K. *J. Am. Chem. Soc.* **1976**, *98*, 1986.
78. Travis, B. R.; Narayan, R. S.; Borhan, B. *J. Am. Chem. Soc.* **2002**, *124*, 3824.

79. Hassall, C. H. *Org. React. (N.Y.)* **1957**, 9, 73.
80. Panda, R.; Panigrahi, A. K.; Patnaik, C.; Sahu, S. K.; Mahapatra, S. K. *Bull. Chem. Soc. Jpn.* **1988**, 61, 1363.

CHAPTER II

THE ANNONACEOUS ACETOGENINS: STRUCTURE, BIOLOGICAL ACTIVITY AND TOTAL SYNTHESIS

A. Historical background

The plant family *annonaceae* has proven to be a rich source of natural products possessing wide variety of biologically and medicinally valuable properties.¹⁻⁵ Traditionally, extracts of many species belonging to this family have been used in folk medicines such as insecticides, fungicides, antiparasitics, antimalarials, emetics, antitumor agents and as a cure for snake bites.⁵ Before the early 1980's, phytochemical studies on these medicinal plants mostly involved the isolation of numerous secondary metabolites including isoquinoline alkaloids, polyphenols, carbohydrates, lipids, proteins, aromatic compounds, essential oils and terpenes.⁶ However, no reports of systematic pharmacological studies aimed towards delineating the bioactive components of these traditional folk therapeutics had been reported. In 1982, Jolad and co-workers discovered uvaricin – a novel antitumor agent, from ethanol root extracts of *Uvaria accuminata* (a member of the Annonaceae family).⁷ Uvaricin was isolated using bioactivity-guided fractionation and was shown to possess high *in vivo* potency as an antileukemic (P-388) agent. Uvaricin demonstrated an activity of 157% test / control (T/C) at 1.4 mg / kg in the PS test system. Activity in the PS test system is defined as an increase in the survival of treated animals over that of controls resulting in a T / C of 125%. In the same report, Jolad and colleagues disclosed the gross chemical structure of uvaricin – determined

using ^1H and ^{13}C NMRs, IR and mass spectroscopic fragmentation pattern. Thus, structurally, uvaricin was shown to be a C34 fatty acid derivative bearing a terminal unsaturated lactone ring and two adjacent tetrahydrofuran (THF) rings flanked by hydroxyl groups along the long aliphatic chain (Figure II-1)

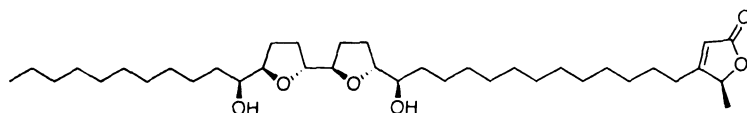


Figure II-1: Uvaricin – the first acetogenin isolated from *Uvaria accuminata*

(Annonaceae)

Since the discovery of uvaricin, its novel structure and promising bio-activity triggered a large body of research in this area which has lead to isolation, structure elucidation and in some cases, biological studies of over 400 related compounds – now termed as the annonaceous acetogenins.^{2,5,8-11} The acetogenins have emerged as a new class of highly potent bioactive compounds, which quite likely were the active ingredients of traditional folk medicines that originated from the Annonaceae family.

B. Structure and proposed biogenesis

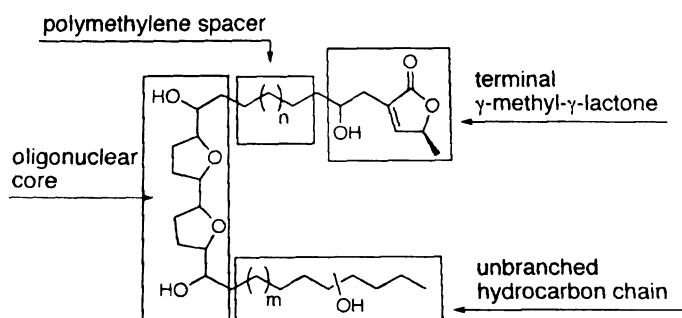


Figure II-2: Generic structure of a binuclear acetogenin

Structurally, the Annonaceous acetogenins are polyunsaturated C32 or C34 fatty acid derivatives that are combined with a 2-propanol unit and cyclized to generate THF or THP unit(s) along the long hydrocarbon chain (Figure II-2).¹² The most commonly found structural features include (a) a long aliphatic chain bearing a terminal methyl-substituted α,β -unsaturated γ -lactone moiety; (b) Up to three THF rings along the hydrocarbon chain; (c) oxygen functionalities such as hydroxyl or acetoxy groups,

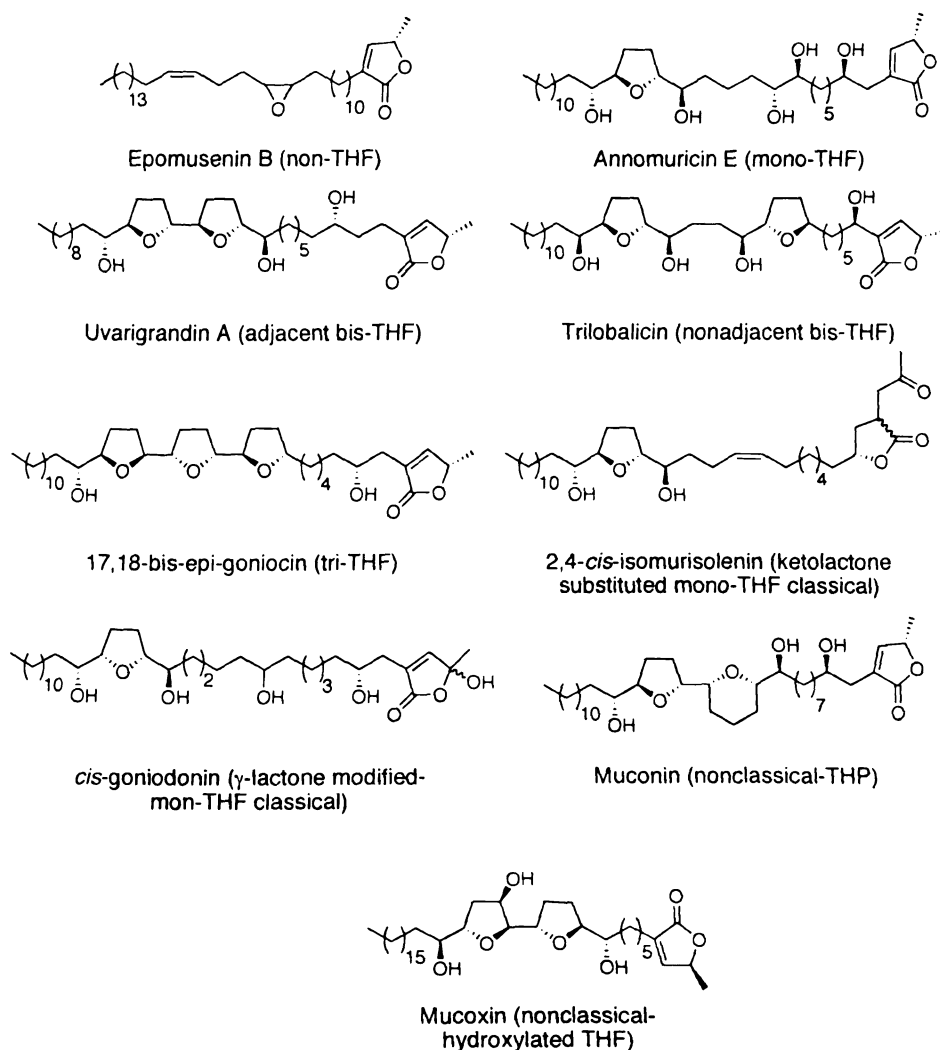


Figure II-3: Classification and representative structures of acetogenins

ketones, epoxides and /or double bonds.

Figure II-3 depicts representative structures of acetogenins with the class name indicated in parentheses. The annonaceous acetogenins are most conveniently classified¹⁰ (based on the number and type of the cyclic ether core structure) into two broad groups, viz., a) classical acetogenins – acetogenins comprising of none to three THF units along with a γ -lactone terminus. This class is subdivided as mono-THF, adjacent bis-THF, nonadjacent bis-THF, tri-THF, non-THF ring containing acetogenins. Each subclass is then further divided according to the nature of the terminal lactone ring. b) Nonclassical acetogenins – structurally, they can be further divided into two broad groups, viz., i) THP ring containing acetogenins: mucocin¹³ (Figure II-3) was the first nonclassical acetogenin with a THP ring nonadjacent to a THF ring. A few more examples of this class of acetogenins (not shown) are muconin¹⁴ (THP ring adjacent to a THF ring), pyranicin¹⁵ (mono-THP ring), jimenezin¹⁶ (hydroxylated THP ring adjacent to a THF ring). ii) Hydroxylated THF ring containing acetogenins: mucoxin¹⁴ (Figure II-3) was the first nonclassical acetogenin reported* containing a hydroxylated THF ring. Two other examples are – goniotriocin¹⁰ and donnaenin.¹⁸

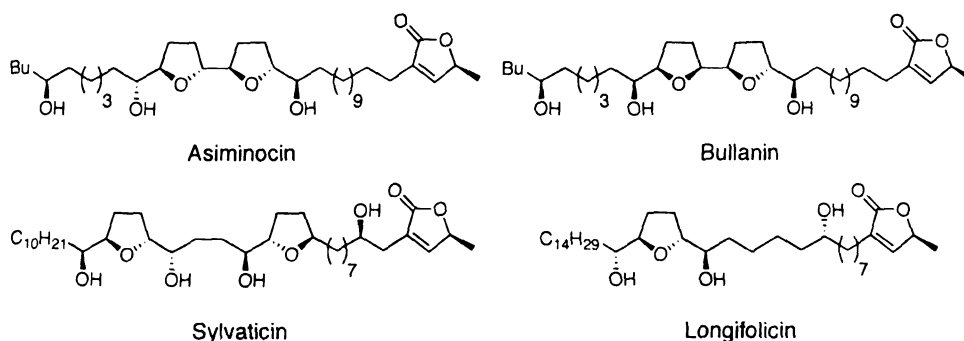
It has been proposed that the THF, THP and epoxide rings in acetogenins arise from isolated double bonds *via* epoxidation / cyclization events as shown in Figure II-4.^{3,4} The *erythro* / *threo* relationship between the carbinol centers and THF rings arises from the olefin geometries while the *trans* / *cis* relationship across the THF rings is a

* Four acetogenins were previously reported to possess hydroxylated THF rings;¹⁷ however their structures were proved erroneous and have been corrected.²

to combat resistance in multidrug resistant (MDR) tumor cells and in pesticide-resistant insects.¹⁹⁻²¹ Some bioactivity studies are briefly described below:

1. *In vitro* studies

In vitro assays have revealed some of the acetogenins to be among the most potent cytotoxic agents known to date. In a recent review, Marshall et al. have summarized²² (Table II-1) relative tumor growth inhibition abilities of representative acetogenins compared to adriamycin (an anticancer drug currently in clinical use).



Compound	Human tumor lines (cell culture)		
	A-549 (lung)	MCF-7(breast)	HT-29 (colon)
Asimocin	3.1×10^{-12}	29×10^{-12}	$<10^{-12}$
Bullanin	3.4×10^{-14}	3.2×10^{-14}	4.8×10^{-12}
Sylvaticin	$<10^{-8}$	3.8×10^{-5}	1.6×10^{-1}
Longifolicin	1.1×10^{-6}	1.2×10^{-5}	—
Adriamycin	2.4×10^{-4}	1.0×10^{-2}	3.8×10^{-2}

Table II-1: Relative tumor growth inhibition (ED_{50} mg / mL) for representative acetogenins compared to adriamycin

These acetogenins were proven to be more potent than adriamycin in preliminary assays. Besides being highly potent, acetogenins have also been shown to exhibit

selective cytotoxicity to tumor cells over other innocent cells.¹⁹ In addition, they have also exhibited selectivities among various cancerous cell lines.²³⁻²⁵

2. *In vivo* studies

Although extensive animal testing of acetogenins has not been done, the studies so far have been promising. Early on, uvaricin (157% T/C at 1.4 mg/kg, *vide infra*)⁷, rollinones (147% T/C at 1.4 mg/kg, Figure II-5) and asimicin (124% T/C at 25 μ g/kg, Figure II-5)⁵ were shown to possess *in vivo* activity against 3PS (murine lymphocytic leukemia). Bullatacin (Figure II-5) effective at 50 μ g/kg against L1210 (murine leukemia) in normal mice was 300 times more potent than paclitaxel.²⁶ Both bullatacin and bullatalicin (effective at 1 mg/kg) were almost equivalent to cisplatin.³

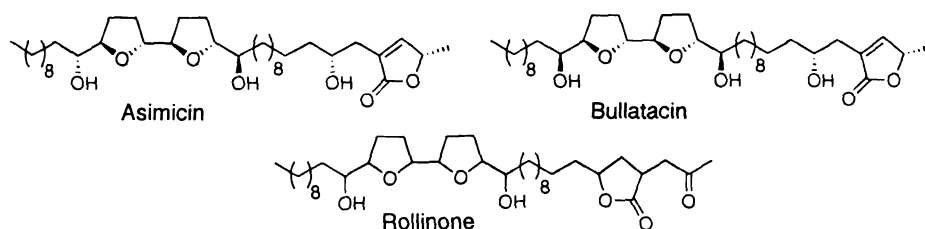


Figure II-5: Some acetogenins that showed high *in vivo* cytotoxicity profiles

3. Activity against multidrug resistant (MDR) cells

The effect of acetogenin treatment on MDR tumor cells is demonstrated by Oberlies and co-workers' *in vitro* studies on wild-type and adriamycin resistant human mammary adenocarcinoma cells (MCF-7/wt and MCF-7/Adr respectively).^{20,21} After treatment of both the cell lines with bullatacin (1.0 μ g/mL) for 48-h, MCF-7/wt cells showed regrowth (comparable to the vehicle treated control) when fed fresh media; while

MCF-7/Adr cells did not. Thus, bullatacin was cytostatic to wild type cells but cytotoxic to the drug resistant cells.

4. Pesticidal activity

Several classes of synthetic compounds such as chlorinated hydrocarbons, organophosphates, carbamates etc. have been used as insecticides against cockroaches. Their repeated use has resulted in development of resistance, which calls for new insecticides with novel mode of action. Alali and co-workers conducted comparative studies of dietary toxicities of acetogenins vs. conventional insecticides on insecticide-resistant as well as susceptible strains of cockroaches.²³ The acetogenins showed lower or comparable LT_{50} values (number of days before death of 50% of the population at a dose of 1000 ppm) in both the strains (Table II-2). Also, in a yellow fever larva assay 44 acetogenins were found to be highly potent.²⁷

Compound type	Active ingredient	Jwax (susceptible strains)	Muncie (resistant strain)
natural	parviflorin	0.8	1.2
	asimicin	2.3	3.8
synthetic	chlorpyrifos	0.5	4.2
	hydramethylnon	10.4	6.1

Table II-2: LT_{50} values for German cockroach fifth instars

D. Mechanism of action

It has been proposed that acetogenins exert their bioactivity *via* inhibition of two target proteins: a) NADH-ubiquinone oxidoreductase (Complex I) which is a membrane bound protein in mitochondrial electron transport system.^{26,28,29} b) ubiquinone-linked NADH oxidase present in the plasma membrane of only tumor cells.³⁰ Both of these binding events result in ATP deprivation, which eventually leads to apoptosis. Weiss and co-workers in 1991²⁸ found that annonin I (Figure II-6) was an excellent inhibitor of Complex I ($IC_{50} = 0.8 \text{ nM/mg}$ for insecticidal mitochondria; $IC_{50} < 0.1 \text{ }\mu\text{M/mg}$ for bovine heart muscle mitochondria). Using ESR spectroscopy they demonstrated that electron transport from Complex I to ubiquinone is interrupted in the presence of annonin I.

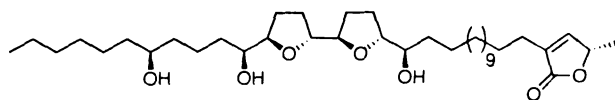


Figure II-6: Annonin I

Complex I has also attracted attention due to its implication in several diseases including idiopathic Parkinson's disease, maturity onset diabetes, stroke-like episodes and Huntington's disease.³¹ Some acetogenins (rolliniastatin-1 and -2) were found to be more potent inhibitors of complex I than piericidin-A (the most potent Complex I inhibitor previously reported).³² Thus, it is of great interest to study the interactions between Complex I and acetogenins in greater detail. While the precise mode of complexation of acetogenins with their target proteins at molecular level is not known, some general proposals have been put forth: a) Shimada et al. studied acetogenin conformations within artificial liposomal membranes using techniques such as ^1H

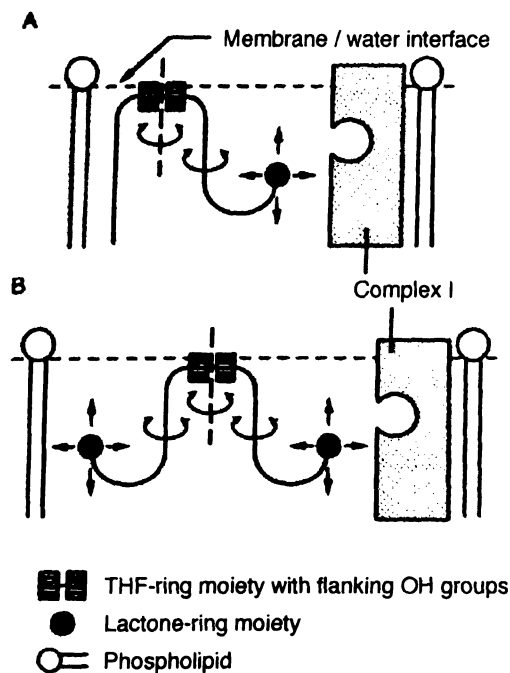


Figure II-7: Model of bis-THF acetogenins interacting with complex I in mitochondrial membrane (Ref. 35)

intermolecular nOe's and differential calorimetric scanning data.^{33,34} They proposed that acetogenins containing mono-, adjacent and nonadjacent bis-THF units had the THF rings residing at the glycerol head region of phosphatidylcholine serving as hydrophilic anchor at the membrane interphase. The γ -lactone ring diffuses in the membrane interior to bind with the target site (Figure II-7).³⁵ Depending upon the length of the linker unit (alkyl chain that connects the lactone to the THF core) the lactone penetrates the lipid bilayer to different depths. Thus, a given acetogenin molecule with specific spacer length can adapt to the geometry of only a specific cell type, hence the observed selectivity in its mode of action. b) Miyoshi and co-workers³⁶ through their studies of 22 representative acetogenins using submitochondrial particles as well as quantum chemical calculations

(MNDO-AM1), proposed that the stereochemistry across the THF rings is not crucial to the activity and that the alkyl spacer connecting the γ -lactone ring and THF core must be of optimal length and flexibility for high potency. c) Studies on ion (Ca^{+2} and Mg^{+2}) complexation abilities of acetogenins have shown that the complexation depends upon the relative configuration of acetogenin molecule and nature of the ion. Considering that NADH – ubiquinone oxidoreductase is an iron cluster enzyme, some researchers³⁷ have proposed iron-mediated complexes between acetogenins and the protein targets.

E. Structure-activity relationships

Because of a lack of understanding of the exact mode of binding of acetogenins with the target proteins, researchers have not been able to design systematic SAR studies. However, based on the work of several investigators,^{15,21,27,32,36,38,39} Alali et al., in a recent review¹⁰, suggested some generalizations on the SARs of the annonaceous acetogenins which are summarized below. 1) The general order of potency of acetogenins is: bis-adjacent THF > bis-nonadjacent THF > mono-THF > non-THF. The ring size (THF vs. THP) and stereochemistry about the rings is practically inconsequential to the potency and selectivity. 2) α,β -unsaturated γ -lactone is an essential feature and any structural modifications lead to diminished activity. 3) The spacer length (distance between the THF ring core and the lactone ring) is critical to the potency. For example, 13-carbon chain in mono- and bis-THF compounds is optimum. 4) Three hydroxyl groups (two flanking the THF core and third somewhere along the long hydrocarbon chain) are responsible for optimal polarity and topology needed for most effective

binding. Beyond four hydroxyl groups activity decreases significantly. 5) In general, a ketone functionality instead of a hydroxyl group reduces the activity.

More recently, Miyoshi and co-workers have reported the first SAR study using a series of synthetic acetogenin analogs, which were designed to delineate structural features critical to activity.³⁶ Bullatacin is one of the most active inhibitors of Complex I. Miyoshi et al. synthesized simplified analogs of bullatacin (Figure II-8) and tested them for NADH-oxidase inhibition. The results (summarized in Figure II-8) clearly indicated that the inhibitory activity was completely lost when the THF core and the terminal lactone ring were decoupled (**G-J**). Also, when the two ring moieties were used in combination in various molar ratios, no synergistic enhancement of activity was observed

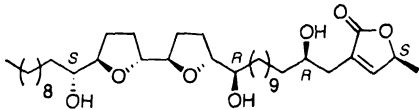
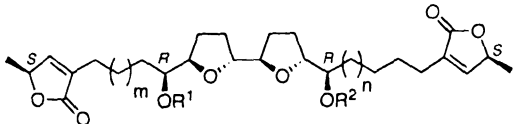
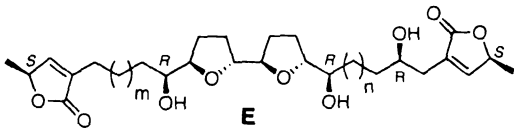
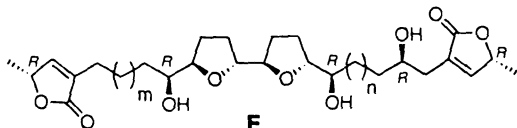
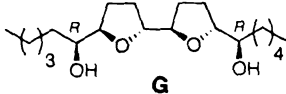
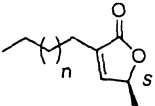
Inhibitor	IC ₅₀ (nm)
 Bullatacin	1.2 (± 0.1)
 A , m=10, n=9, R ¹ = R ² = H B , m=7, n=6, R ¹ = R ² = H C , m=10, n=9, R ¹ = H, R ² = COCH ₃ D , m=10, n=9, R ¹ = COCH ₃ , R ² = COCH ₃	A 1.2 (± 0.1) B 1.9 (± 0.1) C 2.0 (± 0.2) D 18 (± 2)
 E	1.6 (± 0.1)
 F	1.2 (± 0.2)
 G	4500 (± 300)
 H , n=1 I , n=4 J , n=10	H , >20,000 I , >20,000 J , 6200 (± 400)

Figure II-8: NADH-oxidase inhibitory potencies of bullatacin analogs

(data not shown). Among the other modifications – bis-acetogenin (**A**), bis-acetogenin with shorter linkers (**B**), reduced bis-acetogenin (**E**) and bis-acetogenin with inverted lactone configuration (**F**) did not exhibit any perturbation in activity. However, acetylation of the hydroxyl groups flanking the THF core (**C** and **D**) did result in slightly

reduced potency. Thus, it was concluded that the THF (with two flanking hydroxyl groups) and lactone ring systems must be linked together for optimum activity. Since variations in other functional groups did not lead to any significant change in enzyme inhibition, the critical structure features of bullatacin or any further insights into precise mode of binding remain undiscovered.

In separate studies reported earlier, the cytotoxicity of bullatacin against carcinoma cells decreased significantly (about 10^6 -fold) upon saturation of the double bond in the α,β -unsaturated γ -lactone.^{33,40} Curiously, in Miyoshi's studies (*vide supra*) analog **E** (reduced bis-acetogenin) did not show depletion in inhibitory activity compared to bullatacin or analog **A**. Thus, whether or not the cytotoxicity profile of acetogenins correlates to the inhibitory potency remains unclear.

F. Classical vs. nonclassical acetogenins

The annonaceous acetogenins due to their highly potent, selective cytotoxicity and pesticidal activities especially against drug resistant tumor cells and insects are increasingly being looked at as new generation antitumor therapeutics and pesticides. Classical acetogenins have been and continue to be investigated in areas spanning isolation, purification, structure elucidation, semi and total synthesis, bioactivity testing and studies on mechanism of action. In recent years, nonclassical acetogenins with unique structural features have emerged.¹⁰ Novel structures that offer new synthetic challenges and promising bioactivity have prompted total syntheses of some of the THP containing nonclassical acetogenins. In some cases, the originally proposed structure was revised after the total synthesis.⁴¹ To our knowledge, however, none of the hydroxylated

THF containing nonclassical acetogenins have been synthesized or studied in any further detail.

G. Total synthesis of the annonaceous acetogenins

Due to excellent biological and medicinal activities along with unique structural features, the annonaceous acetogenins have attracted the attention of several synthetic groups over the last two decades. Acetogenins, though found in a large number of plant species, exist only in minute amounts as complex mixtures of related isomers. As a result, the isolation and purification process is often tedious. On an average, about 10-20 mg of material can be obtained from 15 kg of stem bark, which requires multistep separation involving partition extraction and chromatography on several different columns followed by repetitive HPLC.⁴² Moreover, since acetogenins are often waxes or gums, their structure elucidation using X-ray crystallography is not possible. Thus, total synthesis has played an important role in this field of research. Synthetic materials have been obtained in sufficient amounts for confirmation (in some cases revision) of proposed structures, establishment of relative absolute configurations and for biological testing. In addition, total synthesis has provided expeditious routes to obtain unnatural stereoisomers and other simplified structural analogs of the natural products to gain insights into SARs.^{35,43} Acetogenins embody adjacent or nonadjacent polyether rings, which in the early years of discovery were unique and challenging structural features from a synthetic point of view. This triggered the development of several elegant methods to synthesize such polycyclic substituted ether units and useful chiral building blocks. Thus acetogenins have served to advance synthetic chemical methodologies.

In 1991, Hoyer and co-workers reported the total synthesis of (+)-(36-*epi*)-*ent*-uvaricin – the first of any member of the acetogenin family (Figure II-9).^{44,45} This classic

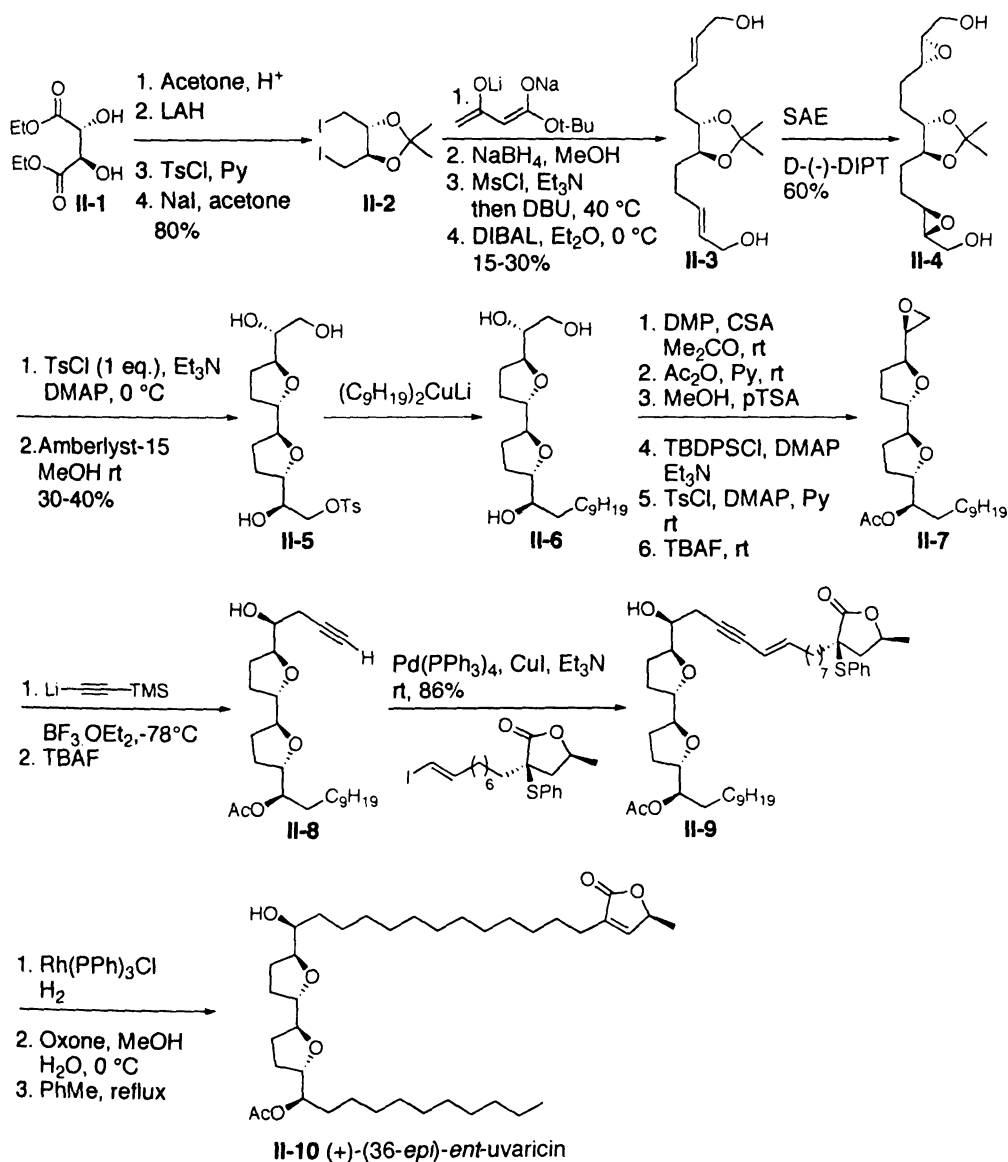


Figure II-9: The first total synthesis of an acetogenin, (+)-(36-*epi*)-*ent*-uvaricin

synthesis involved a bi-directional approach to secure the bis-THF core of the molecule.

The synthetic scheme is described in Figure II-9. Starting from (+)-diethyl tartrate **II-1** derived diiodide **II-2**, *E, E*-bis allylic alcohol **II-3** was obtained using Weiler dianion

alkylation.⁴⁶ Sharpless asymmetric epoxidation of **II-3** furnished the bis-epoxydiol **II-4**. The two ends of C_2 symmetric diol **II-4** were distinguished by formation the monotosylate, which was subjected to one-pot acid promoted acetonide cleavage, epoxide opening reaction, to provide the C15 – C24 bis-THF core **II-5**. Alkylation of the tosylate **II-5** using excess lithium dinonylcuprate furnished intermediate **II-6**, which after protective group manipulations was transformed into epoxide **II-7**. Lithium trimethylsilylacetylide opening of epoxide **II-7** provided alkyne **II-8**, which was coupled to the vinyl iodide **II-9** using the Sonogashira protocol. Enyne reduction, oxidation of sulfide and thermal elimination of the resultant sulfoxide produced compound **II-10** (in total twenty eight steps), which after Mosher's ester analysis and spectroscopic comparison with the natural product was assigned to be a diastereomer of natural uvaricin differing only at C36 stereocenter (**II-10**, Figure II-9).

After Hoye's initial report, a large number of syntheses of natural acetogenins as well their analogs have appeared in the literature. A few recent syntheses are cited here.⁴⁷⁻⁵⁴ Several reviews dedicated to the synthetic approaches have also been published.^{22,55-57} From a synthesis design point of view, acetogenins can be divided into four well-defined domains, viz., the oligonuclear cyclic ether core, terminal γ -methyl- γ -lactone moiety, an acyclic alkyl chain connecting the two cyclic domains and a long unbranched hydrocarbon chain often containing oxygen functionalities. Several elegant routes to construct and couple oligonuclear cyclic ether core and the terminal lactone unit have been described in the total synthesis literature. The long hydrocarbon chain can be easily incorporated using routine chemical transformations at an early or later stage in

synthesis. In most syntheses, the oligo-cyclic ether fragment is constructed first and then is coupled to the terminal γ -methyl- γ -lactone ring with the appropriate linker.

The following sections describe representative total syntheses of the annonaceous acetogenins. Since our own efforts have dealt with method development for highly regio- and stereoselective synthesis of substituted THF rings, the synthetic strategies are described focusing on the construction of cyclic polyether cores; synthesis of the terminal lactone with an appropriate spacer and completion of the total synthesis is mentioned briefly in some cases. The classification is based on strategies used for the construction of the oligonuclear cyclic ether fragments.

1. Multiple intramolecular Williamson etherification strategy

Trost designed a versatile strategy to synthesize structurally related acetogenins using intramolecular double Williamson etherification protocol to construct the bis-THF core.⁵⁸ Synthesis of one of the members, (+)-squamocin K is described in Figures II-10 and II-11.

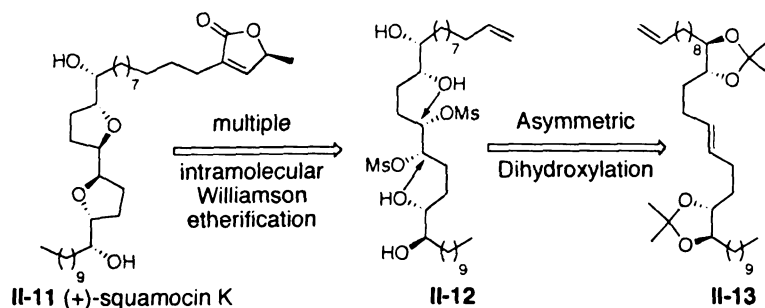


Figure II-10: Trost's synthesis of (+)-squamocin K (key retrosynthetic disconnections)

The total synthesis scheme in a forward sense is depicted in Figure II-11. Standard functional group manipulations of known bis-homoallylic alcohol II-14

provided the Julia olefination precursors **II-17** and **II-18**. The desired *E* olefin **II-13**, albeit obtained in a moderate selectivity (*E* : *Z* = 3 : 1), preferentially reacted in subsequent asymmetric dihydroxylation reaction which obviated the need for separation. The bis-mesylate **II-19** upon acetonide deprotection and exposure to base underwent intramolecular displacement reaction to yield the bis-THF system **II-20**. Finally, the butenolide ring was efficiently introduced using a ruthenium-catalyzed Alder-ene

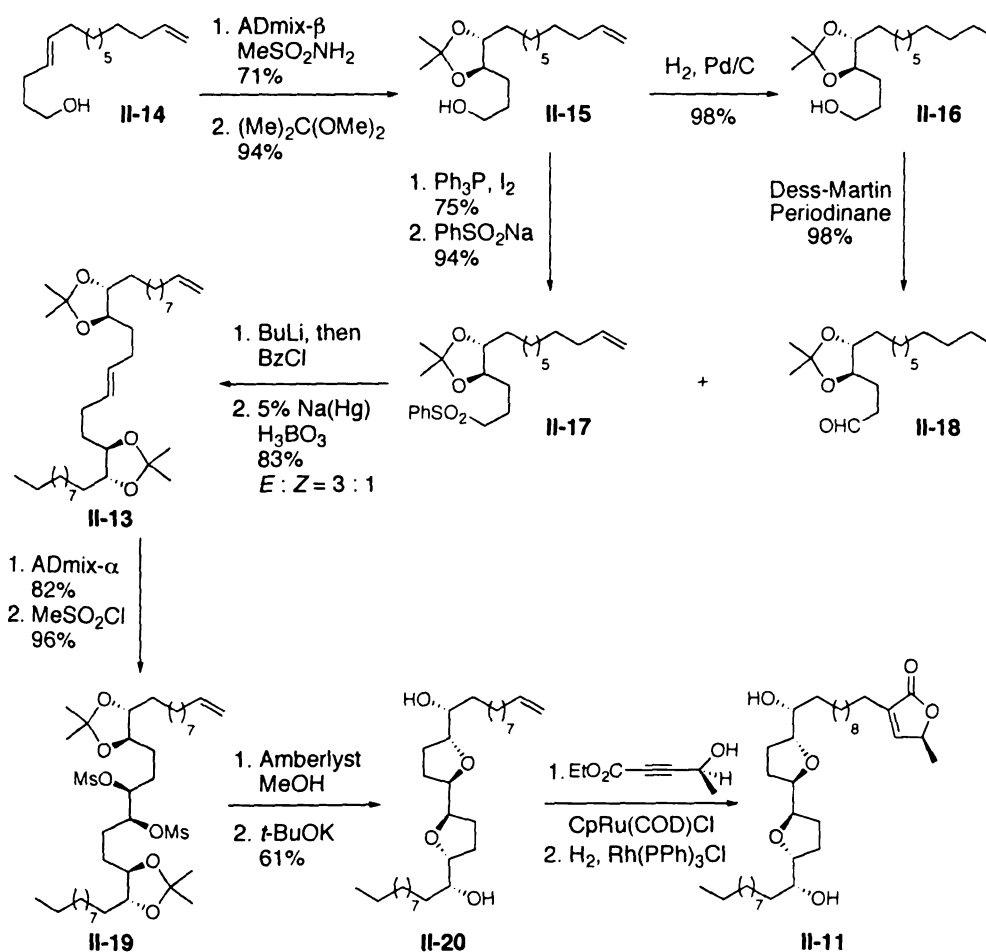


Figure II-11: Trost's synthesis of (+) - squamocin K

protocol.^{59,60} Thus, the total synthesis of (+)-squamocin K (**II-11**) was completed in 15 steps along the longest linear sequence. Since all the oxygenated stereocenters were

established using Sharpless asymmetric dihydroxylation reaction, by merely varying the ligands and the role of oxygen functionalities (as electrophile and nucleophile during etherification process), in principle, a variety of diastereomers can be easily accessed.

Marshall and co-workers in their elegant studies have shown that chiral α -oxygenated stannanes (**II-21**, Figure II-12) undergo stereospecific rearrangement⁶¹⁻⁶³ to produce γ -oxy allylmetallic species (tin **II-22** or indium **II-23** depending on the reagents), which upon addition to aldehydes provide *syn* or *anti* diols, **II-24** and **II-25** respectively. $\text{BF}_3 \cdot \text{OEt}_2$ mediated addition of γ -oxy allyl stannane **II-22** proceeds *via* an acyclic transition state while γ -oxy allyl indium species **II-23** forms a cyclic transition state to afford the corresponding diols as single diastereomers. This asymmetric allylation of suitably functionalized aldehydes in combination with intramolecular Williamson etherification reaction has been effectively used in the total syntheses of several

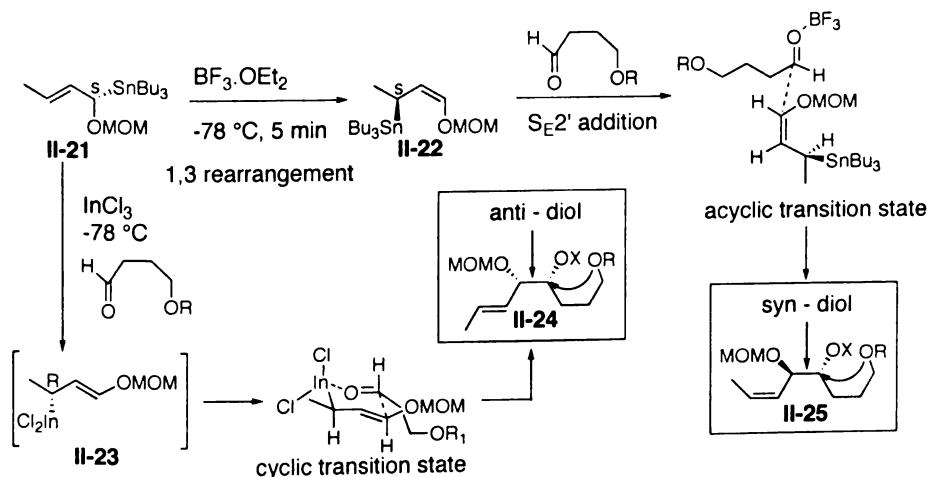


Figure II-12: Marshall's stereoselective $\text{S}_{\text{E}}2'$ addition approach to oxygenated THF precursors

acetogenins.⁵⁴ The synthesis of bullanin (**II-33**) is shown in Figure II-13. $\text{BF}_3 \cdot \text{OEt}_2$ mediated $\text{S}_{\text{E}}2'$ addition of chiral allyl stannane **II-26** to enantiopure γ,δ -bis-alkoxy aldehyde **II-27** resulted in corresponding *syn* diol which was subsequently converted to the tosylate **II-28**. Upon revealing the terminal aldehyde, **II-29** was treated with chiral α -oxy-allyl stannane **II-30**, this time in presence of InBr_3 to afford the corresponding *anti* – diol. Tosylation of the *anti* diol led to the bis-tosylate **II-31**. One-pot silyl deprotection / tosylate displacement reaction of **II-31** furnished the bis-THF scaffold **II-32**. Sonogashira coupling of alkyne **II-32** with appropriate vinyl iodide followed hydrogenation and global deprotection provided the natural product bullanin **II-33**. Either enantiomer of *syn* (**II-24**) and *anti* (**II-25**) adducts is accessible by appropriate choice of chiral α -alkoxy allylic stannanes. In addition, the carbinol stereocenters in aldehyde of type **II-27** are

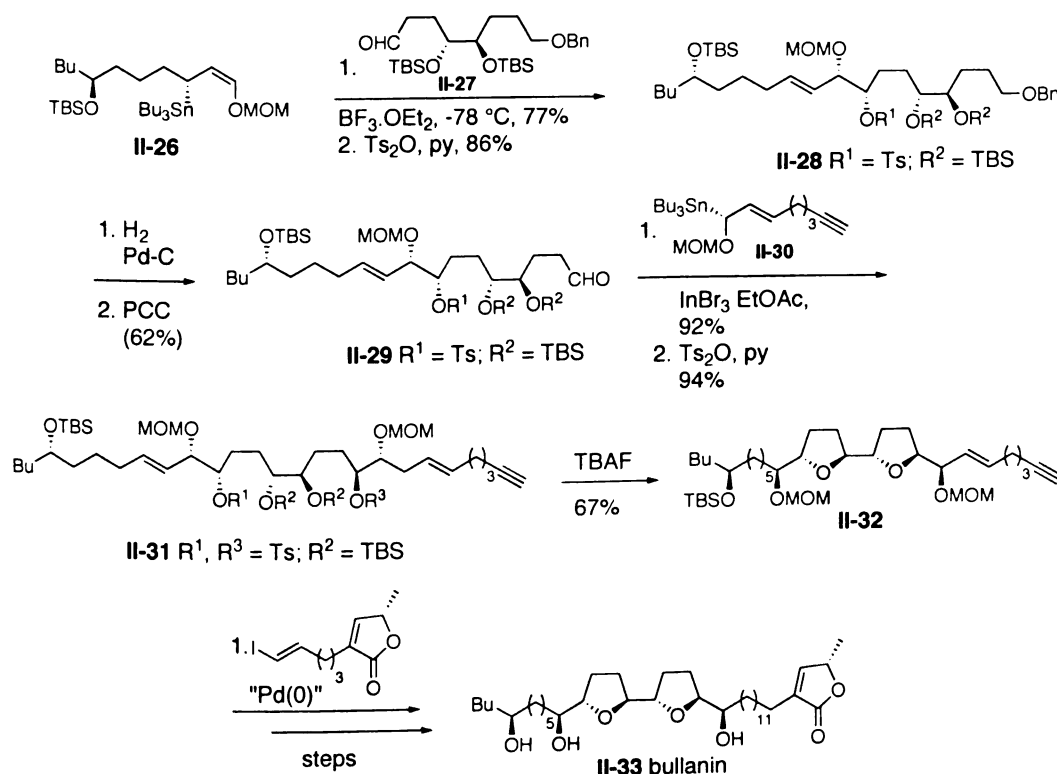


Figure II-13: Marshall's synthesis of bullanin

established using Sharpless asymmetric dihydroxylation. Thus, this approach has proved to be quite versatile due to availability of a stereodiverse pool of chiral building blocks.

2. Epoxide cascade strategy

In 1996, Hoye disclosed a highly efficient approach to build C_2 symmetric bis-THF units in acetogenins using an ‘inside out’ epoxide cascade reaction (Figure II-14).⁶⁴ Bis-epoxy diol **II-35** was synthesized in high yield and enantiomeric purity from bis-allylic diol **II-34**, which in turn was readily prepared from commercially available all *trans* 1,5,9-cyclododecatriene. The bis-epoxy diol intermediate (**II-36**, not isolated) generated after Sharpless asymmetric dihydroxylation reaction spontaneously cyclized in an ‘inside out’ fashion to form the bis-THF unit **II-37**. The corresponding C_2 symmetric bis-epoxide **II-38** was desymmetrized by using trimethylsilyl acetylide as the limiting reagent. Subsequent routine transformations including Sonogashira coupling protocol to

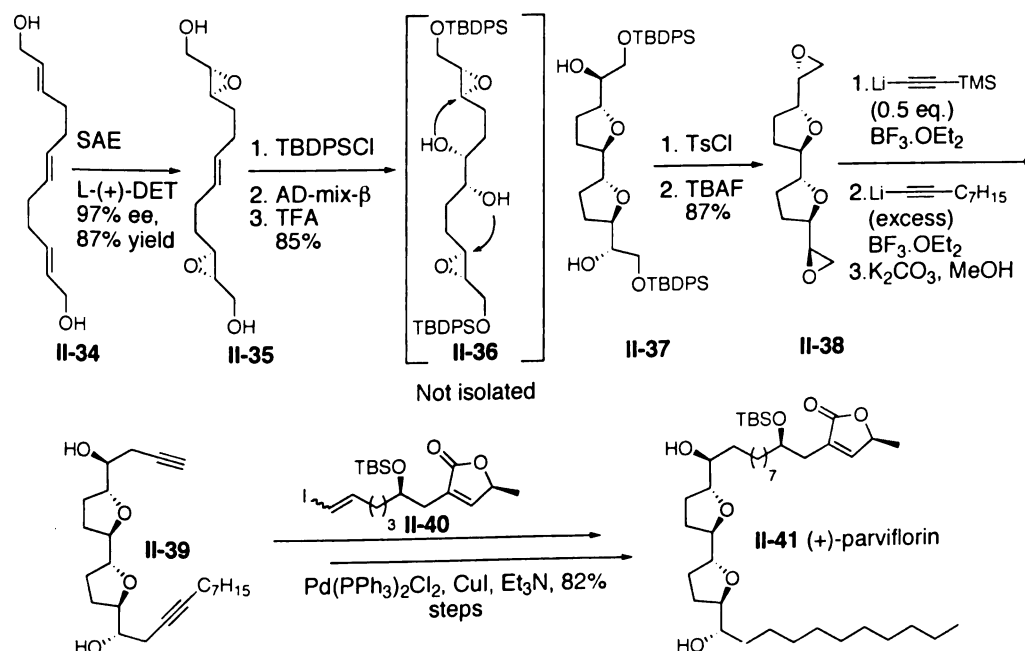


Figure II-14: Hoye's synthesis of (+)-parviflorin

couple vinyl iodide **II-40** with alkyne **II-39** produced (+)-parviflorin (**II-41**) in a concise manner involving longest linear sequence of 14 steps.

3. Biomimetic ‘naked carbon skeleton’ strategy

Townsend and Basak have hypothesized that polyether natural products might arise from a cascade of hydroxy-directed *syn*-oxidative cyclizations^{65,66} rather than the traditional *anti* opening of polyepoxy alcohols (Figure II-15).⁶⁷ *Syn* cyclization involves direct etherification of the olefin moiety, while *anti* cyclization involves intermediacy of an epoxy alcohol, which undergoes intramolecular epoxide opening. The two events result in formation of cyclic ethers bearing complementary stereocenters at the points of cyclization

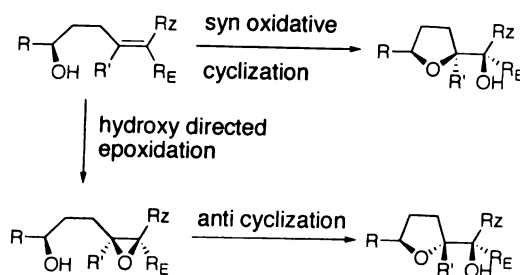


Figure II-15: Syn and anti oxidative cyclizations of hydroxy olefin

Inspired by this proposal, McDonald and co-workers have explored metal mediated *syn*-oxidative polycyclization reaction of hydroxypolyenes.⁶⁸ A representative optimized result is shown in Figure II-16. Upon exposure to dichloroacetyl perhenate reagent, hydroxytriene **II-42** oxidatively cyclized to afford a mixture of products **II-43** and **II-44** in a ratio favoring (4 : 1) the expected all *syn* selective cyclized product **II-43** over the *trans, trans, cis* (*syn, syn, anti* cyclization) product **II-44**. The stereochemistry of tris-THF core of **II-43** matches that of an acetogenin goniocin **II-45**. Although several

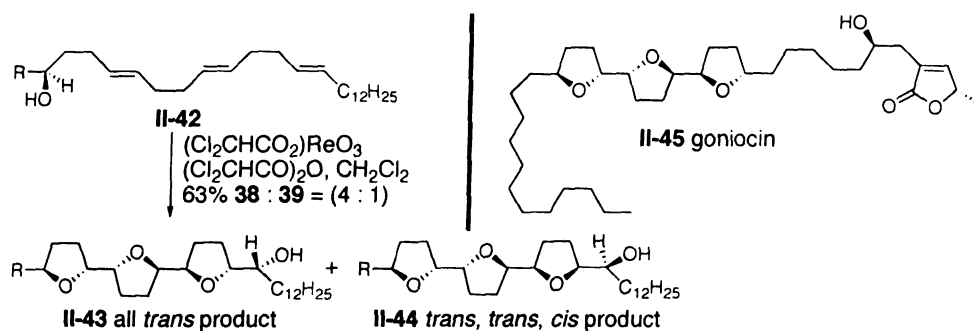


Figure II-16: McDonald's biomimetic oxidative cyclization strategy

stereogenic centers are set during the oxidative cyclization reaction, this approach has not been popular for use in total synthesis. One of the reasons could be that efficiency and selectivity of cyclization decreases with increase in polyene chain length. This has been partly attributed to possible chelation effects of earlier formed ether rings with alkoxyrhenium intermediates as the cyclization proceeds. Along similar lines, in presence of oxygen or any other chelating functionality elsewhere in the molecule, stereochemical outcome of cyclization is not predictable as indicated by Sinha's studies⁶⁹ (not shown) on goniocin synthesis. Also, depending upon the double bond substitution pattern, the reactive conformation in cyclization event is not always predictable. Thus, the overall complexity of the approach has prevented its extensive use in total synthesis of acetogenins.

4. Step-growth oligomerization strategy

Casiraghi has used a vinylogous aldol condensation reaction of heterocyclic silyloxy dienes (Figure II-17) to prepare oligomeric THF systems found in acetogenins.^{70,71} Initial condensation of the diene with chiral aldehyde **II-46** in the presence of $\text{BF}_3 \cdot \text{OEt}_2$, afforded the adduct **II-47** after hydrogenation. After suitable functional groups

manipulations (Figure II-17), 2-acetoxytetrahydrofuran **II-49** was obtained. The next condensation step involved Lewis acid mediated anomeric activation of **II-49** followed by C-glycosidation type coupling thus generating only the *trans* isomer across the THF ring. However both *erythro* and *threo* isomeric products **II-50a** and **II-50b** were formed in equal proportions (separable prior to hydrogenation). Repetition of the same sequence (shown only for **II-50a**) yielded bis-THF units as a diastomeric pair (**II-51** and **II-52**). This approach has also not been used in total synthesis design probably because of the inevitable formation of mixtures.

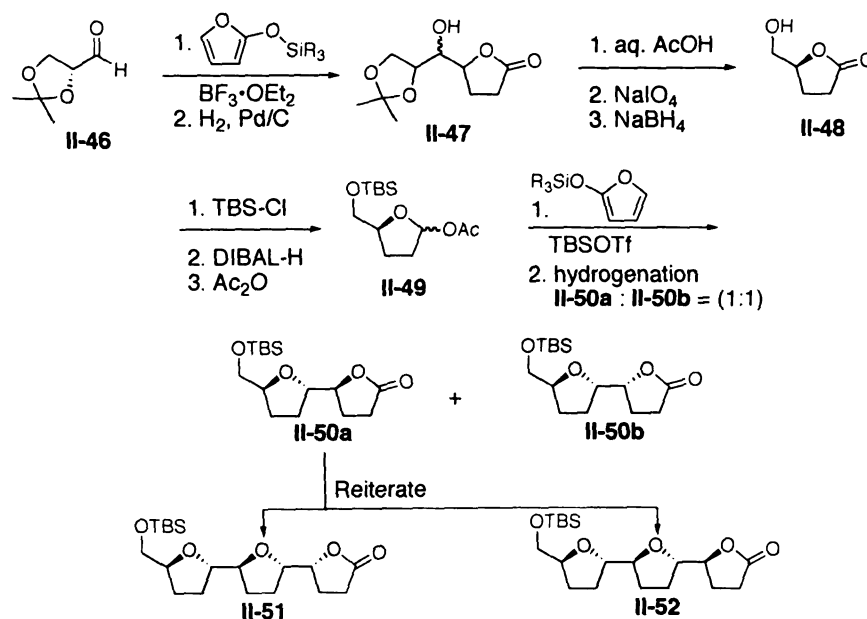


Figure II-17: Casiraghi's iterative vinologous aldol reaction strategy

5. Sequential, modular strategy

In general acetogenins containing adjacent bis-THF core are the most potent of all.¹⁰ A step towards systematic SAR studies of this class of acetogenins would be

development of an expeditious way to construct libraries of stereoisomeric bis – THF cores with appropriate functional group handles for further elaboration.

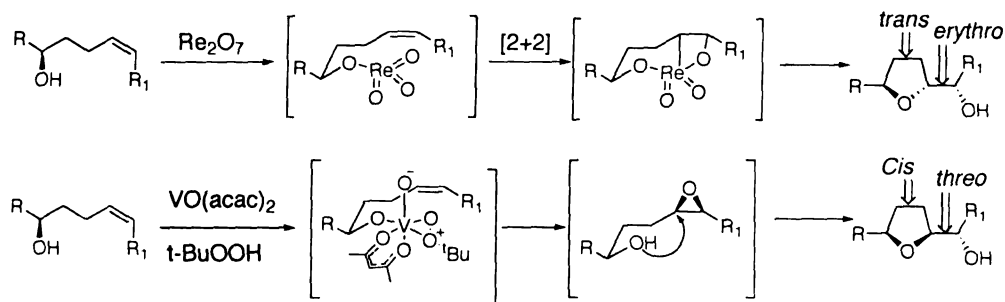


Figure II-18: Proposed mechanisms for metal mediated oxidative cyclization of hydroxy olefins

Sinha and Keinan have developed modular strategies for such library syntheses⁴³ using a combination of the following chemical transformations: a) metal mediated stereospecific oxidative cyclization of 4-alkenols (Figure II-18) – Re₂O₇ mediated cyclization⁷²⁻⁷⁴ generated *syn* while VO(acac)₂ formed *anti* oxidative products. Thus, by appropriate choice of the metal oxidant, two diastereomeric THFs could be obtained from a single hydroxy olefin. b) Sharpless asymmetric dihydroxylation and c) Mitsunobu inversion of chiral alcohols.

Figure II-19 depicts a small library synthesis of bis-THF cores (**II-56-II-63**) by combined use of the above-mentioned protocols. The starting chiral unsaturated hydroxy-lactone **II-53** was prepared from the corresponding olefin precursor (not shown) *via* asymmetric dihydroxylation reaction. Thus, all four stereoisomers of **II-53** were equally accessible. Treatment of **II-53** with Re₂O₇ or VO(acac)₂ generated corresponding *trans* (**II-54**) or *cis* (**II-55**) mono-THF products in high (90%) diastereoselectivity. Reiteration of the sequence along with Mitsunobu inversion of the secondary hydroxyl stereocenter

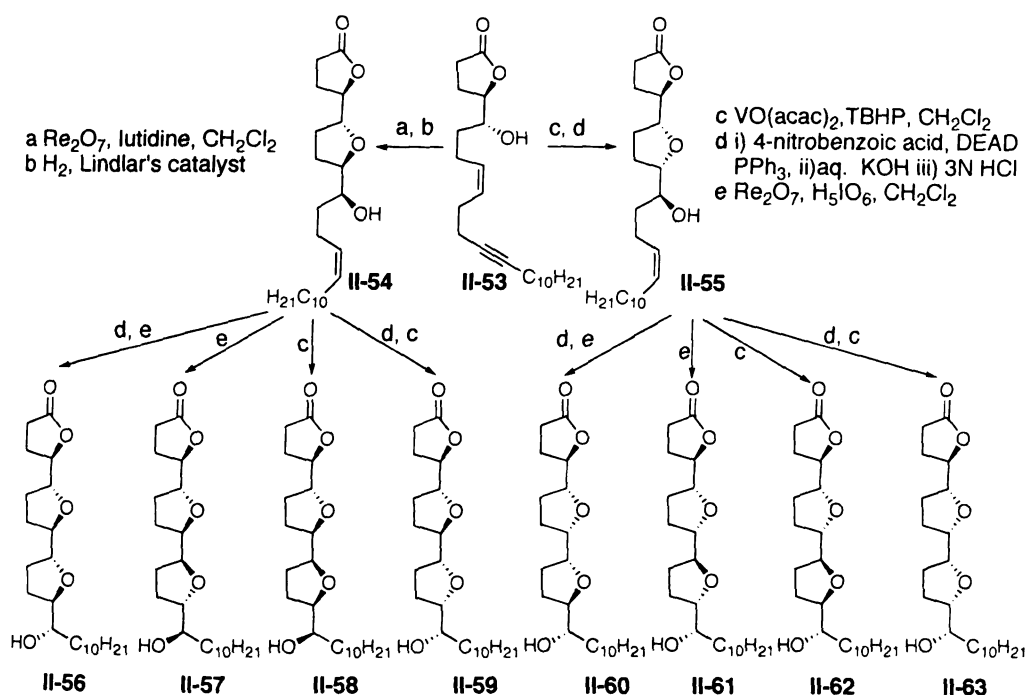


Figure II-19: Sinha and Keinan's library synthesis of bis - THF core units

afforded eight isomeric bis – THF units (**II-56** to **II-63**). In a similar manner, the remaining 56 isomers were synthesized and some of them were used in total syntheses of asimicin, bullatacin, trilobacin, rolliniastatin and solamin.

Koert and co-workers have used another modular strategy (Figure II-20) to sequentially assemble oligo-THF units.^{75,76} Their approach involves the stereoselective addition of a Grignard reagent of type **II-65** or its organozinc counterpart **II-70** to enantiopure mono-THF aldehydes such as **II-64**. The Grignard addition proceeded *via* a chelation controlled transition state to generate the adduct **II-66** in high diastereoselectivity. On the other hand, Lewis acid mediated organozinc addition afforded the Felkin–Ahn product **II-71**, also in very high diastereoselectivity. Each of the adducts **II-66** and **II-71** were transformed to the corresponding bis-THF units **II-68** and **II-73** *via* the intermediacy of epoxy alcohols, **II-67** and **II-72**.

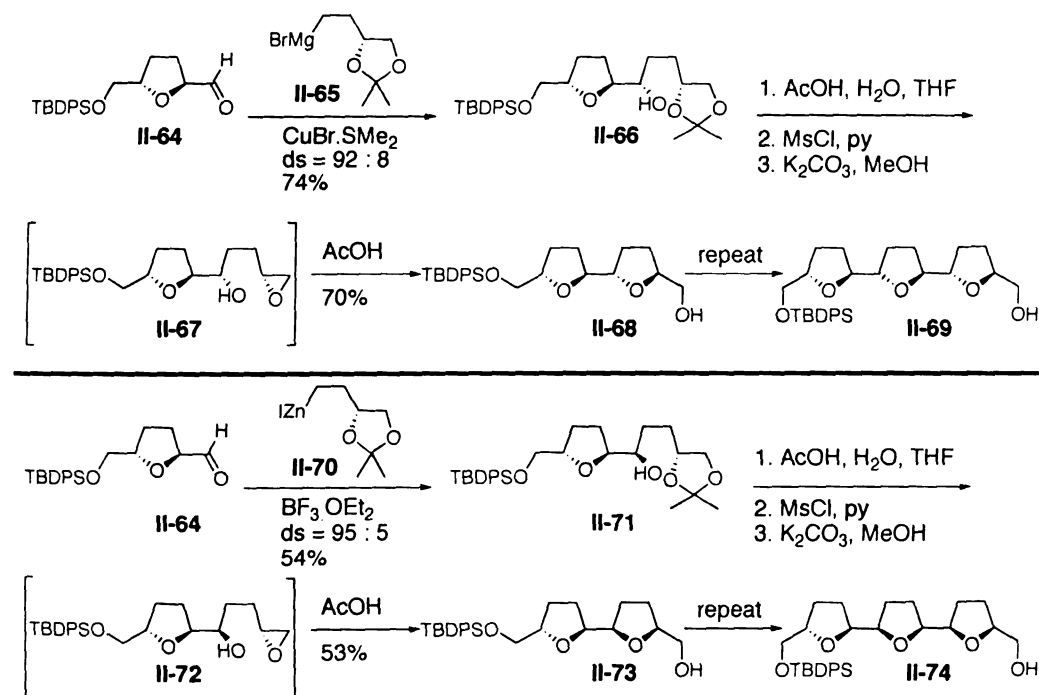


Figure II-20: Koert's modular strategy to construct bis - and tris - THF system

Reiteration of the same sequence provided higher THF units **II-69** and **II-74** following the same mechanism. Since all possible stereoisomers of reactants were available, a series of stereoisomeric THF systems could be generated. However, a limitation of this strategy is that the level of diastereoselection in both, the chelation-controlled and the Felkin–Ahn addition depends on whether the chirality of the organometallic species is matched or mismatched with respect to the facial selectivity of the aldehyde.

6. Miscellaneous

Jacobsen and co-workers synthesized muconin – a THP ring containing nonclassical acetogenin – using an Ireland-Claisen rearrangement and ring closing metathesis as key transformations to construct the THF-THP core (Figure II-21).⁷⁷

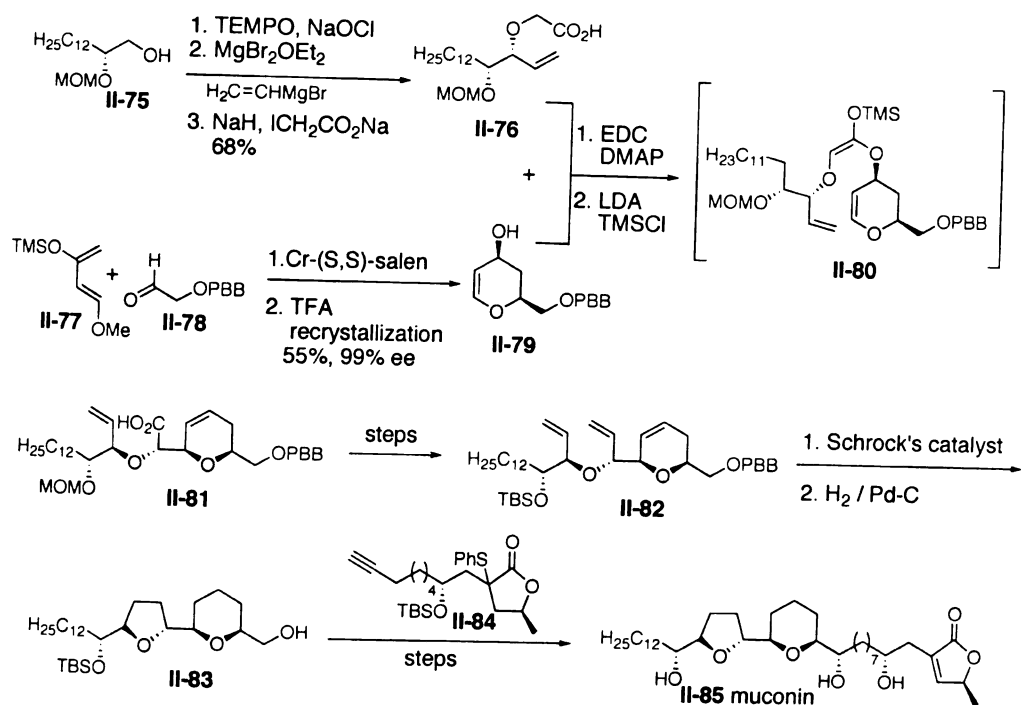


Figure II-21: Jacobsen's synthesis of muconin

The chiral building blocks, viz., diol **II-75** and dihydropyran **II-79** were obtained from inexpensive, racemic materials, commercially available in bulk quantities. Thus, racemic tetradecene oxide (not shown) upon hydrolytic kinetic resolution (HKR) protocol earlier developed in their laboratories, using chiral Co (*S,S*)-salen complex afforded the enantioenriched diol **II-75** (> 99% ee) in good yields.⁷⁸ Also, asymmetric hetero-Diels-Alder reaction of diene **II-77** and dienophile **II-78** catalyzed by Cr-(*S,S*) salen furnished the dihydropyran **II-79** (> 99% ee after recrystallization) in acceptable yields.⁷⁹ Esterification of chiral acid **II-76** with alcohol **II-79** set the stage for the Ireland-Claisen rearrangement, which generated intermediate **II-81**. Transformation of carboxylic acid **II-81** to bis-allyl ether **II-82** and the subsequent RCM reaction installed the THF-THP scaffold **II-83** (after hydrogenation of the RCM product). The butenolide ring was

100

101

102

103

104

105

106

107

108

109

110

111

112

incorporated in the final stages via organozinc mediated addition of the terminal alkyne **II-84** to the aldehyde generated from **II-83**. Muconin **II-85** was thus synthesized in over thirty-six steps.

Tanaka recently reported a straightforward, versatile strategy for construction of adjacent bis-THF units (Figure II-22).⁸⁰ Starting α -tetrahydrofuranic aldehydes of type **II-86** were readily accessible using a method developed in the same laboratory.⁸¹ Zinc mediated asymmetric alkynylation⁸² of **II-86** with alkyne **II-87** using (1*S*,2*R*)-*N*-methylephedrin (NME) as a chiral auxiliary, provided alkynol **II-88** in excellent diastereoselectivity which was manipulated in two different ways (**a** and **b**). Path **a** involved transformation of the 1,2 diol functionality in **II-88** to epoxyalcohol **II-89** which spontaneously cyclized in a 5-*exo-tet* mode to yield the bis-THF unit **II-90**. Along path **b**, the roles of oxygen functionalities were switched. Thus, intramolecular Williamson etherification of tosylate **II-91** lead to diastereomeric bis-THF core **II-92**. Since antipodes of all the chiral materials were available, various diastereomeric bis-THF units could be

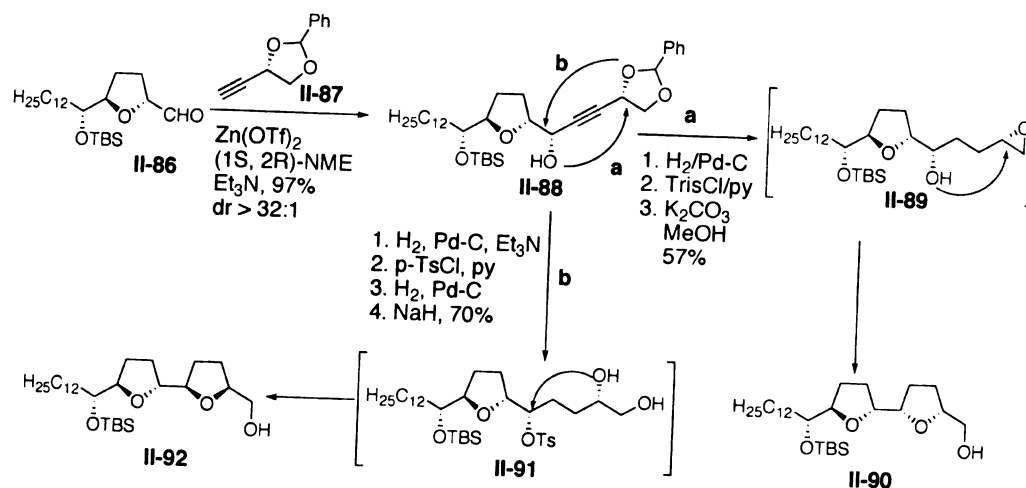


Figure II-22: Tanaka's stereodivergent strategy for construction of adjacent bis-THF systems

accessed efficiently. In principle, this approach can be further extended to construct oligomeric THF cores.

Evans has utilized the temporary silicon-tethered (TST) ring closing metathesis (RCM) method developed earlier in their laboratories,⁸³ for the synthesis of mucocin (Figure II-23).⁵² The appropriately functionalized THP and THF fragments **II-96** and **II-98** respectively, were obtained from a common chiral epoxide **II-93**. THP **II-96** was synthesized using highly diastereoselective, reductive bismuth tribromide mediated cyclization protocol (**II-95** to **II-96**) developed in their laboratories. Cobalt (II) catalyzed oxidative cyclization to construct *trans* THF **II-98** also proved highly stereoselective. Fully functionalized fragments **II-96** and **II-99** were tethered by treatment of **II-96** with excess $^i\text{Pr}_2\text{SiCl}_2$, washing off the excess reagent and then introducing **II-99** in the same

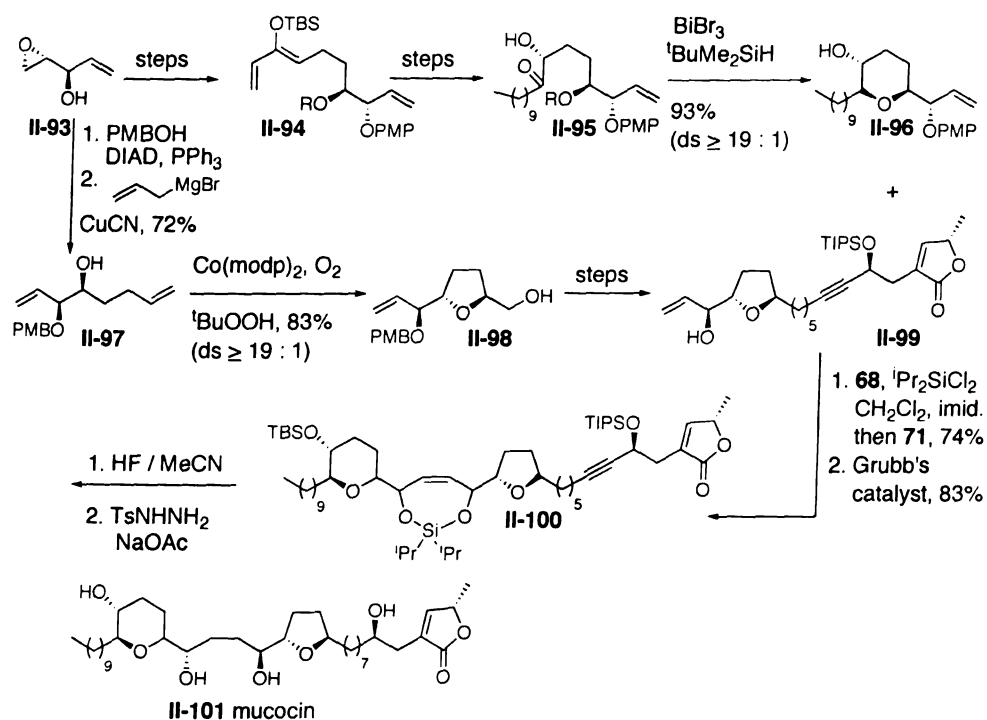


Figure II-23: Evans' synthesis of mucocin

pot. RCM reaction of the tethered product (not shown) furnished fully assembled intermediate **II-100**, which after cleavage of the silyl tether and enyne reduction provided muconin **II-101**. This strategy being highly convergent, offers avenues for structural diversity in the two cyclic ether units to be coupled.

In conclusion, the annonaceous acetogenins have proven to be one of the most potent classes of cytotoxic antitumor agents. More interestingly, they have shown high potency against multidrug resistant tumor cells and pesticide resistant insects. In spite of the promising biological activity, this class of natural products remains under-explored in area of lead development for pharmacological applications. Synthetic chemists can contribute to this area by design and development of rapid syntheses and high-throughput screening of libraries of constitutional and stereoisomers of acetogenins and their

synthetic analogs. Our studies on the synthesis of mucoxin – a novel nonclassical acetogenin are described in chapters III and IV.

H. References

1. Cave, A.; Figadere, B.; Laurens, A.; Cortes, D. in *Progress in the Chemistry of Organic Natural Products*; Herz, W., Kirby, G. W., E., M. R., Steglich, W., Tamm, C., Eds.; Springer-Verlag: New York, 1997; Vol. 70, pp 81-287.
2. Zeng, L.; Ye, Q.; Oberlies, H.; Shi, G.; Gu, Z.-M.; He, K.; McLaughlin, J. L. *Nat. Prod. Rep.* **1996**, *13*, 275.
3. Gu, Z.-M.; Zhao, G.-X.; Oberlies, N. H.; Zeng, L.; McLaughlin, J. L. *Rec. Adv. Phytochem.* **1995**, *29*, 249.
4. Fang, X. P.; Rieser, M. J.; Gu, Z. M.; Zhao, G. X.; McLaughlin, J. L. *Phytochem. Anal.* **1993**, *4*, 27.
5. Rupprecht, J. K.; Hui, Y. H.; McLaughlin, J. L. *J. Nat. Prod.* **1990**, *53*, 237.
6. Leboeuf, M.; Cave, A.; Bhaumik, P. K.; Mukherjee, B.; Mukherjee, R. *Phytochemistry* **1982**, *21*, 2783.
7. Jolad, S. D.; Hoffmann, J. J.; Schram, K. H.; Cole, J. R.; Tempesta, M. S.; Kriek, G. R.; Bates, R. B. *J. Org. Chem.* **1982**, *47*, 3151.
8. Zafra-Polo, M. C.; Gonzalez, M. C.; Estornell, E.; Sahpaz, S.; Cortes, D. *Phytochemistry* **1996**, *42*, 253.
9. Zafra-Polo, M. C.; Figadere, B.; Gallardo, T.; Tormo, J. R.; Cortes, D. *Phytochemistry* **1998**, *48*, 1087.
10. Alali, F. Q.; Liu, X.-X.; McLaughlin, J. L. *J. Nat. Prod.* **1999**, *62*, 504.
11. Johnson, H. A.; Oberlies, N. H.; Alali, F. Q.; McLaughlin, J. L. in *Biologically Active Natural Products: Pharmaceuticals*; Cutler, S. J., Cutler, H. G., Eds.; CRC Press: Boca Raton, FL, 2000, pp 173-183.
12. Gleye, C.; Raynaud, S.; Hocquemiller, R.; Laurens, A.; Fourneau, C.; Serani, L.; Laprevote, O.; Roblot, F.; Leboeuf, M.; Fournet, A.; De Arias, A. R.; Figadere, B.; Cave, A. *Phytochemistry* **1998**, *47*, 749.
13. Shi, G. E.; Alfonso, D.; Fatope, M. O.; Zeng, L.; Gu, Z. M.; Zhao, G. X.; He, K.; Macdougall, J. M.; McLaughlin, J. L. *J. Am. Chem. Soc.* **1995**, *117*, 10409.
14. Shi, G.; Kozlowski, J. F.; Schwedler, J. T.; Wood, K. V.; MacDougall, J. M.; McLaughlin, J. L. *J. Org. Chem.* **1996**, *61*, 7988.

15. Alali, F. Q.; Rogers, L.; Zhang, Y.; McLaughlin, J. L. *Tetrahedron* **1998**, *54*, 5833.
16. Chavez, D.; Acevedo, L. A.; Mata, R. *J. Nat. Prod.* **1998**, *61*, 419.
17. Nonfon, M.; Lieb, F.; Moeschler, H.; Wendisch, D. *Phytochemistry* **1990**, *29*, 1951.
18. Jiang, Z.; Chen, R.-Y.; Chen, Y.; Yu, D.-Q. *J. Nat. Prod.* **1998**, *61*, 86.
19. Oberlies, N. H.; Jones, J. L.; Corbett, T. H.; Fotopoulos, S. S.; McLaughlin, J. L. *Cancer Lett.* **1995**, *96*, 55.
20. Oberlies, N. H.; Croy, V. L.; Harrison, M. L.; McLaughlin, J. L. *Cancer Lett.* **1997**, *115*, 73.
21. Oberlies, N. H.; Chang, C. J.; McLaughlin, J. L. *J. Med. Chem.* **1997**, *40*, 2102.
22. Marshall, J. A.; Hinkle, K. W.; Hagedorn, C. E. *Isr. J. Chem.* **1997**, *37*, 97.
23. Alali, F. Q.; Kaakeh, W.; Bennette, G. W.; McLaughlin, J. L. *Econ. Entomol.* **1998**, *91*, 641.
24. Hopp, D. C.; Zeng, L.; Gu, Z. M.; McLaughlin, J. L. *J. Nat. Prod.* **1996**, *59*, 97.
25. Hopp, D. C.; Zeng, L.; Gu, Z. M.; Kozlowski, J. F.; McLaughlin, J. L. *J. Nat. Prod.* **1997**, *60*, 581.
26. Ahammadsahib, K. I.; Hollingworth, R. M.; McGovren, J. P.; Hui, Y. H.; McLaughlin, J. L. *Life Sci.* **1993**, *53*, 1113.
27. He, K.; Zeng, L.; Ye, Q.; Shi, G. E.; Oberlies, N. H.; Zhao, G. X.; Njoku, J.; McLaughlin, J. L. *Pestic. Sci.* **1997**, *49*, 372.
28. Londershausen, M.; Leicht, W.; Lieb, F.; Moeschler, H.; Weiss, H. *Pestic. Sci.* **1991**, *33*, 427.
29. Lewis, M. A.; Arnason, J. T.; Philogene, B. J. R.; Rupprecht, J. K.; McLaughlin, J. L. *Pestic. Biochem. Physiol.* **1993**, *45*, 15.
30. Morre, D. J.; Decabo, R.; Farley, C.; Oberlies, N. H.; McLaughlin, J. L. *Life Sci.* **1994**, *56*, 343.
31. Weiss, H.; Friedrich, T.; Hofhaus, G.; Preis, D. *Eur. J. Biochem.* **1991**, *197*, 563.

32. Esposti, M. D.; Ghelli, A.; Ratta, M.; Cortes, D.; Estornell, E. *Biochem. J.* **1994**, *301*, 161.
33. Shimada, H.; Grutzner, J. B.; Kozlowski, J. F.; McLaughlin, J. L. *Biochemistry* **1998**, *37*, 854.
34. Shimada, H.; Kozlowski, J. F.; McLaughlin, J. L. *Pharmacol. Res.* **1998**, *37*, 357.
35. Kuwabara, K.; Takada, M.; Iwata, J.; Tatsumoto, K.; Sakamoto, K.; Iwamura, H.; Miyoshi, H. *Eur. J. Biochem.* **2000**, *267*, 2538.
36. Miyoshi, H.; Ohshima, M.; Shimada, H.; Akagi, T.; Iwamura, H.; McLaughlin, J. L. *Biochim. Biophys. Acta* **1998**, *1365*, 443.
37. Hoppe, R.; Flasche, M.; Scharf, H. D. *Tetrahedron Lett.* **1994**, *35*, 2873.
38. Gu, Z. M.; Zeng, L.; Fang, X. P.; Colmansaizarbitoria, T.; Huo, M.; McLaughlin, J. L. *J. Org. Chem.* **1994**, *59*, 5162.
39. Landolt, J. L.; Ahammadsahib, K. I.; Hollingworth, R. M.; Barr, R.; Crane, F. L.; Buerck, N. L.; McCabe, G. P.; McLaughlin, J. L. *Chem.-Biol. Interact.* **1995**, *98*, 1.
40. Mikolajczak, K. J.; Madrigal, R. V.; Rupprecht, J. K.; Hui, Y. H.; Liu, Y. M.; Smith, D. L.; McLaughlin, J. L. *Experientia*, *46*, 324.
41. Takahashi, S.; Maeda, K.; Hirota, S.; Nakata, T. *Org. Lett.* **1999**, *1*, 2025.
42. Zhao, G. X.; Miesbauer, L. R.; Smith, D. L.; McLaughlin, J. L. *J. Med. Chem.* **1994**, *37*, 1971.
43. Keinan, E.; Sinha, A.; Yazbak, A.; Sinha, S. C.; Sinha, S. C. *Pure Appl. Chem.* **1997**, *69*, 423.
44. Hoye, T. R.; Suhadolnik, J. C. *J. Am. Chem. Soc.* **1985**, *107*, 5312.
45. Hoye, T. R.; Hanson, P. R.; Kovelesky, A. C.; Ocain, T. D.; Zhuang, Z. P. *J. Am. Chem. Soc.* **1991**, *113*, 9369.
46. Huckin, S. N.; Weiler, L. *J. Am. Chem. Soc.* **1974**, *96*, 1082.
47. Dixon, D. J.; Ley, S. V.; Reynolds, D. J. *Angew. Chem., Int. Ed.* **2000**, *39*, 3622.
48. Dixon, D. J.; Ley, S. V.; Reynolds, D. J. *Chem. Eur. J.* **2002**, *8*, 1621.
49. Hu, T.-S.; Yu, Q.; Wu, Y.-L.; Wu, Y. *J. Org. Chem.* **2001**, *66*, 853.

50. Harcken, C.; Bruckner, R. *New J. Chem.* **2001**, 25, 40.
51. Hoppen, S.; Baurle, S.; Koert, U. *Chem. Eur. J.* **2000**, 6, 2382.
52. Evans, P. A.; Cui, J.; Gharpure, S. J.; Polosukhin, A.; Zhang, H.-R. *J. Am. Chem. Soc.* **2003**, 125, 14702.
53. Jiang, H. Ph. D. Thesis, University of Virginia, 2000.
54. Marshall, J. A.; Piettre, A.; Paige, M. A.; Valeriote, F. *J. Org. Chem.* **2003**, 68, 8290.
55. Koert, U. *Synthesis* **1995**, 115.
56. Hoppe, R.; Scharf, H. D. *Synthesis* **1995**, 1447.
57. Casiraghi, G.; Zanardi, F.; Battistini, L.; Rassu, G.; Appendino, G. *Chemtracts* **1998**, 11, 803.
58. Trost, B. M.; Calkins, T. L.; Bochet, C. G. *Angew. Chem., Int. Ed.* **1997**, 36, 2632.
59. Trost, B. M.; Shi, Z. P. *J. Am. Chem. Soc.* **1994**, 116, 7459.
60. Trost, B. M.; Muller, T. J. J.; Martinez, J. J. *Am. Chem. Soc.* **1995**, 117, 1888.
61. Marshall, J. A. *Chem. Rev.* **1996**, 96, 31.
62. Marshall, J. A.; Welmaker, G. S.; Gung, B. W. *J. Am. Chem. Soc.* **1991**, 113, 647.
63. Marshall, J. A.; Hinkle, K. W. *J. Org. Chem.* **1995**, 60, 1920.
64. Hoye, T. R.; Ye, Z. X. *J. Am. Chem. Soc.* **1996**, 118, 1801.
65. Townsend, C. A.; Basak, A. *Tetrahedron* **1991**, 47, 2591.
66. Koert, U. *Angew. Chem., Int. Ed.* **1995**, 34, 298.
67. Cane, D. E.; Celmer, W. D.; Westley, J. W. *J. Am. Chem. Soc.* **1983**, 105, 3594.
68. Towne, T. B.; McDonald, F. E. *J. Am. Chem. Soc.* **1997**, 119, 6022.
69. Sinha, S. C.; Sinha, A.; Sinha, S. C.; Keinan, E. *J. Am. Chem. Soc.* **1997**, 119, 12014.
70. Zanardi, F.; Battistini, L.; Rassu, G.; Pinna, L.; Mor, M.; Culeddu, N.; Casiraghi, G. *J. Org. Chem.* **1998**, 63, 1368.

71. Casiraghi, G.; Zanardi, F.; Rassu, G. *Pure Appl. Chem.* **2000**, 72, 1645.
72. Tang, S. H.; Kennedy, R. M. *Tetrahedron Lett.* **1992**, 33, 5303.
73. Tang, S. H.; Kennedy, R. M. *Tetrahedron Lett.* **1992**, 33, 5299.
74. Kennedy, R. M.; Tang, S. *Tetrahedron Lett.* **1992**, 33, 3729.
75. Koert, U.; Stein, M.; Harms, K. *Tetrahedron Lett.* **1993**, 34, 2299.
76. Koert, U.; Wagner, H.; Pidun, U. *Chem. Ber.* **1994**, 127, 1447.
77. Schaus, S. E.; Branalt, J.; Jacobsen, E. N. *J. Org. Chem.* **1998**, 63, 4876.
78. Tokunaga, M.; Larrow, J. F.; Kakiuchi, F.; Jacobsen, E. N. *Science* **1997**, 277, 936.
79. Schaus, S. E.; Branalt, J.; Jacobsen, E. N. *J. Org. Chem.* **1998**, 63, 403.
80. Maezaki, N.; Kojima, N.; Tominaga, H.; Yanai, M.; Tanaka, T. *Org. Lett.* **2003**, 5, 1411.
81. Maezaki, N.; Kojima, N.; Asai, M.; Tominaga, H.; Tanaka, T. *Org. Lett.* **2002**, 4, 2977.
82. Frantz, D. E.; Fassler, R.; Tomooka, C. S.; Carreira, E. M. *Acc. Chem. Res.* **2000**, 33, 373.
83. Evans, P. A.; Murthy, V. S. *J. Org. Chem.* **1998**, 63, 6768.

CHAPTER III

SYNTHESIS OF THE LEFT HAND FRAGMENT (C12-C34) OF MUCOXIN AND PRELIMINARY STUDIES ON ITS COUPLING WITH THE RIGHT HAND FRAGMENT

A. Introduction

The annonaceous acetogenins are C32 or C34 fatty acid derivatives originating from the plant family *annonaceae* found in tropical and sub-tropical regions. In recent years, this class of bioactive compounds has captured the attention of researchers in the chemical, biological and medicinal sciences due to their high potency (sub-nanomolar IC_{50} values) and selective cytotoxicity profiles against a variety of human tumor cell lines including multi-drug resistant tumor cells (Chapter II).¹⁻⁵ Classically, the acetogenins comprise of one or more 2,5-disubstituted THF rings along the long fatty acid chain.

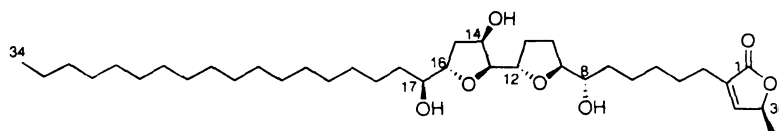


Figure III-1: Mucoxin

More recently, some acetogenins – now termed as nonclassical acetogenins – containing THP or hydroxylated 2,3,5-trisubstituted THF rings have been isolated.⁶ In addition to their biological activities, the novel structural features of nonclassical acetogenins have aroused the interest of synthetic chemists.⁷⁻¹⁰

Mucosin (Figure III-1) is one of the nonclassical acetogenins isolated by McLaughlin and coworkers in 1996 from the bioactive leaf extracts of *Rollinia mucosa*.¹¹ *In vitro* cytotoxicity assays against a panel of six human tumor cell lines showed mucosin to be more potent and selective against MCF-7 (breast carcinoma) cell lines ($ED_{50} = 3.7 \times 10^{-3} \mu\text{g/mL}$) than adriamycin ($ED_{50} = 1.0 \times 10^{-2} \mu\text{g/mL}$). The isolation procedure for mucosin involved activity directed open column fractionation using brine shrimp lethality test and at later stages purification by ^1H NMR-monitored repetitive reverse and normal phase HPLC techniques. As is often the case with acetogenins,¹² after such rigorous purification procedures, only 1.8 mg of mucosin was isolated. Due to a limited supply of the natural sample, only the constitution and the relative configuration of the seven oxygenated stereocenters of the bis-THF core (C8-C17, Figure III-1) of mucosin were established.¹¹ Although, no attempts were made to determine the absolute stereochemistry of C8-C17 portion of mucosin, the absolute configuration at C36 was assigned to be *S* based on the observation that over 400 acetogenins isolated to date have been shown to possess *S* configuration at that carbon.⁶

Mucosin is the first nonclassical acetogenin possessing a hydroxylated THF ring (C13-C17, Figure III-1).^{*} This structural feature adds an element of complexity in the design of its total synthesis. Several chiral building blocks used to construct 2,5-disubstituted THF units have originated from the earlier total syntheses of classical acetogenins (Chapter II). However, it may not be possible to use these building blocks 'as is' to construct the hydroxylated 2,3,5 tri-substituted THF ring of mucosin. Also,

^{*} Four acetogenins were previously reported to possess hydroxylated THF rings;¹³ however their structures were proved erroneous and have been corrected.²

87

88

89

90

91

92

93

straightforward and efficient modifications of such existing building blocks to incorporate the ring hydroxyl group are not readily apparent.

Mucosin attracted our attention as a synthetic target for several reasons. We envisioned that the hydroxylated THF fragment of mucosin could be easily accessed using our method for regio- and stereoselective construction of hydroxylated, tri-substituted THF units (Chapter I).¹⁴ Thus, it would serve to test the viability and generality of our method in a total synthesis setting. A major focus of our laboratories is on developing straightforward and versatile methods to synthesize THF units with various substitution patterns, using regiocontrolled cyclization reactions. Thus, the right-hand portion (C1-C12) of mucosin also attracted our attention as a possible avenue for new method development to install the 2,5-disubstituted THF ring. In light of the fact that the proposed structure of mucosin contains unusual elements (a hydroxylated THF ring), previously unknown in acetogenins, it becomes important to confirm the proposed structure, establish the relative and absolute configuration as well as further explore the bioactivity profile. Total synthesis would provide the material necessary for such investigations on mucosin. Structure-activity relationship studies on classical acetogenins have indicated that adjacent bis-THF acetogenins with three free hydroxyl groups possess the most potent cytotoxic and pesticidal properties.⁶ Mucosin presents itself as an interesting case study since it embodies all the above-mentioned features but at the same time possesses a unique disposition of one of the hydroxyl groups. Also, as in any other total synthesis, an appropriately designed synthetic strategy would provide an expeditious access to unnatural constitutional and stereoisomers of mucosin. Finally, the

1.

2.

B.

P.

e.

2.

intermediates generated during the total synthesis could serve as truncated analogs of mucoxin that can be employed for SAR analysis to delineate essential pharmacophores.

B. Retrosynthesis

Most acetogenin total syntheses reported so far involve first, construction of the polycyclic ether core bearing suitable functional group handles, followed by sequential elaboration to install the long hydrocarbon side chain and the terminal γ -lactone with an appropriate linker.^{12,15-17} From the outset, we sought a more convergent approach that involved coupling the right (C1-C12) and the left (C13-C34) hand fragments of mucoxin in fully elaborated forms. Our strategy, in the form of a retrosynthetic analysis, is summarized in Figure III-2.

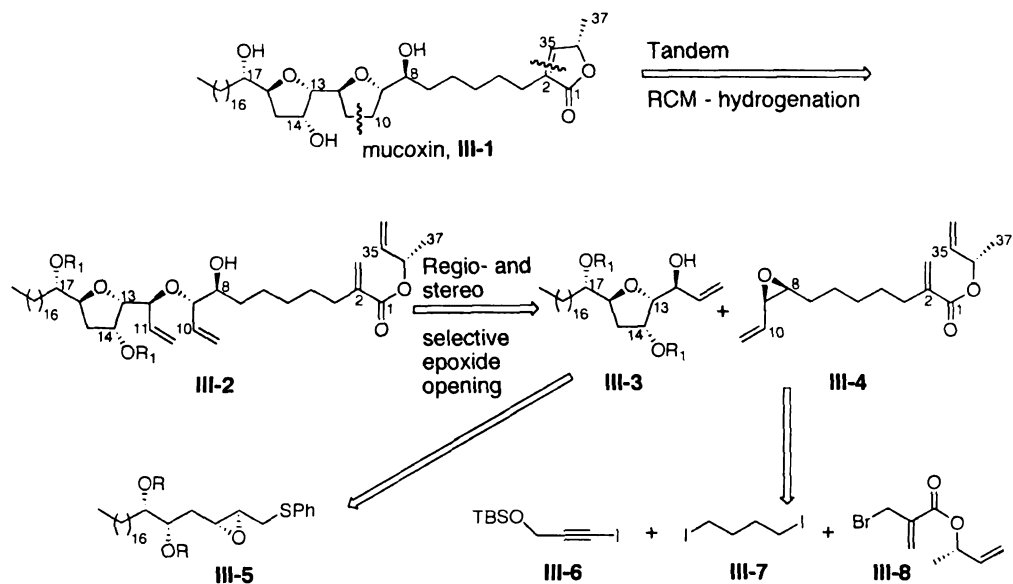


Figure III-2: Mucoxin: retrosynthetic analysis

Since the absolute stereochemistry of the C8-C17 bis-THF core of mucoxin is unknown, we opted to synthesize enantiomer **III-1** (Figure III-2). Our retrosynthesis

began by two simultaneous fragmentations of the natural product along the C2-C35 and the C10-C11 bonds.

Grubbs has recently reported a 'one pot' tandem olefin metathesis hydrogenation sequence to directly obtain reduced metathesis products (Figure III-3).¹⁸ After completion of the metathesis reaction at 40 °C, hydrogen was introduced in the same reaction vessel which generated the active hydrogenation catalyst $\text{RuHCl}(\text{H}_2)(\text{PCy}_3)_2$. Upon increasing the temperature to 70 °C, hydrogenation took place cleanly to afford the corresponding saturated products. Figure III-3 shows examples of this protocol relevant to our total synthesis. The hydrogenation occurred readily in case of bisallyl ether **III-9** at atmospheric pressure, whereas higher pressure (100 psi) was needed to obtain the lactone **III-12** due to the steric and electronic factors. Inspired by this report, we decided to construct the C9-C12 THF and the terminal α,β unsaturated γ -lactone rings of mucoxin using a tandem double RCM / hydrogenation sequence of the precursor **III-2** (Figure III-2).

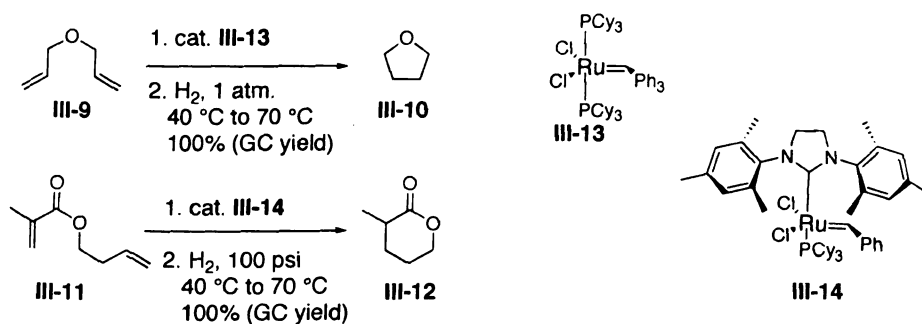


Figure III-3: Grubbs' tandem olefin metathesis - hydrogenation protocol

To finish the retrosynthetic analysis, 2,3,5-trisubstituted THF unit **III-3** would be obtained *via* regio- and stereoselective cyclization of epoxy-diol **III-5** using the methodology described in Chapter I.¹⁴ Finally, vinylic epoxide **III-4** would be

synthesized using a Knochel type three component coupling reaction^{19,20} of alkynyl iodide **III-6**, 1,4 diiodobutane **III-7** and allylic bromide **III-8** (Figure III-2).

We planned to assemble the advanced intermediate **III-2** *via* a regio- and stereoselective intermolecular opening of the vinylic epoxide **III-4** by the allylic alcohol **III-3**. Intramolecular epoxide opening by a hydroxyl nucleophile has been extensively studied and utilized to prepare medium sized cyclic ether units.^{21,22} In fact, it is probably the most commonly used tactic to install multiple cyclic ether segments, as demonstrated in the elegant total syntheses of polyether natural products including marine toxins such as brevetoxins, ciguatoxins, maitotoxin and simpler annonaceous acetogenins.²³ In contrast, the intermolecular version of the process using alcohols as external nucleophiles has been investigated to a much lesser extent.

To the best of our knowledge, intermolecular epoxide ring opening by means of alcohols has remained unused as a strategy in complex total synthesis settings. This could be attributed to several factors. First, alcohols, in general are poor nucleophiles²⁴⁻²⁷ and epoxides, inherently are not very reactive electrophiles.²⁸⁻³⁰ Thus, their union often needs harsh conditions such as the use of alkoxides at elevated temperatures³¹⁻³³ or epoxide activation using strong Lewis or Bronsted acids³⁴⁻³⁷ which could be incompatible with sensitive functionalities present elsewhere in the reacting partners. Moreover, even under such forcing conditions, a large excess of alcohol is required to drive the reaction to completion. Secondly, most intermolecular epoxide opening reactions thus far have involved simple alcohols like MeOH, EtOH, benzyl alcohol and phenol that can be used as solvents.³⁸⁻⁴¹

This, clearly, is not viable from a total synthesis standpoint since complex alcohol coupling partners most likely will not be available in such large quantities. Also, another potential limitation on the use of complex alcohols as nucleophiles is that as the alcohol gets sterically hindered, its nucleophilicity is likely to drop further. Finally, it is more difficult to achieve high levels of regio- and stereocontrol in intermolecular fusion of an alcohol and epoxide (*vide supra*) as compared to its intramolecular counterpart.^{42,43}

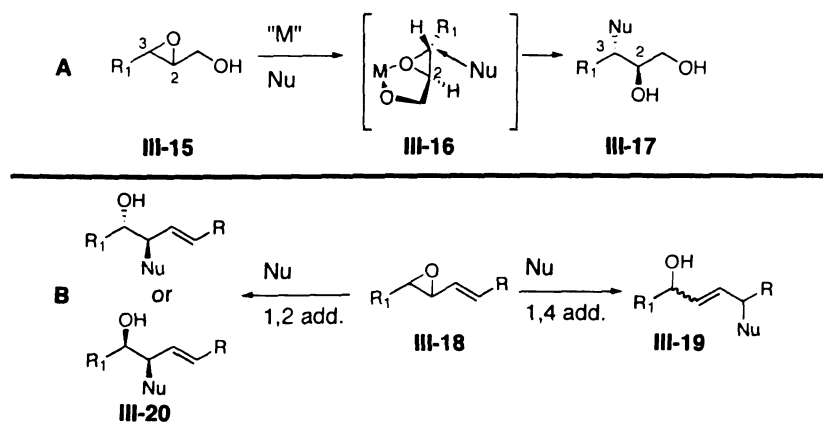


Figure III-4: Common tactics used for regiocontrol in intermolecular epoxide opening reactions

Having mentioned the difficulties in epoxide ring opening by external alcohol nucleophiles, it would be in order to point out a few literature reports that have dealt with the issue. Two commonly used techniques to realize regiocontrol in intermolecular epoxide opening reactions are outlined in Figure III-4. 2,3 Epoxy alcohols (part A, III-15) form bidentate chelates with metal centers (III-16) which leads to selective activation of C3 of the epoxide toward a nucleophilic attack.^{41,44} In case of vinylic epoxides of type III-18, under acidic conditions, the epoxide carbon adjacent to the olefinic moiety is selectively activated toward nucleophilic attack due to resonance

stabilization of partial positive charge. Depending upon the nature of transition metal activator or Lewis acid catalyst the corresponding 1,4 (**III-19**) or 1,2 (**III-20**) addition products can be obtained.^{24,42,45,46} Representative examples of these strategies, specifically, in the context of alcohol nucleophiles are described below.

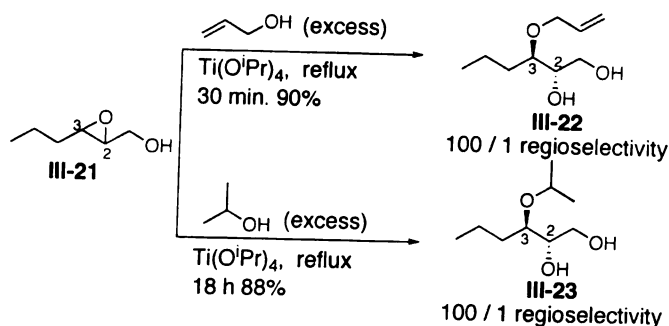


Figure III-5: Sharpless' protocol for C3 selective epoxide ring opening of 2,3 epoxy alcohols

In 1985, Sharpless and co-workers developed a procedure for highly regioselective opening of 2,3 epoxy alcohols using stoichiometric $\text{Ti(O}^i\text{Pr)}_4$ as a chelating agent⁴¹ (Part A, Figure III-4). 2,3 epoxy-1-hexanol **III-21** (Figure III-5) when treated with allyl alcohol produced the corresponding C3 ring opened product **III-22** in excellent yields and regioselectivity. The same transformation using bulkier $i\text{PrOH}$ was sluggish and took prolonged heating for completion. This efficient protocol although widely used, is restricted to sterically unhindered alcohols. It should also be noted that only the alcohol nucleophiles had to be used in large excess at elevated temperatures whereas other nucleophiles including azides, cyanides, thiophenols, and amines reacted efficiently at ambient temperature.

Vinyllic epoxide substrates of type **III-18** (Part B, Figure III-4) have been used more frequently as alkylating agents for alcohols under transition metal catalyzed or

Lewis acidic conditions. Hirama and co-workers showed that the densely functionalized cyclopentadiene monoepoxide (**III-25**, Figure III-6) could be regio- and stereoselectively opened by the azatyrosine **III-24** using CsF as an activator in good yields.⁴⁷ This method though attractive due to the functional group tolerance and reactant stoichiometry, was

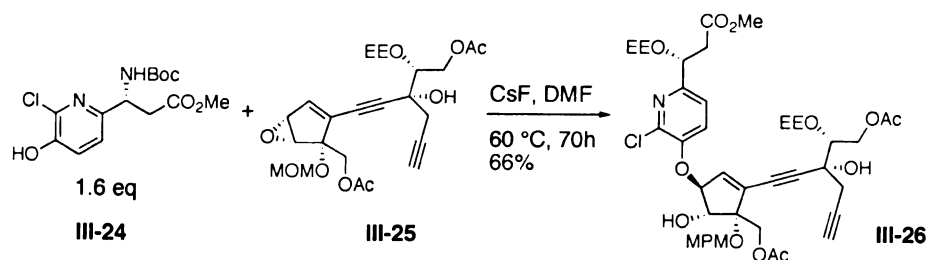


Figure III-6: Hirama's conditions for regio- and stereoselective addition of aromatic alcohols to highly functionalized vinyl epoxides

applicable to very specific aromatic alcohols. Extension of this protocol to other aromatic or aliphatic alcohols has not been reported.

Most transition metal mediated nucleophilic additions to vinylic epoxides have been known to produce 1,4 addition products (**III-19**, Figure III-4).⁴³ However, Trost, in 1988 reported Pd(0) catalyzed regioselective 1,2 addition to vinylic epoxides (Figure III-7).²⁴ The trick was to use a tin ether, which formed an intermediate 'ate' complex thereby tethering the nucleophile to the epoxide prior to attack (**III-28** and **III-29**). The nucleophile was then delivered selectively at the carbon adjacent to the vinyl group.

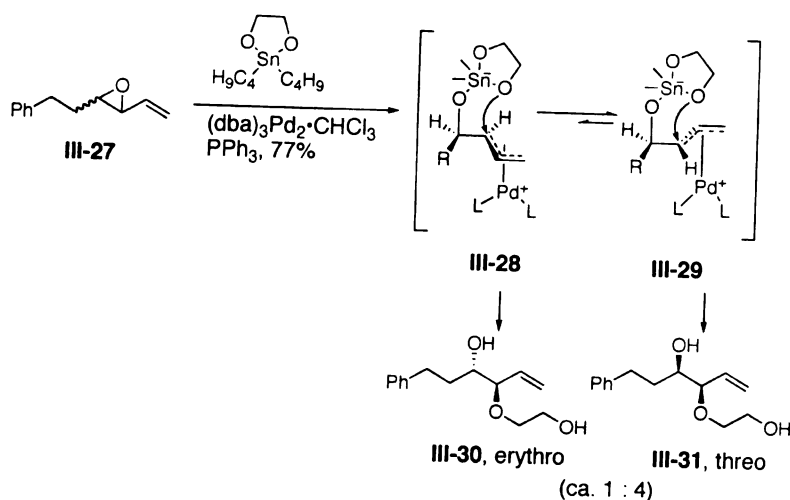


Figure III-7: Trost's strategy for 1,2 addition of alcohols to vinylic epoxides

Thus vinylic epoxide **III-27**, when treated with a cyclic stannane in presence of Pd(0), gave diastereomeric 1,2 addition products **III-30** and **III-31** exclusively in 77% yield. However this methodology is faced with several limitations and is far from being of general applicability. First, the stereochemical fidelity of the starting epoxide is lost during the reaction. It was shown that irrespective of the epoxide geometry, the *threo* ring opened product was always obtained as the major product. To explain the results, Trost proposed that eclipsing interactions of the R group with allyl fragment would destabilize conformation **III-28** (Figure III-7) relative to **III-29**. Secondly, the use of cyclic stannanes was essential. Trialkyl stannanes (**III-33**, Figure III-8) produced the desired products in low (up to 25%) yields and the reaction was accompanied by rearranged products. Thus, complex mono alcohols did not participate effectively.

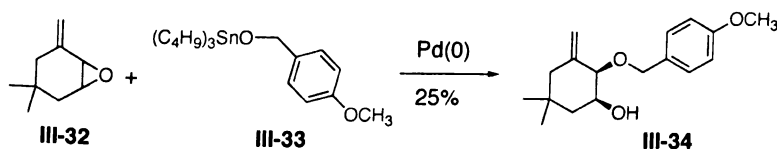


Figure III-8: Trialkyl stannanes proved inefficient as electrophiles in Trost's studies

21.

22.

23.

24.

25.

26.

27.

28.

29.

30.

31.

32.

33.

34.

35.

36.

37.

38.

39.

40.

More recently, Trost has also developed trialkyl borane mediated, Pd(0) catalyzed allylic alkylation of alcohols using racemic vinylic epoxides (Figure III-9).⁴⁶ The proposed mechanism again involves tethering the nucleophile to the epoxide *via* a borate

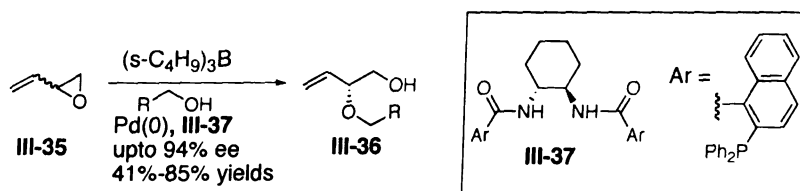


Figure III-9: Trost's two-component catalyst system for asymmetric allylic alkylation of alcohols

complex before ether bond formation. Nevertheless, this method is also restricted to primary alcohol pronucleophiles and has been applied only to terminal vinylic epoxides. Another class of epoxides that participate in intermolecular ring opening is sugar derived 1, 2 oxiranes.

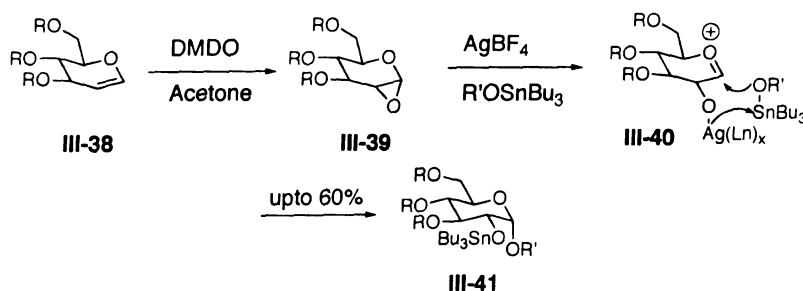


Figure III-10: A representative example of regio- and stereoselective ring opening of sugar derived oxiranes

Danishefsky has extensively studied glycosidation reactions of glycosyl donors such as III-39 using a variety of promoters.⁴⁸⁻⁵⁴ The sequence outlined in Figure III-10, involves AgBF₄ promoted O-glycosidation using stannylated glycosyl acceptors.⁵⁴

Danishefsky has invoked a stannyl group transfer to the C2 oxygen of the donor **III-40** to reason the observed α -selectivity in the glycosidation reaction. The driving force in such an epoxide activation event is the generation of an oxonium ion intermediate.

Mioskowski and Lautens, independently reported their studies on vinyl epoxide ring opening by alcohols about the same time,^{42,55} which were most relevant and promising to us for use in our total synthesis. A representative example from Mioskowski's studies is shown in Figure **III-11**.⁵⁵ Out of a wide range of Lewis acids screened, $\text{BF}_3 \cdot \text{OEt}_2$ worked most efficiently for the regio- and stereoselective opening of **III-42** with a variety of alcohols. The hindered secondary alcohol **III-43**, having an

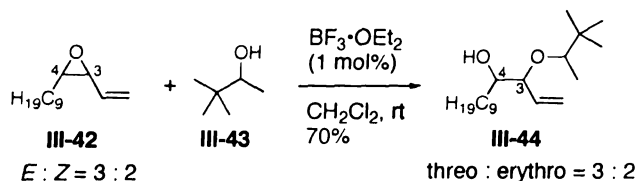


Figure III-11: Mioskowski's conditions for stereoselective $\text{S}_{\text{N}}2$ addition of alcohols to vinyl epoxides

adjacent neopentyl center, also participated efficiently. The ring opening occurred exclusively at C3 of the epoxide **III-42** and the diastereomeric ratio was conserved in the product **III-44**. Also, the reaction was found to be tolerant to different solvents (benzene, Et_2O) and temperatures (-78°C to reflux).

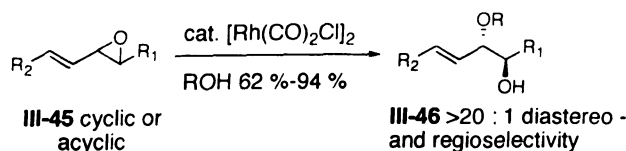


Figure III-12: Lautens' protocol for $\text{S}_{\text{N}}2$ substitution of vinylic epoxides by alcohols under mild conditions

12

13

14

15

16

17

18

19

20

21

22

23

24

25

Lautens used a rhodium(I) catalyst to promote the intermolecular epoxide opening reaction by alcohol nucleophiles (Figure III-12).⁴² A variety of epoxides containing functional groups like esters and silyl ethers elsewhere, reacted efficiently to afford the corresponding S_N2 products with inversion of configuration at the reactive carbon. The alcohol nucleophile however had to be used in excess (10eq.) and only simple unhindered alcohols were examined. Nonetheless, this method seemed promising because of the mild conditions utilized. We also thought that it might be possible to recycle any excess alcohol necessary to promote the reaction.

Encouraged by Mioskowski's and Lautens' studies as well as our own experience in the regioselective epoxide ring opening area, we decided to attempt an intermolecular coupling of the functionalized allylic alcohol **III-3** and the vinylic epoxide **III-4** units (Figure III-2) in the total synthesis of mucoxin. This strategy was particularly attractive to us because of (i) functional group tolerance of the coupling reaction thereby allowing the convergent assembly of advanced intermediates, ii) possible avenues for introducing diversity in terms of the size of the ring (THF and THP) to be installed and (iii) the stereogenic centers (in principle, all four stereoisomers of vinylic epoxide of type **III-4** could be easily accessed using Sharpless asymmetric epoxidation reaction of the appropriate *cis* or *trans* allylic alcohol precursor).

C. Evaluation of the proposed intermolecular regio- and stereoselective epoxide opening strategy

1. Design and synthesis of chiral allylic alcohol **III-3**

During the course of our earlier work (Chapter I), five regio- and stereoisomeric THF diols (**III-54–III-58**, Figure III-14) were accessed using the 2-deoxy-D-ribose derived epoxy diol system **III-53** as the common precursor. Depending upon the epoxide stereochemistry, the choice of the pendant functional group X (**III-53**) and the acid promoter, all five THF diols (**III-54** to **III-58**) were obtained in high yields and enantiopurity, which rendered this method a viable route to access 3-hydroxy-2,3,5-trisubstituted THF motifs for use in total synthesis. We considered the possibility of using one of these available THF diols for further elaboration to the target allylic alcohol **III-3**. As far as the stereochemistry is concerned, of all the isomers, **III-57** most closely resembles the target allylic alcohol **III-3** (Figure III-15).

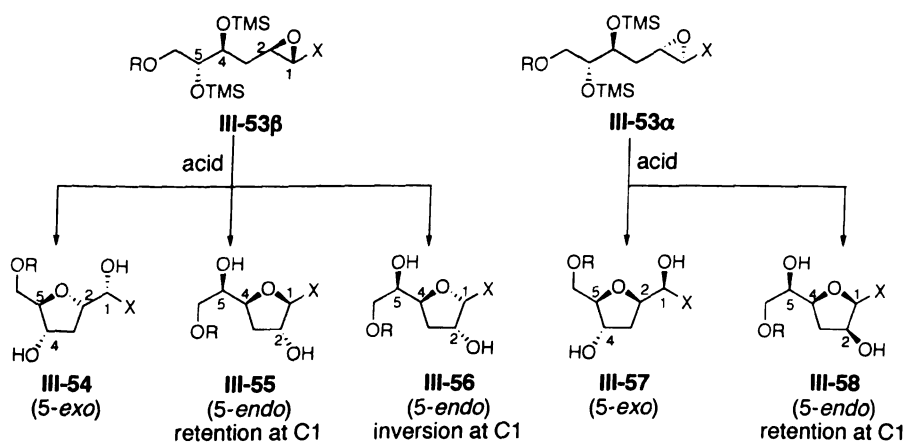


Figure III-14: Isomeric THF diols available from a common epoxy diol precursor

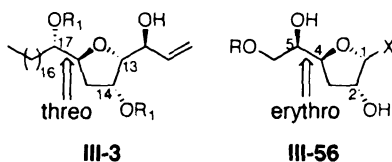


Figure III-15: Stereochemical similarities and differences between the target THF unit

III-3 and an available precursor III-56

Triol **III-56** has the same absolute configuration about the THF ring as that of target triol **III-3**. The only difference lies in the *threo* (**III-3**) vs. *erythro* (**III-56**) relationship between the side chain carbinol stereocenter (C17 in **III-3** and C5 in **III-56**) and the THF ring system. In order to use **III-56** as a precursor to **III-3** following three transformations would be necessary: (i) inversion of the C5 stereocenter (ii) installation of the aliphatic chain and (iii) elaboration of the pendant group (X) to the allylic alcohol functionality.

In case of acetogenins containing 2,5-disubstituted THF rings flanked by hydroxyl groups, inversion of such side chain carbinol stereocenters has been achieved in two major ways:¹⁵ i) using Mitsunobu inversion of alcohols ii) *via* formation of a terminal epoxide that involves S_N2 displacement at the stereocenter in question. It seemed to us that inversion of the C5 stereocenter in **III-56** using one of these protocols would

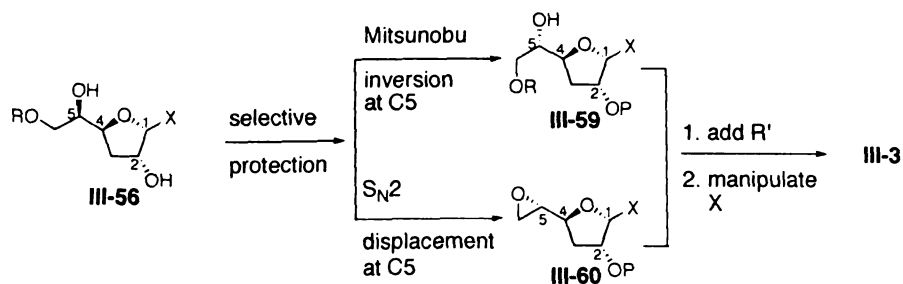


Figure III-16: A route to transform **III-57** to the target allylic alcohol **III-3**

necessitate selective protection of the C2 hydroxyl group (Figure III-16) due to similar steric environments of the two hydroxyl groups. Overall, this approach did not appear concise and straightforward. Also, if the oxygenated stereocenters in cyclization precursor **III-5** (Figure III-2) were derived from asymmetric transformations instead of the naturally available chiral pool, a variety of stereoisomeric epoxydiols of type **III-5** could be easily obtained merely by using enantio- and diastereomeric reagents and reactants. Such a strategy would offer easy access to unnatural analogs of mucoxin.

Sharpless asymmetric dihydroxylation⁵⁶ and epoxidation reactions are extremely reliable^{57,58} to establish oxygenated stereocenters in high enantio- and diastereoselectivity. These methods are also highly versatile since both the antipodes of chiral reagents employed are easily available. Thus, these protocols were ideally suited for our purpose to synthesize epoxy diols of type **III-5**.

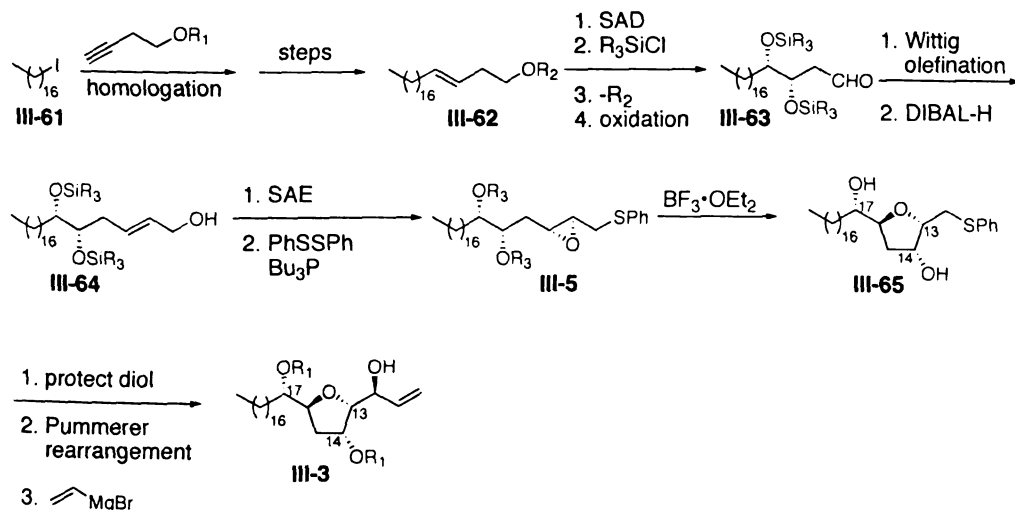
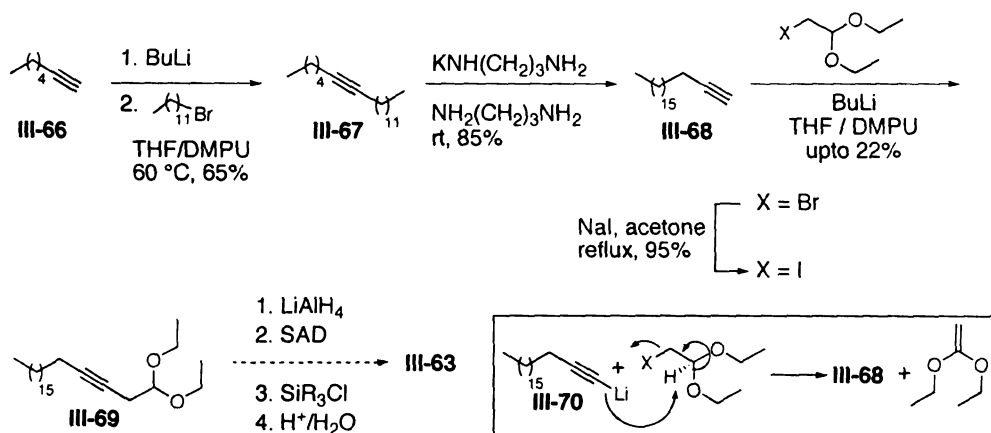


Figure III-17: Proposed synthesis of the left hand (C13-C34) fragment of mucoxin

In our synthetic strategy (Figure III-17), we chose to incorporate the long alkyl chain from the outset. Thus, readily available 1-iodoheptadecane **III-61** would be

homologated using suitably protected 3-butyne-1-ol and the resultant homopropargylic alcohol would be transformed into the homoallylic alcohol **III-62**. Asymmetric dihydroxylation of the *trans* olefin **III-62** should afford diol **III-63**, which after suitable manipulations should generate allylic alcohol **III-64**. Epoxy diol **III-5** would then be accessed *via* asymmetric epoxidation of **III-64** followed by treatment with the Hata reagent to install the thiophenyl group. Exposure of **III-5** to Lewis acid should lead to simultaneous deprotection / cyclization event (Chapter I)¹⁴ to afford the THF diol **III-65** having all the stereogenic centers correctly established. Finally, Pummerer rearrangement to convert the thiophenyl group in **III-65** into an aldehyde functionality and subsequent addition of vinyl magnesium bromide in a chelation controlled manner should provide chiral allylic alcohol **III-3**. The transformations needed to elaborate the β,γ -dihydroxy aldehydes similar to **III-63** to the epoxy diol systems of type **III-5** (Figure **III-17**), were optimized during the course of our method development (Chapter I). Therefore, our immediate goal was to access aldehyde **III-63** in a quick and efficient manner. Several approaches toward this goal were tried.

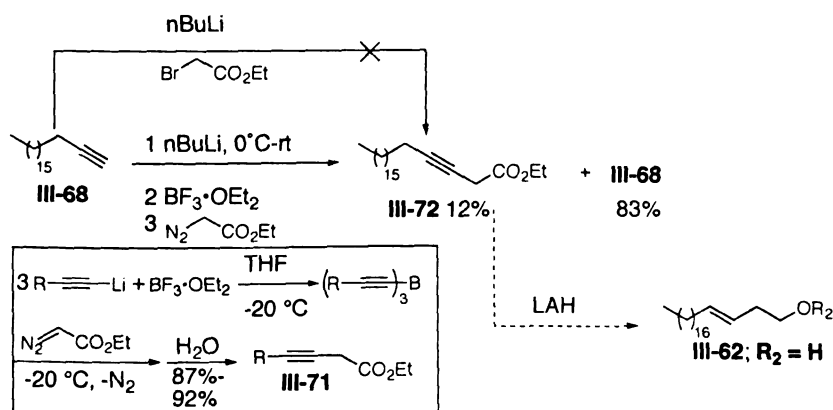
The first approach involved introduction of the aldehyde functionality in a masked form by alkylation of 1-nonadecyne **III-68** with bromoacetaldehyde diethyl acetal (Scheme **III-1**). **III-68** was prepared in good yield *via* alkylation of 1-heptyne (**III-66**) with 1-bromododecane followed by isomerization of the internal alkyne **III-67** to the terminal alkyne **III-68** by way of an alkyne zipper reaction.^{59,60} Homologation of **III-68** with bromo (or iodo) acetaldehyde diethyl acetal^{61,62} to obtain desired alkyne **III-69**, however proved low yielding under a variety of temperature and solvent conditions. The fact that bromo (or iodo) acetaldehyde diethyl acetal was fully consumed in the reaction –



Scheme III-2: Alkyne zipper reaction strategy

as detected by GC analysis and D₂O quenching experiments – suggested that β -elimination of the acetals by lithium acetylide **III-70** (Scheme III-2) might be a side-reaction resulting in lower yields.

We also attempted to prepare propargylic ester **III-72** (Scheme III-3), which upon treatment with LAH would directly provide the homoallylic alcohol **III-62** through simultaneous reduction of the alkyne and ester functionalities. Quenching of lithium acetylide of **III-68** with ethyl bromoacetate however led to decomposition.



Scheme III-3: Propargylic ester strategy

Layton has developed a method for preparation of propargylic esters (**III-71**, Scheme III-3) using trialkynylboranes.⁶³ Treatment of a lithium acetylide with $\text{BF}_3 \cdot \text{OEt}_2$ at -20°C generated the corresponding trialkynylborane which upon immediate exposure to ethyl diazoacetate and subsequent hydrolysis afforded corresponding propargylic ester (**III-71**) in high yields. This protocol was also unsuccessful in our hands. Reaction of 1-nonadecyne **III-68** led to the propargylic ester **III-72** in only 12% yield and the rest of the starting alkyne was recovered unchanged. It must however be noted that, in our case, treatment of the lithium acetylide of **III-68** with $\text{BF}_3 \cdot \text{OEt}_2$ resulted in a white precipitate, which could not be solubilized even after addition of ethyl diazoacetate. Since such precipitation has been reported in the original procedures,⁶³ we think that the organoborane species, due to the long hydrocarbon chain might be insoluble in the reaction medium.

Next, a Wittig olefination approach for the direct preparation of the *trans* homoallylic alcohol **III-62** from a long chain aldehyde was explored. Schlosser has developed a method for the synthesis of *trans*-alkenols using a modified Wittig reaction of ω -hydroxyalkyl-triphenylphosphonium bromides (Figure III-18).^{64,65} ω -Hydroxyalkyl-triphenylphosphonium bromides of varying chain lengths (**III-73**) after conversion to the

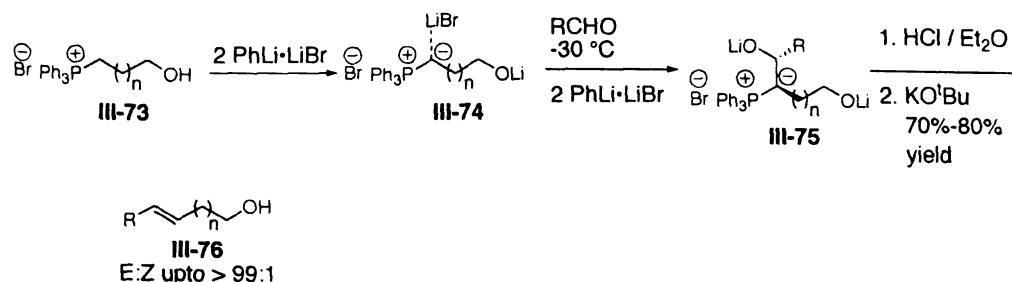
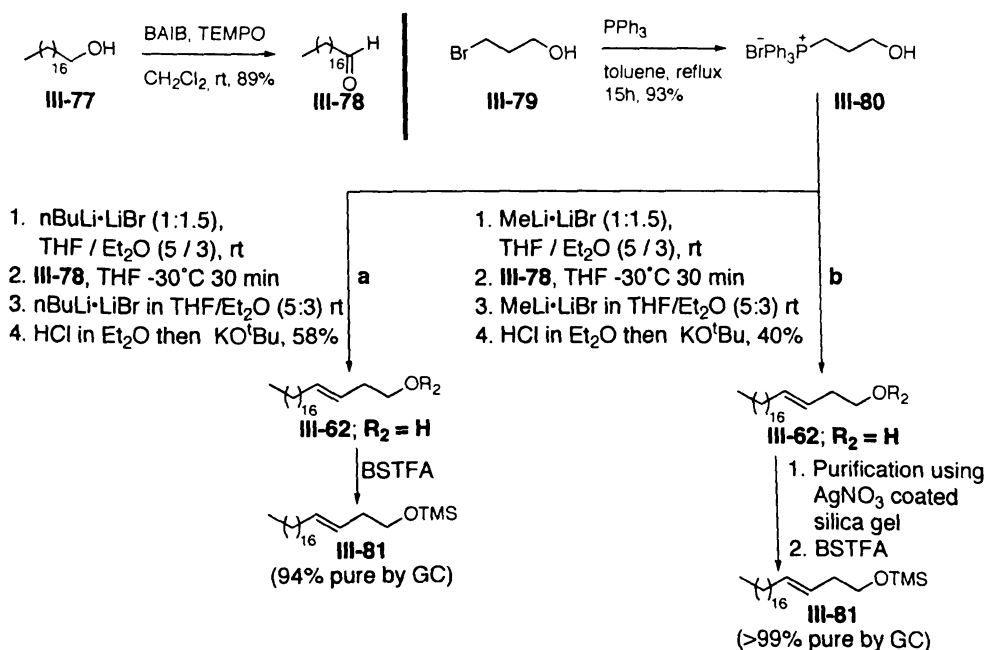


Figure III-18: Schlosser's β -oxido ylide route to *trans* alkenols

corresponding ylides **III-74** were treated with an aldehyde at low temperatures (in order to prevent decomposition of the corresponding oxaphosphetane to the olefin). Treatment of the oxaphosphetane intermediate with $\text{PhLi} \cdot \text{LiBr}$ complex lead to the formation of β -oxido ylide **III-75**, which is allowed to equilibrate to the more stable *trans* isomer. Upon reprotonation with HCl and breaking the oxaphosphetane- LiBr complex with KO^tBu , the corresponding *trans* alkenols **III-76** were isolated in good yields and high selectivity.

In order to explore the possibility of using Schlosser's modified Wittig olefination protocol in our synthesis, octadecanal **III-78** was synthesized by BAIB / TEMPO mediated oxidation of 1-octadecanol (Scheme III-4).⁶⁶ Wittig reaction of **III-78** with 3-hydroxypropyl triphenylphosphonium bromide **III-80**⁶⁷ using $n\text{BuLi} \cdot \text{LiBr}$ complex for ylide generation provided the *trans* alkenol **III-62** in 58% yield. However, we were faced with some difficulties. First, alkenol **III-62** contained minor impurities (possibly the

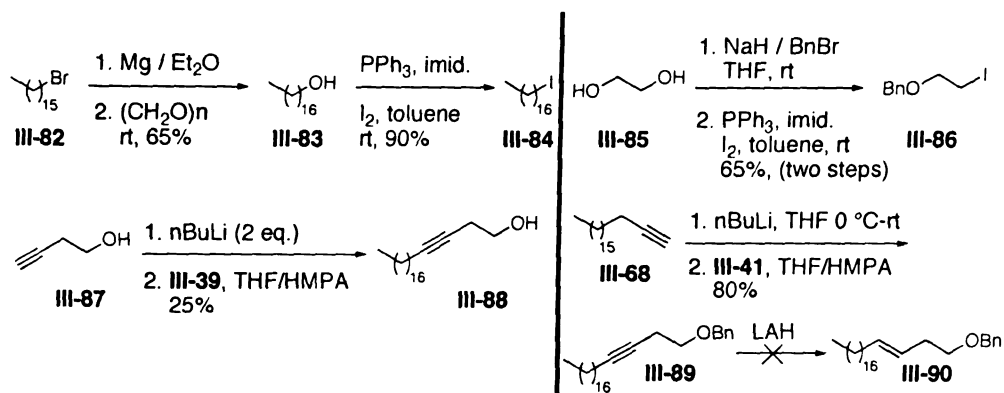


Scheme III-4: Application of Schlosser's method to synthesize *trans* alcohol **III-62**

cis isomer; as indicated by ^1H NMR), which could not be separated *via* column chromatography.* GC analysis of the TMS derivative **III-81** also showed minor impurity peaks. We did not want to proceed with isomeric mixtures at such an early stage in the synthesis. Secondly, use of THF / Et₂O (5/3) solvent mixture was reported to be critical for achieving high *trans* selectivity. Thus, while using the commercially available nBuLi in hexanes, it was necessary to remove hexanes and freshly prepare a stock solution of nBuLi•LiBr complex in THF / Et₂O (5/3) prior to the reaction. This procedure proved tedious and impractical especially for large-scale operations. When we switched to commercially available MeLi in Et₂O as the base, the desired alkenol **III-62** was obtained in lower yields (ca. 40%). Use of AgNO₃ coated silica gel for chromatography is known to facilitate separation of isomeric mixtures of unsaturated hydrocarbons.⁶⁸ Purification of the alkenol **III-62** using this technique indeed separated the impurities to furnish **III-62** in >99% purity as indicated by GC analysis of the TMS derivative **III-81**. However, the yields and efficiency of the purification technique could not be reproduced on large scales needed to bring up multigram quantities of material.

Next, we turned to the alkynylation reaction of a suitable primary iodide *via* an S_N2 displacement reaction to obtain the corresponding long chain homopropargylic alcohol that can be reduced to *trans* homoallylic alcohol **III-62**. The requisite iodide substrates **III-84** and **III-86** were prepared as shown in Scheme III-5. 1-heptadecanol **III-83** although commercially available, is expensive and was therefore prepared from 1-bromohexadecane (**III-82**) by carbon homologation.⁶⁹ After considerable experimentation, we found that the homologation worked reproducibly on large scales

* Due to the presence of the long chain alkyl groups, purification by crystallization was also not feasible.

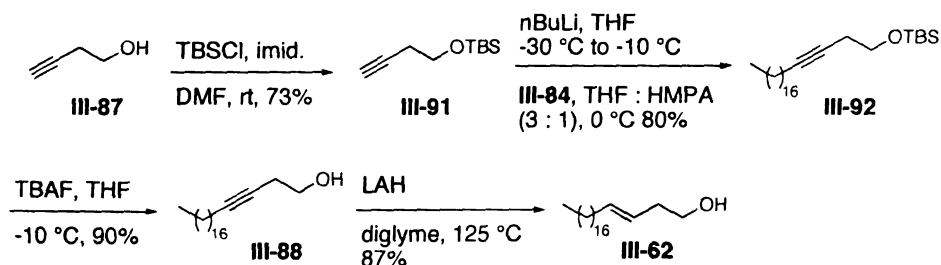


Scheme III-5: Iodide alkynylation route

(200 grams of **III-82**) only when paraformaldehyde was cracked to generate molecular formaldehyde, which was then bubbled through an ethereal solution of 1-hexadecyl magnesium bromide. Iodination of **III-83** using triphenyl phosphine and iodine furnished 1-iodo hexadecane in 90% yield. Similar iodination of mono benzyl protected ethylene glycol **III-85** provided the iodide **III-86**.

Treatment of the dianion of 3-butyn-1-ol **III-87** with iodide **III-84** produced the homopropargylic alcohol **III-88** only in low yields. Under a variety of different reaction conditions which included changing the reactant stoichiometry, solvent proportions and temperature, the yields of **III-88** went up to only ca. 25%.⁷⁰⁻⁷³ 1-octadecene – a β elimination product of the iodide **III-84** was often obtained as a side product. On the other hand, alkynylation of iodide **III-86** with 1-nonadecyne **III-68** under similar conditions (Scheme III-5), met with success and the benzyl protected homopropargylic alcohol **III-89** was isolated in good (80%) yields. Unfortunately, reduction of **III-89** to the corresponding *trans* olefin **III-90** proved difficult, even after refluxing with LAH in diglyme for several hours,⁷⁴ alkyne **III-89** was recovered unaffected. Realizing that LAH

reduction reactions of propargylic and homopropargylic alcohols containing free hydroxyl groups are more facile due to pre formation of organoaluminates,⁷⁵ we finally resorted to a somewhat lengthier route to homoallylic alcohol **III-62** (Scheme III-6).



Scheme III-6: Synthesis of *trans* homoallylic alcohol **III-62**

Thus, reaction of the lithium acetylide of TBS protected 3-butyn-1-ol **III-91** with the iodide **III-84** in THF•HMPA (3:1) at 0 °C afforded the TBS ether **III-92** in consistent yields of 80%.⁷⁶⁻⁷⁸ TBAF mediated deprotection of **III-92** provided the homopropargylic alcohol **III-88** (90%). LAH reduction of the free alcohol **III-88** delivered the homoallylic alcohol **III-62** in high yields (87%) after optimization of the work up procedure. Simply quenching the LAH reaction with 1-2 N HCl, followed by extraction of the aqueous layer,⁷⁹ afforded alcohol **III-62** only in 25%-53% yield depending upon the reaction scale. The optimized work up involved first quenching the reaction by drop wise addition of H₂O and 15% NaOH, heating the resultant mixture at 50 °C for 45 min and filtration to separate the white precipitate.⁸⁰ The precipitate so obtained was further dissolved in 1.5 N HCl (concentration of HCl was critical to ensure maximum recovery of the product) and extracted with EtOAc several times. Following this work up procedure, the alcohol **III-62** was obtained in greater than 85% yields, independent of the reaction scale. With an optimized reaction sequence and sufficient amounts of **III-62** in hand, we now focused

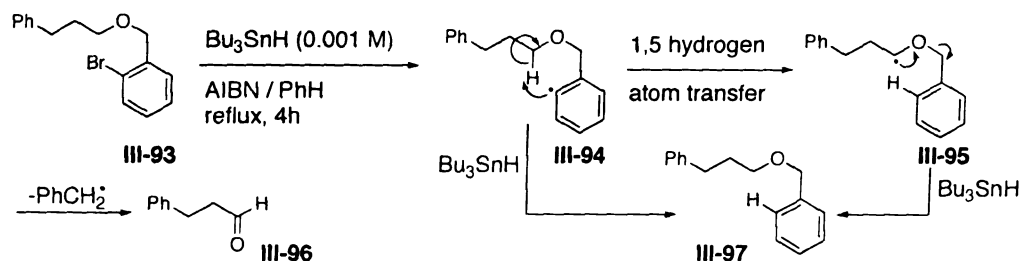
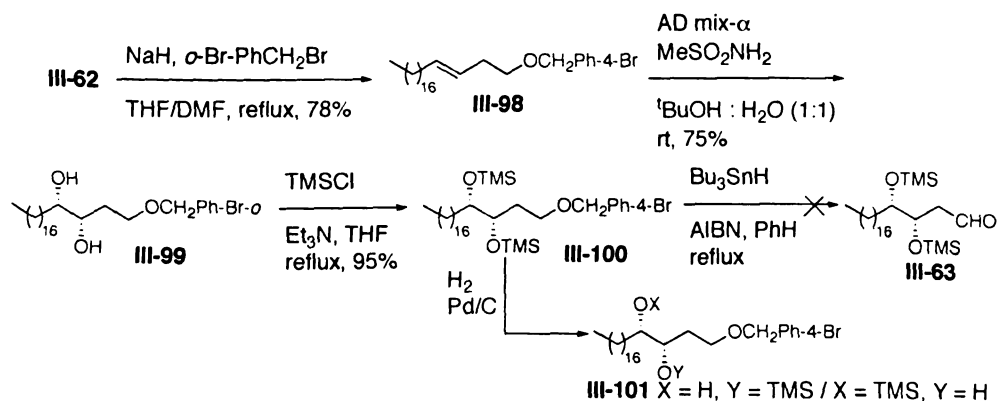


Figure III-19: Curran's self-oxidizing protecting group

our attention on further functionalization of **III-62** to chiral aldehyde **III-63**.

In 1992, Curran introduced a new class of 'self oxidizing' protecting groups.⁸¹ The concept is outlined in Figure III-19. *o*-Bromobenzyl ether of 3-phenyl-1-propanol **III-93**, when treated with Bu_3SnH / AIBN (at 0.001 M), bromine abstraction generated the aryl radical species **III-94**. After a 1,5 hydrogen atom transfer **III-94** is transformed into the α -alkoxy radical **III-95**, which upon spontaneous homolytic fission produces 3-phenyl propanaldehyde **III-96** (typical yields range from 55 to 60%). Maintaining a low concentration of Bu_3SnH is critical because trapping of **III-94** or **III-95** by hydrogen transfer from Bu_3SnH generates the reduced product (**III-97**). Thus, in the process of reductive removal of the protecting group, the substrate undergoes oxidation to the



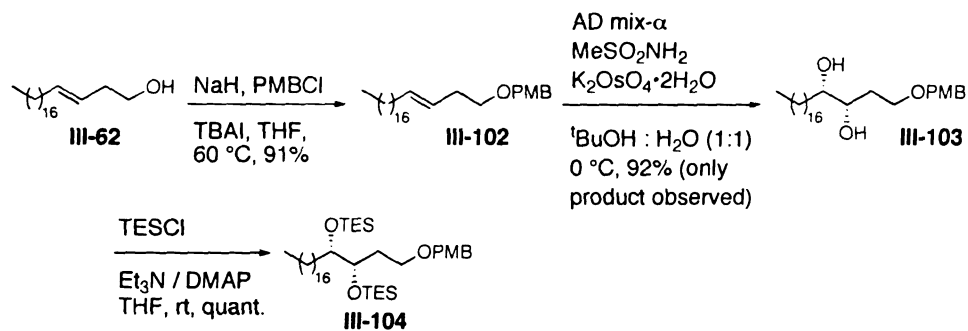
Scheme III-7: Attempted use of Curran's self-oxidizing protecting groups in our system

corresponding aldehyde. This technique seemed useful so as to cut down on the number of steps.

To test the feasibility of this tactic in our synthesis, differentially protected triol **III-100** was synthesized as shown in Scheme III-7. Protection of the homoallylic alcohol **III-62** as *o*-bromo-benzyl ether **III-98** (78% yield), Sharpless asymmetric dihydroxylation of **III-98** (75% yield) and protection of the 1,2 diol **III-99** as the bis-TMS ether (95% yield) produced the required triol **III-100**. Preliminary attempts at oxidative removal of the *o*-bromobenzyl group in **III-100**, following the reported procedures resulted only in recovery of the starting material. The necessity to use high dilutions for the oxidative deprotection reaction posed a practical limitation. In our case, a large amount of solvent was necessary for a small scale reaction (80 mL of PhH for 50 mg of the substrate) in order to maintain 0.001 M concentration, which rendered the process inconvenient especially on multigram scales. Therefore this approach was not pursued further. Also, under hydrogenolysis conditions, one of the TMS groups in **III-100** was cleaved prior to the removal of *o*-bromo-benzyl group (**III-101**).

During a separate project* it was shown that primary benzyl or *p*-methoxybenzyl ethers in triol systems similar to **III-100**, were not amenable to selective cleavage in presence of secondary bis-TMS ether groups. We therefore decided to consider using more robust TES groups to block the 1,2 diol functionality (Scheme III-8). Accordingly, PMB ether **III-102** was synthesized (NaH / PMBCl) in 91% yield. Sharpless asymmetric dihydroxylation reaction of the trans olefin **III-102** at 0 °C was slow (82%, 4 d). However when potassium osmate was added externally so as to increase the amount of

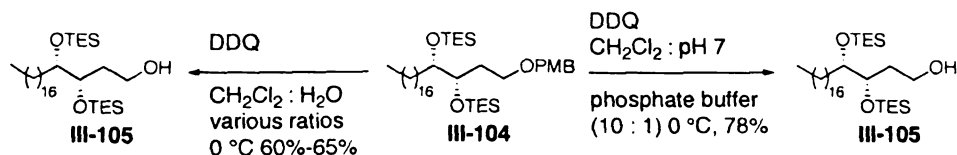
* Borhan, B.; Sivakumar, M. Unpublished results.



Scheme III-8: Synthesis of the differentially protected triol **III-104**

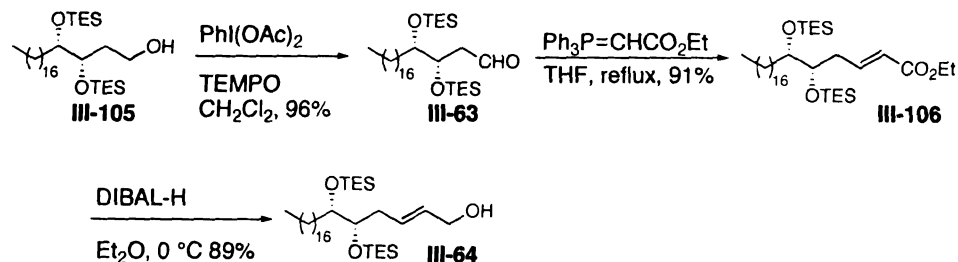
osmium to 0.1 mol%, the reaction was completed in 17 h and furnished the diol **III-103** in 92% yield.⁵⁶ Treatment of diol **III-103** with TESCl, Et₃N / DMAP, produced the differentially protected triol **III-104** in quantitative yields.

Selective deprotection of the primary PMB ether was next examined. DDQ mediated PMB cleavage using a mixture CH₂Cl₂ and H₂O in various ratios provided the alcohol **III-105** in up to 65% yields (Scheme III-9).⁸² Once again, a major side reaction was TES cleavage in addition to the PMB removal, which probably occurred due to the acidity of dichlorodicyano hydroquinone generated during the reaction. Accordingly, the use of pH 7 buffer,⁸³ led to higher yields (78%) of alcohol **III-105**. The isolated yields also depended upon the work up procedure – the optimum work up involved quenching



Scheme III-9: Selective deprotection of the PMB group in **III-104**

the reaction with NaHCO_3 and extraction with CH_2Cl_2 .^{*} With sufficient amount of the bis-TES protected triol **III-105** available, we proceeded with its further elaboration.

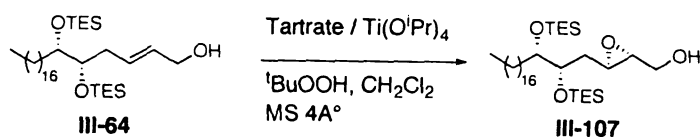


Scheme III-10: Synthesis of allylic alcohol **III-64**

Transformation of **III-105** to allylic alcohol **III-64** proceeded uneventfully (Scheme III-10). Oxidation of **III-105** by means of catalytic TEMPO and bis-acetoxyiodo benzene (BAIB) as a stoichiometric oxidant,⁶⁶ afforded aldehyde **III-63** in excellent yields. This oxidation proved more convenient and efficient with BAIB/TEMPO than conventional Dess-Martin oxidation. Wittig olefination of the aldehyde **III-63** with (carbethoxymethylene)triphenyl phosphorane in refluxing THF generated the α,β unsaturated ester **III-106** (91%) exclusively as the *trans* isomer. Finally, DIBAL-H reduction of **III-106** provided the allylic alcohol **III-64** in 89% yield.

We now directed our efforts toward manipulation of **III-64** to the epoxy sulfide **III-5**. Earlier, we had optimized the Sharpless asymmetric epoxidation conditions for allylic alcohol systems structurally related to **III-64** (Chapter I).^{14,84} Using our optimized conditions (Table **III-1**, entry 1), the epoxyalcohol **III-107** was obtained in a maximum yield of 30% (*dr* = 6.7 : 1) even after careful purification of the reagents and solvents

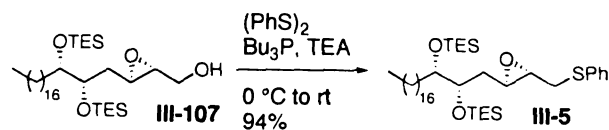
^{*} A non-aqueous workup involving filtration of precipitated salts afforded only 33% yield of product, while the use of other solvents such as EtOAc or CHCl_3 in aqueous extractions resulted in emulsions.



entry	tartrate / Ti(O ⁱ Pr) ₄ (eq. / eq. of III-20)	dr	yield (%)
1	(D)-DET / Ti(O ⁱ Pr) ₄ (5.0 / 3.6)	6.7 : 1	29
2	(D)-DET / Ti(O ⁱ Pr) ₄ (1.2 / 1.0)	4.2 : 1	35
3	(D)-DET / Ti(O ⁱ Pr) ₄ (0.24 / 0.2)	2.5 : 1	68
4	(D)-DIPT / Ti(O ⁱ Pr) ₄ (0.24 / 0.2)	8.3 : 1	67
5	(D)-DIPT / Ti(O ⁱ Pr) ₄ (0.6 / 0.5)	10 : 1	70
6	(D)-DIPT / Ti(O ⁱ Pr) ₄ (1.2 / 1.0)	100 : 1	73

Table III-1: Optimization of the Sharpless asymmetric epoxidation of **III-64**

and utilizing several different work up procedures. Upon decreasing the reagent stoichiometry (entries 2 and 3), the yields went up but only at the cost of the diastereoselectivity. Since the diastereomers were not amenable to separation by column chromatography or crystallization techniques, we decided to maximize the diastereomeric ratios. Epoxidation using catalytic (D)-DIPT instead of (D)-DET (entry 4) significantly improved the diastereoselectivity while keeping the yields high enough for material throughput. With 50% catalyst (entry 5) the diastereoselectivity further increased and gratifyingly, use of a complete equivalent of the catalyst (entry 6) afforded the desired triol **III-107** in excellent diastereomeric ratio (100:1) and good yields (73%). Next, treatment of **III-107** using (PhS)₂ and Bu₃P⁸⁵ efficiently installed the thiophenyl pendant group in one step (Scheme III-11) which provided us with large amounts of epoxysulfide



Scheme III-11: Use of the Hata reagent to install the thiophenyl pendant group

III-5 to further explore the proposed synthetic scheme.

At this point, it is appropriate to discuss the rationale behind our choice of thiophenyl as the directing group. Our total synthesis, by design, called for an *endo* selective epoxide opening of a suitable epoxydiol (**III-108**, Figure III-20) to access the THF diol with appropriately positioned hydroxyl groups (**III-109**) and a functional group handle (X) for further elaboration to bis-THF **III-110**.

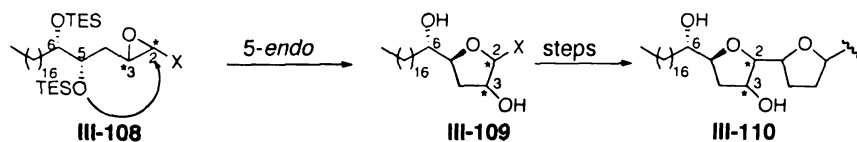


Figure III-20: An *endo* selective epoxide opening of **III-108** to generate 3-hydroxylated trisubstituted THF **III-109**

From our earlier studies (Chapter I), two such directing groups, namely, vinyl and thiophenyl, had emerged that led to *endo* selective epoxide opening. Vinylic epoxide opening reactions involved inversion of configuration at the reactive epoxide carbon whereas ring opening of epoxysulfides resulted in a net retention at the point of cyclization. The major pathway followed in $\text{BF}_3 \cdot \text{OEt}_2$ mediated simultaneous silyl deprotection / epoxide opening reaction of epoxy sulfide systems such as **III-111** (Figure III-21) involved the generation of episulfonium intermediates (**III-112**). These reactive intermediates spontaneously cyclized to produce five membered rings (referred to as THF

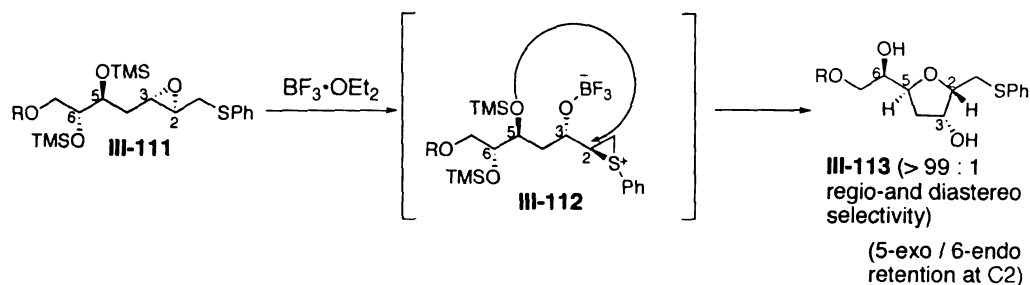


Figure III-21: Cyclization of an epoxy sulfide derived from 2-deoxy-D-ribose (Chapter I)
via episulfonium ion formation

diols) in very high regio- and stereoselectivities (>99%). The THF diols so generated retained (*via* a double inversion) the configuration at C2 (**III-113**). To sum up, during cyclization of an epoxydiol such as **III-108** (Figure III-20), configurations at C1 and C2 in the product **III-109** are determined by (i) the geometry and stereochemistry of the epoxide and (ii) the mode of epoxide opening (inversion vs. net retention at the reactive carbon).

In our case, *trans* allylic alcohol **III-64** was selected as the asymmetric epoxidation precursor since in general, 3-*E* allylic alcohols have been shown to provide the corresponding epoxy alcohols in higher enantiomeric purity than their 3-*Z* counterparts.⁸⁶ With this choice of the double bond (hence the epoxide) geometry, either the 2*R*,3*R* (**III-107**, Figure III-22) or the 2*S*,3*S* epoxy alcohol (**III-114**) could be accessed by appropriate choice of the tartrate reagent. Furthermore, in order to generate a THF diol having 2,3 *cis* relative configuration (**III-65** or **III-115**), the *endo* selective epoxide opening of either of the precursors **III-107** or **III-114** would have to proceed *via* net retention at C2. As described earlier, out of the two *endo* directing groups, viz., vinyl and thiophenyl (Chapter I) only the latter retains the stereochemistry of the carbon atom at the

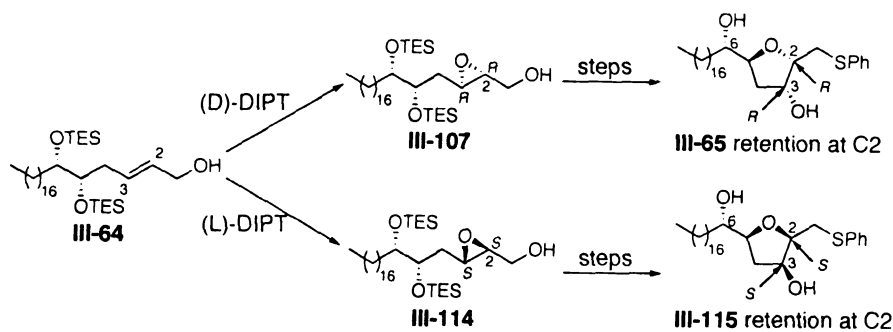


Figure III-22: Stereoisomeric THF diols originating from *trans* alcohol **III-64**

point of cyclization. Finally, of the two epoxides **III-107** and **III-114**, only **III-107** would provide the requisite 2,3-*cis*-5-*trans* relative configuration (**III-65**) across the THF ring.

A THF diol system stereochemically akin to **III-65** but containing a vinyl functional group (**III-119**, Figure III-23) could potentially be accessed from the *cis* vinylic epoxide **III-118** via preferential nucleophilic attack at C2. However, as mentioned earlier, *cis* epoxy alcohols (**III-117**) may not be obtained in high diastereoselectivity using the Sharpless asymmetric epoxidation reaction.⁸⁶ Another complication associated with intramolecular *endo* opening of *cis* vinylic epoxides in general, is that due to steric interactions between the π system and the incoming nucleophile (**III-118**, Figure III-23), the π -bond may not remain aligned parallel to the empty p orbital of the incipient carbocation.⁸⁷⁻⁸⁹

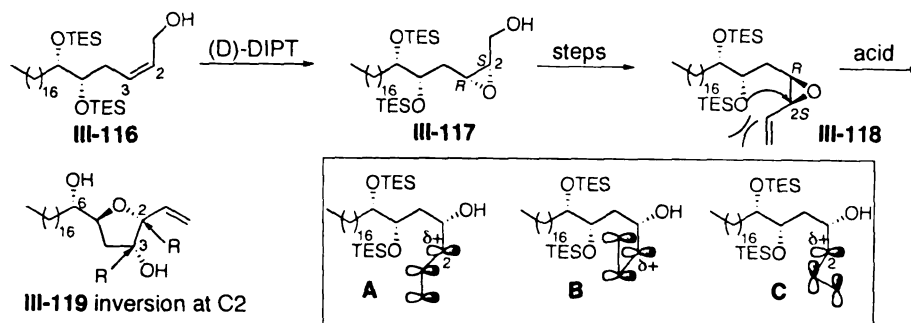


Figure III-23: *Cis*-vinylc epoxide may exhibit reduced *endo*-selectivity during intramolecular cyclization reaction

Thus, the two conformations **A** and **B**, in which the π -bond resides parallel to the p-orbital at C2 would be higher in energy due to the proximity of the π system to the incoming nucleophile. This steric barrier is reduced when the π system rotates away (conformation **C**) which, however, causes loss of π -overlap and hence the carbocation stabilization at C2. This phenomenon is likely to diminish *endo* selectivity in case of *cis* vinylc epoxide opening reactions. Therefore, we anticipated that this tactic would not be applicable in our synthesis.

Taken together, our strategy of using the *trans* epoxysulfide **III-5** as the cyclization precursor was benefited by the fact that **III-5** could be obtained in very high diastereomeric ratios from allylic alcohol **III-64** and that the possibility of any steric interference to cyclization *via* episulfonium formation (as discussed above for the vinyl epoxide case) was minimized.

The stage was now set to investigate the *in situ* deprotection / cyclization reaction of epoxy sulfide **III-5**. When **III-5** was treated with $\text{BF}_3 \cdot \text{OEt}_2$ under previously optimized conditions (Scheme III-12),¹⁴ two sets of products (**III-65** and **III-120**, separable by

colat

to III

2.3-

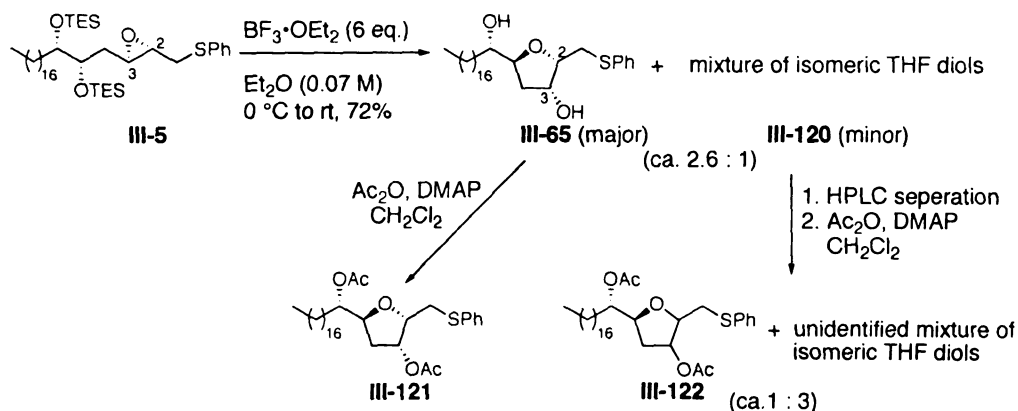
Stets

e

i

s

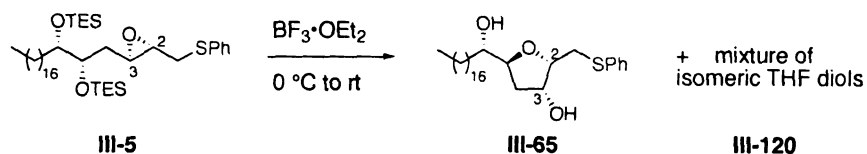
column chromatography) were isolated. The major product, **III-65**, after per-acetylation to **III-121** was shown to be an *endo* selective epoxide opening product having the desired 2,3-*cis*-5-*trans* relative stereochemistry about the THF ring. The structure and relative stereochemistry of **III-121** was established by means of 2D COSY and 1D NOESY



Scheme III-12: $\text{BF}_3 \cdot \text{OEt}_2$ mediated cyclization of the epoxy sulfide **III-5** using previously optimized conditions

experiments. ^1H NMR of the minor product **III-120** (ca 20%) revealed a mixture of isomeric THF diols, which were separable into two fractions by HPLC. The minor fraction (5%) was a single isomer whereas the major portion (15%) was again a mixture of at least two isomeric THF diols (as judged by ^1H NMR). COSY analysis of the per-acetate derivative of the minor fraction suggested another *endo* epoxide opening product (**III-122**). However, no conclusive information regarding the relative stereochemistry of **III-122** could be obtained using 1D NOESY experiments due to overlapping signals. More rigorous stereochemical assignment of **III-122** or structure analysis of the other 15% fraction was not pursued. No further improvement in the *endo* selectivity could be accomplished by varying solvents, concentration or the stoichiometry of $\text{BF}_3 \cdot \text{OEt}_2$ (Table

III-2). Overall, cyclization reaction of **III-5** was clearly not as *endo* selective as that of the original epoxysulfide systems (**III-108**, Figure III-20 and Chapter I).



entry	Solvent (concentration)	BF ₃ •OEt ₂ (eq.)	III-65 : III-120
1	Et ₂ O (0.07 M)	3	2.5 : 1
2	Et ₂ O (0.04 M)	6	2.8 : 1
3	CH ₂ Cl ₂ (0.07 M)	3	trace : major
4	CH ₂ Cl ₂ (0.04 M)	6	trace : major

Table III-2: Cyclization of **III-5** under various conditions

We next tried to understand the reduced regioselectivity in the cyclization of **III-5** and rationally design experiments to improve the same. In order for our strategy (see Figure III-21 and accompanying discussion) to be successful, epoxysulfide **III-121** must rearrange to the episulfonium intermediate (**III-122**) and the major product must arise from intramolecular trapping of **III-122**. However, it is also possible that the pathway involving direct opening of the epoxide at C3 is kinetically competitive with that involving intermediacy of the episulfonium ion (opening at C2).

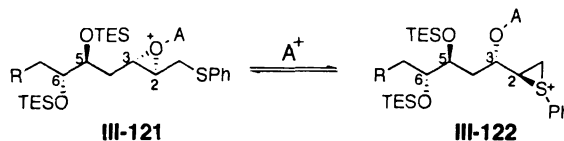


Figure III-24: Payne like equilibration of epoxy sulfide **III-121** under acidic conditions

The

Fig

epi

ep

m

I

s

t

s

This raises the possibility that an acid catalyzed Payne rearrangement-like equilibrium (Figure III-24) may be operative between the activated epoxide (**III-121**) and the episulfonium ion (**III-122**).

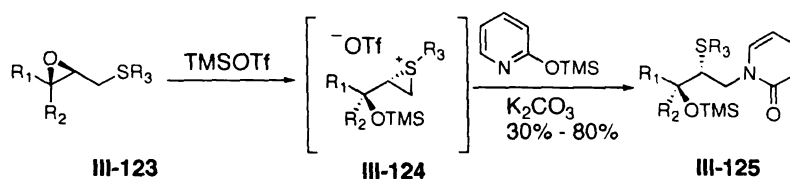


Figure III-25: Rayner's conditions for intermolecular trapping of episulfonium ions

Rayner and co-workers in their studies involving intermolecular trapping of episulfonium ions by nitrogen nucleophiles have suggested that a Payne like equilibration may not be involved.⁹⁰ They proposed that the starting epoxy sulfide (**III-123**, Figure **III-25**) is completely converted to the reactive episulfonium ions (**III-124**), which is subsequently trapped by the external nucleophile. Although the major products isolated in their experiments (for example **III-125**) were *via* trapping of episulfonium ion intermediates, the possibility of an equilibrium between **III-124** and activated **III-123** cannot be ruled out. Thus, the same result would be obtained if the trapping of episulfonium **III-124** with the nucleophile were much faster than of the activated epoxide. In this scenario, the presence of this Payne-like equilibrium would be inconsequential to the product distribution.

Should a Payne-like equilibrium exist in our system, the outcome of the cyclization event would depend upon which of the two activated species, **III-121** or **III-122** (Figure III-26) is trapped faster and that in turn, would be dictated by which of the two hydroxyl groups C5-OH or C6-OH is more available for nucleophilic attack. Thus, in this scenario, three different routes (**a**, **b** or **c**, Figure III-26) leading to three

isomeric products, **III-126** (5-*exo*), **III-127** (5-*endo*) and **III-128** (6-*endo*) are available. Since, in course of our previous studies (Chapter I) products resulting from attack on the less substituted carbon of the episulfonium ion were not observed, those pathways are not shown in Figure III-26. On the other hand, if the starting epoxy sulfide is completely converted into the reactive episulfonium intermediate **III-122** prior to cyclization, only pathways, **b** and **c** are accessible. In either scenario, the major product will be decided by which of the two nucleophiles (C5-OH or C6-OH) is more available for cyclization.

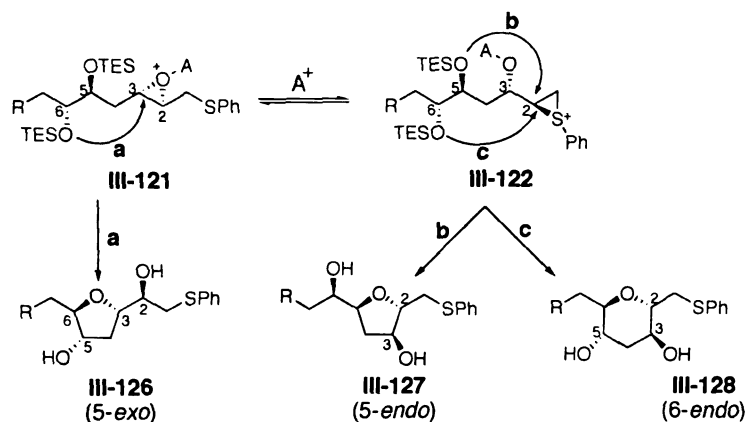


Figure III-26: Possible route for cyclization of epoxy sulfides under acidic conditions;

endo / *exo* notation is relative to epoxide.

Assuming that the hydroxyl groups must be freed from silyl blocking groups prior to cyclization, their availability would be determined by the relative rates of silyl deprotections. The facility of silyl group removal is governed mainly by their nature and the steric environment, which precisely are the major structural differences between our earlier 2-deoxy-D-ribose derived epoxy sulfide **III-129** (Chapter I) and the epoxy sulfide **III-5** (Figure III-27).

in I

the

as

set

tu

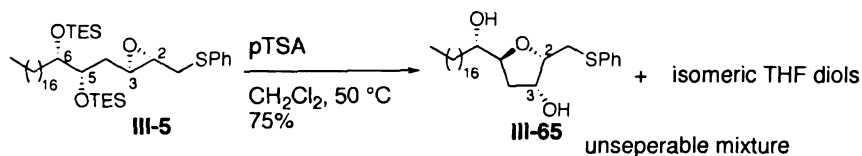
II

O

C

P

The following experiments provided more evidence in that direction. Epoxy sulfide **III-130** containing free hydroxyl groups was prepared in order to decouple the silyl removal and epoxide opening events (Scheme III-13). Exposure of **III-130** to $\text{BF}_3 \cdot \text{OEt}_2$ under the same reaction conditions (Scheme III-12) again afforded a mixture of **III-65** and **III-120** in about the same proportion. We also reprotected the hydroxyl groups as TMS ethers (**III-131**) thinking that TMS groups might provide the right balance of relative rates of silyl deprotection and episulfonium formation. However, treatment of **III-131** with $\text{BF}_3 \cdot \text{OEt}_2$ also produced the same mixture of products. Thus, considering these experiments, a possible explanation for the reduced *endo* selectivity in the cyclization of **III-5** might be that the C6-OH is sterically less hindered and hence more available as a nucleophile (than C6-OH in **III-129**) thereby diverting the reaction along the undesired pathways.

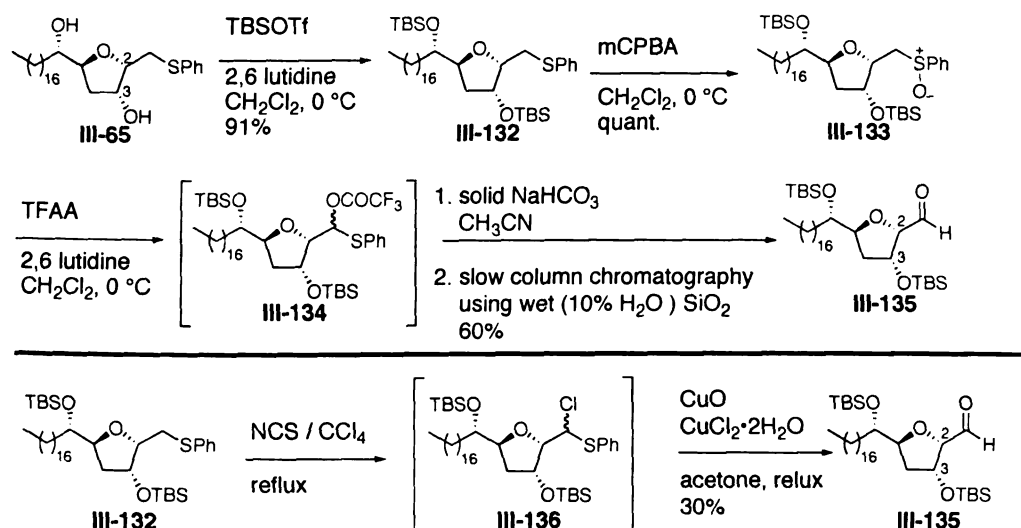


Scheme III-14: Another attempt to improve the *endo* selectivity in the cyclization of

III-5

In a separate project,⁹¹ it was shown that epoxy sulfide **III-129** upon heating with pTSA in CH_2Cl_2 at 50 °C also produced the *endo* selective cyclized product *via* episulfonium formation in high selectivity (ca. 19 : 1). When **III-5** was treated with pTSA under those conditions (Scheme III-12), the desired THF diol **III-65** was produced apparently in higher yields (75% vs. earlier yields of 56%) but unfortunately, even after purification the product contained inseparable isomeric impurities (ca. 20% as judged by

^1H NMR). Since we did not want to proceed with isomeric mixtures at this point in the total synthesis, we decided to go with the conditions that produced the desired product **III-65** in highest selectivity and purity (entry 2, Table **III-2**). The isolated yield (56%) of **III-65** under these conditions was acceptable for purposes of bringing up more material for the total synthesis. Moreover, **III-65** could be easily separated from other isomeric THF products by flash column chromatography.



Scheme III-15: Preparation of the aldehyde **III-135**

Equipped with large amounts of THF diol **III-65**, we set out to investigate its transformation to the key allylic alcohol **III-3**. Scheme III-15 outlines further manipulation of the THF diol **III-65**. TBS protection of **III-65** using more reactive TBSOTf as the silylating agent (reaction using TBSCl was incomplete after 24 h) proceeded smoothly in 91% yield to afford bis-TBS ether **III-132**, which was now set up for a Pummerer rearrangement to install the aldehyde functionality.^{92,93} The rearrangement was carried out in two different ways. First, using conventional Pummerer rearrangement conditions,^{92,93} the phenyl sulfide **III-132** was oxidized to the

center

when

III.

at the

to the

age

Na

W

at

pl

h

P

C

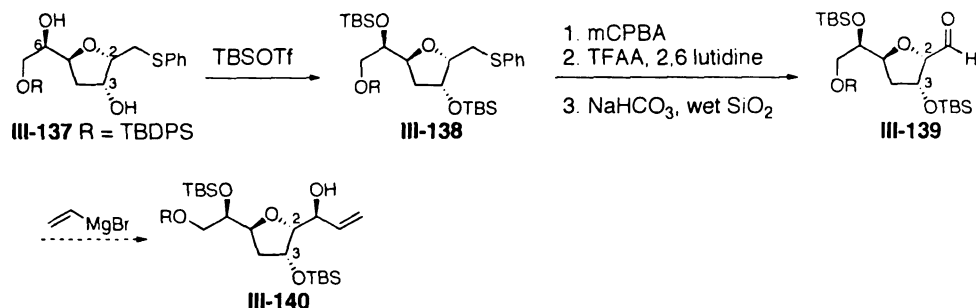
.

corresponding sulfoxide **III-133** by dropwise addition of a CH_2Cl_2 solution of mCPBA which proved critical to avoid over oxidation of **III-132** to sulfone. The crude sulfoxide **III-133** was next treated with TFAA in presence of 2,6 lutidine to obtain the α -trifluoroacetoxy phenyl sulfide **III-134**. Hydrolysis of the rearranged product **III-134** to the aldehyde **III-135** proved tricky. Treatment of **III-134** with a variety of hydrolyzing agents^{94,95} including sat. aq. NaHCO_3 , aq. CuCl_2 , aq. HgCl_2 , wet SiO_2 , 5% HCl , and Na_2CO_3 in MeOH either led to incomplete hydrolysis or decomposition of the material. While the hydrolysis conditions were being explored another route to obtain the desired aldehyde **III-135** was examined. The sulfide **III-132** was directly converted to α -chloro phenyl sulfide **III-136** by treatment with NCS in refluxing CCl_4 , which was then hydrolyzed using cupric salts in acetone.^{96,97} This Pummerer like rearrangement however provided the aldehyde **III-135** in only 30% yield. We then refocused our attention to the α -trifluoroacetoxy phenyl sulfide **III-134** to further explore its hydrolysis. Ultimately, we found that treatment of a CH_3CN solution of **III-134** with solid NaHCO_3 for 18 h followed by slow elution of the product on a wet silical gel (10% H_2O) column provided the aldehyde **III-135** in 60% yield.

a) Synthesis of a model allylic alcohol

We had planned to access the target allylic alcohol **III-3** *via* a 1,2 chelation controlled addition of vinyl magnesium bromide to the aldehyde **III-135**. With the requisite aldehyde available, we were only a step away from **III-3**. In order to extensively investigate the proposed regioselective intermolecular epoxide opening strategy (Figure

III-2), we needed sufficient amount of the allylic alcohol **III-3** in hand. At this point, instead of bringing up more material to acquire adequate quantities of **III-3**, we decided



Scheme III-16: Synthesis of a model aldehyde **III-139**

to switch to a model allylic alcohol (**III-140**, Scheme III-16), which could be obtained *via* a shorter reaction sequence. THF diol **III-137** (derived from 2-deoxy-D-ribose) was available from our earlier studies (Chapter I). Structurally (constitution and stereochemistry), **III-137** is akin to the real THF diol **III-65** (Scheme III-12), the only differences being the stereochemistry at C6 and an alkoxy methyl side chain, instead of the long alkyl chain. Since these differences reside in the side chain remote to the reacting end of the allylic alcohol, we thought that **III-137** would serve as an appropriate model THF diol. The aldehyde **III-139** was synthesized from **III-137** using the same transformations as before (Scheme III-16).

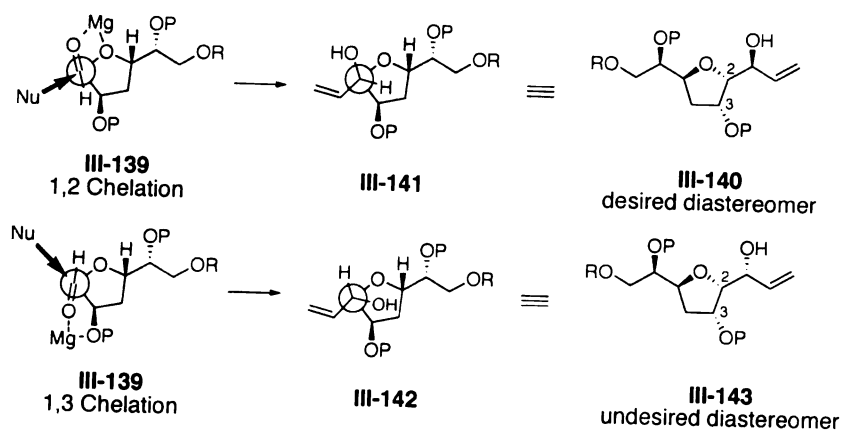
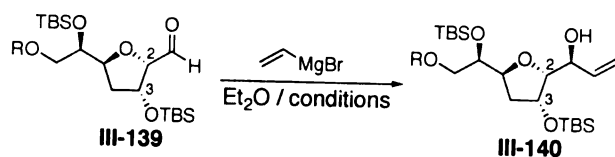


Figure III-28: 1,2 vs. 1,3 Chelation control in addition of vinyl magnesium bromide to aldehyde **III-139**

We then turned to investigate the addition of vinyl magnesium bromide to aldehyde **III-139** to prepare model allylic alcohol **III-140**. 1,2 Chelation controlled addition of organometallic reagents across α -tetrahydrofuranyl aldehydes is well preceded in the acetogenin literature.⁹⁸⁻¹⁰⁰ In our case, in addition to a 1,2 chelation, 1,3 complexation of the aldehydic oxygen with the ring hydroxyl group was likely to occur during organometallic addition reactions.¹⁰¹ As shown in Figure **III-28**, 1,2 chelation (**III-141**) would lead to the desired diastereomer of the allylic alcohol **III-140**, whereas 1,3 complexation (**III-142**), due to attack on the opposite face of the aldehyde would produce the unwanted diastereomer **III-143**, epimeric at the newly formed stereocenter. Thus, to minimize any potential 1,3 chelation event, bulky TBS groups were used to protect the hydroxyl groups in **III-139**.



conditions	yield (%)	dr
MgBr ₂ •OEt ₂ , 0 °C, 2 h	57	7 : 1
-20 °C to -30 °C, 1 h	68	10 : 1
-40 °C, 2 h	80	10 : 1

Table III-3: Synthesis of model allylic alcohol **III-140**

After some experimentation (Table III-3), the desired allylic alcohol **III-140** was obtained in high diastereoselectivity (10:1) and yields (80%). The absolute configuration of **III-140** at the newly formed stereocenter was established by Trost's *O*-methyl mandelate analysis¹⁰² (absolute configuration assignment of chelation controlled addition products of the real aldehyde **III-135**, using Trost and Mosher ester analysis is discussed in detail in Chapter IV)

b) Determination of the enantiomeric excess and the absolute configuration of diol **III-59**

As mentioned earlier (Scheme III-12), the relative configuration of the THF diol **III-65** (which would eventually become the hydroxylated THF portion (C13-C37) of mucoxin, was established by 1D NOESY analysis. Since all the stereocenters in **III-65** originated from asymmetric transformations, we decided to independently confirm the stereochemical outcome of the asymmetric dihydroxylation. For this purpose, the diol **III-103** (Figure III-29) was chosen. **III-103** was obtained from *trans* diol **III-102** via a

Sha

Sha

asy

qua

att

(F

dis

Sharpless asymmetric dihydroxylation reaction (Scheme III-8). According to the Sharpless mnemonic device (Figure III-29) for predicting the enantioselectivity in the asymmetric dihydroxylation reaction,⁵⁶ the northeast (NE) and the southwest (SW) quadrants are more open to the olefin substituents. The SW quadrant is considered an attractive area for large aliphatic groups. If the olefin **III-102** is positioned accordingly (Figure III-29), AD-mix α should react from the bottom face, leading to the desired *S,S* diol **III-103**. The

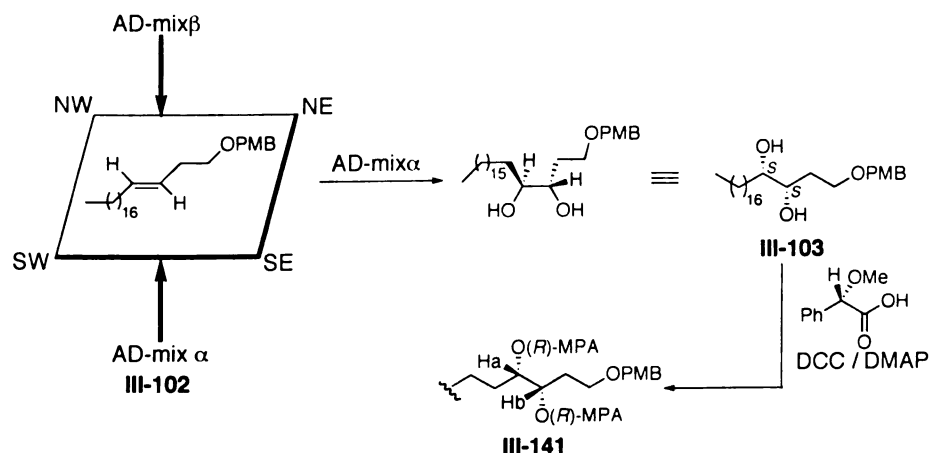


Figure III-29: Mnemonic device for Sharpless asymmetric dihydroxylation reaction as applied to *trans* olefin **III-102**

% ee of **III-103** was determined after its derivatization to the bis-(*R*)-MPA ester **III-141**. ¹H NMR of **III-141** showed only one set of H_a, H_b protons indicating that diastereomeric ratio of **III-141** was >98:2.

In order to independently confirm the absolute configuration of diol **III-103**, we decided to use exciton coupled circular dichroism (ECCD) spectroscopy. Use of ECCD for determination of the absolute configuration of 1,2 and 1,3 diols is well preceded.^{103,104} For this purpose, the diol is first derivatized to install chromophoric

groups at the chiral centers in question. A chromophore, when exposed to circularly polarized light, undergoes electronic excitation. When two such chromophores are close in space, their electronic transition dipole moments interact through space. Consequently, the excited states of the individual chromophores split each other resulting in two excited states having different energy levels for the system as a whole. The CD spectrum of such a coupled chromophoric system becomes bisignate or a 'split' CD. The split CD either shows a positive signal at longer wavelength and a negative signal at shorter wavelength (termed as a positive couplet), or vice versa (negative couplet). A positive CD couplet results from chromophores arranged in positive helicity. A positive helical system, in turn, is defined as one in which the transition dipole moments of the two interacting chromophores are oriented in a clockwise manner going from the front to the back chromophore (Figure III-30).

One of the most common chromophores used for the derivatization of diols is *p*-dimethylamino benzoate group. This group has a large coefficient of absorption ($\epsilon = 28,200$ (CH_3CN); $\lambda_{\text{max}} = 307$ nm), which could lead to strong CD signals. Also, its transition dipole (La, Figure III-30) is oriented parallel to the C-O bond and since the

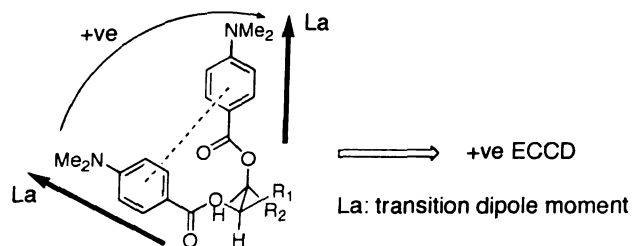


Figure III-30: A positively helical system comprises of two interacting chromophores twisted in a clockwise direction going from the front to the back chromophore

twi

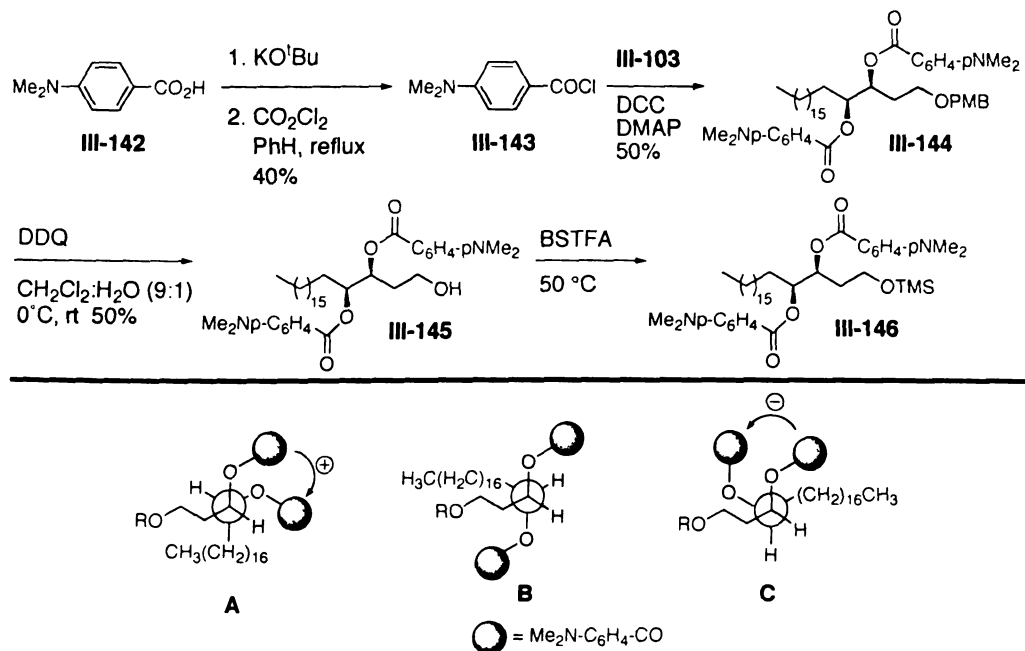
sp-

con

re-

in

twist of the adjacent transition dipoles in turn directly correlates to the sign of the ECCD spectrum, the absolute sense of twist between the vicinal C-O bonds (absolute configuration of the diol) can be predicted from the sign of the ECCD spectrum. The requisite di-benzoate derivative **III-144** was synthesized from the diol **III-103** as shown in Scheme III-17.¹⁰⁵



Scheme III-17: Synthesis of dibenzoate derivatives of the diol **III-103** for ECCD analysis

Out of the three possible staggered conformations (**A**, **B** and **C**) of such a di-benzoate system, **B** is ECCD inactive since the angle between the two transition dipoles is 180°. Conformation **A** bears two gauche interactions and therefore would be lower in energy than **C**, which involves three such interactions. The transition dipoles in the predominant conformation **A** are oriented in a clockwise direction going from the front to the back chromophore and should lead to a positive ECCD signal. Thus, if the absolute

configuration of the original diol is *S,S*, its di-benzoate derivative is expected to produce a positive ECCD signal. With **III-144** in hand we now initiated the ECCD analysis. Unfortunately, no distinct ECCD spectrum was observed for **III-144** in various solvents (CH_2Cl_2 , MeCy and MeCN). We thought that the PMB group might also be behaving as a chromophore causing additional dipole interactions with that of the two benzoate groups. The PMB group, therefore was deprotected to generate the free alcohol **III-145**. The ECCD sign in case of **III-145** was found to be solvent dependent. In polar solvents such as MeCN and CH_2Cl_2 : MeOH (1 : 1) a positive spectrum was obtained while in less polar CH_2Cl_2 , the sign switched to negative. It is likely that the free hydroxyl group in **III-145** developed intra / intermolecular hydrogen bonding with the *p*-dimethylamino benzoate groups thereby affecting the stability and population of the conformations. Moreover, the extent of such hydrogen bonding possibly is dependent on the polarity of solvents. Ultimately the TMS ether **III-146** provided consistent results. In a range of solvents, a positive ECCD was observed. A representative spectrum of **III-146** in MeCN is shown in Figure III-31. Thus, the *S,S* configuration of diol **III-103** was confirmed.

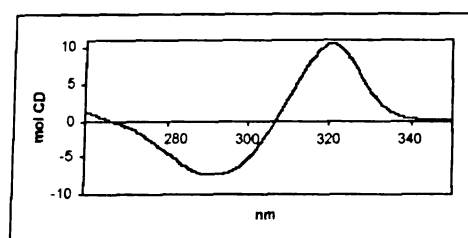


Figure III-31: ECCD spectrum of **III-146** in MeCN

2. Synthesis of vinylic epoxide **III-4**

With model allylic alcohol **III-104** in hand, our next goal was the vinylic epoxide **III-4**. Epoxide opening reactions, in general are facile under acid catalyzed conditions.

W.

ep

un

ac

th

4

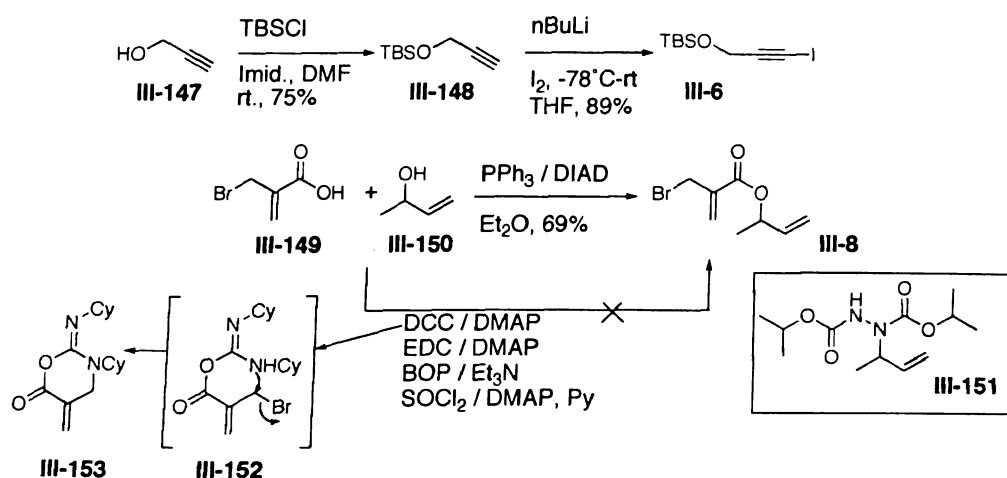
l

I

v

We anticipated that **III-4**, due to carbocation stabilizing vinyl group adjacent to the epoxide moiety, could be activated under mildly acidic conditions^{42,55} and that the α,β – unsaturated ester functionality at the other end should be compatible with such mild acidic medium. As described earlier (Figure **III-2**), we planned to employ Knochel's three component coupling protocol to build the carbon skeleton of the target epoxide **III-4**.²⁰ Retrosynthetically, **III-4** was broken down into three fragments, alkynyl iodide **III-6**, 1,4-diiodobutane **III-7** and (bromomethyl) acrylate **III-8**. Iodide **III-6**¹⁰⁶ and acrylate **III-8**¹⁰⁷ are easily accessible, whereas 1,4-diiodobutane **III-7** is commercially available.

Lithium acetylide of the TBS protected propargyl alcohol (**III-148**) was quenched with I_2 to efficiently obtain the alkynyl iodide **III-6** (67% overall yield Scheme **III-18**). Synthesis of the (bromomethyl) acrylate **III-8** on the other hand proved problematic. Mitsunobu esterification of (bromomethyl) acrylic acid (**III-149**) with 3-buten-2-ol (**III-150**) has been reported to provide acrylate **III-8** in 70% yield.¹⁰⁷ However, initially we only obtained **III-8** in about 30 – 35% yield.



Scheme III-18: preparation of the three component coupling partners, **III-6** and **III-8**

red

im

A-

w

W

a

A

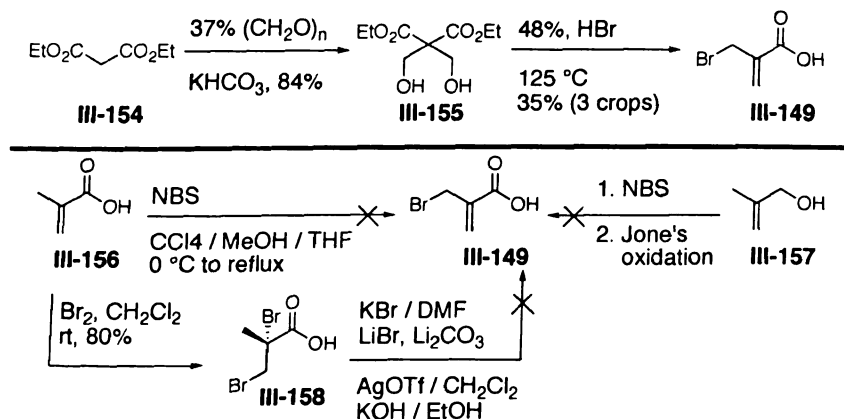
y

t

c

Several Mitsunobu esterification conditions^{28,108} including different solvents, reagent stoichiometry and order of reagent-addition were examined, but did not lead to improved results. During this exploration, a common side product **III-151** (formed by *N*-alkylation of DIAD) was observed. Such *N*-alkylation of diazoesters is known to occur when the acid component is less reactive due to steric bulk or weak nucleophilicity.¹⁰⁹ We were finally, able to obtain a consistent yield (69%) of **III-8** by drop wise addition of an ethereal solution of **III-150** and PPh_3 to a solution of **III-149** and DIAD in ether. Meanwhile, several other esterification reactions involving DCC, EDC, BOP and SOCl_2 were also attempted without any success. Interestingly, in the DCC coupling reactions, the cyclized product **III-153** was cleanly obtained probably *via* an intramolecular displacement of allylic bromide in the DCC-acid complex **III-152**.

(Bromomethyl) acrylic acid **III-149** was prepared following a reported procedure (Scheme III-19).¹¹⁰ Thus, diethyl malonate **III-154** was transformed into the diol **III-155** *via* treatment with formalin solution; **III-155** upon heating with aq. HBr afforded **III-149**



Scheme III-19: Synthesis of bromomethylacrylic acid **III-149**

in a

pre

in

br

at

ll

to

c

e

s

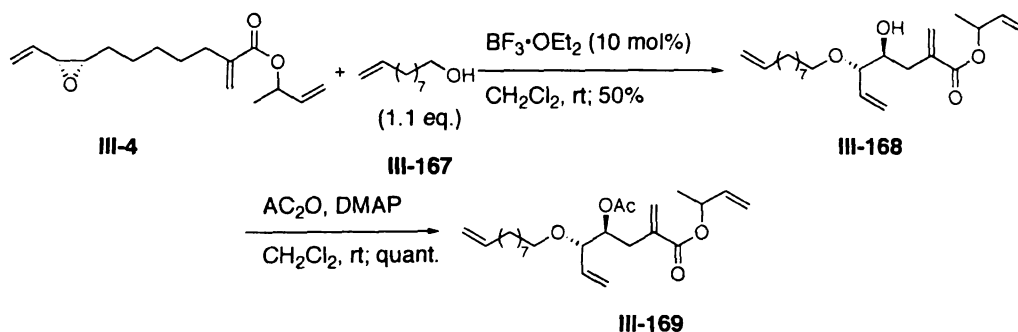
in acceptable yields. Since tedious crystallization was necessary to recover the product prepared using this protocol, we also investigated alternate routes to **III-149** (summarized in Scheme III-19). However, both radical bromination (**III-156** and **III-157**)^{111,112} and bromine addition / elimination (**III-58**)¹¹³⁻¹¹⁵ were unsuccessful.

The three component coupling reaction involved sequential, one pot coupling of alkynyl iodide **III-6** and (bromomethyl) acrylate **III-8** with diiodide **III-7** (Scheme III-20). Treatment of **III-7** with activated metallic zinc at 40 °C and subsequent exposure to CuCN•LiCl complex generates putative bis-heterobimetallic species **III-159**. The organocopper end of **III-159** being more reactive, preferentially couples with the first electrophile **III-6** at low temperatures (-60 °C to -35 °C); the acrylate **III-8**, added second then couples with the organozinc portion to provide the highly functionalized intermediate **III-160** in good yield (45%).^{116,117} It must be pointed out that use of anhydrous pentane as a co-solvent was essential to obtain reasonable (40 to 50%) yields. The yields obtained in our system, albeit lower than in Knochel's systems (60 – 80%), were acceptable since the entire carbon skeleton of the right hand fragment was installed in a single step.

corresponding aldehyde **III-165** (89%) and subsequent Wittig olefination of **III-165** (70%) to secure the target vinylic epoxide **III-4**.

3. Attempted intermolecular epoxide opening

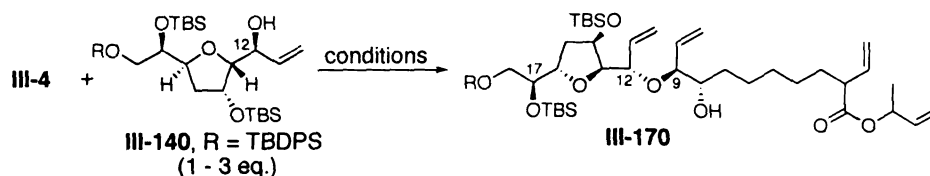
With the requisite substrates, viz. **III-140** and **III-4** available, efforts were now focused on the proposed regio- and stereoselective epoxide ring opening reaction. We first decided to try Mioskowski's optimized conditions⁵⁵ for our epoxide opening reaction. Initially, we chose a commercially available primary alcohol **III-167** as the nucleophile (Scheme III-21). The epoxide **III-4** and the alcohol **III-167** (1.1 eq.) coupled at ambient temperature in presence of catalytic $\text{BF}_3 \cdot \text{OEt}_2$, to afford the ring opened product **III-168** in 50% yields. The regiochemistry of **III-168** was established by COSY analysis of its acetate derivate **III-169**. We were greatly encouraged by this result because the sensitive α, β unsaturated ester functionality seemed to tolerate the reaction conditions reasonably well and excess amount of alcohol was not required.



Scheme III-21: A trial intermolecular ring opening of the vinylic epoxide **III-4** using Mioskowski's conditions

We then decided to move on to model alcohol **III-140** hoping to further optimize the reaction to increase the yields. Reaction of **III-4** and **III-140** under the same

conditions (Table III-4, entry 1) resulted in rapid decomposition, and the desired product was isolated only in 12% yield, after careful chromatographic purification. We then reduced the amount of catalyst and temperature as summarized below (entries 2-4, Table



conditions	result
$\text{BF}_3 \cdot \text{OEt}_2$ (10 mol%), CH_2Cl_2 , rt, 30 min	III-170 (12%)
$\text{BF}_3 \cdot \text{OEt}_2$ (1 mol%), CH_2Cl_2 , 0 °C, 1 h	no reaction
$\text{BF}_3 \cdot \text{OEt}_2$ (4 mol%), CH_2Cl_2 , 0 °C, 4 h	no reaction
$\text{BF}_3 \cdot \text{OEt}_2$ (4 mol%), CH_2Cl_2 , rt, 12 h	III-170 (20%)
$\text{Cu}(\text{OTf})_2$ (10 mol%), CH_2Cl_2 , rt	decomposition

Table III-4: Preliminary attempts at optimization of the coupling of **III-4** and **III-140**

III-4). To our disappointment, the yield increased only up to 20%. Also, the reaction using $\text{Cu}(\text{OTf})_2$ (another catalyst that was shown to be as efficient as $\text{BF}_3 \cdot \text{OEt}_2$ in Mioskowski's studies) lead only to decomposition. In all cases, unreacted alcohol **III-140** was recovered.

At this point, it appeared to us that this reaction might need extensive investigations that would involve screening of a variety of acid promoters, solvents and temperature conditions. We therefore decided to further simplify the system to model vinylic epoxides **III-174** and **III-175** and a model alcohol **III-177**, which could be accessed quickly as shown in Scheme III-22. Commercially available ethyl 6-hydroxy hexanoate **III-171** *via* sequential PCC oxidation and *E*-selective Wittig olefination was

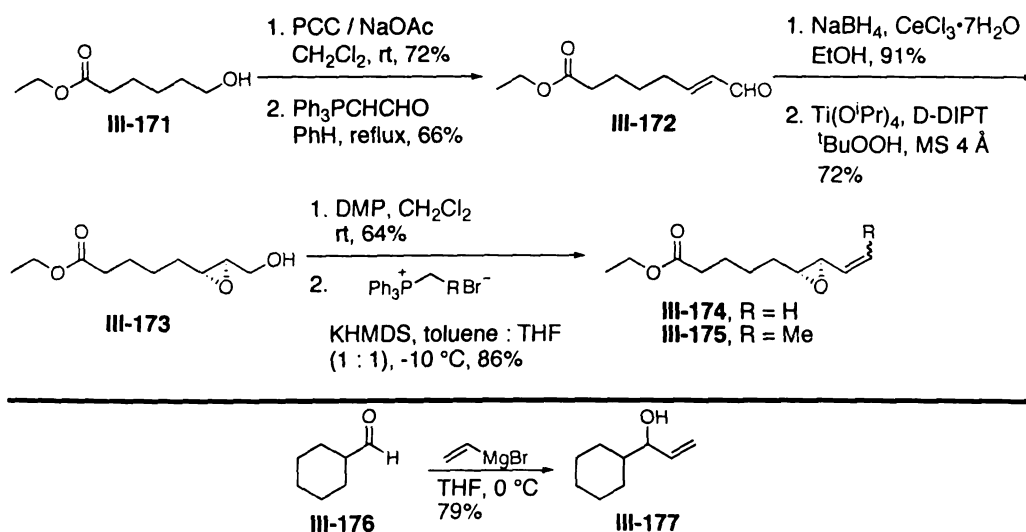
tr

fo

al

v

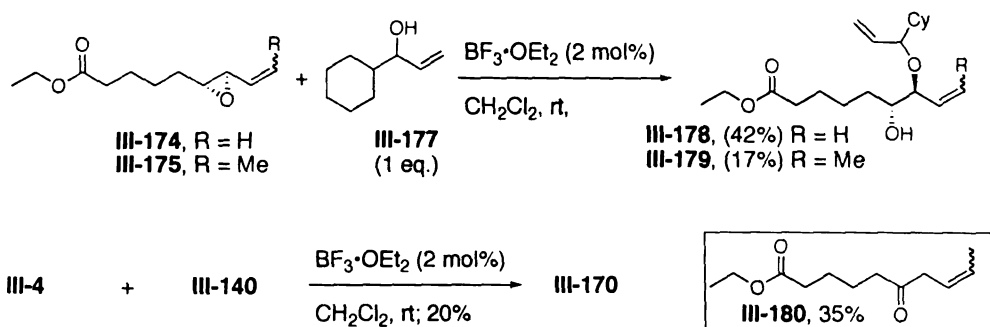
transformed to the α,β -unsaturated aldehyde **III-172**. **III-172** upon Luche reduction^{118,119} followed by SAE furnished epoxy alcohol **III-173**. Finally Wittig olefination of the aldehyde derived from **III-173** with two different ylides provided the corresponding vinylic epoxides **III-174** and **III-175**. The allylic alcohol **III-177** was obtained simply by



Scheme III-22: Synthesis of simplified model vinylic epoxides and an allylic alcohol

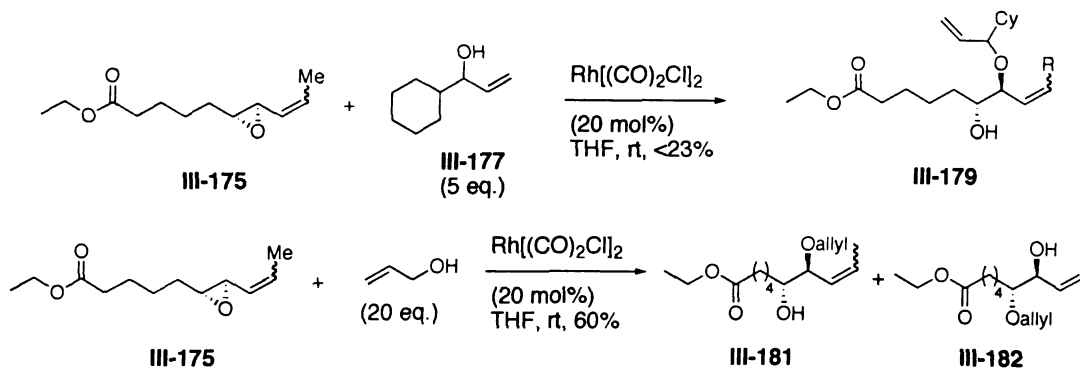
addition of vinyl magnesium bromide to cyclohexane carboxaldehyde **III-176**. With the requisite substrates in hand, the optimization process was continued.

After some experimentation, we found that by slow addition of $\text{BF}_3 \cdot \text{OEt}_2$ (2 mol%) to a mixture of **III-174** and **III-177** (Scheme III-23) at ambient temperature the yield of the desired product **III-178** could be improved to 42%. However, the same



Scheme III-23: Further optimization studies on the ring opening using model systems

procedure failed to improve the efficiency of the coupling of **III-4** and **III-140** beyond 20%. We suspected that in case of the terminal vinylic epoxides such as **III-174** and **III-4**, generation of undetected 1,4 addition products might be responsible for lower yields. Thinking that the methyl substituted vinylic epoxide **III-175** might diminish the likelihood of the 1,4 addition pathway, it was treated with **III-177** under the optimized conditions. This, however led to even lower yield (17%) of the desired product **III-179**. Furthermore, a side product **III-180** formed *via* an intramolecular 1,2 hydride migration¹²⁰ was isolated in 35% yields. The studies described so far indicated that the epoxide opening reaction might be acutely sensitive to the steric environment around the reaction centers.



Scheme III-24: Application of Lautens' conditions to model systems

st

pr

or

le

m

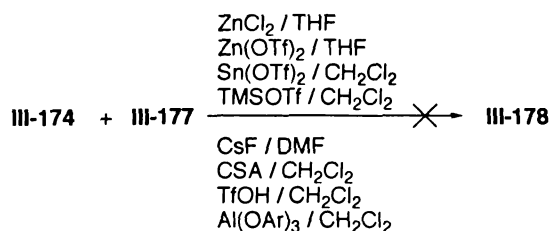
c

u

.

We next turned to examine Lautens' conditions (Scheme III-24).⁴² In their studies, when terminal vinylic epoxides were used, a mixture of 1,4 and 1,2 addition products was produced. We therefore chose **III-175** as the electrophile. Also, in the original report, 10 – 30 equivalents of the alcohol were used with 5 mol% catalyst loading. We modified those conditions to 5 equivalents of the nucleophile **III-177**, 20 mol% catalyst and the reaction was run at 3 M concentration. Under these conditions, only 23% material was recovered which contained the desired product **III-179** along with unidentified side products. Interestingly when allyl alcohol was used, a 1 : 1 mixture of regioisomeric products **III-181** and **III-182** was isolated. No further experimentation using Lautens' rhodium catalyst was continued.

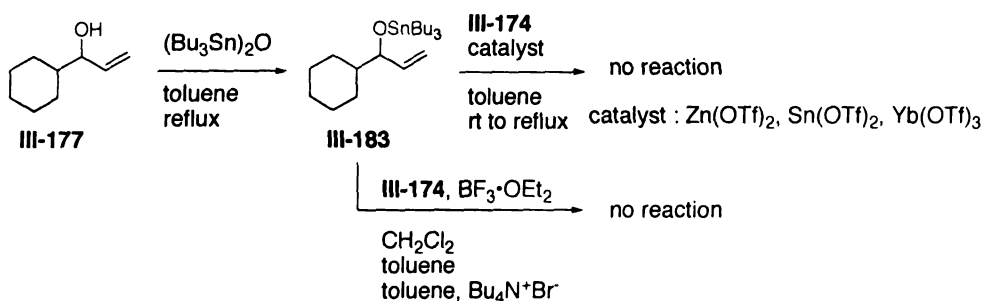
Since the terminal vinylic epoxide **III-174** proved superior to **III-175** in terms of yields and regioselectivity (Scheme III-23), investigations were continued using **III-174**. Using the epoxide **III-174** and the alcohol **III-177**, we now screened a range of Lewis and protic acids (Scheme III-25) under different solvent and a wide window of temperature (-78 °C to reflux). With the exception of Sn(OTf)₂ and TMS(OTf)₂ mediated reactions where the desired product **III-178** was obtained in 25%-40% yields, all other reactions led either to recovery of the starting materials or decomposition.



Scheme III-25: Screening of various acid catalysts for S_N2 opening of the model epoxide

All the trials so far, led to us to think that the nucleophilicity of alcohols decreases significantly with increase in steric bulk and hence under strongly activating conditions, the vinylic epoxides followed intramolecular rearrangement (for example, **III-180**, Scheme III-23) or other decomposition pathways.

One of the tactics used to increase nucleophilicity of such hindered alcohols is their derivatization to the corresponding tin ethers. The enhanced nucleophilicity of tin ethers as compared to the parent alcohols has been attributed to the more polar character of Sn-O bond than H-O bond.¹²¹ In carbohydrate chemistry, hindered glycosyl accepters are often derivatized as tin ethers which facilitates their O-glycosidation reaction.¹²²⁻¹²⁴ This precedent prompted us to explore the use of tributyl tin ether derivative (**III-183**, Scheme III-26) of the model alcohol **III-177** as a nucleophile. **III-183** was conveniently accessed by treatment of **III-177** with bis-tributyl tin oxide in refluxing toluene accompanied by azeotropic removal of H₂O.^{45,123} Typically, tin ethers are used in conjunction with lanthanide triflates. Three different triflates (Scheme III-26) were examined for the coupling of **III-183** and **III-174** in refluxing toluene, all of which resulted only in recovery of the starting materials. In our earlier experiments, BF₃•OEt₂ proved to be most effective catalyst. Unfortunately, in this case, all BF₃•OEt₂ mediated coupling reactions (Scheme III-26) failed. From all our unsuccessful attempts at coupling vinylic epoxides with alcohols as well as other reports, it became clear that activated vinyl epoxides in absence of an effective nucleophile, are notorious for rapidly undergoing internal rearrangement and other decomposition processes.



Scheme III-26: Attempted epoxide opening reactions using a tributyl tin ether

While in search of alternative ways to activate an epoxide, which would avoid other unwanted rearrangement pathways, we thought that the thiophenyl group (i.e., use of an epoxy sulfide instead of a vinylic epoxide) might serve the purpose. In the course of this and the earlier project (Chapter I) we had clearly established the effectiveness of a thiophenyl directing group in epoxide activation *via* an episulfonium ion formation and its subsequent trapping by an internal hydroxyl group. Intermolecular trapping of episulfonium ions (generated from epoxy sulfides) by nitrogen nucleophiles has been reported by Rayner;⁹⁰ however use of alcohols or other oxygen nucleophiles for this purpose is not known. We thought that an epoxy sulfide activated *via* episulfonium ion is less likely to self decompose than activated vinyl epoxides since the former does not

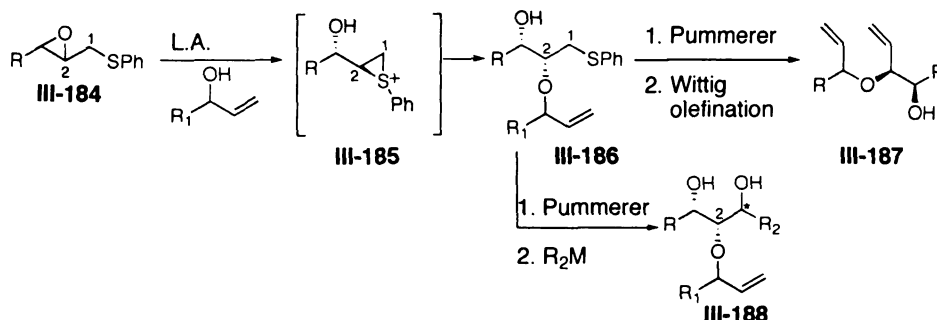


Figure III-32: Design of an epoxy sulfide substrate for regioselective ring opening by alcohols

in

et

C

w

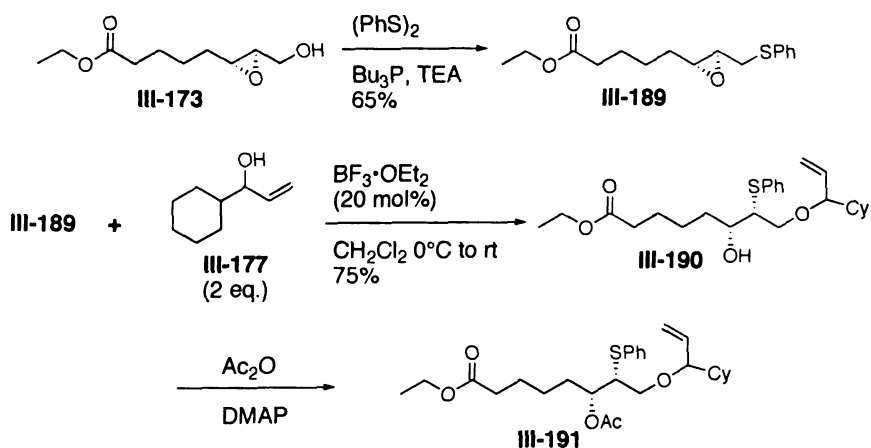
a

u

s

involve highly reactive allyl cation type species which is prone to rearrangements and other decomposition processes. Thus, an episulfonium ion if trapped regioselectively at C2 (**III-185**, Figure III-32) would generate an intermediate phenyl sulfide (**III-186**), which can be easily manipulated to the requisite RCM precursor **III-187**. Moreover, the aldehyde intermediate *en route* to **III-187** could be manipulated into a variety of other useful functionalities (for example **III-188**) thus offering an efficient entry into synthetically useful fragments.

To test our proposal, the required epoxy sulfide **III-189** was quickly obtained from available epoxy alcohol **III-173** using the Hata reagent (Scheme III-27).⁸⁵



Scheme III-27: Synthesis and acid catalyzed intermolecular coupling reaction of an epoxy sulfide with an alcohol nucleophile

After preliminary optimization, we found that slow addition of $\text{BF}_3 \cdot \text{OEt}_2$ to a solution of pre-mixed epoxy sulfide **III-189** and the alcohol **III-177** at 0 °C followed by warming the reaction to ambient temperature provided a ring opened product in 75% yield. COSY experiment of the acetate derivative **III-191**, however, showed that the undesired regioisomer **III-190** was produced *via* a [1,2] thiophenyl migration event. Although the

desired regioselectivity in opening of the epoxy sulfide **III-189** was not obtained, the reaction was much cleaner and higher yielding than any of the attempted vinyl epoxide openings suggesting that rearrangement / decomposition pathways were reduced in this case.

A popular tactic employed for controlling the regioselectivity and increasing the facility of intermolecular epoxide opening reaction is to tether the incoming nucleophile to the epoxide prior to the desired bond formation *via* metal mediated chelate complexes.^{24,125} Miyashita¹²⁶ and Saigo¹²⁷ have independently contributed to this area through the development of stereospecific epoxide substitution by use of

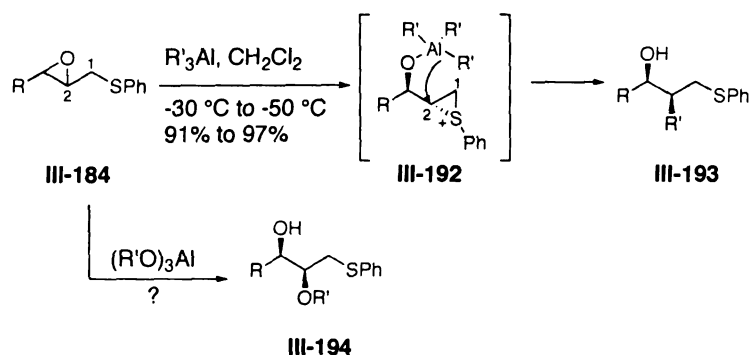
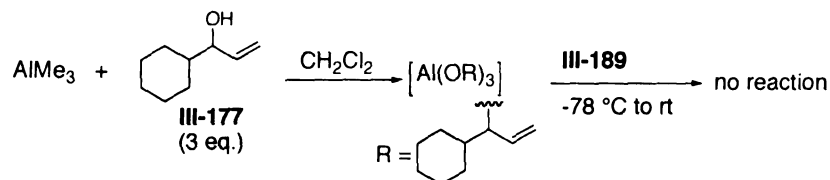


Figure III-33: Regio- and stereoselective alkyl group transfer to epoxy sulfides

organoaluminum reagents. It was shown that organoaluminum reagents efficiently transferred alkyl or alkynyl groups to 2,3 epoxy sulfides (**III-184**, Figure **III-34**) under mild conditions with complete regio- and stereocontrol. Presumably, the trialkyl aluminum initially acts as a Lewis acid to generate the episulfonium intermediate bearing the 'ate' complex (**III-192**). An alkyl group is then transferred to C2 (the choice of solvent was critical to the regioselectivity) to afford the substitution product (**III-193**) with a net retention of configuration.

Inspired by these studies, we set out to investigate whether trialkoxy aluminum species would transfer an alkoxy group in a similar manner, to afford the corresponding C2 ring opened product (**III-194**). Aluminum aryloxides have been known in the literature as effective Lewis acids for oxygen containing substrates. Their Lewis acidity is

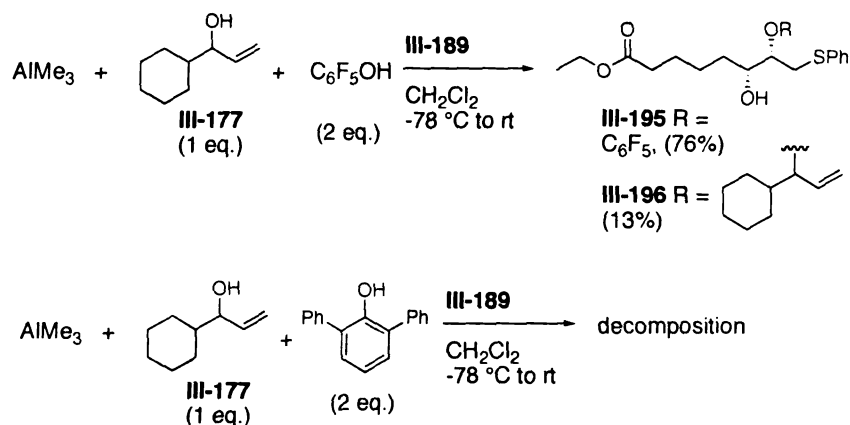


Scheme III-28: Attempted preparation and reaction of a trialkoxy aluminum with the epoxy sulfide **III-189**

tuned by the steric and electronic nature of the aryloxy ligands.¹²⁸⁻¹³⁰ On the other hand, use of alkoxy aluminums in an analogous manner has not been investigated. Aluminum aryloxides can be easily prepared by reacting AlMe_3 with an appropriate aromatic alcohol and depending upon the nature and stoichiometry of the reagents, di-or tri aryloxy aluminums can be generated.¹²⁹ Accordingly, we treated AlMe_3 with our alcohol nucleophile **III-177** (Scheme III-28) and the resultant solution was exposed to epoxy sulfide **III-189**. However **III-189** remained unchanged for a prolonged time even at room temperature. A likely explanation for the lack of reactivity is that alkoxy aluminum species are not acidic enough to generate episulfonium intermediates.

Being aware of a report that used $(\text{C}_6\text{F}_5\text{O})_3\text{Al}$ as a Lewis acid to promote epoxide rearrangements,¹²⁰ we next treated AlMe_3 with a 2 : 1 mixture of $\text{C}_6\text{F}_5\text{OH}$ and **III-177** (hoping to generate an aluminum species that would promote episulfonium generation as well as transfer the desired alkoxy group). When the resultant solution was reacted with

III-189, the epoxy sulfide was completely consumed and two products **III-195** and **III-196** were formed Scheme III-29). Unfortunately, the major product (76%) resulted



Scheme III-29: Attempted alkoxy group transfer to the epoxy sulfide **III-189**

from transfer of pentafluoro phenoxy group transferred to C2 while the minor product (13%) contained the desired product. Lastly, when 2,6-diphenyl phenol was used in a similar manner (in an attempt to prevent aryl group by increasing steric bulk), the reaction resulted in decomposition.

After the unsuccessful attempts at the intermolecular epoxide opening with desired regioselectivity, we considered yet other ways to access the target RCM precursor **III-2**. Cyclic sulfates and sulfites derived from vicinal diols have served as effective epoxide surrogates especially in intermolecular ring opening processes.¹³¹⁻¹³⁵ Cyclic sulfates are inherently reactive toward ring opening than their epoxide analogs possibly due to the internal O-S-O angle strain and a partial double bond character of the ring O-S bond (**III-198**, Figure **III-35**).¹³¹ Cyclic sulfites (such as **III-199**) on the other hand, can be activated by Lewis acids *via* coordination with the lone pair on the sulfur atom.

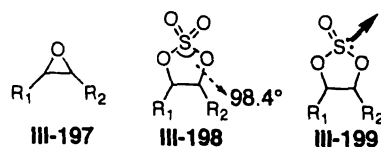
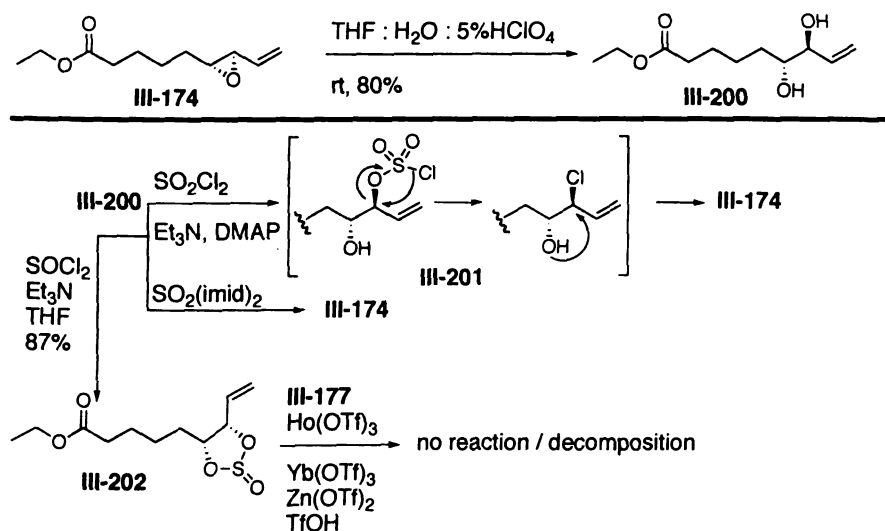


Figure III-34: Cyclic sulfates and sulfites as epoxide surrogates

Accordingly, we decided to explore cyclic sulfate and sulfite analogs of the vinyl epoxide **III-174**. The requisite diol precursor **III-200** was easily obtained by stereoselective hydrolysis of **III-174** (Scheme III-30).¹³⁶ Unfortunately, all attempts to prepare the cyclic sulfate from **III-200** failed.^{132,137} The reaction mediated by sulfuryl chloride produced the vinylic epoxide **III-174** presumable through the intermediacy of chlorohydrin **III-201**.¹³¹ The cyclic sulfite **III-202** which, was accessed from **III-200** in high yields,¹³⁸ failed to combine with the alcohol **III-177** under a variety of acidic conditions.¹³⁹



Scheme III-30: Attempted preparation and ring opening of cyclic sulfates and sulfites

Due to the failure of acid promoted coupling of vinylic epoxides and equivalents thereof with alcohols, we decided to explore the desired C-O bond formation under basic or neutral conditions as a last resort. Given the poor nucleophilicity of alcohols, we decided to employ substrates such as **III-203** (Figure III-35) containing a good leaving group at an allylic position. One might anticipate that such allylic electrophiles would be reactive enough toward nucleophiles under mildly basic or neutral conditions. In the carbohydrate literature, *O*-glycosidation reactions of hindered secondary electrophiles are often

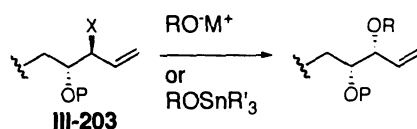
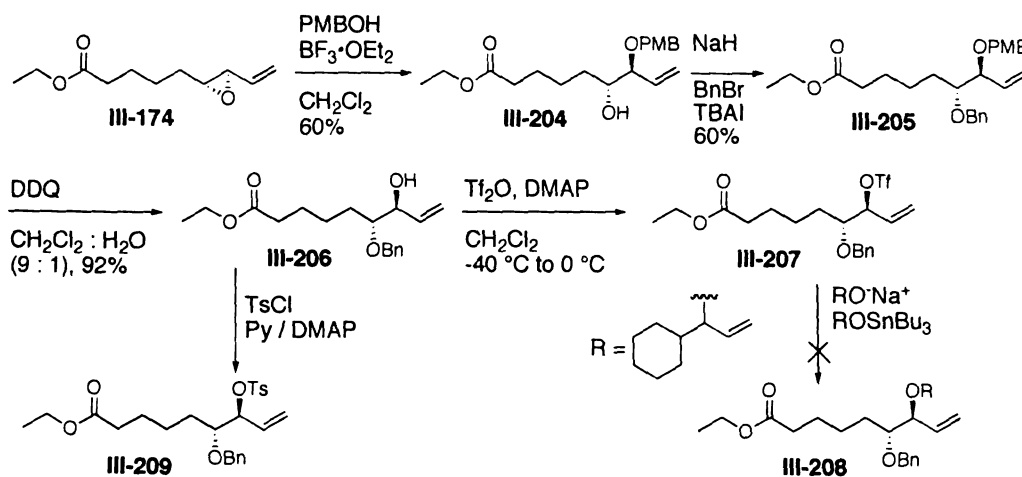


Figure III-35: S_N2 displacement of allylic electrophiles with alkoxides

facilitated by treatment of their triflate derivatives with stannylated glycosyl acceptors.¹²²⁻¹²⁴ These couplings are usually carried out under near neutral conditions and are compatible with benzoate or acetate protecting groups elsewhere in the substrates.

To continue efforts in this direction, the selectively protected diol **III-206** containing a free allylic alcohol functionality was synthesized as shown in Scheme III-31. Synthesis and isolation of triflate **III-207** proved challenging. During the preparation, subzero temperatures had to be maintained along with careful control of the reagent stoichiometry and the order of addition.¹⁴⁰⁻¹⁴² As can be imagined, **III-207** was extremely sensitive to aqueous work up. Even after meticulous non-aqueous work up procedures,^{141,143} **III-207** could not be completely freed of DMAP derived salts. Even when the cleanest samples of **III-207** were treated with sodium or tin alkoxides of **III-177**, no desired product was obtained. Similarly, tosylate **III-199**, though relatively

more stable to isolation procedures, could not be purified from TsCl derived side products.



Scheme III-31: Attempted preparation and displacement reactions of allylic triflate and tosylate

In conclusion, a synthetic scheme involving a convergent assembly of fully functionalized left (C13-C37) and right (C1-C12) hand fragments of mucoxin *via* regio- and selective intermolecular epoxide opening was designed (Figure III-2). The advanced coupling partners, viz., the allylic alcohol III-140 and the vinylic epoxide III-4 were synthesized as planned. However, a maximum yield of only 20% was obtained in the attempted coupling reactions of III-140 and III-4 using conventional acid catalyzed conditions. The desired C-O bond formation was also attempted under several other acidic, basic and neutral conditions using model nucleophiles III-177 and III-183, vinylic epoxides III-174, III-175 and vinylic epoxide equivalents III-189, III-202, III-207 and III-209. None of these attempts met with success. Alcohols, inherently are moderate nucleophiles and in our experience, their nucleophilicity depletes rapidly with increase in their steric bulk. Under acid catalyzed reactions, the nucleophile is unable to

compete with the internal 1,2 hydride transfer and other rearrangement / decomposition pathways of the activated vinylic epoxides, and is recovered unscathed. The ester functionality in all the vinylic epoxides examined may also be responsible for accelerating self-destruction of the epoxides under acidic conditions.

After the failure to access the proposed RCM precursor **III-2**, the global synthetic strategy was revised. The left hand (C12-C37) segment as the aldehyde **III-135** was conserved in the new designs, whereas, the right hand piece (C1-C13) was functionalized in several different ways. The new routes and culmination of the total synthesis of the proposed structure of mucoxin is the subject of Chapter IV.

D. Experimental section

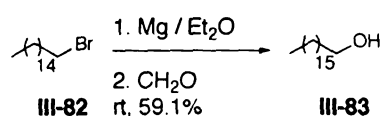
General Procedures:

All reactions were carried out in flame dried glassware under an atmosphere of dry nitrogen or argon. 4 Å molecular sieves were dried at 160 °C under vacuum prior to use. Unless otherwise mentioned, solvents were purified as follows. THF and Et₂O were either distilled from sodium benzophenone ketyl or used as is from a solvent purification system. CH₂Cl₂, toluene, CH₃CN and Et₃N were distilled from CaH₂. DMF, diglyme, and DMSO were stored over 4 Å mol. sieves and distilled from CaH₂. All other commercially available reagents and solvents were used as received.

¹H NMR spectra were measured at 300, 500 or 600 MHz on a Varian Gemini-300, a Varian VXR-500 or a Varian Inova-600 instrument respectively. Chemical shifts are reported relative to residual solvent (δ 7.27, 2.50 and 4.80 ppm for CDCl₃, (CD₃)₂SO and CD₃OD respectively). ¹³C NMR spectra were measured at 125 MHz on a Varian VXR-500 instrument. Chemical shifts are reported relative to the central line of CDCl₃ (δ 77.0 ppm). Infrared spectra were recorded using a Nicolet IR/42 spectrometer FT-IR (thin film, NaCl cells). High resolution mass spectra were measured at the University of South Carolina, Mass Spectrometry Laboratory. Optical rotations were measured on a Perkin–Elmer polarimeter (model 341) using a 1 mL capacity quartz cell with a 10 cm path length.

Analytical thin layer chromatography (TLC) was performed using Whatman glass plates coated with a 0.25 mm thickness of silica gel containing PF254 indicator, and

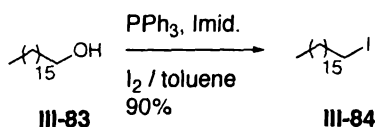
compounds were visualized with UV light, potassium permanganate stain, *p*-anisaldehyde stain, or phosphomolybdic acid in EtOH. Chromatographic purifications were performed using Silicycle 60 Å, 35-75 µm silica gel. All compounds purified by chromatography were sufficiently pure for use in further experiments, unless indicated otherwise. GC analysis was performed using HP (6890 series) GC system containing Altech SE-54, 30 m x 320 mm x 0.25 mm column. Analytical and semi-preparative HPLC normal phase separations were performed using HP 1100 series HPLC system.



A 1-L three-necked round-bottom flask fitted with a reflux condenser and a 100 mL addition funnel was charged with magnesium turnings (24.1 g, 0.99 mol) and Et₂O (300 mL). To this mixture, 1,2 dibromoethane (5.5 mL, 63.9 mmol) was added over 30 min upon which Et₂O started refluxing slowly. To the activated magnesium, 1-bromohexadecane **III-82** (100 mL, 0.33 mol) was added via the addition funnel over 1 h. After completion of the addition, the reaction mixture was stirred for an additional 2 h. The addition funnel was then replaced by a wide glass tube, which was connected to the side-arm of a filtration flask via a rubber tubing. The filtration flask fitted with an inlet for nitrogen was charged with paraformaldehyde (50 g) and heated to 180 °C – 200 °C. The formaldehyde generated by cracking paraformaldehyde in this manner was slowly bubbled into the Grignard reagent by a current of dry nitrogen. After 1 h the bubbling was stopped and the reaction was allowed to stir at ambient temperature for 2 h. The reaction mixture was then diluted with H₂O (200 mL), slowly poured into 300 g of cracked ice, and 320 mL of 30% H₂SO₄ was added to it and stirred at ambient

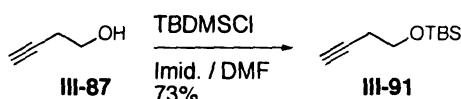
temperature for 30 min. Layers were separated and the aqueous portion was washed with Et₂O (3x300 mL). The combined organic layers were washed with brine (300 mL), dried over MgSO₄, concentrated and the crude product was purified by flash column chromatography [hexanes (1.5 L), 4 : 1 hexanes : EtOAc (3 L)] to yield 1-heptadecanol **III-83** as a white solid (50 g, 59.1%). mp. 54-55 °C; Spectroscopic data for **III-83** matched to that reported by Aldrich.

Partial data for **III-83**: ¹H NMR (500 MHz, CDCl₃) δ 3.66 (t, *J* = 6.6 Hz, 2 H), 1.6-1.53 (m, 2 H), 1.33-1.27 (m, 28 H), 0.90 (t, *J* = 6.6 Hz, 3 H)

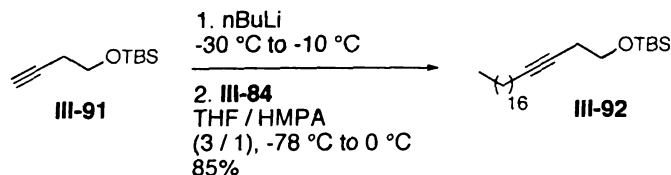


To a solution of 1-heptadecanol **III-83** (68 g, 0.265 mmol) in dry toluene (2.3 L), triphenyl phosphine (171 g, 0.652 mmol), and imidazole (45 g, 0.661 mmol) were added at ambient temperature and stirred under N₂ until a clear solution was obtained. To this solution I₂ (136 g, 0.535 mmol) was added and stirring was continued for 1 h at the same temperature after which the reaction was quenched by adding aqueous saturated sodium sulfite solution until the yellow color disappeared. The layers were then separated, aqueous layer was washed with 1 : 4 EtOAc : hexanes (3x400 mL), and the combined organic layers were dried over Na₂SO₄ and concentrated. Purification by flash column chromatography (hexanes) afforded iodide **III-84** as a white solid (87.3 g, 90%). Data for **III-84**: ¹H NMR (500 MHz, CDCl₃) δ 3.18 (t, *J* = 7.07 Hz, 2 H), 1.82 (q, *J* = 7.06 Hz, 2 H), 1.40-1.22 (m, 28 H), 0.88 (t, *J* = 6.95 Hz, 3 H); ¹³C NMR (125 MHz, CDCl₃) δ 33.9, 32.2, 30.8, 30.0, 29.9, 29.8, 29.7, 29.6, 28.8, 22.9 (multiple carbons), 14.3, 7.2; IR (thin film) 2953, 2916, 2846, 1471, 1423, 1296, 1255, 1213, 1192, 1165, 725, 603 cm⁻¹;

HRMS (EI) calcd for $C_{17}H_{35}I$, 366.1784 m/z (M)⁺; observed, 366.1797 m/z ; mp = 33-34 °C.

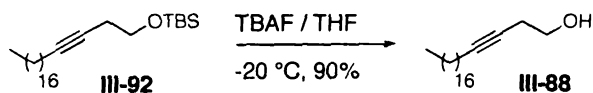


To a solution of 3-butyn-1-ol **III-87** (27 mL, 29.16 g, 0.416 mmol) and imidazole (61 g, 0.896 mmol) in DMF (100 mL) cooled to 0 °C, a solution of t-butyldimethylchlorosilane (64.5 g, 0.428 mmol) in DMF (125 mL) was added and stirred at the same temperature for 40 min under N_2 . The reaction was then warmed to ambient temperature and stirred for 3 h after which H_2O (500 mL) was added. The aqueous layer was extracted with 4:1 hexanes : EtOAc (4x400 mL), and the combined organic layers were dried (Na_2SO_4) and concentrated. After flash column chromatography, the silyl ether **III-91** was obtained as a colorless oil (62 g, 73%). Data for **III-91**: 1H NMR (500 MHz, $CDCl_3$) δ 3.74 (t, J = 7.1 Hz, 2 H), 2.40 (dt, J = 7.2, 2.7 Hz, 2 H), 1.95 (d, J = 2.7 Hz, 1 H), 0.90 (s, 9 H), 0.07 (s, 6 H); ^{13}C NMR (125 MHz, $CDCl_3$) δ 81.7, 69.5, 69.4, 62.0, 26.1, 23.1, 18.5, -5.1; IR (thin film) 3330, 2954, 2860, 2753, 2711, 2123, 1839, 1590, 1471, 1388, 1255, 1106, 1006, 916, 837, 777, 643 cm^{-1} ; HRMS (CI, CH_4) calcd for $C_{10}H_{20}OSi$, 185.1362 m/z ($M + H$)⁺; observed, 185.1361 m/z .



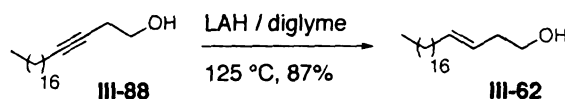
To a solution of the silyl ether **III-91** (13.63 g, 74.08 mmol) in THF (113 mL) cooled to -30 °C, nBuLi (7.8 mL of 9.97 M solution in hexanes, 77.8 mmol) was added dropwise and the solution was warmed to -10 °C over 1 h. The lithium acetylide was

cooled to $-78\text{ }^{\circ}\text{C}$ after which a solution of iodide **III-84** in 3 : 1 THF : HMPA (147 mL) was added and stirred for 10 min at the same temperature. The reaction was then warmed to $0\text{ }^{\circ}\text{C}$ and after 1 h H_2O (300 mL) was added. The aqueous layer was extracted with Et_2O (3x 400 mL). The combined organic layers were dried over MgSO_4 and concentrated to afford a crude oil, which was purified by flash column chromatography (hexanes \rightarrow 19 : 1 hexanes : EtOAc) to yield the silyl protected homopropargylic alcohol **III-92** (26.7 g, 85%) as a yellow oil. Data for **III-92**: ^1H NMR (500 MHz, CDCl_3) δ 3.69 (t, $J = 7.06\text{ Hz}$, 2 H), 2.36 (dt, $J = 7.3, 2.4\text{ Hz}$, 2 H), 2.12 (dt, $J = 7.2, 2.4\text{ Hz}$, 2 H), 1.45 (q, $J = 7.1\text{ Hz}$, 2 H), 1.39-1.23 (m, 30 H), 0.90 (s, 9 H), 0.88 (t, $J = 7.01\text{ Hz}$, 3 H), 0.07 (s, 6 H); ^{13}C NMR (125 MHz, CDCl_3) δ 81.5, 76.8, 62.5, 31.9, 29.7, 29.6, 29.4, 29.2, 29.1, 28.9, 25.9, 23.2, 22.7, 18.2, 18.3, 14.1, -5.3; IR (thin film) 2923, 2854, 1466, 1383, 1362, 1253, 1105, 1059, 1007, 916, 837, 777, 721 cm^{-1} ; HRMS (CI, CH_4) calcd for $\text{C}_{27}\text{H}_{54}\text{OSi}$, 421.3866 m/z ($\text{M} - \text{H}$) $^+$; observed, 421.3874 m/z .



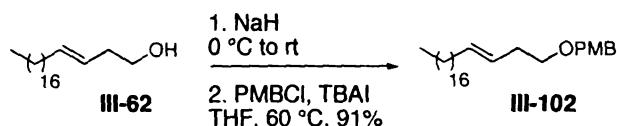
To a solution of the silyl protected homopropargylic alcohol **III-92** (35.9 g, 0.085 mol) in THF (100 mL), TBAF (130 mL of 1M solution in THF, 0.13 mol) was added at $-20\text{ }^{\circ}\text{C}$ under N_2 . After stirring for 30 min at the same temperature, H_2O (200 mL) was added. The layers were separated, aqueous layer was extracted with Et_2O (3x 400 mL). The combined organic layers were dried over MgSO_4 and concentrated. The crude product was purified by flash column chromatography (4 : 1 hexanes : EtOAc) to furnish the homopropargylic alcohol **III-88** as a white solid. Data for **III-88**: ^1H NMR (500 MHz, CDCl_3) δ 3.67 (t, $J = 6.2\text{ Hz}$, 2 H), 2.43 (dt, $J = 6.2, 2.4\text{ Hz}$, 2 H), 2.15 (dt, $J = 7.2,$

2.4 Hz, 2 H), 1.76 (s(br), 1 H), 1.48 (q, $J = 7.1$ Hz, 2 H), 1.37-1.25 (m, 30 H), 0.88 (t, $J = 6.6$ Hz, 3 H); ^{13}C NMR (125 MHz, CDCl_3) δ 82.9, 76.2, 61.4, 31.9, 29.8, 29.7, 29.6, 29.4, 29.2, 29.0, 28.9, 23.2, 22.7, 18.8, 14.1; IR (thin film) 2953, 2914, 2848, 1470, 1049, 1018, 874, 752 cm^{-1} ; HRMS (CI, CH_4) calcd for $\text{C}_{21}\text{H}_{40}\text{O}$, 307.3001 m/z ($\text{M} - \text{H}$) $^+$; observed, 307.3003 m/z ; mp = 61-62 $^\circ\text{C}$.

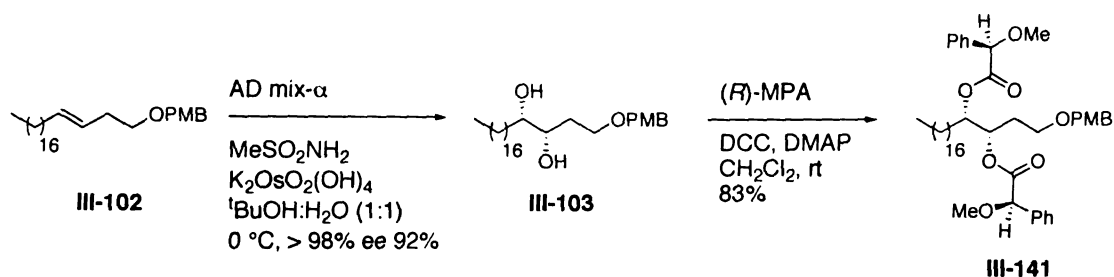


A 1 L two-necked round-bottom flask fitted with a stir bar and a reflux condenser was charged with LAH (7.7 g, 0.203 mol). A solution of the homo propargylic alcohol **III-88** (35 g, 0.113 mol) in diglyme (350 mL) was carefully added dropwise at 0 $^\circ\text{C}$ to the reaction mixture. While stirring vigorously, the mixture was heated to 125 $^\circ\text{C}$. After 17 h, the reaction was cooled to room temperature upon which 7.7 mL of H_2O was added dropwise. 7.7 mL of 15% NaOH was then added followed by 22 mL of H_2O . The resultant mixture was heated at 50 $^\circ\text{C}$ for 45 min and filtered after cooling to ambient temperature. The filtrate was diluted with EtOAc (500 mL) and washed with 1.5 N HCl (5x100 mL) to remove diglyme from the organic layer. The organic layer was dried (Na_2SO_4) and concentrated. Chromatographic purification of the crude product (19 : 1 hexanes : EtOAc \rightarrow 2.3:1 hexanes : EtOAc) yielded the *E*- homo allylic alcohol **III-62** (30.5 g, 87%) as a white solid. Data for **III-62**: ^1H NMR (500 MHz, CDCl_3) δ 5.58-5.52 (m, 1 H), 5.40-5.34 (m, 1 H), 3.62 (t, $J = 6.3$ Hz, 2 H), 2.26 (dt, $J = 12.5, 6.08$, 2 H), 2.00 (dt $J = 14.3, 7.3$ Hz, 2 H), 1.48 (s (br), 1 H), 1.36-1.25 (m, 30 H), 0.88 (t, $J = 6.8$ Hz, 3 H); ^{13}C NMR (125 MHz, CDCl_3) δ 134.4, 125.7, 62.1, 36.1, 32.7, 31.9, 29.7, 29.6, 29.5, 29.4, 29.2, 22.7, 14.1; IR (thin film) 3448, 3136, 2914, 2848, 1637, 1470, 1047, 1020,

926, 890, 715 cm^{-1} ; HRMS (CI, CH_4) calcd for $\text{C}_{21}\text{H}_{42}\text{O}$, 309.3157 m/z ($\text{M} - \text{H}$)⁺; observed, 309.3142 m/z ; mp = 55-56 °C.



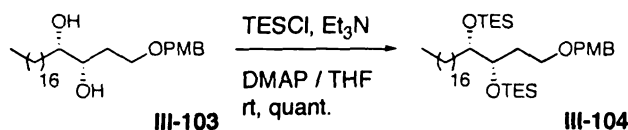
A 1 L round-bottom flask was fitted with a reflux condenser was charged with a stir bar and NaH (14 g of 60 wt% dispersion in oil, 0.36 mol). A solution of the homo allylic alcohol **III-62** (37 g, 0.12 mol) in THF (400 mL) was added dropwise at 0 °C. The mixture was warmed to room temperature and stirred for an additional 1 h. 4-Methoxybenzyl chloride (25 g, 0.16 mmol) and TBAI (16.5 g, 0.045 mol) were added and the reaction mixture was heated to 60 °C for 18 h. The reaction was cooled to ambient temperature and carefully quenched by adding saturated NH_4Cl solution. The layers were separated, and the aqueous layer was extracted with Et_2O (3x300 mL). Combined organic layers were dried (MgSO_4) and concentrated to furnish a crude solid which upon purification by flash column chromatography (49 : 1 hexanes : EtOAc) afforded the PMB protected homo allylic alcohol **III-102** (47 g, 91%) as a white solid. Data for **III-102** ^1H NMR (500 MHz, CDCl_3) δ 7.27 (d, J = 8.7 Hz, 2 H), 6.88 (d, J = 8.7 Hz, 2 H), 5.54-5.48 (m, 1 H), 5.45-5.39 (m, 1 H), 4.46 (s, 2H), 3.81 (s, 3 H), 3.47 (t, J = 7.0 Hz, 2 H), 2.31 (dt, J = 13.5, 6.6 Hz, 2 H), 2.0 (dt, J = 13.9, 6.9 Hz, 2 H), 1.37-1.28 (m, 30 H), 0.9 (t, J = 6.9, 2 H); ^{13}C NMR (125 MHz, CDCl_3) δ 159.2, 132.7, 130.7, 129.4, 129.3, 126.2, 113.8, 113.7, 72.5, 70.1, 55.3, 33.1, 32.7, 32.2, 29.8, 29.7, 29.6, 29.5, 29.4, 29.2, 14.2; IR (thin film) 2954, 2918, 2848, 1969, 1896, 1614, 1522, 1462, 1361, 1246, 1176, 1097, 1030, 964, 822 cm^{-1} ; HRMS (EI) calcd for $\text{C}_{29}\text{H}_{50}\text{O}_2$, 430.3811 m/z (M)⁺; observed, 430.3799 m/z ; mp = 38-39 °C.



A 2 L two-necked round flask fitted with a mechanical stirrer was charged with AD mix- α (97.8 g). $^t\text{BuOH}$ (330 mL) and H_2O (330 mL) were added followed by methanesulfonamide (6.6 g) and $\text{K}_2\text{OsO}_4 \cdot 2\text{H}_2\text{O}$ (144 mg). This mixture was stirred until a clear solution was obtained which was cooled to $0\text{ }^\circ\text{C}$ upon which the olefin **III-102** (30 g, 0.07 mol) was added in one portion. The reaction was vigorously stirred at $0\text{ }^\circ\text{C}$ for 20 h after which time sodium sulfite (100 g) was added at the same temperature. The mixture was then warmed to room temperature and stirred for 45 min, then diluted with EtOAc (500 mL) and washed with H_2O (200 mL). The aqueous layer was extracted with EtOAc (3x300 mL), combined organic layers were dried (Na_2SO_4) and concentrated to yield a crude solid which was purified by flash column chromatography (9 : 1 hexanes : EtOAc \rightarrow 2 : 3 hexanes : EtOAc) to yield the diol **III-103** (32.5 g, 92%, $> 98\%$ ee as determined after derivatization to bis-(*R*)-methoxyphenylacetate). To a solution of **III-103** (50 mg, 0.11 mmol), (*R*)-MPA (54 mg, 0.32 mmol) and DCC (67 mg, 0.32 mmol) in CH_2Cl_2 (2 mL) was added DMAP (2 mg, 0.02 mmol) at room temperature. After 10 h, the reaction was quenched by saturated NaHCO_3 solution (1 mL). The aqueous layer was extracted with CH_2Cl_2 (5x2 mL), combined organic layers were dried, concentrated and the solvent was evaporated to afford bis-(*R*)-methoxyphenylacetate (**III-141**). ^1H NMR of the crude material indicated the presence of a single diastereomer.

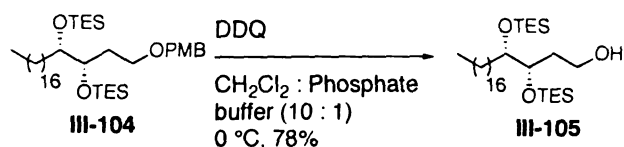
Data for **III-103**: $[\alpha]_D^{20}$ -2.0 (c 1.0, CHCl_3), ^1H NMR (500 MHz, CDCl_3) δ 7.24 (d, $J = 8.4$ Hz, 2 H), 6.88 (d, $J = 8.4$ Hz, 2 H), 4.45 (s, 2 H), 3.80 (s, 3 H), 3.72-3.62 (m, 3 H), 3.42-3.39 (m, 1 H), 1.89-1.74 (m, 2 H) 1.44-1.50 (m 3 H), 1.33-1.21 (m, 31 H), 0.88 (t, $J = 6.8$ Hz, 3 H); ^{13}C NMR (125 MHz, CDCl_3) δ 159.4, 129.8, 129.4, 113.9, 74.3, 73.7, 73.1, 68.3, 55.3, 33.6, 33.2, 32.0, 29.7, 29.6, 29.5, 29.4, 25.8, 22.7, 14.1; IR (thin film) 3354, 2916, 2848, 1612, 1514, 1467, 1369, 1248, 1178, 1114, 1035, 814 cm^{-1} ; HRMS (EI) calcd for $\text{C}_{29}\text{H}_{52}\text{O}_4$, 464.3866 m/z (M^+); observed, 464.3875 m/z ; mp = 75-77 $^\circ\text{C}$.

Data for **III-141**: ^1H NMR (500 MHz, CDCl_3) δ 7.45-7.42 (m, 4 H), 7.39-7.31 (m, 6 H), 7.18 (d, $J = 8.6$ Hz, 2 H), 6.85 (d, $J = 8.6$ Hz, 2 H), 5.11 (dt, $J = 2.4, 6.6$ Hz, 1 H), 4.87-4.84 (m, 1 H), 4.70 (s, 1 H), 4.67 (s, 1 H), 4.20 (dd, $J = 11.5, 19.2$ Hz, 2 H), 3.79 (s, 3 H), 3.39 (s, 3 H), 3.35 (s, 3 H), 3.17-3.13 (m, 1 H), 3.08-3.03 (m, 1 H), 1.43-0.93 (m, 34 H), 0.88 (t, $J = 6.9$ Hz, 3 H); ^{13}C NMR (125 MHz, CDCl_3) δ 170.4, 170.2, 159.4, 136.7, 136.6, 130.5, 129.5, 129.0, 128.9, 128.8, 127.6, 127.5, 127.4, 113.9, 82.7, 82.3, 75.0, 72.7, 71.9, 65.8, 57.5, 57.4, 55.5, 32.2, 30.8, 30.4, 30.0, 29.9, 29.8, 29.7, 29.6, 29.5, 29.4, 25.2, 22.9, 14.3.



To a solution of the diol **III-103** (29 g, 0.062 mol) in THF (600 mL) triethyl amine (202 mL) was added followed by triethylsilyl chloride (63 mL, 0.374 mol) and DMAP (2.9 g, 0.024 mol) at ambient temperature. The reaction was stirred under N_2 for 3 h after which time was quenched by adding saturated NaHCO_3 solution (400 mL). The aqueous layer was extracted with 1 : 5 EtOAc : hexanes (3x500 mL) to afford crude oil which was purified by column chromatography (35 : 1 hexanes : EtOAc) providing the

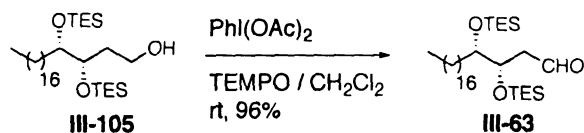
fully protected triol **III-104** as a colorless oil (43 g, quant.). Data for **III-104**: $[\alpha]_D^{20}$ -17.5 (c 3.0, CHCl_3) ^1H NMR (500 MHz, CDCl_3) δ 7.26 (d, $J = 8.6$ Hz, 2 H), 6.87 (d, $J = 8.6$ Hz, 2 H), 4.43 (s, 2 H), 3.81 (s, 3 H), 3.78-3.74 (m, 1 H), 3.58-3.51 (m, 3 H), 2.04-2.00 (m, 1 H), 1.63-1.43 (m, 3 H), 1.35-1.19 (m, 30 H), 1.00-0.88 (m, 21 H), 0.63-0.51 (m, 12 H); ^{13}C NMR (125 MHz, CDCl_3) δ 159.0, 131.0, 129.1, 113.6, 75.3, 72.3, 72.1, 67.5, 55.3, 31.9, 30.6, 30.2, 29.9, 29.7, 29.6, 29.4, 26.7, 22.7, 14.1, 7.0, 6.9, 6.6, 6.4, 5.8, 5.2, 5.1; IR (thin film) 3324, 2924, 2856, 2071, 2003, 1876, 1614, 1587, 1513, 1461, 1414, 1379, 1301, 1247, 1172, 1099, 1014, 825, 738 cm^{-1} ; HRMS (EI) calcd for $\text{C}_{41}\text{H}_{80}\text{O}_4\text{Si}_2$, 692.5595 m/z (M-H) $^+$; observed, 692.5567 m/z .



To a 0 °C solution of PMB ether **III-104** (15 g, 0.02 mol) in 460 mL of CH_2Cl_2 : phosphate buffer (10 : 1), DDQ (5.7 g, 0.03 mol) was added in one portion. After stirring the reaction under N_2 at the same temperature for 90 min, saturated NaHCO_3 solution (200 mL) was added. The mixture was warmed to ambient temperature and carefully extracted with CH_2Cl_2 (3x200 mL) so as to avoid emulsions. The combined organic layers were dried (Na_2SO_4), concentrated and the crude oil was purified by flash column chromatography (3% EtOAc in hexanes) to afford 12.6 g (78%) of the primary alcohol **III-105**.

Data for **III-105**: $[\alpha]_D^{20}$ -24.3 (c 2.34, CHCl_3) ^1H NMR (500 MHz, CDCl_3) δ 3.78-3.58 (m, 4 H), 2.88 (t, $J = 5.7$ Hz, 1 H), 1.95-1.90 (m, 1 H), 1.67-1.57 (m, 2 H), 1.40-1.46 (m, 1 H), 1.37-1.17 (m, 30 H), 0.99-0.90 (m, 18 H), 0.87 (t, $J = 7.0$ Hz, 3 H), 0.63-0.52 (m,

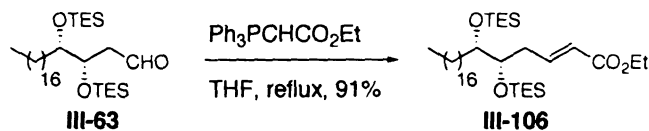
12 H); ^{13}C NMR (125 MHz, CDCl_3) δ 75.9, 75.1, 61.1, 34.7, 32.1, 30.6, 30.0, 29.9, 29.8, 29.5, 26.8, 22.9, 14.2, 7.0, 5.3, 5.2; IR (thin film) 3471, 2928, 2851, 1468, 1411, 1374, 1242, 1080, 1023, 723 cm^{-1} ; HRMS (CI, CH_4) calcd for $\text{C}_{33}\text{H}_{72}\text{O}_3\text{Si}_2$, 571.4942 m/z ($\text{M}-\text{H}^+$); observed, 571.4927 m/z .



To a solution of alcohol **III-105** (15.5 g, 0.03 mol) in CH_2Cl_2 (50 mL) at room temperature, bisacetoxyiodo benzene (9.61 g, 0.03 mol) was added. After addition of TEMPO (437 mg, 3.0 mmol) the clear orange solution was stirred at rt for 2 h. The reaction was then diluted with CH_2Cl_2 (150 mL) and treated with saturated sodium sulfite solution until it became colorless. Upon separation of the layers aqueous layer was extracted with CH_2Cl_2 (3x200 mL). The combined organic layers were dried over Na_2SO_4 , concentrated and purified by column chromatography (2% EtOAc in hexanes) to furnish aldehyde **III-63** as a colorless oil (14.8 g, 96%).

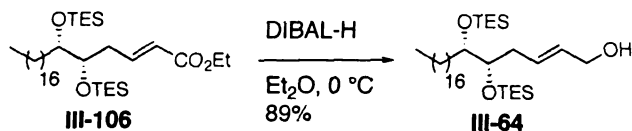
Data for **III-63**: $[\alpha]_{\text{D}}^{20} -21.6$ (c 1.95, CHCl_3) ^1H NMR (500 MHz, CDCl_3) δ 9.67 (t, J = 2.22 Hz, 1 H), 4.20-4.17 (m, 1 H), 3.62-3.59 (m, 1 H), 2.65 (ddd, J = 1.8, 4.0, 15.9 Hz, 1 H), 2.43 (ddd, J = 2.9, 8.2, 15.7 Hz, 1 H), 1.66-1.60 (m, 1 H), 1.47-1.31 (m, 1 H), 1.30-1.12 (m, 30 H), 0.92-0.88 (m, 18 H), 0.86 (t, J = 7.1 Hz, 3 H), 0.62-0.48 (m, 12 H); ^{13}C NMR (125 MHz, CDCl_3) δ 201.9, 75.1, 70.8, 46.1, 32.1, 30.6, 30.0, 29.9, 29.8, 29.5, 26.7, 22.9, 14.2, 7.0, 5.3, 5.1; IR (thin film) 2930, 2978, 2855, 2716, 1732, 1640, 1414,

1381, 1327, 1240, 1103, 1007, 976, 833, 743, 673 cm^{-1} ; HRMS (CI, CH_4) calcd for $\text{C}_{33}\text{H}_{70}\text{O}_3\text{Si}_2$, 569.4785 m/z (M-H) $^+$; observed, 569.4775 m/z .



A solution of aldehyde **III-63** (15.1 g, 0.02 mol) and (carbethoxymethylene)triphenylphosphorane (13.9, 0.05 mol) in THF (245 mL) was heated to reflux for 16 h. After cooling the solution to rt, the solvent was evaporated and the crude product was purified by column chromatography (EtOAc : hexanes = 1 : 99) to afford α,β -unsaturated trans ester **III-106** as a yellow oil (15.1 g, 91%).

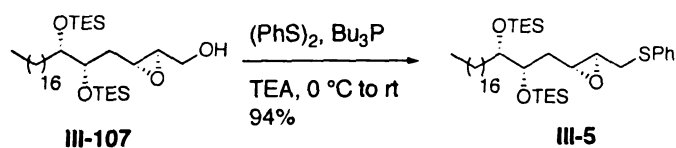
Data for **III-106**: $[\alpha]_D^{20}$ -30.1 (c 1.99, CHCl_3) ^1H NMR (500 MHz, CDCl_3) δ 7.37-6.98 (m, 1 H), 5.85 (d, J = 15.5 Hz, 1 H), 4.19 (q, J = 7.1 Hz, 2 H), 3.71-3.61 (m, 1 H), 3.60-3.58 (m, 1 H), 2.57-2.52 (m, 1 H), 2.23-2.17 (m, 1 H), 1.67-1.20 (m, 35 H), 1.02-0.92 (m, 18 H), 0.90 (t, J = 7.0 Hz, 3 H), 0.65-0.55 (m, 12 H); ^{13}C NMR (125 MHz, CDCl_3) δ 166.6, 147.9, 123.0, 75.6, 75.0, 60.2, 60.1, 34.2, 34.1, 32.1, 30.3, 30.0, 29.9, 29.6, 26.8, 22.9, 14.5, 14.4, 14.3, 7.1, 7.0, 5.4, 5.2; IR (thin film) 2926, 2878, 2855, 1729, 1657, 1464, 1414, 1379, 1368, 1318, 1264, 1238, 1167, 1100, 1047, 1005, 984, 849, 743, 673 cm^{-1} ; HRMS (CI, CH_4) calcd for $\text{C}_{37}\text{H}_{76}\text{O}_2\text{Si}_2$, 639.5204 m/z (M-H) $^+$; observed, 639.5213 m/z .



To a cold (0 $^\circ\text{C}$) solution of ester **III-106** (15.2 g, 23.8 mmol) in diethyl ether (245 mL), DIBAL-H (75 mmol, 50 mL of 1.5 M solution in toluene) was added under

and the mixture was stirred for another 45 min. A solution of allylic alcohol (6.21 g, 10.4 mmol) in CH_2Cl_2 (31 mL) was added via a syringe pump over 45 min. The reaction was warmed to $-20\text{ }^\circ\text{C}$, stirred for 2 h and then quenched by adding saturated Na_2SO_4 and Na_2SO_3 solutions (6.8 mL each). Et_2O (25 mL) was added and the resultant yellow mixture was vigorously stirred at rt for 4 h. The yellow gelatinous mass was further diluted with Et_2O (200 mL), celite was added and the mixture was filtered through a pad of celite. The filter cake was washed with Et_2O (ca. 600 mL) until it turned dry and granular. The filtrate was concentrated and epoxy alcohol **III-107** was isolated in 73% yield after purification by column chromatography (7% EtOAc in hexanes).

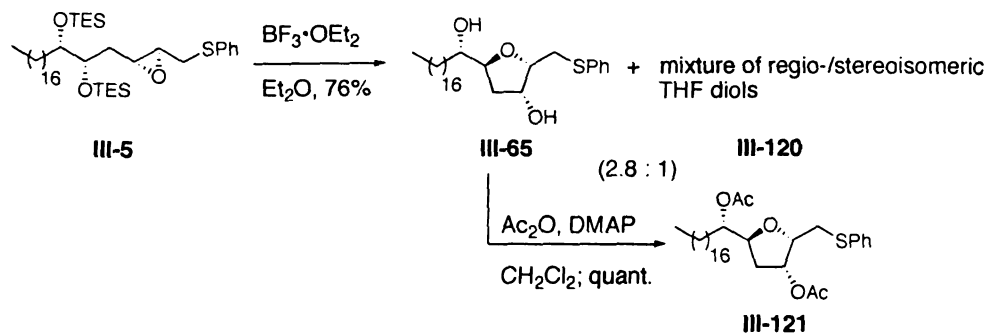
Data for **III-107**: $[\alpha]_D^{20} -16.7$ (c 1.06, CHCl_3) ^1H NMR (500 MHz, CDCl_3) δ 4.05-4.03 (m, 1 H), 3.93 (dt, $J = 4.3, 8.4$ Hz, 1 H), 3.76-3.72 (m, 2 H), 3.23 (dt, $J = 2.3, 7.2$ Hz, 1 H), 3.04 (m, 1 H), 2.09 (s (br), 1 H), 1.98-1.76 (m, 4 H), 1.63-1.37 (m, 30 H), 1.15-1.05 (m, 18 H), 1.03 (t, $J = 7.0$ Hz, 3 H), 0.77-0.67 (m, 12 H); ^{13}C NMR (125 MHz, CDCl_3) δ 75.6, 73.6, 62.2, 58.8, 54.9, 33.7, 32.2, 30.4, 30.0, 29.9, 29.8, 29.6, 26.8, 22.9, 14.4, 7.2, 7.1, 5.3, 5.2; IR (thin film) 3438, 2932, 2878, 2855, 1462, 1414, 1379, 1329, 1238, 1098, 1009, 976, 903, 874, 743, 673 cm^{-1} ; HRMS (CI, CH_4) calcd for $\text{C}_{35}\text{H}_{74}\text{O}_4\text{Si}_2$, 613.5047 m/z ($\text{M}-\text{H}$) $^+$; observed, 613.5052 m/z .



To a solution of diphenyldisulfide (6.4 g, 29.3 mmol) in triethylamine (20 mL), was added tributylphosphine (7.1 mL, 29.3 mmol) at ambient temperature under N_2 . This

solution was cooled to 0 °C and into it was cannulated a pre-cooled solution of epoxy alcohol **III-107** (5.96 g, 9.67 mmol) in Et₃N. The reaction was warmed to ambient temperature over 6 h. The reaction mixture was quenched with water (50 mL) and the aqueous solution extracted with EtOAc (3x150 mL). The combined EtOAc extracts were dried over Na₂SO₄ and concentrated under reduced pressure. The crude product was purified by flash column chromatography (hexanes → 2% EtOAc in hexanes) to afford **III-5** as a colorless oil (6.43 g, 94%).

Data for **III-105**: $[\alpha]_D^{20}$ -26.2 (c 1.62, CHCl₃) ¹H NMR (500 MHz, CDCl₃) δ 7.41 (d, *J* = 1.3 Hz, 2 H), 7.40-7.18 (m, 3 H), 3.75 (dt, *J* = 4.2, 8.2 Hz, 1 H), 3.57-3.55 (m, 1 H), 3.13 (dd, *J* = 5.1, 13.9 Hz, 1 H), 2.97-2.87 (m, 3 H), 1.69-1.31 (m, 4 H), 1.30-1.15 (m, 30 H), 0.98-0.91 (m, 18 H), 0.88 (t, *J* = 7.1 Hz, 3 H), 0.62-0.53 (m, 12 H); ¹³C NMR (125 MHz, CDCl₃) δ 135.9, 130.0, 129.2, 126.7, 75.4, 73.5, 58.2, 57.3, 36.5, 33.9, 32.2, 30.4, 30.1, 30.0, 29.9, 29.8, 29.6, 26.8, 23.0, 14.4, 7.2, 5.3; IR (thin film) 3077, 3061, 2853, 1806, 1586, 1482, 1439, 1416, 1379, 1327, 1302, 1238, 1184, 1092, 1007, 970, 943, 916, 747, 699 cm⁻¹; HRMS (EI) calcd for C₄₁H₇₈O₃SSi₂, 706.5210 *m/z* (M)⁺; observed, 706.5223 *m/z*.

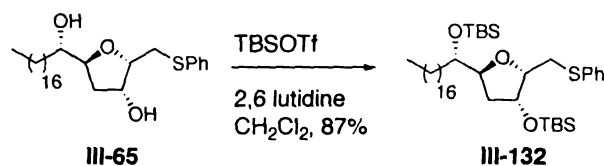


To a solution of **III-5** (4.0 g, 5.66 mmol) in 150 mL Et₂O at 0 °C was added BF₃•OEt₂ (4.3 mL, 33.8 mmol) drop wise. After complete addition, the mixture was slowly allowed to attain room temperature over 5 h. The reaction mixture was quenched with NaHCO₃ solution (50 mL) and extracted with EtOAc (3x100 mL). The combined extracts were dried over MgSO₄ and concentrated under reduced pressure to afford a mixture of regio- and stereoisomeric products. Flash column chromatography provided **III-65** (1.52 g, 56%) as a white solid along with an inseparable mixture of isomers (543 mg). **III-65** (50 mg, 0.11 mmol) was subjected to the acetylation conditions by treatment with acetic anhydride (43 mg, 0.42 mmol) and DMAP (52 mg, 0.42 mmol) in CH₂Cl₂ (1 mL) at room temperature to furnish **III-121** as a colorless oil (61 mg, 99%).

Data for **III-5**: [α]_D²⁰ -36.2 (c 0.32, CHCl₃) ¹H NMR (500 MHz, CDCl₃) δ 7.41-7.20 (m, 5 H), 4.45-4.44 (m, 1 H), 4.10 (dt, *J* = 6.2, 9.5 Hz, 1 H), 4.00 (ddd, *J* = 3.1, 5.4, 8.8 Hz, 1 H), 3.81-3.34 (m, 1 H), 3.27 (dd, 5.3, 13.0 Hz, 1 H), 3.14 (dd, *J* = 9.1, 13.3 Hz, 1 H), 2.17-2.12 (s(br), 1 H), 2.04-1.80 (m, 2 H), 1.58-1.25 (m, 32 H), 0.88 (t, *J* = 7.0 Hz, 3 H); ¹³C NMR (125 MHz, CDCl₃) δ 195.1, 135.6, 129.9, 129.3, 126.8, 100.9, 91.5, 81.5, 74.2, 73.0, 37.7, 33.7, 32.7, 32.2, 29.9, 29.8, 29.6, 25.8, 22.9, 14.3; IR (thin film) 3440, 3400, 2918, 2841, 1585, 1464, 1414, 1325, 1173, 1092, 1026, 964, 949, 879, 810, 729, 683 cm⁻¹; HRMS (CI, CH₄) calcd for C₂₉H₅₀O₃S, 477.3402 *m/z* (M-H)⁺; observed, 477.3398 *m/z*.

Partial data for **III-121**: ¹H NMR (500 MHz, CDCl₃) δ 7.39-7.18 (m, 5 H), 5.34 (m, 1 H), 4.83 (dt, *J* = 4.9, 8.4 Hz, 1 H), 4.21 (m, 1 H), 4.12 (m, 1 H), 3.19 (dd, *J* = 5.7, 13.5, 1 H), 3.06 (dd, *J* = 8.4, 13.4, 1 H), 2.09-1.86 (m, 2 H), 2.05 (s, 3 H) 2.00 (s, 3 H), 1.58-1.49 (m,

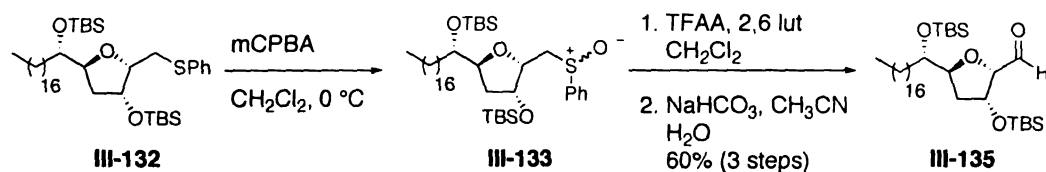
2 H), 1.27-1.21 (m, 30 H), 0.87 (t, $J = 6.6$ Hz, 3 H); ^{13}C NMR (125 MHz, CDCl_3) δ 171.1, 170.0, 135.8, 130.3, 129.2, 126.8, 80.2, 78.7, 75.1, 74.7, 35.6, 32.9, 32.2, 31.0, 29.9, 29.8, 29.7, 29.6, 25.6, 22.9, 21.4, 21.2, 14.4;



2,6-Lutidine (1.3 mL, 11.2 mmol) was added to a 0 °C solution of diol **III-65** (1.72 g, 3.59 mmol) in 18 mL CH_2Cl_2 . A solution of TBS-OTf (1.9 mL, 8.25 mmol) in 10 mL CH_2Cl_2 was then added and the reaction mixture stirred at 0 °C for 30 min. When TLC indicated completion of the reaction, water (50 mL) was added and the aqueous solution was extracted with CH_2Cl_2 (3x100 mL). The combined extracts were dried over Na_2SO_4 and concentrated under reduced pressure to afford the crude product as a colorless oil. After purification by flash column chromatography, 2.26 g of **III-132** was obtained (87%).

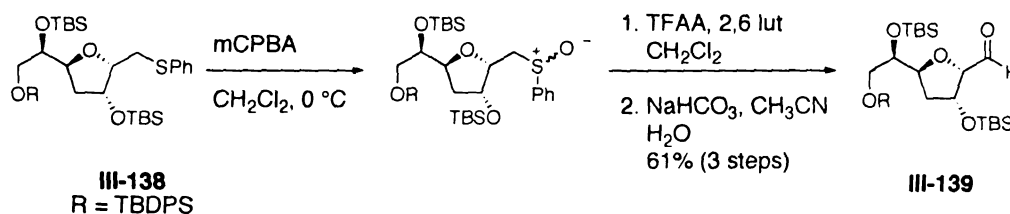
Data for **III-132**: $[\alpha]_{\text{D}}^{20} -71.0$ (c 0.57, CHCl_3) ^1H NMR (500 MHz, CDCl_3) δ 7.37-7.14 (m, 5 H), 4.40 (m, 1 H), 4.21 (dt, $J = 5.3, 10.4$ Hz, 1 H), 3.96 (dt, $J = 3.1, 6.8$ Hz, 1 H), 3.59 (m, 1 H), 3.15 (m, 2 H), 1.88-1.79 (m, 2 H), 1.38-1.22 (m, 32 H), 0.91 (s, 9 H), 0.89 (t, $J = 6.6$ Hz, 3 H), 0.87 (s, 9 H), 0.12 (s, 3 H), 0.11 (s, 3 H) 0.07 (s, 3 H) 0.05 (s, 3 H); ^{13}C NMR (125 MHz, CDCl_3) δ 137.0, 129.1, 128.7, 125.8, 81.7, 80.7, 74.6, 73.0, 37.3, 32.7, 32.2, 30.1, 29.9, 29.8, 29.6, 26.2, 26.0, 22.9, 18.5, 18.3, 14.4, -4.0, -4.2, -4.3, -4.6; IR (thin film) 2926, 2856, 1585, 1470, 1439, 1389, 1362, 1254, 1194, 1078, 1057, 1007,

960, 835, 775, 737, 690 cm^{-1} ; HRMS (ES) calcd for $\text{C}_{41}\text{H}_{78}\text{O}_3\text{SSi}_2$, 707.5289 m/z ($\text{M}+\text{H}^+$); observed, 707.5269 m/z .



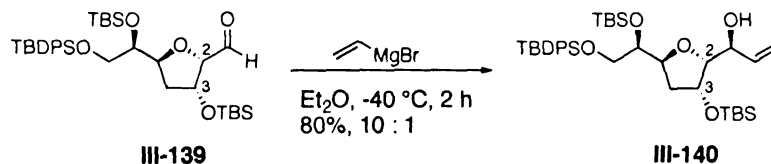
To a 0 °C solution of sulfide **III-132** (1 g, 1.4 mmol) in 16 mL CH_2Cl_2 , was added a solution of mCPBA (350 mg, 1.4 mmol) in CH_2Cl_2 (16 mL). After 30 min at 0 °C, the reaction mixture was quenched with sat. NaHCO_3 solution (30 mL) and the aqueous mixture was extracted with CH_2Cl_2 (3x50 mL). The combined extracts were dried over Na_2SO_4 and concentrated under reduced pressure to afford sulfonamide **III-133** as a mixture of stereoisomers. The crude product so obtained was dissolved in CH_2Cl_2 (11.3 mL), cooled to 0 °C and 2,6-lutidine (0.56 mL) was added. TFAA (0.69 mL, 4.95 mmol) in CH_2Cl_2 (11.3 mL) was then added and the mixture stirred at 0 °C for 1 h. The reaction mixture was quenched with sat. NaHCO_3 solution and extracted with CH_2Cl_2 . The combined extracts were dried over Na_2SO_4 and concentrated under reduced pressure to afford a clear oil. This material was taken up in 1:1 acetonitrile – water (50 mL) and solid NaHCO_3 (2.5 g) was added. The reaction mixture was stirred at ambient temperature for 16 h, upon which the solution was diluted with 25 mL water. The aqueous solution was extracted with CH_2Cl_2 (3x25 mL) and the combined extracts were dried over Na_2SO_4 and concentrated under reduced pressure. Slow chromatography on

(125 MHz, CDCl₃) δ 137.0, 135.8, 133.6, 129.9, 129.1, 128.7, 127.9, 125.9, 81.7, 79.5, 73.3, 73.2, 65.8, 49.7, 34.5, 32.5, 27.0, 19.4, 18.2, 7.0, -4.6, -6.9.



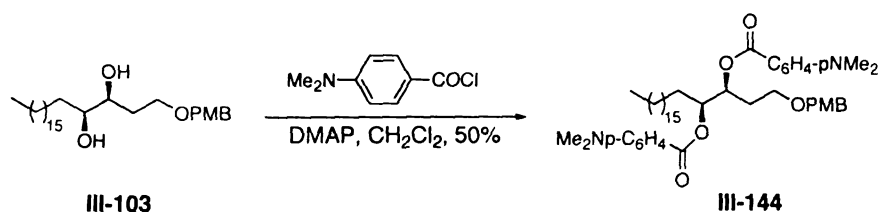
Pummerer rearrangement of sulfide **III-138** (2.51 g, 3.47 mmol) to secure aldehyde **III-139** (1.36 g, 61%) was carried out following the representative procedure described above (for **III-135**). Flash column chromatography was performed using 3% EtOAc in hexanes.

Partial data for **III-139**: $[\alpha]_D^{20}$ -37.9 (c 0.89, CHCl₃) ¹H NMR (500 MHz, CDCl₃) δ 9.62 (d, J = 2.2 Hz, 1 H), 7.67-7.65 (m, 4 H), 7.45-7.37 (m, 6 H), 4.84-4.80 (m, 1 H), 4.77-4.75 (m, 1 H), 4.16-4.10 (m, 1 H), 4.09-4.07 (m, 1 H), 3.60 (dd, J = 4.6, 10.4 Hz, 1 H), 3.43 (dd, J = 7.3, 10.4, 1 H), 2.17-2.19 (m, 1 H), 1.89-1.85 (m, 1 H), 1.05 (s, 9 H), 0.86 (s, 9 H), 0.81 (s, 9 H), 0.07 (s, 3 H), 0.04 (s, 3 H), -0.02 (s, 3 H), -0.07 (s, 3 H); ¹³C NMR (125 MHz, CDCl₃) δ 203.1, 135.8, 135.7, 133.5, 133.4, 130.0, 129.9, 127.9, 127.8, 87.2, 81.7, 76.3, 72.9, 65.9, 35.2, 27.0, 26.0, 25.8, 19.4, 18.2, 18.1, -4.5, -4.6, -5.0; IR (thin film) 2957, 2889, 1959, 1909, 1821, 1736, 1471, 1255, 1151, 1068, 998, 887, 806, 777, 702 cm⁻¹.

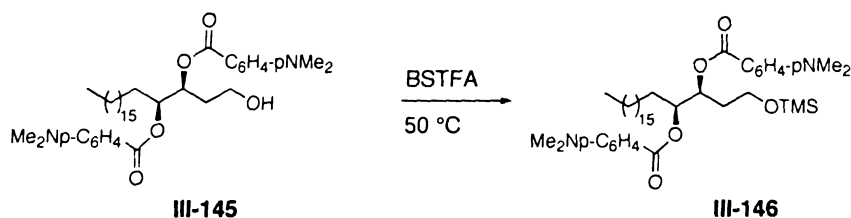


To a solution of aldehyde **III-139** (205 mg, 0.32 mmol) in diethyl ether (4.2 mL), vinylmagnesium bromide (0.8 mL) was added at -40°C and stirred under N_2 for 2 h. The reaction was quenched by addition of saturated NH_4Cl solution (5 mL), layers were separated and the aqueous layer was extracted with Et_2O (3x50 mL). The combined organic layers were dried (MgSO_4), concentrated and the crude product was purified by flash column chromatography to furnish the allylic alcohol **III-140** (170 mg, 80%; dr = 10:1 by ^1H NMR) as a colorless oil.

Partial data for **III-140**: ^1H NMR (300 MHz, CDCl_3) δ 7.68-7.65 (m, 4 H), 7.47-7.37 (m, 6 H), 6.00-5.89 (m, 1 H), 5.43 (d, $J = 17.0$ Hz, 1 H), 5.20 (d, $J = 10.7$ Hz, 1 H), 4.66 (m, 1 H), 4.42-4.40 (m, 2 H), 4.08-4.07 (m, 1 H), 3.75-3.72 (m, 1 H), 3.56 (dd, $J = 4.9, 15.2$ Hz, 1 H), 3.41 (dd, $J = 7.7, 9.9$ Hz, 1 H), 3.29 (s(br), 1 H), 2.25-2.16 (m, 1 H), 1.90-1.83 (m, 1 H), 1.04 (s, 9 H), 0.94 (s, 9 H), 0.82 (s, 9 H), 0.14 (s, 6 H), 0.02 (s, 3 H), -0.06 (s, 3 H).

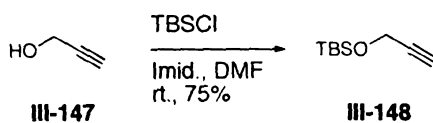


To a solution of diol **III-103** (54 mg, 0.11 mmol) in CH_2Cl_2 (1 mL) *p*-dimethylaminobenzoyl chloride (107 mg, 0.93 mmol) and DMAP (100 mg, 0.82 mmol) were added and stirred for 15 h. The reaction was then quenched with H_2O (3 mL) and the aqueous layer was extracted with CH_2Cl_2 (2x5 mL). The combined organic layers were dried (Na_2SO_4), concentrated under reduced pressure and the crude material was



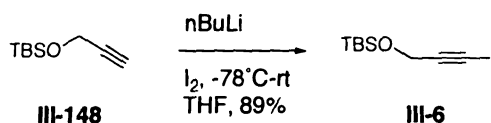
Alcohol **III-145** (15 mg, 0.02 mmol) was dissolved in bis-(trimethylsilyl)trifluoroacetamide (0.2 mL) and the solution was heated to 50 °C for 30 min. After cooling to room temperature, the volatiles were removed under reduced pressure and the TMS derivative **III-146** was used for ECCD analysis without further purification.

Partial data for **III-146**: ^1H NMR (500 MHz, CDCl_3) δ 8.00-7.94 (m, 4 H), 6.69-6.65 (m, 4 H), 5.47-5.44 (m, 1 H), 5.35-5.32 (m, 1 H), 3.68-3.65 (m, 2 H), 3.05 (s, 6 H), 3.04 (s, 6 H), 2.01-1.94 (s, 2 H), 1.73-1.69 (s, 2 H), 1.37-1.21 (m, 30 H), 0.89 (t, $J = 7.1$ Hz, 3 H), 0.08 (s, 3 H), 0.07 (s, 6 H); ^{13}C NMR (125 MHz, CDCl_3) δ 166.7, 166.5, 153.5, 131.7, 117.5, 117.4, 110.9, 74.2, 71.4, 59.2, 40.3, 34.5, 32.1, 31.3, 30.0, 29.9, 29.8, 29.7, 29.6, 29.5, 25.5, 22.9, 14.3, 1.2, -0.4.



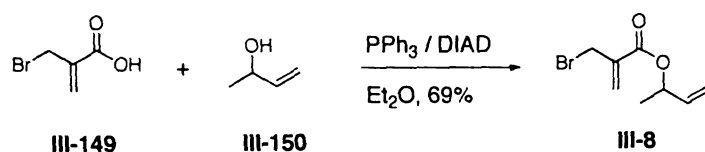
To a solution of propargyl alcohol **III-147** (11.2 g, 0.20 mol) in DMF (70 mL), *t*-butyldimethylchlorosilane (36.2 g, 0.24 mmol) and imidazole (34 g, 0.50 mol) was added. After stirring for 15 h, the reaction was poured in H_2O (200 mL) and extracted with pentane (3x300 mL). Purification by vacuum distillation afforded the TBS protected propargyl alcohol **III-148** as a colorless oil (25.5 g, 75%). Spectroscopic properties of **III-148** match those reported.¹⁰⁶

Partial data for **III-148**: ^1H NMR (500 MHz, CDCl_3) δ 4.30 (t, $J = 2.2$ Hz, 2 H), 2.38 (t, $J = 2.2$ Hz, 1 H), 0.9 (s, 9 H), 0.2 (s, 6 H).



To a -78°C solution of **III-148** (11 g, 64.7 mmol) in THF (60 mL), *n*-BuLi (32 mL of 2.02 M solution in hexanes, 64.7 mmol) was added. After stirring for 1 h, a solution of I_2 (18.9 g, 74.4 mmol) in THF (35 mL) was added and the reaction was warmed to rt. After 15 min, the reaction was diluted with Et_2O (200 mL) and washed with saturated sodium thiosulfate solution (3x150 mL). The organic layer was dried, concentrated and purified by column chromatography (2% EtOAc in hexanes) to afford 17.0 g of alkynyl iodide **III-6** as a brown liquid (89% yield). Spectroscopic properties of **III-6** match those reported.¹⁰⁶

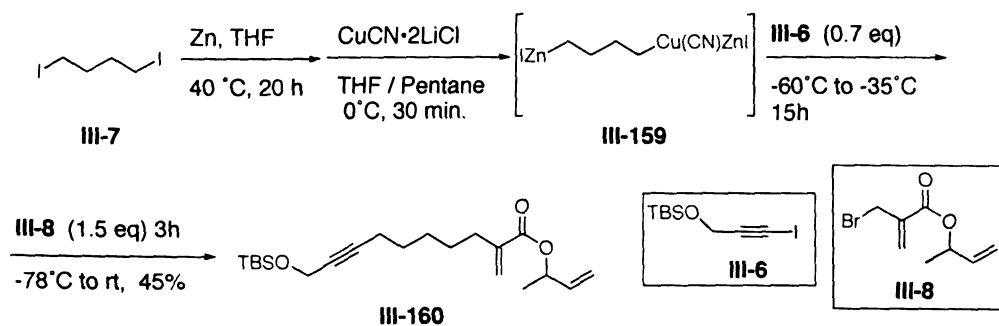
Partial data for **III-6**: ^1H NMR (500 MHz, CDCl_3) δ 4.47 (s, 2 H), 0.92 (s, 9 H), 0.13 (s, 6 H).



To a solution of bromomethylacrylic acid **III-149** (7 g, 42.4 mmol) and DIAD (8.34 mL, 42.4 mmol) in ether (64 mL), was added a solution of alcohol **29** (5.52 mL, 63.6 mol) and Ph_3P (11.1 g, 42.4 mol) in ether (64 mL), dropwise at 0°C . The reaction was stirred at the same temperature for 30 min, and then at room temperature for 16 h. The mixture was filtered and washed with Et_2O (100 mL). After concentration of the

filtrate, the crude product was purified by flash column chromatography (3% EtOAc in hexanes) to furnish acrylate **III-8** as a yellow liquid (6.5 g, 69%). Spectral properties of **III-8** matched those reported.¹⁰⁷

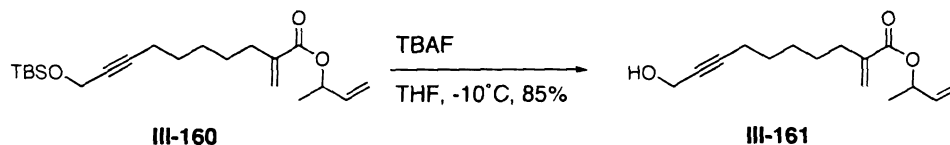
Partial data for **III-8**: ¹H NMR (500 MHz, CDCl₃) δ 6.31 (app s, 1 H), 5.95 (app s, 1 H), 5.88-5.82 (m, 1 H), 5.46 (quin, *J* = 6.4 Hz, 1 H), 5.26 (d, *J* = 16.7 Hz, 1 H), 5.18 (d, *J* = 10.1 Hz, 1 H), 4.19 (s, 2 H), 1.38 (d, *J* = 6.7 Hz, 3 H).



1,2 dibromoethane (27 μL, 5 mol%) in THF (1.5 mL) was added to zinc dust (398 mg, 6.08 mmol) and the suspension was refluxed for 30 min. Upon cooling the mixture to rt, TMSCl (23 μL, 3 mol%) and 1,4 diiodobutane **III-7** (0.2 mL, 1.52 mmol) in THF (5 mL) were added and the mixture was heated at 40 °C for 20 h after which CG analysis indicated complete consumption of the diiodide. The suspension was then allowed to settle at room temperature. The supernatant liquid was transferred to a pre-cooled (-60 °C) solution of CuCN (136 mg, 1.52 mmol) and LiCl (129 mg, 3.04 mmol) in 3 : 1 THF : pentane (2 mL). The resulting mixture was stirred at 0 °C for 1 h after which alkynyl iodide **III-6** (315 mg, 1.06 mmol) in 1 : 1 THF : pentane (1.5 mL) was added at -60 °C, stirred at -35 °C for 20 h and again cooled to -78 °C. Allyl bromide **III-8** (500 mg, 2.28 mmol) was added at -78 °C and the reaction was warmed to room temperature.

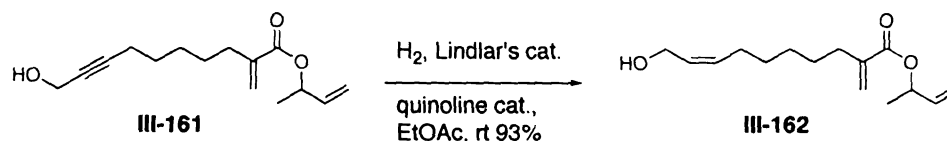
After 4 h saturated NH_4Cl solution (15 mL) was added to quench the reaction. The aqueous layer was extracted with Et_2O (3x50 mL), organic layers were combined, dried (Na_2SO_4), concentrated and the product was purified by column chromatography (1% – 4% EtOAc in hexanes) to afford **III-160** as a yellow liquid (174 mg, 45% yield).

Partial data for **III-160**: ^1H NMR (300 MHz, CDCl_3) δ 6.16 (app s, 1 H), 5.95-5.83 (m, 1 H), 5.52 (app s, 1 H), 5.44-5.40 (m, 1 H), 5.23 (d, $J = 17.2$, 1 H), 5.15 (d, $J = 11.2$, 1 H), 4.30-4.28 (m, 2 H), 2.31 (t, $J = 6.6$ Hz, 2 H), 2.21 (t, $J = 6.6$ Hz, 2 H), 1.58-1.42 (m, 6 H), 1.36 (d, $J = 6.6$ Hz, 3 H), 0.97 (s, 9 H), 0.13 (s, 6 H).



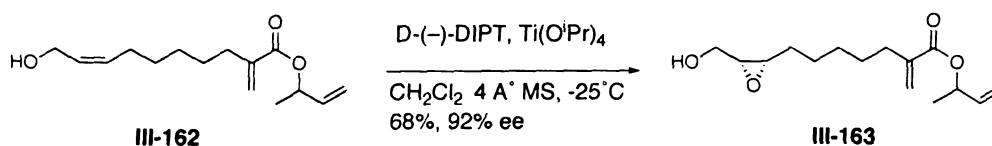
To a solution of **III-160** (650 mg, 1.78 mmol), in THF (10 mL) cooled to -10°C , TBAF (3.6 mL of 1.0 M solution in THF, 3.6 mmol) was added and stirred for 45 min after which the reaction was poured into water (15 mL) and extracted with Et_2O (3x15 mL). Combined organic layers were dried over Na_2SO_4 , concentrated and crude product was purified by column chromatography (5% EtOAc in hexanes) to furnish propargylic alcohol **III-161** as a colorless liquid (378 mg, 85% yield).

Partial data for **III-161**: ^1H NMR (300 MHz, CDCl_3) δ 6.16 (app s, 1 H), 5.89-5.84 (m, 1 H), 5.54 (app s, 1 H), 5.48-5.41 (m, 1 H), 5.25 (d, $J = 17.5$ Hz, 1 H), 5.16 (d, $J = 10.4$ Hz, 1 H), 4.34-4.26 (m, 2 H), 2.33 (t, $J = 6.2$ Hz, 2 H), 2.23 (t, $J = 6.6$ Hz, 2 H), 1.76-1.36 (m, 9 H).



A mixture of propargylic alcohol **III-61** (600 mg, 2.4 mmol), Lindlar's catalyst (110 mg) and quinoline (0.3 mL) in ethyl acetate (20 mL) was vigorously stirred under H_2 (1 atm) for 2 h. The reaction mixture was then filtered over a pad of celite and the residue was washed with ethyl acetate (40 mL). The filtrate was washed with 5% CuSO_4 (2x5 mL). The organic portion was dried (Na_2SO_4), concentrated and the crude product was purified by flash column chromatography to afford the *cis* allylic alcohol **III-162** as a colorless liquid (562 mg, 93%).

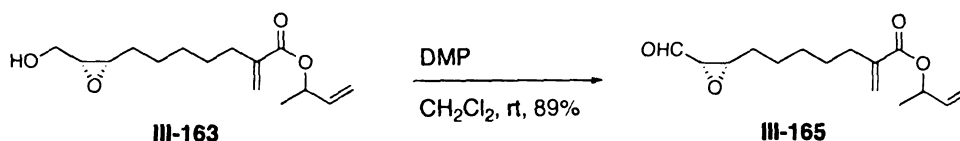
Partial data for **III-162**: ^1H NMR (300 MHz, CDCl_3) δ 6.16 (app s, 1 H), 5.94-5.83 (m, 1 H), 5.62-5.53 (m, 3 H), 5.44-5.40 (m, 1 H), 5.30 (d, $J = 16.0$, 1 H), 5.20 (d, $J = 10.4$ Hz, 1 H), 4.20 (d, $J = 6.3$ Hz, 1 H), 2.31 (t, $J = 7.3$ Hz, 2 H), 2.12-2.05 (m, 2 H), 1.48-1.27 (m, 9 H).



To a flame dried round bottom flask charged with pre-activated 4 Å MS (100 mg) and CH_2Cl_2 (3 mL), $\text{Ti}(\text{O}^i\text{Pr})_4$ (230 mg, 2.5 mmol) was added and the mixture was cooled to -30°C . To this, a solution of D-(-)-DIPT (225 mg, 0.95 mmol) in CH_2Cl_2 (3 mL) was added and the mixture was stirred for 30 min before $t\text{-BuOOH}$ (0.9 mL of 4.01 M solution in toluene, 3.52 mmol) was added to it. After stirring for another 30 min at the same temperature, a solution of allylic alcohol **III-162** (400 mg, 1.59 mmol) in CH_2Cl_2 (6

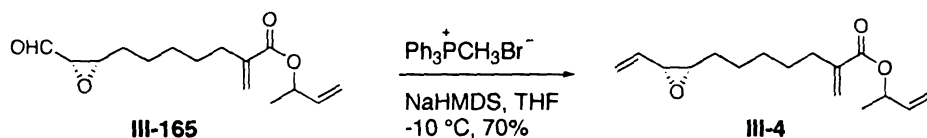
mL) was added dropwise and the reaction was stirred at -25°C for 18 h. Saturated Na_2SO_4 solution (0.8 mL) and saturated Na_2SO_3 (1.6 mL) were added and the reaction was diluted with ether (12 mL). The mixture was stirred vigorously for 3 h, stored at 0°C overnight and then filtered through a celite pad. The filtrate was washed with anhydrous ether (500 mL), concentrated and the crude product was purified by column chromatography (5% EtOAc in hexanes) to furnish the epoxy alcohol **III-163** as faint pink liquid (290 mg 68% yield, 92% ee). The % ee of **III-163** was determined after derivatization to the corresponding (*S*)-MPA ester.

Partial data for **III-163**: ^1H NMR (300 MHz, CDCl_3) δ 6.24 (app s, 1 H), 5.94-5.82 (m, 1 H), 5.52 (app s, 1 H), 5.43-5.39 (m, 1 H), 5.25 (d, $J = 17.5$ Hz, 1 H), 5.14 (d, 10.9 Hz, 1 H), 3.84 (dd, $J = 3.9, 12.1$ Hz, 1 H), 3.67 (dd, $J = 6.7, 12.1$ Hz, 1 H), 3.18-3.13 (m, 1 H), 3.05-3.00 (m, 1 H), 2.31 (t, $J = 6.7$ Hz, 2 H), 2.05 (s(br), 1 H), 1.55-1.23 (m, 11 H).



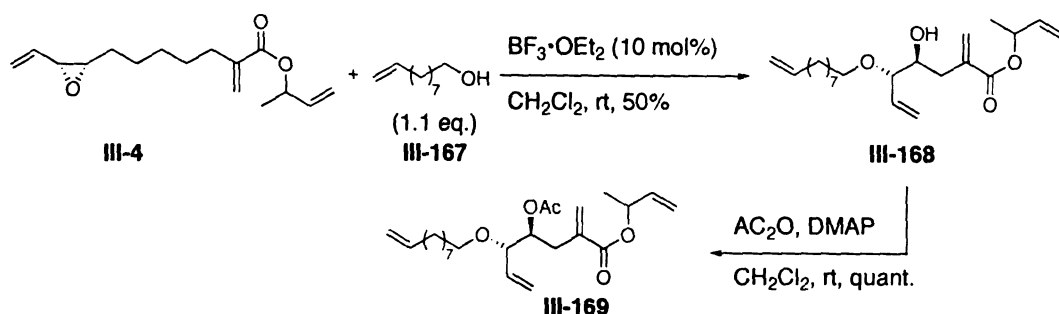
To a suspension of DMP reagent (3.2 g, 7.55 mmol) in CH_2Cl_2 (20 mL), a solution of the epoxy alcohol **III-163** (1.19 g, 4.44 mmol) in CH_2Cl_2 (10 mL) was added at rt and the reaction was stirred for 2 h. After diluting with Et_2O (26 mL), the mixture was poured in a saturated solution of NaHCO_3 (26 mL) containing $\text{Na}_2\text{S}_2\text{O}_3$ (9.5 g) and stirred vigorously for 5 min. The layers were separated and the aqueous layer was washed with CH_2Cl_2 (2x30 mL). The combined organic layers were dried, concentrated and the crude product was purified by flash column chromatography (2% EtOAc in hexanes) to afford epoxy aldehyde **III-165** (1.05 g, 89%).

Partial data for **III-165**: ^1H NMR (300 MHz, CDCl_3) δ 9.31 (d, $J = 2.7$, 1 H), 6.14 (app s, 1 H), 5.93-5.82 (m, 1 H), 5.51 (app s, 1 H), 5.24 (d, $J = 17.2$ Hz, 1 H), 5.13 (d, $J = 10.5$ Hz, 1 H), 3.35-3.32 (m, 1 H), 3.28-3.24 (m, 1 H), 2.30 (t, $J = 6.7$ Hz, 1 H), 1.8-1.34 (m, 8 H), 1.23 (t, $J = 6.7$ Hz, 3 H).



To a suspension of methyl triphenylphosphonium bromide (710 mg, 1.99 mmol) in THF (10 mL), NaHMDS (1.58 mL of 1.0 M solution, 1.58 mmol) was added at 0°C and stirred at rt for 30 min. The resultant ylide was cooled back to -10°C . To this cooled mixture, a solution of aldehyde **III-165** (350 mg, 1.32 mmol) in THF (3 mL) was added dropwise. After 10 min at -10°C , the reaction was quenched with sat. NH_4Cl (20 mL) diluted with ether (50 mL). The organic layer was washed with H_2O (10 mL), brine (10 mL), dried and concentrated. The crude product was purified by column chromatography to afford vinylic epoxide **4** as a colorless liquid (244 mg, 70% yield).

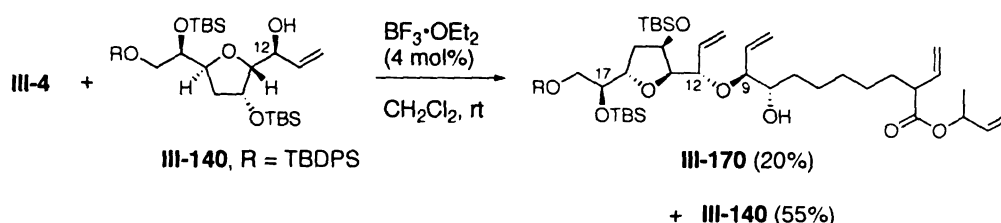
Partial data for **III-4**: ^1H NMR (300 MHz, CDCl_3) δ 6.10 (app s, 1 H), 5.85-5.79 (m, 1 H), 5.69-5.62 (m, 1 H), 5.45 (app s, 1 H), 5.43 (d, $t = 17.7$ Hz, 1 H), 5.35-5.33 (m, 1 H), 5.28 (d, $J = 10.6$ Hz, 1 H), 5.20 (d, $J = 17.6$ Hz, 1 H), 5.08 (d, $J = 10.6$ Hz, 1 H), 3.33 (m, 1 H), 3.00 (m, 1 H), 2.52 (d, $J = 7.7$ Hz, 3 H); ^{13}C NMR (125 MHz, CDCl_3) δ 166.5, 141.3, 138.0, 132.9, 124.5, 120.4, 115.7, 71.3, 58.8, 57.3, 31.9, 29.1, 28.5, 27.8, 26.2, 20.1.



A mixture of vinylic epoxide **III-4** (22 mg, 83.0 μ mol) and alcohol **III-167** (15 mg, 92.0 μ mol) was dissolved in CH_2Cl_2 (0.18 mL). To this, $BF_3 \cdot OEt_2$ (10 μ L of 0.83 M solution in CH_2Cl_2 , 8.3 μ mol) was added at once at room temperature. After 15 min, the epoxide was completely consumed and several other spots appeared as judged by TLC. The reaction was then diluted with CH_2Cl_2 (10 mL) and quenched with H_2O (2 mL). The aqueous layer was extracted with CH_2Cl_2 (2x10 mL), combined organic layers were dried, concentrated. Careful chromatographic purification (5% – 7% EtOAc in hexanes) afforded the adduct **III-168** (17 mg, 50%). Structure of **III-168** was confirmed by 1H homo decoupling experiments of the acetate derivative **III-169**.

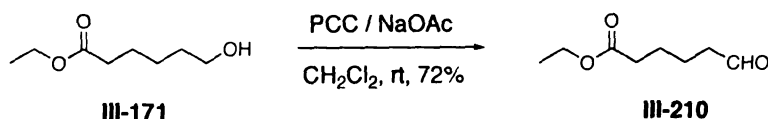
Partial data for **III-168**: 1H NMR (500 MHz, $CDCl_3$) δ 6.15 (app s, 1 H), 5.95-5.81 (m, 2 H), 5.78-5.60 (m, 1 H), 5.57 (app s, 1 H), 5.45-5.39 (m, 1 H), 5.30-5.24 (m, 3 H), 5.18-5.13 (m, 1 H), 5.03-4.93 (m, 2 H), 3.59-3.39 (m, 3 H), 3.28-3.23 (m, 1 H), 2.77 (s (br), 1 H), 2.31 (t, J = 7.1 Hz, 2 H), 2.09-2.04 (t, 6.6 Hz, 2 H), 1.57-1.27 (m, 15 H).

Partial data for **III-169**: 1H NMR (500 MHz, $CDCl_3$) δ 6.15 (app s, 1 H), 5.95-5.88 (m, 2 H), 5.83-5.87 (m, 1 H), 5.42 (app s, 1 H), 5.39 (m, 1 H), 5.21-5.25 (m, 3 H), 5.18 (m, 1 H), 4.95-5.10 (m, 3 H), 3.63-3.69 (m, 2 H), 3.45-3.55 (m, 1 H), 3.31-3.27 (m, 1 H), 2.28 (t, J = 6.7 Hz, 1 H), 1.98-2.04 (m, 5 H), 1.81-1.20 (m, 23 H).



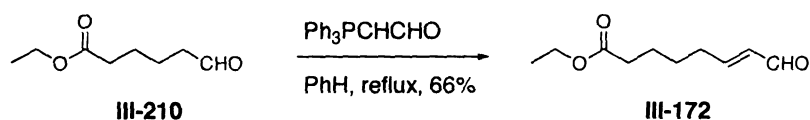
Intermolecular ring opening of vinyl epoxide **III-4** (20 mg, 76 μmol) with alcohol **III-140** (51 mg, 77 μmol) using $\text{BF}_3 \cdot \text{OEt}_2$ (3.5 μl of 0.9 M solution in CH_2Cl_2 , 3.2 μmol) was effected by the procedure described above. Adduct **III-170** was obtained in 20 % yield (14 mg) along with recovered alcohol **III-140** (28 mg, 55%).

Partial data for **III-170**: ^1H NMR (500 MHz, CDCl_3) δ 7.62-7.78 (m, 5 H), 7.32-7.48 (m, 5 H), 6.15 (app s, 1 H), 5.98-5.62 (m, 3 H), 5.45 (app s, 1 H), 5.39-5.42 (m, 1 H), 5.15-5.30 (m, 6 H), 4.69-4.57 (m, 1 H), 4.20-4.37 (m, 2 H), 4.01-4.13 (m, 1 H), 3.78-3.60 (m, 2 H), 3.59-3.42 (m, 2 H), 3.38-3.29 (m, 1 H), 2.89 (s(br), 1 H), 2.23 (t, $J = 6.7$, Hz, 2 H), 2.02-2.18 (m, 1 H), 1.98-1.80 (m, 1 H), 1.43-.120 (m, 11 H), 1.04 (s, 9 H), 0.9 (s, 9 H), 0.8 (s, 9 H), 0.1 (s, 3 H), 0.08 (s, 3 H), 0.06 (s, 3 H), -0.02 (s, 3 H).



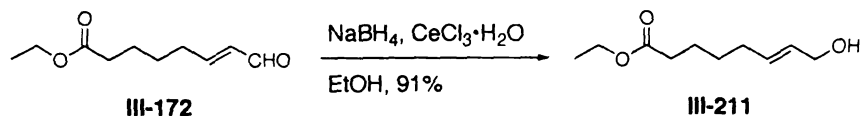
To a suspension of PCC (22.9 g, 0.11 mol) and sodium acetate (2.4 g, 0.03 mol) in CH_2Cl_2 (100 mL), was added a solution of ethyl 6-hydroxyhexanoate **III-171** (9.85 g, 0.06 mol) in CH_2Cl_2 (24 mL) at room temperature. After 2 h, the reaction was diluted with Et_2O (150 mL) and filtered through a celite pad. The filtrate was concentrated under reduced pressure and the crude material was purified by column chromatography (5% EtOAc in hexanes) to afford aldehyde **III-210** (6.83 g, 72%).¹⁴⁴

Partial data for **III-210**: ^1H NMR (500 MHz, CDCl_3) δ 9.76 (t, $J = 1.7$ Hz, 1 H), 4.11 (q, $J = 7.1$ Hz, 2 H), 2.48-2.43 (m, 2 H), 2.36-2.08 (m, 2 H), 1.69-1.63 (m, 4 H), 1.24 (t, $J = 7.3$ Hz, 3 H); ^{13}C NMR (125 MHz, CDCl_3) δ 202.4, 173.5, 60.6, 43.7, 34.2, 24.5, 21.7, 14.5.



Aldehyde **III-210** (6.8 g, 43.0 mmol) in benzene (30 mL) was added to a suspension of (triphenylphosphoranylidene)acetaldehyde (13.1 g, 43.0 mmol) in benzene (30 mL). The mixture was heated to reflux for 15 h and then cooled to room temperature. Volatiles were evaporated and the crude product was purified by flash column chromatography (15% EtOAc in hexanes) to obtain 5.2 g of α,β -unsaturated aldehyde **III-172** (66%) as a colorless liquid.

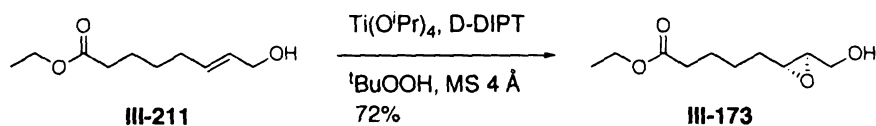
Partial data for **III-172**: ^1H NMR (500 MHz, CDCl_3) δ 9.51 (d, $J = 7.7$ Hz, 1 H), 6.84 (dt, $J = 6.7, 8.8$ Hz, 1 H), 6.18-6.09 (m, 1 H), 4.13 (q, $J = 7.15$ Hz, 2 H), 2.41-2.31 (m, 4 H), 1.74-1.53 (m, 4 H), 1.24 (t, $J = 7.1$ Hz, 3 H).



To a solution of aldehyde **III-172** (5.2 g, 28.3 mmol), cerium trichloride (10.6 g, 28.3 mmol) and sodium borohydride (1.07 g, 28.3 mmol) were added at room temperature. After completion of the reaction (30 min), H_2O (3.5 mL) was added and the volatiles were removed under reduced pressure. The residue was taken up in Et_2O (300 mL) and H_2O (150 mL). Layers were separated, the aqueous layer was extracted with

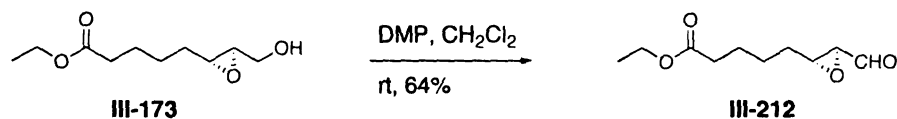
Et₂O (3x150 mL), the combined organic layers were dried (MgSO₄) and concentrated. After purification by column chromatography (30% EtOAc in hexanes), allylic alcohol **III-211** was produced in 91% yield (4.78 g).

Partial data for **III-211**: ¹H NMR (500 MHz, CDCl₃) δ 5.70-5.66 (m, 2 H), 4.17-4.10 (m, 4 H), 2.31 (t, *J* = 7.2 Hz, 2 H), 2.11-2.05 (m, 2 H), 1.70-1.60 (m, 2 H), 1.58-1.38 (m, 2 H), 1.27 (t, *J* = 7.14 Hz, 3 H).



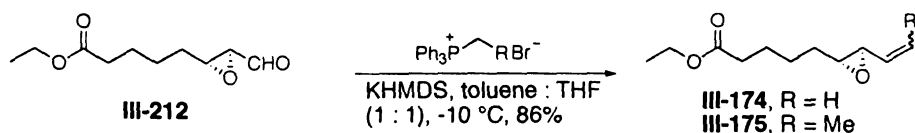
To a flame dried round bottom flask charged with pre-activated 4 Å MS (1.54 g) and CH₂Cl₂ (46 mL), Ti(O^{*i*}Pr)₄ (1.5 mL, 5.14 mmol) was added and the mixture was cooled to −30°C. To this, a solution of D-(−)-DIPT (1.3 mL, 6.17 mmol) in CH₂Cl₂ (46 mL) was added and the mixture was stirred for 30 min before t-BuOOH (13.9 mL of 4.01 M solution in toluene, 56.0 mmol) was added to it. After stirring for another 30 min at the same temperature, a solution of allylic alcohol **III-211** (4.78 g, 25.7 mmol) in CH₂Cl₂ (18 mL) was added dropwise and the reaction was stirred at −25°C for 18 h. Saturated Na₂SO₄ solution (5.4 mL) and saturated Na₂SO₃ (30.8 mL) were added and the reaction was diluted with ether (150 mL). The mixture was stirred vigorously for 3 h and then filtered through a celite pad. The filtrate was washed with anhydrous ether (1 L), concentrated and the crude product was purified by column chromatography (5% EtOAc in hexanes) to furnish the epoxy alcohol **III-173** as colorless liquid (3.74 72% yield, >99% ee). The % ee of **III-173** was determined after derivatization to the corresponding (*S*)-MPA ester.

Partial data for **III-173**: ^1H NMR (500 MHz, CDCl_3) δ 4.12 (q, $J = 7.14$ Hz, 2 H), 3.88 (dd, $J = 2.2, 12.6$ Hz, 1 H), 3.61 (dd, $J = 4.1, 12.6$ Hz, 1 H), 2.97-2.90 (m, 2 H), 2.31 (t, $J = 7.4$ Hz, 2 H), 1.72-1.42 (m, 6 H), 1.25 (t, $J = 7.14$ Hz, 3 H).



To a suspension of DMP reagent (10.2 g, 24.0 mmol) in CH_2Cl_2 (40 mL), a solution of the epoxy alcohol **III-173** (2.42 g, 12.0 mmol) in CH_2Cl_2 (20 mL) was added at rt and the reaction was stirred for 2 h. After diluting with Et_2O (50 mL), the mixture was poured in a saturated solution of NaHCO_3 (80 mL) containing $\text{Na}_2\text{S}_2\text{O}_3$ (20 g) and stirred vigorously for 5 min. The layers were separated and the aqueous layer was washed with CH_2Cl_2 (2x100 mL). The combined organic layers were dried, concentrated and the crude product was purified by flash column chromatography (2% EtOAc in hexanes) to afford epoxy aldehyde **III-212** (1.53 g, 64%).

Partial data for **III-212**: ^1H NMR (500 MHz, CDCl_3) δ 9.01 (d, $J = 6.04$ Hz, 1 H), 4.13 (q, $J = 7.1$ Hz, 2 H), 3.26-3.22 (m, 1 H), 3.16-3.13 (m, 1 H), 2.33 (t, $J = 2.5$ Hz, 2 H), 1.78-1.52 (m, 6 H), 1.26 (t, $J = 7.1$ Hz, 3 H).



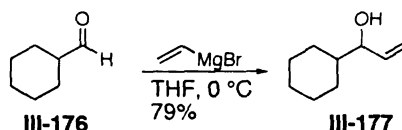
To a slurry of ethyltriphenylphosphonium bromide (1.97 g, 5.3 mmol) in 4 : 1 toluene : THF (10.6 mL) at -20 $^\circ\text{C}$, KHMDs (9.16 mL of 0.5 M solution in toluene, 4.58 mmol) was added and the orange mixture was warmed to room temperature. After 1 h, the ylide was cooled back to -20 $^\circ\text{C}$ and a solution of aldehyde **III-212** (530 mg, 2.65

mmol) in THF (5.3 mL) was added. The reaction was continued at $-10\text{ }^{\circ}\text{C}$ for 1 h after which EtOH (0.19 mL) was added and the solids were filtered off through a celite pad. The crude material was purified by column chromatography (10% EtOAc in hexanes) to furnish vinylic epoxide **III-175** in 86% yield (483 mg) as colorless oil.

Vinyl epoxide **III-174** was prepared by the same procedure using methyltriphenyl-phosphonium bromide. Thus 446 mg (85%) of **III-174** was obtained from 530 mg of **III-212**.

Partial data for **III-175**: ^1H NMR (500 MHz, CDCl_3) δ 5.79-5.73 (m, 1 H), 5.08-5.04 (m, 1 H), 4.15 (q, $J = 7.3$ Hz, 2 H), 3.38-3.34 (m, 1 H), 2.84-2.80 (m, 1 H), 2.31 (t, $J = 7.1$ Hz, 2 H), 1.79 (dd, $J = 1.7, 7.1$ Hz, 3 H), 1.75-1.48 (m, 6 H), 1.24 (t, $J = 7.3$ Hz, 3 H).

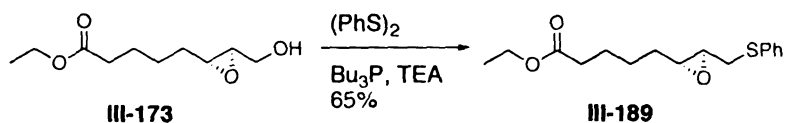
Partial data for **III-174**: ^1H NMR (500 MHz, CDCl_3) δ 5.62-5.40 (m, 2 H), 5.26-5.23 (m, 1 H), 4.11 (q, $J = 7.1$ Hz, 2 H), 3.10-3.07 (m, 1 H), 2.84-2.80 (m, 1 H), 2.31 (t, $J = 7.1$ Hz, 2 H), 1.72-1.45 (m, 6 H), 1.25 (t, $J = 7.2$ Hz, 3 H).



Cyclohexylcarboxaldehyde **III-176** (1.12 g, 10 mmol) in THF (10 mL) was added to a solution of vinylmagnesium bromide (12 mL of 1.0 M solution, 12 mmol) in THF (10 mL) at $0\text{ }^{\circ}\text{C}$. After 3 h, the reaction was quenched by addition of saturated NH_4Cl solution (10 mL). The layers were separated and aqueous layer was extracted with Et_2O (3x15 mL). The combined organic layers were dried over MgSO_4 , concentrated and the crude material was purified by flash column chromatography (20% EtOAc in hexanes) to

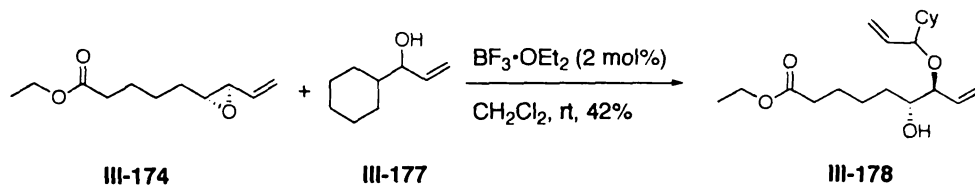
afford alcohol **III-177** as a colorless oil (1.1 g, 79%). Spectral data for **III-177** matched that of the reported.¹⁴⁵

Partial data for **III-177**: ¹H NMR (500 MHz, CDCl₃) δ 5.92-5.81 (m, 1 H), 5.24-5.12 (m, 2 H), 3.87-3.45 (m, 1 H), 1.87-0.99 (m, 11 H).



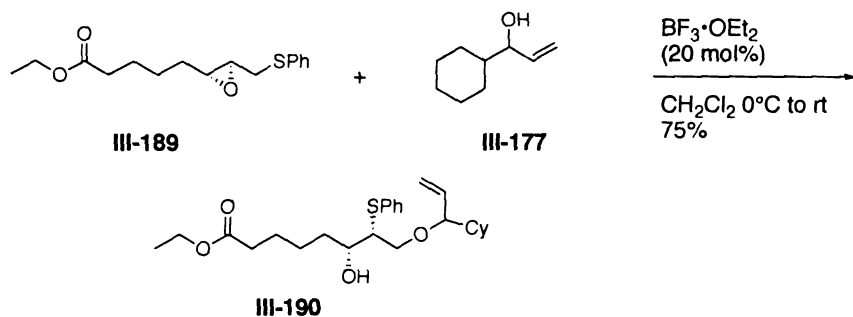
To a solution of diphenyldisulfide (3.28 g, 15.0 mmol) in triethylamine (9 mL), was added tributylphosphine (3.5 mL, 15.0 mmol) at ambient temperature under N₂. This solution was cooled to 0 °C and to it was cannulated a pre-cooled solution of epoxy alcohol **III-173** (1.0 g, 5.0 mmol) in Et₃N. After stirring at ambient temperature for 6 h, the reaction mixture was quenched with water (50 mL) and the aqueous solution extracted with EtOAc (3x150 mL). The combined EtOAc extracts were dried over Na₂SO₄ and concentrated under reduced pressure. The crude product was purified by flash column chromatography (5% EtOAc in hexanes) to afford epoxy sulfide **III-189** as a colorless oil (955 mg, 65%).

Partial data for **III-189**: ¹H NMR (500 MHz, CDCl₃) δ 7.44-7.19 (m, 5 H), 4.11 (q, *J* = 7.1 Hz, 2 H), 3.21-3.12 (m, 1 H), 2.96-2.86 (m, 2 H), 2.68-2.61 (m, 1 H), 2.27 (t, *J* = 7.3 Hz, 2 H), 1.67-1.24 (m, 6 H), 1.26 (t, *J* = 7.2 Hz, 3 H).



Coupling of vinylic epoxide **III-174** (50 mg, 0.25 mmol) and alcohol **III-177** (35 mg, 0.25 mmol) was performed using the same representative procedure as above but by dropwise addition of $\text{BF}_3 \cdot \text{OEt}_2$ (6 μL of 0.85 M solution in CH_2Cl_2 , 5 μmol) at room temperature. Adduct **III-178** was obtained in 42% yield as a mixture of diastereomers (35 mg).

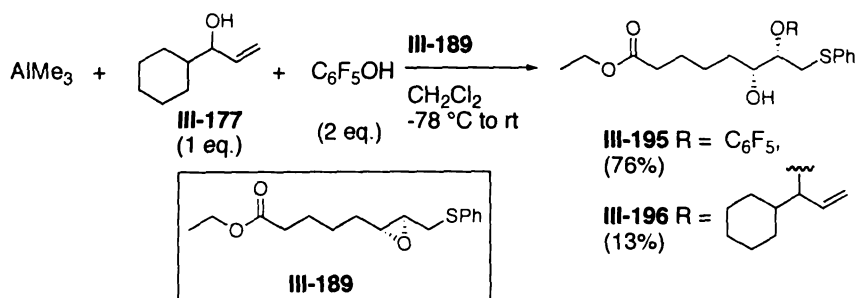
Partial data for **III-178**: ^1H NMR (500 MHz, CDCl_3) δ 5.84-5.74 (m, 1 H), 5.64-5.72 (m, 2 H), 5.52-5.62 (m, 1 H), 5.32-5.28 (m, 1 H), 5.24-5.18 (m, 3 H), 5.16-5.04 (m, 4 H), 4.08-4.14 (m, 4 H), 3.74-3.68 (m, 3 H), 3.64-3.59 (m, 1 H), 3.55 (t, $J = 7.0$ Hz, 1 H), 3.46 (t, $J = 6.9$ Hz, 1 H), 2.38-2.21 (m, 4 H), 2.02 (s(br), 2 H), 1.82-0.90 (m, 40 H); ^{13}C NMR (125 MHz, CDCl_3) δ 174.0, 173.9, 138.2, 137.7, 135.4, 135.3, 120.0, 118.4, 118.3, 117.1, 84.6, 82.4, 82.1, 80.5, 73.6, 72.4, 60.4, 60.3, 42.5, 34.5, 34.4, 32.0, 31.9, 29.3, 29.2, 29.1, 29.0, 26.8, 26.7, 26.4, 26.3, 26.2, 26.1, 25.7, 25.5, 25.2, 14.4.



A solution of epoxy sulfide **III-189** (30 mg, 0.1 mmol) and alcohol **III-177** (29 mg, 0.2 mmol) in CH_2Cl_2 (1 mL) was cooled to -10°C . $\text{BF}_3 \cdot \text{OEt}_2$ (24 μL of 0.8 M, 0.02 mmol) was added dropwise and the reaction was stirred at -10°C to 0°C for 10 h. Saturated NaHCO_3 solution (0.5 mL) was then added dropwise and the reaction was diluted with CH_2Cl_2 (10 mL) and H_2O (5 mL). After separation of layers, the aqueous

layer was extracted with CH₂Cl₂ (2x10 mL), combined organic layers were dried, concentrated to afford a crude oil. Purification by flash column chromatography (5% – 7% EtOAc in hexanes) furnished ring opened product **III-190** (32 mg, 75%).

Partial data for **III-190**: ¹H NMR (500 MHz, CDCl₃) δ 7.43-7.20 (m, 5 H), 5.64-5.60 (m, 1 H), 5.21-5.06 (m, 3 H), 4.12 (q, *J* = 7.3, 2 H), 3.70-3.66 (m, 1 H), 3.56-3.49 (m, 1 H), 3.44-3.39 (m, 1 H), 3.36-3.29 (m, 1 H), 2.26 (dt *J* = 1.6, 7.5 Hz, 2 H), 1.91 (d, *J* = 5.5 Hz, 3 H), 1.78-1.22 (m, 17 H).



To a solution of pentafluorophenol (110 mg, 0.60 mmol) and alcohol **III-177** (42 mg, 0.30 mmol) in CH₂Cl₂ (1 mL) was added trimethyl aluminum (0.15 mL of 2 M solution in toluene, 0.30 mmol) dropwise at room temperature. After 1 h, the brown solution was cooled to -78 °C and epoxy sulfide **III-189** in CH₂Cl₂ (0.6 mL) was added. The reaction was then warmed to room temperature over 90 min, after which saturated NaHCO₃ solution (2 mL) was added dropwise. The mixture was diluted with CH₂Cl₂ (5 mL) and H₂O (3 mL) and the layers were separated. The aqueous layer was extracted with CH₂Cl₂ (3x5 mL), the combined organic layers were dried, concentrated to obtain a crude oil. Upon purification by column chromatography (5% EtOAc in hexanes), two ring opened products **III-195** (37 mg, 76%) and **III-196** (6 mg, 13%) were isolated as colorless liquids.

Partial data for **III-195**: ^1H NMR (500 MHz, CDCl_3) δ 7.30-7.21 (m, 5 H), 4.21-4.20 (m, 1 H), 4.14 (q, $J = 7.1$ Hz, 2 H), 3.97-3.96 (m, 1 H), 3.39 (dd, $J = 7.3, 14.1$ Hz, 1 H), 3.13 (dd, $J = 4.9, 13.9$ Hz, 1 H), 2.32-2.29 (m, 2 H), 2.03 (s(br), 1 H), 1.71-1.29 (m, 6 H), 1.25 (t, $J = 7.3$ Hz, 3 H); ^{13}C NMR (125 MHz, CDCl_3) δ 173.9, 137.2, 135.1, 132.5, 130.5, 129.5, 129.3, 128.0, 127.2, 86.0, 71.6, 71.4, 60.5, 55.8, 34.9, 34.3, 33.8, 33.1, 29.9, 25.7, 25.5, 24.9, 14.4.

Partial data for **III-196**: ^1H NMR (500 MHz, CDCl_3) δ 7.42-7.25 (m, 5 H), 5.68-5.50 (m, 2 H), 5.22-5.12 (m, 2 H), 4.25 (q, $J = 7.1$ Hz, 2 H), 3.90-3.81 (m, 1 H), 3.80-3.65 (m, 1 H), 3.60-3.54 (m, 1 H), 3.42-3.48 (m, 1 H), 3.38-3.25 (m, 3 H), 3.18-2.98 (m, 1 H), 2.21-2.35 (m, 2 H), 1.78-1.20 (m, 20 H).

E. References

1. Cave, A.; Figadere, B.; Laurens, A.; Cortes, D. in *Progress in the Chemistry of Organic Natural Products*; Herz, W., Kirby, G. W., E., M. R., Steglich, W., Tamm, C., Eds.; Springer-Verlag: New York, 1997; Vol. 70, pp 81-287.
2. Zeng, L.; Ye, Q.; Oberlies, H.; Shi, G.; Gu, Z.-M.; He, K.; McLaughlin, J. L. *Nat. Prod. Rep.* **1996**, *13*, 275.
3. Gu, Z.-M.; Zhao, G.-X.; Oberlies, N. H.; Zeng, L.; McLaughlin, J. L. *Rec. Adv. Phytochem.* **1995**, *29*, 249.
4. Fang, X. P.; Rieser, M. J.; Gu, Z. M.; Zhao, G. X.; McLaughlin, J. L. *Phytochem. Anal.* **1993**, *4*, 27.
5. Rupprecht, J. K.; Hui, Y. H.; McLaughlin, J. L. *J. Nat. Prod.* **1990**, *53*, 237.
6. Alali, F. Q.; Liu, X.-X.; McLaughlin, J. L. *J. Nat. Prod.* **1999**, *62*, 504.
7. Schaus, S. E.; Branalt, J.; Jacobsen, E. N. *J. Org. Chem.* **1998**, *63*, 4876.
8. Evans, P. A.; Cui, J.; Gharpure, S. J.; Polosukhin, A.; Zhang, H.-R. *J. Am. Chem. Soc.* **2003**, *125*, 14702.
9. Takahashi, S.; Nakata, T. *J. Org. Chem.* **2002**, *67*, 5739.
10. Yang, W. Q.; Kitahara, T. *Tetrahedron* **2000**, *56*, 1451.
11. Shi, G.; Kozlowski, J. F.; Schwedler, J. T.; Wood, K. V.; MacDougall, J. M.; McLaughlin, J. L. *J. Org. Chem.* **1996**, *61*, 7988.
12. Marshall, J. A.; Hinkle, K. W.; Hagedorn, C. E. *Isr. J. Chem.* **1997**, *37*, 97.
13. Nonfon, M.; Lieb, F.; Moeschler, H.; Wendisch, D. *Phytochemistry* **1990**, *29*, 1951.
14. Narayan, R. S.; Sivakumar, M.; Bouhlel, E.; Borhan, B. *Org. Lett.* **2001**, *3*, 2489.
15. Koert, U. *Synthesis* **1995**, 115.
16. Hoppe, R.; Scharf, H. D. *Synthesis* **1995**, 1447.
17. Casiraghi, G.; Zanardi, F.; Battistini, L.; Rassu, G.; Appendino, G. *Chemtracts* **1998**, *11*, 803.
18. Louie, J.; Bielawski, C. W.; Grubbs, R. H. *J. Am. Chem. Soc.* **2001**, *123*, 11312.

19. Knochel, P.; Yeh, M. C. P.; Berk, S. C.; Talbert, J. *J. Org. Chem.* **1988**, *53*, 2390.
20. Achyutharao, S.; Knochel, P. *J. Org. Chem.* **1991**, *56*, 4591.
21. Alvarez, E.; Candenas, M. L.; Perez, R.; Ravelo, J. L.; Martin, J. D. *Chem. Rev.* **1995**, *95*, 1953.
22. Marmsater, F. P.; West, F. G. *Chem. Eur. J.* **2002**, *8*, 4347.
23. Koert, U. *Angew. Chem., Int. Ed.* **1995**, *34*, 298.
24. Trost, B. M.; Tenaglia, A. *Tetrahedron Lett.* **1988**, *29*, 2931.
25. Sinou, D.; Frappa, I.; Lhoste, P.; Porwanski, S.; Kryczka, B. *Tetrahedron Lett.* **1995**, *36*, 1251.
26. Godleski, S. A. in *Comprehensive Organic Synthesis*; 1st ed.; Trost, B. M., Fleming, I., Eds.; Pergamon Press: Oxford, 1991; Vol. 4, pp 585-662.
27. Fournier-Nguefack, C.; Lhoste, P.; Sinou, D. *Tetrahedron* **1997**, *53*, 4353.
28. Mitsunobu, O. in *Comprehensive Organic Synthesis*; 1st ed.; Trost, B. M., Fleming, I., Eds.; Pergamon Press: Oxford, 1991; Vol. 6, pp 88-93.
29. Trost, B. M.; Fleming, I., Eds. *Comprehensive Organic Synthesis*; 1st ed.; Pergamon Press: Oxford, 1991; Vol. 6.
30. Birkinshaw, T. N. in *Comprehensive Organic Functional Group Transformations*; Katritzky, A. R., Meth-Cohn, O., Rees, C. W., Roberts, S. M., Eds.; Pergamon Press: Oxford, 1990; Vol. 1, pp 204-220.
31. Wood, H. B.; Ganem, B. *J. Am. Chem. Soc.* **1990**, *112*, 8907.
32. Toda, J.; Sano, T.; Tsuda, Y.; Itatani, Y. *Chem. Pharm. Bull.* **1982**, *30*, 1322.
33. Schultz, A. G.; Lucci, R. D.; Fu, W. Y.; Berger, M. H.; Erhardt, J.; Hagmann, W. K. *J. Am. Chem. Soc.* **1978**, *100*, 2150.
34. Voyle, M.; Kyler, K. S.; Arseniyadis, S.; Dunlap, N. K.; Watt, D. S. *J. Org. Chem.* **1983**, *48*, 470.
35. Schwartz, R. E.; Helms, G. L.; Bolessa, E. A.; Wilson, K. E.; Giacobbe, R. A.; Tkacz, J. S.; Bills, G. F.; Liesch, J. M.; Zink, D. L.; Curotto, J. E.; Pramanik, B.; Onishi, J. C. *Tetrahedron* **1994**, *50*, 1675.
36. Ley, S. V.; Sternfeld, F. *Tetrahedron* **1989**, *45*, 3463.

37. Peredamiranda, R.; Garcia, M.; Delgado, G. *Phytochemistry* **1990**, 29, 2971.
38. Posner, G. H.; Rogers, D. Z. *J. Am. Chem. Soc.* **1977**, 99, 8214.
39. Otera, J.; Yoshinaga, Y.; Hirakawa, K. *Tetrahedron Lett.* **1985**, 26, 3219.
40. Iranpoor, N.; Baltork, I. M. *Tetrahedron Lett.* **1990**, 31, 735.
41. Caron, M.; Sharpless, K. B. *J. Org. Chem.* **1985**, 50, 1557.
42. Fagnou, K.; Lautens, M. *Org. Lett.* **2000**, 2, 2319.
43. Trost, B. M.; VanVranken, D. L. *Chem. Rev.* **1996**, 96, 395.
44. Righi, G.; Pescatore, G.; Bonadies, F.; Bonini, C. *Tetrahedron* **2001**, 57, 5649.
45. Keinan, E.; Sahai, M.; Roth, Z.; Nudelman, A.; Herzig, J. *J. Org. Chem.* **1985**, 50, 3558.
46. Trost, B. M.; McEachern, E. J.; Toste, F. D. *J. Am. Chem. Soc.* **1998**, 120, 12702.
47. Kawata, S.; Hiramata, M. *Tetrahedron Lett.* **1998**, 39, 8707.
48. Friesen, R. W.; Danishefsky, S. J. *J. Am. Chem. Soc.* **1989**, 111, 6656.
49. Halcomb, R. L.; Danishefsky, S. J. *J. Am. Chem. Soc.* **1989**, 111, 6661.
50. Gordon, D. M.; Danishefsky, S. J. *Carbohydr. Res.* **1990**, 206, 361.
51. Randolph, J. T.; Danishefsky, S. J. *J. Am. Chem. Soc.* **1993**, 115, 8473.
52. Danishefsky, S. J.; McClure, K. F.; Randolph, J. T.; Ruggeri, R. B. *Science* **1993**, 260, 1307.
53. Liu, K. K. C.; Danishefsky, S. J. *J. Org. Chem.* **1994**, 59, 1892.
54. Liu, K. K. C.; Danishefsky, S. J. *J. Org. Chem.* **1994**, 59, 1895.
55. Prestat, G.; Baylon, C.; Heck, M. P.; Mioskowski, C. *Tetrahedron Lett.* **2000**, 41, 3829.
56. Kolb, H. C.; Vannieuwenhze, M. S.; Sharpless, K. B. *Chem. Rev.* **1994**, 94, 2483.
57. Katsuki, T.; Sharpless, K. B. *J. Am. Chem. Soc.* **1980**, 102, 5974.

58. Gao, Y.; Hanson, R. M.; Klunder, J. M.; Ko, S. Y.; Masamune, H.; Sharpless, K. B. *J. Am. Chem. Soc.* **1987**, *109*, 5765.
59. Brown, C. A.; Yamashita, A. *J. Am. Chem. Soc.* **1975**, *97*, 891.
60. Kimmel, T.; Becker, D. *J. Org. Chem.* **1984**, *49*, 2494.
61. Speicher, A.; Eicher, T. *Synthesis* **1995**, 998.
62. Tsuboi, S.; Masuda, T.; Takeda, A. *Chem. Lett.* **1983**, 1829.
63. Hooz, J.; Layton, R. B. *Can. J. Chem.* **1972**, *50*, 1105.
64. Schlosser, M.; Christmann, K. F. *Angew. Chem., Int. Ed.* **1966**, *5*, 126.
65. Schlosser, M.; Tuong, H. B.; Schaub, B. *Tetrahedron Lett.* **1985**, *26*, 311.
66. DeMico, A.; Margarita, R.; Parlanti, L.; Vescovi, A.; Piancatelli, G. *J. Org. Chem.* **1997**, *62*, 6974.
67. Couturier, M.; Dory, Y. L.; Rouillard, F.; Deslongchamps, P. *Tetrahedron* **1998**, *54*, 1529.
68. Heath, R. R.; Tumlinson, J. H.; Doolittle, R. E.; Duncan, J. H. *J. Chromatogr. Sci.* **1977**, *15*, 10.
69. Gilman, H.; Catlin, W. E. *Org. Synth., CV I*, 188.
70. Mori, K.; Tomioka, H. *Liebigs Ann. Chem.* **1992**, 1011.
71. Mori, K.; Ogita, H. *Liebigs Ann. Chem.* **1994**, 1065.
72. Freeman, F.; Kim, D. *Synthesis* **1989**, 698.
73. Bengtsson, M.; Liljefors, T. *Synthesis* **1988**, 250.
74. Magoon, E. F.; Slaugh, L. H. *Tetrahedron* **1967**, *23*, 4509.
75. Doolittle, R. E. *Synthesis* **1984**, 730.
76. Chattopadhyay, S.; Mamdapur, V. R.; Chadha, M. S. *Synth. Commun.* **1990**, *20*, 1299.
77. Sankaranarayanan, S.; Chattopadhyay, S. *Tetrahedron-Asymmetry* **1998**, *9*, 2627.
78. Fisher, I. G.; Tyman, J. H. P. *Synth. Commun.* **1998**, *28*, 1323.

79. Baurle, S.; Peters, U.; Friedrich, T.; Koert, U. *Eur. J. Org. Chem.* **2000**, 2207.
80. Paquette, L. A. in *Encyclopedia of Reagents for Organic Synthesis*; Paquette, L. A., Ed.; Wiley: Chichester ; New York, 1995; Vol. 5, pp 3009-3014.
81. Curran, D. P.; Yu, H. S. *Synthesis* **1992**, 123.
82. Horita, K.; Yoshioka, T.; Tanaka, T.; Oikawa, Y.; Yonemitsu, O. *Tetrahedron* **1986**, 42, 3021.
83. Evans, D. A.; Kaldor, S. W.; Jones, T. K.; Clardy, J.; Stout, T. J. *J. Am. Chem. Soc.* **1990**, 112, 7001.
84. Reed, L. A.; Ito, Y.; Masamune, S.; Sharpless, K. B. *J. Am. Chem. Soc.* **1982**, 104, 6468.
85. Sekine, M.; Kume, A.; Hata, T. *J. Chem. Soc., Chem. Commun.* **1981**, 969.
86. Johnson, R. A.; Sharpless, K. B. in *Catalytic Asymmetric Synthesis*; 2nd ed.; Ojima, I., Ed.; Wiley-VCH: New York, 2000, pp 231-280.
87. Nicolaou, K. C.; Duggan, M. E.; Hwang, C. K.; Somers, P. K. *J. Chem. Soc., Chem. Commun.* **1985**, 1359.
88. Nicolaou, K. C.; Prasad, C. V. C.; Somers, P. K.; Hwang, C. K. *J. Am. Chem. Soc.* **1989**, 111, 5330.
89. Nicolaou, K. C.; Prasad, C. V. C.; Somers, P. K.; Hwang, C. K. *J. Am. Chem. Soc.* **1989**, 111, 5335.
90. Gill, D. M.; Pegg, N. A.; Rayner, C. M. *J. Chem. Soc., Perkin Trans. I* **1993**, 1371.
91. Sivakumar, M.; Borhan, B. *Tetrahedron Lett.* **2003**, 44, 5547.
92. De Lucchi, O.; Miotti, U.; Modena, G. *Org. React. (N.Y.)* **1991**, 40, 157.
93. Padwa, A.; Gunn, D. E., Jr.; Osterhout, M. H. *Synthesis* **1997**, 1353.
94. Sugihara, H.; Tanikaga, R.; Kaji, A. *Synthesis* **1978**, 881.
95. Dilworth, B. M.; McKervery, M. A. *Tetrahedron* **1986**, 42, 3731.
96. Bakuzis, P.; Bakuzis, M. L. F.; Fortes, C. C.; Santos, R. *J. Org. Chem.* **1976**, 41, 2769.

97. Imbroisi, D. D.; Simpkins, N. S. *J. Chem. Soc., Perkin Trans. 1* **1991**, 1815.
98. Koert, U.; Wagner, H.; Pidun, U. *Chemische Berichte* **1994**, 127, 1447.
99. Berninger, J.; Koert, U.; Eisenberghohl, C.; Knochel, P. *Chem. Ber.* **1995**, 128, 1021.
100. Arndt, S.; Emde, U.; Baurle, S.; Friedrich, T.; Grubert, L.; Koert, U. *Chem. Eur. J.* **2001**, 7, 993.
101. Reetz, M. T. *Angew. Chem., Int. Ed.* **1984**, 23, 556.
102. Trost, B. M.; Belletire, J. L.; Godleski, S.; McDougal, P. G.; Balkovec, J. M.; Baldwin, J. J.; Christy, M. E.; Ponticello, G. S.; Varga, S. L.; Springer, J. P. *J. Org. Chem.* **1986**, 51, 2370.
103. Harada, N.; Nakanishi, K. *Circular Dichroic Spectroscopy : Exciton Coupling in Organic Stereochemistry*; University Science Books: Mill Valley, CA, 1983.
104. Berova, N.; Nakanishi, K.; Woody, R. *Circular Dichroism : Principles and Applications*; 2nd ed.; Wiley-VCH: New York, 2000.
105. Harada, N.; Chen, S. L.; Nakanishi, K. *J. Am. Chem. Soc.* **1975**, 97, 5345.
106. Trost, B. M.; Tanoury, G. J.; Lautens, M.; Chan, C.; Macpherson, D. T. *J. Am. Chem. Soc.* **1994**, 116, 4255.
107. Furstner, A.; Dierkes, T. *Org. Lett.* **2000**, 2, 2463.
108. Mitsunobu, O. *Synthesis* **1981**, 1.
109. Hughes, D. L.; Reamer, R. A.; Bergan, J. J.; Grabowski, E. J. J. *J. Am. Chem. Soc.* **1988**, 110, 6487.
110. Singh, R.; Whitesides, G. M. *J. Am. Chem. Soc.* **1990**, 112, 1190.
111. Inokuchi, T.; Asanuma, G.; Torii, S. *J. Org. Chem.* **1982**, 47, 4622.
112. Jorapur, V. S.; Duffley, R. P.; Razdan, R. K. *Synth. Commun.* **1984**, 14, 655.
113. Ando, M.; Wada, T.; Isogai, K. *J. Org. Chem.* **1991**, 56, 6235.
114. Oki, M.; Shionoiri, K.; Otake, K.; Ono, M.; Toyota, S. *Chem. Lett.* **1991**, 597.
115. Nakamura, K.; Kimura, T.; Kanno, H.; Takahashi, E. *J. Antibiot.* **1995**, 48, 1134.

116. Knochel, P.; Jeong, N.; Rozema, M. J.; Yeh, M. C. P. *J. Am. Chem. Soc.* **1989**, *111*, 6474.
117. Knochel, P.; Achyutharao, S. *J. Am. Chem. Soc.* **1990**, *112*, 6146.
118. Luche, J. L. *J. Am. Chem. Soc.* **1978**, *100*, 2226.
119. Luche, J. L.; Rodriguezhahn, L.; Crabbe, P. *J. Chem. Soc., Chem. Commun.* **1978**, 601.
120. Kita, Y.; Furukawa, A.; Futamura, J.; Ueda, K.; Sawama, Y.; Hamamoto, H.; Fujioka, H. *J. Org. Chem.* **2001**, *66*, 8779.
121. David, S.; Hanessian, S. *Tetrahedron* **1985**, *41*, 643.
122. Blunden, S. J.; Cusack, P. A.; Smith, P. J. *J. Organomet. Chem.* **1987**, *325*, 141.
123. Danishefsky, S. J.; Gervay, J.; Peterson, J. M.; McDonald, F. E.; Koseki, K.; Griffith, D. A.; Oriyama, T.; Marsden, S. P. *J. Am. Chem. Soc.* **1995**, *117*, 1940.
124. Hodosi, G.; Kovac, P. *Carbohydr. Res.* **1998**, *308*, 63.
125. Sasaki, M.; Miyazawa, M.; Tanino, K.; Miyashita, M. *Tetrahedron Lett.* **1999**, *40*, 9267.
126. Sasaki, M.; Tanino, K.; Miyashita, M. *J. Org. Chem.* **2001**, *66*, 5388.
127. Liu, C. Q.; Hashimoto, Y.; Kudo, K.; Saigo, K. *Bull. Chem. Soc. Jpn.* **1996**, *69*, 2095.
128. Maruoka, K.; Oishi, M.; Shiohara, K.; Yamamoto, H. *Tetrahedron* **1994**, *50*, 8983.
129. Saito, S.; Yamamoto, H. *Chem. Commun.* **1997**, 1585.
130. Marx, A.; Yamamoto, H. *Synlett* **1999**, 584.
131. Byun, H. S.; He, L. L.; Bittman, R. *Tetrahedron* **2000**, *56*, 7051.
132. Gao, Y.; Sharpless, K. B. *J. Am. Chem. Soc.* **1988**, *110*, 7538.
133. Berridge, M. S.; Franceschini, M. P.; Rosenfeld, E.; Tewson, T. J. *J. Org. Chem.* **1990**, *55*, 1211.
134. Tewson, T. J. *J. Org. Chem.* **1983**, *48*, 3507.
135. He, L. L.; Byun, H. S.; Bittman, R. *J. Org. Chem.* **1998**, *63*, 5696.

- 136. Moghaddam, M. F.; Motoba, K.; Borhan, B.; Pinot, F.; Hammock, B. D. *Biochim. Biophys. Acta* **1996**, 1290, 327.
- 137. Myers, A. G.; Goldberg, S. D. *Angew. Chem., Int. Ed.* **2000**, 39, 2732.
- 138. Bianco, A.; Brufani, M.; Manna, F.; Melchioni, C. *Carbohydr. Res.* **2001**, 332, 23.
- 139. Sanders, W. J.; Kiessling, L. L. *Tetrahedron Lett.* **1994**, 35, 7335.
- 140. Capaccio, C. A. I.; Varela, O. *Tetrahedron-Asymmetry* **2000**, 11, 4945.
- 141. Corey, E. J.; Helal, C. J. *Tetrahedron Lett.* **1996**, 37, 5675.
- 142. Galinis, D. L.; Fuller, R. W.; McKee, T. C.; Cardellina, J. H.; Gulakowski, R. J.; McMahon, J. B.; Boyd, M. R. *J. Med. Chem.* **1996**, 39, 4507.
- 143. Shinkai, S.; Tsuji, H.; Hara, Y.; Manabe, O. *Bull. Chem. Soc. Jpn.* **1981**, 54, 631.
- 144. Trost, B. M.; Verhoeven, T. R. *J. Am. Chem. Soc.* **1980**, 102, 4743.
- 145. Bergmeier, S. C.; Stanchina, D. M. *J. Org. Chem.* **1997**, 62, 4449.

CHAPTER IV

TOTAL SYNTHESIS OF THE PROPOSED STRUCTURE OF MUCOXIN

A. Revised strategies for the coupling of left- (C13-C37) and right-hand (C1-C12) fragments of mucoxin

As discussed in Chapter III, our original synthetic approach to mucoxin called for a late stage coupling of the fully functionalized allylic alcohol **IV-1** and vinylic epoxide **IV-2** (Figure IV-1) *via* a regioselective C-O bond formation. Since the proposed intermolecular allylic alkylation strategy was not successful, we turned to explore alternative routes to couple the two halves. In redesigning the synthesis, we decided to rely on C-C bond forming reactions because we felt that, a broader range of methodologies could be explored for intermolecular C-C bond formation as compared to C-O bond formation.¹ Nonetheless, in order to keep the synthesis concise and convergent, we wanted to conserve the global strategy to couple the two fragments in their functionally elaborated forms.

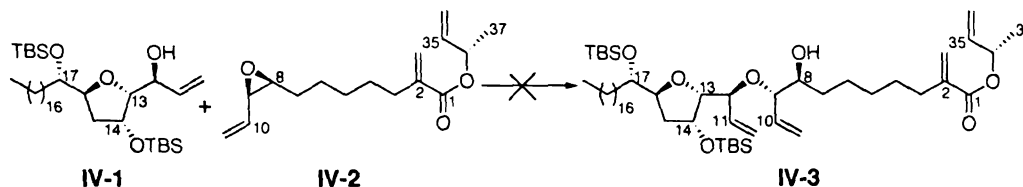


Figure IV-1: Original regio- and stereoselective intermolecular epoxide opening strategy

The hydroxylated THF portion (C12-C37) of mucoxin was available from earlier studies (Chapter III) in the form of an aldehyde (**IV-4**; X = H, Figure IV-2). Since carbonyl group is a versatile functionality and has been used extensively in C-C bond

forming reactions both as an electrophile as well as a nucleophile,² we decided to conserve aldehyde **IV-4** as the left hand coupling partner in our revised synthetic plan. A general design of the right hand segment **IV-5** is shown in Figure IV-2. Accordingly, the plan required accessing a fragment containing a terminal acrylate (**IV-5**), an appropriate reactive group (M) at the other end and a suitable functionality along the linker that can be elaborated to a 2,5 di-substituted THF ring.

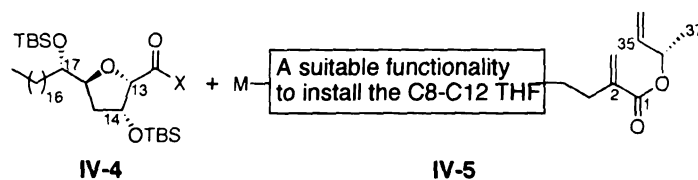


Figure IV-2: General representation of the revised strategy

An obvious C-C bond forming reaction involving a carbonyl reacting partner is addition of an organometallic reagent to the carbonyl group. Organomagnesium (Grignard)^{3,4} and organolithium⁵ reagents are probably the most commonly used species for this purpose. Although carbonyl addition reactions of magnesium and lithium organics are highly facile and reliable, these organometallics, owing to the highly polar nature of the metal-carbon bond, exhibit low chemoselectivity in their reactions.³⁻⁵ Thus in addition to carbonyl functionalities, they also react with several moieties including epoxides, nitriles, halides and in some cases even silyl and benzyl protecting groups.⁶ Their reactivity can be attenuated by techniques such as transmetallation to the corresponding copper⁷ or titanium⁸ species. Nevertheless, since such transition metal reagents were derived from the corresponding organomagnesiums or organolithiums, highly functionalized organometallics are not accessible. Clearly, in our case, the right

hand piece **IV-5** could not be derivatized as a Grignard or organolithium species due to the sensitive ester group.

Functionalized organozinc reagents bearing electrophilic carbonyl groups and their equivalents are stable and can be generated from the corresponding alkyl halides. Although organozinc compounds have been known for several decades,^{9,10} they have found only limited utility in organic synthesis possibly due to their lack of inherent reactivity. However, the discovery that organozincs can be efficiently transmetallated to a variety of more reactive transition metal salts,^{11,12} opened avenues for new applications. During the past few years, mostly through the work of Knochel, these reagents have emerged as effective alternatives to the conventional main group organometallic reagents.¹³⁻¹⁵ Organozincs can be prepared under mild conditions (that not require pre-formation of the corresponding organomagnesium or lithium species) by direct insertion of elemental zinc into carbon-halogen bonds, or *via* zinc-iodine or boron-zinc exchange.^{11,16,17} Due to the availability of such methods of preparation and their inherent low reactivity, several organozinc reagents containing reactive functional groups like esters, ketones, nitriles, amides, nitro groups and epoxides have been prepared. Organozincs so generated can be reacted with various electrophiles with or without transition metal catalysts depending upon the reactivity of the latter.¹⁵ Thus, organozinc mediated coupling reactions offer an attractive strategy to combine fragments bearing sensitive functional groups.

1. Evaluation of coupling strategies involving organozinc additions

Being aware of the scope and recent discoveries on organozinc reagents, our first plan was to couple tri-substituted THF aldehyde **IV-4** with an organozinc species derived from a suitably functionalized right hand fragment of type **IV-5** ($M = \text{Zn}$, Figure IV-2). To quickly test the feasibility of this approach, our immediate target was to access the functionalized primary iodide **IV-6** (Figure IV-3) designed as a model system. Also, a model tetrahydrofuranaldehyde **IV-8** that closely mimicked the real aldehyde **IV-4** was available from our earlier studies (Chapter III). Chelation controlled addition of the organozinc obtained from iodide **IV-6** to aldehyde **IV-8** would afford the corresponding coupled product (**IV-9**).^{18,19} A subsequent stereoselective epoxidation / cyclization of the bis-homoallylic alcohol **IV-9**²⁰ should install the 2,5 di-substituted THF ring to complete assembly of the bis-THF core unit.

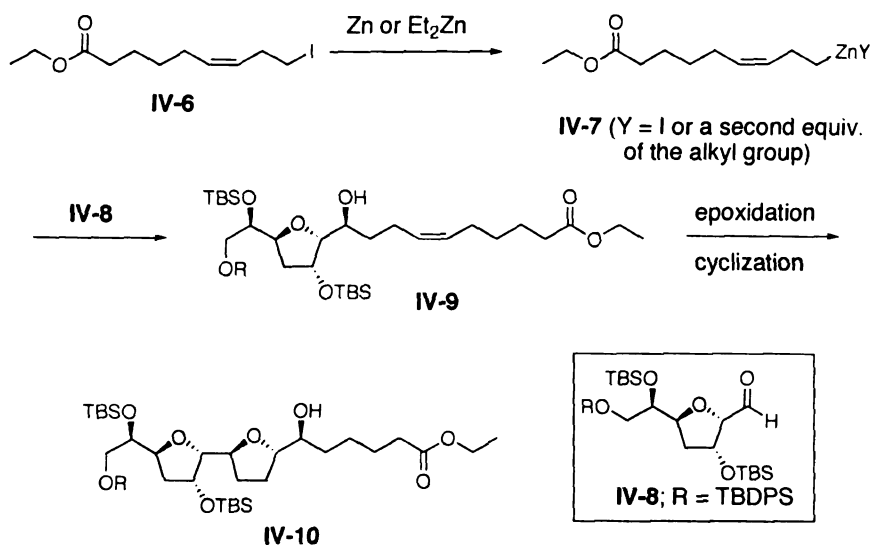
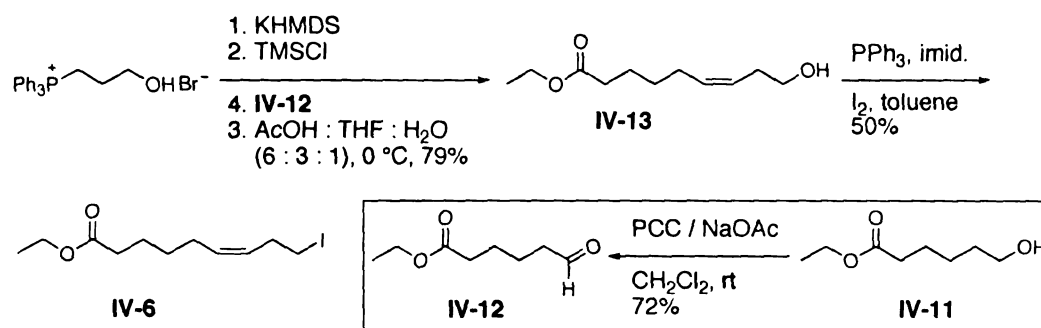


Figure IV-3: Design of the new synthetic strategy

The requisite primary iodide **IV-6** was readily obtained from the commercially available ethyl 6-hydroxyhexanoate **IV-11** following a three-step sequence (Scheme

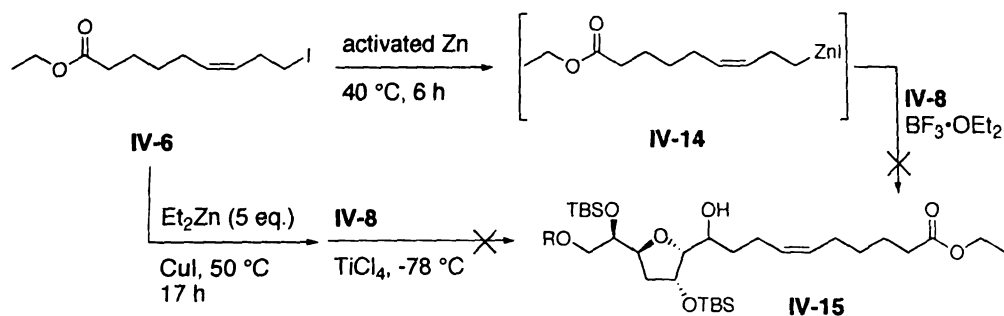


Scheme IV-1: Synthesis of the model iodide

IV-1). PCC oxidation of **IV-11** (72%) delivered the aldehyde **IV-12**. Wittig olefination of **IV-12** with 3-hydroxy-propyltriphenylphosphonium bromide was carried out by *in situ* TMS protection of the ylide prior to addition of the aldehyde.^{21,22} After treatment of the reaction mixture with aqueous acid in the same pot, *cis* homoallylic alcohol **IV-13** was obtained in >95% diastereoselectivity. Finally, PPh_3 / I_2 mediated iodination of **IV-13** produced the desired iodide **IV-6**.²³

Organozincs are known to undergo nucleophilic addition to aliphatic aldehydes in the presence of Lewis acids or transition metal activators.²⁴⁻²⁷ First, iodide **IV-6** was treated with activated metallic zinc to generate the organozinc iodide intermediate **IV-14**, which was then reacted with aldehyde **IV-8** that had been pre-complexed with $\text{BF}_3 \cdot \text{OEt}_2$ (Scheme IV-2). Although **IV-8** was usually recovered unchanged, iodide **IV-6** was always completely consumed (as indicated by GC and TLC analysis). Based on this as well as our previous experience with alkylzinc reagents (Chapter III), we think that the

desired alkylzinc iodide (**IV-14**) was generated but probably was not reactive enough to add to the activated aldehyde.

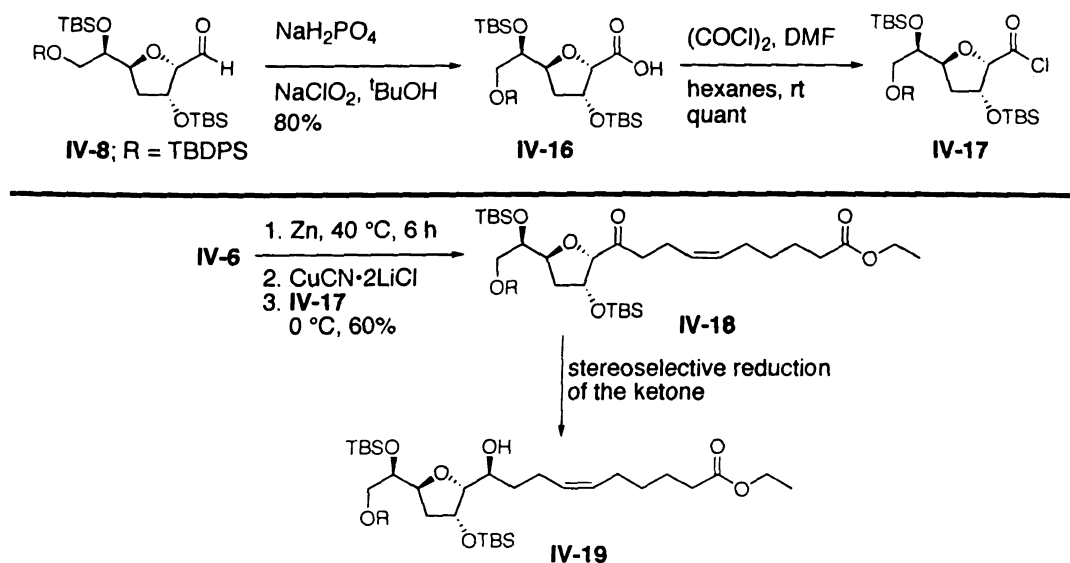


Scheme IV-2: Attempted organozinc additions to aldehyde **IV-8**

Since dialkylzinc reagents are known to be more reactive than alkylzinc halides, we next attempted to generate the dialkyl zinc species from **IV-6**. Thus, **IV-6** was treated with Et_2Zn and catalytic CuI to obtain the corresponding dialkyl zinc *via* zinc-halogen exchange.^{28,29} However, when aldehyde **IV-8** was added to the dialkyl zinc reagent in the presence of TiCl_4 , no desired secondary alcohol (**IV-15**) was obtained. In all of our attempts, a part of the starting material (iodide **IV-6**) was always recovered unchanged indicating that the exchange process remained incomplete.

In addition, a number of operational difficulties were encountered. First, the process³⁰ calls for the use of neat Et_2Zn which is extremely flammable when exposed to atmosphere. Therefore all the operations needed to be carried out in a dry box. Secondly, this protocol typically uses excess Et_2Zn to drive the equilibrium towards the product side. The excess reagent then has to be carefully and completely removed under vacuum before treatment with the aldehyde, in order to avoid competing ethyl group transfer. We felt that such a procedure would be cumbersome and unsafe especially on multi-gram scales. Hence the zinc-halogen exchange route was abandoned.

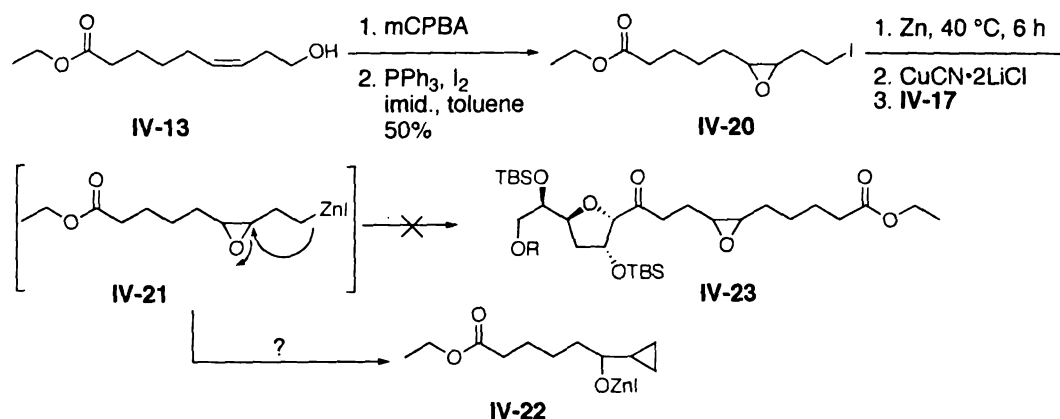
In absence of Lewis acids or transition metal catalysts, aldehydes are not reactive towards alkyl zincs. On the other hand, the coupling of acid chlorides with organozinc reagents is much more efficient, and requires no further activation. Therefore we redirected our attention toward using the corresponding acid chloride as the electrophile (**IV-17**, Scheme IV-3). **IV-17** was prepared by NaClO₂ / NaH₂PO₄ mediated oxidation³¹ of **IV-8** to the corresponding acid (**IV-16**, 80%) and its subsequent treatment with (COCl)₂ / DMF.³² Gratifyingly, the primary iodide (**IV-6**) derived alkyl zinc, after transmetallation to the corresponding organocopper species, reacted with acid chloride **IV-17** to afford ketone **IV-18** in 60% yield (Scheme IV-3). We anticipated that stereoselective carbonyl reduction of **IV-18** would generate the desired *threo* α-tetrahydrofuranyl secondary alcohol (**IV-19**).



Scheme IV-3: Synthesis of ketone **IV-18** via organozinc addition to acid chloride **IV-17**

Along similar lines, we also tried to access epoxy ketone **IV-23** (Scheme IV-4) by addition of the epoxy iodide (**IV-20**) derived organozinc reagent to acid chloride **IV-17**. If successful, this strategy would bypass the proposed stereoselective epoxidation /

cyclization sequence (Figure IV-3) to install the second (C8-C12) THF ring of mucosin, thereby making the synthesis more convergent. Stereoselective ketone reduction and *in situ* cyclization of **IV-24** would directly afford bis-THF unit **IV-10** (Figure IV-3). However, in the attempted coupling of **IV-20** with **IV-17**, the crude product did not show any diagnostic ^1H NMR peaks corresponding to the desired product **IV-23** (for example, the epoxy methines or α -keto methylene protons). Instead, unusual upfield signals belonging to a cyclopropyl ring were observed. Although epoxides are known to be compatible with organozincs and the corresponding organocopper reagents, we surmised that juxtaposition of the two functionalities in **IV-21**, might trigger an internal rearrangement to produce cyclopropyl alkoxide **IV-22**.



Scheme IV-4: Attempted addition of epoxy iodide **IV-20** to acid chloride **IV-17** via the organozinc reagent

With ketone **IV-18** (Scheme IV-3) in hand, we focused our attention on its stereoselective reduction. α -Oxygenated ketones, by appropriate choice of the hydride source and nature of the oxygen substituent, can be reduced to the corresponding *erythro* or *threo* α -oxy alcohols. Using metal hydrides such as LiAlH_4 , NaBH_4 and ZnBH_4 , *erythro* products can be obtained, provided that an α -oxygen is available for chelation (as

in α -hydroxy ketones, α -keto lactones and α -keto tetrahydrofurans, etc.). These reactions occur *via* a chelation controlled transition state.³³⁻³⁵ On the other hand, bulky, non-chelating metal hydrides such as L- and K-selectride afford the corresponding *threo* products through a Felkin-Anh transition state, irrespective of the nature of the α -oxygen substituent in the parent ketone.³⁶⁻³⁸ Hydride reduction of ketone **IV-18** following these two routes is shown in Figure IV-4. In our case, the desired *threo* isomer (**IV-19**) would be obtained *via* a Felkin-Anh transition state **IV-26**.

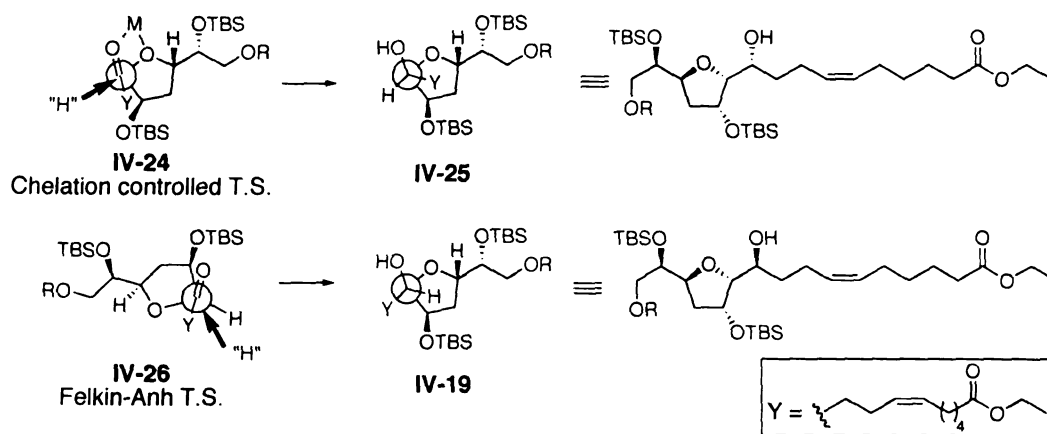
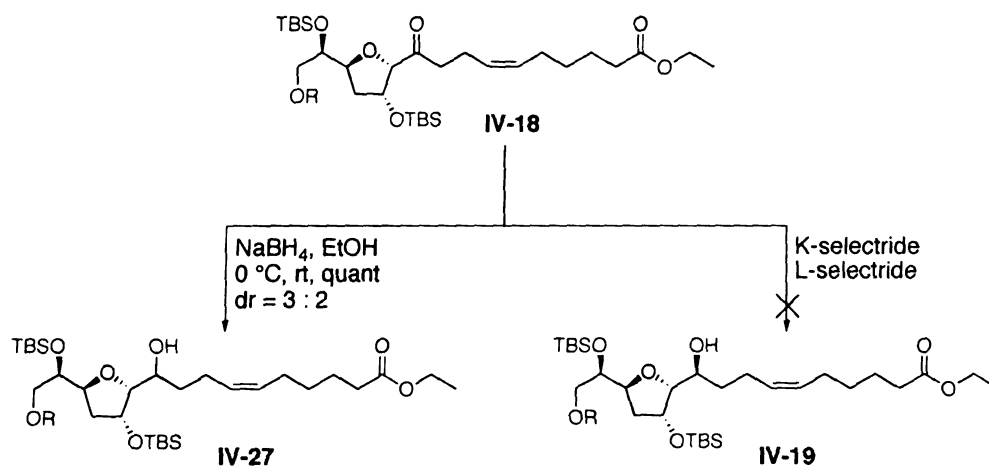


Figure IV-4: Chelation controlled vs. Felkin-Anh transition state for reduction of ketone **IV-18**

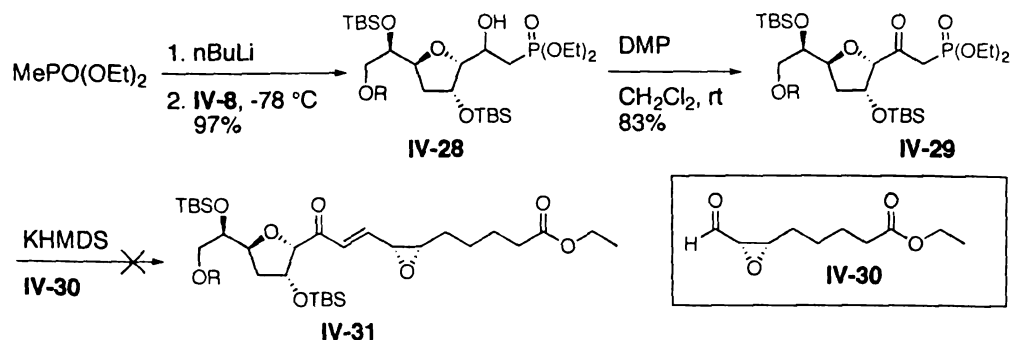
In preliminary studies, we found that NaBH_4 reduction of ketone **IV-18** produced alcohol **IV-27** quantitatively, but in poor diastereoselectivity ($\text{dr} = 3 : 2$, Scheme IV-5). Also, the diastereomers were not separable by column chromatography. On the other hand, exposure of **IV-18** to the selectrides (Scheme IV-5) resulted in complete consumption of the starting material, but no desired product could be isolated. It appeared that the hydride transfer step was occurring and the intermediate borinate was being produced. However oxidation of the borinate species to free the alcohol product appeared



Scheme IV-5: Attempted hydride reduction reactions of ketone **IV-18**

to be the problematic step. Overall, the stereoselective ketone reduction approach proved synthetically unviable.

Concurrent with the organozinc addition approach, another strategy involving a HWE olefination reaction³⁹ to couple the right and the left hand portions of mucosin was also examined. For this purpose, aldehyde **IV-8** was further functionalized to generate β -keto phosphonate **IV-29** (Scheme IV-6). Addition of the anion of diethyl methylphosphonate furnished β -hydroxyphosphonate **IV-28**, which was oxidized to β -ketophosphonate **IV-29** in 83% yield with the Dess–Martin periodinane.⁴⁰ The



Scheme IV-6: Model studies on HWE olefination approach

aldehyde partner **IV-30** was similarly prepared by oxidation of the corresponding epoxy alcohol (not shown), which was available from earlier studies (Chapter III). Unfortunately, the intended HWE olefination to acquire α,β -unsaturated ketone **IV-31** was unsuccessful. When NaH was used as the base, the starting materials were recovered unchanged. Furthermore, the use of KHMDS as the base afforded an intractable mixture, containing none of the desired enone – discerned from the ^1H NMR spectrum of the cure product.

2. Conventional organometallic addition using chelation control to couple the two halves of mucoxin

In view of the failed coupling strategies described above, we decided to move away from our original plan of combining the two halves of mucoxin in fully functionalized forms. In search of more a straightforward, workable route while still keeping the synthesis concise, we came up with the following design (Figure IV-5). Chelation controlled addition of an organomagnesium or lithium reagent of general structure **IV-32** to aldehyde **IV-8** should produce the bis-homoallylic alcohol **IV-33**. Further, one pot stereoselective epoxidation / cyclization* of **IV-33** would furnish bis-THF containing compound **IV-34**. Finally, the primary iodide derived from **IV-34** would be coupled to the α -bromomethyl lactone **IV-35** *via* formation of the corresponding organozinc. From our earlier experience (Chapter III) and literature reports,⁴¹ we anticipated that alkylzinc iodides would couple efficiently with bromomethyl acrylate type substrates such as **IV-35**.

* Several possible methods for stereoselective epoxidation of **IV-33** are discussed later in the same section.

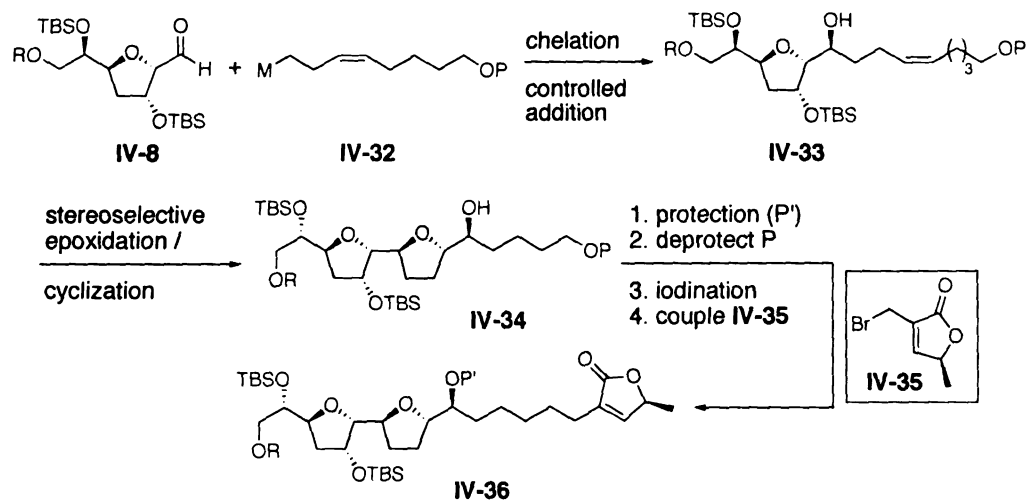
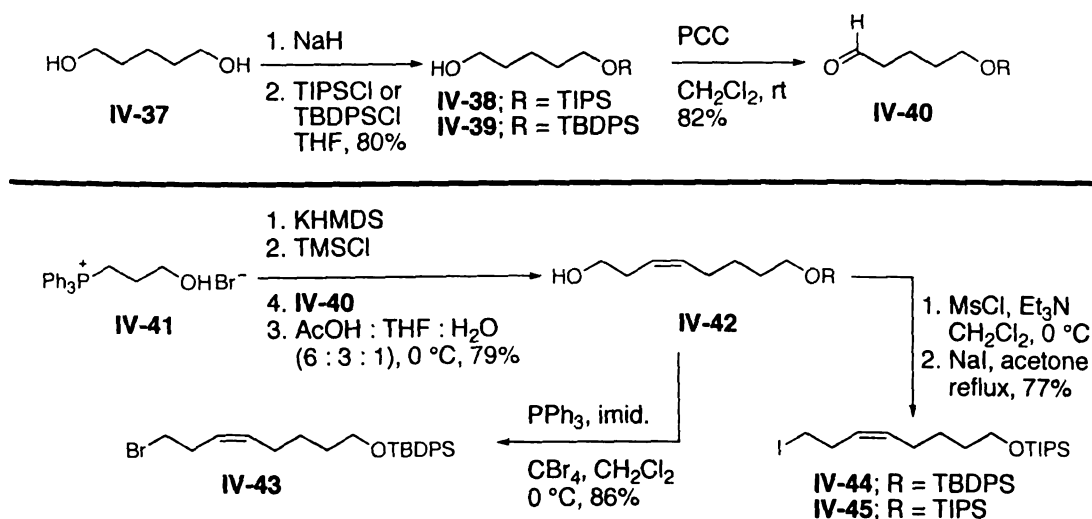


Figure IV-5: Revised stepwise strategy to assemble fragments **IV-8**, **IV-32** and **IV-35**

As part of the revised synthetic strategy, our immediate goal was to optimize the chelation controlled addition of an appropriate organometallic reagent (**IV-32**) to aldehyde **IV-8**. We began by synthesizing suitable homoallylic halide precursors that would allow access to the corresponding organometallic reagent. Commercially available 1,5-pentanediol after mono protection and PCC oxidation afforded aldehyde **IV-40** in 66% overall yield (Scheme IV-8). Z-selective Wittig olefination of **IV-40** by way of

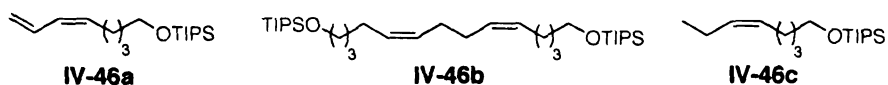


Scheme IV-7: Synthesis of the requisite homoallylic halides

in situ TMS protection of the ylide derived from 3-hydroxypropyltriphenylphosphonium bromide as described earlier (Scheme IV-1),^{21,42} delivered homoallylic alcohol **IV-42**. Bromide **IV-43** was prepared by bromination⁴³ of the alcohol using PPh₃ / CBr₄, while iodides **IV-44** and **IV-45** were accessed *via* displacement of the corresponding mesylates by NaI.⁴⁴

The chelation controlled addition of Grignard reagents⁴⁵⁻⁴⁸ derived from halides **IV-43**, **IV-44** and **IV-45** to aldehyde **IV-8** required some optimization. These studies are summarized in Table IV-1.

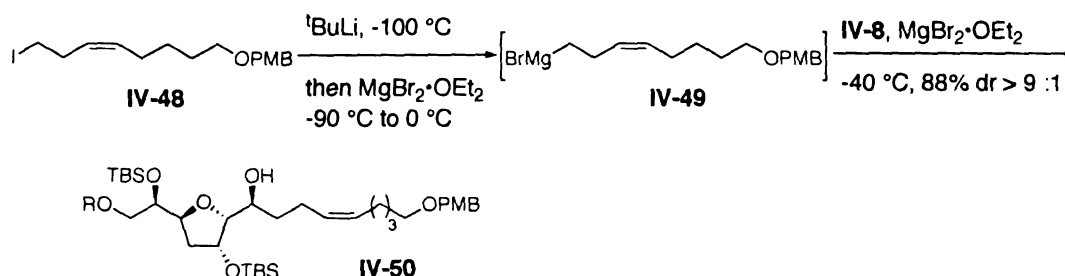
Initially, the formation of the Grignard reagent proved to be tricky. When iodide **IV-45** (entry 1) was treated with activated Mg in refluxing diethyl ether^{3,4} and aldehyde **IV-8** subsequently added (entries 1 and 2),⁴⁹ no addition products were obtained. Under these conditions, dienes **IV-46a** and **IV-46b** were obtained as major products along with the reduced product **IV-46c**. We surmised that the enhanced reactivity of the allylic iodide might be responsible for the relative facility of the competing β -elimination and homo-coupling pathways.



Accordingly, when bromide **IV-43** was subjected to the same reaction conditions (entry 3), the desired product was obtained in 30% yield along with a significant amount of recovered aldehyde. Notably, when the alkylmagnesium iodide (entry 4) was generated at low temperature *via* lithium-halogen exchange (^tBuLi, -90 °C) followed by

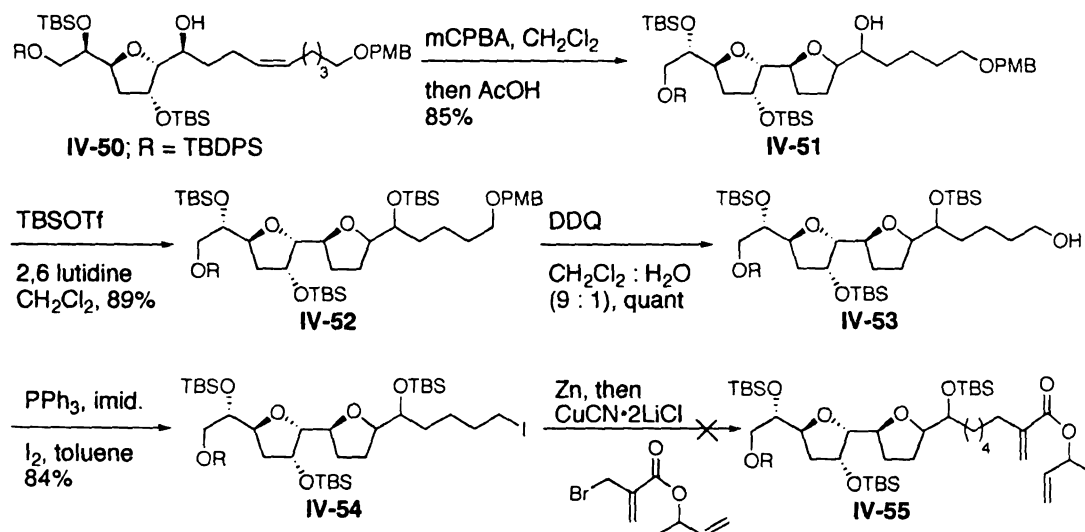
commercially available solid $\text{MgBr}_2 \cdot \text{OEt}_2$ contained enough moisture to quench the metallated species (entry 4). Indeed, when freshly prepared^{52,53} $\text{MgBr}_2 \cdot \text{OEt}_2$ was used (entry 5), the yield of the desired adduct jumped to 67% (dr = 4 : 1). The yield and diastereoselectivity were further improved (entry 6) when Et_2O was used as a solvent instead of THF.

Before further investigations began, homoallylic alcohol **IV-50** bearing a terminal PMB ether (instead of silyl ether **IV-47**) was synthesized (Scheme IV-8) in order to facilitate protecting group manipulations. Iodide **IV-48** was obtained following a similar sequence as before (Scheme IV-7). By carefully controlling the temperature and amount of $\text{MgBr}_2 \cdot \text{OEt}_2$, adduct **IV-50** was obtained in 88% yield as a single diastereomer after chromatographic purification.



Scheme IV-8: Synthesis of bis-homoallylic alcohol **IV-50**

As the first step toward investigations on the proposed stereoselective epoxidation-cyclization sequence to install the di-substituted THF ring (Figure IV-5), bis-homoallylic alcohol **IV-50** was subjected to mCPBA mediated epoxidation (Scheme IV-9). As expected, no diastereoselectivity was observed and after treatment of the reaction mixture with glacial AcOH in the same pot, the bis-THF unit **IV-51** was obtained as an inseparable mixture of diastereomers (ca. 1:1). Since **IV-51** was easily synthesized, we



Scheme IV-9: Feasibility studies of the new strategy described in Figure IV-5

decided to test the viability of further transformations in our proposed synthetic plan (Figure IV-5, Scheme IV-9). TBS protection of **IV-51** to produce tris-TBS ether **IV-52** (89%) and subsequent PMB deprotection of **IV-52** to reveal the primary alcohol **IV-53** proceeded smoothly. Iodination of **IV-53** secured the target iodide **IV-54** in 84% yield. However, our preliminary attempts toward organozinc mediated coupling of the iodide with the bromomethyl acrylate were unsuccessful.

At this point, the two issues that needed to be addressed were stereoselective epoxidation of bis-homoallylic alcohol **IV-50** and the final coupling of iodide **IV-54** with the bromomethyl acrylate. Several methods for the stereoselective epoxidation reaction were considered. The most commonly used tactic for the conversion of stereodefined bis-homoallylic alcohols to the corresponding THF units is a one pot, hydroxyl directed $\text{VO}(\text{acac})_2$ / $t\text{-BuOOH}$ mediated epoxidation / cyclization reaction.²⁰ Transition metal catalyzed, *tert*-butyl peroxide mediated epoxidation of olefins was first reported by

Indictor and Brill.⁵⁴ Among various transition metal catalyzed epoxidations, vanadium-catalyzed hydroxyl directed epoxidation of alkenols has been used most commonly in

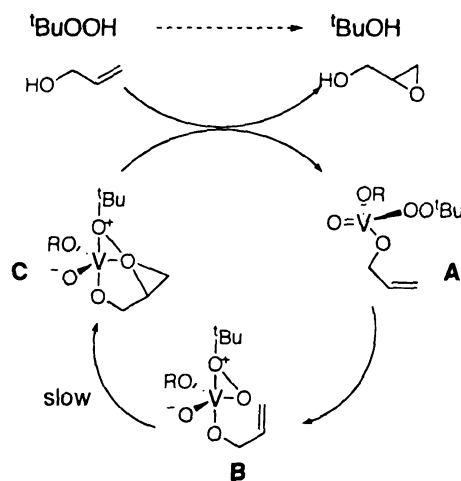


Figure IV-6: Sharpless' mechanism for vanadium catalyzed epoxidation of allylic alcohols

organic synthesis. The first mechanistic proposal for $\text{VO}(\text{acac})_2$ catalyzed epoxidation of allylic alcohols was put forth by Sharpless and co-workers (Figure IV-6).⁵⁵ After initial oxidation and ligand exchange at the metal center (**A**), the peroxide is activated by bidentate coordination to vanadium (**B**). The subsequent rate-determining step (**C**) involves oxygen transfer to the olefin.

This mechanism has been extended to construct working transition state models to explain the observed diastereoselectivities in epoxidation of various allylic, homoallylic, bis- and tris-homoallylic alcohols.²⁰ In particular, such a transition state model for secondary bis-homoallylic alcohols containing trisubstituted olefins was originally proposed by Kishi.⁵⁶ A representative example from Kishi's studies is shown in Figure IV-7. During epoxidation / cyclization of trisubstituted alkenol **IV-56**, THF **IV-58** was

produced as the major diastereomer *via* intermediacy of epoxide (**IV-57**). To explain the facial selectivity of the olefin epoxidation, two transition states **A** and **B** were invoked. Irrespective of the nature of R and R', **A** is the lower energy TS since the ⁱPr group

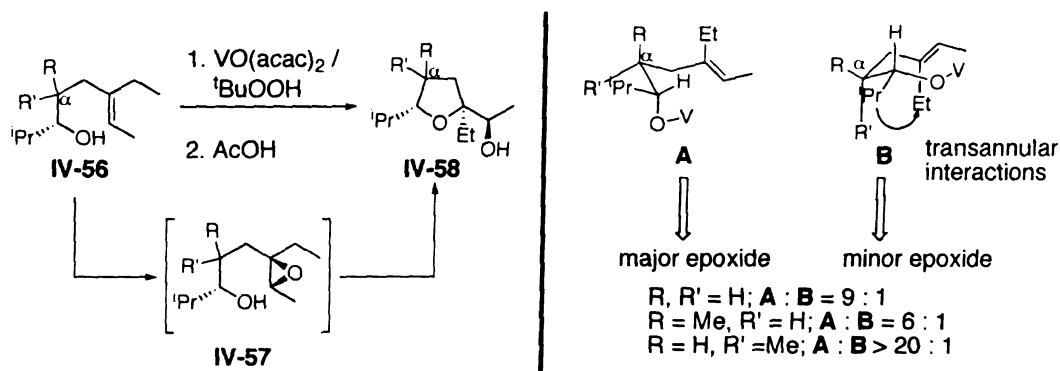


Figure IV-7: Kishi's transition state analysis to explain the diastereoselectivity observed in directed epoxidation of bis-homoallylic alcohols

occupies an 'outside' position whereas **B**, due to the proximity of the ⁱPr and Et groups suffers from transannular interactions. In the absence of any substitution at the α carbon (R, R' = H) a 9:1 selectivity in favor of **IV-57** was obtained. When R = Me and R' = H, the selectivity was lowered due to additional 1,3 diaxial interactions (of R and Et) in **A**. Finally, when the configuration at the α-carbon is switched (R = H and R' = Me), **B** is highly disfavored due to the 1,3 diaxial interactions (of R' and Et) in addition to the preexisting transannular interactions.

Applying a similar model to our secondary bis-homoallylic alcohol (**IV-50**), two transition states, **A** and **B** (Figure IV-8) can be drawn. Due to the *cis*-1,2 substitution pattern of the olefin, transition state **A** suffers from steric interactions between X and the incoming electrophilic oxygen. **B**, though devoid of such steric compression, experiences an allylic A^{1,3} strain⁵⁷ between X and the axial hydrogen. From this analysis, the relative

preference for the two transition states was not readily apparent. Moreover, a brief literature search revealed that high diastereoselectivities for $\text{VO}(\text{acac})_2$ promoted directed epoxidations of secondary bis- homoallylic alcohols have been observed only in the case

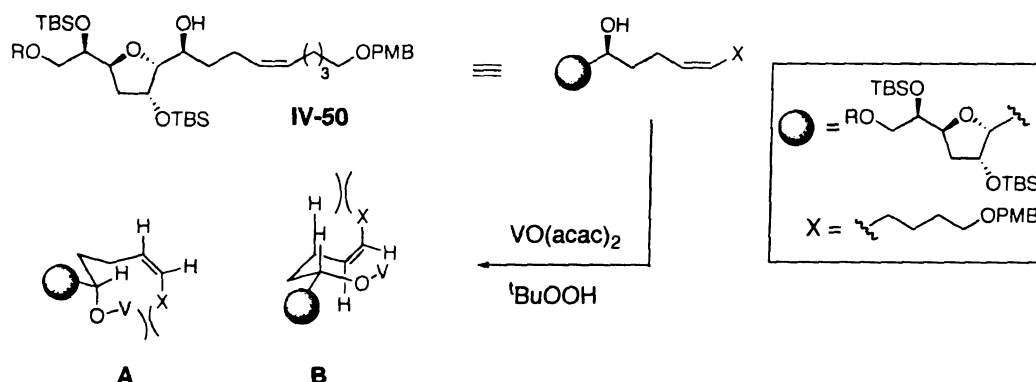


Figure IV-8: Application of Kishi's T.S. models to bis-homoallylic alcohol **IV-50**

of trisubstituted olefins.

Also, in our hands, preliminary trials to epoxidize **IV-50** using $\text{VO}(\text{acac})_2$ / $t\text{BuOOH}$ were not successful. Under several different conditions (ranging from ambient temperature to 80 °C), no epoxide product was ever observed. This indicated that olefin **IV-50** was inherently unreactive towards epoxidation under these conditions. Even if this type of epoxidation were successful, the strategy suffers from an inherent deficiency. The stereoselectivity of the epoxidation would be derived from the substrate (existing carbinol stereocenter) rather than from the reagents. Thus, diastereomeric THFs that would result from cyclization of the opposite epoxide stereoisomer would be difficult. Since we were aiming to establish a versatile synthesis of mucoxin, that would allow access to unnatural stereoisomers, the directed metal catalyzed strategy was not pursued further.

Among other protocols for the asymmetric epoxidation of unfunctionalized olefins, are methods developed by Shi and Jacobsen / Katsuki.⁵⁸ Recently, Shi and co-workers have developed a new chiral ketone catalyst (**IV-59**, Figure IV-9) for

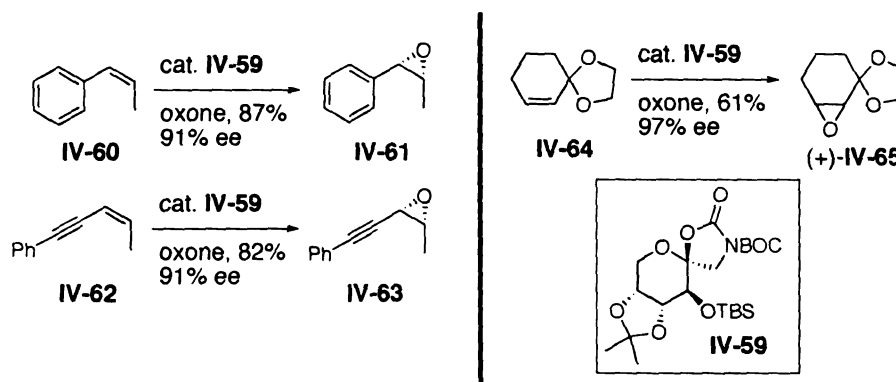


Figure IV-9: Representative examples of Shi asymmetric epoxidation of *cis* olefins

asymmetric epoxidations of *cis*- and terminal olefins.* Although the corresponding oxiranes were obtained in high enantiopurities and complete diastereospecificity, a major limitation of this method is only conjugated olefins or olefins bearing an adjacent acetal functionality (for example, **IV-60**, **IV-62** and **IV-64**) are optimal substrates. In case of alkyl substituted olefins (only one example reported) ca. 65% ee was obtained.⁶¹ Moreover, no further data on the diastereoselectivity of such unconjugated olefins is available.

In 1990, Jacobsen⁶² and Katsuki⁶³ independently reported asymmetric epoxidation of unfunctionalized olefins using Mn-salen complexes as chiral catalysts. Although 1,2 di-substituted *cis*-olefins produced the corresponding epoxides in high enantiopurities, as in Shi epoxidations, the optimum results were obtained only for

* The earlier ketone catalysts proved to be highly enantioselective only for *trans* and trisubstituted olefins.^{59,60}

conjugated and acetal containing olefins.⁵⁸ In addition, during epoxidation, the diastereomeric purity of the starting olefin was lost. For example, *cis*- β -methylstyrene (**IV-66**, R = Me, Figure IV-10) produced a mixture of the corresponding *cis*- and *trans*

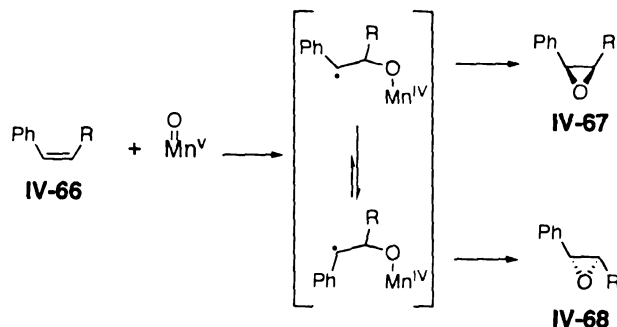


Figure IV-10: Proposed radical intermediate during oxygen transfer step in Jacobsen epoxidation

epoxides. It is believed that a radical intermediate is involved during the oxygen transfer, which undergoes bond rotation to favor formation of the *trans* epoxide (**IV-68**).⁶³ Taken together, none of the above-mentioned epoxidation protocols appeared feasible for use in our system.

In this context, we were also aware of Sharpless' method for the stereospecific conversion of 1,2-diols to epoxides (Figure IV-11).⁶⁴ Thus, vicinal diol **IV-69** is first converted to the corresponding ortho acetate (**IV-70**), which when treated with an acyl or TMS halide, leads to formation of regioisomeric acetoxy halides (**IV-72** and **IV-73**) via the intermediacy of acetoxonium ion **IV-71**. Upon basic hydrolysis, the halohydrin esters

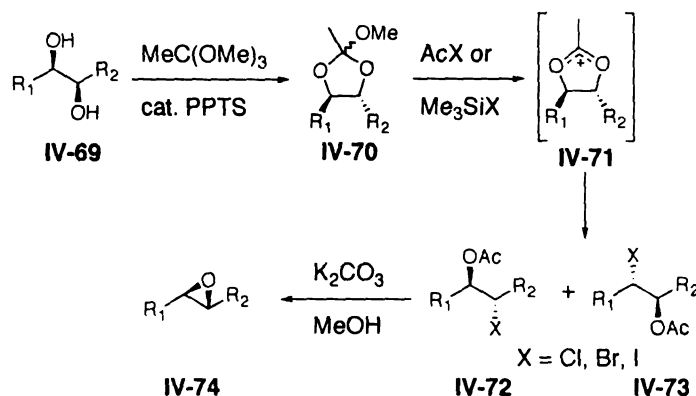


Figure IV-11: Sharpless' protocol for stereospecific conversion of vicinal diols into epoxides

undergo intramolecular halide displacement to generate the corresponding epoxide (IV-74). After each step, the corresponding intermediate is isolated simply by evaporation of the volatiles and the epoxides are obtained in 82% – 97% yield with complete retention of configuration at both the vicinal carbinol centers. Formation of both acetoxy halohydrin IV-72 and IV-73 involves inversion at one of the original diol stereocenters, which undergoes another inversion during epoxide ring formation. Thus the regioselectivity in acetoxy halohydrin formation is immaterial and the final epoxide is obtained with complete stereochemical fidelity.

We felt that this type of stereoselective epoxide formation was suitable in our synthesis for several reasons. First, asymmetric dihydroxylation unlike asymmetric epoxidation reactions, does not require any specific structural elements in the parent olefin and thus is a much more general way to oxidatively functionalize olefins. Secondly, the dihydroxylation process has been optimized for a variety of olefins with different substitution patterns to obtain the corresponding diols in high enantioselectivity and yields.^{65,66} In particular, for *cis* 1,2-di-substituted olefins (which is the substitution

pattern of our substrate **IV-50**), with appropriate choice of ligands, upto 90% ee has been obtained. Also, all four stereoisomeric epoxides are accessible from the appropriate diol precursors, which in turn are easily available simply by permutations of the olefin geometry and both antipodes of the chiral ligand. This would allow stereochemical diversity in our synthetic scheme to efficiently access the unnatural isomers of the natural product.

Since our ultimate goal was to construct the bis-THF unit **IV-51** (Scheme IV-9) starting from bis-homoallylic alcohol **IV-50** (whether or not *via* an epoxide intermediate),

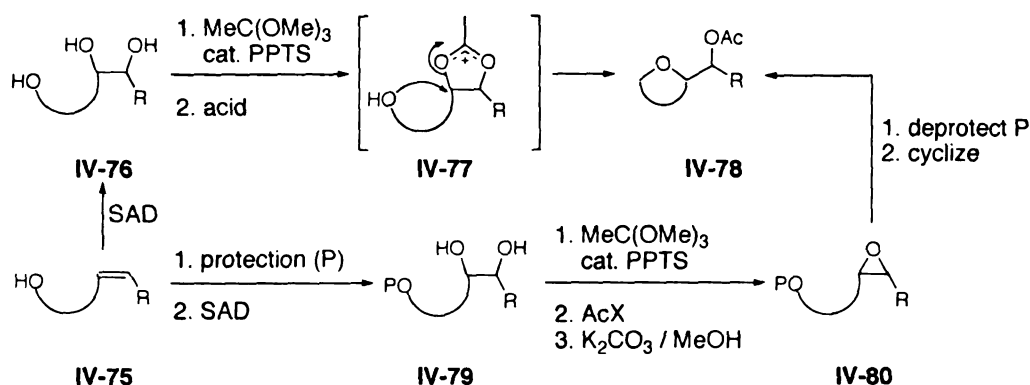


Figure IV-12: Proposed one pot cyclization of triols (**IV-76**) to the corresponding cyclic hydroxy ethers (**IV-78**)

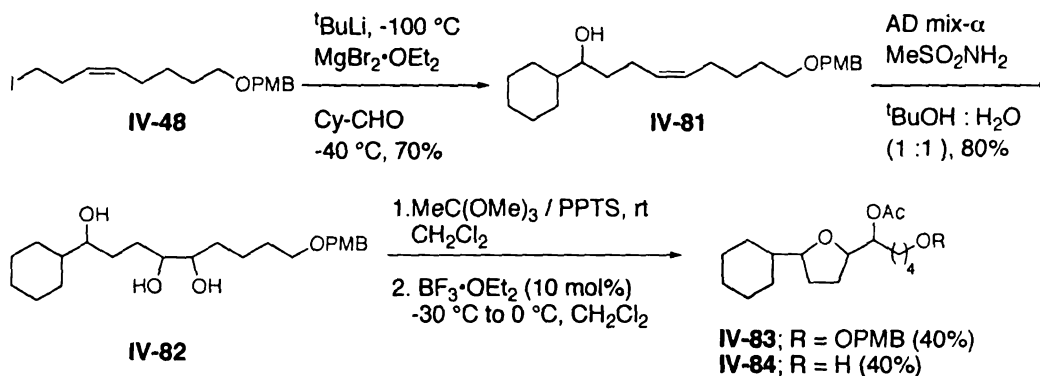
based on Sharpless' proposed mechanism for diol to epoxide conversion,⁶⁴ we put forth the following proposal (Figure IV-12).

An acetoxonium ion containing an appropriately positioned hydroxyl group (**IV-77**) may be intramolecularly trapped by the hydroxyl nucleophile. This event should result in formation of the corresponding cyclic ether unit defined by the general representation **IV-78**. We anticipated that in a triol system such as **IV-76**, the 1,2 ortho acetate would be preferentially generated leaving the isolated hydroxyl free for

nucleophilic attack. Also, the acid used for generation of the acetoxonium intermediate preferably should not contain a good nucleophile unlike in Sharpless' protocol (Figure IV-11), which might compete to trap the cation. Certainly, one might predict that even in presence of an external nucleophile, intramolecular trapping of the acetoxonium ion would be faster. In the ring closure of medium sized (5-7) cyclic ethers, an *exo-tet* mode is generally favored over an *endo-tet* according to Baldwin's rules.⁶⁷ Accordingly we anticipated that cyclization of hydroxy olefin **IV-50** (Scheme IV-9), following this route, should lead to the required 2,5 di-substituted THF ring (**IV-51**) bearing an adjacent secondary carbinol on the side chain. If successful, this strategy (from now on referred to as 1,2,n triol cyclization) would offer a quick and efficient entry to cyclic ethers of type **IV-78** (Figure IV-12) starting from alkenols such as **IV-75** in two steps, namely, Sharpless asymmetric dihydroxylation and a one-pot triol cyclization. Clearly, the alternative route involving pre-formation an epoxide (**IV-80**, Figure IV-12) would be lengthy and less efficient since it would call for additional protection / deprotection steps. In addition this sequence would obviate the need for a hydroxyl (or other) functionality in the substrate to direct the epoxidation, allowing us to generate stereoisomeric analogs of mucoxin as described in Chapter III.

Our immediate goal now, was to test the feasibility of the proposal. We decided to use a simplified model triol **IV-82** (Scheme IV-10) for this purpose. **IV-82** would also serve to test the compatibility of the PMB protecting group (which was present in the real substrate **IV-50**) with the cyclization conditions. The triol was obtained by dihydroxylation of the bis-homoallylic alcohol (**IV-81**), which in turn was prepared using

Grignard addition of the available iodide (**IV-48**) to cyclohexane carboxaldehyde. The stage was now set to attempt the proposed triol cyclization reaction.



Scheme IV-10: One pot cyclization of a model triol **IV-82**

From the outset, $\text{BF}_3 \cdot \text{OEt}_2$ was chosen as the acid promoter as it is an effective oxygen-coordinating Lewis acid in epoxide activations. After treatment of **IV-82** with trimethyl orthoacetate and catalytic PPTS, rapid consumption of the starting material was accompanied by appearance of two new spots on TLC at higher R_f values. Volatiles were then evaporated and the crude product was exposed to $\text{BF}_3 \cdot \text{OEt}_2$ (10 mol%, $-30\text{ }^{\circ}\text{C}$) in CH_2Cl_2 . Upon warming to $0\text{ }^{\circ}\text{C}$, the reaction was quenched and the purification of the crude material afforded two products **IV-83** and **IV-84** (each as a mixture of diastereomers) in 80% overall yield. No other regioisomeric cyclic products were detected. Although PMB deprotection under the reaction conditions could not be prevented, we were pleased to obtain the desired cyclized products. Later, we also found that isolation of the ortho acetate intermediate was not necessary and similar yields of **IV-83** and **IV-84** were obtained by addition $\text{BF}_3 \cdot \text{OEt}_2$ in the same pot. Thus, the triol cyclization, as proposed, was efficiently accomplished in a two-step one-pot procedure. Further studies to improve functional group compatibility of the reaction and to expand

its scope to access a variety of heterocycles have been undertaken by another graduate student in our laboratories.

B. Completion of the total synthesis of the proposed structure of mucoxin

Encouraged by the model studies, our next goal was to test the applicability of the triol cyclization with a bis-homoallylic alcohol such as **IV-50**. Since **IV-50** was also a model system derived from a model aldehyde **IV-8** (Scheme IV-8), we first decided to synthesize the real trisubstituted THF containing bis-homoallylic alcohol **IV-85** (Figure IV-13), which would be used for completion of the total synthesis.

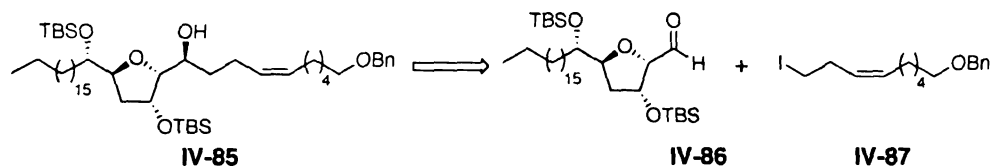
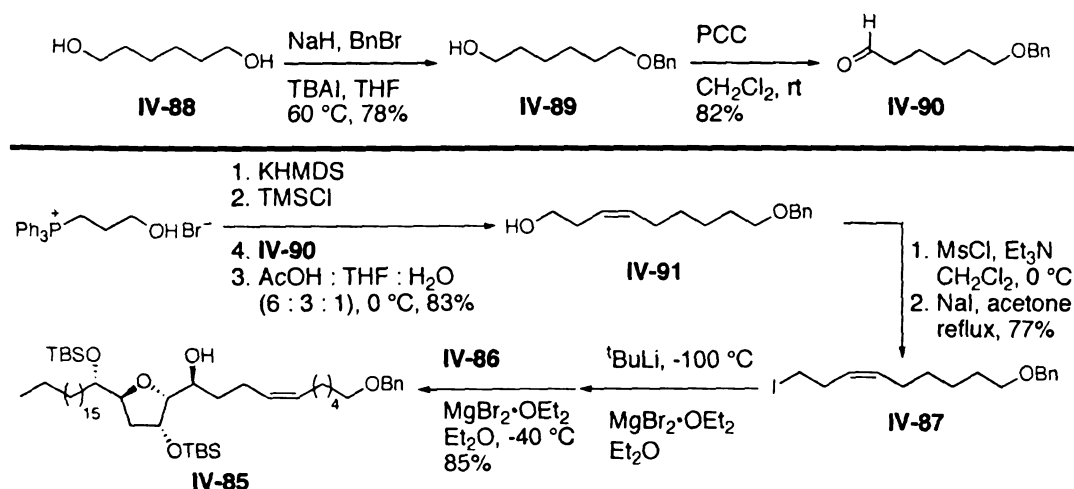


Figure IV-13: Assembly of the real aldehyde (**IV-86**) and partially functionalized right hand piece **IV-87**

The aldehyde precursor (**IV-86**) was available from earlier studies (Chapter III). Chelation controlled addition of the Grignard reagent derived from iodide **IV-87** to aldehyde **IV-86**, should furnish the requisite substrate **IV-85**. We decided to use iodide **IV-87** – a slightly modified version of the previous iodide (**IV-48**, Scheme IV-9), for two reasons. First, since the PMB protecting was found to be unstable to the $\text{BF}_3 \cdot \text{OEt}_2$ mediated triol cyclization reaction (Scheme IV-10), it was replaced by a more robust benzyl group.^{6,68} Second, in view of our unsuccessful attempts to couple iodide **IV-54** (Scheme IV-9) with (bromomethyl) acrylate, we decided to explore alternative ways

(*vide infra*) to install the terminal butenolide ring. This required the use of a nine carbon iodide (**IV-87**) rather than the earlier eight carbon unit **IV-48**.

Our efforts began by synthesis of **IV-87** (Scheme IV-11). Commercially available 1,6 hexanediol (**IV-88**) was transformed into aldehyde **IV-90** *via* mono benzylation (78%) followed by PCC oxidation (82%). *Cis*-selective Wittig olefination of **IV-90** with 3-hydroxypropyltriphenylphosphonium bromide *via* in situ TMS protection of the ylide⁴² generated the homoallylic alcohol **IV-91** (83%, > 10:1 diastereoselectivity). Displacement of the mesylate obtained from **IV-91** by NaI afforded the requisite iodide in 77% yield.⁴⁴ Chelation controlled addition involved first, generation of Grignard



Scheme IV-11: Synthesis of the real bis-homoallylic alcohol (**IV-85**)

reagent from **IV-87** by low temperature lithium-halogen exchange / transmetalation sequence, followed by treatment with $\text{MgBr}_2 \cdot \text{OEt}_2$ pre-complexed aldehyde **IV-86** at -40 $^\circ\text{C}$. The adduct (**IV-85**) was obtained in 85% yield as a single diastereomer (> 20:1 selectivity based on ^1H NMR of the crude product) after chromatographic purification.

With the desired bis-homoallylic alcohol **IV-85** in hand, we now set out to examine the triol cyclization reaction. This required first accessing the corresponding triol using Sharpless asymmetric dihydroxylation reaction. According to the empirical mnemonic device to predict enantioselectivity in the dihydroxylation reaction,^{65,69} the southwest (SW) and the northeast (NE) quadrants are more open to accommodate the olefinic substituents (Figure IV-14). The SW quadrant is considered an attractive area for soft, large and / or flat groups. Thus is it preferentially occupied by aryl and large alkyl groups in that order. Moreover oxygen-containing groups have a lesser tendency to occupy this position.⁷⁰ This mnemonic is most reliable in case of monosubstituted and *trans* 1,2 di-substituted olefins. When an olefin is oriented according to the constraints,

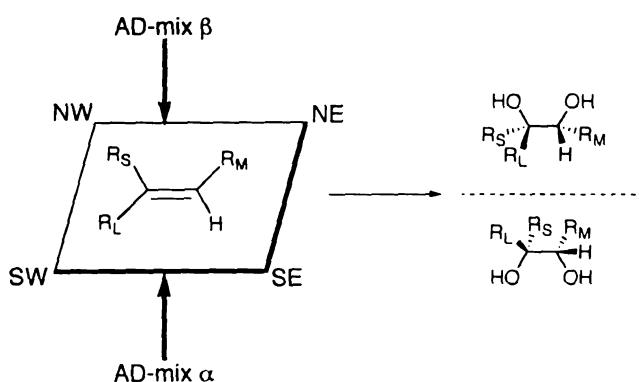


Figure IV-14: Empirical mnemonic device for the asymmetric dihydroxylation reaction

AD-mix- α reacts from the bottom face.

While positioning olefin **IV-85** according to the mnemonic, we reasoned that the unbranched alkyl portion might preferentially occupy the SW corner. The highly oxygenated THF ring containing substituent would then be placed in the SE area (Figure IV-15). **IV-85**, so oriented, would generate corresponding triol **IV-94** when treated with AD-mix- α . Subsequent triol cyclization involving inversion of configuration at the point

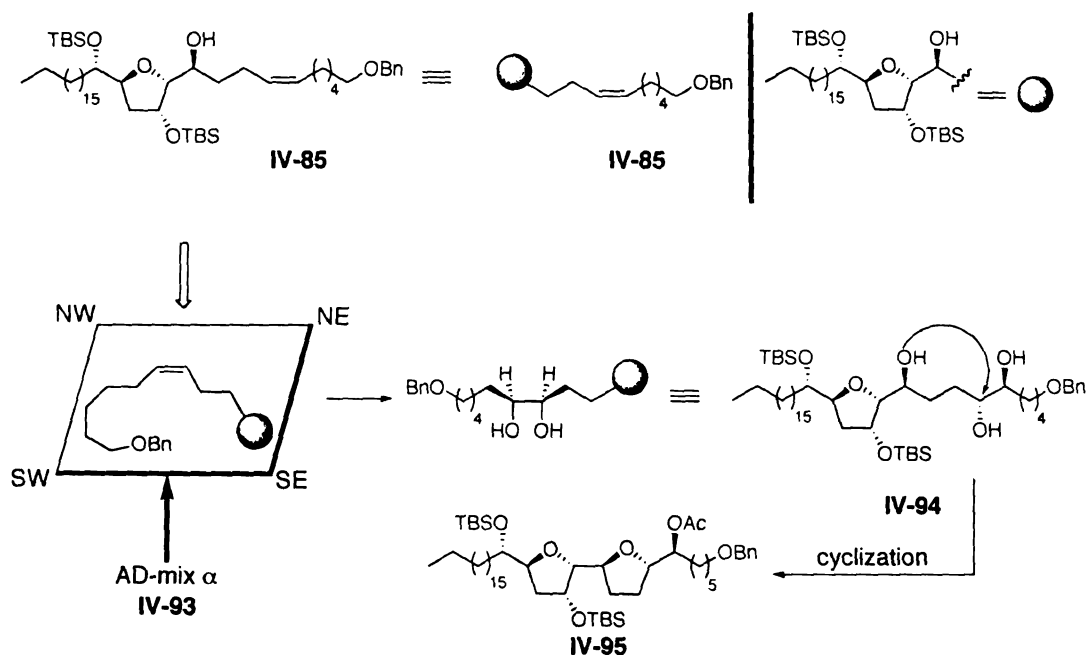
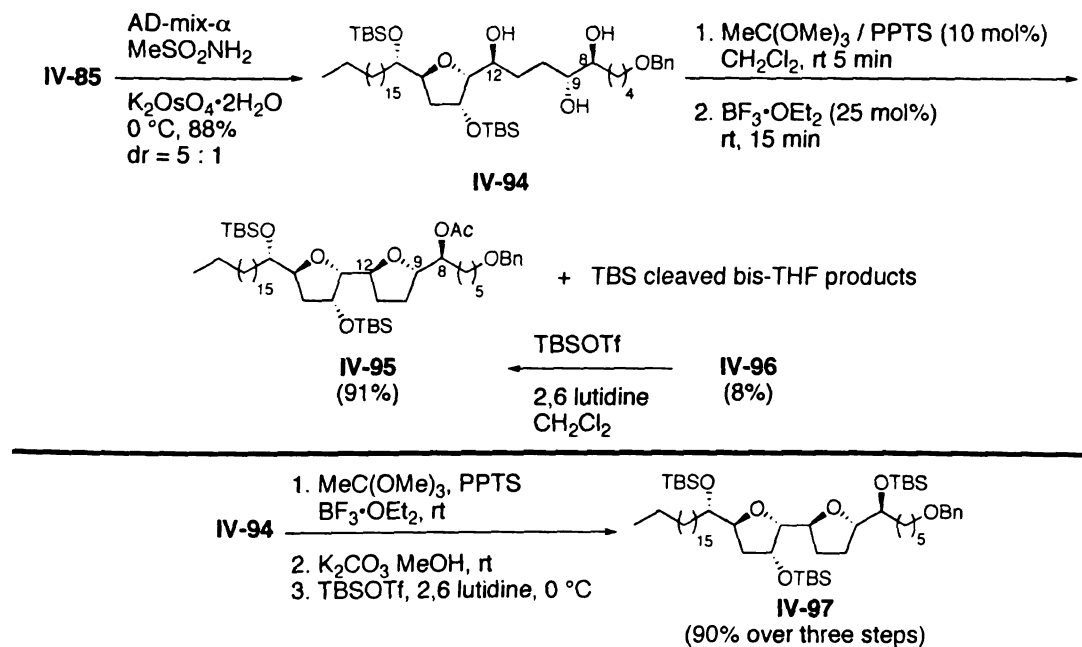


Figure IV-15: Application of the asymmetric dihydroxylation mnemonic to olefin **IV-85**



Scheme IV-12: Application of triol cyclization method to the real system

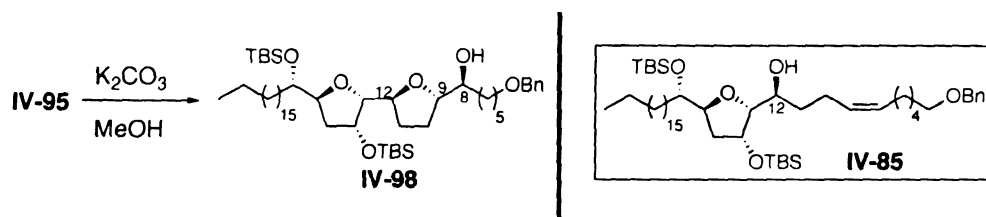
of cyclization, should lead to bis-THF unit (**IV-95**) bearing correct configuration at all the stereocenters.

Accordingly, asymmetric dihydroxylation of **IV-85** with AD-mix- α afforded the triol (**IV-94**, Scheme IV-12, only the major isomer shown) in 88% combined yield and ca. 5:1 diastereoselectivity. The diastereomers were easily separable by flash column chromatography and the major isomer was isolated in 73% yield. *Cis* 1,2-di-substituted olefins are known to be the most difficult class of substrates for the asymmetric dihydroxylation. Use of new chiral ligands, viz., DHQD-IND and DHQ-IND has significantly improved the enantioselectivities in certain substrates.⁷¹ In our case, since the major diol (**IV-94**) was isolated in enantiopure form and in good yields no further attempts were made to improve the diastereoselectivity by variation of the chiral ligands).

Armed with sufficient amounts of the triol **IV-94** we next investigated its cyclization reaction (Scheme IV-12). Using our original conditions (Scheme IV-10), i.e., 10 mol% $\text{BF}_3 \cdot \text{OEt}_2$, $-30\text{ }^\circ\text{C}$ to $0\text{ }^\circ\text{C}$, **IV-95** was obtained as the major (55%) product along with 20% of a mixture of TBS deprotected bis-THF products. After some experimentation, it was found that rapid addition of 25 mol% of $\text{BF}_3 \cdot \text{OEt}_2$ at ambient temperature and immediate (10-15 min) quenching of the reaction maximized the yield of the desired bis-THF (**IV-95**) up to 91%. Furthermore, reprotection on the small amount of cyclized product that had lost one of the silyl groups afforded **IV-95** in >95% yield. Thus, under these optimized conditions, the triol cyclization of **IV-94** proceeded almost quantitatively to afford **IV-95** as a single regio- and stereoisomer. Furthermore, we found that triol **IV-94** could be converted to fully protected bis-THF unit **IV-97** following a three-step sequence, viz., cyclization, acetate hydrolysis and TBS protection (Scheme IV-12) in excellent yield without purifying any of the intermediates. Differentially protected

bis-THF **IV-97** was suitable for further elaboration along the proposed synthetic scheme (Figure IV-5).

The mnemonic for asymmetric dihydroxylation is not completely reliable to predict facial selectivity of complex unknown olefins, particularly with a *cis*-1,2 substitution pattern.^{65,69} Therefore, before proceeding further, we decided to independently establish the absolute configuration of the vicinal diol generated *via* the asymmetric dihydroxylation reaction of **IV-85** (Scheme IV-12).

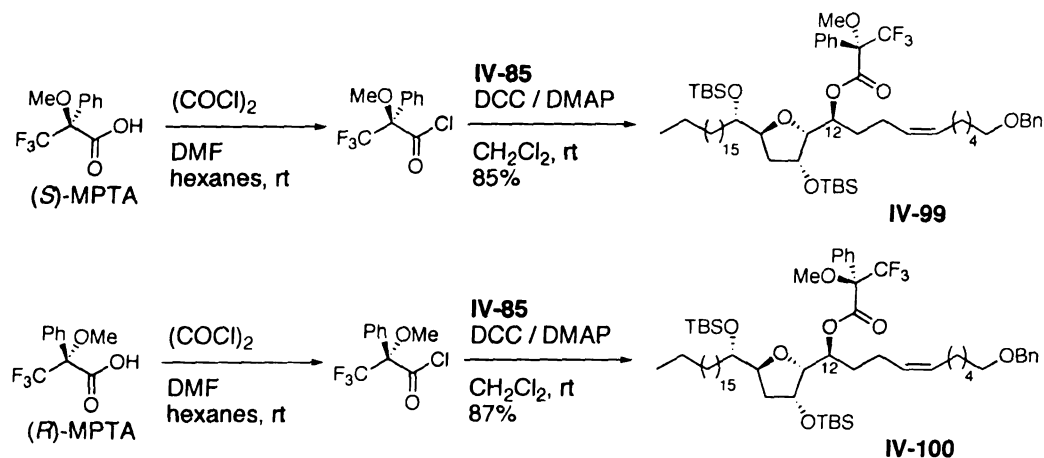


Scheme IV-13: Chiral alcohols (**IV-85** and **IV-98**) used in Mosher's ester analysis

We planned to use Mosher's ester analysis for this purpose.⁷² The three free hydroxyl groups in **IV-94**, being sterically similar would be hard to differentiate while forming the Mosher's monoester derivative. To simplify the derivatization and analysis process, we decided to use cyclized product **IV-98** (Scheme IV-13). **IV-98** was prepared by base hydrolysis of acetate **IV-95**. Mosher's ester analysis of **IV-98** would establish the absolute configuration at C8 and indirectly that of C9 since both C8 and C9 carbinols originated *via* dihydroxylation of *cis* olefin **IV-85**. Also, a similar Mosher's ester analysis of **IV-85** (Scheme IV-13) would ascertain the configuration at C12. Finally, NOESY experiments would confirm the relative stereochemistry across the C9-C12 THF ring.

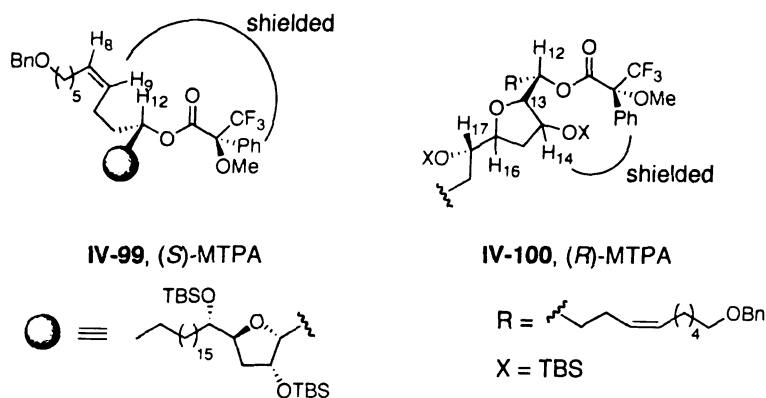
As per the plan, both, (*S*)- and (*R*)- α -methoxy- α -trifluoromethylphenylacetate (MTPA) ester derivatives of **IV-85** were synthesized (**IV-99** and **IV-100**, Scheme IV-14).

The DCC / DMAP mediated coupling was most efficient when freshly prepared MTPA chlorides were used.³²



Scheme IV-14: Synthesis of Mosher's esters of **IV-85**

Table IV-2 shows esters **IV-99** and **IV-100** drawn (only relevant structural features shown for clarity) in conformations proposed by Mosher* that explain the correlation between observed ¹H NMR chemical shifts and the absolute configuration of the parent alcohol **IV-85** at C12.⁷²



* Based on ORD and CD studies,⁷³ it has been proposed that the electronegative CF₃ group eclipses the carbonyl group in the CD active conformation. No detailed explanation of this conformational bias is provided.

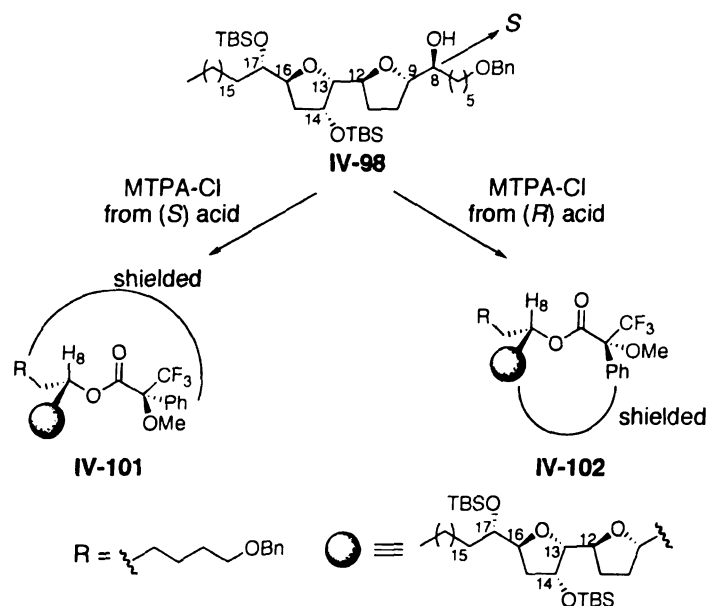
proton	chemical shift (δ) in IV-99	chemical shift (δ) in IV-100
H ₈	5.30	5.34
H ₉	5.22	5.30
H ₁₂	5.46	5.40
H ₁₄	4.37	4.33
H ₁₆	4.32	4.25
H ₁₇	3.65	3.59

Table IV-2: Mosher's ester analysis of **IV-99** and **IV-100**

Also, listed in Table IV-2 are chemical shifts of protons relevant in determination of the configuration. In **IV-99**, the olefin containing side chain is juxtaposed with the phenyl group of the MTPA ester. Therefore, those protons fall within the shielding cone of the phenyl group and are expected to shift upfield compared to the same protons in the other diastereomer (**IV-100**). As can be seen in Table IV-2, H₈ (5.30 δ) and H₉ (5.22 δ) in **IV-99** are more upfield than H₈ (5.34 δ) and H₉ (5.30 δ) in **IV-100**. Similarly, the trisubstituted THF ring in the (*R*)-MTPA derivative (**IV-100**), is shielded by the phenyl group and all the oxygenated methines (H₁₂, H₁₄, H₁₆ and H₁₇) in that portion of the molecule are shifted upfield compared to the corresponding protons in **IV-99** (Table IV-2). From this analysis, the stereocenter at C12 was established to be (*S*) which is also the expected configuration based on a chelation controlled transition state.

Next, we attempted to determine the configuration of bis-THF **IV-98** at C8 carbinol using the same technique. **IV-98** was derivatized as *S* (**IV-101**) and *R* (**IV-102**)

MTPA esters, again *via* DCC / DMAP mediated coupling with appropriate acetyl chlorides (Table IV-3). In **IV-101**, the alkyl side chain is shielded by the phenyl group of the MTPA ester and hence is expected to show upfield ^1H chemical shifts compared to the same protons in **IV-102**. On the other hand, the bis-THF portion in **IV-102**, being in the phenyl-shielding cone, would exhibit relatively upfield-shifted ^1H signals than those protons in **IV-101**. In both the derivatives, ^1H NMRs signals of the short, five carbon alkyl side chain overlapped with that of the THF ring methylenes (C10, C11 and C15) as well as the long, 17 carbon side chain on the other side. Therefore, the short alkyl chain portion was not used for the analysis. As indicated in Table IV-3, all the oxygenated methines (proton numbering corresponds to the carbon numbering in **IV-98**) belonging to the bis-THF portion in **IV-102** are shifted upfield relative to those in **IV-101** as expected.*



* Only H₉ did not fit in the trend, possibly because it resided outside shielding cone of the phenyl group.

proton	chemical shift (δ) in IV-101	chemical shift (δ) in IV-102
H ₈	5.14	5.12
H ₉	4.04	4.08
H ₁₂	4.31	4.27
H ₁₃	3.66	3.61
H ₁₄	4.22	4.16
H ₁₆	4.26	4.24
H ₁₇	3.71	3.70

Table IV-3: Mosher's ester analysis of **IV-101** and **IV-102**

Thus, the configuration of **IV-98** at C8 was determined to be (*S*). Also, since asymmetric dihydroxylation of a *cis*-olefin can in principle, produce only 1*R*, 2*S* or 1*S*, 2*R* diols, the original configuration at C9 (in **IV-94**, Scheme IV-12) is expected to be (*R*). Since the cyclization of **IV-94** to produce bis-THF **IV-95** (Scheme IV-12) involves inversion of configuration at the point of cyclization, the configuration of C9 in **IV-95** must be (*S*).

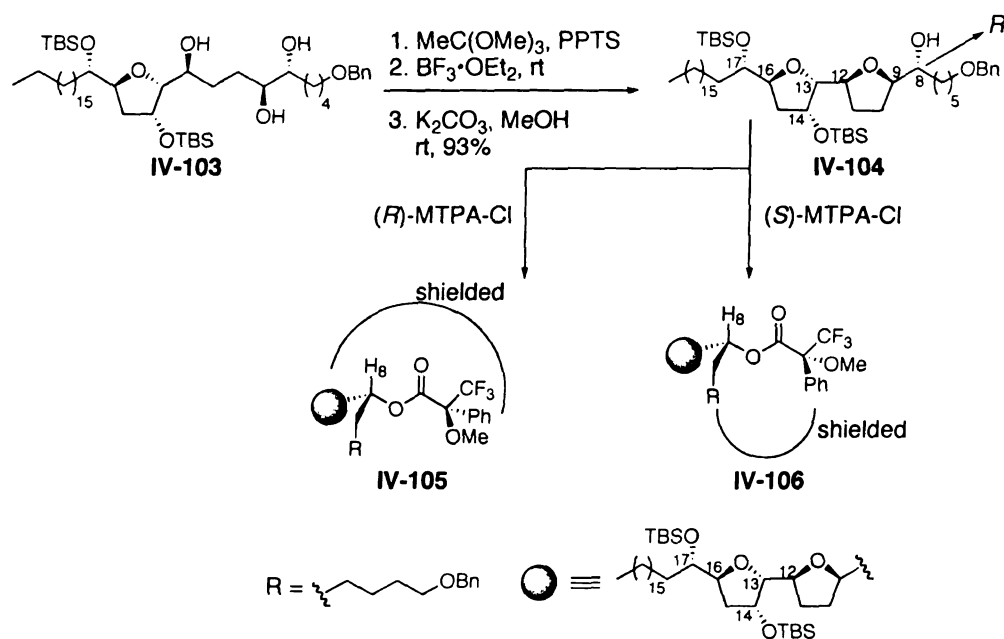
In order to further confirm our stereochemical assignment of **IV-98**, bis-THF **IV-104** (Table IV-4), epimeric at C8 and C9 was similarly analyzed. Triol **IV-103** was obtained via asymmetric dihydroxylation of **IV-85** (Scheme IV-12) using AD-mix- β , which upon cyclization and acetate deprotection furnished the bis-THF (**IV-104**, Table IV-4). The corresponding (*S*) (**IV-105**) and (*R*) (**IV-106**) MTPA esters were accessed as before. As expected the bis-THF portion of **IV-105** showed upfield ¹H NMR shifts relative to that of **IV-106** (Table IV-4), which verified the (*R*) configuration at C8 (and hence again (*R*) at

C9 as discussed before) in **IV-104**. Furthermore, 1D NOESY experiments clearly showed a strong nOe correlation between H₉ and H₁₂ (Figure IV-16) indicating a *cis* geometry across the THF ring, whereas no nOe correlations were observed across the di-substituted THF ring in **IV-101**.



Figure IV-16: nOe correlations in **IV-101** and **IV-105** containing *trans* and *cis* di-substituted THF rings respectively

The Mosher's ester analysis taken together with the nOe correlations confirmed that bis-THF **IV-98** (produced as the major diastereomer), possessed the requisite relative stereochemistry in C8-C12 portion. The minor diastereomer **IV-104** on the other hand,

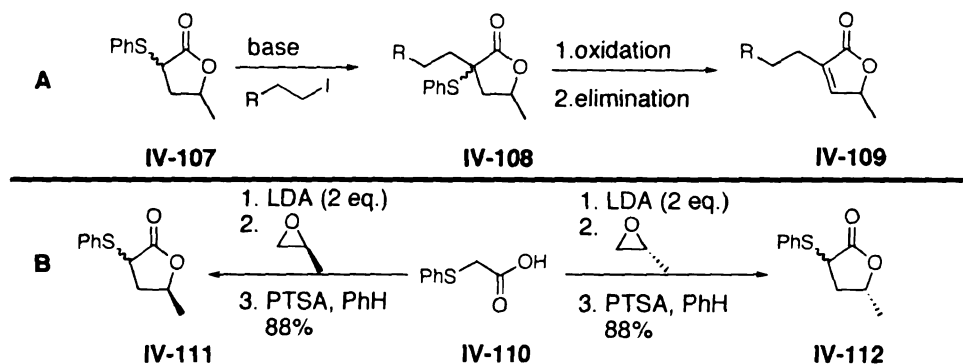


proton	chemical shift (δ) in IV-105	chemical shift (δ) in IV-106
H ₈	5.07	5.04
H ₉	4.02	4.07
H ₁₂	4.26	4.13
H ₁₃	3.60	3.52
H ₁₄	4.02	3.96
H ₁₆	4.30	4.28
H ₁₇	3.72	3.75

Table IV-4: Mosher's ester analysis of **IV-105** and **IV-106**

contained the undesired *cis*-di-substituted THF ring. Equipped with sufficient amounts of the fully protected version (**IV-97**, Scheme IV-12) of the desired diastereomer we then proceeded toward the final stages of the synthesis.

One of the tactics used to install the terminal butenolide in acetogenins, is outlined in Scheme IV-15 (A).^{38,74} α -Phenylthio lactone (**IV-107**) is alkylated to produce α -di-substituted derivative **IV-108**. The thiophenyl group is then oxidized to the corresponding sulfoxide, which upon heating undergoes *syn*-elimination to furnish the corresponding internal α,β -unsaturated lactone (**IV-109**).



Scheme IV-15: Synthesis of α -SPh lactones **IV-111** and **IV-112**

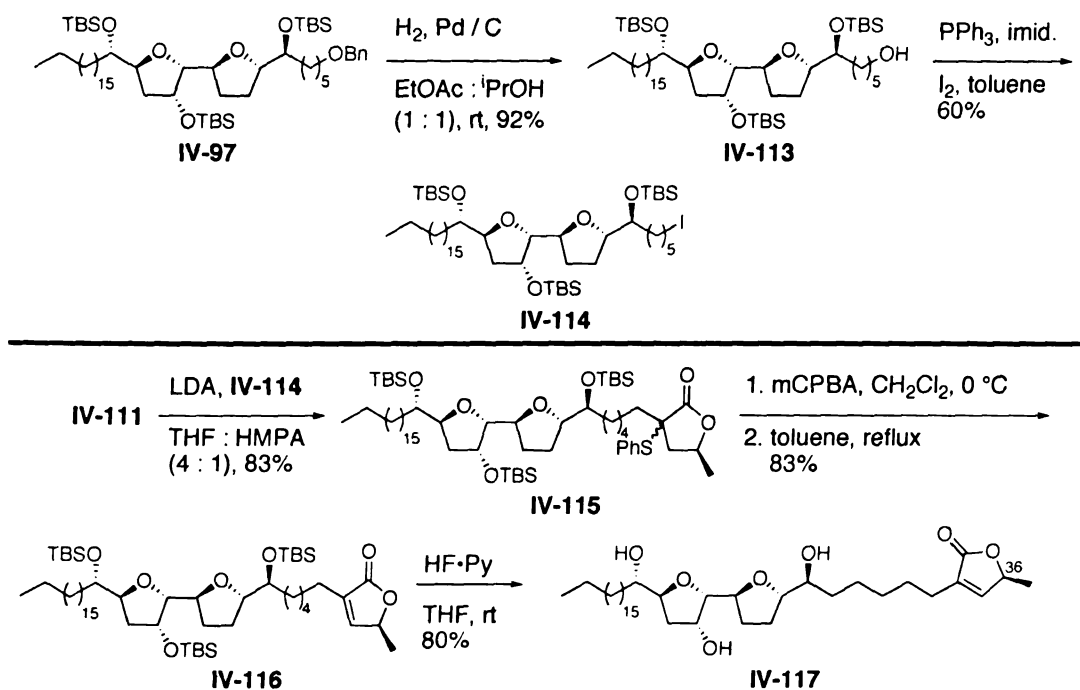
We decided to adopt this strategy to introduce the terminal lactone in mucoxin. Known α -SPh lactones **IV-111** and **IV-112**⁷⁵ were efficiently accessed from commercially available phenylthioacetic acid **IV-110**. Di-anion of **IV-110** when treated with (*S*)- and (*R*)-propylene oxides generated the corresponding γ -hydroxy acids (not shown) which spontaneously cyclized upon exposure to catalytic PTSA in benzene. Thus, both diastereomers **IV-111** and **IV-112** – referred to as *S*- γ -methyl and *R*- γ -methyl lactones respectively, were conveniently synthesized. This was particularly advantageous since we had randomly targeted an enantiomer of the bis-THF core (C8-C17) of mucoxin.* By reacting the iodide derived from **IV-97**, (Scheme IV-12) with *S*- γ -methyl lactone **IV-111** either natural mucoxin or its diastereomer would be produced. On the other hand, combination of the iodide with **IV-112** would furnish either the enantiomer or C36 epimer of natural mucoxin. In either case, by comparison of the optical rotation of the synthetic samples with that of the natural product,[#] the absolute stereochemistry of

* The absolute stereochemistry of that part of mucoxin is unknown, However, the γ -methyl stereocenter has been assigned *S* configuration.⁷⁶

[#] Although the α_D of mucoxin has not been reported, we hoped to obtain an authentic sample.

mucoxin should be established. Accordingly, having the lactones (**IV-111** and **IV-112**) in hand, we now turned to orthogonally protected bis-THF **IV-97** for further manipulations.

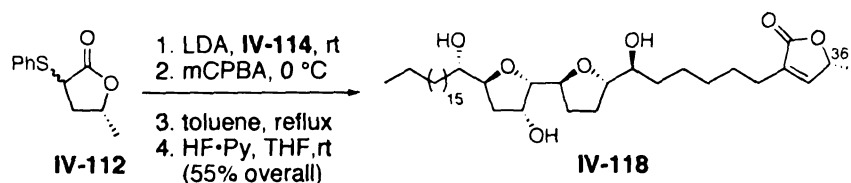
Iodide **IV-114** was obtained in a straightforward manner from **IV-97** by sequential debenzylation (H_2 , Pd/C, 92%)⁷⁷ and iodination (PPh_3/I_2 , 60%) of the resultant primary alcohol (Scheme IV-16).²³



Scheme IV-16: Completion of the total synthesis of proposed structure of mucoxin (**IV-117**)

After some experimentation,^{38,74} alkylation of α -SPh lactone **IV-111** with iodide **IV-114** was effected in 83% yield to secure intermediate **IV-115** which contained the complete carbon skeleton on mucoxin. The stage was now set for the β -elimination and final deprotection reactions. **IV-115** when submitted to mCPBA oxidation, afforded the corresponding sulfoxide in quantitative yield. The crude sulfoxide upon heating (refluxing toluene) underwent *syn*- β -elimination to provide internal α,β -unsaturated

lactone **IV-116**. Finally, global deprotection of **IV-116** using $\text{HF}\cdot\text{Py}^{74}$ occurred uneventfully to furnish target molecule **IV-117**, which was isolated in high purity after HPLC purification. Also, coupling of iodide **IV-114** with lactone **IV-112** in an analogous manner (Scheme IV-17) provided **IV-118**, which was exactly identical to **IV-117** in all respects except the absolute configuration at C36.



Scheme IV-17: Synthesis of C36 epimer of **IV-117**

C. Comparison of spectroscopic data and conclusions

The structures (constitution) of **IV-117** and **IV-118** as shown (Schemes IV-16 and IV-17), were confirmed by COSY experiments.

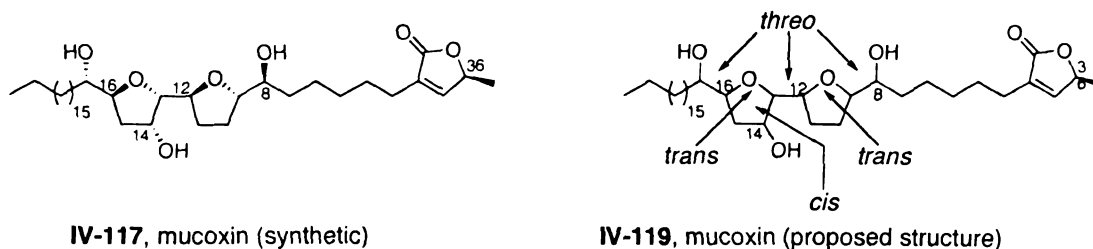


Figure IV-17: Mucoxin: synthetic and originally proposed structures

^1H and ^{13}C NMR spectra of **IV-117** and **IV-118** were found to be exactly identical indicating that stereochemistry at C36 was inconsequential as far as NMR spectra were concerned. However, both ^1H and ^{13}C spectra of **IV-117** differed from the corresponding published spectra of natural mucoxin having the proposed structure **IV-119** (Figure IV-17). Partial ^1H NMR spectra of the synthetic and natural samples are shown in Figure

IV-18. Since the major differences in the spectra reside in the hydroxyl-flanked bis-THF (C8-C17) region, only that portion in each spectrum is shown (proton numbering corresponds to the carbon numbering shown in the drawings above the spectra).

Table IV-5 shows comparison of ^1H chemical shifts of bis-THF portions of **IV-117** vs. natural mucoxin. The following differences and similarities in the spectra can be noted. Oxymethines that show largest differences in chemical shifts are H_{17} , and H_{14} , which are part of the trisubstituted THF ring. Other oxymethines, though slightly different in chemical shifts ($\Delta\delta = \text{ca. } 0.01 \text{ to } 0.09$), have the same splitting pattern. H_{13} in the natural spectrum appears as a triplet with $J = 3 \text{ Hz}$. McLaughlin has used this splitting pattern and the J value of H_{13} along with preliminary molecular modeling to propose the relative stereochemistry of C12, C13 and C14 triad (Figure IV-17) of mucoxin.*⁷⁶ In view of this, it becomes important to note that H_{13} in the synthetic spectrum appears as a triplet as well with the exact same coupling constant. Finally, chemical shifts of the THF ring methylenes (H_{10} , H_{11} , and H_{15}) also differ significantly. Moreover, of all three methylenes, δ value of H_{15} , which again is part of the trisubstituted THF ring, deviates the most.

* The basis for this stereochemical assignment is discussed in more detail later.

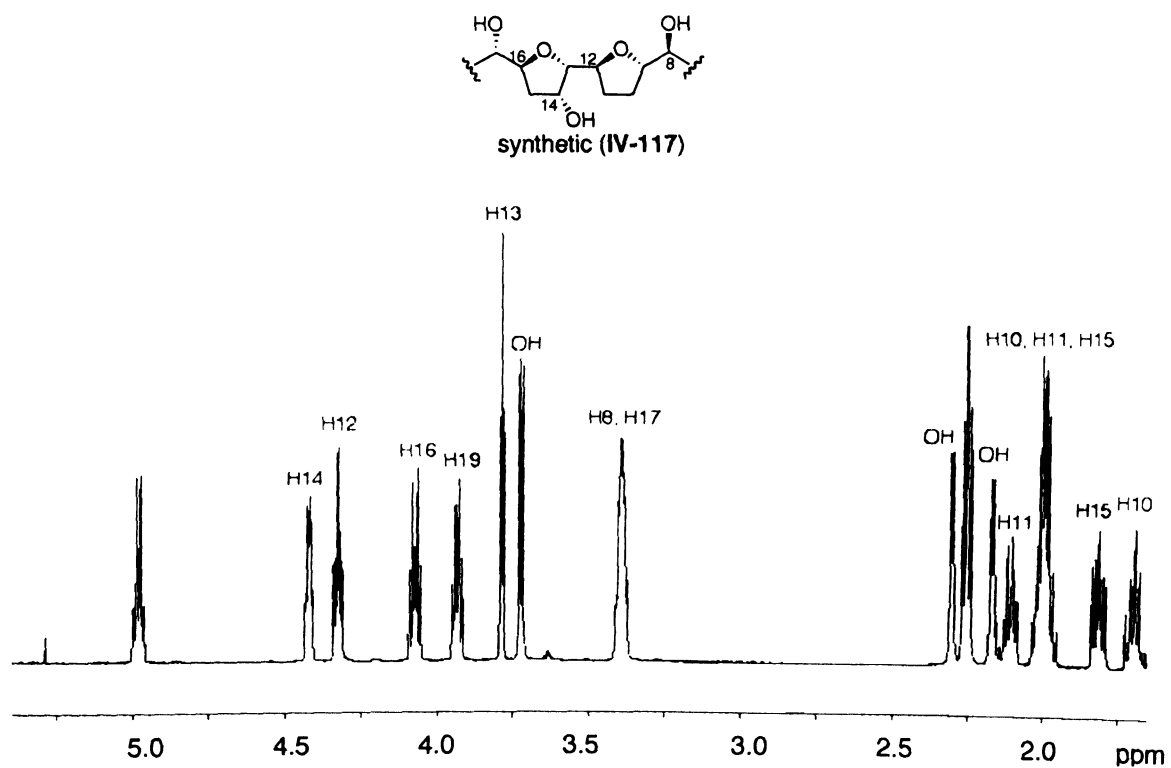
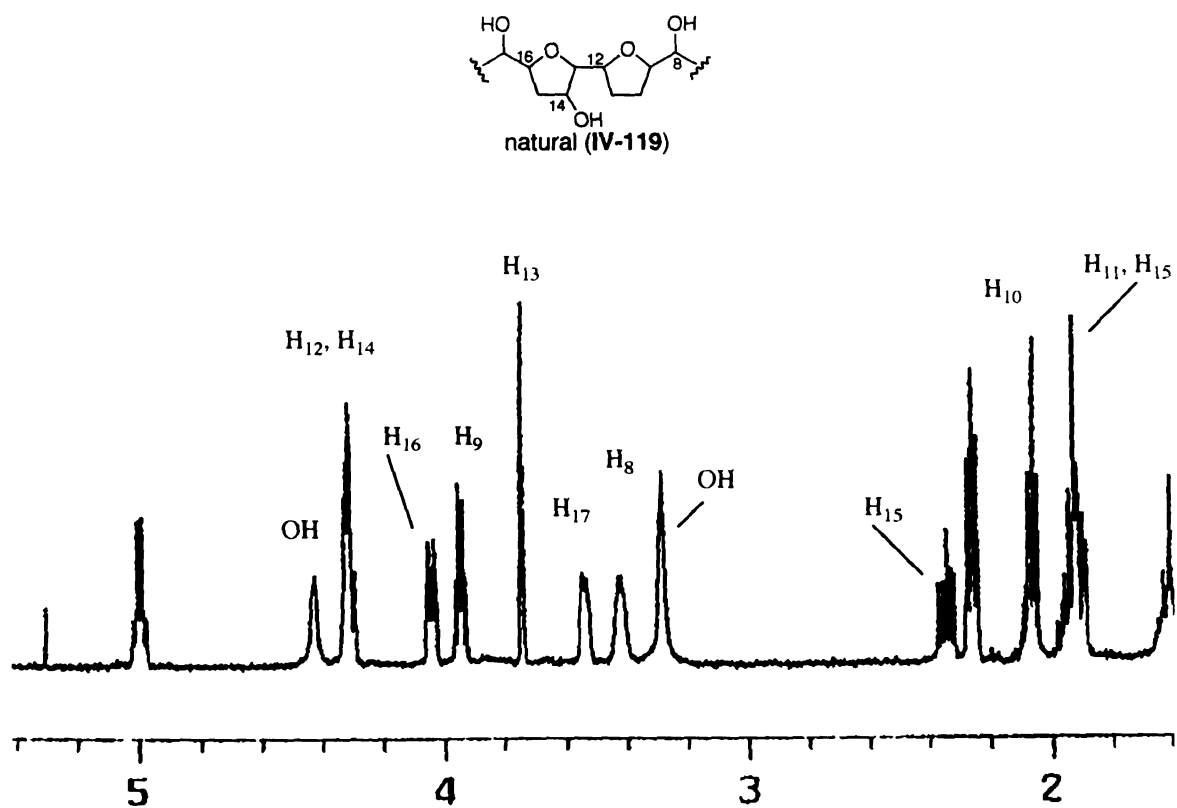
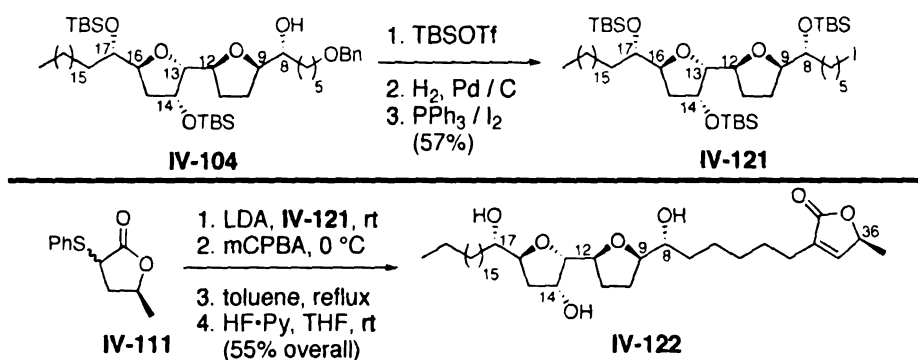


Figure IV-18: Comparison of partial ^1H NMR spectra of the natural mucoxin and IV-117

proton	IV-117	natural mucoxin	$\Delta\delta$ (IV-117-natural)
H ₈	3.41	3.42	-0.01
H ₉	3.96	3.95	+0.01
H ₁₀	1.84, 2.02	1.91, 2.05	-0.07, -0.03
H ₁₁	2.02, 2.13	1.91, 2.05	0.11, 0.08
H ₁₂	4.35	4.31	0.04
H ₁₃	3.80	3.71	0.09
H ₁₄	4.44	4.32	0.12
H ₁₅	1.84, 2.02	1.91, 2.35	-0.07, -0.33
H ₁₆	4.09	4.04	0.05
H ₁₇	3.41	3.53	-0.12

Table IV-5: Comparison of ¹H NMR chemical shifts of bis-THF portions (C8-C17) of natural mucoxin vs. **IV-117**

Since neither a natural sample of mucoxin nor any other characterization data besides the published spectra were available, we began further investigations using the existing information. As a part of our efforts to locate the source of the discrepancies, **IV-122** – a diastereomer of **IV-117** (epimeric at C8 and C9) was synthesized (Scheme IV-18). Bis-THF intermediate **IV-104**, which was available *via* cyclization of triol **IV-103** (Table IV-4) was converted to the corresponding iodide (**IV-121**). Coupling of iodide **IV-121** with lactone **IV-111** following a similar reaction sequence as before (Scheme IV-18) afforded **IV-122**.



Scheme IV-18: Synthesis of (8,9-*epi*) **IV-117**

Comparison of ^1H NMRs of **IV-122** and the natural sample indicated that chemical shifts of all the oxymethines in the bis-THF (C8-C17) portion differed (Figure IV-19 and Table IV-6). The diagnostic H_{13} signal (t, $J = 3$ Hz) in the natural spectrum, which was used to propose the relative configuration of C12, C13 and C14 stereocenters (*vide supra*), is a dd ($J = 1.5, 3.4$ Hz) in **IV-122**. $\Delta\delta$ for H_9 in case of **IV-122** is much greater than that in **IV-117** (Tables IV-5 and IV-6), which suggests that stereochemistry of the di-substituted THF ring in **IV-117** matches more closely to that in the natural product. Also, the THF methylenes (H_{10} , H_{11} and H_{15}) in **IV-122** differ widely from those in natural mucoxin. Taken together, ^1H NMR of **IV-117** matches more closely with the natural spectrum than that of **IV-122**.

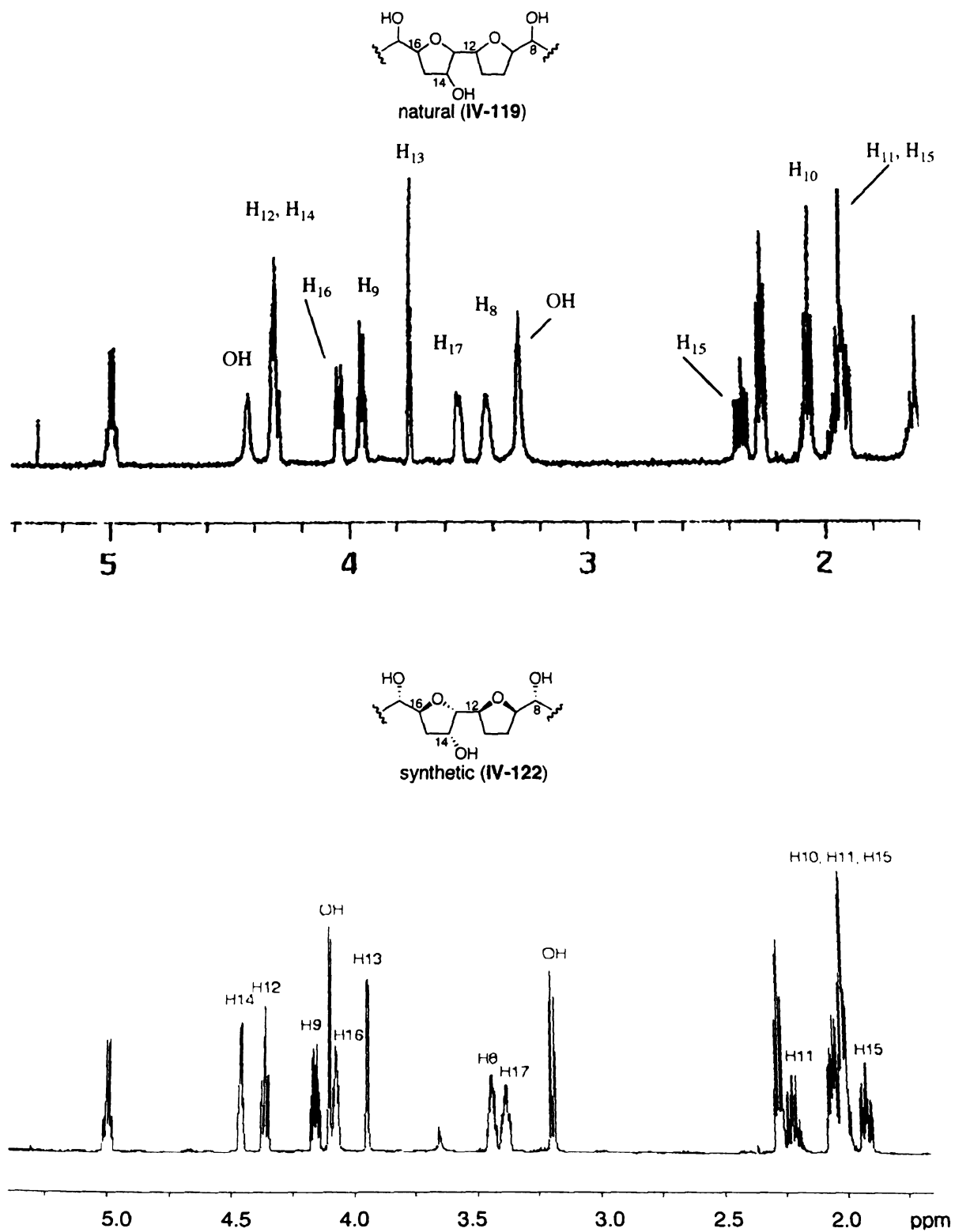


Figure IV-19: Comparison of partial ^1H NMR spectra of natural mucoxin and IV-122

proton	IV-122	natural mucoxin	$\Delta\delta$ (IV-122-natural)
H ₈	3.44	3.42	0.02
H ₉	4.16	3.95	0.21
H ₁₀	2.04, 2.04	1.91, 2.05	0.13, -0.01
H ₁₁	2.04, 2.22	1.91, 2.05	0.13, 0.17
H ₁₂	4.37	4.31	0.06
H ₁₃	3.95	3.71	0.24
H ₁₄	4.46	4.32	0.14
H ₁₅	1.92, 2.04	1.91, 2.35	0.01, -0.31
H ₁₆	4.08	4.04	0.04
H ₁₇	3.39	3.53	-0.14

Table IV-6: Comparison of ¹H chemical shifts of bis-THF portions (C8-C17) of natural mucoxin vs. **IV-122**

At this point, we decided to re-examine Mclaughlin's reasoning for structure elucidation of mucoxin. In the process we hoped to delineate any ambiguities in their proposed structure and possible sources of discrepancies between the synthetic and the natural spectra.

Based on the reported COSY and HRMS analysis of the natural sample of mucoxin, the proposed structure (constitution) appears to be correct. Figure IV-20 shows the HRMS (EI) fragmentation pattern of the tris-TMS derivative of mucoxin (**IV-120**).⁷⁶

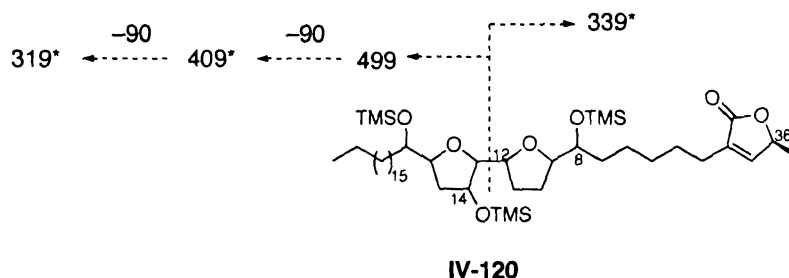


Figure IV-20: HRMS fragmentation pattern of the tris-TMS derivative of mucoxin. (* = observed peak)

Also, as mentioned earlier, using COSY experiments the structure (constitution) of our synthetic sample (**IV-117**) was clearly established. Therefore we felt that the differences in the synthetic vs. natural spectra are most likely due to stereochemical mismatches. In case of natural mucoxin, the relative configuration across both the THF rings (C9-C12 and C13-C16, **IV-119**, Figure IV-17) was suggested to be *trans* based on the lack of NOESY correlations. 1D NOESY correlations for synthetic compounds **IV-117** and **IV-122** are shown in Figure IV-21. No nOe correlation peaks across either of the THF rings (H_{16} – H_{13} or H_{12} – H_9) were observed in **IV-117** (only relevant partial structure shown). On the other hand, in case of **IV-122**, a strong nOe correlation was observed across the di-substituted THF ring (H_9 – H_{12}) while no nOe signals were seen between H_{13} and H_{16} . This clearly suggests 2,5-*cis* relationship across the

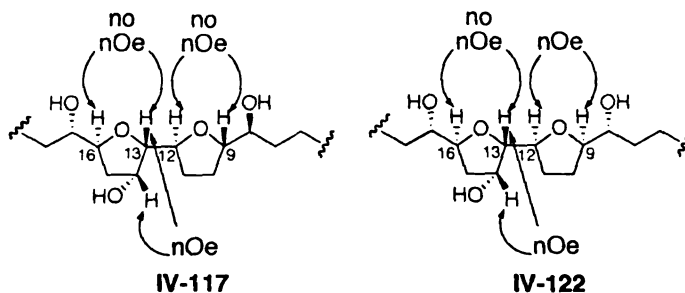


Figure IV-21: nOe correlations in the two synthetic diastereomers

di-substituted THF and 2,5-*trans* relation across C13-C16 THF ring in **IV-122**. Moreover, since we have independently established the absolute configurations at C9, C12 and C16 using Mosher's ester analysis and ECCD techniques, it can be unambiguously stated that both the THFs in **IV-117** are *trans*. nOe correlations have been routinely used to predict 2,5 relative configuration of di-substituted THFs in acetogenins. Such stereochemical assignments have proved reliable as confirmed by total synthesis or X-ray analysis of these natural products.⁷⁸ Thus, based on the above analysis we reasoned that 2,5 stereochemical assignment across the two THF rings in natural mucoxin might be correct. Also, strong nOe correlations between H₁₃ and H₁₄ in **IV-117** and **IV-122** (Figure IV-21) confirmed *cis*-relation between them.

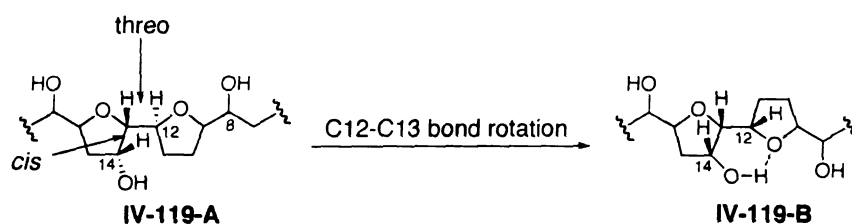


Figure IV-22: Intramolecular hydrogen bonding in mucoxin as proposed by McLaughlin

We next turned to evaluate McLaughlin's assignment of the relative configuration of C12, C13, C14 triad (Figure IV-22, only relevant structural features shown). In ¹H NMR of natural mucoxin, H₁₃ appeared as a pseudotriplet with 3 Hz coupling constant. Based on this and molecular models, McLaughlin proposed that the C12-C13 bond rotation might be restricted possibly due to intramolecular hydrogen bonding between C14 hydroxyl and C9-C12 THF ring oxygen (**IV-119-B**, Figure IV-22). In such a rigid conformation, for H₁₃ to maintain 3 Hz coupling constant with H₁₂ and H₁₄, the two THF

rings must be *threo* to each other and C14-OH must be *cis* to the C13 side chain as shown in **IV-119-A** (Figure IV-22).

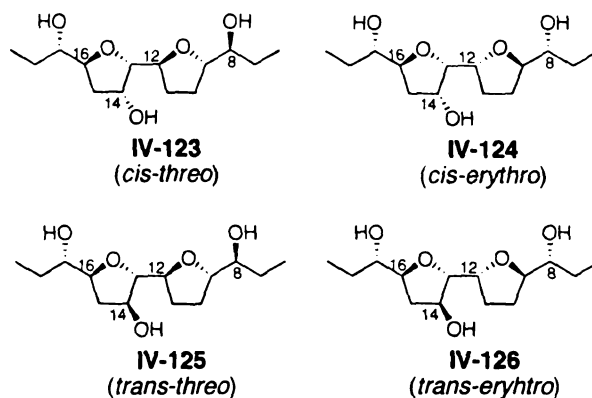
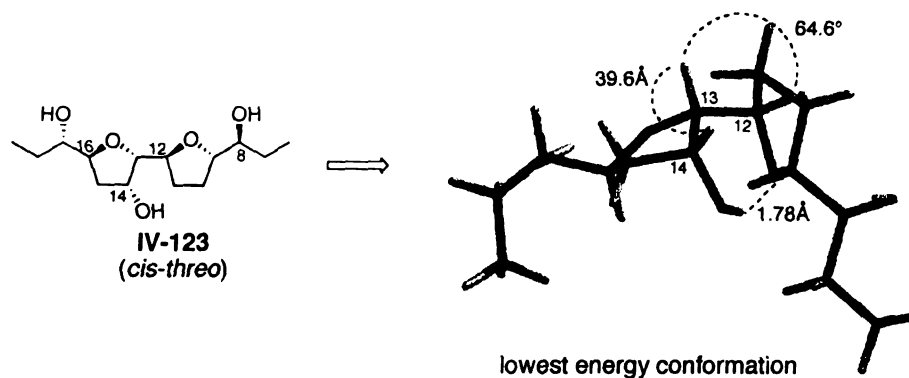


Figure IV-23: Truncated stereoisomeric bis-THF analogs of proposed structure of mucoxin

This stereochemical assignment seems tenuous since the only experimental evidence presented is the coupling constant of H_{13} with H_{12} and H_{14} . To gain further insight into the conformations of the natural product, we decided to carry out basic molecular modeling studies. Using molecular mechanics (MMFF94 force field), conformational searches and energy minimizations of four diastereomeric bis-THF units **IV-123** – **IV-126** (Figure IV-23) were carried out.* **IV-123** is McLaughlin's proposed stereoisomer containing H_{13} and H_{14} *cis* to each other, and H_{12} and H_{13} in a *threo* relationship. **IV-123** is referred to as the *cis-threo* isomer and all the remaining structures are named similarly to reflect the relative configurations at the C12, C13, C14 triad (Figure IV-23). **IV-124** – **IV-126** are hypothetical diastereomers containing different relative stereochemistries at the C12, C13, C14 triad. However, *threo* relation of the side

* Spartan V 5.1.3, Wavefunction, Inc., 18401 Von Karman Avenue, Suite 370, Irvine CA 92612, U.S.A.

chain hydroxyls with the THFs and 2,5 *trans* configuration across both the THFs in **IV-124 – IV-126** is conserved. Also, in all four diastereomers, the original long hydrocarbon



Conformation	Relative energy (Kcal/mol)	OH—O ^a Distance (Å)	θ_{13-14} (degrees) ^b	θ_{12-13} (degrees) ^c
1	0.00	1.78	-39.7	64.3
2	0.07	1.77	-39.7	64.5
3	0.37	1.77	-39.3	64.7
4	0.45	1.77	-40.2	64.2
5	0.47	1.78	-40.4	63.9
6	0.73	1.77	-40.2	64.2
7	0.75	1.77	-40.4	63.9
8	0.78	1.78	-40.2	63.9
9	1.06	1.77	-40.2	63.9
10	1.55	1.79	-38.3	65.7

^a distance between C14-OH and C9-C12 THF oxygen. ^b H₁₃-H₁₄ dihedral angle. ^c H₁₂-H₁₃ dihedral angle.

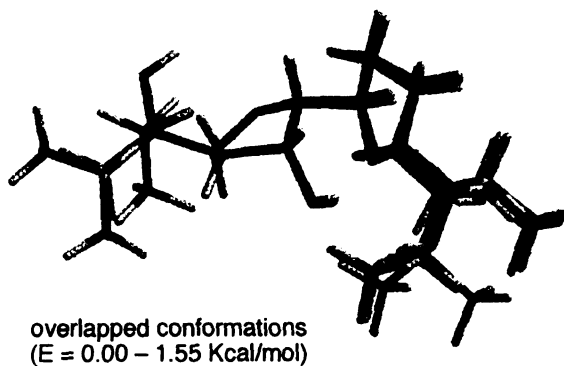


Figure IV-24: Low energy conformations of *cis-threo* isomer **IV-123**

chains are truncated to ethyl groups for ease of energy minimizations.

Figure IV-24 shows conformations of **IV-123** within 2 Kcal/mol of the lowest energy conformation. In all the conformations, the OH—O distance between C14-OH and C9-C12 THF oxygen is ca. 1.78 Å, which is within hydrogen bonding range. The average H_{12} - H_{13} and H_{13} - H_{14} dihedral angles are 64.6° and 39.6° respectively with variation of ca. 2° in each case. The overlapped conformations indicate that both the THF rings are superimposable and only the side chains have different rotations. Using these average dihedral angles, the corresponding theoretical coupling constants between H_{12} - H_{13} and H_{13} - H_{14} can be estimated based on Karplus equation.⁷⁹

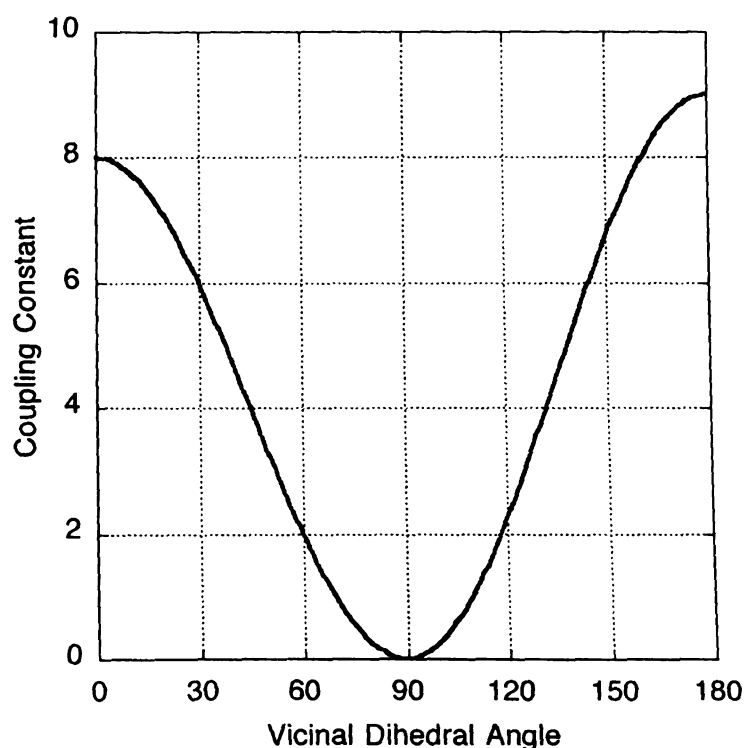


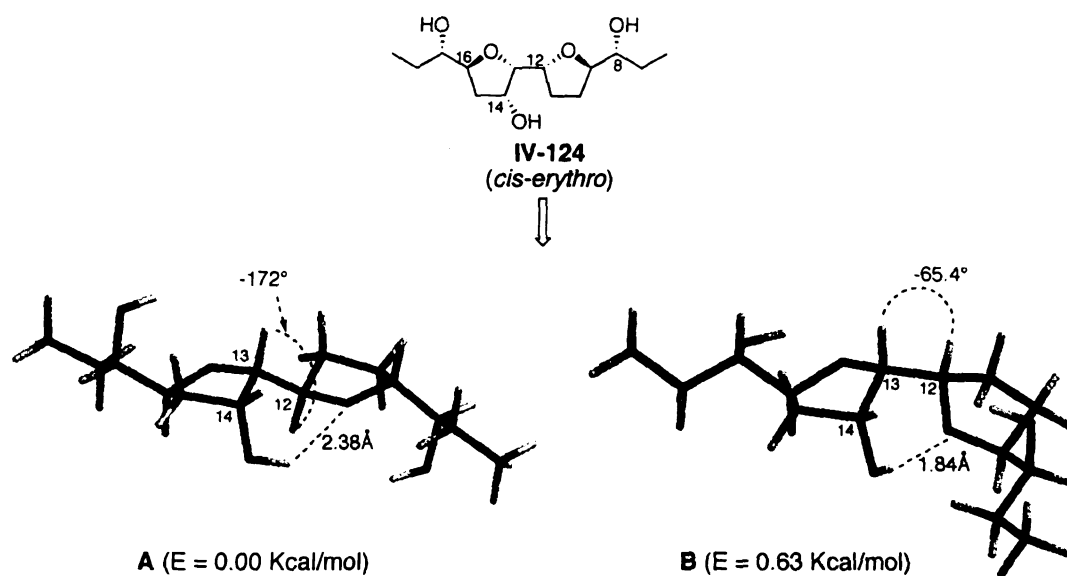
Figure IV-25: Karplus equation plot for vicinal oxygenated systems

Besides dihedral angle, vicinal ^1H - ^1H coupling constants also depend upon the nature of substituents. Figure IV-25 shows variation of coupling constant (J) with dihedral angle according to Karplus equation in case of vicinal oxygenated systems.^{79,80} From the graph, $\theta_{12-13} = 65^\circ$ corresponds to $J = \text{ca. } 1.9 \text{ Hz}$ and $\theta_{13-14} = 40^\circ$ correspond to $J = 4.2 \text{ Hz}$. Thus, the estimated coupling constants are close to the experimentally observed value of 3 Hz.

Similar analysis of *cis-erythro* diastereomer **IV-124** provided interesting results (Figure IV-26). In this case, the low energy ($< 2 \text{ Kcal/mol}$) conformations can be divided into two sets – one having $\theta_{12-13} = 65^\circ$ (A, Figure IV-26) and the other with $\theta_{12-13} = 172^\circ$ (B).^{*} Again from the Karplus equation plot (Figure IV-25) H_{12} - H_{13} coupling constant in conformations **A** is estimated to be 9.0 Hz while that in conformations **B** would be ca. 1.9 Hz. As can be seen from the table (Figure IV-26), 60% of the population constitutes conformations **B**. Notably, the OH–O distance between C14-OH and C9-C12 THF oxygen in **B** is ca. 1.84 Å whereas that in **A** is 2.38 Å. Thus, the conformations with $\theta_{12-13} = 65^\circ$ are more within hydrogen bonding distance than those with $\theta_{12-13} = 172^\circ$. If such an intramolecular hydrogen bonding exists, conformations **B** are likely to be favored.

Furthermore, when the ^1H NMR spectrum of the synthetic material (**IV-117**) was measured in methanol, H_{13} appeared as a doublet of a doublet ($J = 3.3$ and 7.3 Hz). While the coupling constant between H_{13} and H_{14} would be expected to be more or less independent of the solvent, that between H_{12} and H_{13} could vary with the nature of the

^{*} Average values listed in both cases.



Conformation	Relative energy (Kcal/mol)	OH—O ^a Distance (Å)	θ_{13-14} (degrees) ^b	θ_{12-13} (degrees) ^c
1	0.00	2.38	-33.2	-171
2	0.48	2.37	-32.9	-171
3	0.51	2.44	-34.2	-173
4	0.63	1.84	-40.1	-65.4
5	0.82	2.43	-34.1	-173
6	0.93	1.84	-39.9	-65.4
7	1.03	1.84	-40.2	-65.6
8	1.19	1.85	-39.4	-64.4
9	1.33	1.84	-40.0	-65.6
10	1.53	1.85	-39.5	-64.5

^a distance between C14-OH and C9-C12 THF oxygen. ^b H_{13} - H_{14} dihedral angle. ^c H_{12} - H_{13} dihedral angle.

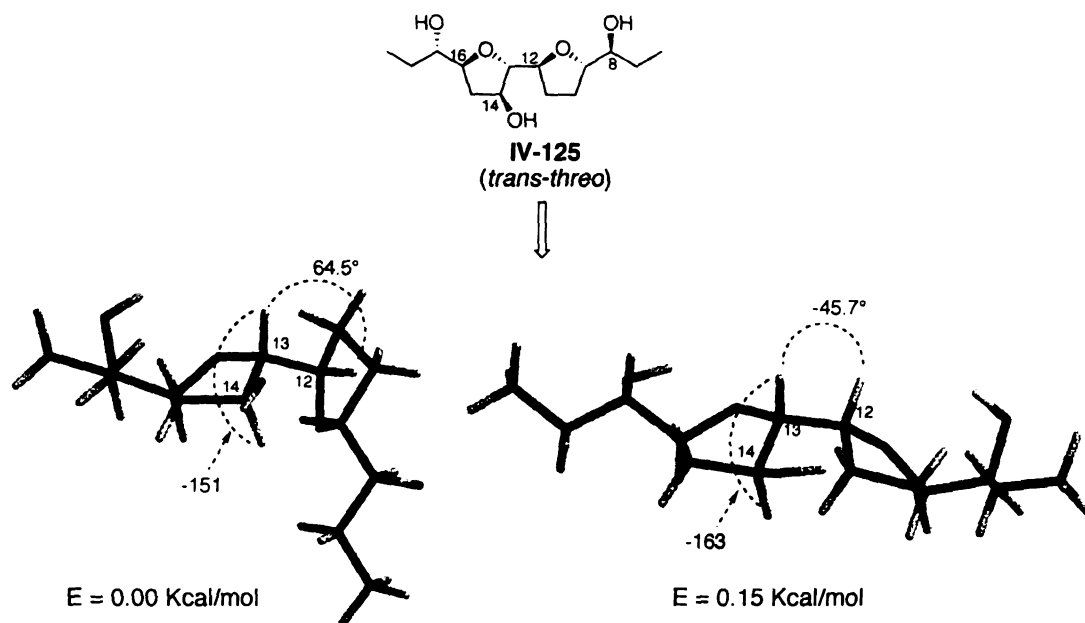
Figure IV-26: Low energy conformations of *cis-erythro* isomer **IV-124**

solvent due to the possibility of hydrogen bonding. Thus, it is conceivable that the intramolecular hydrogen bond between the C14-OH and the THF oxygen (Figure IV-22) is broken in CD_3OD , thereby allowing free rotation about the C_{12} - C_{13} bond. In this case, the molecule is capable of attaining a conformation with a large value for θ_{12-13} ($\sim 152^\circ$)

which corresponds to $J = 7.3$ Hz. In our conformational analysis, only **IV-124** was found to possess low energy conformations (set A) that would fit these observations. Conversely in **IV-123**, θ_{12-13} is close to 65° ($J = 1.9$ Hz) in all of the low energy conformations, which would not fit the observed coupling constant in CD_3OD .

From the above conformational analysis of **IV-123** and **IV-124**, it can be stated that the 3 Hz coupling constant may be maintained between H_{12} and H_{13} , irrespective of the *threo/erythro* relation between the two THFs. Thus, the possibility that the two rings may be *erythro* cannot be ruled out just based on the observed coupling constants. Certainly, such modeling studies are not reliable to decisively assign configurations of unknown stereocenters without experimental evidence, but the analysis definitely suggests a viable alternative to the originally proposed structure of mucoxin.

The C13-C14 *trans* diastereomers **IV-125** and **IV-126** were analyzed along similar lines. In case of the *trans-threo* isomer **IV-125**, low energy conformations can again be divided into two sets based on θ_{12-13} values (Figure IV-27). $\theta_{12-13} = 65^\circ$ corresponds to $J = 1.9$ Hz while $\theta_{12-13} = 45^\circ$ corresponds to $J = 4.0$ Hz according to the Karplus plot (Figure IV-25). However, the θ_{13-14} values in the two sets of conformations are -151° and -163° which would give coupling constants of about 6.8 Hz and 7.8 Hz respectively. Thus, because the estimated *trans* H_{13} - H_{14} coupling constants greatly deviate from the observed value (3 Hz), *trans-threo* isomer **IV-125** is not considered as a valid alternative stereoisomer.

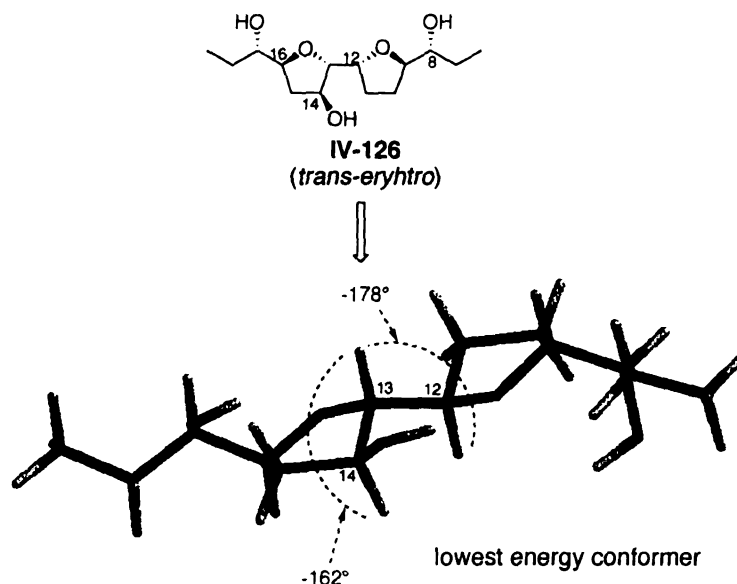


Conformation	Relative energy (Kcal/mol)	OH—O ^a Distance (Å)	θ_{13-14} (degrees) ^b	θ_{12-13} (degrees) ^c
1	0.00	4.61	-151	64.5
2	0.03	4.54	-153	63.9
3	0.15	2.18	-163	-45.7
4	0.22	4.52	-155	63.2
5	0.30	4.65	-148	65.6
6	0.32	4.65	-147	64.6
7	0.33	4.61	-151	64.2
8	0.48	2.19	-162	-45.7
9	0.53	4.53	-154	63.3
10	0.55	4.53	-155	63.3
11	0.60	4.66	-146	64.9
12	0.64	2.22	-162.5	-46.7
13	0.79	2.18	-162.8	-45.8
14	0.85	4.53	-154.5	63.4
15	0.88	2.18	-162.5	-45.6
16	0.91	4.73	-142.4	64.6
17	0.97	2.22	-162.4	-46.7

^a distance between C14-OH and C9-C12 THF oxygen. ^b $H_{13}-H_{14}$ dihedral angle. ^c $H_{12}-H_{13}$ dihedral angle.

Figure IV-27: Low energy conformations of *trans-threo* isomer IV-125

In the case of *trans-erythro* isomer **IV-126**, all the low energy conformations were found to have large dihedral angles (Figure IV-28). The estimated coupling constants, viz., 9 Hz ($\theta_{12-13} = 178^\circ$) and 7.8 Hz ($\theta_{13-14} = 162^\circ$) do not match the observed value of 3 Hz. Thus, **IV-126** is also not considered a viable option.



Conformation	Relative energy (Kcal/mol)	OH—O ^a Distance (Å)	θ_{13-14} (degrees) ^b	θ_{12-13} (degrees) ^c
1	0.00	2.20	-162	-178
2	0.34	2.20	-162	-178
3	0.37	2.23	-161	-178
4	0.69	2.23	-162	-178
5	0.71	2.23	-161	-178
6	0.78	2.20	-162	-178
7	1.03	2.23	-161	-178
8	1.07	2.20	-162	-178
9	1.34	2.23	-162	-178
10	1.51	2.24	-161	-178
11	1.83	2.23	-161	-178

^a distance between C14-OH and C9-C12 THF oxygen. ^b H_{13} - H_{14} dihedral angle. ^c H_{12} - H_{13} dihedral angle.

Figure IV-28: Low energy conformations of *trans-erythro* isomer **IV-126**

Interestingly, during the total synthesis of another nonclassical acetogenin – jimenezin⁸¹ (Figure IV-29), it was found that in the original proposed structure (**IV-127** containing 19- α -H) the relative stereochemistry between the two rings was incorrectly assigned. Diastereomer **IV-126** (containing 19- β -H) was found to match the reported spectra of natural jimenezin rather than **IV-125**.

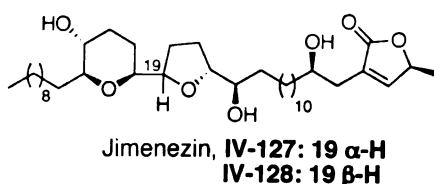


Figure IV-29: Jimenezin: proposed structure (**IV-125**) vs. real structure (**IV-126**)

Finally, based on X-ray crystal structures of previously known related acetogenins⁷⁸, McLaughlin has suggested that both the hydroxyl groups (C8 and C17) flanking the bis-THF unit must be *threo* to the ring system (**IV-119**, Figure IV-17) in mucoxin.

From all the above analysis, we propose **IV-129** and its C8-C17 enantiomer **IV-130** (Figure IV-30) as valid alternatives to the originally proposed structure (**IV-119** Figure IV-17) of natural mucoxin. Both the THFs in **IV-129** and **IV-130** are 2,5 *trans* and therefore are not expected to show any NOESY correlations across the rings. Also, H₁₃ and H₁₄ being *syn* oriented should have the observed 3 Hz coupling constant. Finally, as discussed above, we believe that the *threo* vs. *erythro* relationship between the two rings is inconsequential for maintaining the 3 Hz coupling constant between H₁₂ and H₁₃. Thus, both structures **IV-129** and **IV-130** are consistent with the experimental spectroscopic data for mucoxin.

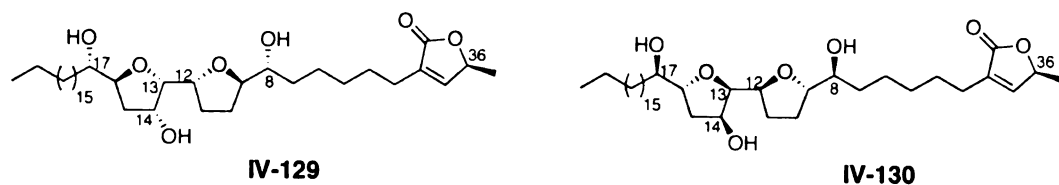
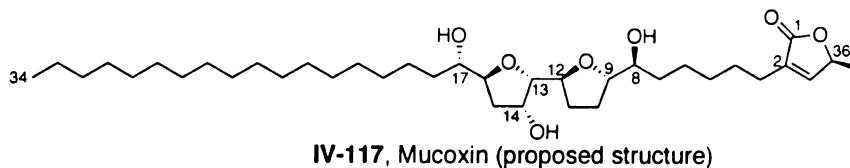


Figure IV-30: Possible alternative structure of mucoxin

In conclusion, total synthesis of the proposed structure of mucoxin (**IV-117**) has been accomplished in 32 steps (26 steps along the longest linear sequence).



Figures IV-31 and IV-32 depict the final synthetic scheme. The key transformations are described below. The trisubstituted hydroxy THF portion (C12-C34) was synthesized in the form of aldehyde **IV-86** (Figure IV-31). The THF core of **IV-86**

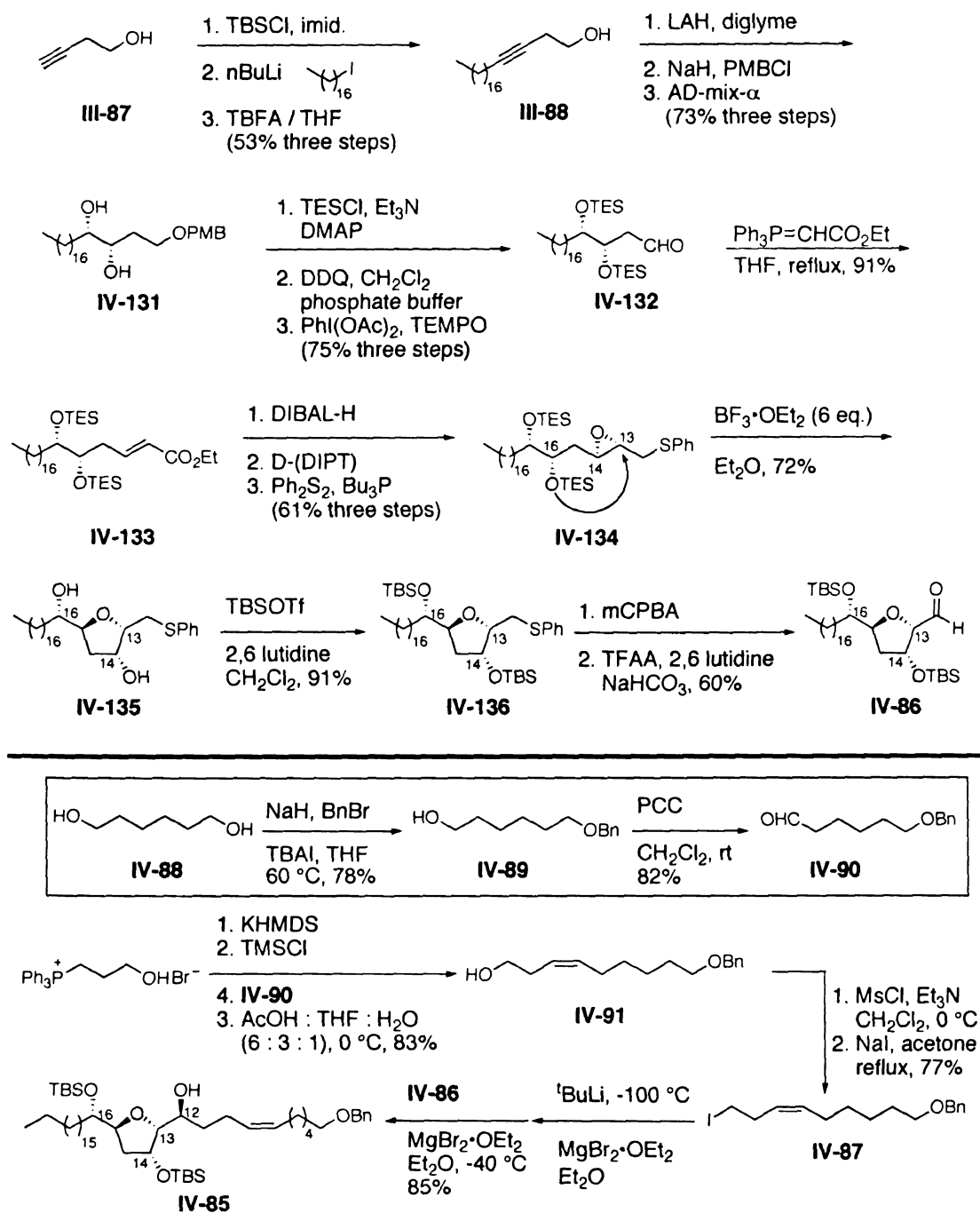


Figure IV-31: Synthesis of hydroxy THF (C12-C34) portion and its union with iodide

IV-87 *via* chelation controlled addition

was assembled using the method developed earlier (Chapters I and III) *via endo* selective cyclization of epoxy sulfide **IV-134**. The cyclization involved net retention of

configuration at C13, which provided the requisite C13-C14 *cis* relative configuration. Pummerer rearrangement of the cyclized product (**IV-136**) afforded aldehyde **IV-86**. **IV-86** was then combined with iodide **IV-87** by way of chelation controlled addition of the corresponding Grignard derivative to furnish adduct **IV-85** in high yield and diastereoselectivity.

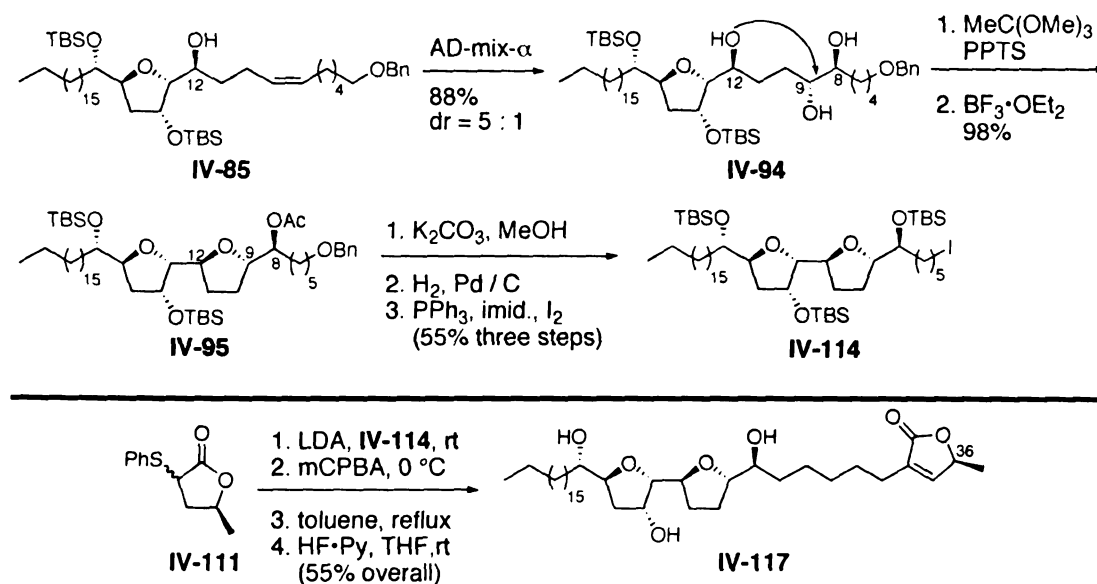


Figure IV-32: Completion of the total synthesis

Sharpless asymmetric dihydroxylation of **IV-85** (Figure IV-32) afforded the requisite triol **IV-94** in high yield (88%), albeit in modest diastereomeric ratio. However, the 5 : 1 ratio was acceptable to us since the desired isomer **IV-94** was easily separable from the minor diastereomer by flash column chromatography and could be isolated in good (73%) yield.

In order to install the di-substituted THF (C8-C12) a novel triol cyclization method was developed. Triol **IV-94** was converted to bis-THF **IV-95** in a single transformation involving generation and intramolecular trapping of acetoxonium ion of the vicinal diol functionality. This triol cyclization proved highly efficient (98% yield)

and the desired bis-THF was obtained in a completely regio- and stereoselective manner. Further investigations to expand the scope of this methodology are being pursued by another graduate student in our laboratory. The two step protocol involving sequential asymmetric dihydroxylation and triol cyclization to transform bis-homoallylic alcohol such as **IV-85** to bis-THF **IV-95** is more efficient and versatile (in terms of yields and potentially accessible stereoisomers) than traditional vanadium catalyzed directed epoxidation / cyclization route. Finally, the terminal butenolide was introduced using known α -SPh lactone **IV-111**.

^1H and ^{13}C NMR spectra of synthetic product **IV-117** differed from that of those of natural mucoxin. Based on the reported COSY and HRMS analysis of the natural sample and our own COSY experiments on synthetic **IV-117**, we believe that constitutionally, the structures of synthetic and natural mucoxin are identical. Therefore, it was reasoned that the discrepancies in the spectra are most likely due to stereochemical mismatches. In our total synthesis, all the stereocenters were established using either highly reliable asymmetric reactions, viz., Sharpless asymmetric epoxidation and

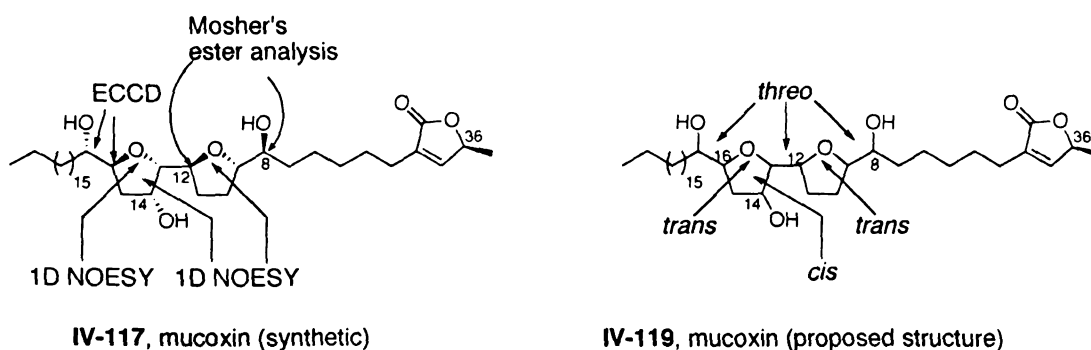


Figure IV-33: Summary of structure proof of synthetic material (**IV-117**)

dihydroxylation or well preceded transformations such as chelation controlled organometallic addition and intramolecular epoxide opening whose stereochemical

outcomes are definitively predictable. Moreover as shown in Figure IV-33, configurations at all stereogenic centers have been independently confirmed using Mosher's ester analysis, nOe correlations and ECCD techniques.

Therefore, we believe that the relative stereochemistry of **IV-117** exactly matches the proposed structure and that the differences in the synthetic vs. natural spectra are due to incorrect stereochemical assignment in the original proposed structure (**IV-119**, Figure IV-27). After closer examination of McLaughlin's reasoning in allocating the relative configuration, we feel that assignment of the *threo* relationship between the two THF rings, which was based on coupling constant between H₁₂ and H₁₃, is unconvincing. Accordingly, our modeling studies (MM2) indicate that *threo* or *erythro* relationship between the rings may be inconsequential to explain the observed coupling constant. Thus, we propose two alternative structures (**IV-129** and **IV-130**, Figure IV-30) containing *erythro* THFs, which also fit the reported spectroscopic data for natural mucoxin.

D. Experimental section

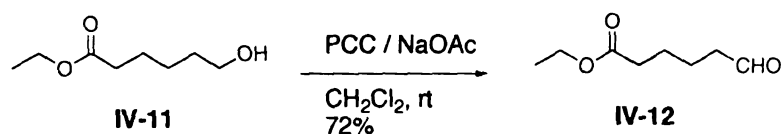
General Procedures

All reactions were carried out in flame-dried glassware under an atmosphere of dry nitrogen or argon. 4 Å molecular sieves were dried at 160 °C under vacuum prior to use. Unless otherwise mentioned, solvents were purified as follows. THF and Et₂O were either distilled from sodium benzophenone ketyl or used as is from a solvent purification

system. CH_2Cl_2 , toluene, CH_3CN and Et_3N were distilled from CaH_2 . DMF, diglyme, and DMSO were stored over 4 Å mol. sieves and distilled from CaH_2 . All other commercially available reagents and solvents were used as received.

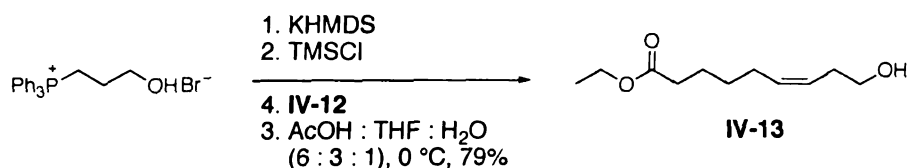
^1H NMR spectra were measured at 300, 500 or 600 MHz on a Varian Gemini-300, a Varian VXR-500 or a Varian Inova-600 instrument respectively. Chemical shifts are reported relative to residual solvent (δ 7.27, 2.50 and 4.80 ppm for CDCl_3 , $(\text{CD}_3)_2\text{SO}$ and CD_3OD respectively). ^{13}C NMR spectra were measured at 125 MHz on a Varian VXR-500 instrument. Chemical shifts are reported relative to the central line of CDCl_3 (δ 77.0 ppm). Infrared spectra were recorded using a Nicolet IR/42 spectrometer FT-IR (thin film, NaCl cells). High-resolution mass spectra were measured at the University of South Carolina, Mass Spectrometry Laboratory using micromass VG-70 s mass spectrometer. Optical rotations were measured on a Perkin–Elmer polarimeter (model 341) using a 1 mL capacity quartz cell with a 10 cm path length.

Analytical thin layer chromatography (TLC) was performed using Whatman glass plates coated with a 0.25 mm thickness of silica gel containing PF254 indicator, and compounds were visualized with UV light, potassium permanganate stain, *p*-anisaldehyde stain, or phosphomolybdic acid in EtOH. Chromatographic purifications were performed using Silicycle 60 Å, 35–75 μm silica gel. All compounds purified by chromatography were sufficiently pure for use in further experiments, unless indicated otherwise. GC analysis was performed using HP (6890 series) GC system containing Altech SE-54, 30 m x 320 mm x 0.25 mm column. Analytical and semi-preparative HPLC normal phase separations were performed using HP 1100 series HPLC system.



To a suspension of PCC (22.9 g, 0.11 mol) and sodium acetate (2.4 g, 0.03 mol) in CH_2Cl_2 (100 mL), was added a solution of ethyl 6-hydroxyhexanoate **IV-11** (9.85 g, 0.06 mol) in CH_2Cl_2 (24 mL) at room temperature. After 2 h, the reaction was diluted with Et_2O (150 mL) and filtered through a Celite pad. The filtrate was concentrated under reduced pressure and the crude material was purified by column chromatography (5% EtOAc in hexanes) to afford aldehyde **IV-12** (6.83 g, 72%). Spectroscopic data for **IV-12** was found to be identical to that reported previously.⁵⁵

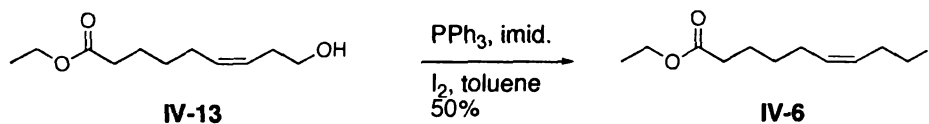
Partial data for **IV-12**: ^1H NMR (500 MHz, CDCl_3) δ 9.76 (t, $J = 1.7$ Hz, 1 H), 4.11 (q, $J = 7.1$ Hz, 1 H), 2.48-2.43 (m, 2 H), 2.36-2.08 (m, 2 H), 1.69-1.63 (m, 4 H), 1.24 (t, $J = 7.3$ Hz, 3 H); ^{13}C NMR (125 MHz, CDCl_3) δ 202.4, 173.5, 60.6, 43.7, 34.2, 24.5, 21.7, 14.5.



KHMDs (57 mL of 0.5 M solution in toluene, 28.5 mmol) was added to a -20 $^\circ\text{C}$ slurry of 3-hydroxypropyltriphenylphosphonium bromide (5.72 g, 14.25 mmol) in THF (30 mL). The mixture was brought to room temperature and stirred for 1 h. After cooling back to 0 $^\circ\text{C}$, TMSCl (1.34 mL, 10.5 mmol) was added and stirring was continued at the same temperature for 15 min. The reaction was then cooled to -78 $^\circ\text{C}$ upon which a THF solution of aldehyde **IV-12** (1.5 g, 9.5 mmol in 20 mL) was added. The reaction was

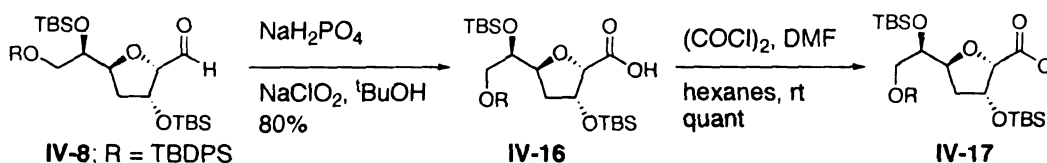
warmed to $-10\text{ }^{\circ}\text{C}$ over 1 h and then treated with AcOH : H₂O : THF (6 : 3 : 1, 100 mL). After being stirred at room temperature for 15 h, the reaction mixture was neutralized by saturated NaHCO₃. The aqueous layer was extracted with EtOAc (3x 200 mL), combined organic layers were dried over Na₂SO₄, concentrated and purified by column chromatography (20%-10% EtOAc in hexanes) to secure the homoallylic alcohol **IV-13** (1.5 g, 79% *Z* : *E* > 10 : 1).

Partial data for **IV-13**: ¹H NMR (500 MHz, CDCl₃) δ 5.50-5.44 (m, 1 H), 5.39-5.27 (m, 1 H), 4.08 (q, *J* = 7.0 Hz, 2 H), 3.59 (t, *J* = 6.7 Hz, 2 H), 3.40 (s(br), 1 H), 2.31-2.23 (m, 4 H), 2.08-2.00 (m, 2 H), 1.65-1.55 (m, 2 H), 1.40-1.33 (m, 2 H), 1.21 (t, *J* = 7.2 Hz, 3 H); ¹³C NMR (125 MHz, CDCl₃) δ 174.05, 132.5, 125.9, 62.4, 60.5, 34.4, 31.0, 29.3, 27.1, 24.7, 14.4.



To a solution of alcohol **IV-13** (580 mg, 2.90 mmol) in toluene (20 mL), triphenyl phosphine (1.91 g, 7.28 mmol), imidazole (500 mg, 7.34 mmol) and iodine (1.47 g, 5.79 mmol) were added at room temperature. After 30 min, saturated sodium sulfite solution was added to the yellowish brown mixture until it turned colorless. Layers were separated, the aqueous layer was extracted with EtOAc (3x20 mL), and the combined organic layers were dried (Na₂SO₄) and concentrated. Upon purification by column chromatography (2% EtOAc in hexanes), iodide **IV-6** was isolated in 50% yield (450 mg).

Partial data for **IV-6**: ^1H NMR (500 MHz, CDCl_3) δ 5.52-5.48 (m, 1 H), 5.35-5.31 (m, 1 H), 4.11 (q, $J = 7.1$ Hz, 2 H), 3.12 (t, $J = 7.3$ Hz, 2 H), 2.64-2.59 (m, 2 H), 2.29 (t, $J = 7.5$ Hz, 2 H), 2.06-2.02 (m, 2 H), 1.66-1.60 (m, 2 H), 1.43-1.37 (m, 2 H), 1.25 (t, $J = 6.4$ Hz, 3 H); ^{13}C NMR (125 MHz, CDCl_3) δ 173.8, 132.2, 128.5, 60.4, 34.4, 31.7, 29.2, 27.3, 24.8, 14.5, 5.5.

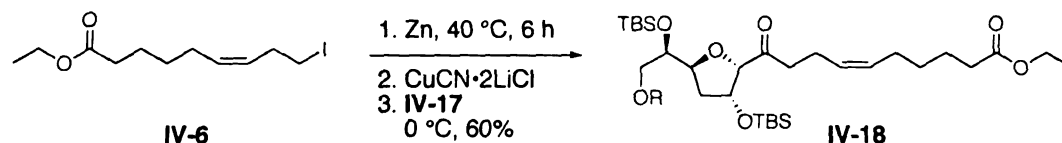


An aqueous solution of sodium chlorite (105 mg, 1.0 mmol) was added to a solution of aldehyde **IV-8** (200 mg, 0.32 mmol) in $^t\text{BuOH}$ (2.5 mL) followed by 0.75 mL of 2-methyl-1-butene in THF (2 M, 1.5 mmol). Monobasic sodium phosphate (95 mg, 0.5 mmol) was added in one portion upon which the solution turned yellow. After stirring for 17 h, volatiles were evaporated and the residue was taken up in CH_2Cl_2 . The salts were removed by filtration and crude acid **IV-16** was used without further purification. To a solution of **IV-16** (197 mg, 0.30 mmol) in hexanes (5 mL), oxalyl chloride (132 μL , 1.5 mmol) and DMF (26 μL , 0.30 mL) were added and the mixture was stirred at room temperature for 1 h. Supernatant liquid was separated from the solids and concentrated under reduced pressure. The crude acid chloride **IV-17** was dried under high vacuum (0.05 mm) and used without purification.

Partial data for **IV-16**: ^1H NMR (500 MHz, CDCl_3) δ 7.68-7.64 (m, 4 H), 7.47-7.36 (m, 6 H), 4.81-4.76 (m, 1 H), 4.67-4.62 (m, 1 H), 4.37 (d, $J = 3.3$ Hz, 1 H), 4.18-4.11 (m, 1 H), 3.57 (dd, $J = 4.7, 10.7$ Hz, 1 H), 3.40 (dd, $J = 7.1, 10.5$ Hz, 1 H), 2.37-2.22 (m, 1 H),

1.94-1.88 (m, 1 H), 1.05 (s, 9 H), 0.89 (s, 9 H), 0.82 (s, 9 H), 0.10 (s, 3 H), 0.08 (s, 3 H), -0.01 (s, 3 H), -0.08 (s, 3 H).

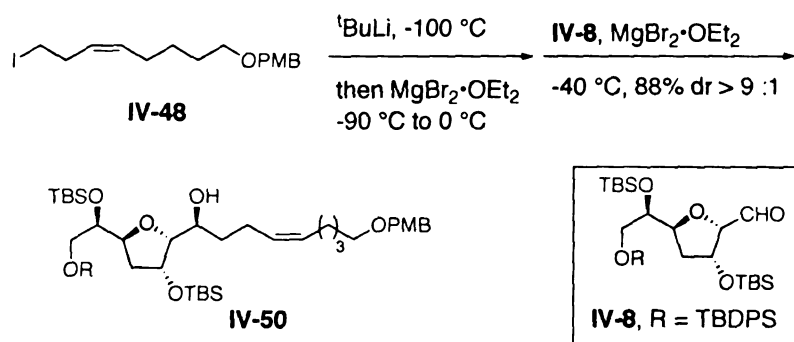
Partial data for **IV-17**: ^1H NMR (500 MHz, CDCl_3) δ 7.68-7.63 (m, 4 H), 7.45-7.27 (m, 6 H), 4.89-4.75 (m, 2 H), 4.74 (d, $J = 4.4$ Hz, 1 H), 4.08-4.05 (m, 1 H), 3.58 (dd, $J = 4.5$, 10.4 Hz, 1 H), 3.40 (dd, $J = 7.6$, 10.5 Hz, 1 H), 2.19-2.14 (m, 1 H), 1.95-1.91 (m, 1 H), 1.04 (s, 9 H), 0.90 (s, 9 H), 0.82 (s, 9 H), 0.13 (s, 3 H), 0.12 (s, 3 H), -0.01 (s, 3 H), -0.09 (s, 3 H); ^{13}C NMR (125 MHz, CDCl_3) δ 171.9, 135.8, 135.7, 133.4, 130.0, 127.9, 90.0, 82.6, 75.1, 72.4, 65.7, 34.2, 27.0, 26.0, 25.8, 19.4, 18.2, 18.1, 1.3, -4.3, -4.6, -4.7, -5.0.



A flask charged with Zn powder (55 mg, 0.84 mmol) was flame dried and flushed with Ar. THF (0.8 mL) and 1,2 dibromoethane (2.6 μL , 0.03 mmol) were added and the mixture was heated to 65 $^\circ\text{C}$ for 30 min. After cooling to room temperature, TMSCl , (3.1 μL , 0.02 mmol) was introduced and the mixture was heated back up to 40 $^\circ\text{C}$ for 15 min. Again after cooling to room temperature, a solution of iodide **IV-6** (130 mg, 0.42 mmol) in THF (0.5 mL) was added and the mixture was further heated to 40 $^\circ\text{C}$ for 6 h. The suspension of organozinc reagent so generated was allowed to settle at room temperature. In the mean time, a mixture of CuCN (38 mg, 0.42 mmol) and LiCl (36 mg, 0.84 mmol) was dissolved in THF (0.5 mL). After cooling the solution to -60°C , the organozinc reagent was cannulated into the $\text{CuCN}\cdot\text{2LiCl}$ complex. This mixture was warmed to 0 $^\circ\text{C}$, stirred for 45 min and cooled back to -25°C . Acid chloride **IV-17** (217 mg, 0.32 mmol) was added as a THF solution (0.5 mL) and the reaction was stirred overnight at 0 $^\circ\text{C}$.

was purified by column chromatography (20% EtOAc in hexanes) to afford alcohol **IV-27** as an inseparable mixture of diastereomers.

Partial data for **IV-27**: ^1H NMR (500 MHz, CDCl_3) δ 7.66-7.63 (m, 4 H), 7.44-7.36 (m, 6 H), 5.43-5.35 (m, 2 H), 4.61-4.44 (m, 3 H), 4.14-3.82 (m, 3 H), 3.67-3.54 (m, 2 H), 3.42-3.38 (m, 1 H), 2.31-2.07 (m, 6 H), 1.85-1.80 (m, 1 H), 1.67-1.58 (m, 3 H), 1.47-1.43 (m, 1 H), 1.41-1.37 (m, 3 H), 1.05 (s, 9 H), 0.85 (s, 9 H), 0.81 (s, 9 H), 0.06 (s, 3 H), 0.01 (s, 3 H), -0.05 (s, 3 H), -0.07 (s, 3 H); ^{13}C NMR (125 MHz, CDCl_3) δ 174.0, 163.1, 135.8, 135.7, 133.5, 130.5, 130.4, 130.3, 130.2, 130.0, 129.9, 129.8, 127.9, 84.5, 84.1, 79.3, 78.9, 75.6, 75.5, 74.7, 73.4, 73.1, 70.7, 65.9, 65.8, 60.4, 35.2, 34.5, 34.4, 34.2, 33.8, 33.6, 32.4, 29.9, 29.5, 29.4, 29.3, 29.0, 27.1, 27.0, 26.1, 26.0, 25.8, 24.9, 24.7, 23.8, 19.4, 18.2, 18.1, 14.5, -4.05, -4.21, -4.52, -4.62, -4.65, -4.79.



Preparation of 1.0 M solution of $\text{MgBr}_2 \cdot \text{OEt}_2$ in diethyl ether:⁵³

A two necked round bottom flask fitted with a reflux condenser was charged with Mg turnings (875 mg, 36 mmol) and a stir bar. After flame drying the flask under N_2 , Et_2O (30 mL) was added. 1,2 dibromoethane (2.6 mL, 30 mmol) was then added drop wise with gentle stirring upon which the solvent started refluxing slowly. When the addition was complete and refluxing ceased, the mixture was stirred for additional 1 h to

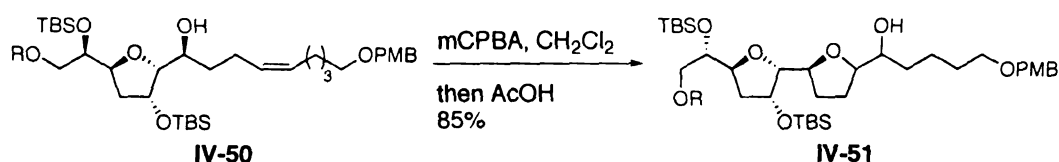
ensure completion of the $\text{MgBr}_2 \cdot \text{OEt}_2$ formation. The solution so prepared was used immediately.

$^t\text{BuLi}$ (4.0 mL of 1.3 M solution in pentane, 5.16 mmol) was added drop wise to pre-cooled ($-100\text{ }^\circ\text{C}$) Et_2O (9mL). To this, a solution of iodide **IV-48** (1.78 g, 4.97 mmol) in Et_2O (14 mL) was added over 10 min.* After stirring for 5 min at $-100\text{ }^\circ\text{C}$ to $-90\text{ }^\circ\text{C}$, $\text{MgBr}_2 \cdot \text{OEt}_2$ in Et_2O (5.2 mL of 1.0 M solution (freshly prepared as described above), was added and the mixture was warmed $0\text{ }^\circ\text{C}$ over 1 h. Meanwhile, a solution of aldehyde **IV-8** (660 mg, 1.03 mmol) in Et_2O (9 mL) was cooled to $-40\text{ }^\circ\text{C}$. $\text{MgBr}_2 \cdot \text{OEt}_2$ in Et_2O (3.9 mL of 1.0 M solution, 3.9 mmol) was added and stirred for 10 min. To this pre-complexed aldehyde, solution of the above mentioned Grignard reagent was cannulated at $-40\text{ }^\circ\text{C}$ and stirred overnight at the same temperature. The reaction was then quenched by slow addition of saturated NH_4Cl solution (10 mL) and H_2O (20 mL). The aqueous layer was extracted with Et_2O (3x100 mL). Combined organic layers were dried (Na_2SO_4), concentrated under reduced pressure to afford a yellow oil. Purification by column chromatography (2% EtOAc in hexanes) furnished the adduct **IV-50** (808 mg, 88%) as a single diastereomer.

Partial data for **IV-50**: ^1H NMR (500 MHz, CDCl_3) δ 7.67-7.64 (m, 4 H), 7.44-7.35 (m, 6 H), 7.26-7.24 (m, 2 H), 6.89-6.86 (m, 2 H), 5.40-5.35 (m, 2 H), 4.61-4.57 (m, 1 H), 4.44-4.42 (m, 2 H), 4.43 (s, 2 H), 4.06-4.04 (m, 1 H), 3.86-3.82 (m, 1 H), 3.80 (s, 3 H), 3.66 (t, $J = 4.0\text{ Hz}$, 1 H), 3.57 (dd, $J = 4.9, 10.4\text{ Hz}$, 1 H), 3.45 (t, $J = 6.6\text{ Hz}$, 2 H), 2.27-2.07 (m,

* Iodide **IV-48** was prepared using the same procedure as for iodide **IV-87**, which is described later in this section.

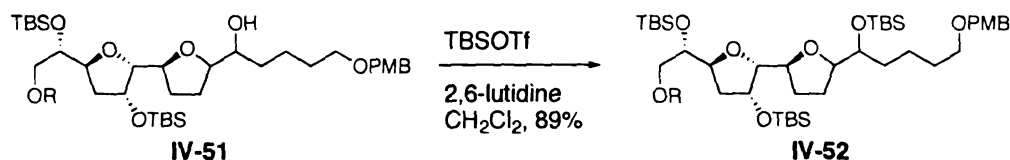
3 H), 1.86-1.82 (m, 1 H), 1.65-1.42 (m, 3 H), 1.21 (t, $J = 7.0$ Hz, 2 H), 0.90 (s, 9 H), 0.70 (s, 9 H), 0.60 (s, 9 H), -0.09 (s, 3 H), -0.11 (s, 3 H), -0.12 (s, 3 H), -0.23 (s, 3 H); ^{13}C NMR (125 MHz, CDCl_3) δ 158.8, 135.3, 133.0, 130.0, 129.7, 129.5, 129.3, 129.0, 127.5, 120.1, 113.5, 100.1, 84.0, 78.8, 75.2, 72.6, 72.3, 70.2, 69.8, 65.4, 55.0, 34.7, 33.3, 29.2, 27.3, 26.8, 26.5, 26.1, 25.6, 25.5, 23.3, 18.9, 17.7, 17.6, -4.7, -5.0, -5.1, -5.3; IR (thin film) 2953, 2930, 2858, 1514, 1429, 1361, 1250, 1151, 1113, 1076, 1007, 835, 777, 702 cm^{-1} .



mCPBA (172 mg, 1.00 mmol) in CH_2Cl_2 (9 mL) was added to a CH_2Cl_2 solution of hydroxy alkene **IV-50** (430 mg, 0.48 mmol in 9 mL) and the reaction was stirred at room temperature for 30 min. 10 mL glacial acetic was then added and after 10 h, the reaction was quenched by saturated NaHCO_3 solution (15 mL). Upon separation of the layers, the aqueous layer was extracted with CH_2Cl_2 (3x15 mL), combined organic layers were dried, concentrated and the crude material was purified by column chromatography (20% EtOAc in hexanes) to afford bis-THF **IV-51** as an inseparable mixture of diastereomers (ca. 1 : 1 ratio).

Partial data for **IV-51**: ^1H NMR (500 MHz, CDCl_3) δ 7.50-7.48 (m, 4 H), 7.29-7.21 (m, 6 H), 7.11 (d, $J = 8.5$ Hz, 2 H), 6.72 (d, $J = 8.7$ Hz, 2 H), 4.56-4.53 (m, 1 H), 4.27 (s, 2 H), 4.18-3.96 (m, 3 H), 3.66-3.62 (m, 1 H), 3.64 (s, 3 H), 3.60-3.45 (m, 1 H), 3.40-3.18 (m, 5 H), 2.00-1.30 (m, 12 H), 0.90 (s, 9 H), 0.70 (s, 9 H), 0.60 (s, 9 H), -0.09 (s, 3 H), -0.11 (s, 3 H), -0.12 (s, 3 H), -0.23 (s, 3 H); ^{13}C NMR (125 MHz, CDCl_3) δ 158.8, 135.3, 133.1,

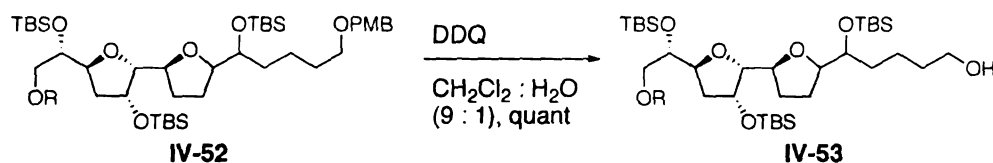
133.0, 130.5, 129.5, 129.4, 129.0, 127.4, 120.2, 113.5, 85.3, 82.1, 79.2, 78.9, 74.0, 73.7, 73.4, 72.5, 72.3, 69.9, 65.2, 55.0, 53.9, 47.3, 33.7, 33.5, 29.6, 29.5, 28.0, 27.9, 27.7, 26.5, 25.6, 25.4, 22.2, 18.8, 17.8, 17.6, -4.3, -5.0, -5.1, -5.2; IR (thin film) 3583, 3470, 2932, 2859, 2256, 2968, 1887, 1818, 1718, 1605, 1514, 1429, 1361, 1250, 1151, 1072, 939, 910, 808, 734, 702 cm^{-1} .



To a 0 °C solution of alcohol **IV-51** (315 mg, 0.35 mmol) in CH_2Cl_2 (10 mL), 2,6-lutidine (0.28 mL, 2.43 mmol) and TBSOTf (0.24 mL, 1.04 mmol) were added in that order. After 30 min at the same temperature, saturated NaHCO_3 solution (5 mL) was added and the layers were separated. The aqueous layer was extracted with CH_2Cl_2 (3x15 mL), combined organic layers were dried over Na_2SO_4 , and concentrated under reduced pressure to afford a crude oil. Upon purification of the oil by column chromatography (1% EtOAc in hexanes), tris-TBS ether **IV-52** was obtained in 89% yield (323 mg).

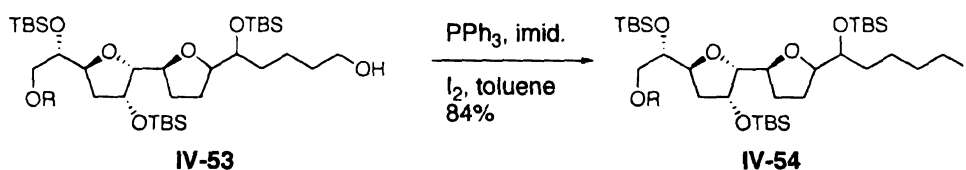
Partial data for **IV-52**: ^1H NMR (500 MHz, CDCl_3) δ 7.65-7.63 (m, 4 H), 7.44-7.35 (m, 6 H), 7.26-7.25 (m, 2 H), 6.88-6.86 (m, 2 H), 4.68-4.63 (m, 1 H), 4.42 (d, $J = 2.4$ Hz, 2 H), 4.32-4.30 (m, 1 H), 4.14-4.09 (m, 1 H), 4.00-3.92 (m, 2 H), 3.80 (s, 3 H), 3.76-3.72 (m, 1 H), 3.63 (dt, $J = 2.9, 8.8$ Hz, 1 H), 3.53-3.50 (m, 1 H), 3.45-3.34 (m, 3 H), 2.17-1.24 (m, 12 H), 0.88 (s, 9 H), 0.86 (s, 9 H), 0.80 (s, 9 H), 0.78 (s, 9 H), 0.10-0.05 (m, 18 H); ^{13}C NMR (125 MHz, CDCl_3) δ 159.2, 135.8, 133.7, 133.5, 131.1, 129.9, 129.8, 129.4, 129.3, 127.9, 127.8, 113.9, 86.8, 85.3, 81.1, 81.0, 79.8, 79.6, 79.3, 79.1, 74.3, 74.1, 73.9, 73.8, 73.3, 72.8, 72.7, 72.6, 70.6, 70.5, 65.9, 65.8, 55.5, 34.4, 34.3, 31.5, 31.4, 30.6, 30.3, 30.2,

29.9, 28.5, 28.0, 27.0, 26.9, 26.8, 26.3, 26.2, 26.1, 26.0, 25.9, 25.8, 23.0, 19.3, 19.2, 18.4, 18.3, 18.2, 18.1, 18.0, -2.7, -3.7, -3.8, -4.0, -4.1, -4.3, -4.4, -4.5, -4.7, -4.8, -4.9.



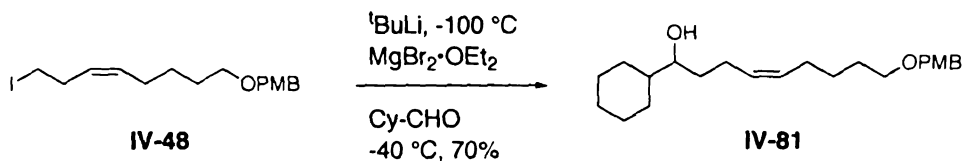
DDQ (94 mg, 0.41 mmol) was added to a solution of PMB ether **IV-52** (330 mg, 0.32 mmol) in 10% wet chloroform (7.1 mL) and the mixture was stirred for 30 min at 0 °C. The reaction was then poured into saturated NaHCO_3 solution (5 mL), layers were separated and the aqueous layer was extracted with CH_2Cl_2 (3x10 mL). Combined organic layers were dried (Na_2SO_4), concentrated and the crude product was purified by column chromatography (5% EtOAc in hexanes) to furnish alcohol **IV-53** as a colorless oil (287 mg, quant.).

Partial data for **IV-53**: ^1H NMR (500 MHz, CDCl_3) δ 7.66-7.63 (m, 4 H), 7.41-7.34 (m, 6 H), 4.67-4.60 (m, 1 H), 4.33-4.23 (m, 1 H), 4.13-4.01 (m, 1 H), 3.98-3.88 (m, 1 H), 3.74-3.72 (m, 2 H), 3.68-3.62 (m, 1 H), 3.62 (t, $J = 6.0$ Hz, 2 H), 3.53-3.46 (m, 1 H), 3.37-3.34 (m, 1 H), 2.19-1.18 (m, 12 H), 1.01-0.09 (m, 36 H), 0.05-0.08 (m, 18 H); ^{13}C NMR (125 MHz, CDCl_3) δ 135.8, 133.7, 133.6, 133.5, 132.2, 129.9, 129.8, 127.9, 127.8, 114.5, 86.8, 85.3, 81.1, 81.0, 79.8, 79.6, 79.3, 79.2, 74.3, 74.0, 73.9, 66.1, 65.9, 65.8, 63.2, 63.1, 55.8, 34.4, 34.3, 33.3, 33.2, 31.8, 31.5, 31.4, 29.9, 28.6, 28.1, 27.0, 26.4, 26.3, 26.2, 26.1, 26.0, 25.9, 25.8, 25.7, 22.9, 22.4, 19.3, 18.4, 18.3, 18.2, 18.1, 18.0, 15.5, 14.3, -3.8, -3.9, -4.0, -4.1, -4.2, -4.3, -4.5, -4.7, -4.8, -4.9; IR (thin film) 3441, 3073, 2955, 2893, 2853, 1911, 1887, 1822, 1701, 1601, 1512, 1471, 1429, 1362, 1257, 1113, 1074, 1005, 939, 885, 775, 702 cm^{-1} .



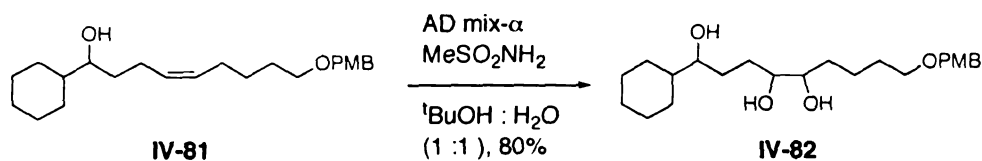
To a solution of alcohol **IV-53** (260 mg, 0.29 mmol) in toluene (10 mL), triphenyl phosphine (192 mg, 0.73 mmol), imidazole (52 mg, 0.73 mmol) and iodine (160 mg, 0.57 mmol) were added at room temperature. After 30 min, saturated sodium sulfite solution was added to the yellowish brown mixture until it turned colorless. Layers were separated, the aqueous layer was extracted with EtOAc (3x10 mL), combined organic layers were dried (Na_2SO_4) and concentrated. Upon purification by column chromatography (2% EtOAc in hexanes), iodide **IV-54** was isolated in 84% yield (253 mg).

Partial data for **IV-54**: ^1H NMR (500 MHz, CDCl_3) δ 7.66-7.64 (m, 4 H), 7.43-7.36 (m, 6 H), 4.70-4.64 (m, 1 H), 4.33-4.31 (m, 1 H), 4.14-4.10 (m, 1 H), 4.03-3.92 (m, 2 H), 3.76-3.75 (m, 1 H), 3.65 (dt, $J = 2.9, 7.5$ Hz, 1 H), 3.54-3.50 (m, 1 H), 3.39-3.35 (m, 1 H), 3.21-3.16 (m, 2 H), 2.19-1.77 (m, 6 H), 1.63-1.53 (m, 3 H), 1.44-1.26 (m, 3 H), 1.01 (s, 9 H), 0.89 (s, 9 H), 0.81 (s, 9 H), 0.10-0.04 (m, 18 H); ^{13}C NMR (125 MHz, CDCl_3) δ 135.8, 133.6, 133.5, 133.4, 129.9, 129.8, 128.0, 127.9, 86.8, 85.3, 81.0, 79.8, 79.6, 79.3, 79.2, 74.3, 73.9, 73.8, 73.5, 73.3, 72.8, 65.8, 65.7, 34.4, 34.3, 34.2, 34.1, 30.5, 30.3, 28.5, 28.0, 27.6, 27.6, 27.0, 26.9, 26.3, 26.2, 26.1, 26.0, 25.9, 25.8, 19.4, 19.3, 18.4, 18.3, 18.2, 18.1, 18.0, 7.5, 7.3, -3.8, -3.9, -4.0, -4.1, -4.3, -4.5, -4.6, -4.7, -4.8; IR (thin film) 2955, 2930, 2856, 1471, 1429, 1361, 1253, 1113, 1074, 1005, 939, 835, 775, 702 cm^{-1} .



Alcohol **IV-81** was prepared using the same representative procedure as described above for **IV-50**. Thus, 1.14 g (3.04 mmol) of iodide **IV-48** afforded 766 mg (70%) of alcohol **IV-81**.

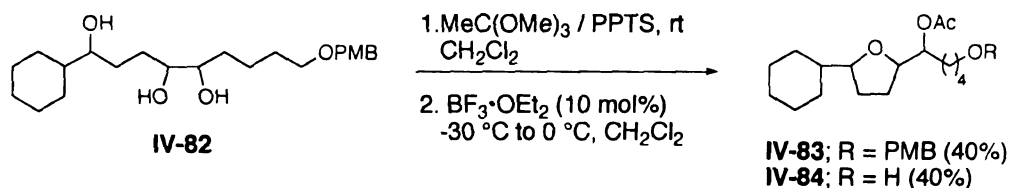
Partial data for **IV-81**: ^1H NMR (500 MHz, CDCl_3) δ 7.24 (d, $J = 8.8$ Hz, 2 H), 6.85 (d, $J = 8.6$ Hz, 2 H), 5.41-5.34 (m, 2 H), 4.40 (s, 2 H), 3.78 (s, 3 H), 3.44-3.32 (m, 3 H), 2.12-1.98 (m, 4 H), 1.78-0.99 (m, 17 H).



AD-mix- α (700 mg) was dissolved in 1 : 1 $^t\text{BuOH} : \text{H}_2\text{O}$ (5 mL). To this clear, orange solution, methane sulfonamide (47.5 mg, 0.50 mmol) and potassium osmate (1 mg) were added and stirred until all the solids dissolved. The solution was then cooled to 0 $^\circ\text{C}$ upon which olefin **IV-81** (180 mg, 0.50 mmol) was added in one portion. The reaction was vigorously stirred for 16 h after which solid sodium sulfite (750 mg) was then added at the same temperature. The mixture was warmed to room temperature and stirring was continued for 45 min. EtOAc (20 mL) and H_2O (5 mL) were added and the layers were separated. The aqueous layer was extracted with EtOAc (4x20 mL), combined organic layers were dried over Na_2SO_4 , concentrated and the crude product

was purified by column chromatography (EtOAc). Triol **I-82** was isolated in 80% yield (158 mg) as a colorless oil.

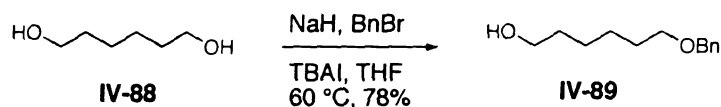
Partial data for **IV-82**: ^1H NMR (500 MHz, CDCl_3) δ 7.25 (d, J = 8.5 Hz, 2 H), 6.86 (d, J = 8.6 Hz, 2 H), 4.93-4.83 (m, 1 H), 4.41 (s, 2 H), 3.92-3.84 (m, 1 H), 3.80 (s, 3 H), 3.57-3.52 (m, 1 H), 2.06 (d, J = 12.1 Hz, 1 H), 1.92-0.87 (m, 20 H).



PPTS (0.5 mg, 1.98 μmol) was added to a solution of triol **IV-82** (80 mg, 0.20 mmol) and trimethylorthoacetate (33 μL , 0.22 mmol) in CH_2Cl_2 (1.5 mL) at 0 °C. After 1 h, the volatiles were removed under reduced pressure and the residue was taken up in CH_2Cl_2 (1 mL). Upon cooling this solution to -30 °C, $\text{BF}_3 \cdot \text{OEt}_2$ (2.7 μL , 0.02 mmol) was added and the reaction was warmed to 0 °C over 30 min. Saturated NaHCO_3 solution (2 mL) was slowly added, the layers were separated and the aqueous layer was extracted with CH_2Cl_2 (3x20 mL). Combined organic layers were dried (Na_2SO_4), concentrated under reduced pressure and the crude product was purified by flash column chromatography (2% EtOAc in hexanes) to furnish cyclized products **IV-83** (35 mg, 40%) and **IV-84** (25 mg, 40%).

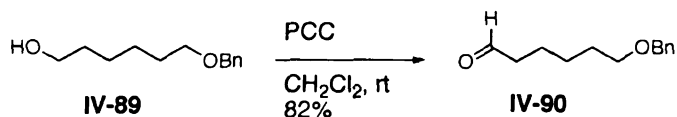
Partial data for **IV-83**: ^1H NMR (500 MHz, CDCl_3) δ 7.22 (d, J = 8.4 Hz, 2 H), 6.85 (d, J = 8.6 Hz, 2 H), 4.90-4.83 (m, 1 H), 4.39 (s, 2 H), 3.91-3.83 (m, 1 H), 3.78 (s, 3 H), 3.57-3.50 (m, 1 H), 3.40 (t, J = 6.4, 2 H), 2.05 (s, 3 H), 1.92-1.80 (m, 3 H), 1.70-1.52 (m, 10 H), 1.40-1.32 (m, 3 H), 1.28-1.15 (m, 4 H), 0.08-0.04 (m, 1 H); ^{13}C NMR (125 MHz,

CDCl₃) δ 171.1, 79.9, 79.8, 75.6, 75.4, 68.5, 68.4, 68.3, 31.9, 31.3, 28.1, 26.1, 25.2, 22.7, 21.4, 21.3, 14.2, 14.1,



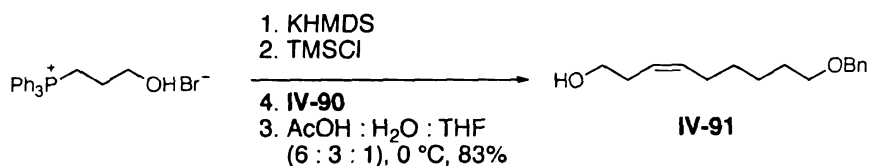
To a slurry of NaH (7 g, 0.18 mol) in THF (300 mL), 1,6 hexanediol **IV-88** (20 g, 0.17 mol) was added at 0 °C and stirred for 1 h while warming to rt. Benzyl bromide (20 mL, 0.17 mmol) was added drop wise followed by TBAI (2.6 g). The reaction was heated to 60 °C for 15 h. After cooling to room temperature H₂O (150 mL) was carefully added. The layers were separated, aqueous layer was extracted with Et₂O (3x300 mL) and the combined organic layers after drying (MgSO₄) were concentrated. Monobenzyl ether **IV-89** was obtained as clear oil (35.4 g, 78%) after chromatographic purification (30% EtOAc in hexanes). This material was spectroscopically identical to a previously reported compound.⁸²

Data for **IV-89**: ¹H NMR (500 MHz, CDCl₃) δ 7.35-7.25 (m, 5 H), 4.50 (s, 2 H), 3.56 (t, J = 6.6 Hz, 2 H), 3.47 (t, J = 6.6 Hz, 2 H), 1.63 (quint, J = 6.6 Hz, 2 H), 1.54 (quint, J = 7.0 Hz, 2 H), 1.38-1.32 (m, 4 H); ¹³C NMR (125 MHz, CDCl₃) δ 138.8, 128.6, 127.9, 127.8, 73.1, 70.6, 62.8, 32.9, 29.9, 26.2, 25.9; IR (thin film) 3393, 3063, 2933, 2859, 1951, 1874, 1810, 1603, 1454, 1363, 1309, 1251, 1205, 1099, 1028, 909, 735, 675 cm⁻¹; HRMS (EI) calcd for C₁₃H₂₀O₂, 208.1458 m/z (M)⁺; observed, 208.1463 m/z .



To a slurry of PCC (31.6 g, 0.15 mol) in CH₂Cl₂ (300 mL), a solution of alcohol **IV-89** (20.4 g, 98.1 mmol) in CH₂Cl₂ (100 mL) was added at room temperature under N₂ with vigorous stirring. After 2 h, anhydrous Et₂O (400 mL) was added and the reaction mixture was filtered through a celite pad. The filtrate was concentrated and the crude brown oily material was purified by flash column chromatography (10% EtOAc in hexanes) to afford aldehyde **IV-90** as a clear liquid (16.6 g, 82%).

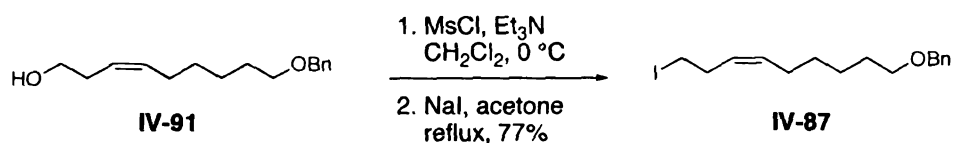
Data for **IV-90**: ¹H NMR (500 MHz, CDCl₃) δ 9.75 (t, *J* = 2.2 Hz, 1 H), 7.39-7.20 (m, 5 H), 4.49 (s, 2 H), 3.47 (t, *J* = 6.4, 2 H), 2.40-2.48 (m, 2 H), 1.72-1.61 (m, 4 H), 1.46-1.38 (m, 2 H); ¹³C NMR (125 MHz, CDCl₃) δ 202.8, 138.8, 128.6, 127.8, 127.7, 73.1, 70.2, 44.0, 29.7, 26.0, 22.1; IR (thin film) 3031, 2936, 2860, 2720, 1954, 1875, 1724, 1453, 1409, 1363, 1391, 1101, 1026, 906, 737, 703 cm⁻¹; HRMS (EI) calcd for C₁₃H₁₈O₂, 206.1307 *m/z* (M)⁺; observed, 206.1309 *m/z*.



KHMDs (175 mL of 0.5 M solution in toluene, 87.5 mmol) was added to a -20 °C slurry of 3-hydroxypropyltriphenylphosphonium bromide (17.6 g, 43.7 mmol) in THF (55 mL). The mixture was brought to room temperature and stirred for 1 h. After cooling back to 0 °C, TMSCl (5.8 mL, 43.7 mmol) was added and stirring was continued at the same temperature for 15 min. The reaction was then cooled to -78 °C upon which a THF solution of aldehyde **IV-90** (5 g, 24.3 mmol in 40 mL) was added. The reaction was warmed to -10 °C over 1 h and then treated with AcOH : H₂O : THF (6 : 3 : 1, 250 mL). After 15 h stirring at room temperature the reaction mixture was neutralized by saturated NaHCO₃.

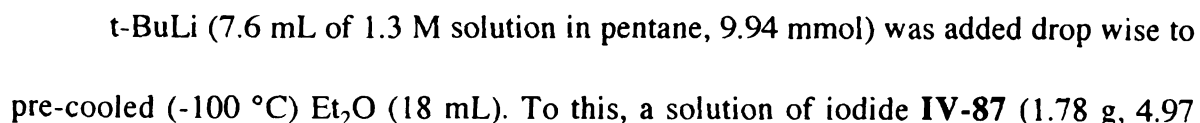
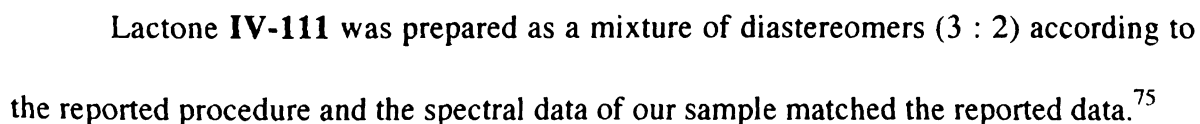
The aqueous layer was extracted with EtOAc (3x 400 mL), combined organic layers were dried over Na₂SO₄, concentrated and purified by column chromatography (10% EtOAc in hexanes) to secure the homoallylic alcohol **IV-91** (9 g, 83%). The sample contained < 5% of the *Z* isomer; however the exact ratio could not be determined due to overlapping signals in the ¹H NMR spectrum.

Data for **IV-91**: ¹H NMR (500 MHz, CDCl₃) δ 7.37-7.25 (m, 5 H), 5.55-5.51 (m, 1 H), 5.39-5.34 (m, 1 H), 4.50 (s, 2 H), 3.60 (t, *J* = 6.9 Hz, 2 H), 3.47 (t, *J* = 6.9 Hz, 2 H), 2.32-2.28 (m, 2 H), 2.08-2.04 (m, 3 H), 1.66-1.60 (m, 2 H), 1.42-1.37 (m, 4 H); ¹³C NMR (125 MHz, CDCl₃) δ 175.5, 138.8, 133.0, 128.6, 127.9, 127.7, 125.5, 73.1, 70.6, 62.4, 30.9, 29.8, 29.7, 27.5, 26.0, 20.9; IR (thin film) 3386, 3028, 2861, 2063, 1950, 1872, 1809, 1714, 1654, 1605, 1453, 1366, 1250, 1204, 1050, 872, 735, 695 cm⁻¹; HRMS (EI) calcd for C₁₆H₂₄O₂, 248.1776 *m/z* (M)⁺; observed, 248.1769 *m/z*.



A solution of alcohol **IV-91** (9.1 g, 36.7 mmol) in CH₂Cl₂ (140 mL) was cooled to 0 °C. To this, mesyl chloride (8.55 mL, 0.11 mol) and triethyl amine (17 mL) were added and stirring was continued at the same temperature for 30 min. The reaction was quenched with H₂O (100 mL). The aqueous layer was extracted with CH₂Cl₂ (3x200 mL) and combined organic layers were concentrated. The residue and sodium iodide (25 g, 0.17 mol) were taken up in acetone (150 mL) and refluxed for 2 h. Upon cooling to room temperature, the reaction was treated with saturated sodium sulfite until it became

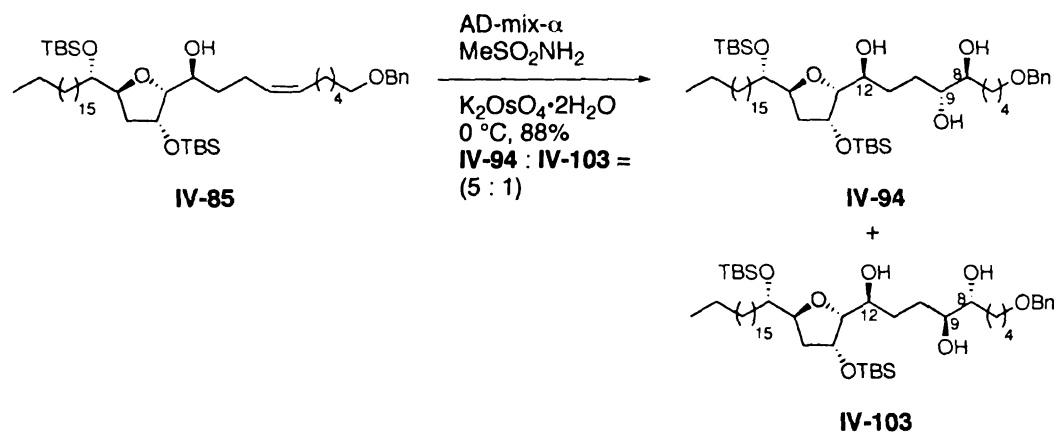
Data for **IV-87**: ^1H NMR (500 MHz, CDCl_3) δ 7.36-7.28 (m, 5 H), 5.55-5.52 (m, 1 H), 5.35-5.32 (m, 1 H), 4.52 (s, 2 H), 3.48 (t, $J = 6.6$ Hz, 2 H), 3.14 (t, $J = 7.3$ Hz, 2 H), 2.66-2.61 (m, 2 H), 2.06-2.04 (m, 2 H), 1.66-1.63 (m, 2 H), 1.42-1.39 (m, 4 H); ^{13}C NMR (125 MHz, CDCl_3) δ 138.9, 132.7, 128.6, 128.2, 127.9, 127.7, 73.1, 70.6, 31.8, 29.9, 29.6, 27.7, 26.1, 5.7; IR (thin film) 3028, 3009, 2932, 2855, 2791, 1920, 1850, 1790, 1495, 1454, 1361, 1242, 1169, 1105, 1028, 734, 698 cm^{-1} ; HRMS (EI) calcd for $\text{C}_{16}\text{H}_{23}\text{IO}$, 358.0794 m/z (M) $^+$; observed, 358.0800 m/z .



mmol) in Et₂O (14 mL) was added over 10 min. After stirring for 5 min at –100 °C to –90 °C, MgBr₂•OEt₂ in Et₂O (12.4 mL of 1.0 M solution (freshly prepared as described on page 288), was added and the mixture was warmed 0 °C over 1 h. Meanwhile, a solution of aldehyde **IV-86** (1 g, 1.63 mmol) in Et₂O (18 mL) was cooled to –40 °C. MgBr₂•OEt₂ in Et₂O (5.0 mL of 1.0 M solution, 5.0 mmol) was added and stirred for 10 min. To this pre-complexed aldehyde, solution of the above mentioned Grignard reagent was cannulated at –40 °C and the reaction mixture was stirred overnight at the same temperature. The reaction was then quenched by slow addition of saturated NH₄Cl solution (20 mL) and H₂O (50 mL). The aqueous layer was extracted with Et₂O (3x100 mL). Combined organic layers were dried (Na₂SO₄), concentrated under reduced pressure to afford a yellow oil. Purification by column chromatography (2% EtOAc in hexanes) furnished the adduct **I-85** (1.17 g, 85%) as a single diastereomer.

Data for **I-85**: $[\alpha]_D^{20}$ –17.1 (c 0.97, CHCl₃) ¹H NMR (500 MHz, CDCl₃) δ 7.33-7.25 (m, 5 H), 5.39-5.33 (m, 2 H), 4.52 (s, 2 H), 4.50-4.39 (m, 1 H), 4.25-4.21 (m, 1 H), 3.8 (dt, *J* = 4.3, 8.8 Hz, 1 H), 3.68-3.62 (m, 2 H), 3.46 (t, *J* = 6.6 Hz, 2 H), 2.96 (s (br), 1 H), 2.29-2.05 (m, 4 H), 1.88-1.86 (m, 2 H), 1.65-1.47 (m, 4 H), 1.38-1.23 (m, 36 H), 0.91 (s, 9 H), 0.90 (s, 9 H), 0.88 (t, *J* = 7.0 Hz, 3 H), 0.11 (s, 3 H), 0.10 (s, 3 H), 0.08 (s, 3 H), 0.06 (s, 3 H); ¹³C NMR (125 MHz, CDCl₃) δ 139.0, 130.3, 129.7, 128.5, 127.8, 127.6, 85.0, 80.5, 75.0, 74.6, 73.1, 70.7, 38.2, 33.4, 32.9, 30.1, 29.9, 29.8, 29.6, 27.4, 26.2, 26.1, 26.0, 25.8, 23.7, 22.9, 18.4, 18.1, 14.3, –4.0, –4.1, –4.3, –4.8; IR (thin film) 3596, 3521, 3031, 3004, 2928, 2856, 1464, 1406, 1389, 1362, 1256, 1190, 1076, 1005, 955, 939, 835, 808, 775,

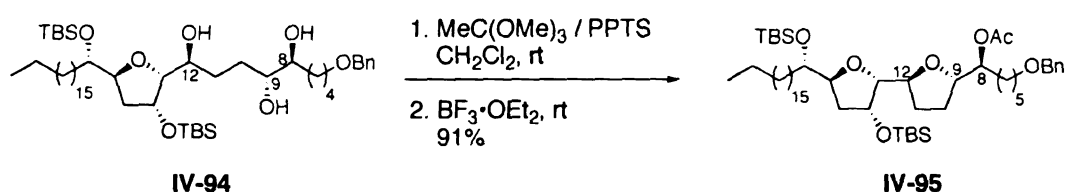
733, 696, 662 cm^{-1} ; HRMS (EI) calcd for $\text{C}_{51}\text{H}_{96}\text{O}_5\text{Si}_2$, 844.6796 m/z (M^+); observed, 844.6789 m/z .



AD-mix- α (1.26 g) was dissolved in 1 : 1 tBuOH : H_2O (13 mL). To this clear, orange solution, methane sulfonamide (86 mg, 0.9 mmol) and potassium osmate (19 mg) were added and stirred until all the solids dissolved. The solution was then cooled to $0\text{ }^\circ\text{C}$ upon which olefin **IV-85** (760 mg, 0.90 mmol) was added in one portion. The reaction was vigorously stirred for 16 h after which solid sodium sulfite (1.35 g) was then added at the same temperature. The mixture was warmed to room temperature and stirring was continued for 45 min. EtOAc (50 mL) and H_2O (20 mL) were added and the layers were separated. The aqueous layer was extracted with EtOAc (4x50 mL), combined organic layers were dried over Na_2SO_4 , concentrated and the crude product was purified by column chromatography (8% EtOAc in hexanes). The desired diastereomer **I-94** was isolated in 73% (577 mg) yield as a colorless oil.

Data for **I-94**: $[\alpha]_{\text{D}}^{20} -16.2$ (c 0.87, CHCl_3) ^1H NMR (500 MHz, CDCl_3) δ 7.33-7.24 (m, 5 H), 4.49 (s, 2 H), 4.42-4.41 (m, 1 H), 4.22-4.20 (m, 1 H), 3.88-3.87 (m, 1 H), 3.71-3.69 (m, 1 H), 3.64-3.58 (m 3 H), 3.47 (t, $J = 6.6$ Hz, 2 H), 3.23 (s (br), 1 H), 3.03 (s (br), 1 H), 1.88-1.86 (m 2 H), 1.68-1.22 (m, 44 H), 0.90 (s, 9 H), 0.89 (s, 9 H), 0.88 (t, $J = 7.0$

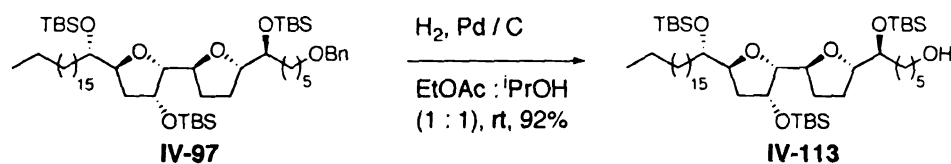
Hz, 3 H), 0.10 (s, 3 H), 0.09 (s, 3 H), 0.07 (s, 3 H) 0.06 (s, 3 H); ^{13}C NMR (125 MHz, CDCl_3) δ 138.9, 128.5, 127.8, 127.7, 85.0, 80.6, 74.9, 74.8, 74.5, 74.4, 73.1, 71.3, 70.6, 38.3, 32.9, 32.1, 31.9, 30.1, 29.9, 29.8, 29.6, 27.7, 26.5, 26.1, 25.9, 25.8, 22.9, 18.4, 18.1, 14.3, -4.0, -4.2, -4.3, -4.9; IR (thin film) 3596, 3521, 3031, 3004, 2928, 2856, 1464, 1406, 1389, 1362, 1256, 1190, 1076, 1005, 955, 939, 835, 808, 775, 733, 696, 662 cm^{-1} ; HRMS (ES) calcd for $\text{C}_{51}\text{H}_{98}\text{O}_7\text{Si}_2$, 879.6929 m/z ($\text{M}+\text{H}$) $^+$; observed, 879.6931 m/z .



PPTS (6 mg, 0.02 mmol) was added to a solution of triol **IV-94** (200 mg, 0.22 mmol) and trimethylortho acetate (36 μL , 0.23 mmol) in CH_2Cl_2 (3 mL) at rt. After complete consumption of the triol (ca. 5 min, as judged by TLC), a solution of $\text{BF}_3 \cdot \text{OEt}_2$ (8 μL , 0.06 mmol) in CH_2Cl_2 (1 mL) was rapidly added to the reaction. After 10 min, the reaction was slowly poured into saturated NaHCO_3 solution (5 mL) and the aqueous layer was extracted with CH_2Cl_2 (3x20 mL). Combined organic layers were dried (Na_2SO_4), concentrated under reduced pressure and the crude product was purified by flash column chromatography (2% EtOAc in hexanes) to furnish bis-THF acetate **IV-95** (187 mg, 91%) as a clear oil.

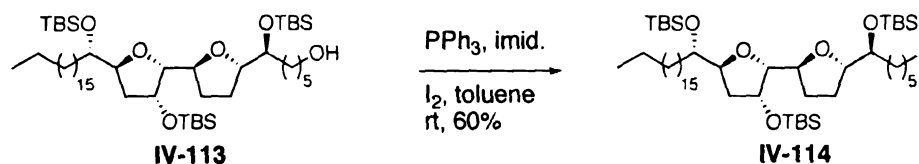
Data for **I-95**: $[\alpha]_{\text{D}}^{20}$ -29.3 (c 0.47, CHCl_3) ^1H NMR (500 MHz, CDCl_3) δ 7.35-7.25 (m, 5 H), 4.91-4.87 (m, 1 H), 4.48 (s, 2 H), 4.29-4.18 (m, 3 H), 4.05-4.01 (m, 1 H), 3.74-3.71 (m, 1 H), 3.63 (dd, J = 3.6, 7.7 Hz, 1 H), 3.44 (t, J = 6.4 Hz, 2 H), 2.08-2.00 (m, 1 H), 2.04 (s, 3 H), 1.96-1.80 (m, 4 H), 1.66-1.51 (m, 6 H), 1.48-1.18 (m, 35 H), 0.88 (s, 9 H),

18.1, 14.3, -3.9, -4.1, -4.4, -4.8; IR (thin film) 2904, 2855, 1990, 1871, 1463, 1366, 1254, 1098 cm^{-1} ; HRMS (ES) calcd for $\text{C}_{57}\text{H}_{110}\text{O}_6\text{Si}_3$, 975.7689 m/z ($\text{M}+\text{H}$)⁺; observed, 975.7697 m/z .



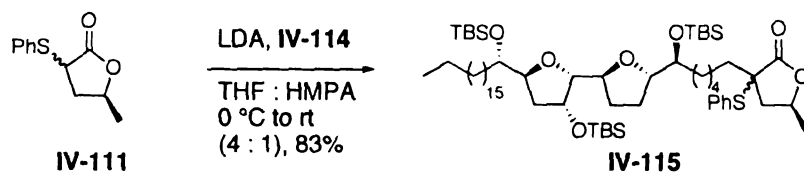
Benzyl ether **IV-97** (390 mg, 0.40 mmol) was dissolved in 1 : 1 EtOAc : iPrOH (20 mL). To this solution, 10% Pd-C (111 mg) was added and the mixture was stirred vigorously under H_2 (1 atm). The hydrogenolysis was complete in 1 h after which the reaction was filtered through a celite pad. The filtrate was concentrated and the crude product was purified by flash column chromatography (5% EtOAc in hexanes) to furnish alcohol **IV-113** in 92% yield (326 mg) as a colorless oil.

Data for **I-113**: $[\alpha]_{\text{D}}^{20}$ -29.4 (c 0.83, CHCl_3) ^1H NMR (500 MHz, CDCl_3) δ 4.30-4.26 (m, 2 H), 4.17-4.13 (m, 1 H), 3.97-3.93 (m, 1 H), 3.76-3.72 (m, 2 H), 3.65-3.63 (m, 1 H), 3.62 (t, $J = 6.6$ Hz, 2 H), 2.00-1.64 (m, 4 H) 1.59-1.12 (m, 44 H), 0.89 (t, $J = 7.0$ Hz, 3 H), 0.88 (s, 9 H), 0.87 (s, 9 H), 0.86 (s, 9 H), 0.07 (s, 3 H), 0.05 (s, 3 H), 0.04 (s, 6 H), 0.04 (s, 6 H); ^{13}C NMR (125 MHz, CDCl_3) δ 85.9, 81.6, 80.5, 79.2, 74.3, 74.0, 73.6, 63.2, 36.3, 33.0, 32.1, 31.9, 31.5, 29.9, 29.8, 29.7, 29.6, 28.7, 26.5, 26.4, 26.2, 26.1, 26.0, 25.9, 22.9, 18.4, 18.3, 18.1, 14.3, 1.2, -3.9, -4.0, -4.1, -4.4, -4.8; IR (thin film) 3385, 2926, 2855, 1600, 1463, 1360, 1255, 1079, 835, 774 cm^{-1} ; HRMS (ES) calcd for $\text{C}_{50}\text{H}_{104}\text{O}_6\text{Si}_3$, 885.7219 m/z ($\text{M}+\text{H}$)⁺; observed, 885.7217 m/z .



Alcohol **IV-133** (304 mg, 0.34 mmol), triphenylphosphine (223 mg, 0.85 mmol) and imidazole (61 mg, 0.90 mmol) were dissolved in toluene (12 mL). Upon addition of iodine (231 mg, 0.91 mmol) the clear, colorless solution turned yellowish brown and turbid. After 1 h vigorous stirring at room temperature, saturated sodium sulfite solution was added to the reaction until the yellowish brown color disappeared. The layers were separated and the aqueous layer was washed with EtOAc (3x15). After evaporation of the solvent form combined and dried (Na_2SO_4) organic layers a gummy material was obtained. Purification of the crude material by column chromatography (3% EtOAc in hexanes) afforded iodide **IV-114** (203 mg, 60%) as a colorless oil.

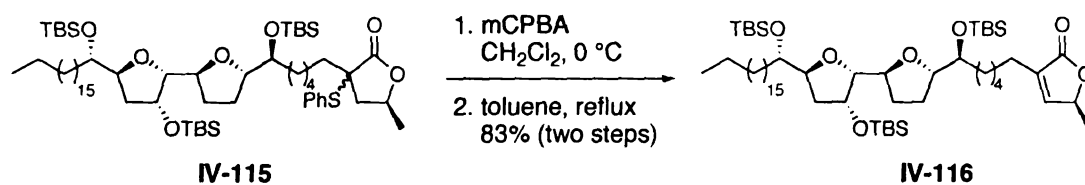
Data for **I-114**: $[\alpha]_D^{20}$ -27.7 (c 1.09, CHCl_3) ^1H NMR (500 MHz, CDCl_3) δ 4.32-4.29 (m, 2 H), 4.19-4.15 (m, 1 H), 3.98-3.94 (m, 1 H), 3.78-3.72 (m, 2 H), 3.65 (dd, $J = 3.5$, 7.7 Hz, 1 H), 3.18 (t, $J = 6.6$ Hz, 2 H), 2.00-1.23 (m, 46 H), 0.90 (t, $J = 7.0$ Hz, 3 H), 0.89 (s, 9 H), 0.88 (s, 9 H), 0.87 (s, 9 H), 0.08 (s, 3 H), 0.07, (s, 3 H), 0.06 (s, 6 H), 0.05 (s, 6 H); ^{13}C NMR (125 MHz, CDCl_3) δ 85.9, 81.6, 80.6, 79.3, 77.5, 77.2, 77.0, 74.2, 74.0, 73.6, 36.3, 33.8, 32.1, 31.7, 31.5, 31.0, 30.1, 29.9, 29.8, 29.6, 28.7, 26.5, 26.4, 26.2, 26.1, 26.0, 25.2, 22.9, 18.4, 18.3, 18.1, 14.3, 7.3, -3.9, -4.0, -4.1, -4.3, -4.4, -4.8; IR (thin film) 2925, 2854, 1597, 1462, 1359, 1253, 1076, 835, 775 cm^{-1} ; HRMS (ES) calcd for $\text{C}_{50}\text{H}_{103}\text{O}_5\text{ISi}_3$, 995.6236 m/z ($\text{M}+\text{H}$) $^+$; observed, 995.6259 m/z .



A solution of diisopropylamine (5.8 μL , 0.06 mmol) in THF (0.5 mL) was cooled to -78°C and *n*-BuLi (24 μL of 2.5 M solution, 0.06 mmol) was added to it. After 15 min, lactone **IV-111** (12.6 mg, 0.06 mmol) in THF (0.4 mL) was added and stirring was continued for 30 min during which time the solution was warmed to 0°C . Iodide **IV-115** (30 mg, 0.03 mmol) was then added as a solution in 1 : 1 THF : HMPA (0.5 mL). The reaction was allowed to attain room temperature. After 15 h, H_2O (1 mL) and EtOAc (5 mL) were added and the layers were separated. The aqueous layer was extracted with EtOAc (3x5 mL), combined organic layers were dried (Na_2SO_4), concentrated and the crude product was purified by column chromatography (1% – 3% EtOAc in hexanes) to afford sulfide **IV-115** as a mixture of diastereomers (27 mg, 83%).

Data for **I-115**: ^1H NMR (500 MHz, CDCl_3) δ 7.56-7.52 (m, 2 H), 7.43-7.33 (m, 3 H), 4.53-4.46 (m, 1 H), 4.32-4.28 (m, 2 H), 4.19-4.15 (m, 1 H), 3.97-3.93 (m, 1 H), 3.78-3.72 (m, 2 H), 3.65 (dd, $J = 3.5, 7.7$ Hz, 1 H), 2.52 (dd, $J = 3.5, 7.7$, 1 H), 2.01-1.91 (m, 2 H), 1.90-1.21 (m, 50 H), 0.90 (t, $J = 7.0$ Hz, 3 H), 0.89 (s, 9 H), 0.88 (s, 9 H), 0.87 (s, 9 H), 0.08 (s, 3 H), 0.07 (s, 3 H), 0.06 (s, 12 H); ^{13}C NMR (125 MHz, CDCl_3) δ 177.3, 137.3, 137.1, 130.8, 130.1, 129.9, 129.2, 129.1, 85.9, 81.6, 80.6, 79.3, 74.3, 74.0, 73.7, 73.6, 73.4, 56.4, 40.3, 36.7, 36.3, 32.1, 31.8, 31.5, 30.2, 30.1, 29.9, 29.6, 28.7, 26.5, 25.4, 26.2, 26.2, 26.0, 25.0, 22.9, 21.7, 18.4, 18.1, 14.3, -3.9 , -4.0 , -4.1 , -4.3 , -4.4 , -4.8 ; IR (thin film) 2926, 2854, 1770, 1464, 1385, 1360, 1255, 1184, 1068, 968, 939, 835, 806, 775,

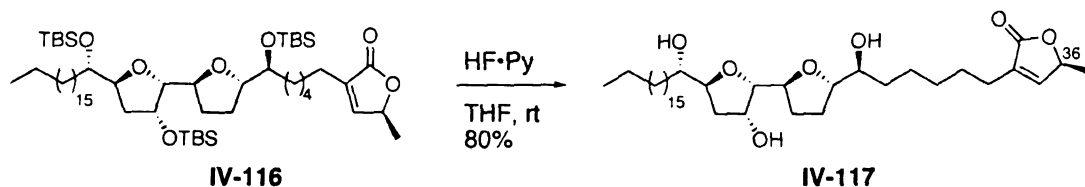
705, 692 cm^{-1} ; HRMS (ES) calcd for $\text{C}_{62}\text{H}_{114}\text{O}_7\text{Si}_3$, 1075.7671 m/z ($\text{M}+\text{H}^+$); observed, 1075.7690 m/z .



To an ice cold solution of **IV-115** (30 mg, 0.03 mmol) in CH_2Cl_2 (1 mL), ca. 75% mCPBA (6.8 mg, 0.03 mmol) in CH_2Cl_2 (1 mL) was added drop wise. After 20 min, saturated NaHCO_3 solution (1 mL) was carefully added and the layers were separated. The aqueous layer was extracted with CH_2Cl_2 (3x5 mL). The combined organic layers were dried and concentrated to afford the corresponding sulfoxide. The crude sulfoxide was taken up in toluene (2 mL) and heated to reflux for 4h. After cooling the solution to room temperature, the solvent was evaporated under reduced pressure and the crude material was purified by column chromatography (5% EtOAc in hexanes) to afford **IV-116** (24 mg, 83%).

Data for **I-116**: $[\alpha]_{\text{D}}^{20} -17.9$ (c 0.42, CHCl_3) ^1H NMR (500 MHz, CDCl_3) δ 6.99 (d, $J = 1.6$ Hz, 1 H), 5.00-4.99 (m, 1 H), 4.31-4.28 (m, 2 H), 4.19-4.15 (m, 1 H), 3.98-3.94 (m, 1 H), 3.78-3.74 (m, 2 H), 3.65 (dd, $J = 3.5, 7.7$ Hz, 1 H), 2.27 (t, $J = 7.3$ Hz, 2 H), 2.02-1.12 (m, 49 H), 0.92-0.88 (m, 30 H), 0.08-0.05 (m, 18 H); ^{13}C NMR (125 MHz, CDCl_3) δ 174.0, 149.0, 134.5, 85.9, 81.6, 80.6, 79.3, 74.3, 74.0, 73.7, 36.3, 32.1, 31.7, 31.5, 30.1, 29.9, 29.8, 29.7, 29.6, 28.7, 27.6, 26.5, 26.4, 26.2, 26.1, 26.0, 25.4, 22.9, 19.4, 18.3, 18.1, 14.3, 1.2, -3.9, -4.0, -4.1, -4.4, -4.8; IR (thin film) 2954, 2927, 2854, 1761, 1463, 1361,

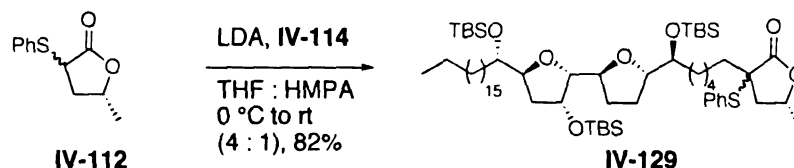
1319, 1257, 1081, 1026, 835, 802, 775 cm^{-1} ; HRMS (ES) calcd for $\text{C}_{55}\text{H}_{108}\text{O}_7\text{Si}_3$, 965.7481 m/z ($\text{M}+\text{H}$)⁺; observed, 965.7480 m/z .



To a solution of **IV-116** (9 mg, 9.31 μmol) in THF (0.5 mL) taken in a polyethylene vial, HF·pyridine (32 μL) was added at room temperature. After stirring for 12 h, the reaction was neutralized by saturate NaHCO_3 solution. H_2O (1 mL) and EtOAc (5 mL) were added and the layers were separated. The organic layer was washed with saturated CuSO_4 (2x2 mL) and the combined aqueous layers were extracted with EtOAc (3x5 mL). The organic layers were mixed, dried over Na_2SO_4 , and the solvent was evaporated to afford a waxy material. Sequential purification by column chromatography (EtOAc, 10% MeOH in EtOAc) and HPLC (10% $i\text{PrOH}$ in Et_2O) triol **IV-117** as a colorless wax (4.6 mg, 80%).

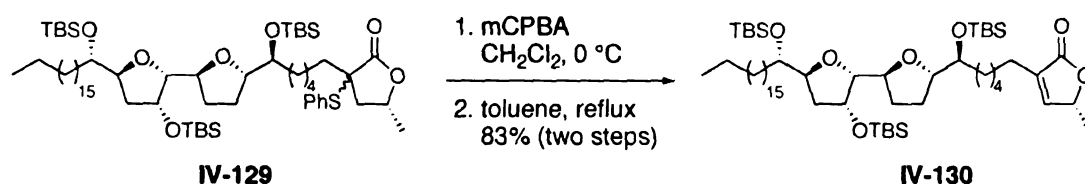
Data for **I-117**: $[\alpha]_{\text{D}}^{20} +3.2$ (c 0.40, CHCl_3) ^1H NMR (500 MHz, CDCl_3) δ 7.00 (d, $J = 1.5$ Hz, 1 H), 5.02-4.98 (m, 1 H), 4.46-4.43 (m, 1 H), 4.35 (dt, $J = 3.4, 6.8$ Hz, 1 H), 4.11-4.08 (m, 1 H), 3.97-3.94 (m, 1 H), 3.81 (t, $J = 3.1$ Hz, 1 H), 3.75 (d, $J = 5.4$ Hz, 1 H), 3.43-3.40 (m, 2 H), 2.32 (d, $J = 4.4$ Hz, 1 H), 2.28 (dt, $J = 1.5, 7.8$ Hz, 2 H), 2.19 (d, $J = 5.4$ Hz, 1 H), 2.15-2.11 (m, 1 H), 2.06-1.98 (m, 3 H), 1.84 (ddd, $J = 4.4, 9.5$ Hz, 13.4 Hz, 1 H), 1.75-1.69 (m, 1 H), 1.57-1.26 (m, 43 H), 0.89 (t, $J = 6.9, 3$ Hz); ^{13}C NMR (125 MHz, CDCl_3) δ 174.0, 149.2, 134.4, 84.1, 83.3, 81.6, 79.3, 77.6, 74.7, 74.3, 73.6, 48.9, 39.0, 34.0, 33.6, 32.1, 29.9, 29.8, 29.7, 29.6, 29.4, 29.3, 28.0, 27.6, 25.8, 25.6, 25.3, 22.9

(multiple carbons), 19.4, 14.3; IR (thin film) 3404, 2917, 2850, 1749, 1590, 1465, 1319, 1072, 1045, 995, 873, 798, 719 cm^{-1} ; HRMS (ES) calcd for $\text{C}_{37}\text{H}_{66}\text{O}_7$, 623.4887 m/z ($\text{M}+\text{H}^+$); observed, 623.4879 m/z .



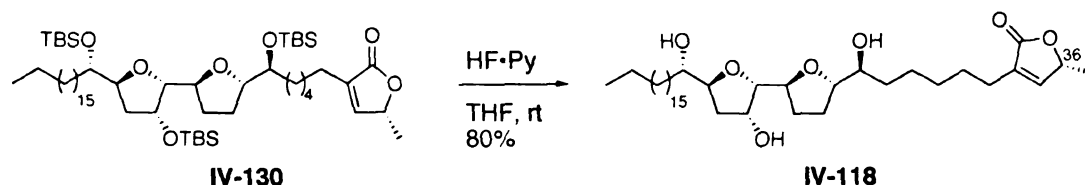
Sulfide **IV-129** was prepared following the same procedure as for **IV-115** using lactone **IV-112** (17.6 mg, 0.08 mmol) and iodide **IV-114** (42 mg, 0.04 mmol). Other reagents and solvents were used in appropriate proportions. **IV-129** was obtained in 82% yield (37 mg).

Data for **I-129**: ^1H NMR (500 MHz, CDCl_3) δ 7.56-7.51 (m, 2 H), 7.40-7.33 (m, 3 H), 4.50-4.46 (m, 1 H), 4.30-4.26 (m, 2 H), 4.18-4.13 (m, 1 H), 3.96-3.92 (m, 1 H), 3.78-3.72 (m, 2 H), 3.65 (dd, $J = 3.5, 7.7$ Hz, 1 H), 2.52 (dd, $J = 3.5, 7.7$ Hz, 1 H), 2.01-1.91 (m, 2 H), 1.90-1.21 (m, 50 H), 0.90 (t, $J = 7.0$ Hz, 3 H), 0.89 (s, 9 H), 0.88 (s, 9 H), 0.87 (s, 9 H), 0.08 (s, 3 H), 0.07 (s, 3 H), 0.06 (s, 12 H); ^{13}C NMR (125 MHz, CDCl_3) δ 171.2, 137.1, 130.8, 130.2, 129.9, 129.2, 129.1, 85.9, 81.6, 80.5, 79.3, 74.3, 74.0, 73.7, 73.4, 56.4, 42.7, 40.4, 36.7, 36.3, 32.1, 31.8, 31.5, 30.2, 29.9, 29.8, 29.6, 28.7, 26.6, 26.4, 26.3, 26.2, 26.1, 26.0, 25.9, 24.9, 22.9, 21.7, 20.9, 18.3, 18.1, 14.3, -3.9, -4.0, -4.1, -4.3, -4.4, -4.8; IR (thin film) 2927, 2854, 1770, 1463, 1385, 1359, 1255, 1184, 1070, 939, 835, 775, 692 cm^{-1} ; HRMS (ES) calcd for $\text{C}_{62}\text{H}_{114}\text{O}_7\text{SSi}_3$, 1075.7671 m/z ($\text{M}+\text{H}^+$); observed, 1075.7632 m/z .



Oxidation of **IV-129** to the corresponding sulfoxide and subsequent elimination was carried out by the same procedure as described for **IV-116**. Thus, 42 mg of **IV-129** afforded 33 mg (83%) of **IV-130**.

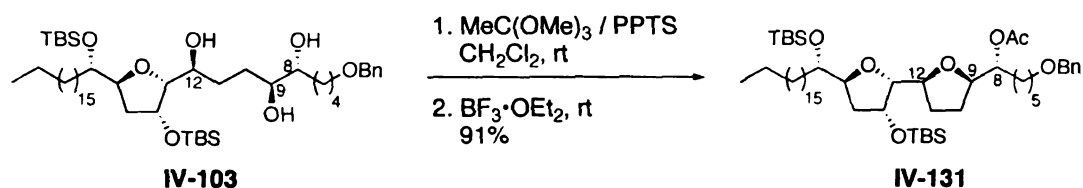
Data for **I-130**: $[\alpha]_D^{20}$ -30.6 (c 0.68, CHCl_3) ^1H NMR (500 MHz, CDCl_3) δ 6.99 (d, $J = 1.6$ Hz, 1 H), 5.00-4.99 (m, 1 H), 4.31-4.28 (m, 2 H), 4.19-4.15 (m, 1 H), 3.98-3.94 (m, 1 H), 3.78-3.74 (m, 2 H), 3.65 (dd, $J = 3.5, 7.7$ Hz, 1 H), 2.27 (t, $J = 7.3$ Hz, 2 H), 2.02-1.12 (m, 49 H), 0.92-0.88 (m, 30 H), 0.08-0.05 (m, 18 H); ^{13}C NMR (125 MHz, CDCl_3) δ 174.0, 149.0, 134.5, 85.9, 81.6, 80.6, 79.3, 74.3, 74.0, 73.7, 36.3, 32.1, 31.7, 31.5, 30.1, 29.9, 29.8, 29.7, 29.6, 28.7, 27.6, 26.5, 26.4, 26.2, 26.1, 26.0, 25.4, 22.9, 19.4, 18.3, 18.1, 14.3, 1.2, -3.9 , -4.0 , -4.1 , -4.4 , -4.8 ; IR (thin film), 2927, 2859, 1761, 1463, 1359, 1319, 1257, 1080, 939, 835, 806, 775 cm^{-1} ; HRMS (ES) calcd for $\text{C}_{55}\text{H}_{108}\text{O}_7\text{Si}_3$, 965.7481 m/z ($\text{M}+\text{H}^+$); observed, 965.7473 m/z .



Triol **IV-118** was obtained by TBS ether removal of **IV-130** using the same procedure as for **IV-117**. Thus, 11 mg (0.01 mmol) of **IV-130** furnished 5.6 mg of **IV-118** (80% yield).

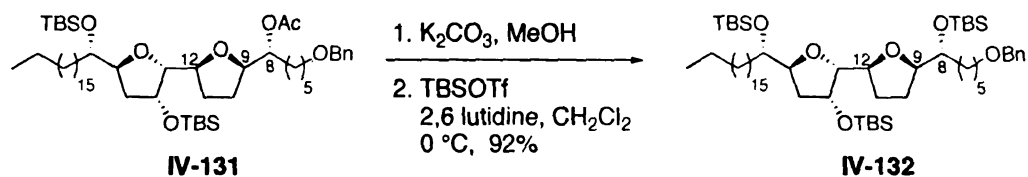
Data for **I-118**: $[\alpha]_D^{20}$ -23.8 (c 0.50, CHCl_3) ^1H NMR (500 MHz, CDCl_3) δ 7.00 (d, $J = 1.5$ Hz, 1 H), 5.02-4.98 (m, 1 H), 4.44-4.42 (m, 1 H), 4.34 (dt, $J = 3.4, 6.8$ Hz, 1 H), 4.11-

4.08 (m, 1 H), 3.97-3.93 (m, 1 H), 3.80 (t, $J = 3.1$ Hz, 1 H), 3.76 (d, $J = 5.4$ Hz, 1 H), 3.43-3.40 (m, 2 H), 2.42 (s (br), 1 H), 2.34 (s (br), 1 H), 2.28 (dt, $J = 1.5, 7.8$ Hz, 2 H), 2.15-2.11 (m, 1 H), 2.06-1.96 (m, 3 H), 1.83 (ddd, $J = 4.4, 9.5, 13.4$ Hz, 1 H), 1.75-1.69 (m, 1 H), 1.57-1.26 (m, 43 H), 0.88 (t, $J = 6.9$, 3 H); ^{13}C NMR (125 MHz, CDCl_3) δ 174.0, 149.2, 134.4, 84.1, 83.4, 81.6, 79.3, 77.6, 74.7, 74.3, 73.6, 48.9, 39.0, 34.0, 33.6, 32.1, 29.9, 29.8, 29.7, 29.6, 29.4, 29.3, 28.0, 27.6, 25.8, 25.6, 25.3, 22.9, 19.4, 14.3; IR (thin film) 3374, 2919, 2848, 1756, 1465, 1439, 1319, 1201, 1076, 952, 873, 800, 721 cm^{-1} ; HRMS (ES) calcd for $\text{C}_{37}\text{H}_{66}\text{O}_7$, 623.4887 m/z ($\text{M}+\text{H}$) $^+$; observed, 623.4888 m/z .



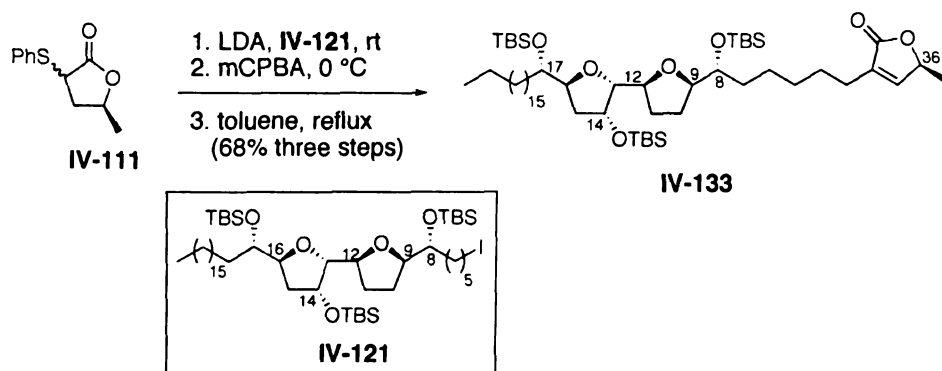
Cyclization of triol **IV-103** to bis-THF **IV-131** was carried using the same procedure as for **IV-95**. Thus, 80 mg (0.09 mmol) of **IV-103** produced 75 mg of **IV-131** (91%).

Partial data for **I-131**: ^1H NMR (500 MHz, CDCl_3) δ 7.39-7.23 (m, 5 H), 4.87-4.81 (m, 1 H), 4.46 (s, 2 H), 4.28-4.21 (m, 2 H), 4.03-3.91 (m, 2 H), 3.72-3.71 (m, 1 H), 3.63 (dd, $J = 3.3, 8.0$ Hz, 1 H), 3.42 (t, $J = 6.3$ Hz, 2 H), 2.02 (s, 3 H), 1.90-1.22 (m, 46 H), 0.88 (t, $J = 7.0$ Hz, 3 H), 0.85 (s, 9 H), 0.84 (s, 9 H), 0.04 (s, 6 H), 0.02 (s, 6 H); ^{13}C NMR (125 MHz, CDCl_3) δ 171.1, 138.9, 135.0, 129.8, 128.5, 127.9, 127.8, 127.7, 86.3, 80.9, 79.7, 79.6, 75.6, 74.3, 73.8, 73.1, 70.6, 36.7, 32.1, 31.8, 31.0, 30.1, 29.9, 29.8, 29.6, 27.9, 27.8, 26.8, 20.4, 26.3, 26.2, 25.9, 25.6, 22.9, 21.4, 18.4, 18.1, 14.3, -3.8, -4.0, -4.5, -4.8.



Tri-TBS ether **IV-132** was prepared by basic hydrolysis and subsequent TBS protection of acetate **IV-131** following the same procedure as described for acetate **IV-95**. 75 mg (92%) of **IV-132** was obtained from 75 mg (0.08 mmol) of **IV-131**.

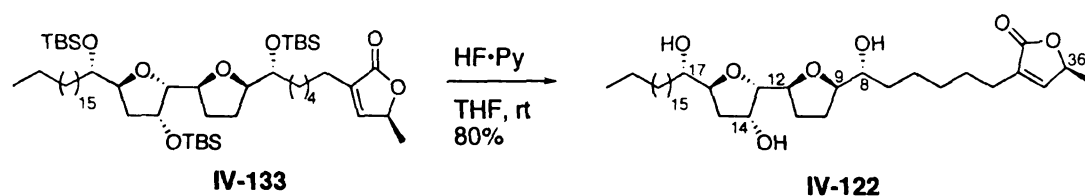
Partial data for **I-132**: ^1H NMR (500 MHz, CDCl_3) δ 7.37-7.22 (m, 5 H), 4.49 (s, 2 H), 4.34-4.27 (m, 2 H), 4.02-3.97 (m, 1 H), 3.94-3.90 (m, 1 H), 3.82-3.78 (m, 1 H), 3.72-3.70 (m, 1 H), 3.65 (dd, $J = 3.1, 8.1$ Hz, 1 H), 3.46 (t, $J = 6.6$ Hz, 2 H), 1.92-1.84 (m, 4 H), 1.82-1.12 (m, 42 H), 0.90-0.87 (m, 30 H), 0.08-0.02 (m, 18 H); ^{13}C NMR (125 MHz, CDCl_3) δ 139.0, 128.5, 127.8, 127.6, 86.9, 81.7, 80.5, 79.6, 74.2, 73.9, 73.8, 73.1, 70.7, 36.3, 32.1, 31.9, 31.4, 30.2, 30.0, 29.9, 29.8, 29.7, 29.6, 28.2, 26.7, 26.5, 26.4, 26.2, 26.1, 26.0, 25.9, 25.8, 22.9, 18.4, 18.1, 14.3, -3.8, -4.0, -4.1, -4.3, -4.4, -4.9.



Alkylation of lactone **IV-111** with iodide **IV-121**, oxidation of the resultant sulfide and elimination of the sulfoxide were effected as in case of **IV-114**. Thus, 40 mg of **IV-121** afforded 26 mg of **IV-133** (68% overall yield).

Partial data for **I-133**: ^1H NMR (500 MHz, CDCl_3) δ 6.98 (d, $J = 1.5$ Hz, 1 H), 5.02-4.88 (m, 1 H), 4.35-4.28 (m, 2 H), 4.04-3.98 (m, 1 H), 3.96-3.88 (m, 1 H), 3.81-3.75 (m, 1 H),

3.71-3.69 (m, 1 H), 3.63 (dd, $J = 3.3, 7.5$ Hz, 1 H), 2.26 (t, $J = 7.2$ Hz, 2 H), 1.91-1.72 (m, 3 H), 1.59-1.18 (m, 46 H), 0.91-0.87 (m, 30 H), 0.08-0.05 (m, 18 H); ^{13}C NMR (125 MHz, CDCl_3) δ 174.0, 149.0, 134.5, 86.9, 81.6, 80.5, 79.6, 74.1, 73.9, 73.7, 36.3, 32.1, 31.4, 30.2, 29.9, 29.6, 28.2, 27.7, 26.4, 26.3, 26.2, 26.0, 25.9, 25.8, 25.4, 22.9, 19.5, 19.4, 18.4, 18.3, 18.1, 14.4, 14.3, -3.8, -3.9, -4.0, -4.1, -4.4, -4.9.



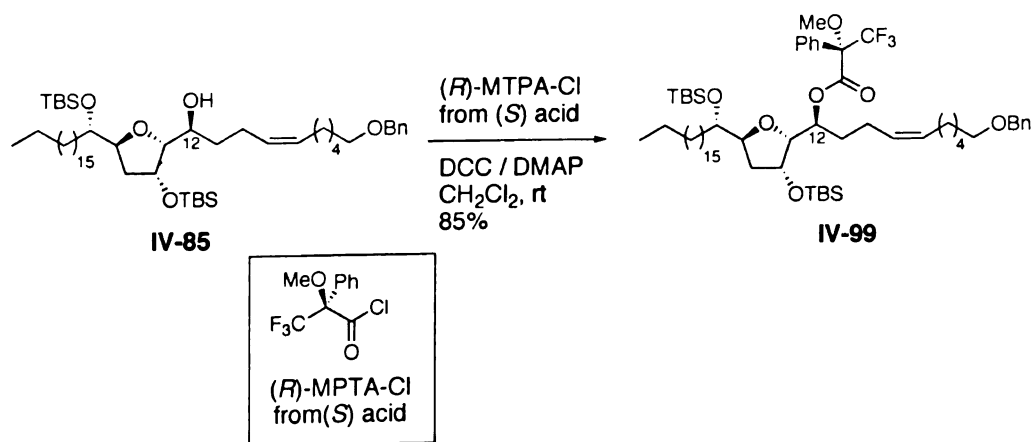
HF•pyridine mediated TBS cleavage of **IV-133** (10 mg, 0.01 mmol) to afford triol **IV-122** (5 mg, 80%) was performed as described before (for **IV-116**).

Data for **I-122**: $[\alpha]_{\text{D}}^{20} -22.0$ (c 0.30, CHCl_3) ^1H NMR (500 MHz, CDCl_3) δ 7.00 (d, $J = 1.5$ Hz, 1 H), 5.02-4.98 (m, 1 H), 4.47-4.46 (m, 1 H), 4.37 (dt, $J = 1.5, 7.6$ Hz, 1 H), 4.18-4.14 (m, 1 H), 4.09-4.07 (m, 1 H), 3.95 (dd, $J = 1.5, 3.4$ Hz, 1 H), 3.46-3.42 (m, 1 H), 3.41-3.37 (m, 1 H), 3.19 (d, $J = 8.8$ Hz, 1 H), 2.27 (dt, $J = 1.5, 7.8$ Hz, 2 H), 2.24-2.19 (m, 1 H), 2.08-1.99 (m, 5 H), 1.92 (ddd, $J = 4.4, 9.5, 13.4$ Hz, 1 H), 1.58-1.25 (m, 40 H), 0.89 (t, $J = 6.9$ Hz, 3 H); ^{13}C NMR (125 MHz, CDCl_3) δ 174.0, 149.1, 134.5, 83.5, 83.1, 81.8, 79.2, 77.6, 74.8, 74.7, 73.8, 38.6, 35.1, 34.0, 32.1, 29.9, 29.8, 29.7, 29.6, 29.5, 29.4, 28.3, 27.6, 25.9, 25.3, 22.9, 19.4, 14.3; IR (thin film) 3378, 2919, 2848, 1751, 1467, 1319, 1029, 873, 794 cm^{-1} ; HRMS (ES) calcd for $\text{C}_{37}\text{H}_{66}\text{O}_7$, 623.4887 m/z ($\text{M}+\text{H}$) $^+$; observed, 623.4874 m/z .

Preparation of Mosher's ester derivatives:

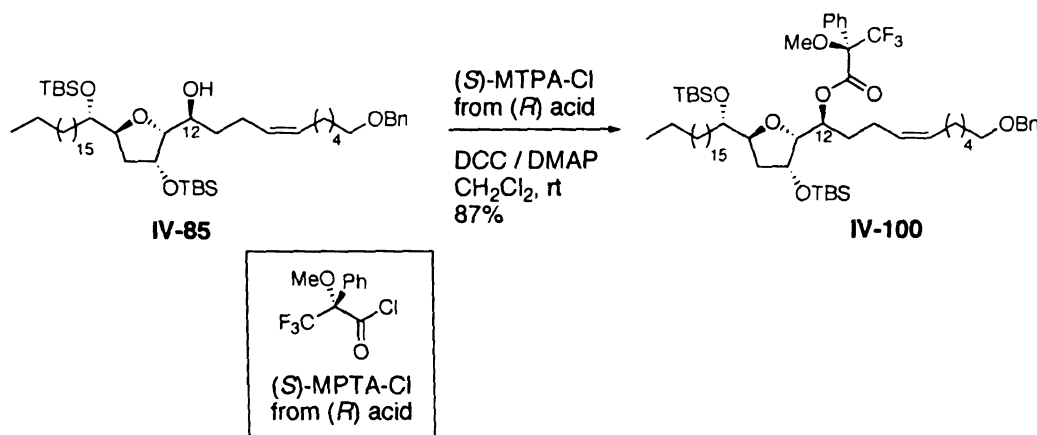
General procedure

To a solution of methoxytrifluoromethylphenylacetic acid (21 mg, 0.09 mmol) in hexanes (1 mL), oxalyl chloride (38 μ L, 0.42 mmol) and DMF (7.5 μ L, 0.09 mmol) were added at room temperature. After 1 h, the reaction mixture was centrifuged to separate the solid residues and supernatant clear liquid was concentrated under reduced pressure (using a water aspirator) to afford methoxytrifluoromethylphenylacetyl chloride. The acid chloride was dissolved in CH_2Cl_2 (1 mL). To this was added a mixture of the alcohol (0.02 mmol), DMAP (1.3 mg, 0.01 mmol) and triethyl amine (31 mL, 0.23 mmol) as a solution in CH_2Cl_2 (1 mL). After stirring overnight at room temperature, the reaction was quenched by saturated NH_4Cl (5 mL) solution and the aqueous layer was extracted with CH_2Cl_2 (3x5 mL). The combined organic layers were dried over Na_2SO_4 , concentrated and crude material was purified by column chromatography to afford the corresponding Mosher's ester (typical yields 85%-88%).



(S)-MTPA derivative **IV-99** (18 mg, 85%) was obtained from alcohol **IV-85** (15 mg, 17.7 μ mol) following the general procedure described above.

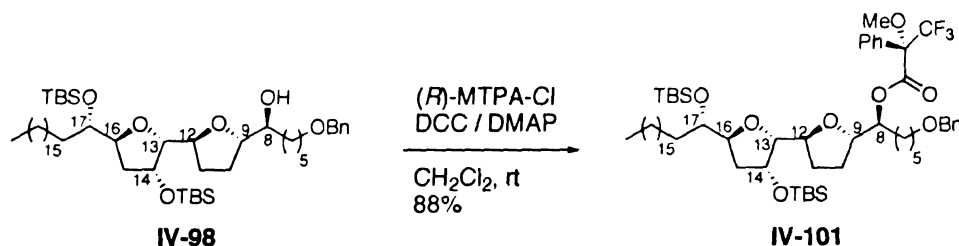
Partial data for **I-99**: ^1H NMR (500 MHz, CDCl_3) δ 7.68-7.67 (m, 2 H), 7.36-7.28 (m, 8 H), 5.45 (dt, $J = 2.4, 8.8$ Hz, 1 H), 5.30-5.19 (m, 2 H), 4.51 (s, 2 H), 4.36-4.34 (m, 1 H), 4.31-4.28 (m, 1 H), 3.85 (dd, $J = 3.5, 9.1$ Hz, 1 H), 3.65 (s, 3 H), 3.64-3.62 (m, 1 H), 3.46 (t, $J = 7.1$ Hz, 2 H), 2.00-1.83 (m, 6 H), 1.63-1.18 (m, 40 H), 0.92 (s, 9 H), 0.88 (t, $J = 7.0$ Hz, 3 H), 0.87 (s, 9 H), 0.10 (s, 3 H), 0.08 (s, 3 H), 0.05 (s, 3 H), 0.04 (s, 3 H); ^{13}C NMR (125 MHz, CDCl_3) δ 166.3, 139.0, 133.1, 130.1, 129.5, 128.6, 128.4, 128.3, 127.8, 127.7, 127.6, 84.0, 79.5, 76.4, 73.6, 73.4, 73.1, 70.6, 55.9, 36.6, 32.4, 32.1, 31.0, 30.1, 29.9, 29.8, 29.7, 29.6, 29.5, 27.3, 26.4, 26.1, 26.0, 23.1, 22.9, 18.3, 18.1, 14.3, 1.2, -3.8, -4.1, -4.3, -4.8.



(*R*)-MTPA derivative **IV-100** (18.5 mg, 87%) was obtained from alcohol **IV-85** (15 mg, 17.7 μmol) following the general procedure described above.

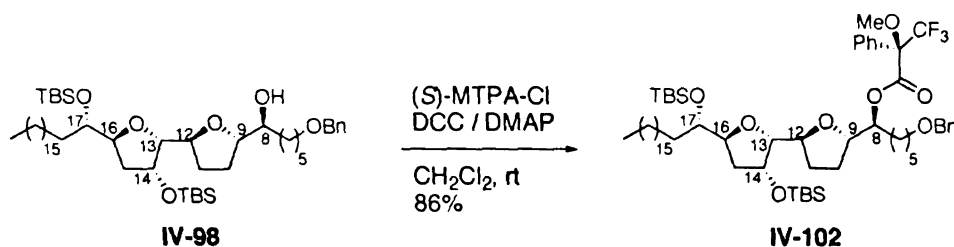
Partial data for **I-100**: ^1H NMR (500 MHz, CDCl_3) δ 7.65-7.64 (m, 2 H), 7.34-7.25 (m, 8 H), 5.40-5.28 (m, 3 H), 4.50 (s, 2 H), 4.33-4.32 (m, 1 H), 4.25-4.23 (m, 1 H), 3.85 (dd, $J = 3.4, 9.0$ Hz, 1 H), 3.59-3.57 (m, 1 H), 3.53 (s, 3 H), 3.46 (t, $J = 6.6$ Hz, 2 H), 2.15-1.88 (m, 5 H), 1.76-1.23 (m, 41 H), 0.91 (s, 9 H), 0.88 (t, $J = 7.0$ Hz, 3 H), 0.86 (s, 9 H), 0.08 (s, 3 H), 0.07 (s, 3 H), 0.03 (s, 6 H); ^{13}C NMR (125 MHz, CDCl_3) δ 166.1, 139.0, 132.5,

130.9, 129.5, 128.5, 128.4, 128.3, 127.8, 127.8, 127.6, 83.3, 79.6, 76.7, 73.8, 73.2, 73.1, 70.6, 55.5, 36.3, 32.1, 31.9, 31.0, 30.0, 29.9, 29.8, 29.7, 29.6, 29.5, 27.4, 26.3, 26.1, 26.0, 23.5, 22.9, 18.3, 18.2, 14.3, 1.2, -3.9, -4.2, -4.8.



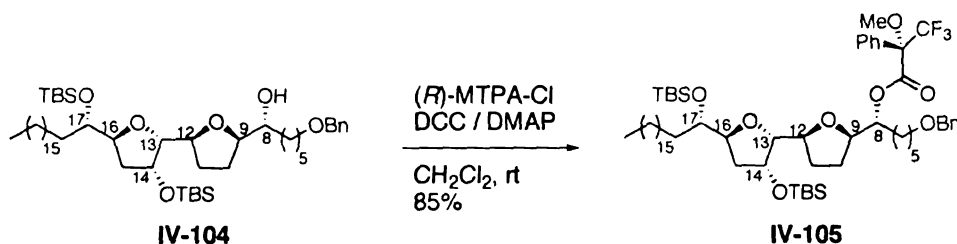
(*S*)-MTPA derivative **IV-101** (19 mg, 88%) was obtained from alcohol **IV-98** (15 mg, 17.4 μ mol) following the general procedure described above.

Partial data for **I-101**: ^1H NMR (500 MHz, CDCl_3) δ 7.66-7.64 (m, 2 H), 7.41-7.27 (m, 8 H), 5.15-5.12 (m, 1 H), 4.49 (s, 2 H), 4.31-4.19 (m, 3 H), 4.06-4.02 (m, 1 H), 3.72-3.65 (m, 2 H), 3.61 (s, 3 H), 3.41 (t, J = 6.7 Hz, 2 H), 2.1-1.81 (m, 4 H), 1.63-1.20 (m, 42 H), 0.90 (s, 9 H), 0.89 (t, J = 7.0 Hz, 3 H), 0.88 (s, 9 H), 0.08 (s, 6 H), 0.06 (s, 6 H); ^{13}C NMR (125 MHz, CDCl_3) δ 166.6, 138.9, 132.7, 129.5, 128.6, 128.5, 127.9, 127.8, 127.7, 85.8, 80.4, 79.3, 79.1, 78.3, 74.0, 73.6, 73.1, 70.5, 56.0, 36.4, 32.1, 31.9, 30.6, 30.1, 29.9, 29.8, 29.7, 29.6, 29.5, 28.7, 28.4, 26.5, 26.2, 26.1, 25.9, 25.0, 22.9, 18.3, 18.1, 14.3, -3.9, -4.2, -4.3, -4.8.



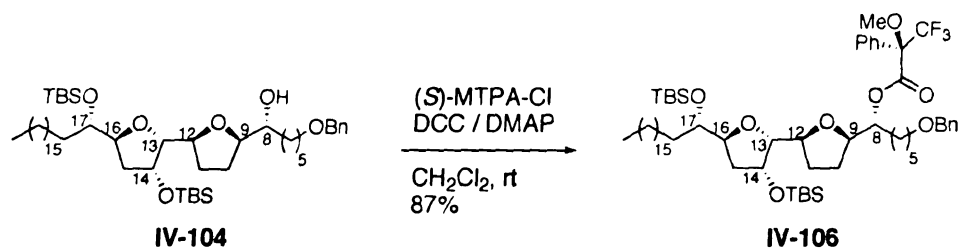
(*R*)-MTPA derivative **IV-102** (18.5 mg, 86%) was obtained from alcohol **IV-98** (15 mg, 17.4 μ mol) following the general procedure described above.

Partial data for **I-102**: ^1H NMR (500 MHz, CDCl_3) δ 7.62-7.60 (m, 2 H), 7.43-7.21 (m, 8 H), 5.12 (m, 1 H), 4.50 (s, 2 H), 4.28-4.22 (m, 2 H), 4.18-4.13 (m, 1 H), 4.08-4.06 (m, 1 H), 3.74-3.68 (m, 1 H), 3.60 (dt, $J = 3.5, 7.5$ Hz, 1 H), 3.56 (s, 3 H), 3.46 (t, $J = 6.7$ Hz, 2 H), 1.87-1.21 (m, 46 H), 0.90 (s, 9 H), 0.89 (t, $J = 7.0$ Hz, 3 H), 0.88 (s, 9 H), 0.08 (s, 6 H), 0.06 (s, 6 H); ^{13}C NMR (125 MHz, CDCl_3) δ 166.5, 138.9, 132.5, 129.6, 128.6, 128.5, 127.9, 127.8, 127.7, 85.6, 80.7, 79.4, 78.5, 78.4, 74.2, 73.6, 73.1, 70.5, 55.8, 36.5, 32.2, 31.8, 30.1, 30.0, 29.9, 29.8, 29.7, 29.6, 29.5, 28.5, 27.5, 26.4, 26.3, 26.2, 25.9, 22.9, 18.4, 18.1, 14.4, -3.9, -4.1, -4.4, -4.8.



(*S*)-MTPA derivative **IV-105** (18 mg, 85%) was obtained from alcohol **IV-104** (15 mg, 17.4 μmol) following the general procedure described above.

Partial data for **I-105**: ^1H NMR (500 MHz, CDCl_3) δ 7.60-7.59 (m, 2 H), 7.40-7.29 (m, 8 H), 5.31-5.02 (m, 1 H), 4.50 (s, 2 H), 4.29-4.24 (m, 1 H), 4.13-4.10 (m, 1 H), 4.09-4.06 (m, 1 H), 4.00-3.95 (m, 1 H), 3.77-3.73 (1 H), 3.58 (s, 3 H), 3.52 (dt, $J = 3.0, 8.0$, Hz, 1 H), 3.46 (t, $J = 6.6$ Hz, 2 H), 1.84-1.19 (m, 46 H), 0.90 (t, $J = 7.0$ Hz, 3 H), 0.88 (s, 9 H), 0.86 (s, 9 H), 0.08 (s, 3 H), 0.07 (s, 3 H), 0.06 (s, 3 H), 0.01 (s, 3 H); ^{13}C NMR (125 MHz, CDCl_3) δ 166.5, 138.9, 132.9, 129.6, 128.5, 128.4, 127.8, 127.7, 127.6, 86.4, 80.9, 80.1, 78.7, 78.4, 74.2, 73.8, 73.1, 70.5, 55.9, 36.7, 32.1, 31.6, 30.5, 30.1, 29.9, 29.8, 29.7, 29.6, 29.5, 27.7, 27.4, 26.3, 26.2, 25.9, 22.9, 18.4, 18.1, 14.3, -3.8, -4.0, -4.5, -4.9.



(*R*)-MTPA derivative **IV-106** (19 mg, 87%) was obtained from alcohol **IV-104** (15 mg, 17.4 μmol) following the general procedure described above.

Partial data for **I-106**: ^1H NMR (500 MHz, CDCl_3) δ 7.62-7.61 (m, 2 H), 7.40-7.27 (m, 8 H), 5.31-5.07 (m, 1 H), 4.49 (s, 2 H), 4.31-4.27 (m, 2 H), 4.04-3.98 (m, 2 H), 3.74-3.72 (m, 1 H), 3.63-3.61 (m, 1 H), 3.61 (s, 3 H), 3.41 (t, $J = 6.6$ Hz, 2 H), 1.95-1.84 (m, 4 H), 1.82-1.26 (m, 42 H), 0.90 (t, $J = 7.0$ Hz, 3 H), 0.88 (s, 18 H), 0.09 (s, 3 H), 0.07 (s, 3 H), 0.06 (s, 3 H), 0.05 (s, 3 H); ^{13}C NMR (125 MHz, CDCl_3) δ 166.7, 138.9, 132.8, 129.6, 128.6, 128.5, 127.8, 127.7, 127.6, 86.3, 80.7, 80.1, 79.0, 78.5, 74.0, 73.8, 73.1, 70.5, 56.0, 36.2, 32.1, 31.5, 30.7, 30.1, 30.0, 29.9, 29.8, 29.7, 29.6, 28.1, 27.7, 26.5, 26.2, 26.1, 25.9, 25.0, 22.9, 18.3, 18.1, 14.3, -3.8, -4.1, -4.4, -4.9.

E. References

1. Trost, B. M.; Fleming, I., Eds. *Comprehensive Organic Synthesis*; 1st ed.; Pergamon Press: Oxford, 1991; Vol. 1,2.
2. Otera, J. *Modern Carbonyl Chemistry*; Wiley-VCH: Weinheim ; New York, 2000.
3. Wakefield, B. J. *Organomagnesium Methods in Organic Synthesis*; Academic Press: London ; San Diego, 1995.
4. Silverman, G. S.; Rakita, P. E. *Handbook of Grignard Reagents*; Marcel Dekker: New York, 1996.
5. Wakefield, B. J. *Organolithium Methods*; Academic Press: London ; San Diego, 1988.
6. Kocienski, P. J. *Protecting Groups*; 2nd ed.; G. Thieme: Stuttgart, 2000.
7. Lipshutz, B. H.; Sengupta, S. *Org. React. (N.Y.)* **1992**, *41*, 135.
8. Weidmann, B.; Seebach, D. *Angew. Chem., Int. Ed. Engl.* **1983**, *22*, 31.
9. Simmons, H. E.; Cairns, T. L.; Vladuchick, A.; Hoiness, C. M. *Org. React. (N.Y.)* **1972**, *20*, 1.
10. Furstner, A. *Synthesis* **1989**, 571.
11. Knochel, P.; Yeh, M. C. P.; Berk, S. C.; Talbert, J. J. *Org. Chem.* **1988**, *53*, 2390.
12. Negishi, E. I. *Acc. Chem. Res.* **1982**, *15*, 340.
13. Knochel, P.; Singer, R. D. *Chem. Rev.* **1993**, *93*, 2117.
14. Knochel, P.; Perea, J. J. A.; Jones, P. *Tetrahedron* **1998**, *54*, 8275.
15. Knochel, P.; Millot, N.; Rodriguez, A. L.; Tucker, C. E. *Org. React. (N.Y.)* **2001**, *58*, 417.
16. Hupe, E.; Calaza, M. I.; Knochel, P. *Tetrahedron Lett.* **2001**, *42*, 8829.
17. Langer, F.; Schwink, L.; Devasagayaraj, A.; Chavant, P. Y.; Knochel, P. *J. Org. Chem.* **1996**, *61*, 8229.
18. Reetz, M. T.; Kessler, K.; Schmidtberger, S.; Wenderoth, B.; Steinbach, R. *Angew. Chem., Int. Ed. Engl.* **1983**, *22*, 989.

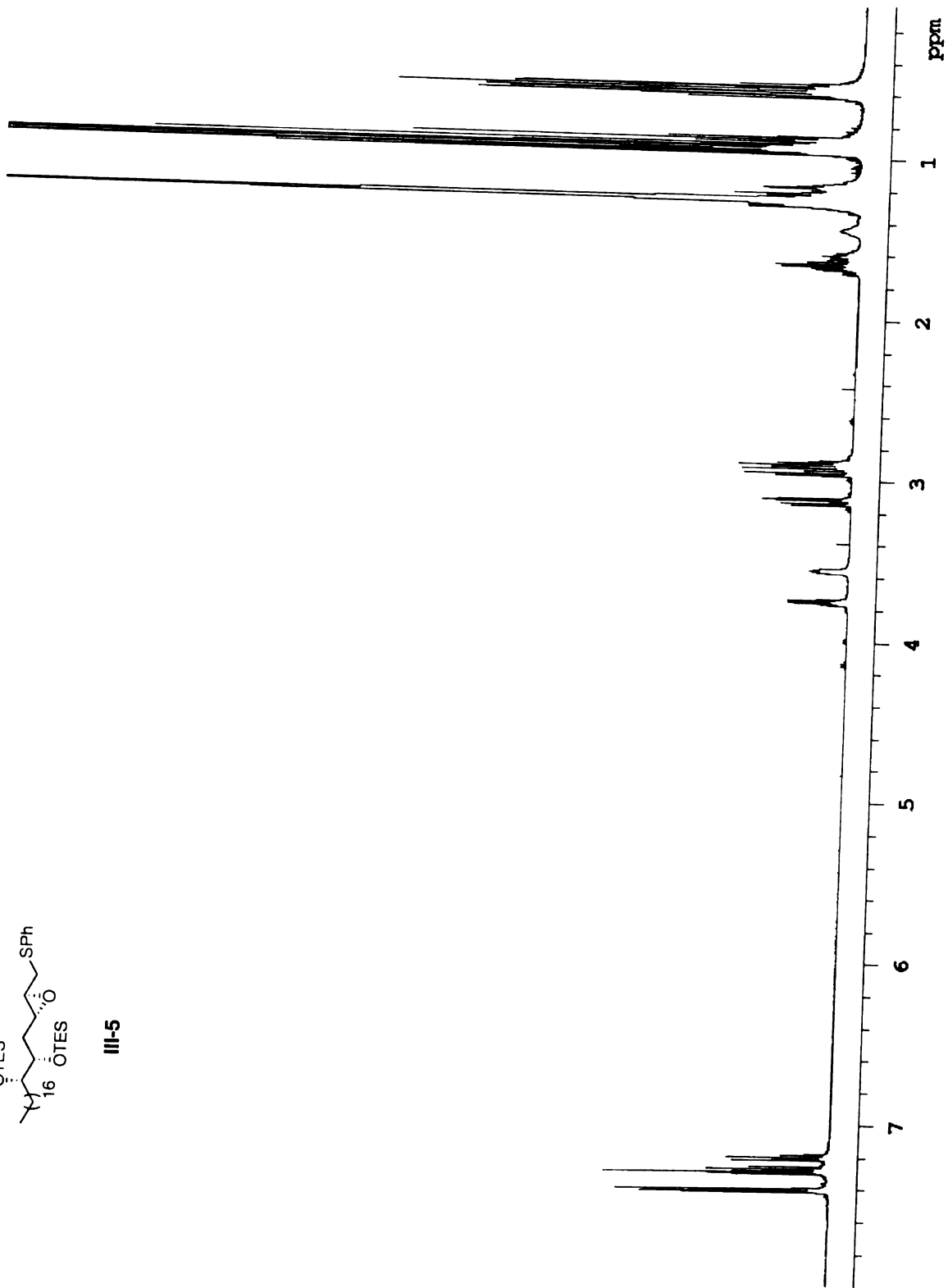
19. Reetz, M. T.; Kessler, K.; Jung, A. *Tetrahedron Lett.* **1984**, 25, 729.
20. Hoveyda, A. H.; Evans, D. A.; Fu, G. C. *Chem. Rev.* **1993**, 93, 1307.
21. Rodefeld, L.; Tochtermann, W. *Tetrahedron* **1998**, 54, 5893.
22. Couturier, M.; Dory, Y. L.; Rouillard, F.; Deslongchamps, P. *Tetrahedron* **1998**, 54, 1529.
23. Anan, H.; Seki, N.; Noshiro, O.; Honda, K.; Yasumuro, K.; Ozasa, T.; Fusetani, N. *Tetrahedron* **1996**, 52, 10849.
24. Yeh, M. C. P.; Knochel, P.; Santa, L. E. *Tetrahedron Lett.* **1988**, 29, 3887.
25. Decamp, A. E.; Kawaguchi, A. T.; Volante, R. P.; Shinkai, I. *Tetrahedron Lett.* **1991**, 32, 1867.
26. Tamaru, Y.; Nakamura, T.; Sakaguchi, M.; Ochiai, H.; Yoshida, Z. *J. Chem. Soc., Chem. Commun.* **1988**, 610.
27. Ochiai, H.; Nishihara, T.; Tamaru, Y.; Yoshida, Z. *J. Org. Chem.* **1988**, 53, 1343.
28. Rozema, M. J.; Sidduri, A.; Knochel, P. *J. Org. Chem.* **1992**, 57, 1956.
29. Rozema, M. J.; Eisenberg, C.; Lutjens, H.; Ostwald, R.; Belyk, K.; Knochel, P. *Tetrahedron Lett.* **1993**, 34, 3115.
30. Knochel, P.; Jones, P., Eds. *Organozinc Reagents: A Practical Approach*; Oxford University Press: Oxford ; New York, 1999.
31. Hanessian, S.; Moitessier, N.; Wilmouth, S. *Tetrahedron* **2000**, 56, 7643.
32. Ward, D. E.; Rhee, C. K. *Tetrahedron Lett.* **1991**, 32, 7165.
33. Larcheveque, M.; Lalande, J. *J. Chem. Soc., Chem. Commun.* **1985**, 83.
34. Overman, L. E.; McCready, R. J. *Tetrahedron Lett.* **1982**, 23, 2355.
35. Nakata, T.; Tanaka, T.; Oishi, T. *Tetrahedron Lett.* **1983**, 24, 2653.
36. Brown, H. C.; Krishnan, S. *J. Am. Chem. Soc.* **1972**, 94, 7159.
37. Rueger, H.; Stutz, S.; Goschke, R.; Spindler, F.; Maibaum, J. *Tetrahedron Lett.* **2000**, 41, 10085.
38. Yang, W. Q.; Kitahara, T. *Tetrahedron* **2000**, 56, 1451.

39. Ley, S. V.; Meek, G. *J. Chem. Soc., Perkin Trans. I* **1997**, 1125.
40. Boger, D. L.; Ichikawa, S.; Zhong, W. *J. Am. Chem. Soc.* **2001**, *123*, 4161.
41. Achyutharao, S.; Knochel, P. *J. Org. Chem.* **1991**, *56*, 4591.
42. Couturier, M.; Dory, Y. L.; Rouillard, F.; Deslongchamps, P. *Tetrahedron* **1998**, *54*, 1529.
43. Peng, S.; Okeley, N. M.; Tsai, A. L.; Wu, G.; Kulmacz, R. J.; van der Donk, W. A. *J. Am. Chem. Soc.* **2002**, *124*, 10785.
44. Nicolaou, K. C.; Ritzen, A.; Namoto, K.; Buey, R. M.; Diaz, J. F.; Andreu, J. M.; Wartmann, M.; Altmann, K. H.; O'Brate, A.; Giannakakou, P. *Tetrahedron* **2002**, *58*, 6413.
45. Reetz, M. T. *Angew. Chem., Int. Ed. Engl.* **1984**, *23*, 556.
46. Reetz, M. T. *Acc. Chem. Res.* **1993**, *26*, 462.
47. Still, W. C.; Schneider, J. A. *Tetrahedron Lett.* **1980**, *21*, 1035.
48. Still, W. C.; McDonald, J. H. *Tetrahedron Lett.* **1980**, *21*, 1031.
49. Asami, M.; Kimura, R. *Chem. Lett.* **1985**, 1221.
50. Koert, U.; Wagner, H.; Pidun, U. *Chem. Ber.* **1994**, *127*, 1447.
51. Arndt, S.; Emde, U.; Baurle, S.; Friedrich, T.; Grubert, L.; Koert, U. *Chem. Eur. J.* **2001**, *7*, 993.
52. Black, T. H. in *Encyclopedia of Reagents for Organic Synthesis*; Paquette, L. A., Ed.; Wiley: Chichester ; New York, 1995; Vol. 5, pp 3197-3199.
53. Black, T. H.; Mcdermott, T. S.; Brown, G. A. *Tetrahedron Lett.* **1991**, *32*, 6501.
54. Indictor, N.; Brill, W. F. *J. Org. Chem.* **1965**, *30*, 2074.
55. Trost, B. M.; Verhoeven, T. R. *J. Am. Chem. Soc.* **1980**, *102*, 4743.
56. Fukuyama, T.; Vranesic, B.; Negri, D. P.; Kishi, Y. *Tetrahedron Lett.* **1978**, 2741.
57. Hoffmann, R. W. *Chem. Rev.* **1989**, *89*, 1841.
58. Katsuki, T. in *Catalytic Asymmetric Synthesis*; 2nd ed.; Ojima, I., Ed.; Wiley-VCH: New York, 2000, pp 287-325.

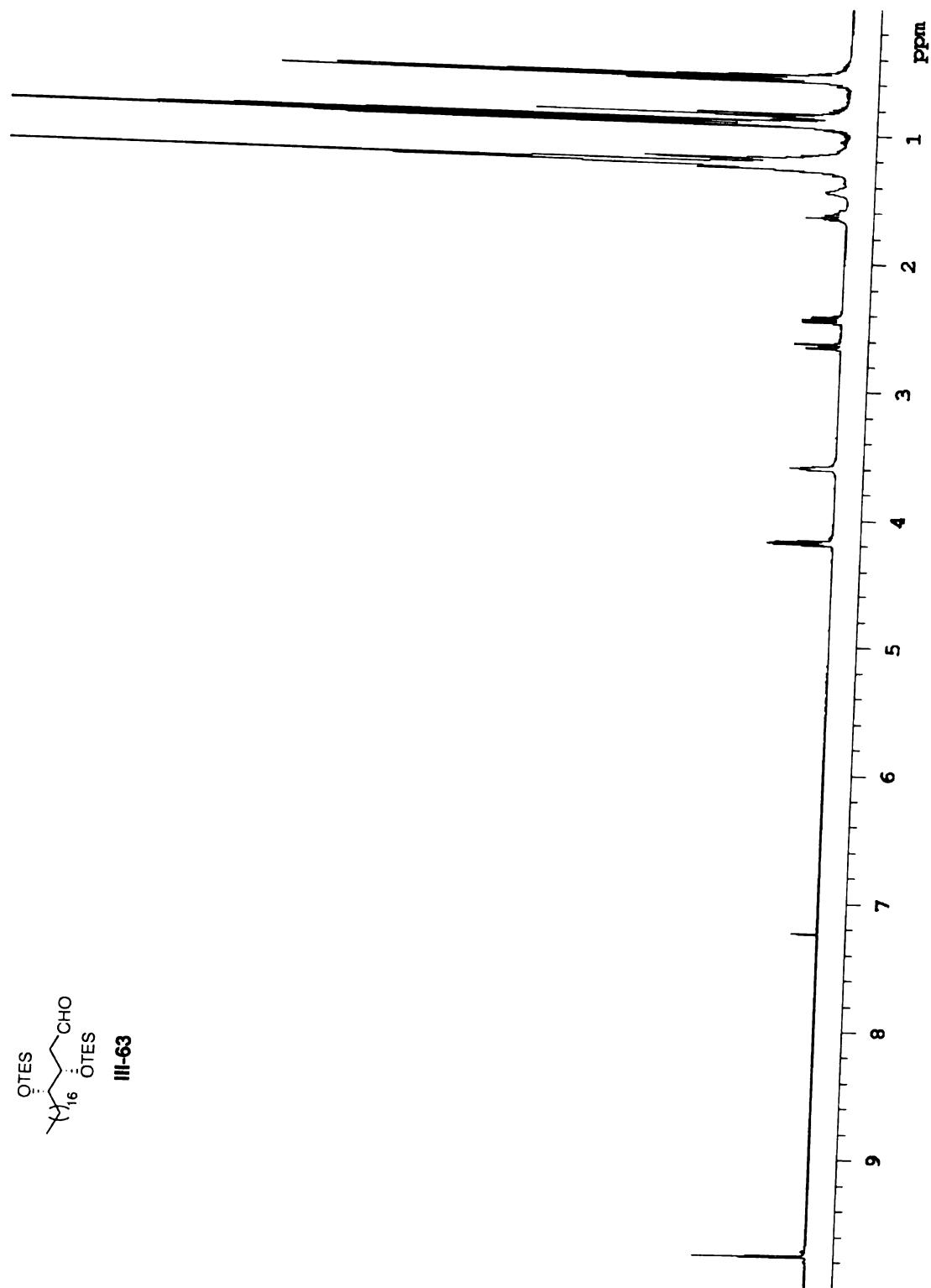
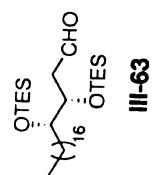
59. Tu, Y.; Wang, Z. X.; Shi, Y. *J. Am. Chem. Soc.* **1996**, *118*, 9806.
60. Wang, Z. X.; Shi, Y. A. *J. Org. Chem.* **1997**, *62*, 8622.
61. Tian, H. Q.; She, X. G.; Shu, L. H.; Yu, H. W.; Shi, Y. *J. Am. Chem. Soc.* **2000**, *122*, 11551.
62. Jacobsen, E. N.; Zhang, W.; Loebach, J. *Abstr. Pap. Am. Chem. S.* **1990**, *199*, 241.
63. Irie, R.; Noda, K.; Ito, Y.; Matsumoto, N.; Katsuki, T. *Tetrahedron Lett.* **1990**, *31*, 7345.
64. Kolb, H. C.; Sharpless, K. B. *Tetrahedron* **1992**, *48*, 10515.
65. Kolb, H. C.; Vannieuwenhze, M. S.; Sharpless, K. B. *Chem. Rev.* **1994**, *94*, 2483.
66. Johnson, R. A.; Sharpless, K. B. in *Catalytic Asymmetric Synthesis*; 2nd ed.; Ojima, I., Ed.; Wiley-VCH: New York, 2000, pp 231-280.
67. Baldwin, J. E. *J. Chem. Soc., Chem. Commun.* **1976**, 734.
68. Greene, T. W.; Wuts, P. G. M. *Protective Groups in Organic Synthesis*; 3rd ed.; Wiley: New York, 1999.
69. Johnson, R. A.; Sharpless, K. B. in *Catalytic Asymmetric Synthesis*; 2nd ed.; Ojima, I., Ed.; Wiley-VCH: New York, 2000, pp 357-398.
70. Hale, K. J.; Manaviazar, S.; Peak, S. A. *Tetrahedron Lett.* **1994**, *35*, 425.
71. Wang, L.; Sharpless, K. B. *J. Am. Chem. Soc.* **1992**, *114*, 7568.
72. Dale, J. A.; Mosher, H. S. *J. Am. Chem. Soc.* **1973**, *95*, 512.
73. Barth, G.; Voelter, W.; Mosher, H. S.; Djerassi, C. *J. Am. Chem. Soc.* **1970**, *92*, 875.
74. Marshall, J. A.; Piettre, A.; Paige, M. A.; Valeriote, F. *J. Org. Chem.* **2003**, *68*, 1771.
75. White, J. D.; Somers, T. C.; Reddy, G. N. *J. Org. Chem.* **1992**, *57*, 4991.
76. Shi, G.; Kozlowski, J. F.; Schwedler, J. T.; Wood, K. V.; MacDougall, J. M.; McLaughlin, J. L. *J. Org. Chem.* **1996**, *61*, 7988.
77. Emde, U.; Koert, U. *Eur. J. Org. Chem.* **2000**, 1889.

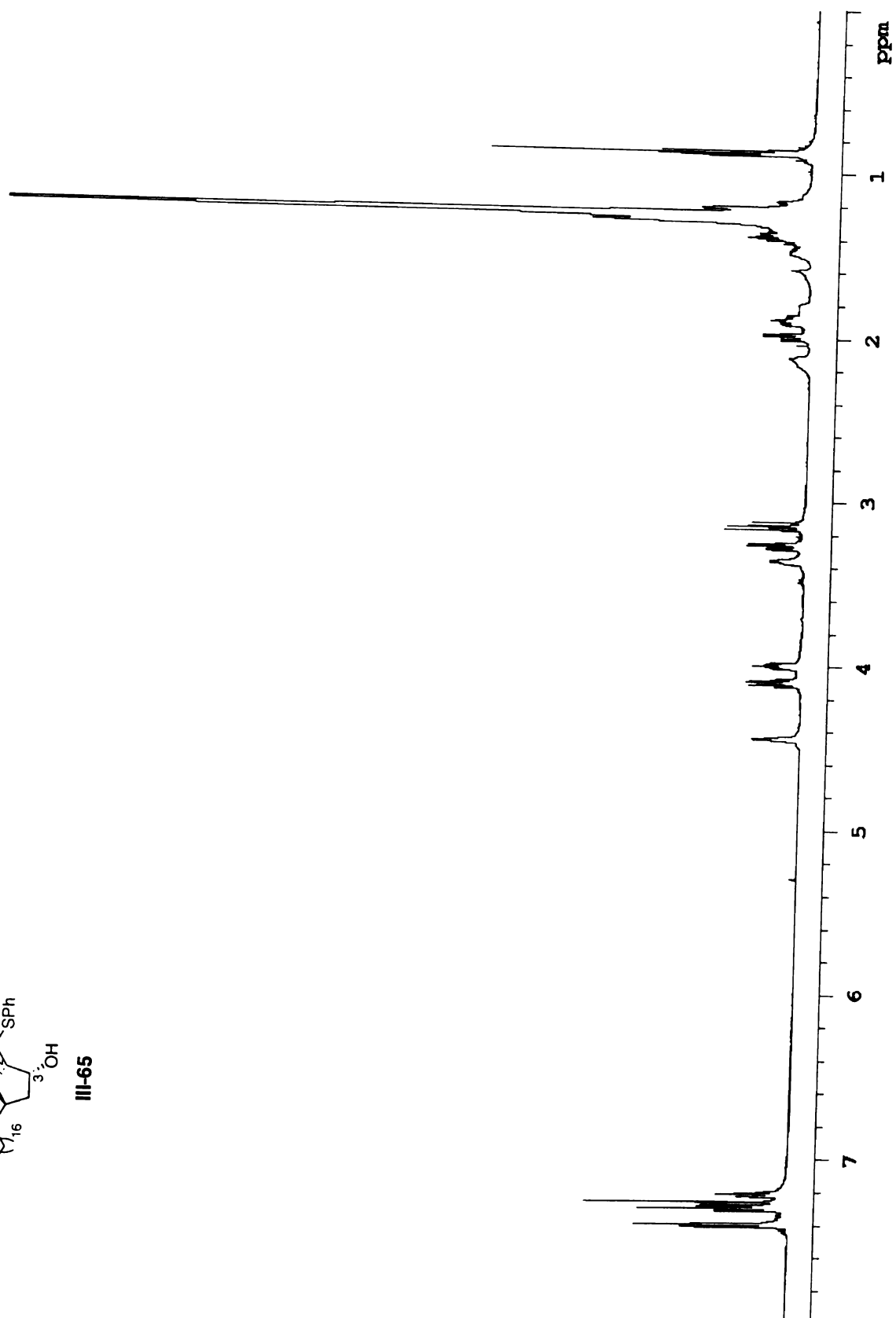
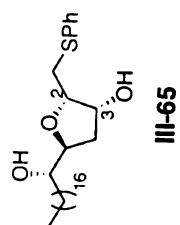
78. Born, L.; Lieb, F.; Lorentzen, J. P.; Moeschler, H.; Nonfon, M.; Sollner, R.; Wendisch, D. *Planta Med.* **1990**, *56*, 312.
79. Pretsch, E. *Tables of Spectral Data for Structure Determination of Organic Compounds*; 2nd ed.; Springer-Verlag: Berlin ; New York, 1989.
80. Homann, R. W.; Kruger, J.; Bruckner, D. *New J. Chem.* **2001**, *25*, 102.
81. Takahashi, S.; Maeda, K.; Hirota, S.; Nakata, T. *Org. Lett.* **1999**, *1*, 2025.
82. Shimojo, M.; Matsumoto, K.; Hatanaka, M. *Tetrahedron* **2000**, *56*, 9281.

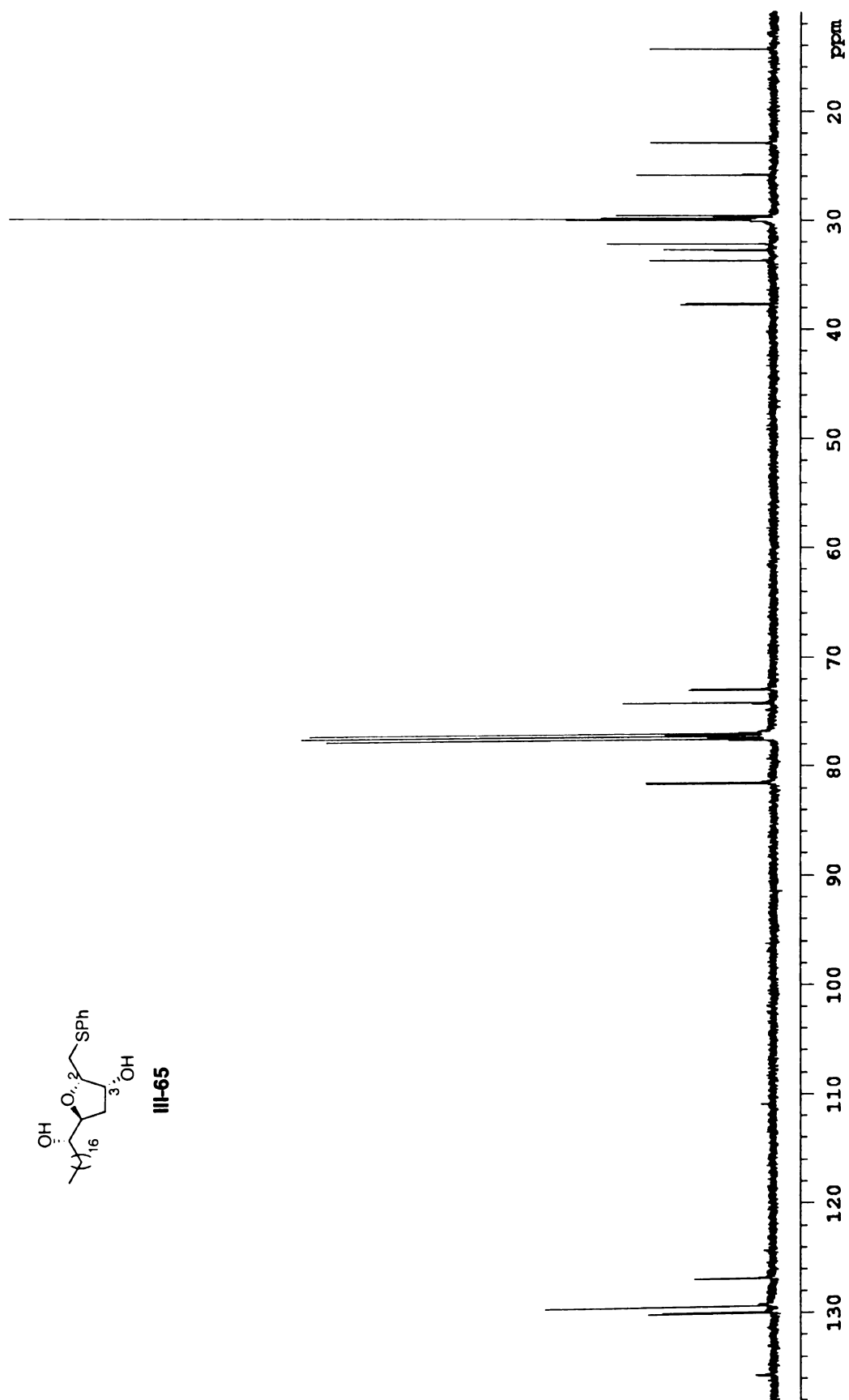
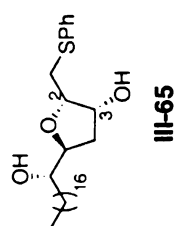
APPENDIX

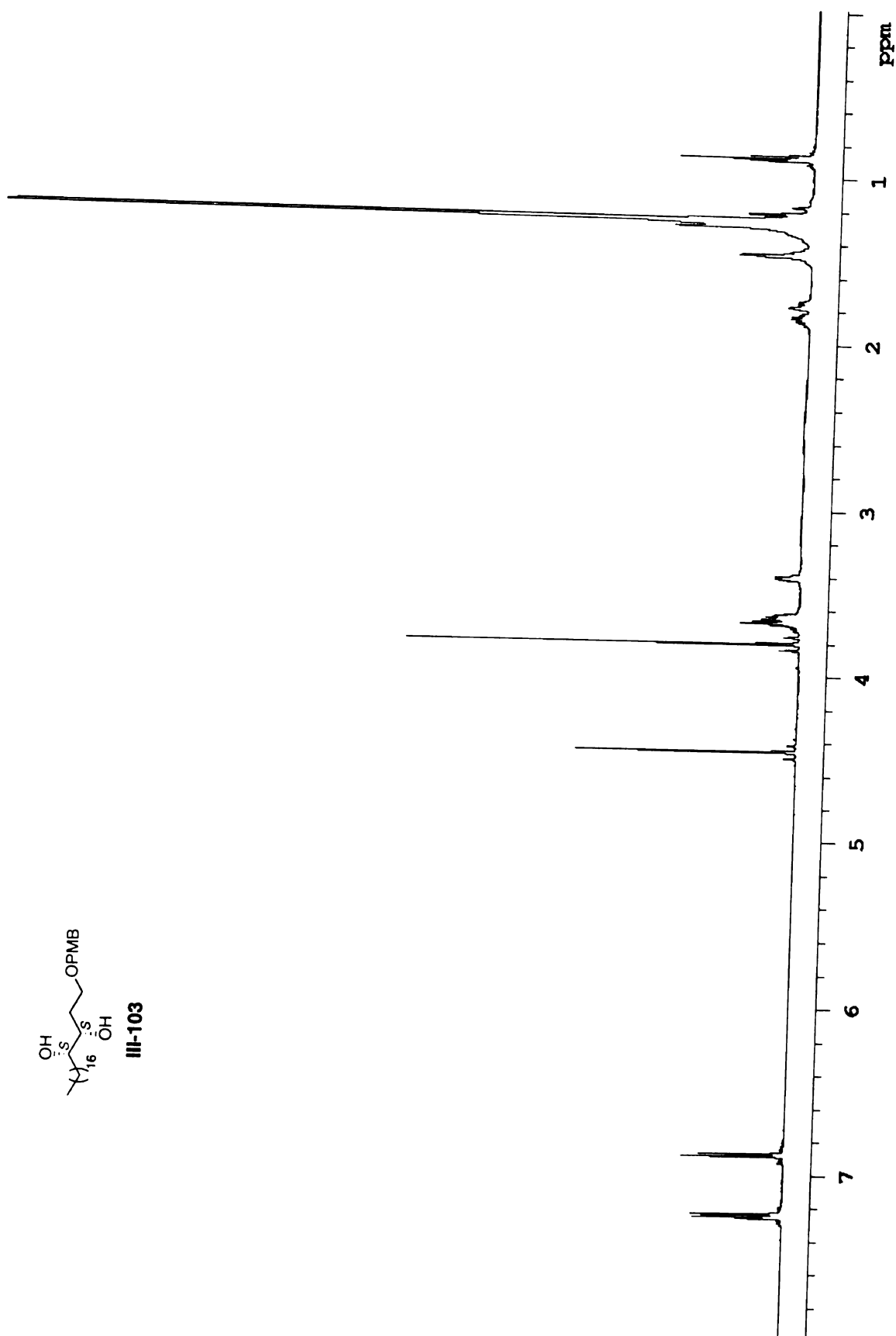


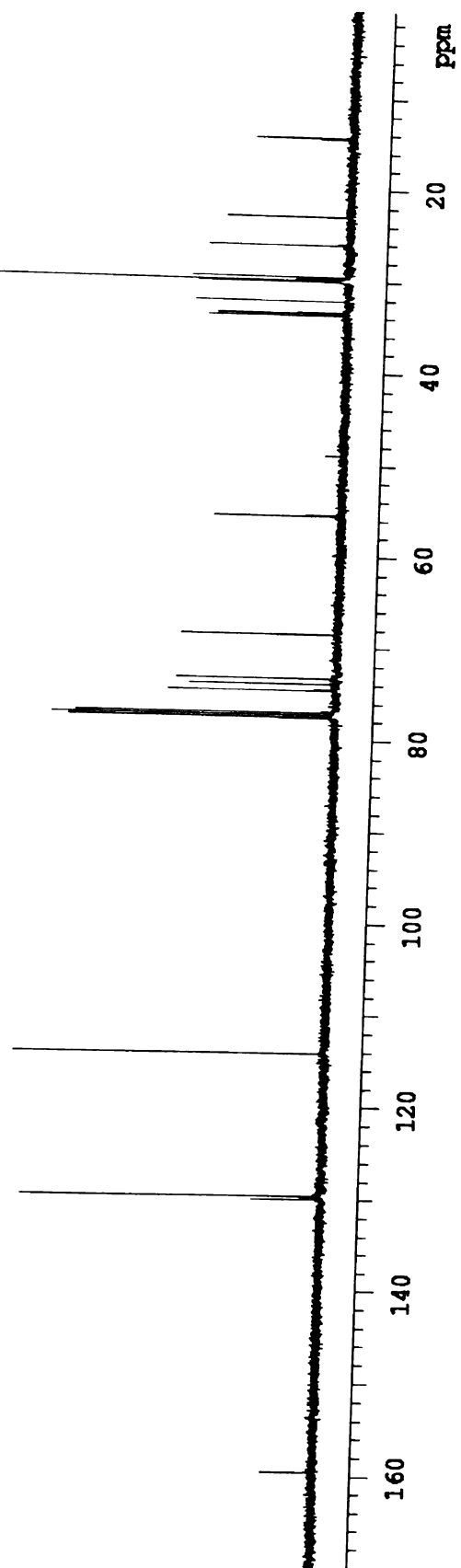
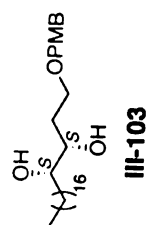










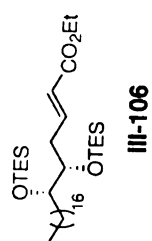
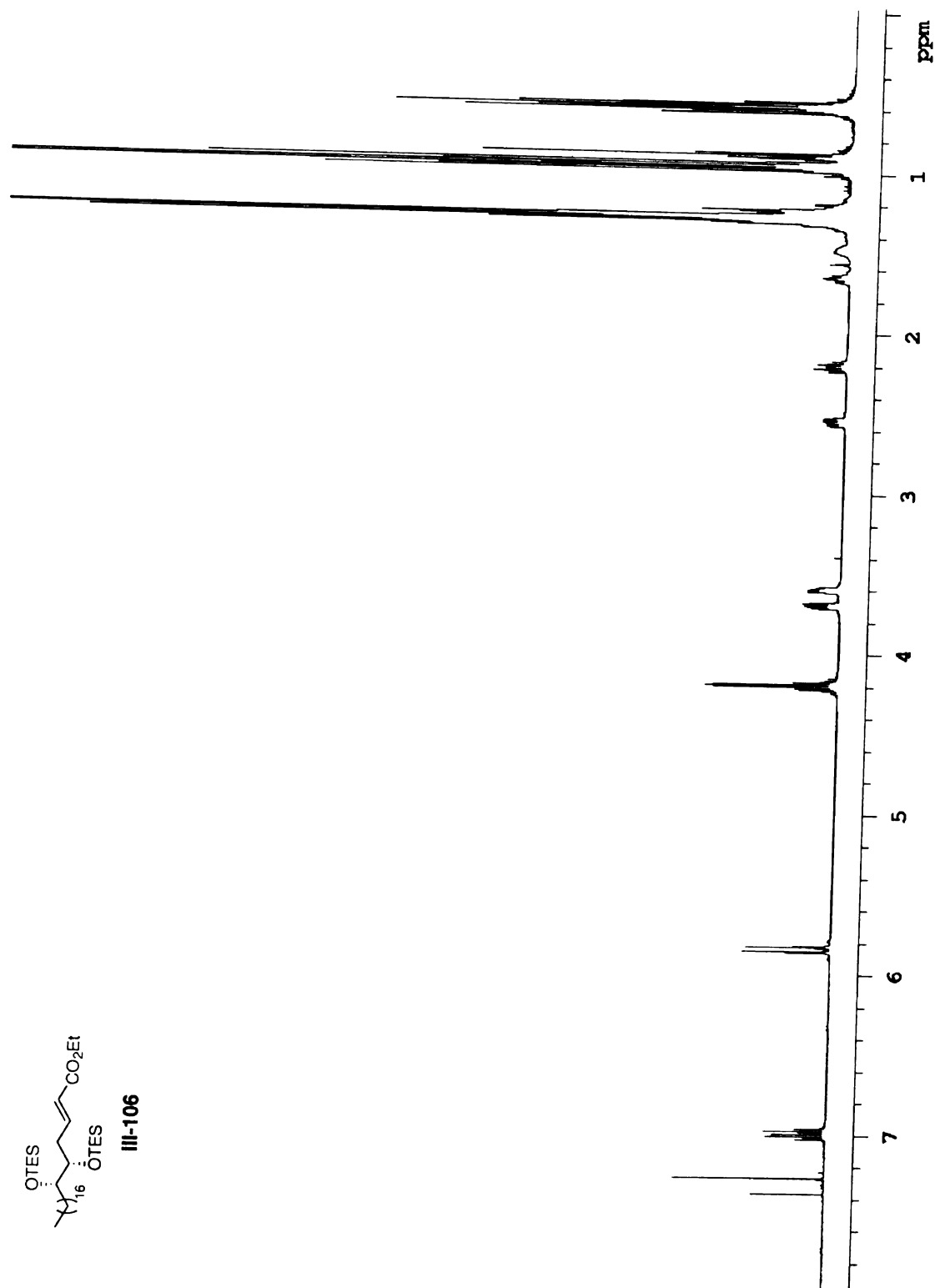


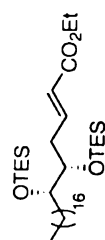




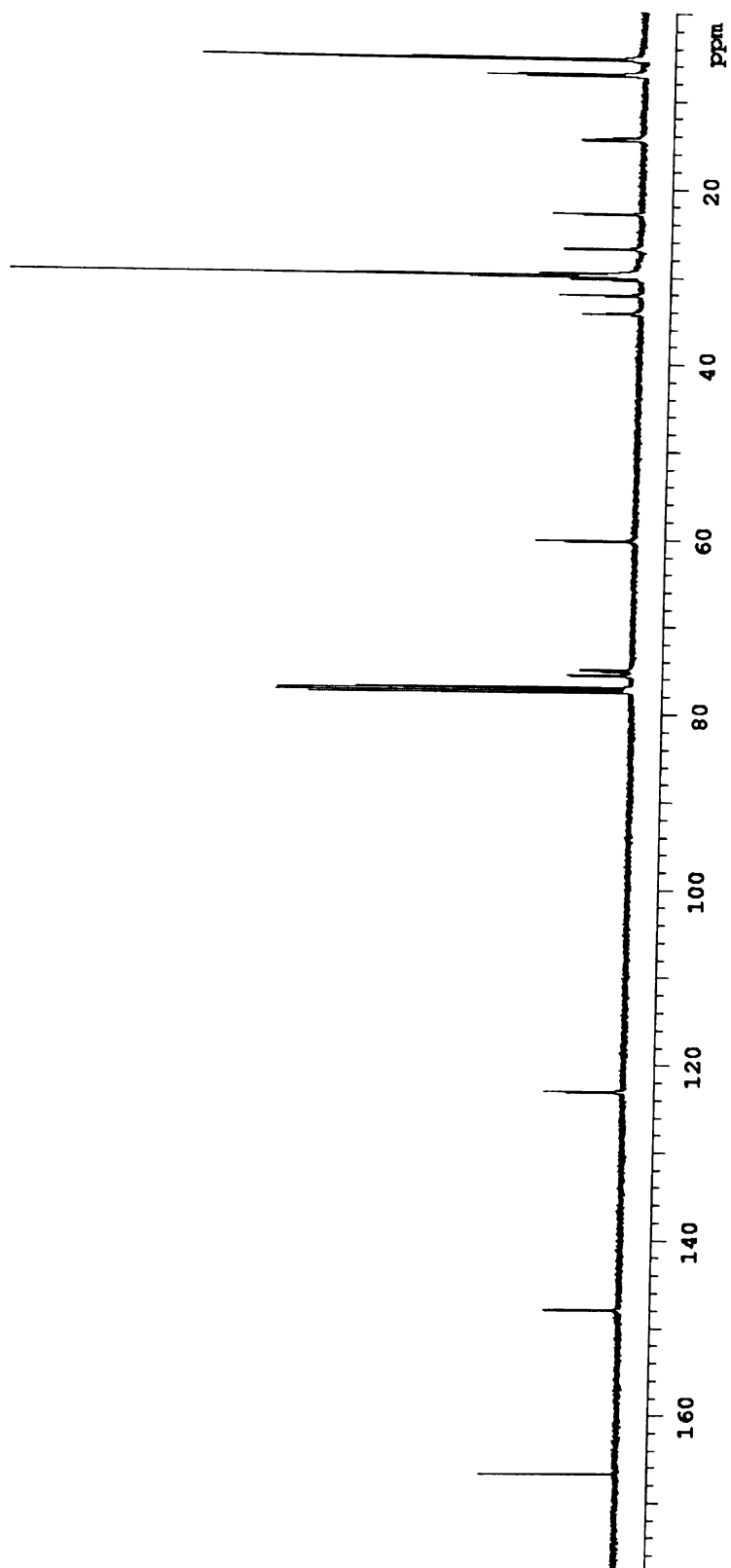








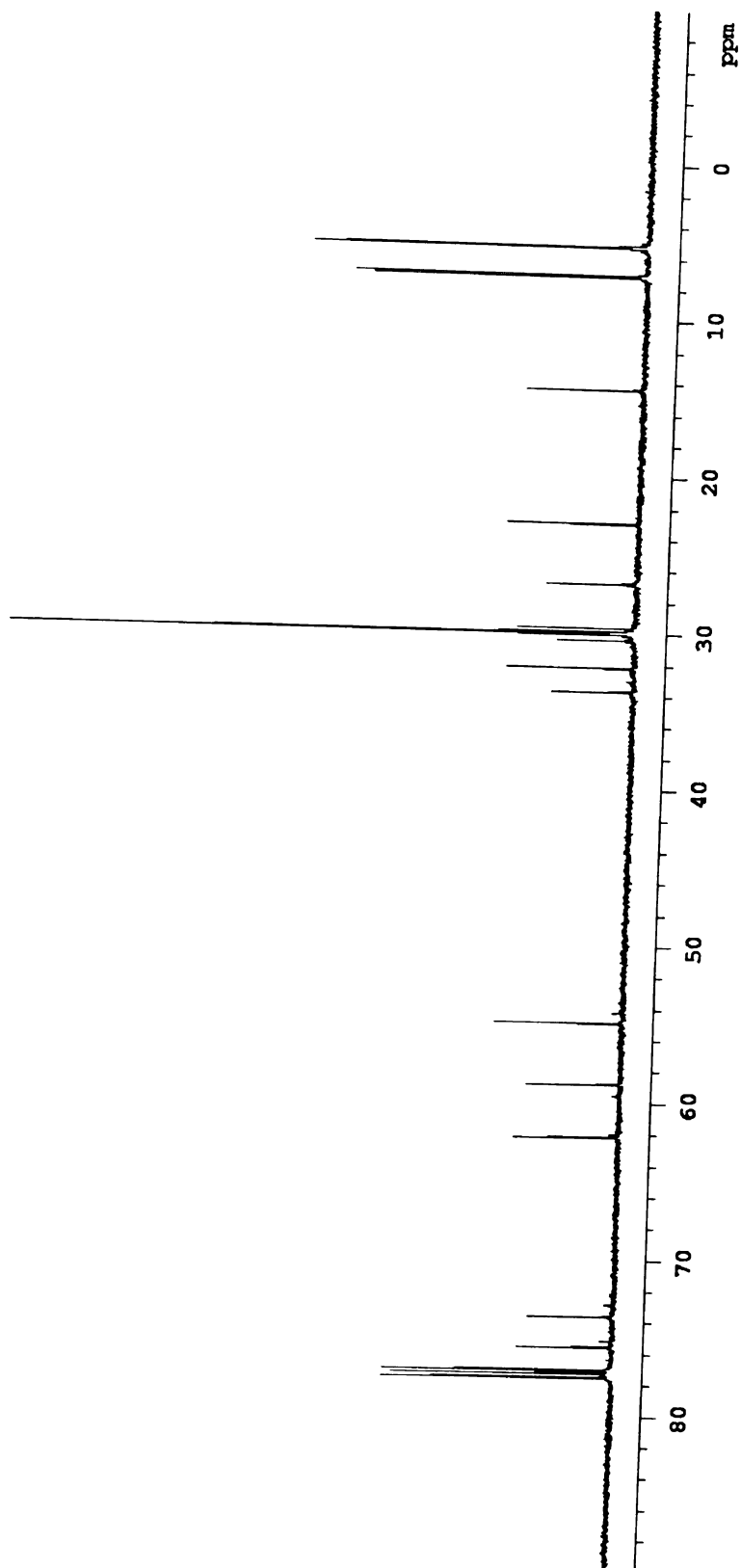
III-106

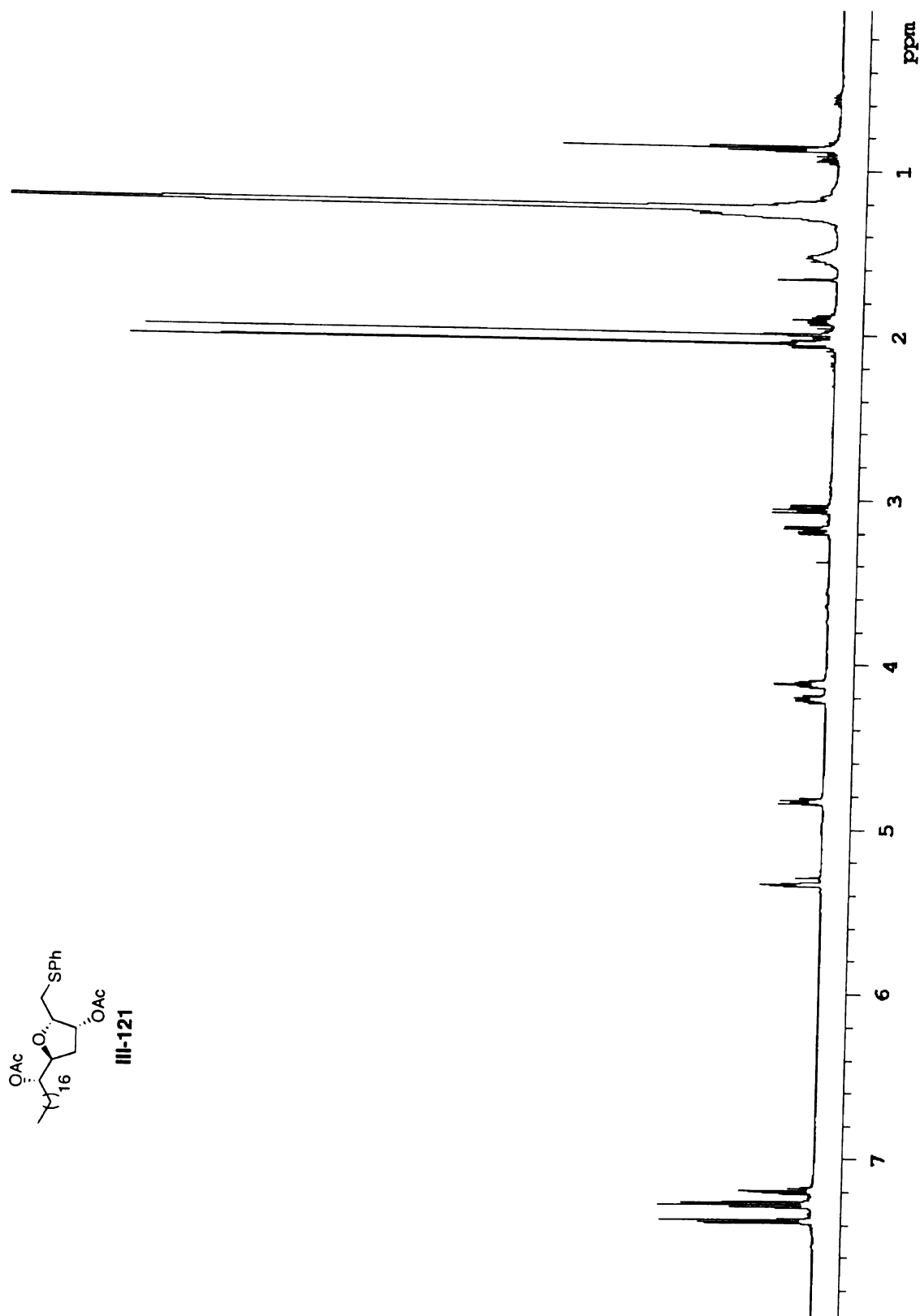


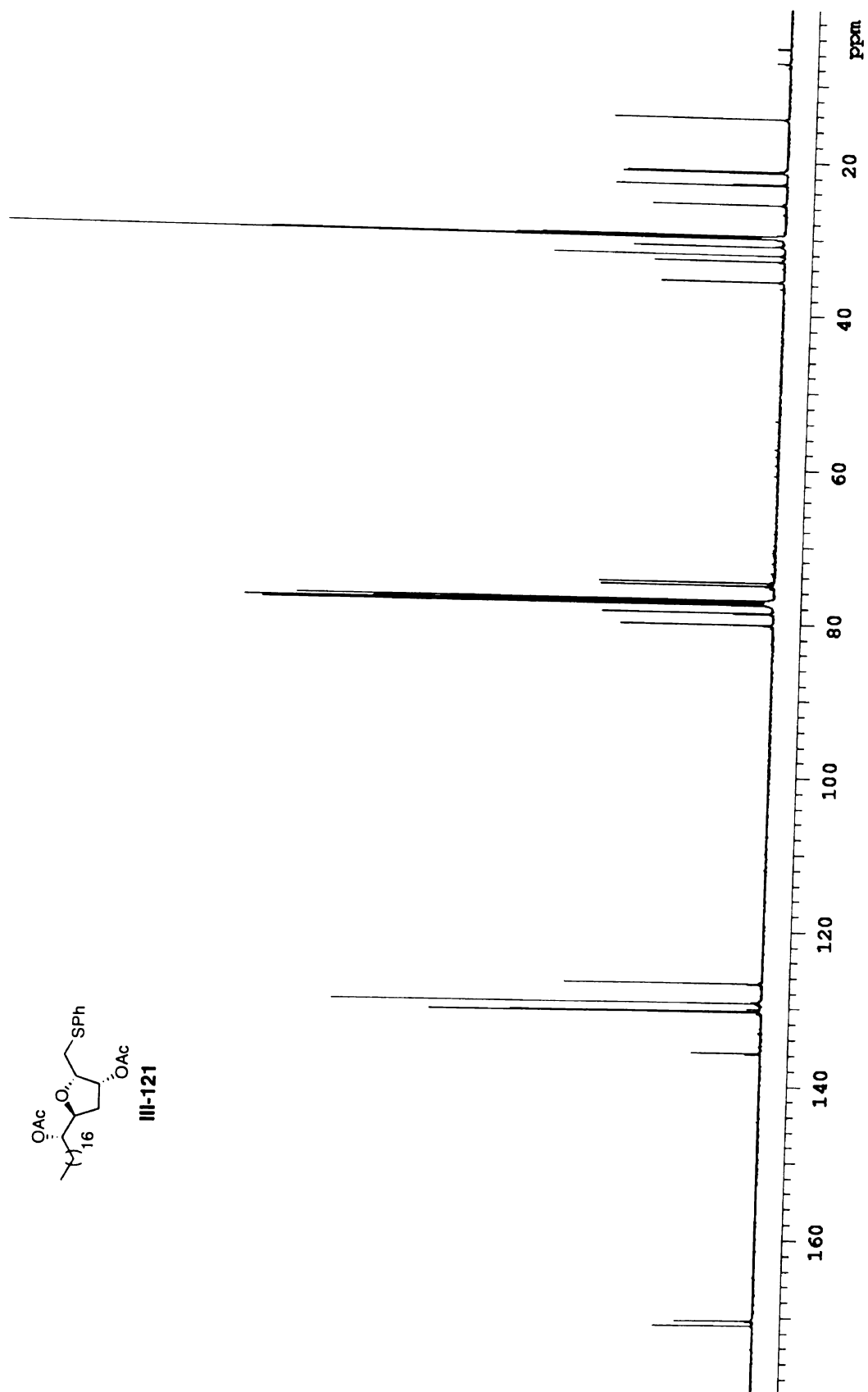


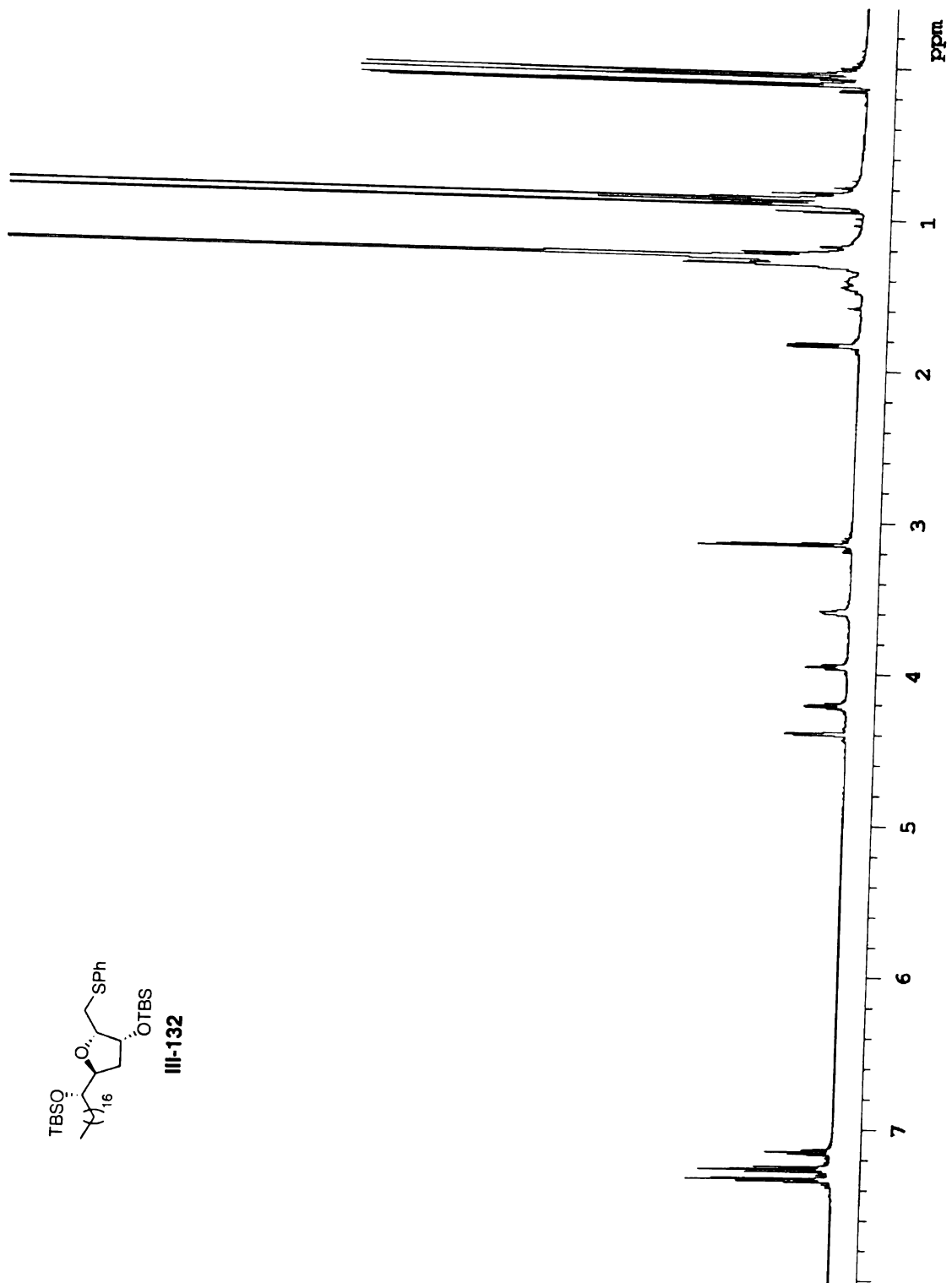


III-107







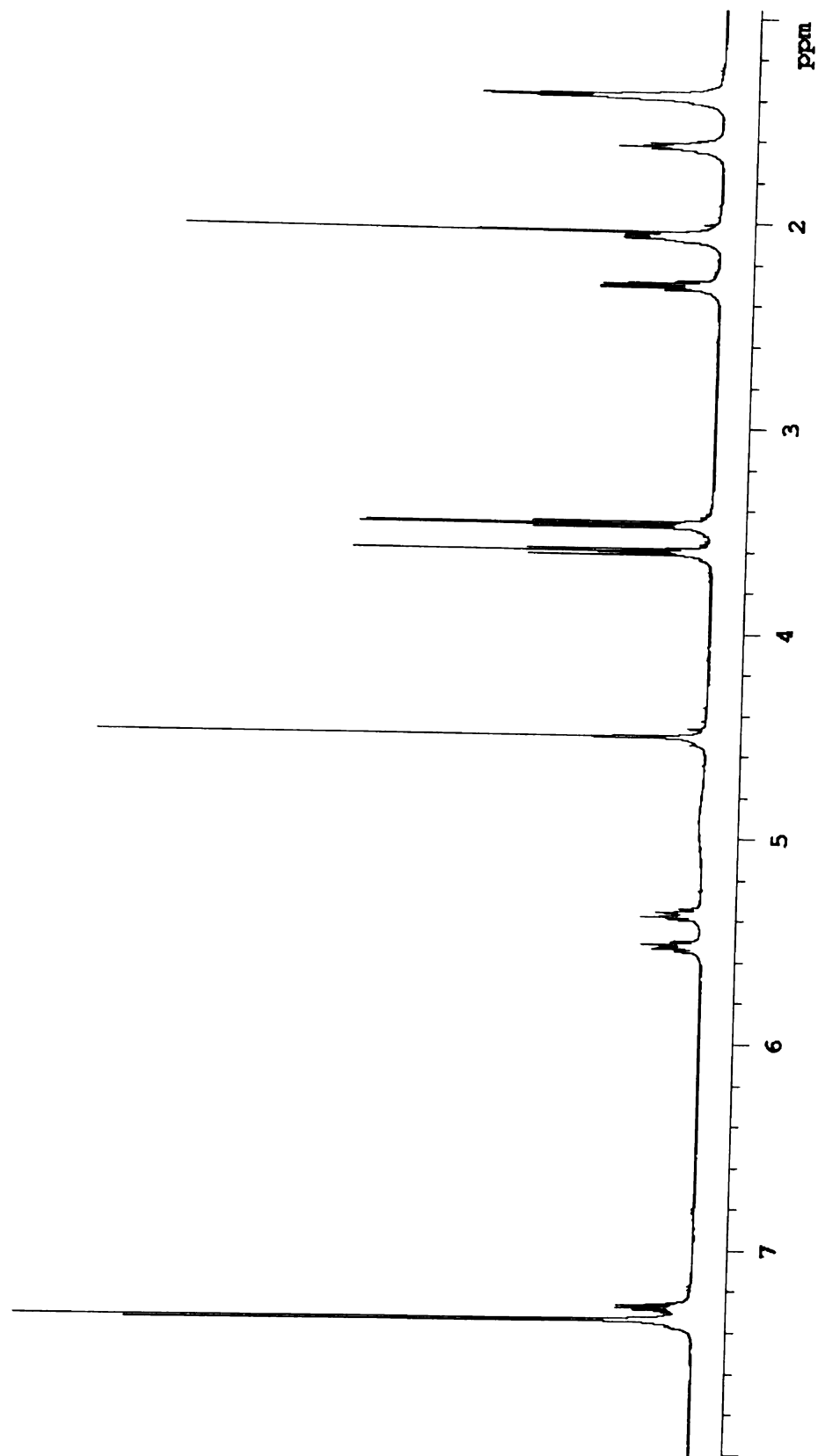






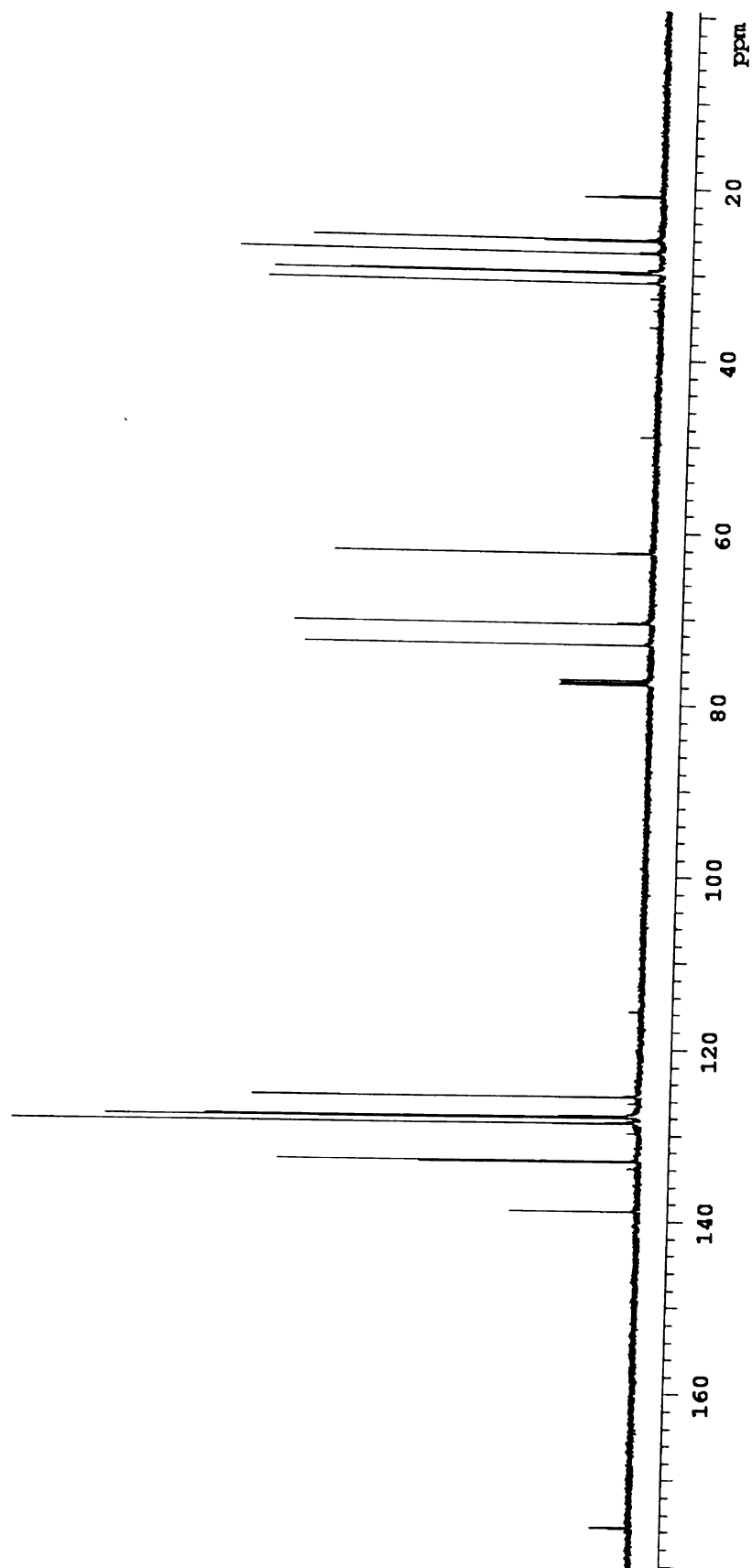


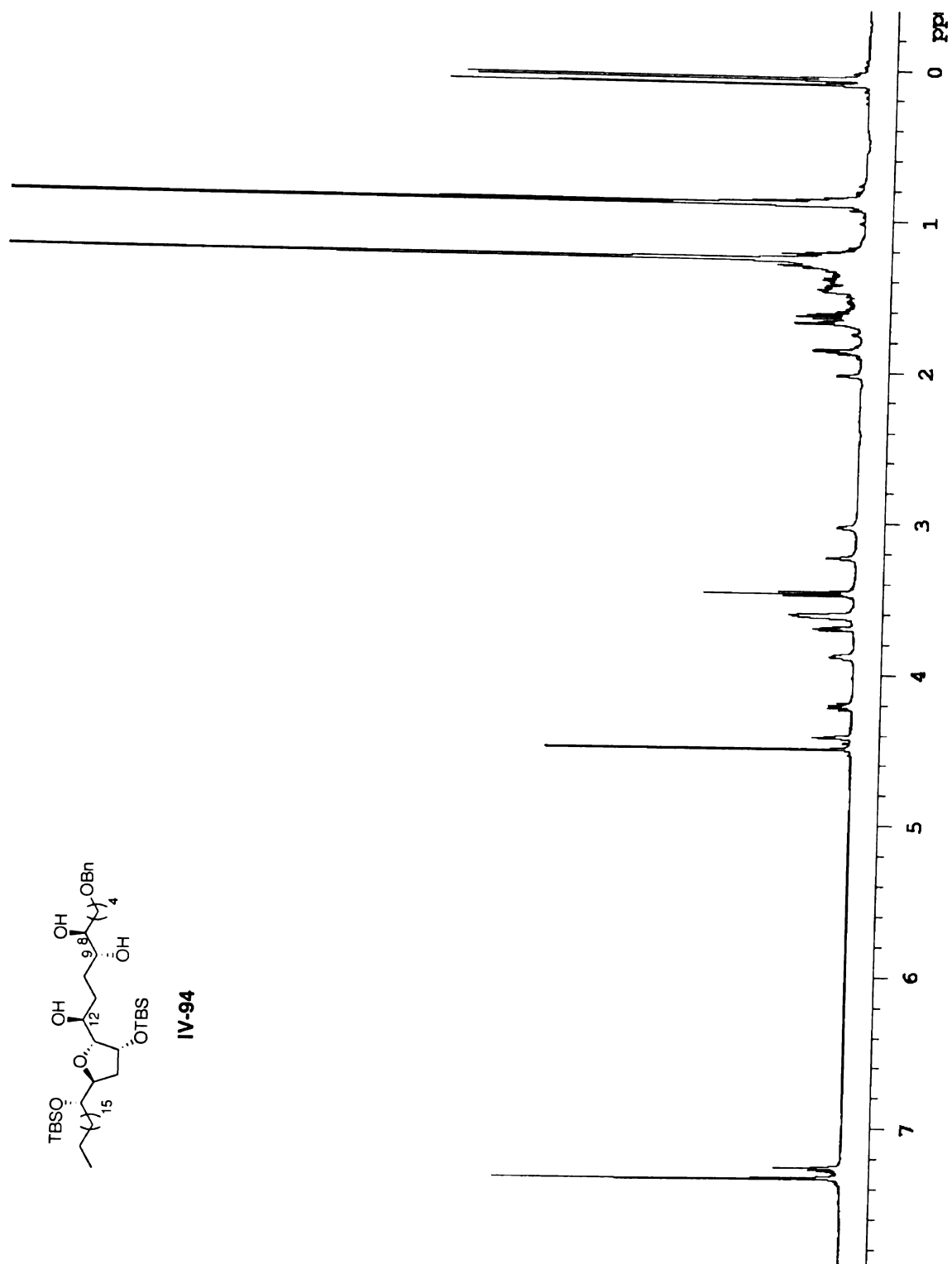
IV-91



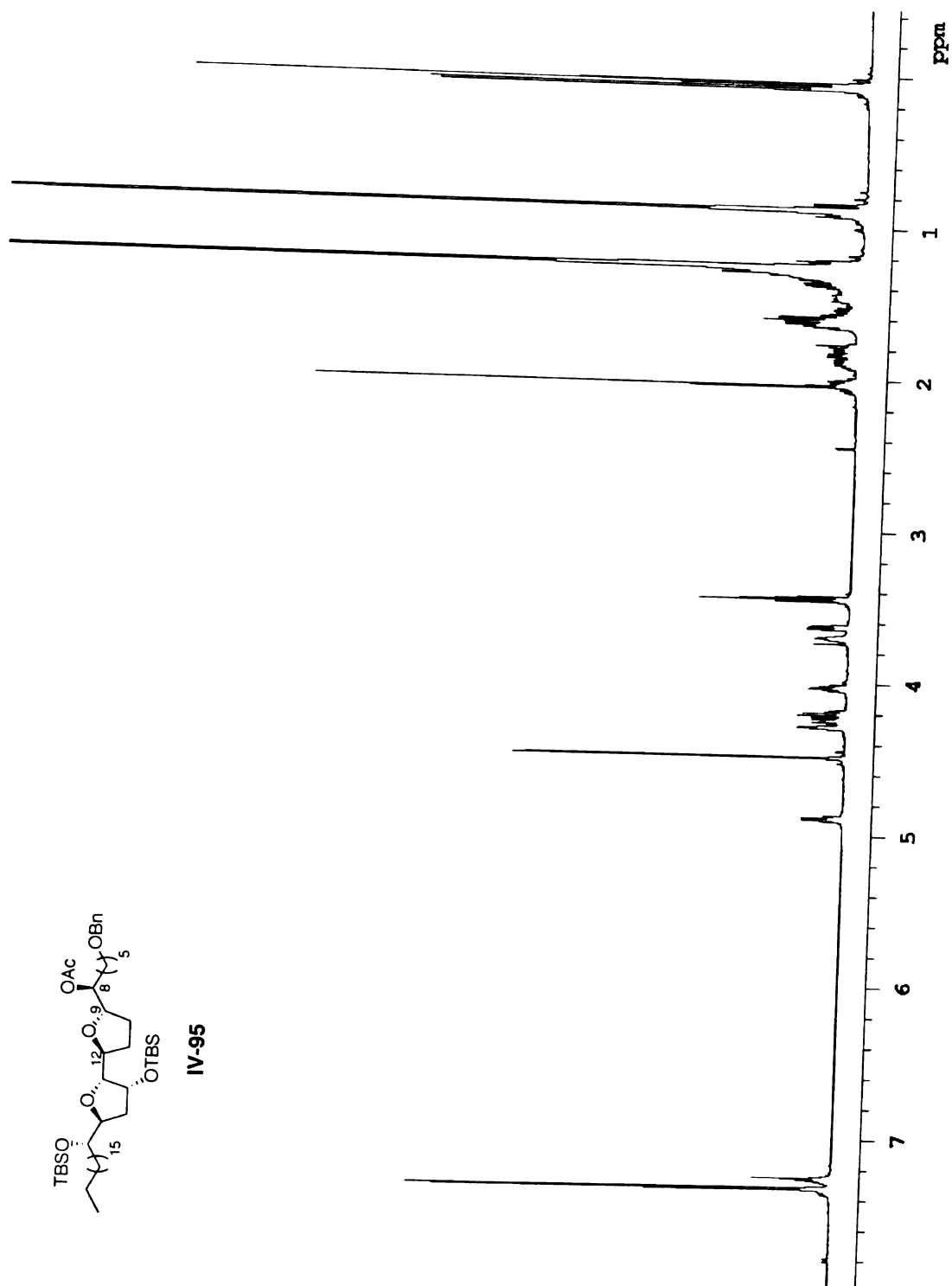
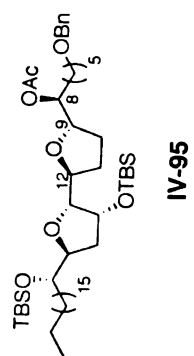


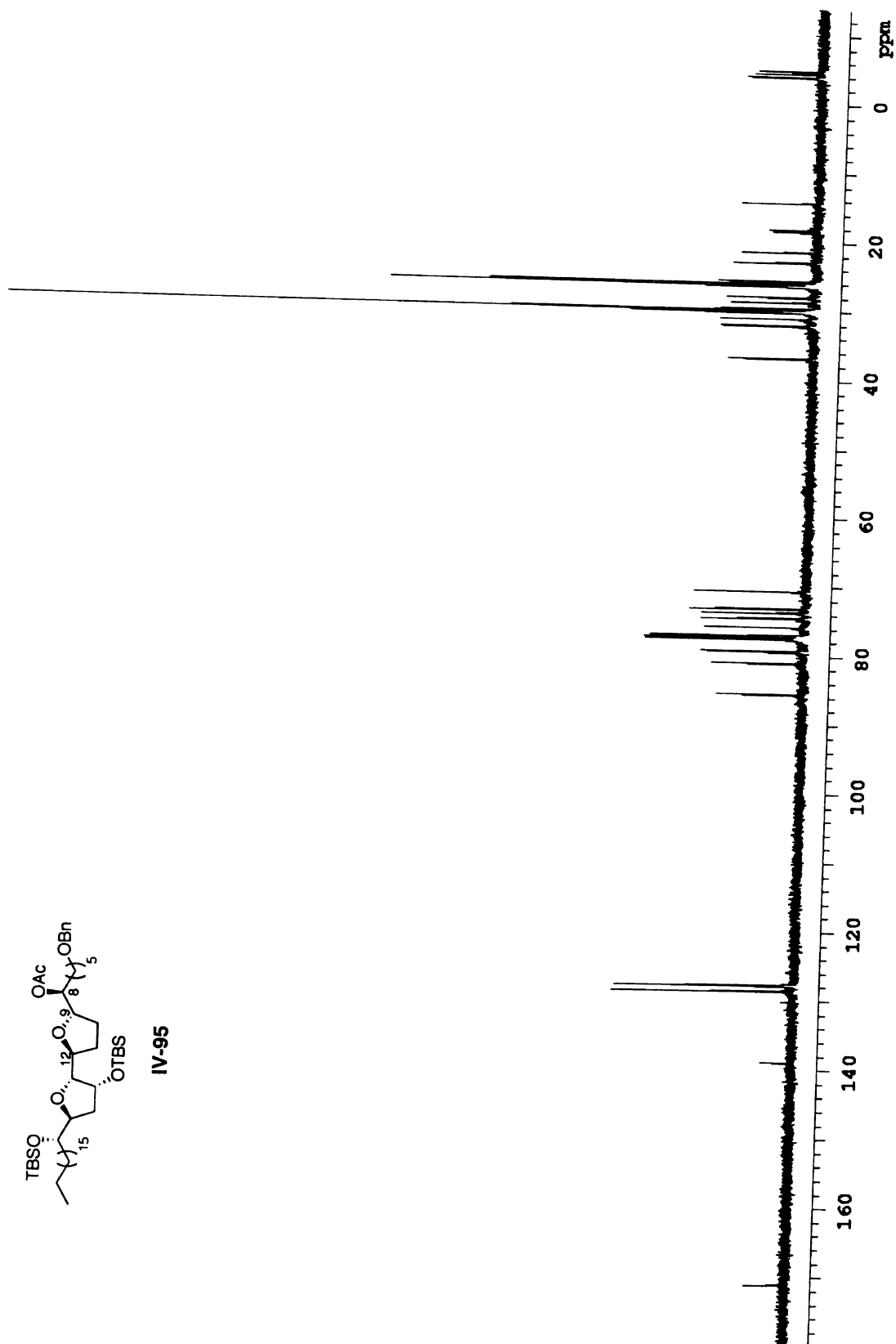
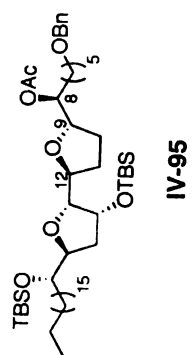
IV-91

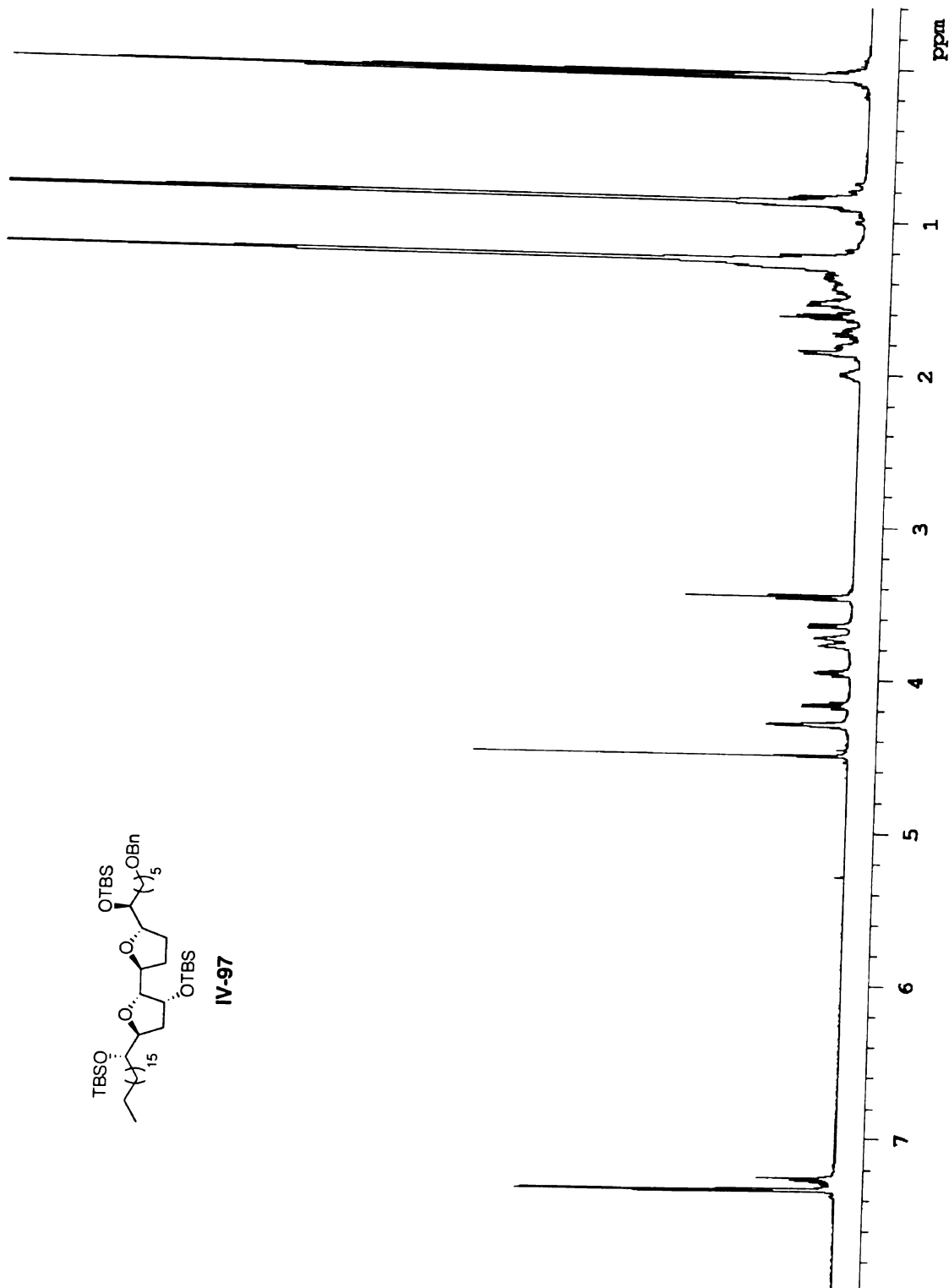




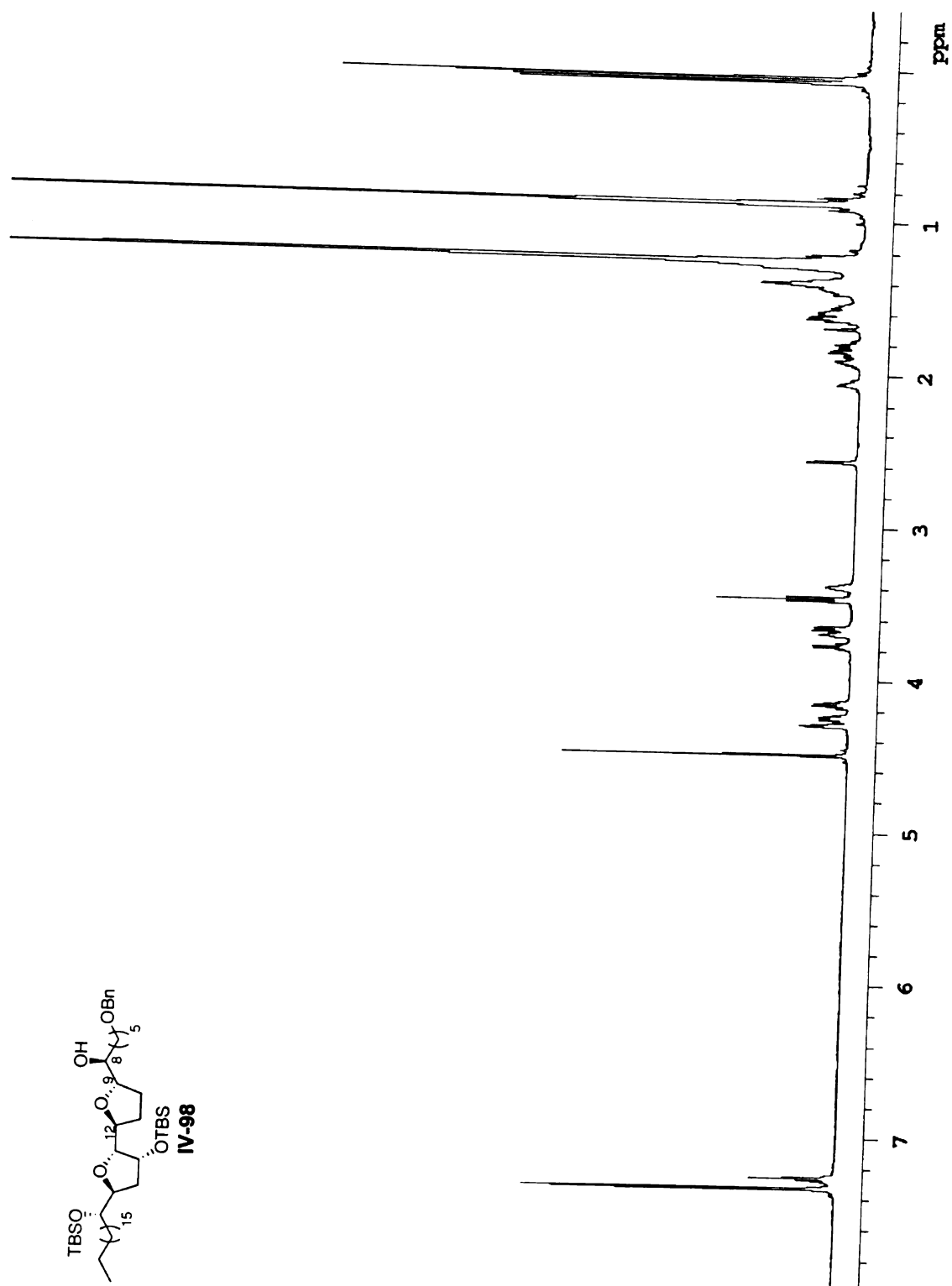
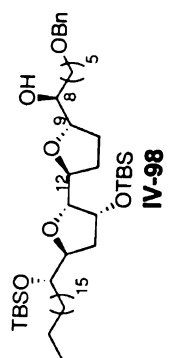


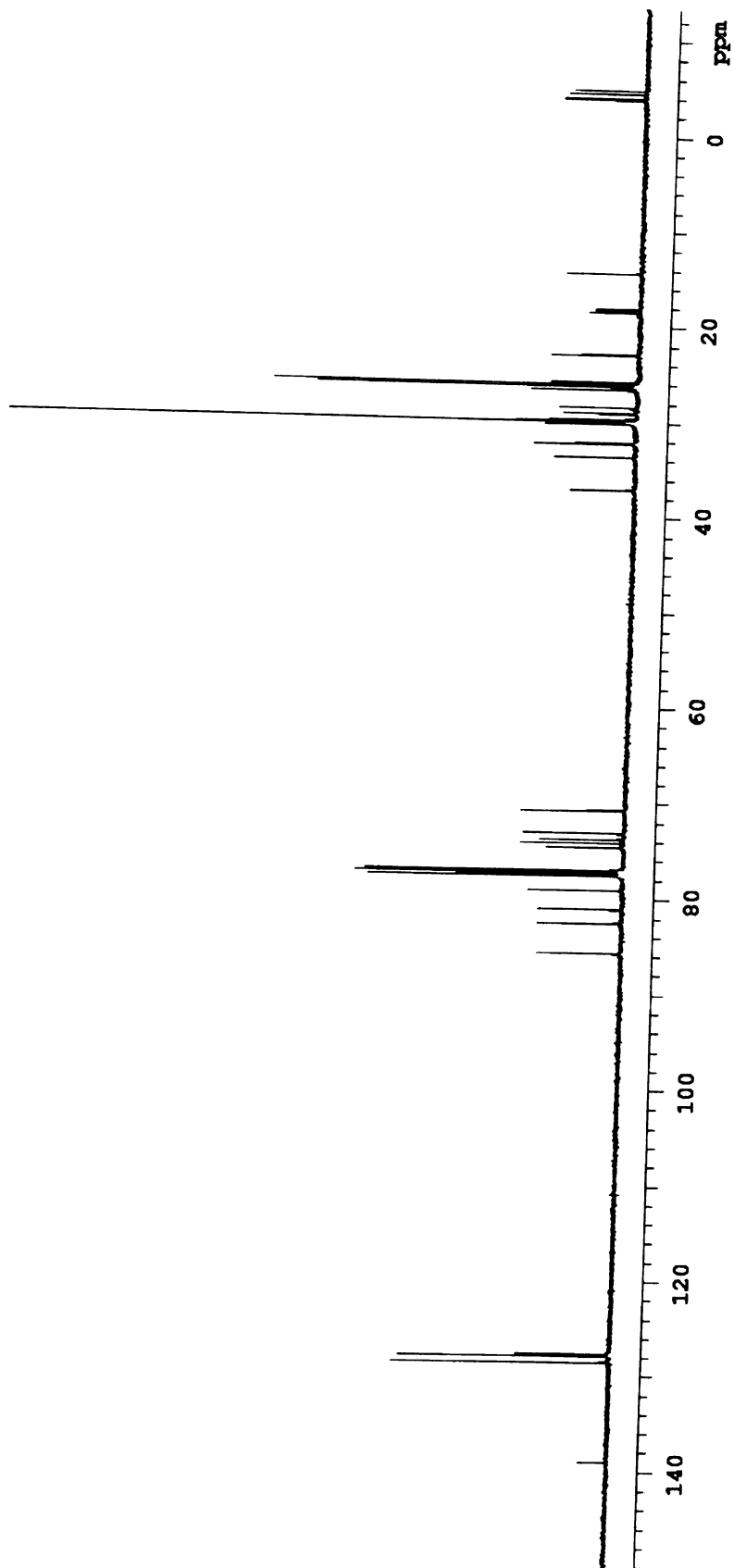
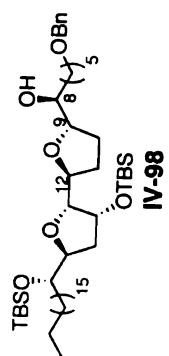


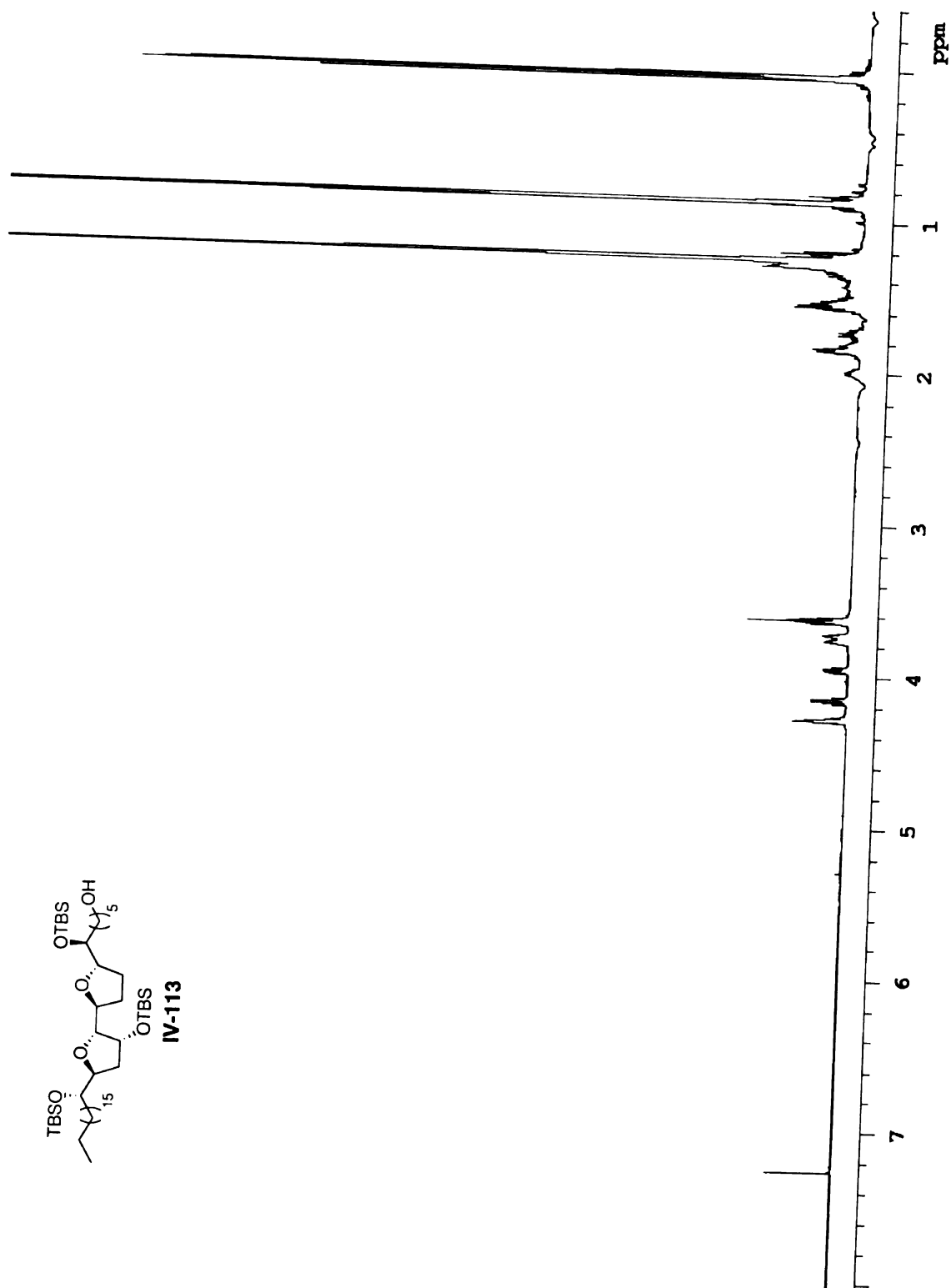




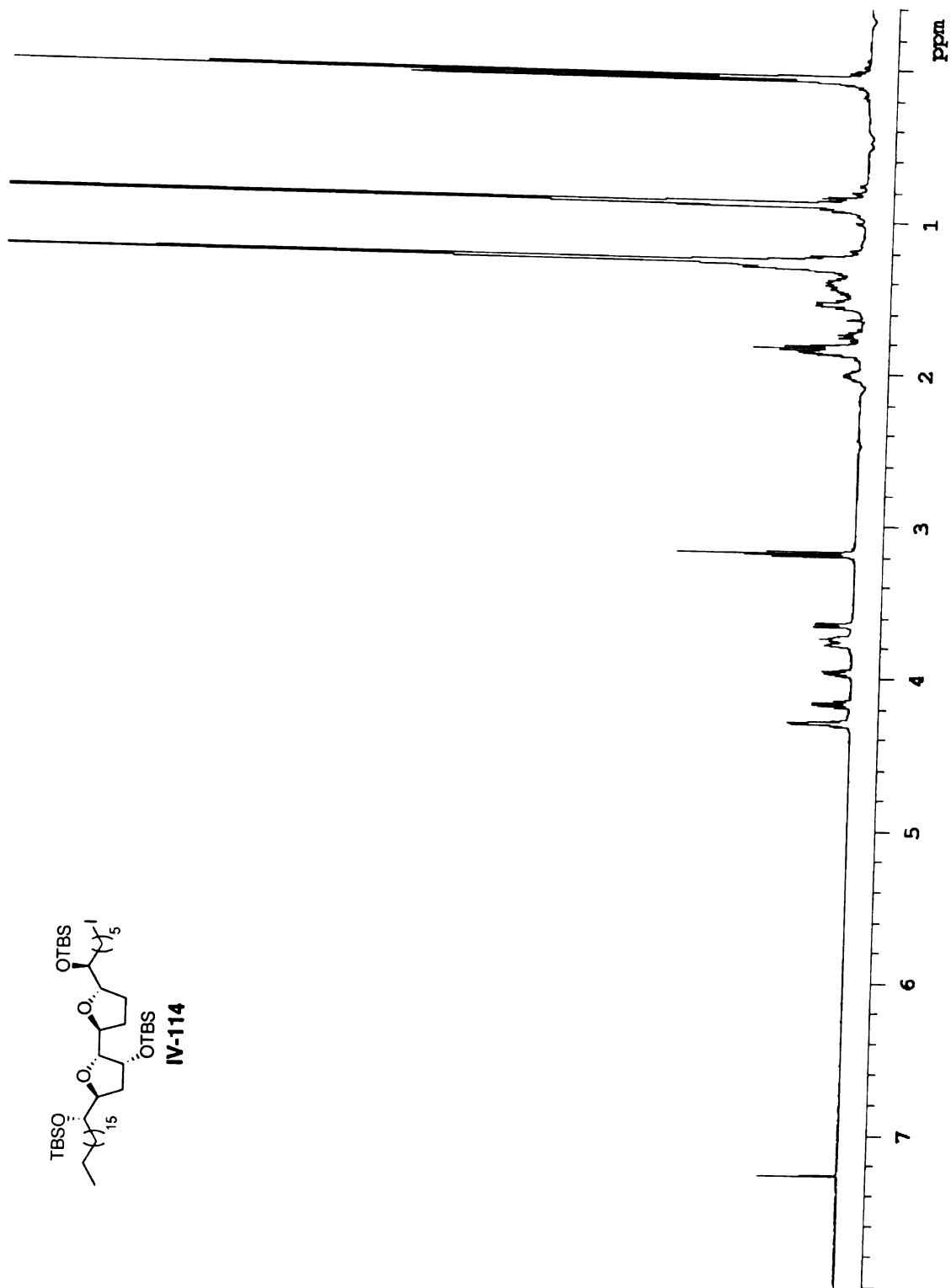




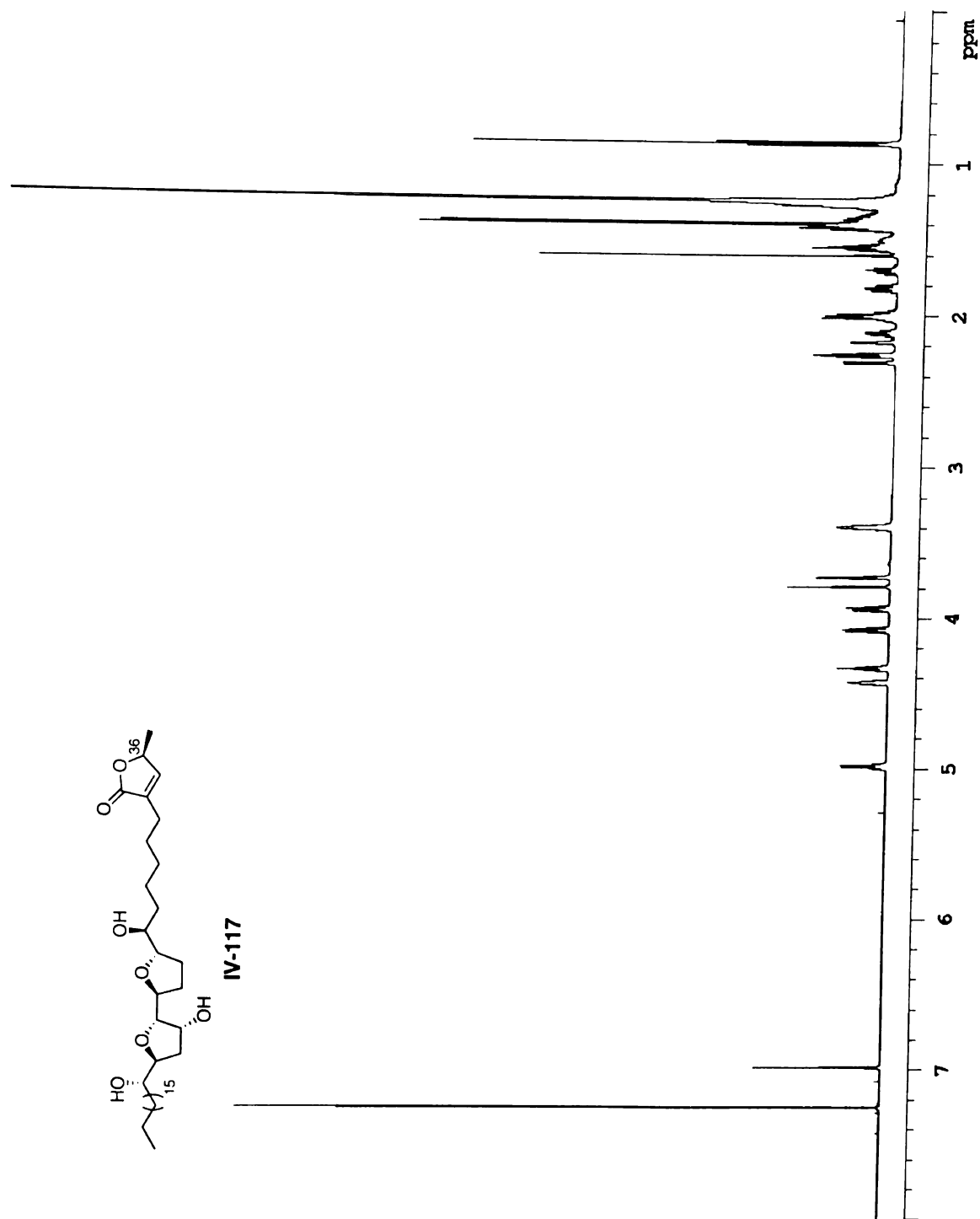


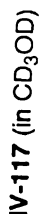


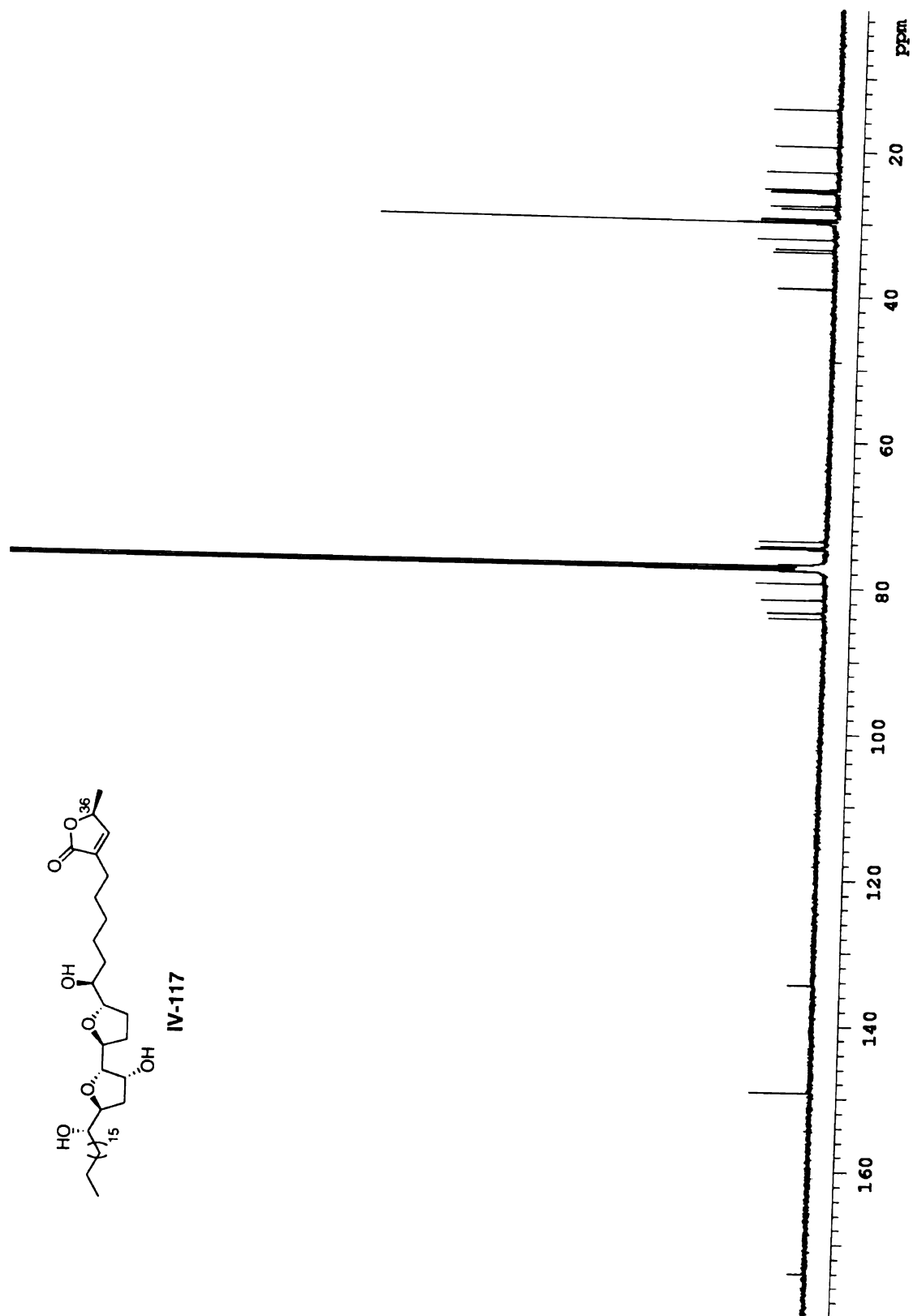


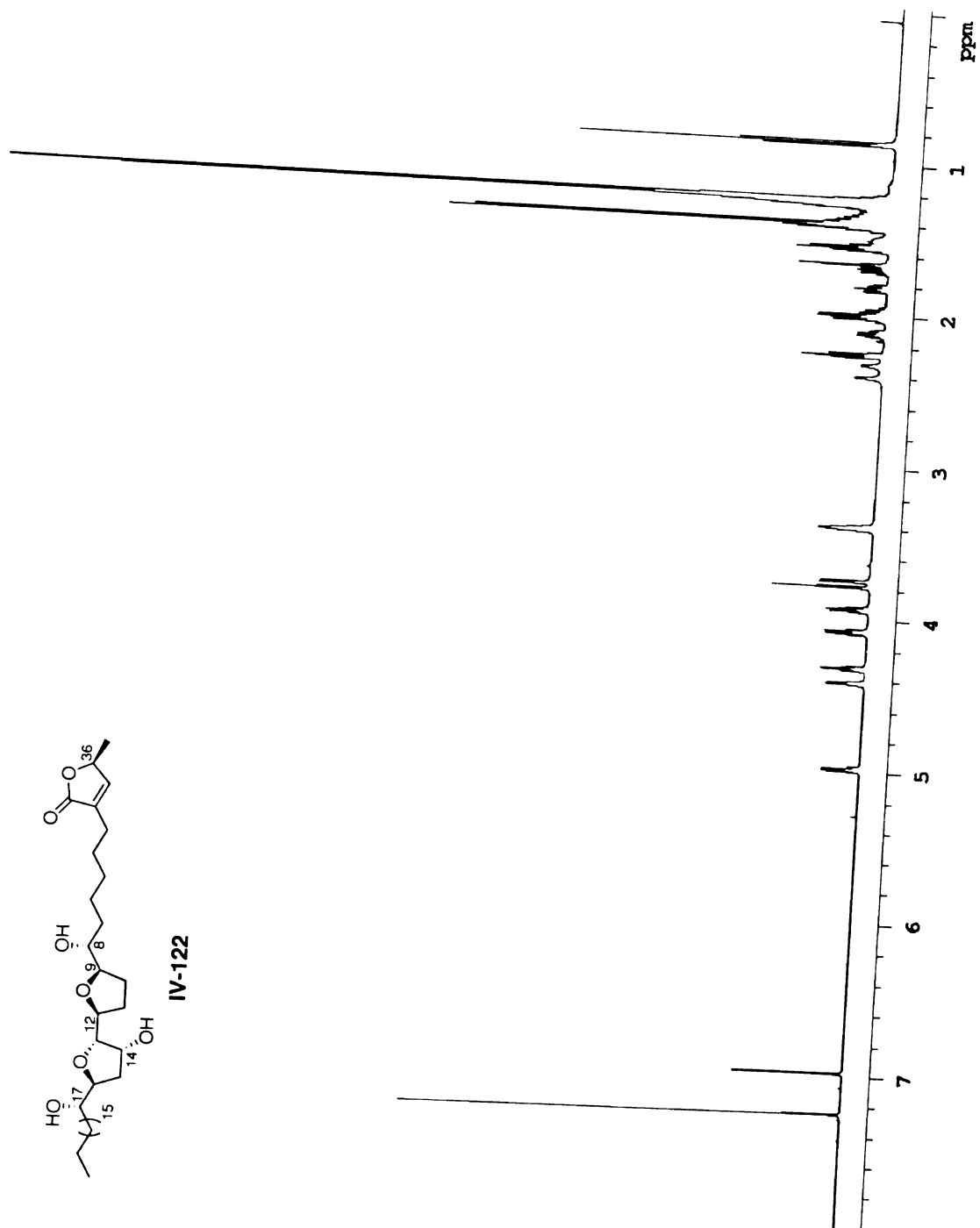


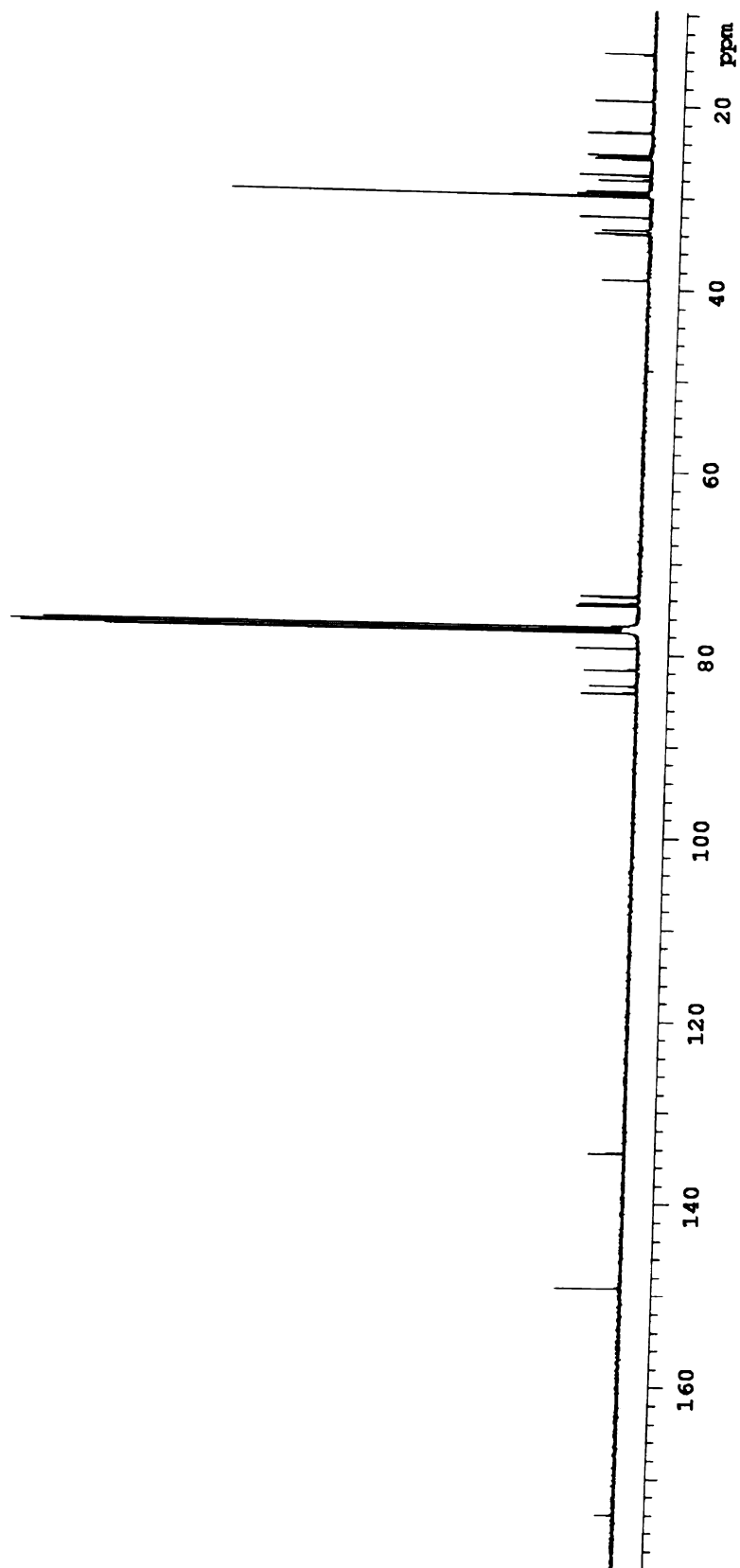
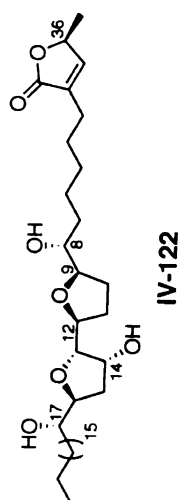












MICHIGAN STATE UNIVERSITY LIBRARIES



3 1293 02551 6380

